GP 223 Part II: Stratigraphic interpretation of reflection seismic data--"Seismic Stratigraphy"

Payton, 1977, Seismic Stratigraphy-Applications to Hydrocarbon Exploration: AAPG Memoir 26

Sheriff, 1980, Seismic Stratigraphy: IHRDC (Boston)

Anstey, 1978, Seismic Exploration for Sandstone Reservoirs: IHRDC (Boston)

Berg and Woolverton, 1985, Seismic Stratigraphy II-An Integrated Approach: AAPG Memoir 39

Abbott, 1979, Atlas of Seismic Stratigraphy: Shell Oil Company

Bally, 1987, 1988, Atlas of Seismic Stratigraphy: AAPG Studies in Geology #27

Cross and Lessenger, 1988, Seismic stratigraphy: Annual Reviews of Earth and Planetary Sciences, v. 16, p. 319-354.

Weimer and Link, 1991, Seismic facies and sedimentary processes of submarine fans and turbidite systems: Spriner Verlag

Biddle, et al, 1992, Seismic model of a progradational carbonate platform....: AAPG Bulletin, v. 76, p. 14-30.

Brown, A.R., 1999, Interpretation of three-dimensional seismic data, 5th edition: American Association of Petroleum Geologists Memoir 42, 514 p. (this volume is periodically updated)

Posamentier, H., and Kolla, V., 2003, Seismic geomorphology and stratigraphy of depositional elements in deep-water settings: Journal of Sedimentary Research, v. 73, p. 367-388

Allen, M.R. et al., 2006, The deliberate search for the stratigraghic trap: Geologic Society of London Sp Pub 254.

Davies, R.J., et al., eds., 2007, Seismic geomorphology: Applications to hydrocarbon exploration and production: Geological Society Special Publication 277, 274 p.

'Classic' reference:

AAPG Memoir 26. "Seismic Stratigraphy-Applications to Hydrocarbon Exploration"
Sections relevant to GP183: Section 2, Parts 1, 2, 5; Parts 6, 9, 10; Parts 3, 4, 7, 8

Modern reference:

Emery, D., and Myers, K.J., eds., 1996, Sequence stratigraphy: Blackwell Science, Oxford, 297 p.

Scales of investigation:

-Detailed borehole- and intra-borehole-scale prediction of lithology, with or without borehole data

-Delimiting depositional packages

-Basin analysis

'Sequence stratigraphy' versus 'seismic stratigraphy'

Definition: Seismic stratigraphy is a geologic approach to stratigraphic interpretation of seismic data

Fundamental Premise ("The Chronostratigraphic Assumption"):

Assuming that data and processing are in order, reflections arise from physical surfaces in the rocks--mainly bedding surfaces and unconformities--characterized by velocity-density contrasts (with a few exceptions like certain fluid contacts, etc.). Therefore, superposition works, i.e.. reflections have chronstratigraphic significance and are not geologically time-transgressive (don't follow lithofacies boundaries)

If the chronostratigraphic assumption is true (and we'll look more closely at this later), then:

1. We can read post-depositional structure regardless of facies changes
2. We can make stratigraphic interpretations, such as:
    a. Geologic time correlation
    b. Definition of genetically related depositional units
    c. Thickness and depositional environment of such units
    d. Paleobathymetry
    e. Burial history
    f. Relief and topography on unconformities
    g. Paleogeography and history (in combination with other info)

Serious limitation: Seismic stratigraphy is largely a geometric method and as such offers no direct, positive identification of lithology.

Examining the chronstratigraphic assumption:

1. Bedding surfaces

-Depositional surfaces mark "momentary" nondeposition

-There may or may not be a lithologic contrast across such surfaces in the geologic record, so they will be seismically recognizable only if there is an acoustic impedance contrast.

-Depositional surfaces are paleoland surfaces and so have geologic time significance. This idea, plus the increasingly widespread acquisition of 3-D seismic data volumes, give rise to the subdiscipline of 'seismic geomorphology' (see Posamentier and Kolla, 2003, Journal of Sedimentary Research, v. 73, p. 367-388).

examples: deep-sea: a turbidite event/bed; subaerial--Mt. St. Helens ashfall

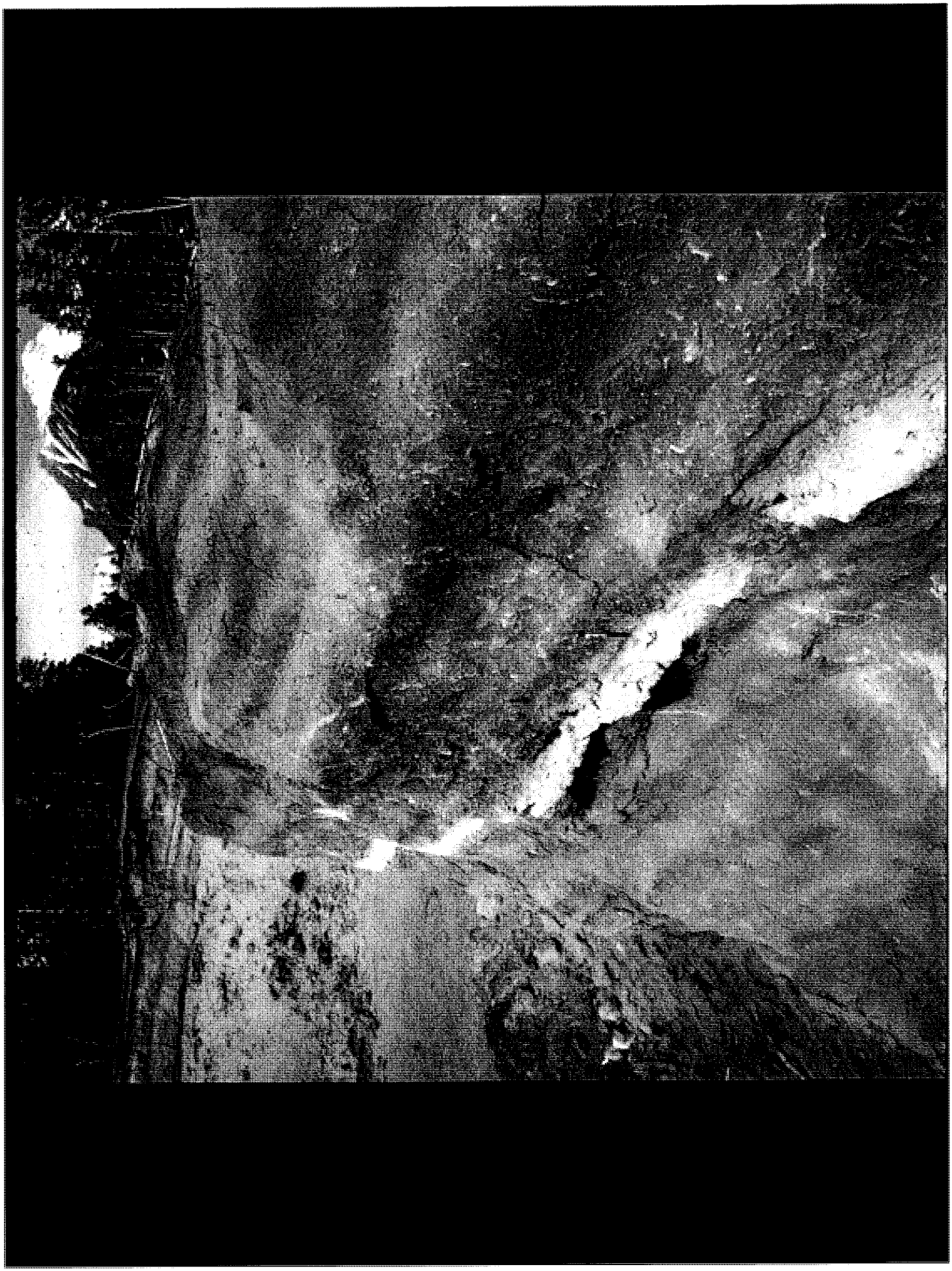

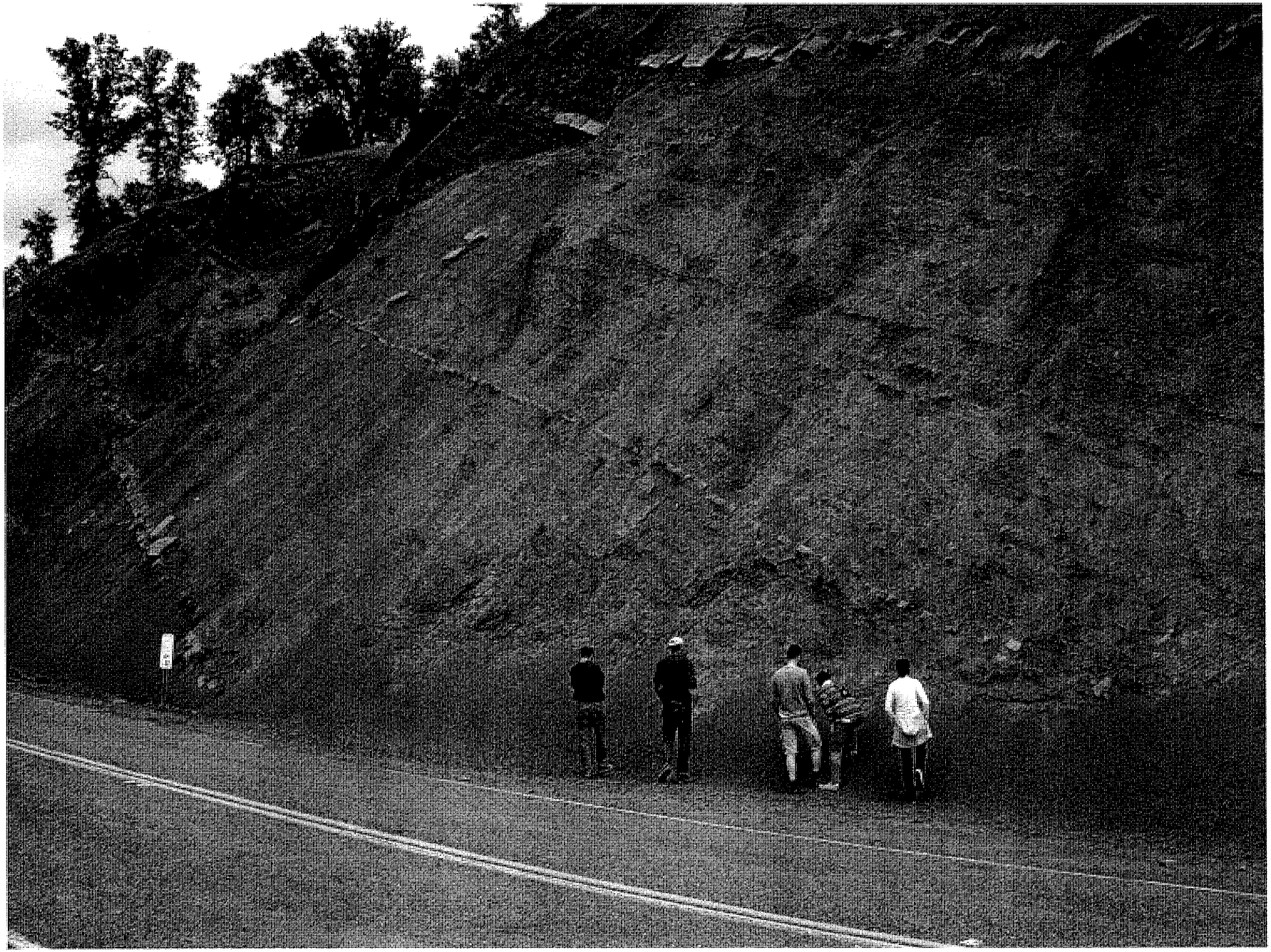

These examples seem obvious, but how about a typical geologic cross-section?

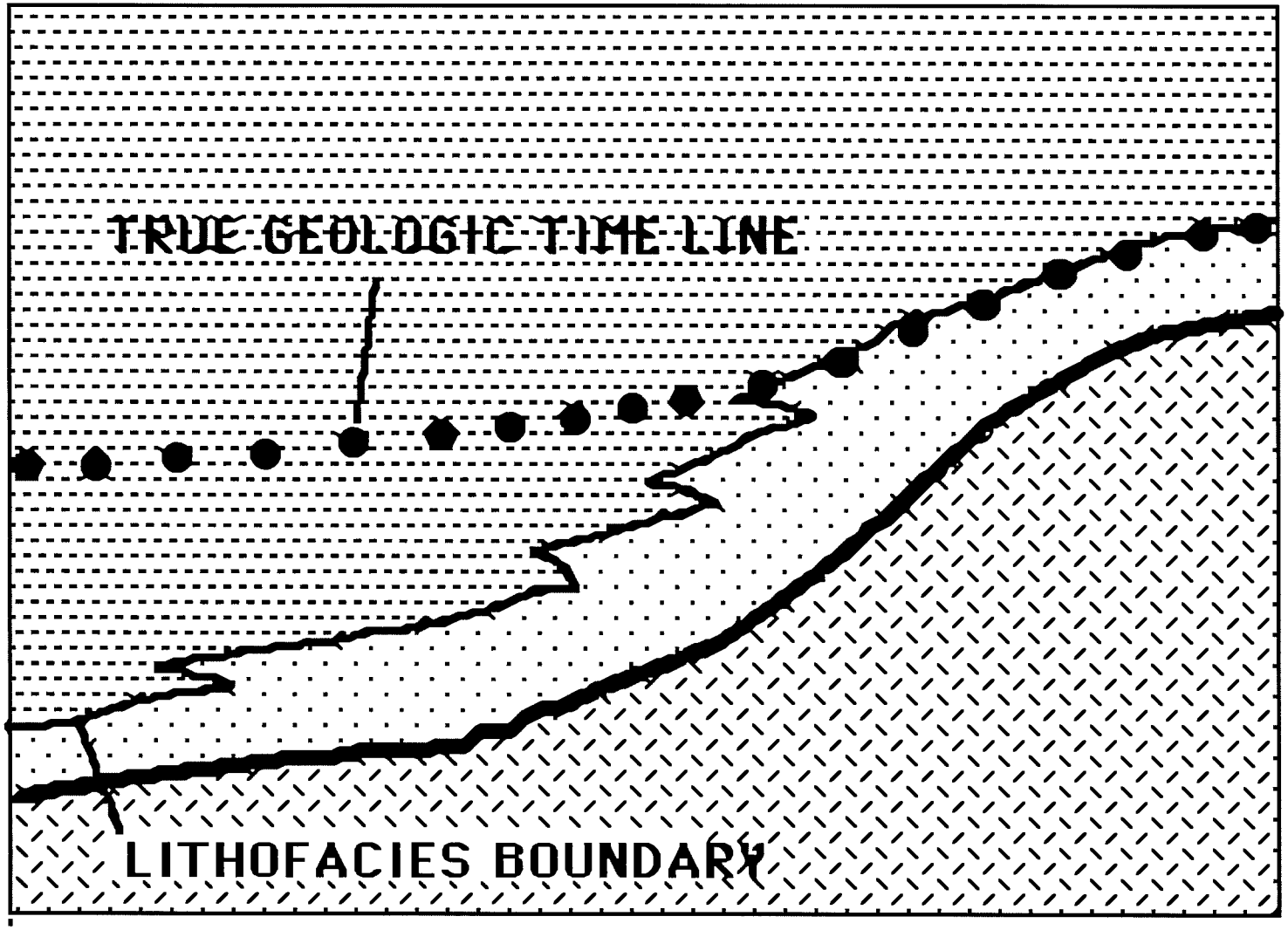

Why should the "true geologic time line" give rise to a reflection, rather than the "lithofacies boundary" ???

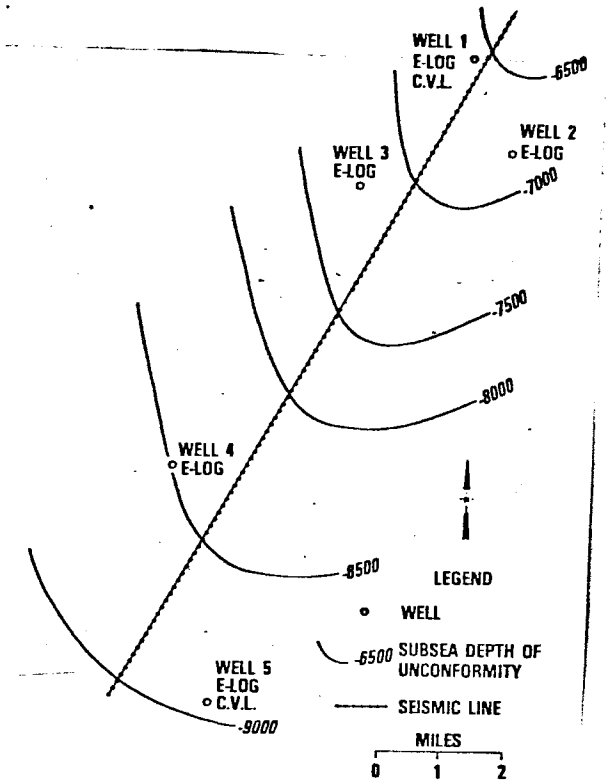

FIG. 1—Location of wells used in Tertiary example, South America.

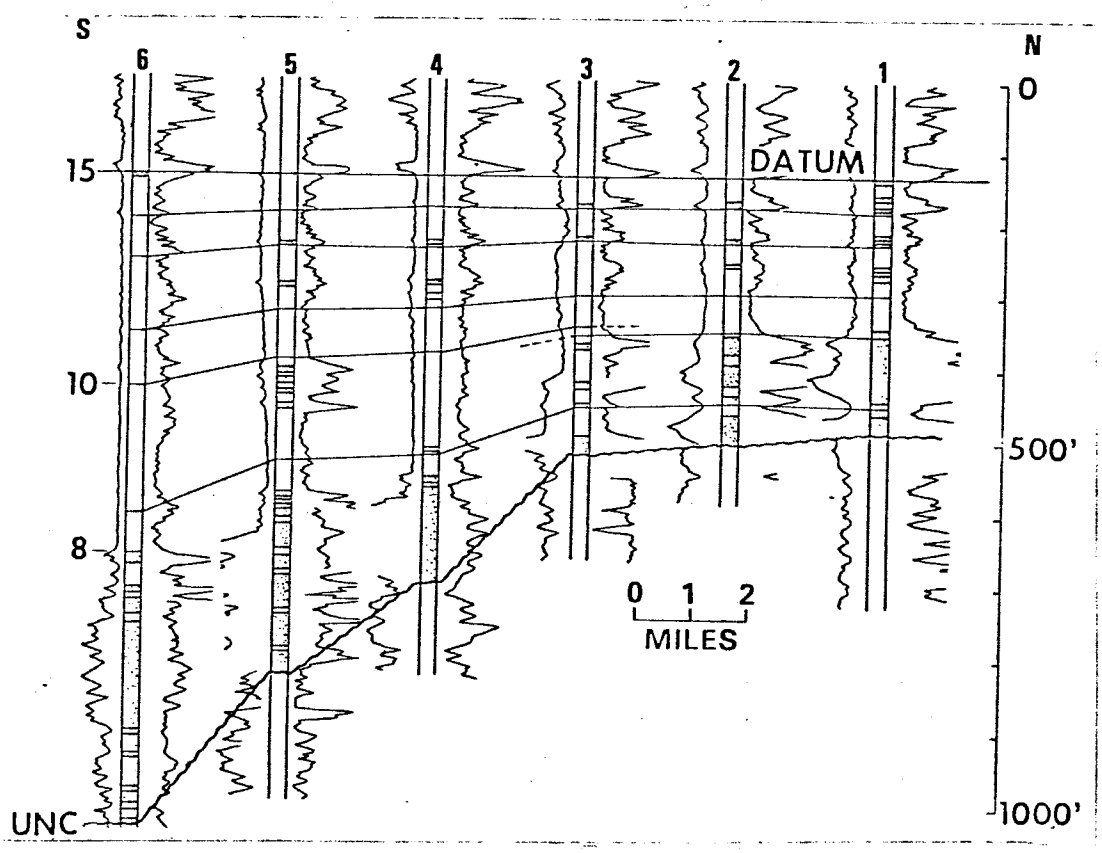

FIG. 2—Geologic cross section showing electric-log correlations, Tertiary example, South America. Stippled pattern in well bore represents sandstone. Key horizons indicated on left.

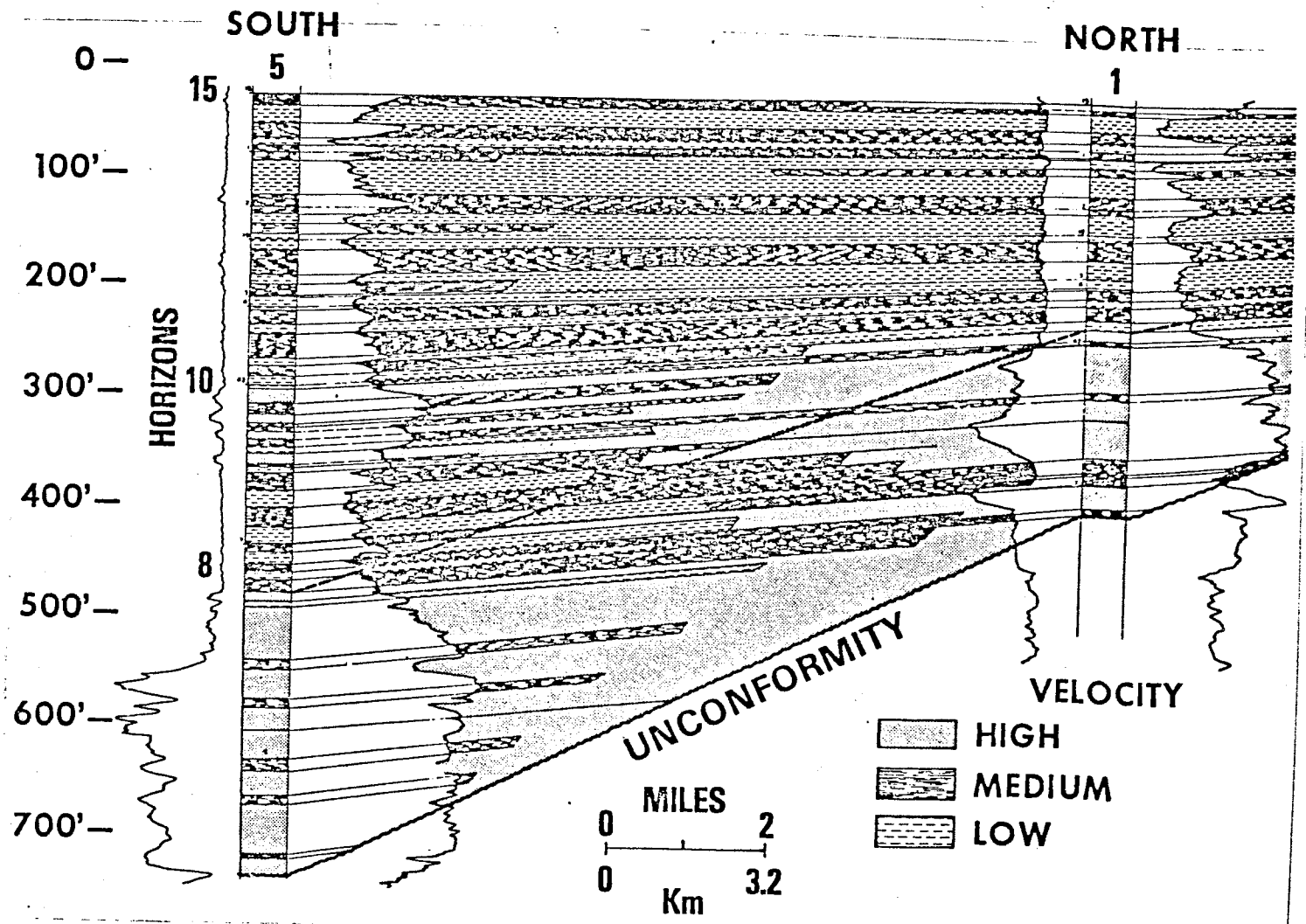

FIG. 3—Distribution of velocity for Tertiary example, South America. Velocity was obtained from CVLs for wells 5 and 1 and distributed laterally using stratal surface correlations.

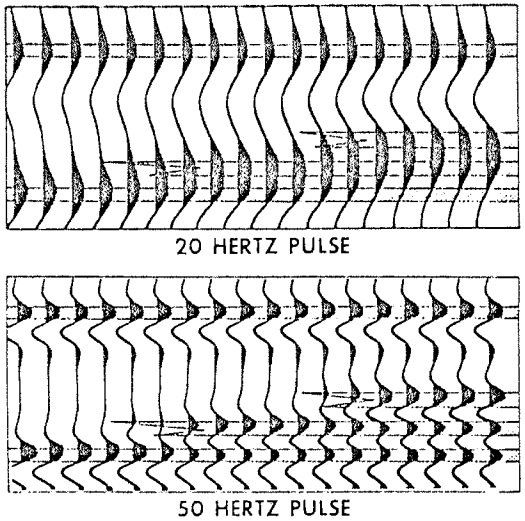

FIG. 17—Comparison of resolving power between 50-Hz and 20-Hz pulse.

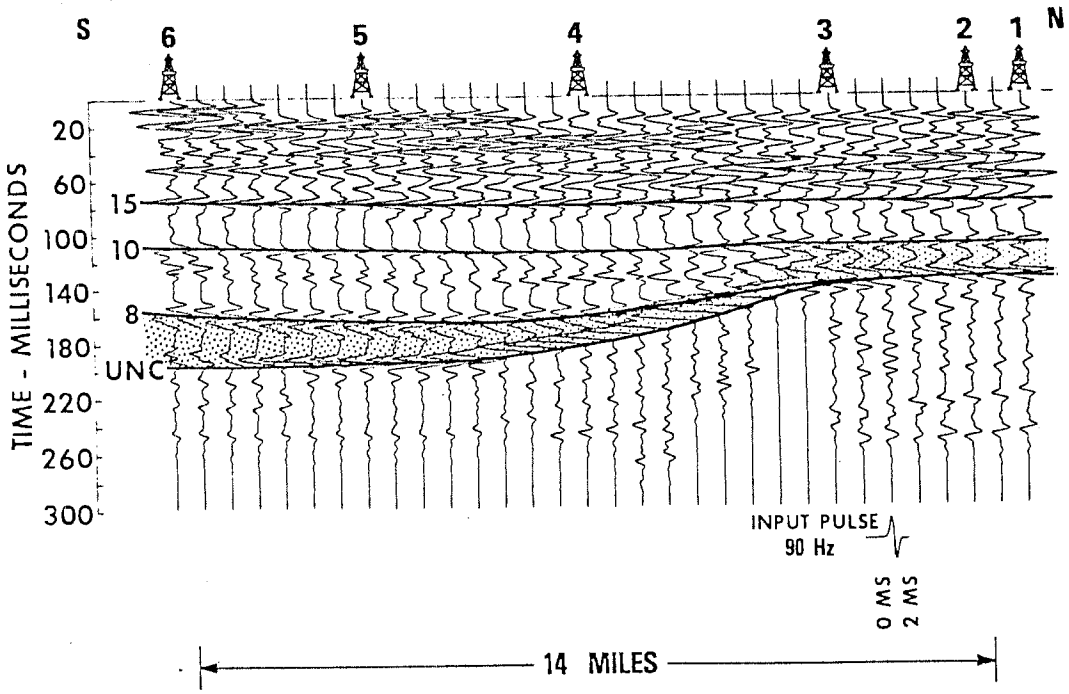

FIG. 4—High frequency synthetic seismic section constructed by inputting 90-Hz sine wave. Stipple pattern represents sandstone.

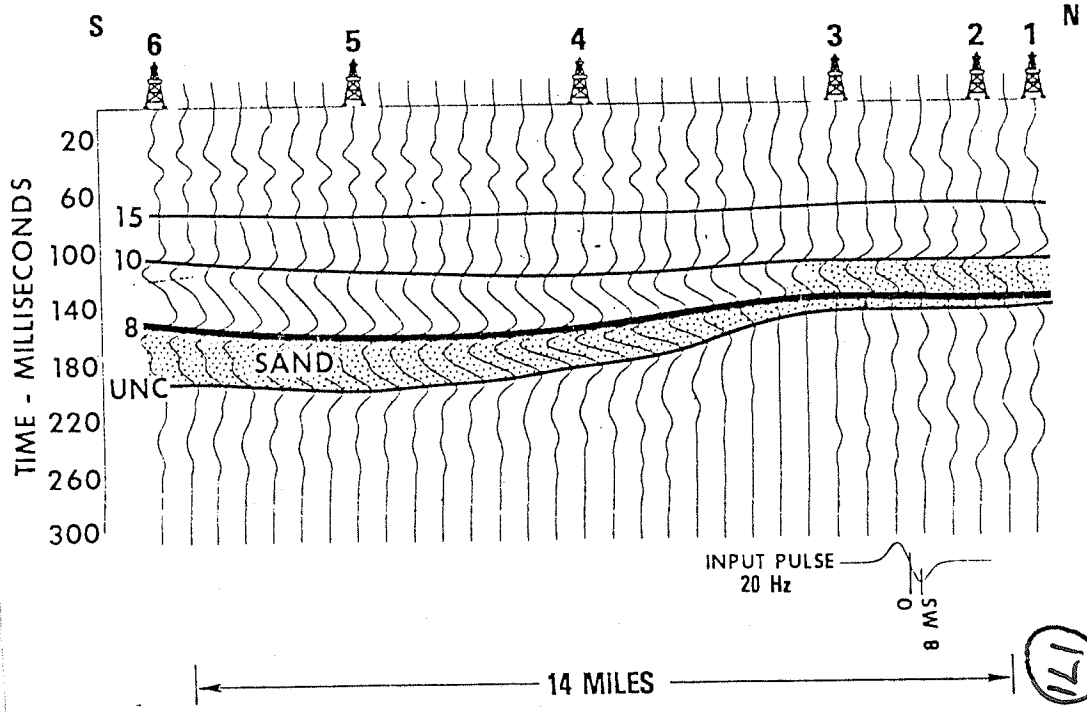

FIG. 5—Normal frequency synthetic seismic section constructed by inputting 20-Hz sine wave. Stipple pattern represents sandstone.

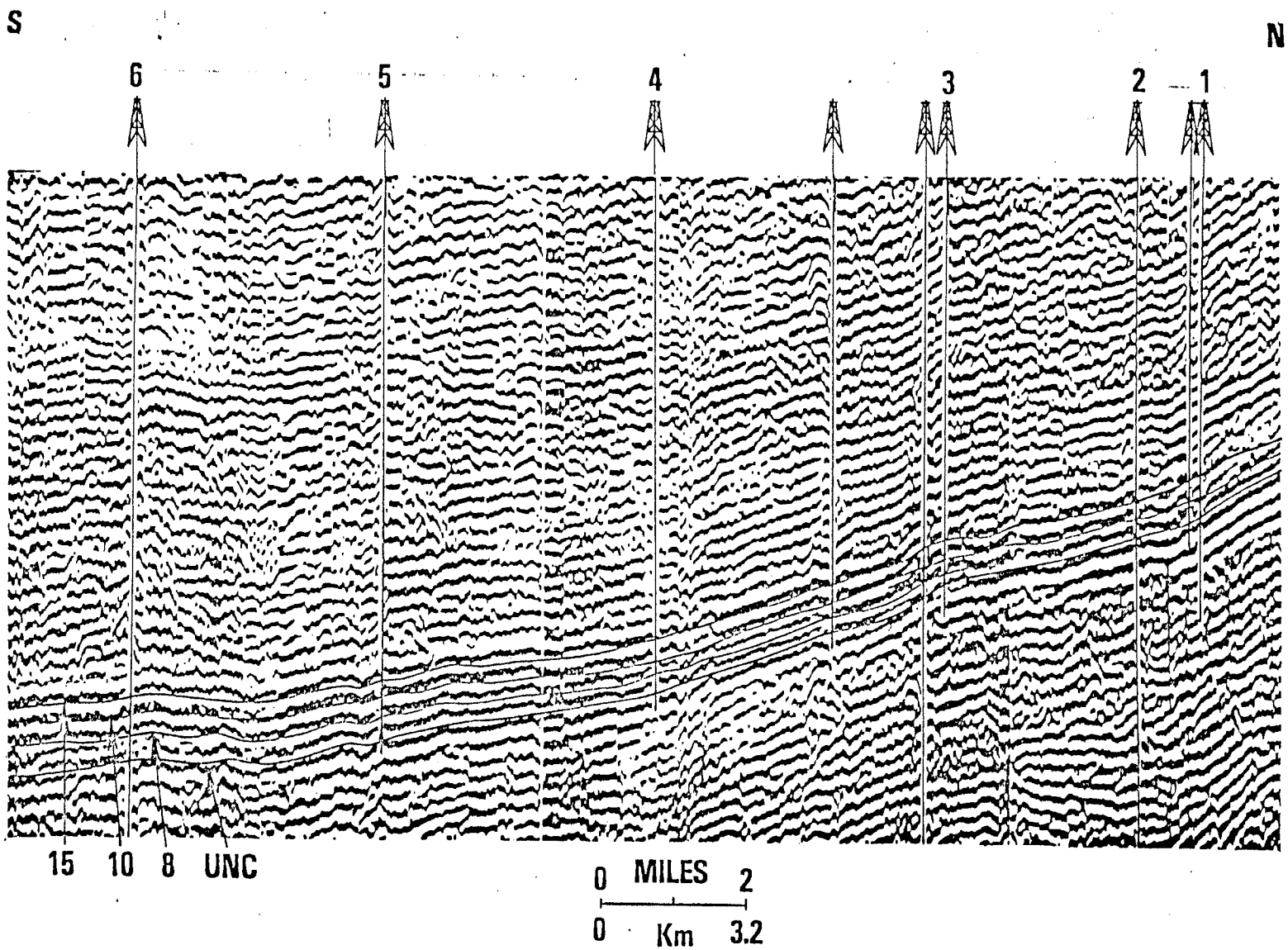

FIG. 6—Single-fold VDF magnetic tape seismic section from a Tertiary basin in South America.

- Unconformities

Geologic time significance: Everything below the unconformity surface is older than everything above, but the surface is not synchronous (like a bedding plane) over its entire extent. The time duration of an unconformity varies from place to place, in general.

They are seismically evident if angular.

Disconformities/paraconformities may not be at all obvious seismically; only if there's an acoustic impedance contrast due to differential lithification, or if traceable into an angular relation.

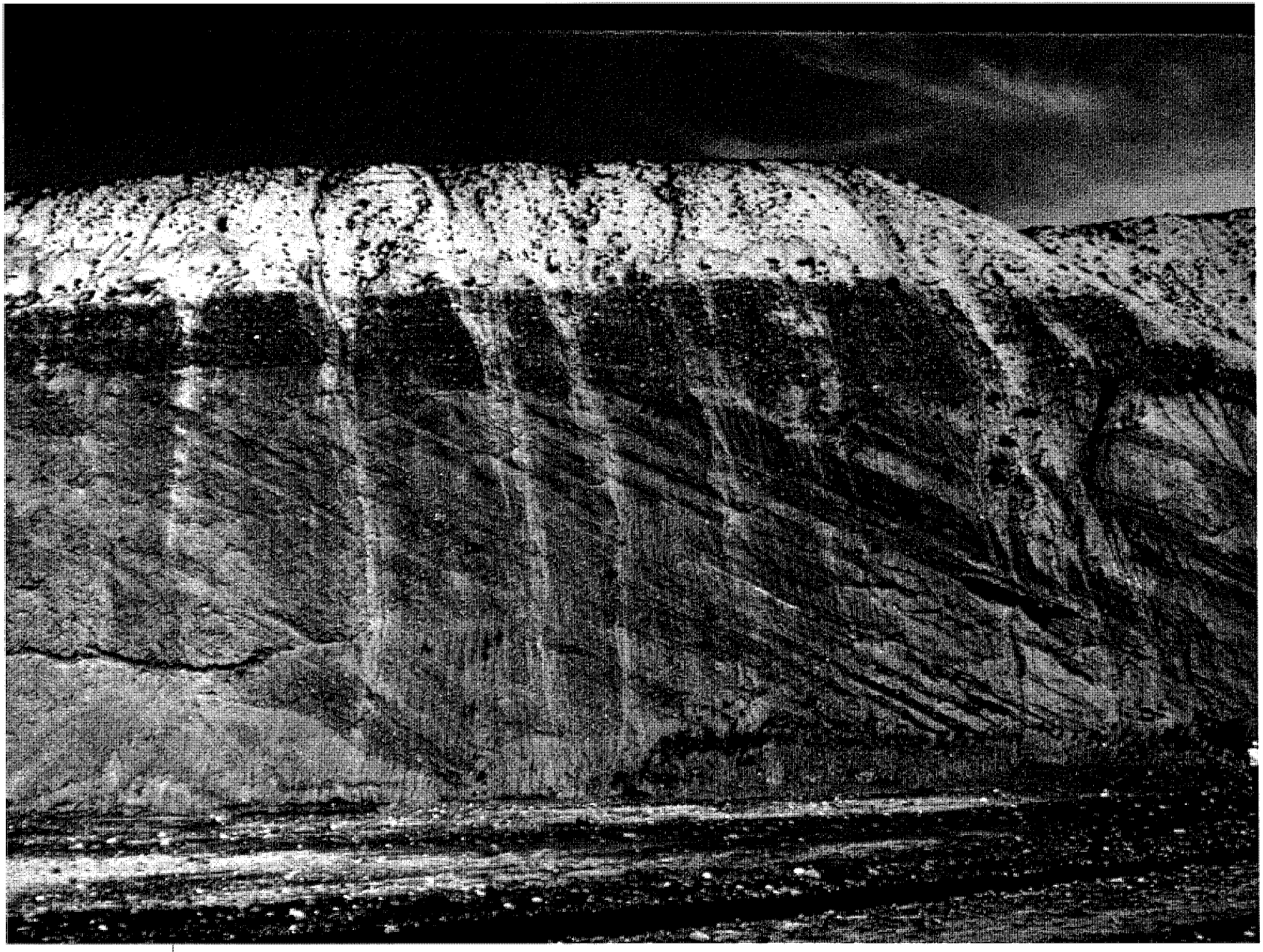

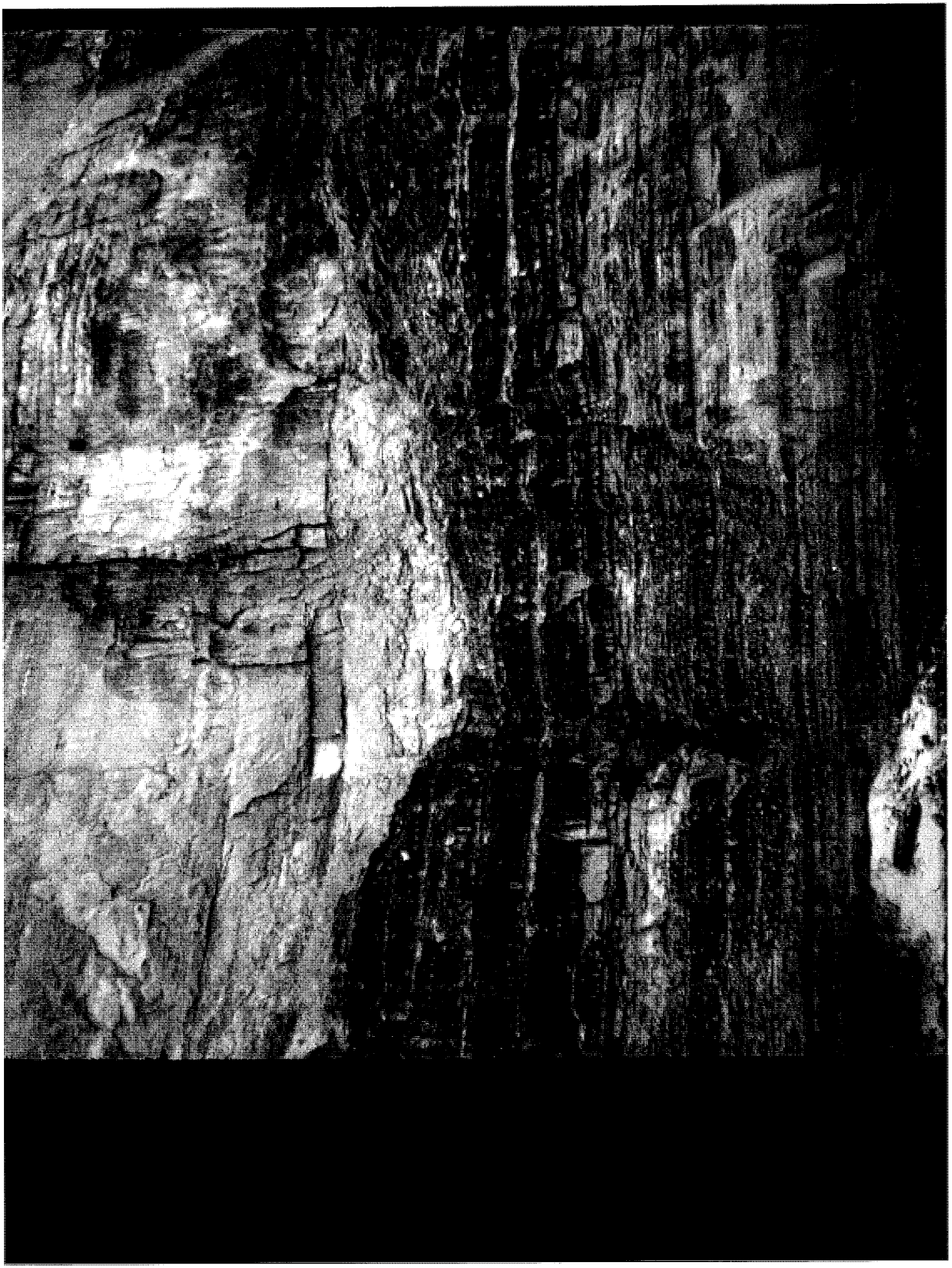

Pitfalls

Artifacts such as multiples

Resolutional limits

Other, nonstratigraphic, seismically imageable phenomena (gas, diagenetic boundaries)

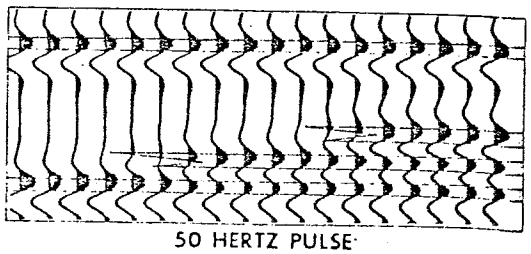

50 HERTZ PULSE

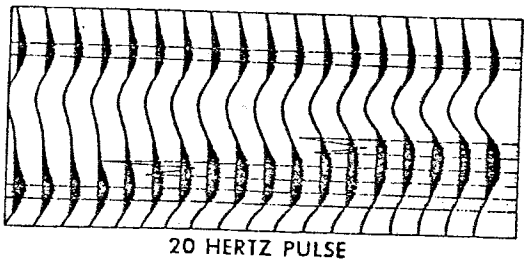

20 HERTZ PULSE

FIG. 17—Comparison of resolving power between 50-Hz and 20-Hz pulse.

AAPG Bull Dec 82

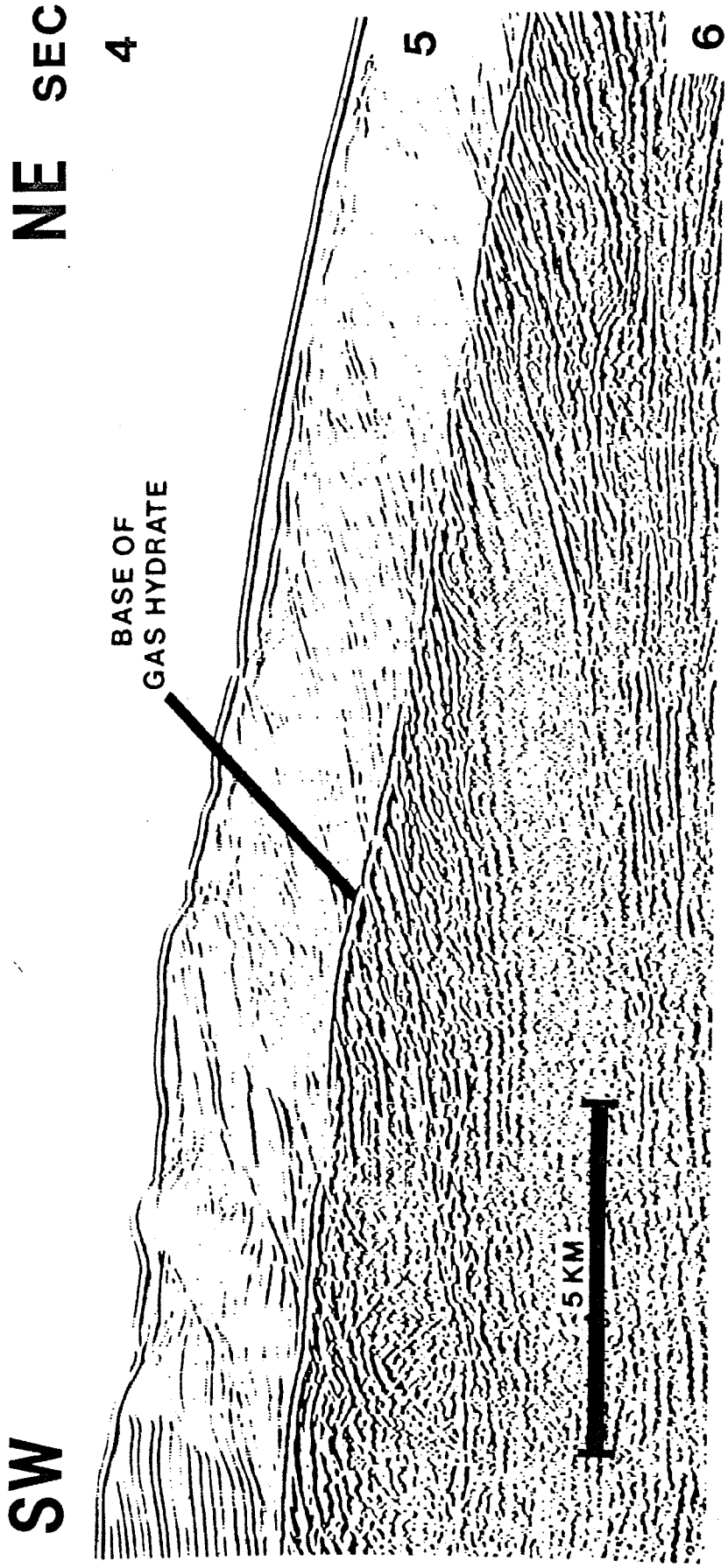

FIG. 1 — Multichannel seismic reflection profile from Blake Outer Ridge (Shipley et al, 1979).

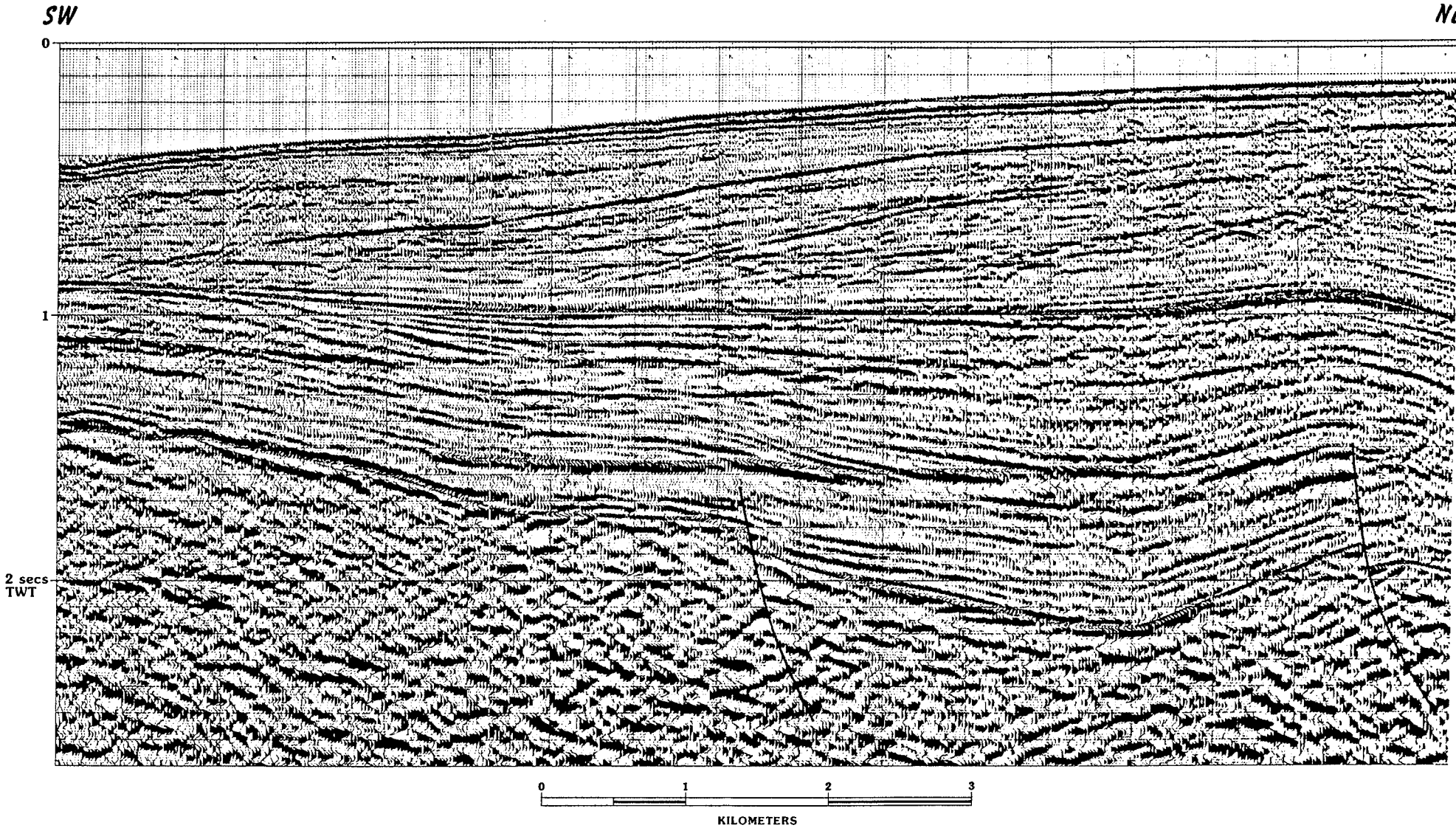

Figure 5. Seismic line showing the distinction between a seismic sequence boundary and a seismic facies boundary. The sequence boundaries are shown in blue and the facies boundary in yellow. The seismic line is taken from the Santa Maria basin, offshore California. The lower sequence boundary is the mid-Tertiary unconformity and the upper sequence boundary is the near base Pliocene unconformity. The Monterey and Sisquoc formations occupy the interval between. A sharp facies boundary is seen at 1.55 secs two-way traveltime which cuts horizontally across the dipping stratal surfaces. This is actually a diagenetic facies boundary between opal-CT porcellanites above and quartz cherts below, but it demonstrates the same principle as a diachronous depositional facies boundary. With an eye of faith, a shallower facies boundary can also be seen at 1.2 secs two-way traveltime. This approximates to the diagenetic facies boundary between opal-A above and opal-CT below.

Hubbard etal 1985a

Controls on stratigraphic accumulations and seismic stratigraphic practices

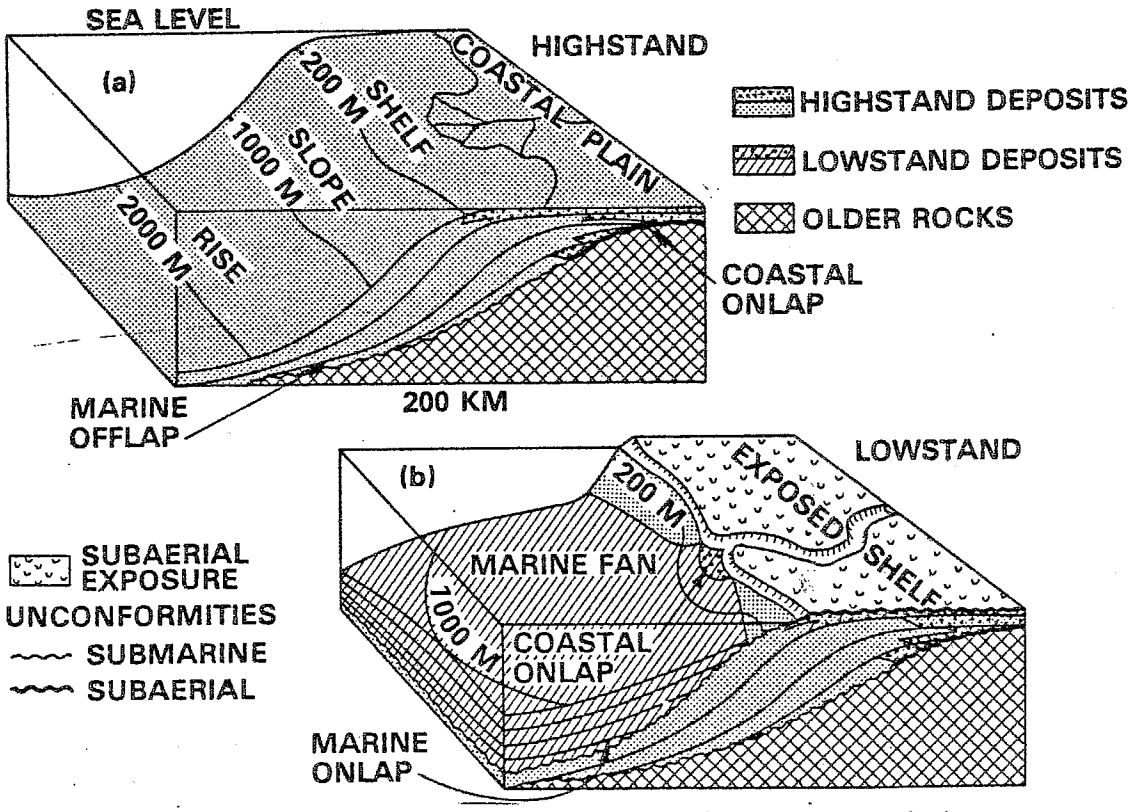

FIG. 9—Depositional patterns during highstand (a) and lowstand (b) of sea level.

AAPG Mem 26 (1977)

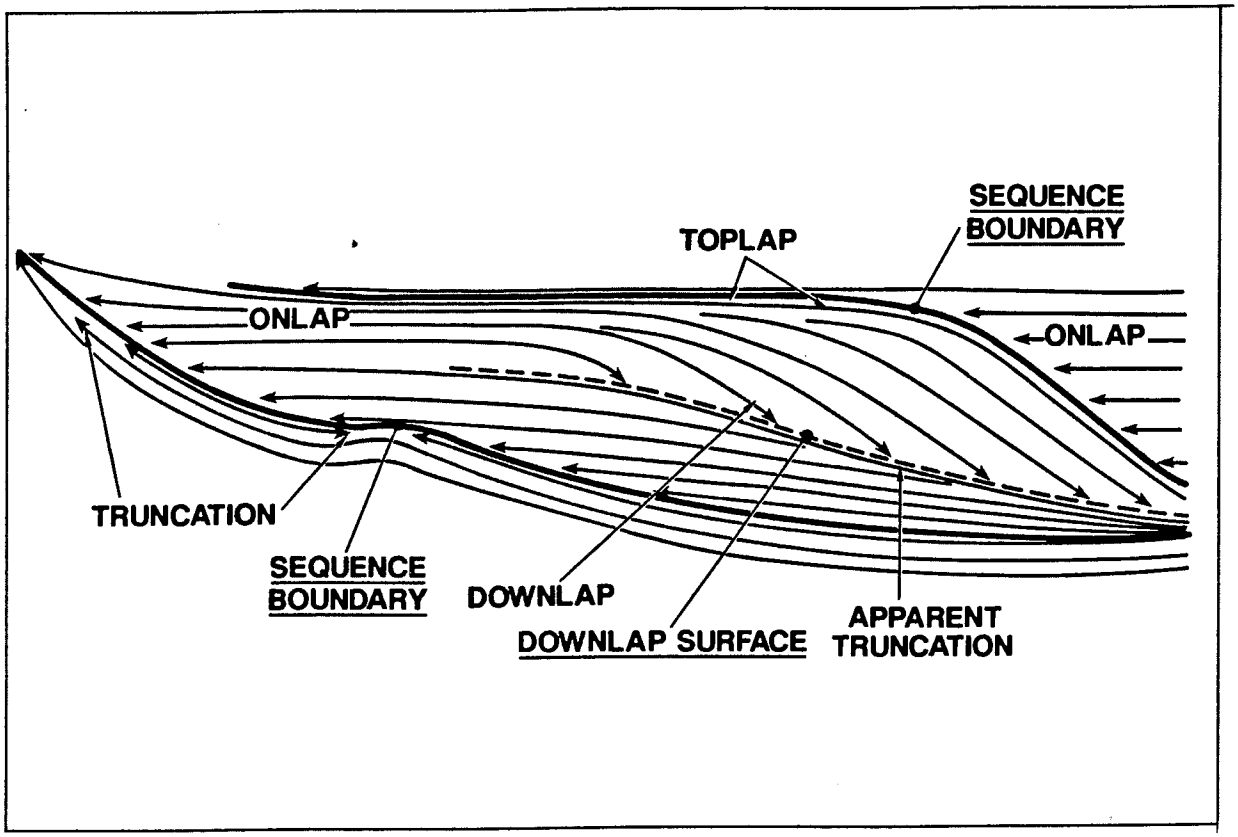

Figure 1. Diagram showing reflection termination patterns and types of discontinuities. Discontinuity names are underlined.

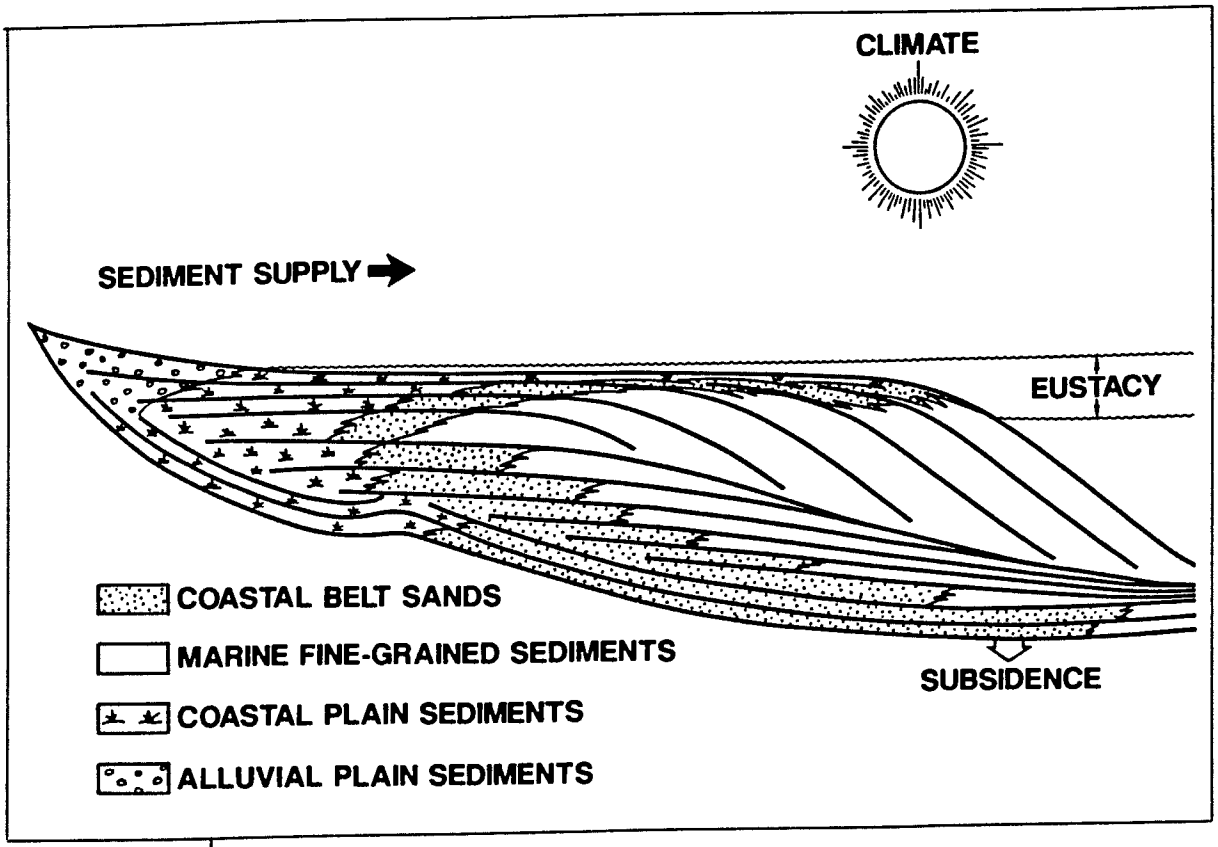

Figure 3. Diagram of seismic reflections, lithofacies, and major variables affecting stratigraphy.

Vail in Bally

SEQUENCE-STRATIGRAPHY
an integrated approach to basin analysis

A discussion of the Sequence Stratigraphic Conceptual Model

John M. Armentrout

Sequence Stratigraphy is the study of stratigraphic relationships within a time-stratigraphic framework. The mapping of depositional facies within each descret time-interval results in paleogeographic maps suitable for predicting the distribution of reservoir, seal and petroleum source rocks. This paper presents a very general overview of the fundamentals of sequence stratigraphy.

Each depositional sequence consists of repetitive, genetically related strata bounded by surfaces of erosion or non-deposition or their correlative conformities (Van Wagoner et al., 1987). Figure D-1 illustrates the geometry of the unconformity-bounded depositional sequence, the basic stratal unit of sequence stratigraphy as defined by the Vail-Exxon conceptual model. The Vail-Exxon model has evolved significantly since it was first introducted in Patton (1977). Some of the changes are most graphically illustrated by comparing the 1977 sequence diagram (Figure D-2) with the 1987 sequence diagram (Figure D-1).

Although the Vail-Exxon model was developed for siliciclastic passive continental margins, the concepts and methodology can be applied in any depositional setting if the interpreter takes care to modify or redefine the generalized model based on the local data. The following discussion focuses on siliciclastic systems (Figure D-3). Interpreters working carbonate systems can use the general principles of this text, but should refer to Sarg (1988) for specifics on carbonate sequence stratigraphy (Figure D-4).

A **depositional sequence** within the context of the Vail-Exxon model is a group of strata deposited during one sea-level cycle (regression-transgression). The sequence is bounded by regional (i.e. basin-wide) unconformities or their correlative conformities (Figure D-1). The original diagram for the depositional sequence displays a very simple geometry (Figure 2)(Mitchum et al., 1977). This original diagram and subsequent revised drawings are here referred to as the Vail-Exxon model, to acknowledge the primary role of Peter Vail in defining sequence stratigraphy along with his many co-workers at Exxon Production Research. The integration of geologic concepts with higher resolution seismic-reflection profiles has resulted in definition of both a more holistic and geologically sound depositional sequence model including predictions of possible lithofacies (Figure 3)(Vail, 1987).

This more holistic sequence stratigraphic depositional model is constructed of a hierarchy of three-dimensional stratal packages, each of which has a specific spatial and temporal relation to the others. These stratal packages and their bounding surfaces are illustrated on Figure D-6 and are defined below. For a more complete discussion see Wilgus et al. (1988), and Van Wagoner et al. (1990).

Since the original publication of the sequence stratigraphic model by Vail and associates (1977), two other primary types of sequences have been introduced: the genetic sequence by

Galloway (1990) following work by Frasier (1976); and the T/R (Transgressive/Regressive) cycle of Embry (1993). These models will be discussed later.

Throughout the definitions of the Vail-Exxon model, the phrase "**genetically related**" is used. The phrase genetically related refers to an interval of conformable strata deposited with no significant disruptions by hiatus or unconformity.

A second nomenclatural note concerns the depositional reference point against which relative sealevel is measured. In the 1977 through 1989 literature the shelf-slope break is used to separate the shelfal transgressive and highstand deposition versus the more basinal lowstand deposition. In Van Wagner et al. (1990) the reference point became the depositional shore-line break, a position which coincides approximately with the seaward end of the stream-mouth bar in a delta or with the upper shoreface in a beach (see also Posamentier et al., 1988). The depositional shore-line break has a relief of several feet to tens of feet, and is a useful reference point in outcrop studies or high resolution reflection profiles, but it is below the resolution of most seismic reflection profiles. **Therefore, the reference datum for description of all sequence stratigraphic patterns during this short course will be the <u>shelf/slope break</u>.** It is essential that the reference datum used in each study be clearly identified for effective communication of sequence scale.

Another general note concerning this short course is that all units of measure will be US Standard (and not metric), as most of the data sets were originally collected using feet and miles.

ELEMENTS OF THE SEQUENCE STRATIGRAPHIC MODEL

The fundamental elements of the sequence stratigraphic model are:

SEQUENCE: a relatively conformable succession of genetically related strata bounded by unconformities and their correlative conformities (Mitchum et al., 1977). **Sequence** implies regional to global significance and can range in duration from first-order sequences with a duration of 100 to 200 million years to fourth-order sequences of approximately 100,000 years. The operational sequence of most seismic interpretations is the third-order cycle of 1 to 10 million years duration. In tectonically active areas second-order sequences of 10 to 80 million years duration are often the dominant sequence. Figure D-1 illustrates a single depositional sequence between two unconformities. Figures D-10 through D-14 present different elements of the sequence hierarchy.

A depositional sequence is subdivided into specific subunits by the relationship of three primary stratigraphic surfaces: the **sequence boundary, transgressive surface** and **maximum flooding surface.** The subdivisions of the sequence consist of **systems tracts** composed of **depositional systems**, and are recognized in outcrop, on wireline logs, and on seismic reflection profiles by the stacking patterns of **parasequences** and **parasequence sets <u>referenced to the</u> shelf/slope break.**

SHELF/SLOPE BREAK: the modern shelf/slope break is marked by the change in surface gradient for the gently dipping shelf (commonly less than 1:1000) to the more steeply dipping continental slope (commonly greater than 1:40)(Heezen et al., 1959). Both shelf and slope gradients vary from basin to basin but the inflection-point at the change in gradients is a geometry frequently observable on seismic reflection profiles. This geometry is imaged at the inflection from topset to foreset of large scale clinoforms (10s to 100s of milliseconds)(Figures D-6 and D-20).

SEQUENCE BOUNDARY: a depositional sequence is bounded by unconformities and their correlative conformity. An **unconformity** is a surface separating younger strata from older strata, along which there is evidence of subaerial erosional truncation or subaerial exposure, with a significant hiatus [a break in the continuity of the stratigraphic record). The rock eroded at the unconformity, and sediment that by-passes across a surface of erosion or non-deposition, accumulates as a conformable succession of strata coeval with the unconformity; the conformable surface (stratum) correlative with the most basinward part of the unconformity is interpreted to be the correlative conformity. This relationship is illustrated on Figure D-3. **The unconformity is assigned the geologic age of this correlative conformity.**

TRANSGRESSIVE SURFACE: the first significant marine-flooding surface across the shelf within the sequence is termed the transgressive surface. In the 1977 through 1989 publications of Vail and associates this suface was recognized at seismic reflection profile scale and was identified by the first onlapping reflection shoreward of the shelf/slope break. This relation is illustrated on Figure 1. In outcrop and on wireline logs, the first landward stepping coarsening upward cycle (parasequence) in interpreted as the first transgressive deposit (Figure D-21). Because the scale of outcrop and log data allows recognition of transgressive deposits below the resolution of the seismic reflection profiles, some initial transgressive deposits are identified as lying stratigraphically below the regional transgressive surface, especially in areas of incised valleys and submarine canyons (see Figure D-9).

MAXIMUM FLOODING SURFACE: the maximum flooding surface is defined by the maximum landward onlap of marine strata on the basin margin and represents the maximum relative rise of sea level.

SYSTEMS TRACT: a set of linked contemporaneous depositional systems that are transitional into one another during a specific phase of a transgressive-regressive cycle (Brown and Fisher, 1977). The systems tracts that make up a single depositional sequence are the **lowstand systems tract**, the **transgressive systems tract**, the **highstand systems tract** , and the **shelf-margin systems tract** (Van Wagoner et al., 1987). Systems tracts are objectively identified on the basis of bounding surface types, their position within the sequence, and the stacking-pattern of component parasequences and parasequence sets indicative of specific depositional systems within the lowstand, transgressive and highstand systems tracts. Systems tracts can often be identified on seismic-reflection profiles.

DEPOSITIONAL SYSTEM: a three-dimensional assemblage of lithofacies (Fisher and McGowan, 1967) such as the deltaic lithofacies package deposited by a fluvial system or a submarine fan deposited from gravity-flow currents such as turbidity flows. Contemporaneous depositional systems form systems tracts, for example, the alluvial fan-fluvial plain-coastal delta-shelf-slope-basin floor depositional systems of the highstand systems tract. Depositional systems can often be identified from seismic-reflection profiles by careful analysis of seismic-facies patterns calibrated with well data. On Figure D-1, depositional systems are illustrated as separate compartments lateral to each other and bounded by the time-significant surfaces of parasequences.

PARASEQUENCE: A relatively conformable succession of genetically related beds or bedsets bounded by marine flooding surfaces and their correlative surfaces (Van Wagoner et al., 1987). Beds, bedsets, laminasets and lamina are defined and illustrated in Van Wagoner et al (1990). Parasequences are progradational, and therefore the beds within each parasequence shoal upward and are capped by a marine-flooding surface indicating a deepening of water depth. Thick parasequences can sometimes be imaged as single seismic

reflections in areas of very high sediment-accumulation rates, but commonly they can only be recognized on wireline-logs or in outcrops. On Figures D-1 through D-7, parasequences are represented as horizontal "time-slices" of laterally gradational and coeval facies thinning in a basinward direction.

PARASEQUENCE SET: a succession of genetically related parasequences forming a distinctive stacking pattern and commonly bounded by major marine flooding surfaces and their correlative surfaces (Van Wagoner et al., 1987). Stacked parasequences prograding into the basin may define a highstand, shelf-margin or lowstand/prograding complex systems tract, depending on the location of up-dip lapout. Stacked parasequences that step-landward at both the proximal and distal ends define transgressive parasequence sets (=transgressive systems tract). Parasequence sets and systems tracts are illustrated on Figures D-1 through D-7. Parasequence sets may be imaged on seismic reflection sections in areas of thick sediment accumulation, but often require collaborative wireline-log data.

CAVEATS IN USING THE VAIL-EXXON MODEL

Three caveats need to be considered when using the Vail-Exxon depositional model: 1) geologic setting of the original model; 2) physiographic provinces to which the model applies; and 3) the scale of stratal elements within the diagrammed model.

The first caveat is that the original model was developed for a siliciclastic-dominated, tectonically stable, passive, continental margin with a relatively wide continental shelf. Subsequently, variations on that model have been developed. Sarg (1988) has published a carbonate model based largely on the Permian strata of the Guadalupe Mountains of west Texas (Figure D-4). Sangree et al. (1988) have published a model for a growth-fault modified depositional sequence based on Gulf of Mexico Neogene examples (Figure D-5). Van Wagoner et al. (1990) present examples of shelf and cratonic basin sequence analysis with a detailed discussion of parasequence cycles (Figure D-6) and for a siliciclastic ramp margin (Figure D-7). As the concept of systems tracts is applied more widely, we can expect many more models on these local variations to be developed. *Our task as interpreters is to honor the local data and to use the most appropriate aspects of the published models in order to construct a depositional model that best represents local observations.*

The second caveat relates to the physiographic provinces encompassed by the Vail-Exxon diagram. The Vail-Exxon diagram was drawn to convey the two dimensional geometry commonly observed on seismic-reflection profiles across continental margins. The three dimensional geometry has been compressed into a two dimensional display. Consequently, the diagram is over-simplified. Additionally, the Vail-Exxon sequence-stratigraphic diagram defining systems tracts (Baum and Vail, 1987) is constructed to illustrate the stratal geometries observed along a continental shelf-slope cross-section where a major river supplies sediment to deposit thick systems tracts. The diagram traverses a passive margin from a river-fed delta across the continental shelf and down a submarine canyon to an aggradational continental-slope submarine-fan system (Figure D-8). Any adjacent parallel cross-section to the river-fed depositional thicks will intersect a much thinner and geometrically different depositional pattern (Figure D-9). Thus, systems tracts can only be uniquely identified by assembling observations throughout a geographically significant area. Although intuitively obvious, these geomorphic relationships in three-dimensions must be kept in mind when examining seismic-reflection profiles or regional stratigraphic correlation cross-sections for systems tracts.

The third caveat for applying the Vail-Exxon sequence stratigraphic model is one of scale. The Vail-Exxon depositional diagram has no vertical or horizontal scale. Thus, it theoretically allows the interpreter to adjust the scale to fit the geometries observed in each study. Van Wagoner

et al. (1990) have presented a set of scales to "bracket" the temporal and spatial scales of sequences, parasequence sets, parasequences, and smaller scale depositional units of beds and laminae (Figure D-10). For example, a sequence has a lateral extent in excess of 1000 square miles (Van Wagoner et al., 1990) Although only an approximation, this number indicates the sequence is bounded by unconformities of regional extent that result from major basin wide, or global, changes in tectonics and sea-level (see the base-level transit cycle of Wheeler, 1964). Smaller scale, local "sequences" may be systems tracts within a sequence, higher-order (shorter duration) cycle sequences, or local sequences related to the balance of sediment supply and accomodation space.

It is important to note the change in the sequence stratigraphy diagrammatic section of 1977 versus 1987 (Figures D-2 and D-1). The geologically constrained model of 1987 (Baum and Vail, 1987) recognized depositional systems tracts, separated by downlap surfaces but each being part of a genetically related depositional cycle bounded by a regional unconformity (Figure 1). The 1977 diagram (Mitchum et al, 1977) considered each depositional package separated by a lapout surface to be a separate sequence (Figure 2). Thus, many 1977 sequences became 1987 systems tracts which stack into sequences bounded by regionally significant unconformities. These relationships help clarify the importance of clearly identifiying both the sequence boundary and the primary downlap surface (the maximum flooding surface) for each depositional cycle.

The primary depositional sequences of the 1977 cycle chart were defined as third-order cycles with a duration of 1 to 10 million years (Vail et al., 1977). Second-order cycles have durations of 10 to 80 million years, and first-order cycles have durations of 100 to 200 million years (Figure D-11). The third-order cycles were defined by those sequences most readily interpretable on 1970 vintage seismic-reflection profiles. With improved acquisition and processing it is now sometimes possible to recognize higher frequency cycles, referred to as fourth-order and possibly fifth-order cycles (Mitchum and Van Wagoner, 1990). Vail and Wornardt (1990a) provide a refinement of estimates for the duration of the dominant (third-order) cycles of the Phanerozoic (Figure D-12). When conducting sequence-stratigraphic analysis and correlating sequences to the global cycle chart (Figure D-13)(Haq et al., 1988), we need to keep in mind the scale of our observations and integrate biostratigraphic and chronostratigraphic data to calibrate the temporal resolution of the sequences we are interpreting.

ELEMENTS OF THE VAIL-EXXON MODEL

The **sequence** is defined as a relatively conformable, genetically related succession of strata bounded by unconformities or their correlative conformities (Mitchum, 1977)(Figure D-1). An unconformity is a surface of erosion or nondeposition that separates younger strata from older rocks and represents a significant hiatus. Unconformities are classified on the basis of the structural relations between the underlying and overlying rocks. They represent breaks in the stratigraphic sequence, that is, they record periods of time that are not represented in the stratigraphic column. Unconformities also record a fundamental change in the environment from one of deposition to one of nondeposition and/or erosion, which often represents an important tectonic event.

The recognition and mapping of unconformities is one of the first steps in understanding the geologic history of a basin or a geologic province. Unconformities are recognized in outcrop, seismic and well data and are used as boundaries of stratigraphic units. They are best seen in a vertical section exposed in a canyon wall, road cut, or quarry, where they appear as an irregular line, often truncating underlying strata and being onlapped or downlapped by overlying strata.. Unconformities can be recognized on seismic dip and strike lines and on detailed well log correlation charts. Major stratigraphic units that are bounded by regional unconformities form an effective means of mapping the distribution in space and time of local and regional stratigraphic and

tectonic events and reconstructing the changing framework of a geologic province or sedimentary basin through time. These unconformity-bounded units have been treated as lithostratigraphic units and referred to as sequences by Sloss (1963). Vail and others (1977) apply the term sequence to a relatively conformable succession of genetically-related strata bounded at its top and base by unconformities or their correlative conformities. These sequences are interpreted as depositional sequences, which can be defined on seismic, well and outcrop data.

In sequence stratigraphy, two primary types of unconformity-bounded sequences are recognized: Type-1 and Type-2 sequences (Van Wagoner et al., 1987). A **Type-1 sequence** is bounded below by a Type-1 sequence boundary and above by either a Type-1 or Type-2 sequence boundary. **A Type-2 sequence** is bounded below by a Type-2 sequence boundary and above by either a Type-1 or a Type-2 sequence boundary. The stratal patterns of each of these sequence types is illustrated in Figure D-6.

A Type-1 sequence boundary is a regional surface characterized by subaerial exposure and concurrent subaerial erosion associated with stream rejuvenation and downward cutting, a basinward shift of facies, a downward shift in coastal onlap, and onlap of overlying strata. **A Type-1 sequence boundary is interpreted to form when the rate of eustatic fall exceeds the rate of basin subsidence at the depositional-shoreline break, producing a relative fall in sea level at that position** (Van Wagoner et al., 1987). The **depositional-shoreline break** is a position on the shelf, landward of which the depositional surface is at or near base level (usually sea level), and seaward of which the depositional surface is below base level (Posamentier et al., 1988)(Figure D-6). This position coincides approximately with the seaward end of the stream-mouth bar in a delta or with the upper shoreface in a beach. In pre-1987 publications (eg. Vail and Todd, 1981; Vail et al, 1984), the depositional-shoreline break was considered to be the shelf edge. In many basins, the depositional-shoreline break may actually be 100 miles or more landward of the actual shelf edge, which is marked by a change in dip from the gently dipping shelf (commonly less than 1:1000) to the more steeply dipping continental slope (commonly greater than 1:40) (Heezen et al., 1959). In other basins the depositional-shoreline break may be coincident with the shelf edge (Van Wagoner et al., 1987). Because of these relationships, most unconformities vary in type from basin to basin. The differentiation of Type-1 and Type-2 unconformities on the Mesozoic-Cenozoic Cycle Chart of Haq et al. (1988) is very misleading. Type-1 unconformities may be a Type-2 if the local tectonic rate of subsidence exceeds the rate of sea-level fall.

A **Type-2 sequence boundary** is a regional surface characterized by subaerial exposure of preceding marine areas, and a downward shift in coastal onlap landward of the depositional-shoreline break; however, it lacks both subaerial erosion associated with stream rejuvenation and a basinward shift in facies (Van Wagoner et al., 1987). Onlap of overlying strata landward of the depositional-shoreline break also marks a Type-2 sequence boundary. **A Type-2 sequence boundary is interpreted to form when the rate of eustatic fall is less than the rate of basin subsidence at the depositional-shoreline break, so that no relative fall in sea level occurs at this shoreline position.**

The Mesozoic-Cenozoic Cycle Chart (Haq et al., 1988) illustrates the first-, second- and third-order sequences for the last 250 million years (Figures D-13 and D-14). The cycle boundaries on that Mesozoic-Cenozoic chart are interpreted to be 48 Type-1 and 68 Type-2 sequence boundaries, but as mentioned above, the specific Type-1 versus Type-2 nature of an unconformity will vary from basin to basin.

The interpretation of a Type-1 sequence boundary implies that a "basin-floor" submarine fan should exist, and the chart is so annotated with an "F" in the systems tracts column where fans have been observed or interpreted (Figure D-14). But again, because of the local variability of depositional rates, tectonic rates and the effect of eustatic change, the chart cannot be used to

predict sequence boundary type -- the local patterns must be interpreted, mapped and correlated to generate a local chart. And it is that local chart that becomes the potentially "predictive" cycle chart.

A cycle chart offers the opportunity to compare local observations with the global synthesis of the Vail-Exxon sequence-stratigraphy team's observations. It is very important that each area be interpreted using wireline-log-calibrated regional, seismic reflection-profile grids, and that the local cycle chart be developed and then compared to the Mesozoic-Cenozoic Cycle Chart (Haq et al., 1988) to check for the possibility that either new cycles are observed in the local data, or that some of the cycles on the global chart are not observed locally. Either of these cases may reflect local variations in tectonics or sediment supply and may lead to recognition of an additional exploration play. Care must be taken to correlate the local data with the cycle chart using biostratigraphic markers. The sequence chronostratigraphy of the Haq et al. (1988) chart has been tied to the absolute age and magnetostratigraphic scales using fossil evidence (Figure D-13). Because the numeric time scales of various authors differ, each sequence-stratigraphy study must involve biostratigraphers to help calibrate and correlate local cycle patterns with the interpreted global patterns. The average Mesozoic and Cenozoic third-order cycles have a duration of only 2.16 million years. Small errors in chronostratigraphy will result in miscorrelations.

PRIMARY MAPPING DATUMS

The primary horizons utilized in sequence stratigraphy are the **sequence boundary (SB)** and the **maximum flooding surface (mfs)** (Figure D-1). These represent two important time-datums in the history of a sequence: the maximum relative lowstand of sea level (SB) and maximum relative highstand of sea level (mfs), respectively. Additionally, downlap surfaces are used to separate systems tracts within the sequence. The sequence boundary and maximum flooding surface are used for regional correlation and subdivision of the depositional sequence as observed on seismic data. These surfaces are recognized on the seismic profile by specific patterns of reflection terminations and reflection configurations, and can be correlated to electric logs, and lithologic and biostratigraphic data through specific combinations of observations.

The recognition of depositional sequences is dependent on the resolution of the data used. Thin sequences may be recognized in outcrop or on wireline logs, but may be below the resolution of the seismic data. Only by careful integration of all data sets can all significant sequences be recognized. Figure D-1 shows the conceptual diagram for a sequence-stratigraphic depositional model and Figure D-15 shows an interpreted seismic profile for comparison to the conceptual model. Once all faults and lapouts have been mapped and the sequence boundaries and maximum flooding surfaces have been identified and correlated, the depositional package within each sequence can be interpreted in terms of candidates for systems tracts. Each of these systems tracts can subsequently be interpreted for seismic facies analysis to define possible depositional systems and exploration plays within each systems tract (see Armentrout el al, 1993).

The mapped patterns of the systems-tracts candidates provide a test of the initial interpretation. Lowstand systems tracts are thickest basinward of the shelf/slope inflection point of the preceding depositional sequence; whereas, transgressive and highstand systems tracts are **generally** thickest at or landward of the shelf/slope inflection point. The shelf/slope inflection point (also termed shelf-break, shelf-edge, or shelf/slope transition) represents the physiographic break in gradient between the shelf and slope of the basin, and can often be recognized on the seismic profile by the topset/foreset inflection point of clinoforms. In areas of growth-faults, this inflection point is often masked by the expanded depositional section and the growth-fault itself approximates the location of the shelf/slope inflection point because these faults generally develop at or near that point (Winker and Edwards, 1983).

SEQUENCE BOUNDARY

The **sequence boundary** is an unconformity that extends laterally into correlative conformities (Figure D-1). Unconformities of regional significance are most extensively developed during times when the rate of sea-level fall is at a maximum. Relative sea-level fall causes a basinward shift of deposition and consequent erosion of the area emerging above **base level,** defined as the surface above which erosion occurs and below which deposition occurs (Wheeler, 1964). The area of erosion will be marked by an unconformity above base level and a correlative conformity with local erosion (submarine canyons, slump scars, basin floor channels or scour) in those areas below regional base level. Lacking recognizable erosion because of sediment bypass, an unconformity may be inferred from depositional onlap or basinward shift in depositional facies.

Unconformities are easily recognized where they remove large thicknesses of strata. This most often occurs at major changes in relief, such as along mountain fronts or the outer shelf and upper slope of a basin. The unconformity is best (but not uniquely) observed on seismic sections parallel to depositional-strike and perpendicular to depositional dip-oriented streams, where rivers or submarine canyons have incised the underlying strata. The erosion surface is recognized by the erosional truncation (termination) of strata (Figure D-16). The subsequent interval of deposition that overlies the unconformity is recognized by depositional onlap of younger strata onto the unconformity (erosion surface) at that location (Figure D-16). Chronostratigraphic data from wells correlated to the seismic profile should be used to confirm the occurrence of a hiatus associated with an unconformity.

Candidates for a **sequence boundary** can be recognized on wireline logs and biostratigraphic checklists. These local candidates must be correlated with regionally significant data sets before they can correctly be called sequence boundaries. Where the sequence boundary is an unconformity, there may be a very marked change in facies across the boundary. For example, on a marine shelf the unconformity will have eroded down into the underlying facies and will be onlapped by deposition of the overlying sequence. The onlapping facies will be a shallow-water transgressive facies or coastal-plain facies, possibly with a basal sand, and will probably overlie either transgressive facies or shallower water to nonmarine progradational facies of the preceding sequence. The change in facies types, reflected by a change in stacking patterns on wireline-log profiles (electrofacies) from progradational funnel-shaped to retrogradational funnel- to bell-shaped patterns, suggests the occurrence of a sequence-boundary candidate (see Van Wagoner et al., 1987). Commonly this change occurs at the base of a very sharp increase in spontaneous potential (?sand) and gamma-ray minimum (?sand). On a basin shelf, this pattern may indicate a lowstand incised valley at the sequence boundary which is filled with sand during late lowstand or early transgressive sytems tract deposition (Figure D-17). In deep-water basinal settings far removed from the active erosion along the basin margin, the sequence boundary is sometimes marked by the rapid influx of coarser sediment resulting in a spontaneous potential maximum and gamma-ray minimum (Figure D-5). This influx of gravity-flow sand and mud into the basin depocenter results from bypass of the shelf and slope caused by a rapid basinward shift of falling base level resulting in the development of an unconformity. These sediments usually occur within basin-floor thicks and may be interpreted as debris-flow or turbidity-flow deposits.

Biostratigraphic data facilitate identification of sequence-stratigraphic boundaries (Figure D-18). The sequence boundary is often associated with a shift in the biofacies assemblage for the same reasons that a shift occurs in the stacking pattern of the wireline-log profiles. The biofacies shift is likely to be very dramatic in shallow marine waters where the neritic (0 to 600 foot) biofacies zones are quite restricted and change rapidly as a result of relatively minor changes in water depth, and accordingly dramatic changes in biofacies occur with as little as 50 to 100 feet of change in water depth. In deeper environments, the bathyal (greater than 600 feet) biofacies zones

are more expansive, encompassing a water-depth range of hundreds of feet. In bathyal environments, a change in water depth of more than 1000 feet is usually needed in order to be reflected by a change in the biofacies assemblages (see Armentrout, 1991 for further discussion).

The near base-level environments, associated with erosion at the sequence boundary, are inhospitable to many organisms because of rapid changes in sediment accumulation rates, temperature changes, availability of fresh versus salt water, and other environmental factors. Consequently, there tends to be a low-diversity assemblage (few species of organisms), despite high abundances (number of individual organisms) of a few very hardy species that flourish in these stressful environments. Near base-level environments include rivers, beaches, and submarine valleys and canyons. Additionally, the rapid accumulation of sediment within the often sandy, transgressive onlapping facies immediately overlying basin margin and shelf unconformities, or gravity-flow-deposited basinal sands, will result in a relative dilution of the fossils preserved.

Fossil dilution events, plus the low diversity in the assemblage, can be identified on faunal or floral checklists as abundance and diversity minima (Figure D-19). Therefore, abundance and diversity minima may mark candidates for sequence boundaries, with the sequence boundary most likely positioned somewhat above the next downhole major increase in fossil abundance (see Figures D-18 and D-19). However, rapid sediment accumulation resulting in fossil dilution also occurs within channel complexes on the slope, and in sand-prone facies of the prograding lowstand wedge, and within sand-prone topset intervals of both lowstand and highstand systems tracts. Careful analysis of the local stratigraphic position and regional correlation of each faunal dilution event must be considered before interpreting the event as a sequence boundary. Additionally, fossil-occurrence information in wells is based on well-cutting samples collected from regular intervals. The observed patterns are therefore for an interval, and the selection of the sequence boundary can be more precisely picked from wireline log patterns within the interval associated with the marked decrease in fossil abundance. The use of biostratigraphy in the context of sequence stratigraphy is further discussed in Armentrout (1991).

In using borehole data, a sequence boundary candidate may be suggested by the (1) fossil abundance and diversity minima, (2) the sharp-based, spontaneous-potential profiles, and (3) a change from progradational to aggradational/retrogradational stacking patterns of wireline-log profiles (Figure D-17). The sequence boundary candidate must correlate through a regionally significant area. Only those sequence-boundary candidates that correlate and map as regionally significant surfaces between stratal intervals are true sequence boundaries in the context of the Vail-Exxon conceptual model.

Dating the sequence boundary is often difficult. Inspection of Figure D-1 illustrates the problem. The unconformity surface represents that interval of geologic time not recorded in the stratal record. This time interval consists of both the hiatus (non-deposition) and the degradational vacuity (removed deposits) (see Wheeler, 1963). Only strata above and below the unconformity can be dated, and the duration of the missing interval will vary across the unconformable surface. By the Vail-Exxon convention, the sequence boundary is dated at the correlative conformity. On Figure D-1 this is that point where the underlying sequence is overlain by the basin-floor fan. Finding this precise location within outcrops or wells correlated to seismic reflection profiles is often difficult, and age-diagnostic fossils often do not occur within the rocks of this interval. Consequently, most sequence boundaries are dated by superposition of diagnostic fossil assemblages from strata some distance above and below the unconformity and interpolated using assumptions of relative rates of sediment accumulation (see Figures D-13 and D-14 for ages assigned to sequence boundaries and maximum flooding surfaces).

MAXIMUM FLOODING SURFACE and CONDENSED SECTION

The **maximum flooding surface (mfs)** is defined by the maximum landward onlap of marine strata on the basin margin and represents the maximum relative rise of sea level. The maximum flooding surface is downlapped by the overlying progradational strata, but the downlap surface will be progressively younger in a seaward direction as each cycle of prograding-downlap sediment occurs above the bottomset beds of the preceding progradational unit (Figure D-20). The maximum flooding surface represents the maximum marine transgression, and can commonly be traced basinward where it occurs within the laterally continuous layer of sediment deposited by hemipelagic and pelagic processes. These hemipelagic and pelagic sediments form the **condensed section**, an interval of fine-grained sediment accumulating at very slow rates during times of late transgression and early highstand of sea level (Loutit et al., 1988). During transgression most of the sediment entering the basin will be trapped within river valleys, coastal embayments and estuaries. When those areas become filled, the sediment will begin prograding basinward and downlap onto the maximum flooding surface or, in more basinward areas, the upper surface of the condensed section within which the maximum flooding surface occurs. Downlap surfaces also occur between other stratal units, but are less regionally extensive. These subordinate downlap surfaces occur at the top of the basin floor thicks and slope thicks. Identification of the maximum flooding surface on a seismic-reflection profile for a depositional cycle requires the recognition of a major onlapping package capped by a downlap surface, and correlated throughout the basin.

It is important to note that the maximum flooding surface may not represent the time of deepest water in the basin, nor the maximum landward coastal onlap of nonmarine deposits. This is because the relative rise in sea level can continue after local progradation initiates coastal regression and continued aggradation of the coastal plain which onlaps the basin margin. This relationship is illustrated on the Haq et al. (1988) cycle chart where the apex of the maximum flooding surface and associated condensed section are shown slightly below the maximum highstand of the short-term (third-order) eustatic curve (Figure D-14). As a consequence of local controls on the age of the maximum flooding surface, this surface will not be precisely the same age everywhere (i.e. diachronous), but may appear to be of uniform age within the resolution of most geochronostratigraphic tools.

Because the maximum flooding surface forms during maximum effective transgression at a relative high stand of sea level, the basin receives sediment only through hemipelagic and pelagic processes. These hemipelagic and pelagic sediments are termed a **condensed section**, because they were deposited at relatively low sedimentation rates, and represent relatively long intervals of time compressed into relatively thin intervals of strata (Loutit et al., 1988). In siliciclastic depositional systems, these sediments are dominated by clays and biogenic materials, are usually thin, often drape the basin topography, and frequently contain authigenic minerals which reflect the slow rates of terrigenous clastic sedimentation, such as glauconite, siderite, and phosphorite. In carbonate depositional systems, condensed sections are commonly characterized by hardgrounds, bored surfaces and phosphate nodules. Organic matter may be abundant.

Stratigraphic sections with intervals of time missing due to erosion or nondeposition are unconformities, not condensed sections. Definitive rates of sediment accumulation for condensed sections cannot be stated because they vary from basin to basin. Therefore, the condensed section as used in sequence stratigraphy is a relative term. Operationally, much of the transgressive systems tract and some of the more basinward highstand systems tract are included in the condensed section and are represented on the seismic reflection profiles by relatively thin intervals of seldom more than two or three reflections.

The condensed section associated with the maximum flooding surface is a regionally correlative datum. Additional intervals of local condensed sedimentation occur when areas of high sediment accumulation rates switch to low sediment accumulation rates. These local condensed intervals occur at downlap surfaces on the top of basin floor and slope gravity-flow systems (Figure D-1), and at the top of abandoned prograding lobes within both highstand and lowstand prograding deltaic systems. These local condensed intervals may have some of the same lithologic characteristics of the condensed section, but will only correlate across local areas. It is very important not to confuse these local condensed intervals with the condensed section associated with the maximum flooding surface. Careful analysis of the local context of these intervals (eg., at the top of a basin floor gravity-flow system within a lowstand systems tract), the lateral distribution of the surface within a data set, and correlation with a regional depositional cycle chart, should help separate local condensed intervals from the regionally significant condensed section between the transgressive and highstand systems tracts (see Armentrout et al.,1990; Schaffer, 1990; and Vail and Wornardt, 1990b for discussions of condensed sections).

The condensed section can be identified in outcrop, core and well cuttings by the lithologic components listed above, and may be recognizable on wireline logs by the maximum-value gamma-ray excursion within a depositional cycle (Figure D-17). The condensed section may be identified in fossil assemblages by zones of maximum faunal abundance which occur as a consequence of relatively low terrigenous-sediment dilution, and by the association of biofacies assemblages which commonly reflect the deepest water of the depositional cycle. As used here, the condensed section is, in reality, an interval of late transgressive and early highstand systems tract deposits that accumulate very slowly. Their mineralogic and biologic content is a consequence of this slow rate of sediment accumulation.

The seismic reflection associated with the condensed section is generally best imaged in basin margin areas where the most landward prograding clinoforms of the highstand systems tract downlap onto it. The late stage of the highstand systems tract progradation may downlap onto distal deposits of the early part of the highstand systems tract, and this downlap surface can be confused with the maximum flooding surface (Figure D-20). On seismic reflection profiles, condensed sections correlate with regionally extensive reflections, commonly parallel high-amplitude reflections formed by the impedence contrasts at the top and bottom of the condensed section. These reflections are conformable to the underlying topography in areas of outer shelves, slopes and basin plains, where sedimentation is dominated by hemipelagic drape.

Reflections from condensed sections almost always exhibit a more uniform amplitude and greater continuity than other reflections. In general, this is because of the regional uniformity of their depositional environment. However, the seismic signature of the condensed section changes both in shoreward and basinward directions. Shoreward, the input of terrigenous sediment dilutes the condensed interval and it is displaced by the oldest downlapping clinoform. Basinward, the reflection thickens in areas of maximum sediment accumulation from hemipelagic sources such as seaward of major rivers, and then thins where only pelagic deposition occurs (Figure D-9). The seismic signature of these changes will be reflected in lateral changes in the maximum flooding surface reflection(s), with lateral changes in amplitude and reflection thickness and overall thickness of the transgressive systems tract. Despite these lateral variations, **the seismic signature of the condensed section and associated maximum flooding surface is generally the most regionally correlatable reflection and often a good correlation interval on wireline logs where it is recognized by ghe highest gamma-ray values within a depositional cycle.**

When basin-margin progradation or regression occurs, the input of terrigenous sediment dilutes the biogenic supply and prevents development of many of the authigenic minerals which characterize the condensed section. This initiation of increased terrigenous sedimentation may be recognized by decreased gamma-ray response, decrease in fossil abundance, and progradation with

REFERENCES CITED

Armentrout, J. M., 1991, Paleontologic constraints on depositional modeling: Examples of integration of biostratigraphy and seismic stratigraphy, Pliocene-Pleistocene, Gulf of Mexico, *in* P. Weimer and M. H. Link, eds., Seismic Facies and Sedimentary Processes of Submarine Fans and Turbidite Systems: Springer-Verlag, New York, p. 137-170.

Armentrout, J. M., and Clement, J. F., 1990, Biostratigraphic calibration of depositional cycles: a case study in High Island-Galveston-East Breaks areas, offshore Texas, *in* J. M. Armentrout and B. F. Perkins, eds., Sequence stratigraphy as an exploration tool: concepts and practices in the Gulf Coast: Gulf Coast Section SEPM Foundation Eleventh Annual Research Conference, Program and Abstracts, p. 21-51.

Armentrout, J. M., Echols, R. J., and Lee, T. D, 1990, Patterns of foraminiferal abundance and diversity: implications for sequence stratigraphic analysis, *in* J. M. Armentrout and B. F. Perkins, eds., Sequence stratigraphy as an exploration tool: concepts and practices in the Gulf Coast: Gulf Coast Section SEPM Foundation Eleventh Annual Research Conference, Program and Abstracts, p. 53-58.

Armentrout, J. M., Malecek, S. J., Fearn, L. B., Sheppard, C. E., Naylor, P. H., Miles, A. W., Demarais, R. J., and Dunay, R. E., 1993, Log-motif analysis of Paleogene depositional systems tracts, Central and Northern North Sea: defined by sequence stratigraphic analysis: Proceedings of the 4th Conference on Petroleum Geology of NW Europe, London, in press.

Baum, G. R., and Vail, P. R., 1987, Sequence stratigraphy, allostratigraphy, isotope stratigraphy and biostratigraphy: putting it all together in the Atlantic and Gulf Paleogene, *in* Innovative biostratigraphic approaches to sequence analysis: new exploration opportunities: Gulf Coast Section SEPM Foundation Eighth Annual Research Conference, Program and Abstracts, p. 15-23.

Brown, L. F., and Fisher, W. L., 1977, Seismic-stratigraphic interpretation of depositional systems: examples from Brazil rift and pull-apart basins, *in* C. E. Payton, ed, Seismic stratigraphy -- applications to hydrocarbon exploration: AAPG Memoir 26, p. 213-248.

Fisher, W. L., and McGowan, J. H., 1967, Depositional systems in the Wilcox Group of Texas and their relationship to occurrence of oil and gas: Gulf Coast Association of Geological Societies, Transactions, v. 17, p. 213-248.

Galloway, W. E., 1989, Genetic stratigraphic sequences in basin analysis I: architecture and genesis of flood-surface bounded depositional units: AAPG Bulletin, v. 73, p. 125-143

Haq, B. U., Hardenbol, J., and Vail, P. R., 1988, Mesozoic and Cenozoic chronostratigraphy and cycles of sea-level change, *in* C. K. Wilgus, H. W. Posamentier, C. A. Ross, and C. G. St. C. Kendall, eds., Sea-level changes: an integrated approach: SEPM Special Publication 42, p.71-108 (NOTE: this chart was first published in Science (1987) but was updated and corrected as chart 3.1B for the 1988 publication cited here).

Heezen, B. C., Tharp, M., and Ewing, M., 1959, The floors of the ocean, I: The North Atlantic: GSA Special Paper 65, 122 p.

Loutit, T. S., Hardenbol, J., Vail, P. R. and Baum, G. R., 1988, Condensed sections: the key to age determinations and correlation of continental margin sequences, *in* C. K. Wilgus, H. W. Posamentier, C. A. Ross, and C. G. St. C. Kendall, eds., Sea-level changes: an integrated approach: SEPM Special Publication 42, p.183-213.

Mitchum, R. M., Jr., 1977, Seismic stratigraphy and global changes of sea level, Part 1: Glossary of terms used in seismic stratigraphy, *in* C.E. Payton, ed., Seismic stratigraphy: applications to hydrocarbon exploration: AAPG Memoir 26, p. 205-212.

Mitchum, R. M., Jr., Vail, P. R., and Thompson, S., III, 1977, Seismic stratigraphy and global changes in sea level, Part 2: The depositional sequence as a basic unit for stratigraphic analysis, *in* C.E. Payton, ed., Seismic stratigraphy: applications to hydrocarbon exploration: AAPG Memoir 26, p. 53-62.

Mitchum, R. M., Jr., and Van Wagoner, J. C., 1990, High-frequency sequences and eustatic cyles in the Gulf of Mexico basin, *in* J. M. Armentrout and B. F. Perkins, eds., Sequence stratigraphy as an exploration tool: concepts and practices in the Gulf Coast: Gulf Coast Section SEPM Foundation Eleventh Annual Research Conference Program and Abstracts, p. 257-267.

Moore, D. G., 1969, Reflection profiling studies of the California Continental Boarderland -- structure and Quaternary turbidite basins: Geological Society of America Special Paper 107, 142 p.

Posamentier, H. W., Jervey, M. T., and Vail, P. R., 1988, Eustatic controls on clastic deposition I -- Conceptual framework, *in* C. K. Wilgus, H. W. Posamentier, C. A. Ross, and C. G. St. C. Kendall, eds., Sea-level changes: an integrated approach: SEPM Special Publication 42, p.109-124.

Sangree, J. B, Vail, P. R., and Sneider, R. M., 1988, Evolution of facies interpretation of the shelf-slope: application of the new eustatic framework to the Gulf of Mexico: Twentieth Annual Offshore Technology Conference, Houston, Texas, OTC no. 5695, p. 133-144.

Sangree, J. B., Vail, P. R., and Mitchum, R. M., Jr., 1990, A summary of exploration applications of sequence stratigraphy, *in* J. M. Armentrout and B. F. Perkins, eds., Sequence stratigraphy as an exploration tool: concepts and practices in the Gulf Coast: Gulf Coast Section SEPM Foundation Eleventh Annual Research Conference Program and Abstracts, p. 321-327.

Sarg, J. F., 1988, Carbonate sequence stratigraphy, *in* C. K. Wilgus, H. W. Posamentier, C. A. Ross, and C. G. St. C. Kendall, eds., Sea-level changes: an integrated approach: SEPM Special Publication 42, p.155-181.

Schaffer, B. L., 1990, The nature and significance of condensed sections in Gulf Coast late Neogene sequence stratigraphy: Gulf Coast Association of Geological Societies Transactions, v. XL, p. 186-195.

Serra, O., 1985, Sedimentary environments from wireline logs: Schlumberger, 211 p..

Sloss, L. L., 1963, Sequences in the cratonic interior of North America: Geol. Soc. America Bulletin, v. 74, p. 93-114.

Vail, P. R., 1987, Seismic stratigraphy interpretation procedure, *in* A. W. Bally, ed., Atlas of Seismic Stratigraphy: AAPG Studies in Geology No. 27, p.1-10.

Vail, P. R., Mitchum, R. M., Jr., and Thompson, S., III, 1977, Seismic stratigraphy and global changes in sea level, part 4: global cycles of relative changes in sea level, *in* C. E. Payton, ed., Seismic stratigraphy: applications to hydrocarbon exploration: AAPG Memoir 26, p. 83-97.

Vail, P. R., Hardenbol, J., and Todd, R. G., 1984, Jurassic unconformities, chronostratigraphy, and sea-level changes from seismic stratigraphy and biostratigraphy, *in* J. S. Schlee, ed., Interregional unconformities and hydrocarbon accumulations: AAPG Memoir 36, p. 129-144.

Vail, P. R., and Todd., R. G., 1981, North Sea Jurassic unconformities, chronostratigraphy and sea-level changes from seismic stratigraphy: Proceedings of the Petroleum Geology of the Continental Shelf, Northwest Europe, p. 216-235.

Vail, P. R., and Wornardt, W. W., 1990a, Well-log and seismic sequence stratigraphy course: Micro-Strat Inc., Houston, Texas, 181 p.

Vail, P. R., and Wornardt, W. W., 1990b, Well-log seismic sequence stratigraphy: an integrated tool for the 90's, *in* J. M. Armentrout and B. F. Perkins, eds., Sequence stratigraphy as an exploration tool: concepts and practices in the Gulf Coast: Gulf Coast Section SEPM Foundation Eleventh Annual Research Conference Program and Abstracts, p. 379-388.

Van Wagoner, J. C., Mitchum, R. M., Jr., Posamentier, H. W., and Vail, P. R., 1987, Key definitions of sequence stratigraphy, *in* A. W. Bally, ed., Atlas of seismic stratigraphy: AAPG Studies in Geology No. 27, p. 11-14.

Van Wagoner, J. C., Mitchum, R. M., Jr., Campion, K. M., and Rahmanian, V. D., 1990, Siliciclastic sequence stratigraphy in well logs, cores, and outcrops: concepts for high-resolution correlation of time and facies: AAPG Methods in Exploration Series, No. 7, 55 p.

Wheeler, H.E., 1964, Base level, lithosphere surface, and time-stratigraphy: Geol. Soc. America Bulletin, v. 75, p. 599-610.

Winker, C. D, and Edwards, M. B., 1983, Unstable progradational clastic shelf margins, *in* D. J. Stanley and G. T. Moore, eds., The shelfbreak: critical interface on continental margins: SEPM Special Publication 13, p. 139-157.

Wilgus, C. K., Posamentier, H. W., Ross, C. A., and Kendall, C. G. St. C. (Editors), 1989, Sea level changes - an integrated approach: SEPM Special Publication 42, 407 p.

SEISMIC STRATIGRAPHIC ANALYSIS TECHNIQUES

Seismic (depositional sequence identification)

Seismic facies identification

Definition of 'Depositional Sequence' (as per Exxon):

'A seismic stratigraphic unit is composed of a relatively conformable succession of genetically related strata bounded above and below by unconformities (or their equivalent conformities).'

Value as an approach: Objective, depends only on geometry of strata (within limit of resolution) and so is not inferential.

Defining sequences

-Boundaries are unconformities, detected by geometric discordance above and below

-Problem of paraconformities

-Nature of discordance:

Structural (angular unconformity)=> truncation

Depositional

Lapout: lateral termination that is original depositional limit

Truncation: lateral termination that is result of erosional cut off from original depositional limit

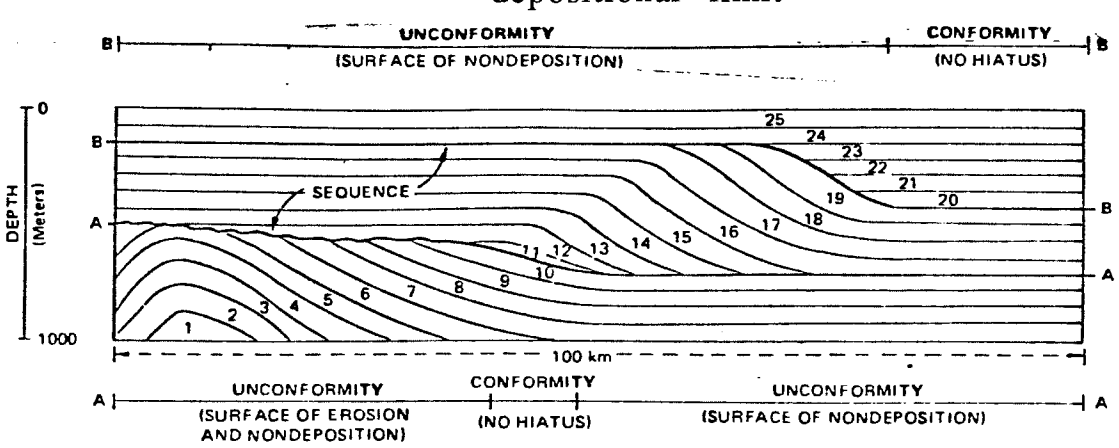

Upper and lower sequence boundaries exhibit certain distinctive geometrical relations

Lower Boundary

Baselap: **Onlap** horizontal or low angle lapout onto slope of greater angle

Downlap inclined lapout onto a gentler slope

Concordance

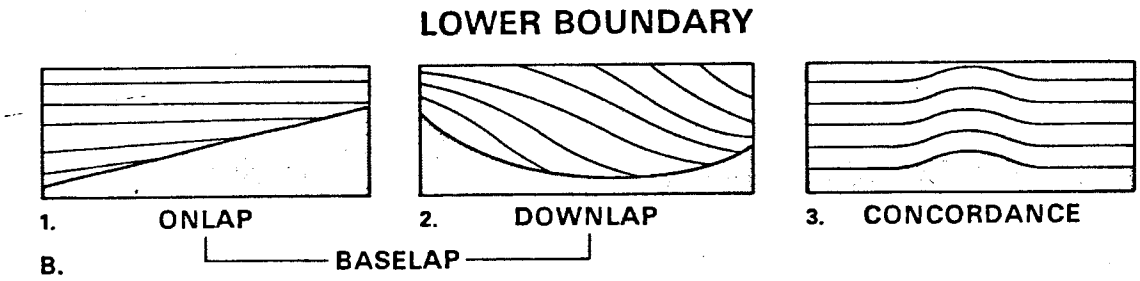

B. Relations of strata to lower boundary surface of a sequence. **B1.** Onlap: at base of sequence initially horizontal strata terminate progressively against initially inclined surface, or initially inclined strata terminate updip progressively against surface of greater initial inclination. **B2.** Downlap: at base of sequence initially inclined strata terminate downdip progressively against initially horizontal or inclined surface (e.g., initially inclined strata terminating against underlying initially horizontal surface). **B3.** Base-concordance: strata at base of sequence do not terminate against lower boundary.

Upper Boundary

Toplap: initial slope of strata at upper boundary, like foresets of dunes (evidence of lateral transport and topset nondeposition

Truncation: obscures original depositional limits (evidence of erosion)

Concordance

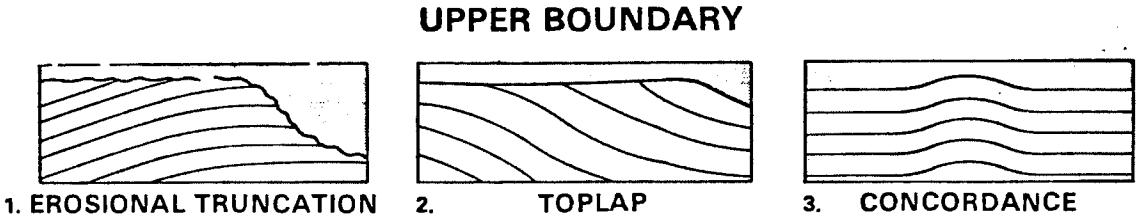

A. Relations of strata to upper boundary of a sequence. **A1.** Erosional truncation: strata at top of given sequence terminate against upper boundary mainly as result of erosion (e.g., tilted strata terminating against overlying horizontal erosion surface, or horizontal strata terminating against later channel surface). **A2.** Toplap: initially inclined strata at top of given sequence terminate against upper boundary mainly as result of nondeposition (e.g., foreset strata terminating against overlying horizontal surface at base-level equilibrium where no erosion or deposition took place). **A3.** Top-concordance: relation in which strata at top of given sequence do not terminate against upper boundary.

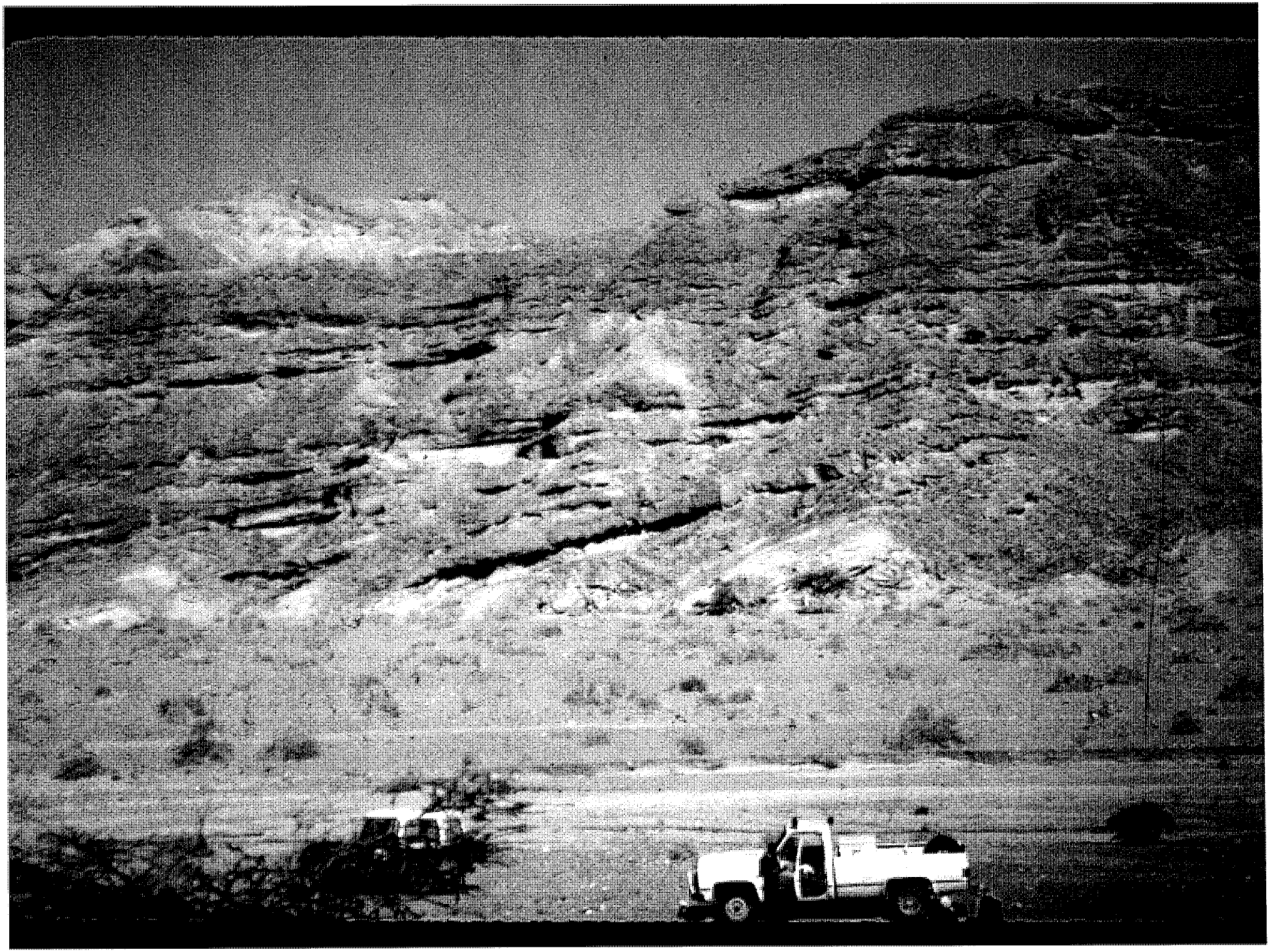

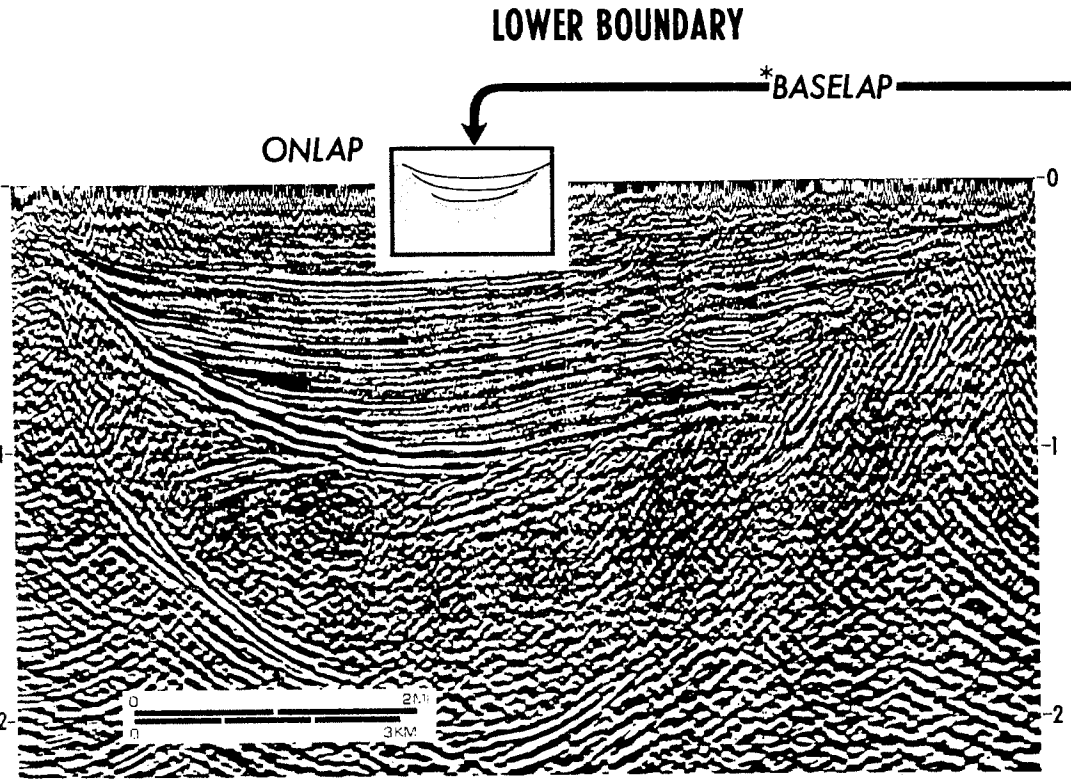

FIGURE 9

*BASELAP IF ONLAP CANNOT BE DISTINGUISHED FROM DOWNLAP BECAUSE OF SUBSEQUENT DEFORMATION, THE MORE INCLUSIVE TERM BASELAP MAY BE NECESSARY.

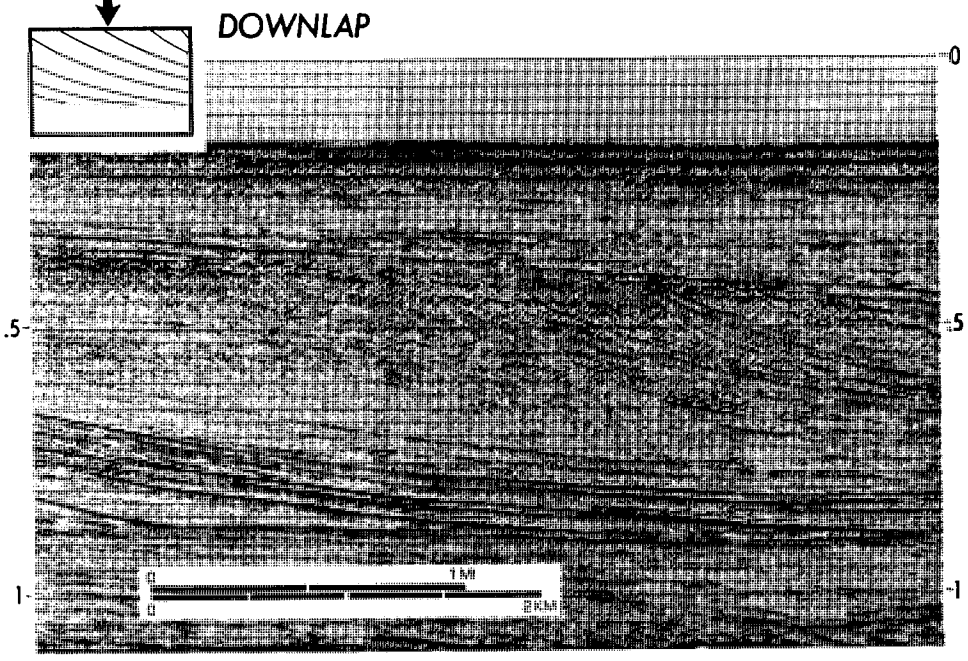

DOWNLAP IS A RELATION IN WHICH SEISMIC REFLECTION OF INCLINED STRATA TERMINATE DOWNDIP AGAINST AN INCLINED OR HORIZONTAL SURFACE. NOTE: DOWNDIP IS A STRATAL TERM, NOT SOLELY RESTRICTED TO SEISMIC REFLECTION PATTERNS.

FIGURE 10

UPPER BOUNDARY

DOWN CUTTING EROSIONAL TRUNCATION

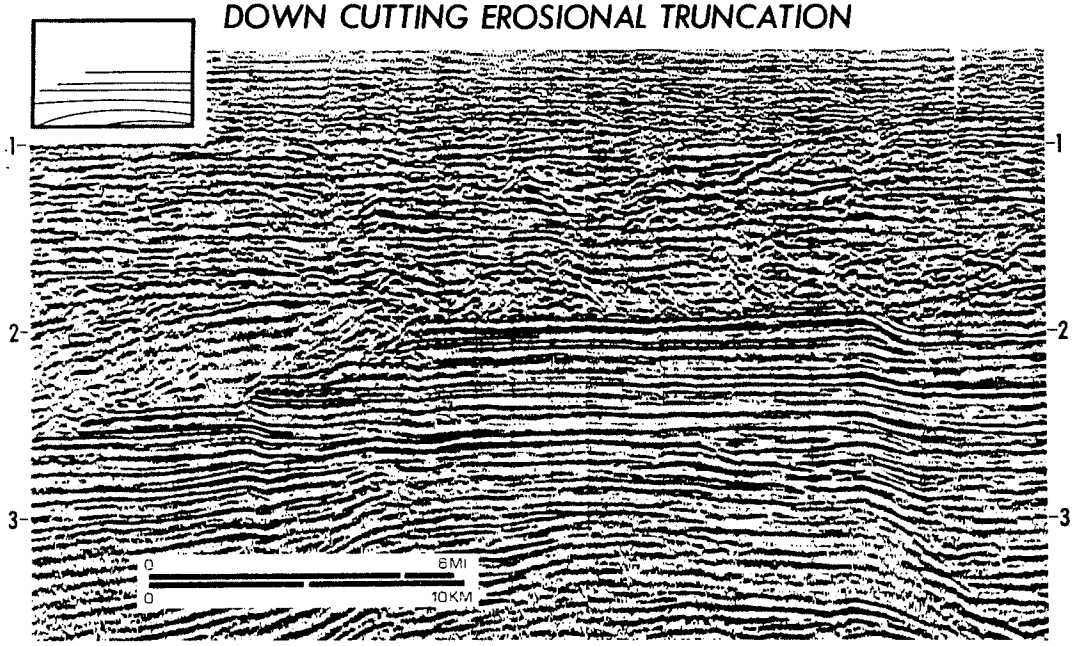

DOWN-CUTTING EROSIONAL TRUNCATION IS WHERE HORIZONTAL STRATA TERMINATE AGAINST AN EROSIONAL SURFACE - IN THIS INSTANCE AGAINST A CHANNEL OR GORGE.

FIGURE 6

Abbott 79

TOPLAP

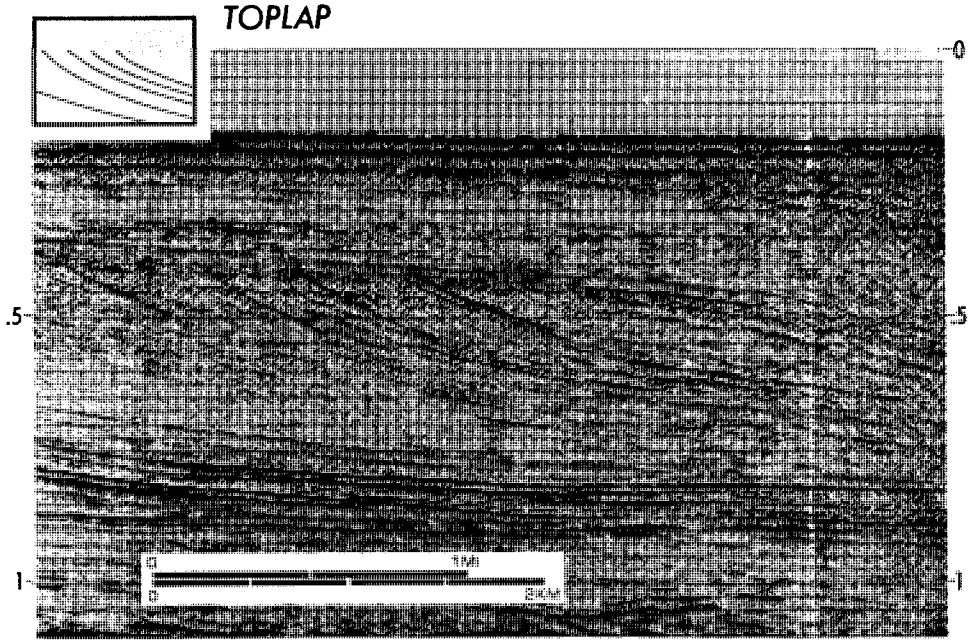

TOPLAP IS THE TERMINATION OF REFLECTIONS INTERPRETED AS STRATA AGAINST AN OVERLYING SURFACE AS A RESULT OF NONDEPOSITION (SEDIMENTARY BYPASSING) AND ONLY MINOR EROSION.

FIGURE 7

Abbott 79

EROSIONAL TRUNCATION

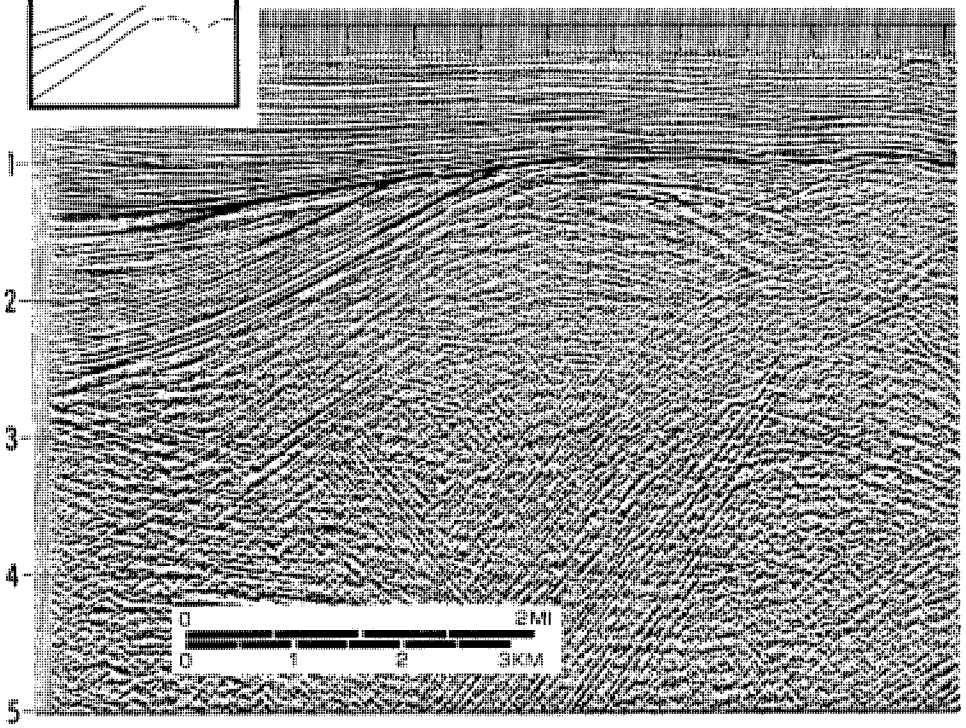

Abbott 79

EROSIONAL TRUNCATION IMPLIES THE DEPOSITION OF STRATA AND THEIR SUBSEQUENT TILTING AND REMOVAL ALONG AN UNCONFORMITY SURFACE. IT IS THE MOST RELIABLE TOP-DISCORDANT CRITERION OF A SEQUENCE BOUNDARY.

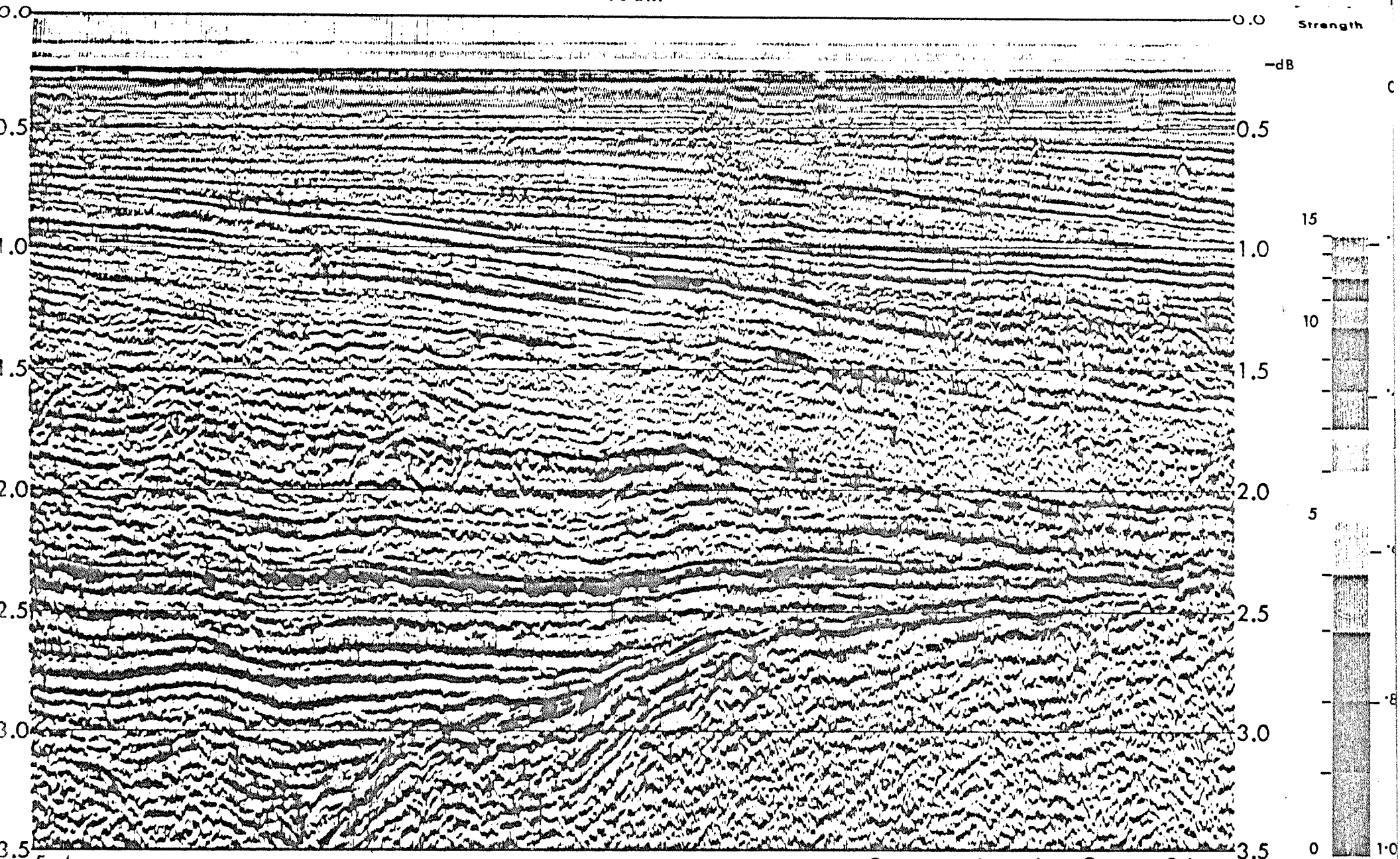

5-4

Anstey, New Seismic Interpreter Courtesy Seiscom

(181)

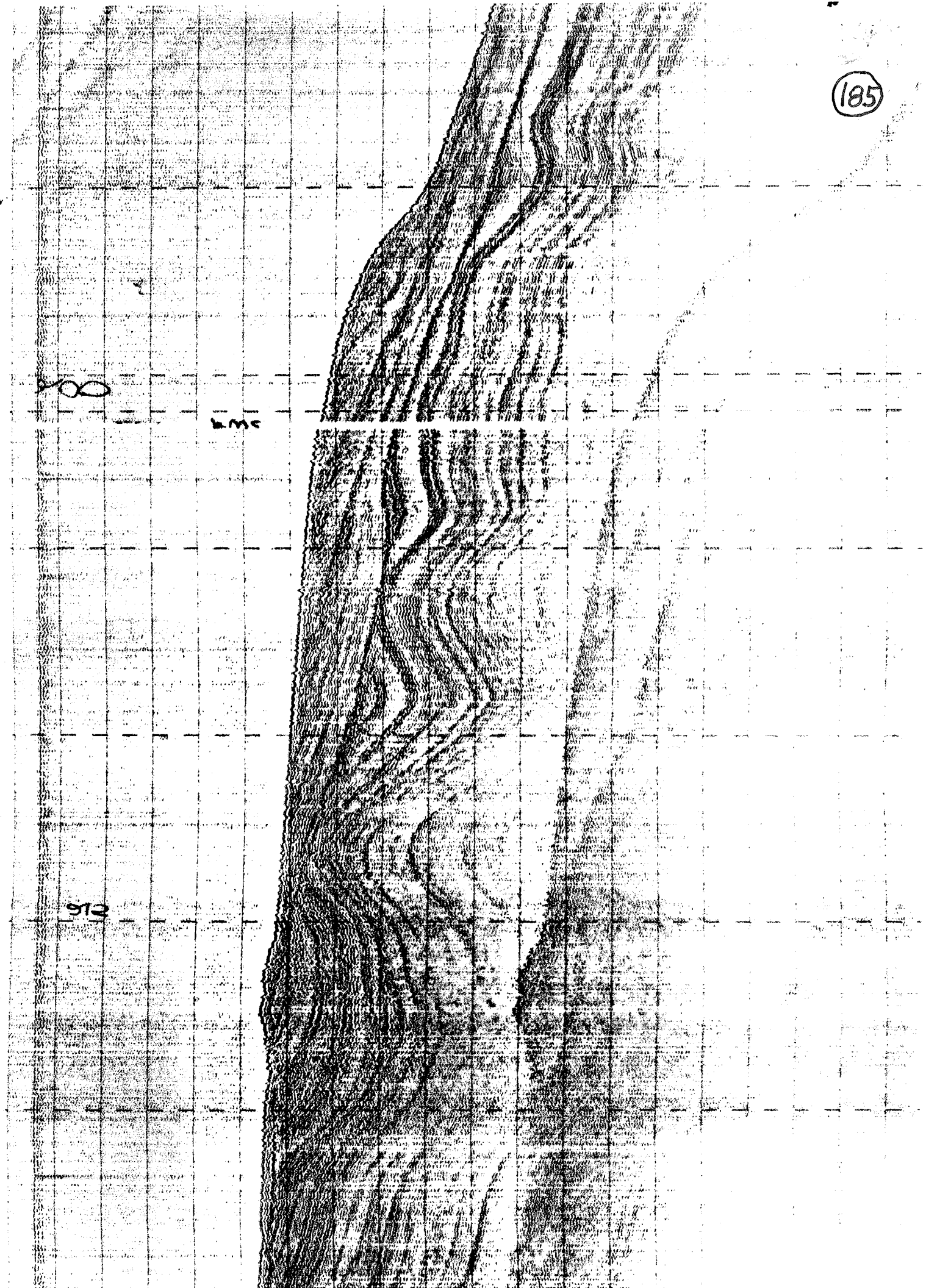
700
bmc
912

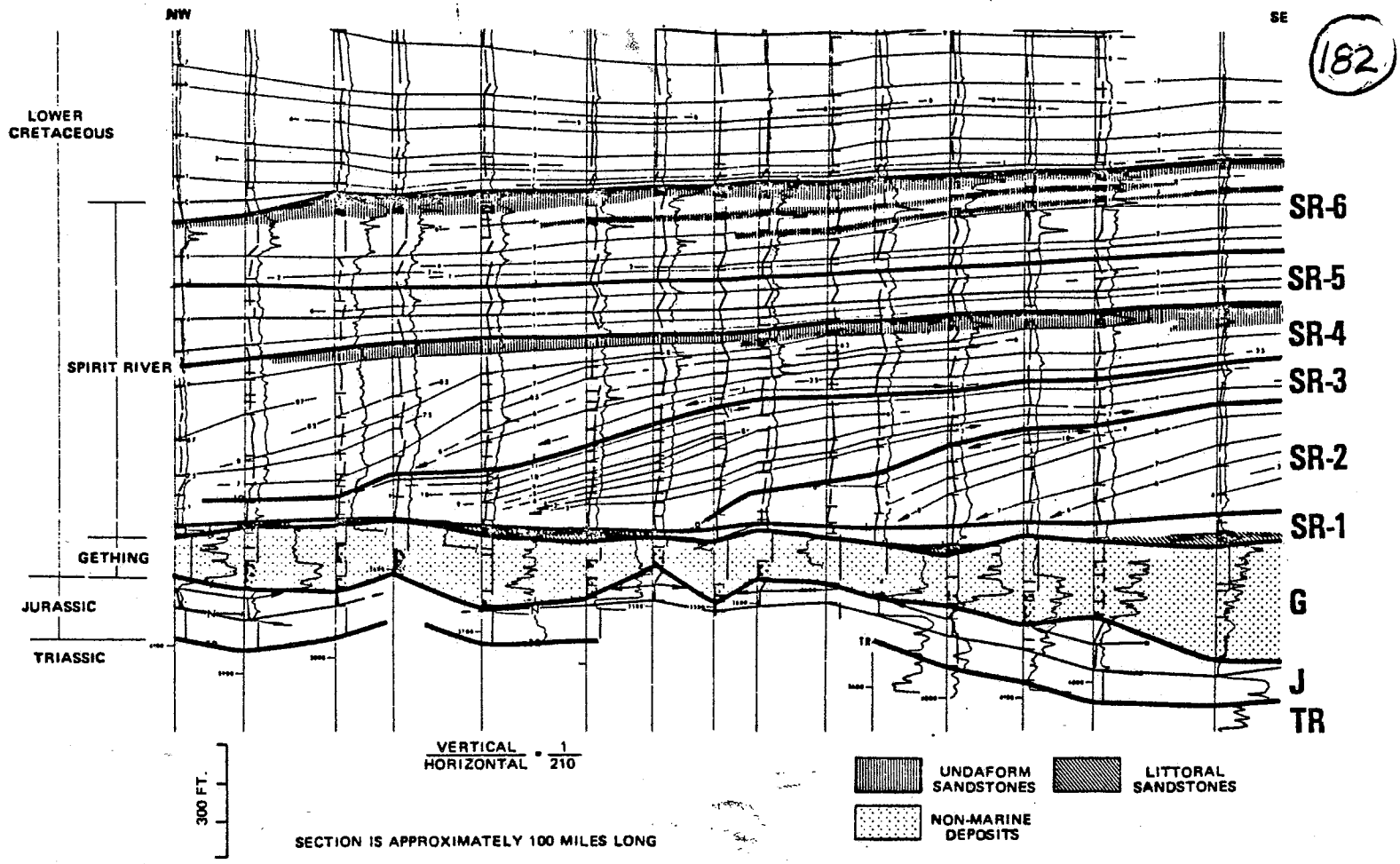

FIG. 3—Subsurface section from western Canada showing sequences defined by well-log marker correlation (prepared by G. T. MacCallum, and provided by mperial Oil, Ltd.) Marker correlation of closely spaced well logs displays depositional patterns of Lower Cretaceous strata in northwestern British Columbia. Erosion runcation of Jurassic beds (surface J), onlap of lowermost Spirit River onto Gething (surface G), and progressive downlap and minor onlap of prograding upper Spirit tiver beds are used to determine several sequence boundaries.

AAPG Mem 26 (1977)

CHRONOSTRATIGRAPHIC SIGNIFICANCE OF DEPOSITIONAL (SEISMIC) SEQUENCES —

AAPG Memoir 26 (1977)

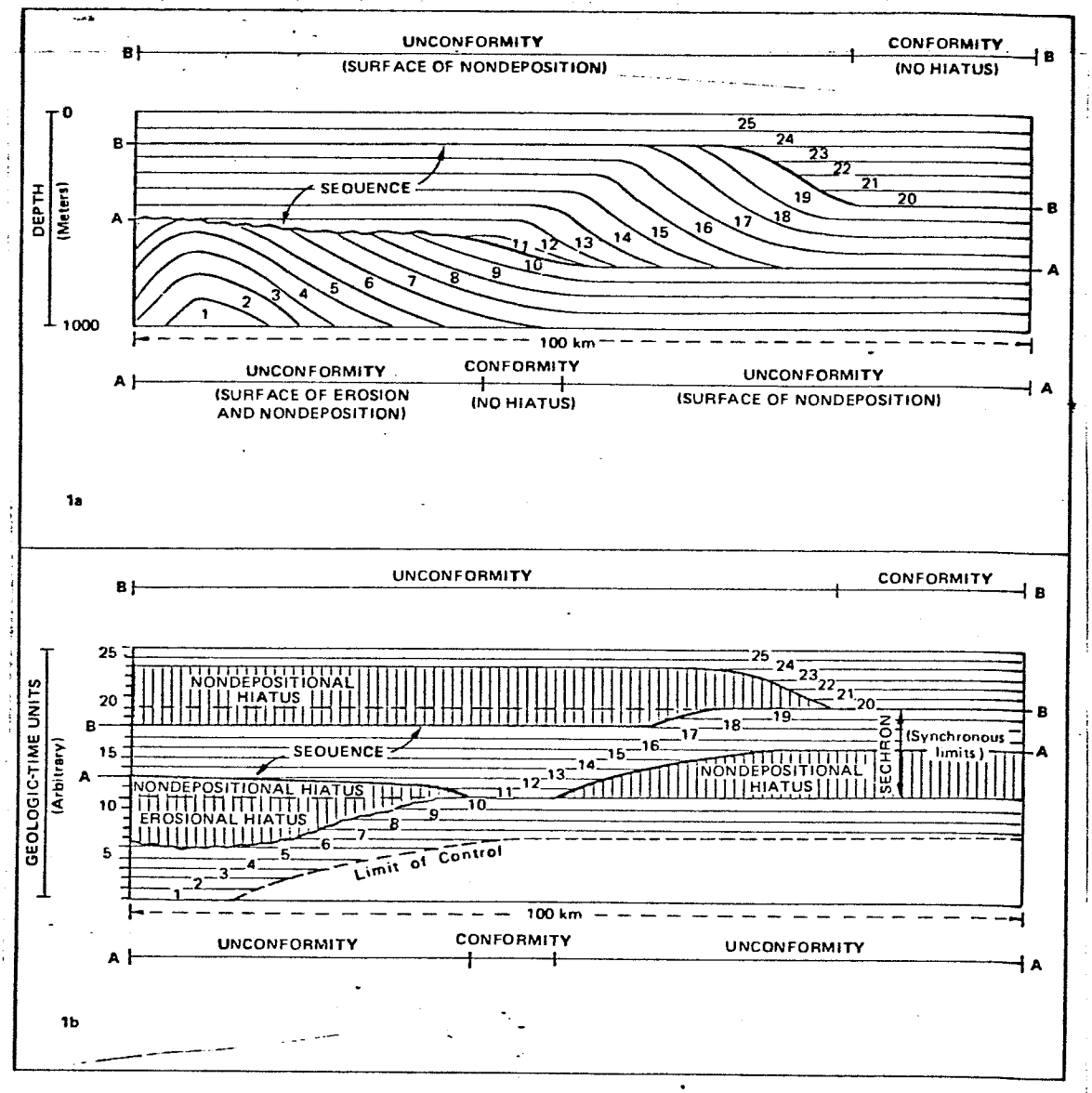

FIG. 1—Basic concepts of depositional sequence. A depositional sequence is a stratigraphic unit composed of relatively conformable successions of genetically related strata and bounded at its top and base by unconformities or their correlative conformities.

A. Generalized stratigraphic section of a sequence. Boundaries defined by surfaces A and B which pass laterally from unconformities to correlative conformities. Individual units of strata 1 through 25 are traced by following stratification surfaces, and assumed conformable where successive strata are present. Where units of strata are missing, hiatuses are evident.

B. Generalized chronostratigraphic section of a sequence. Stratigraphic relations shown in A are replotted here in chronostratigraphic section (geologic time is the ordinate). Geologic-time ranges of all individual units of strata given as equal. Geologic-time range of sequence between surfaces A and B varies from place to place, but variation is confined within synchronous limits. These limits determined by those parts of sequence boundaries which are conformities. Here, limits occur at beginning of unit 11 and end of unit 19. A sechron is defined as maximum geologic-time range of a sequence.)

Seismic resolution
and
stratigraphic interpretation

SEISMIC RESOLUTION & STRATIGRAPHIC INTERPRETATION

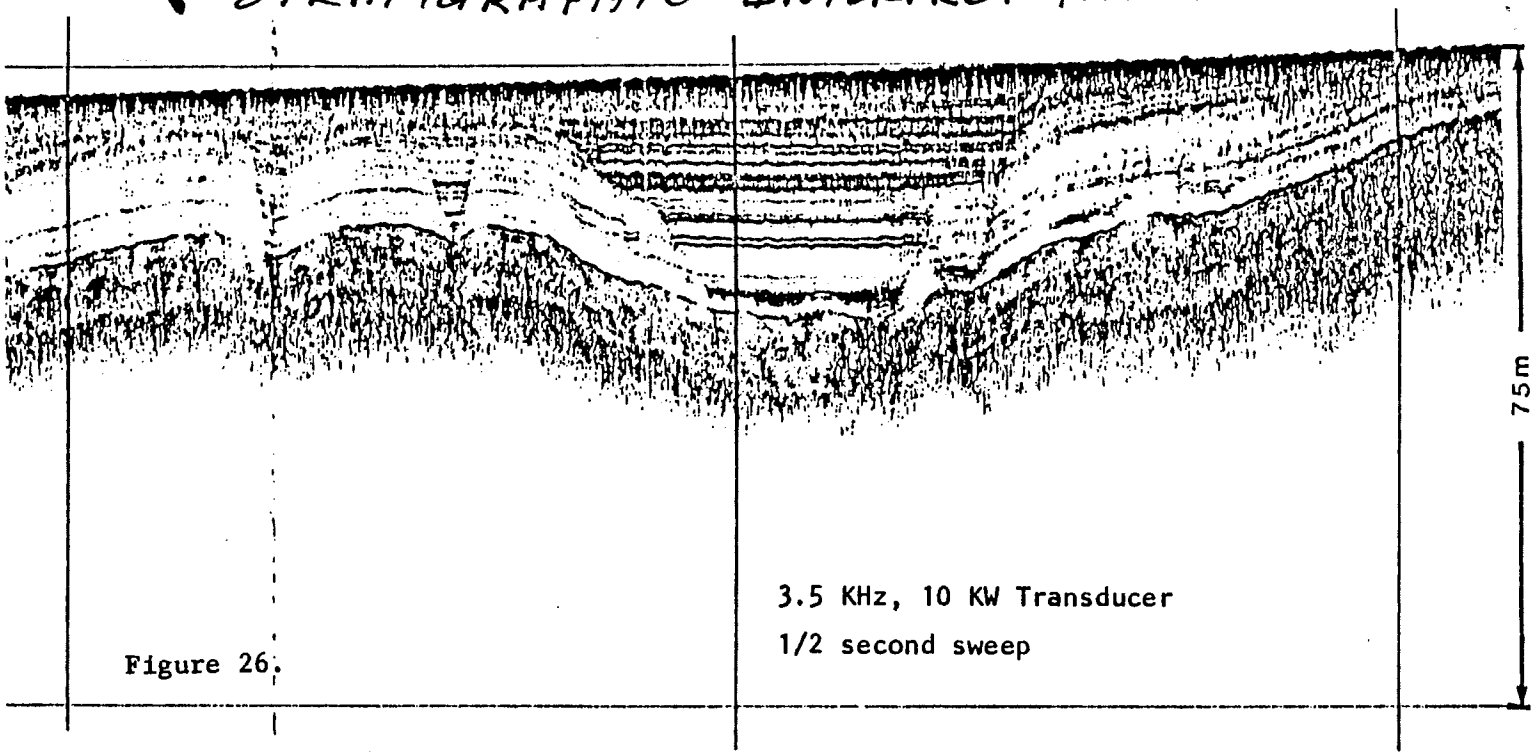

Figure 26.

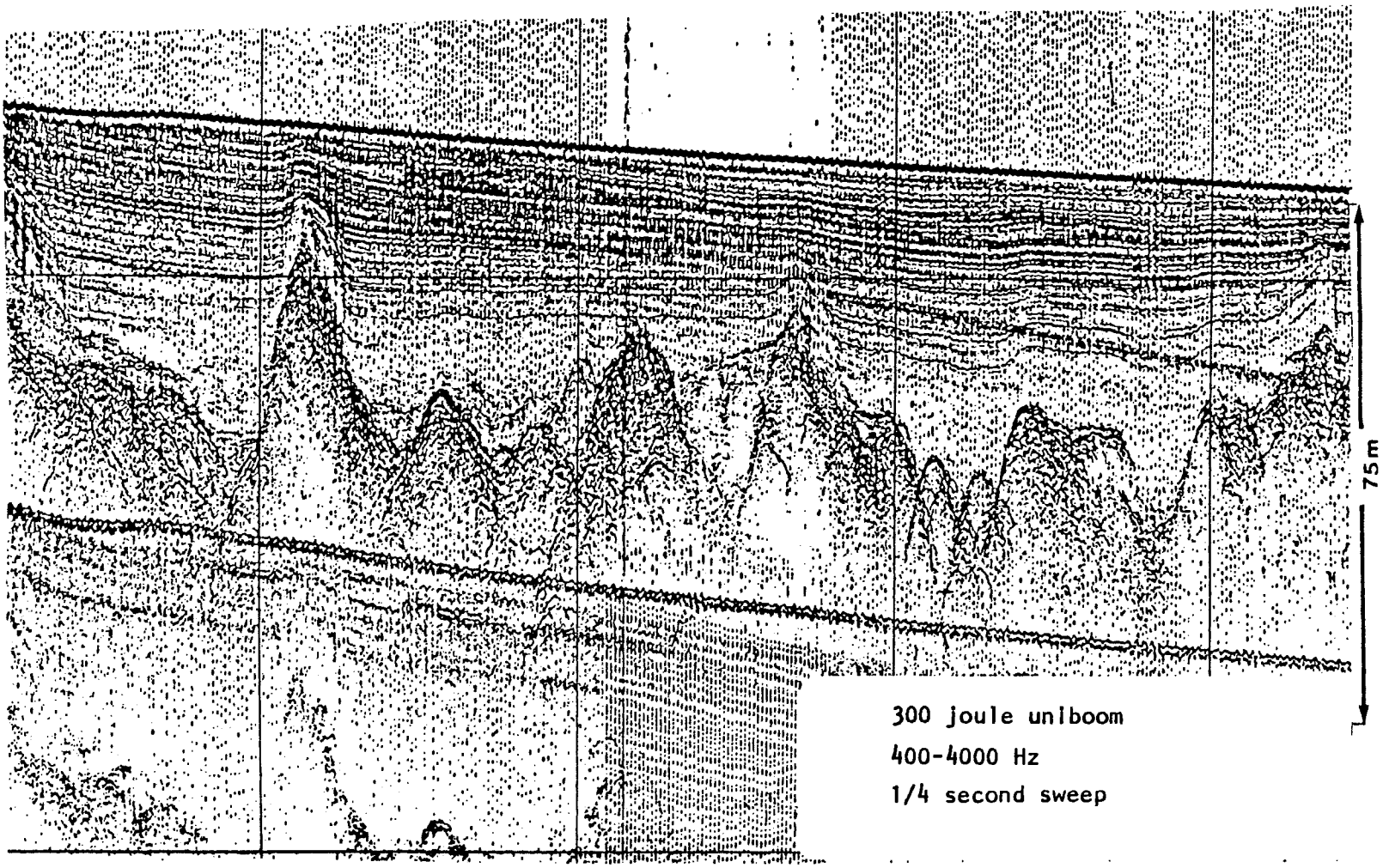

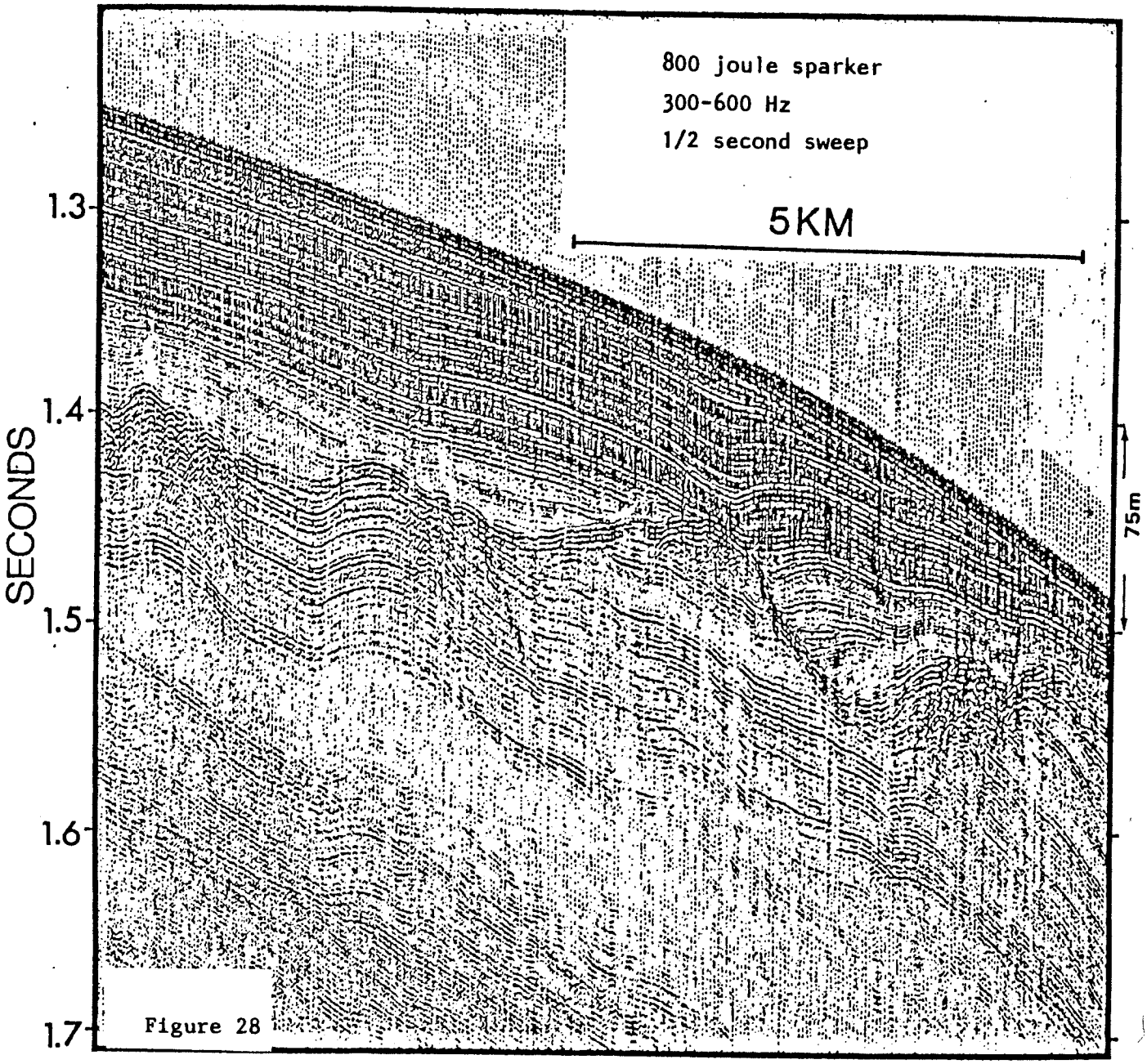
800 joule sparker
300-600 Hz
1/2 second sweep
5KM
SECONDS
1.3
1.4
1.5
1.6
1.7
75m

Figure 28

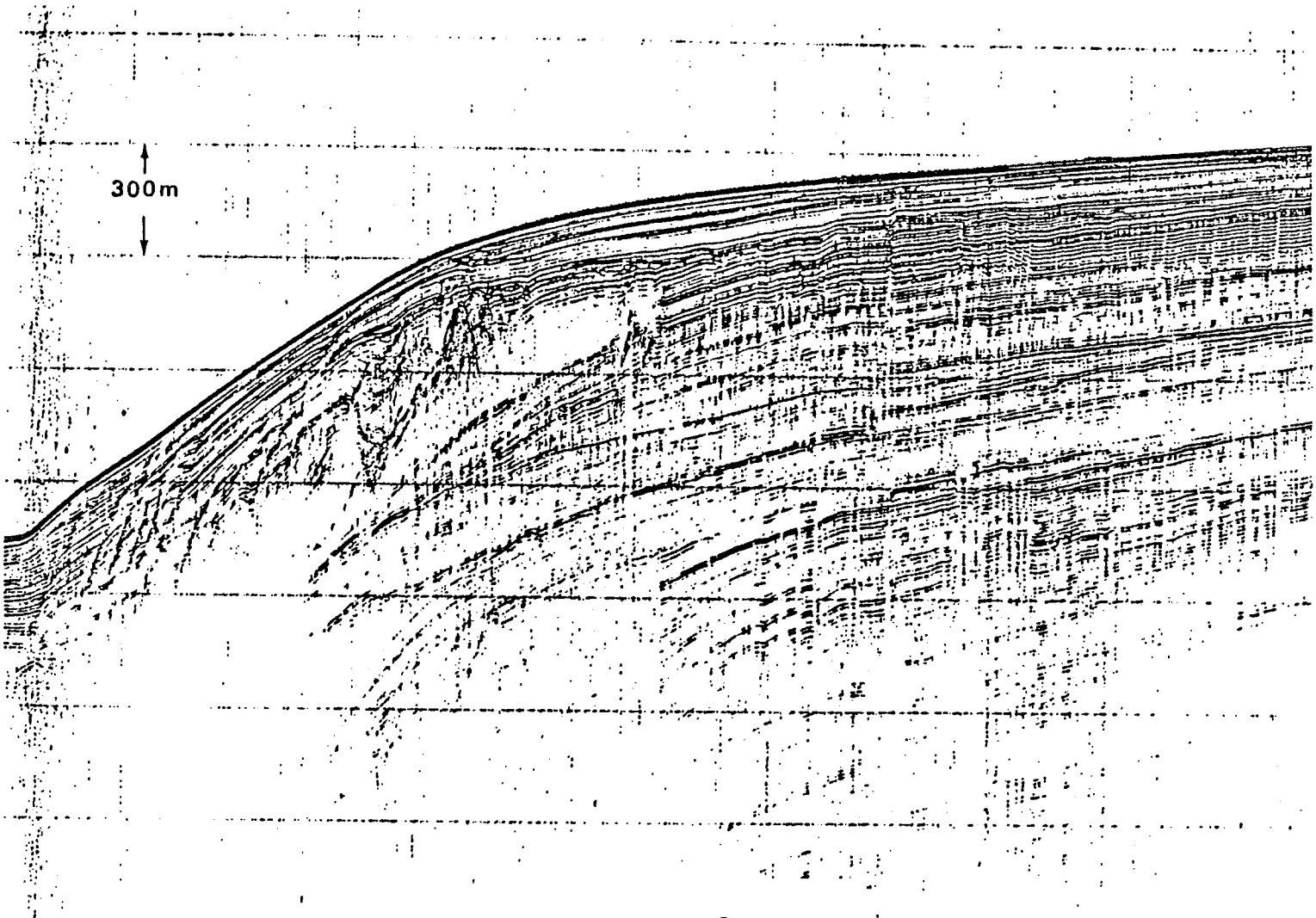

Figure 29.

40 in^3 airgun
55-170 Hz
4 second sweep

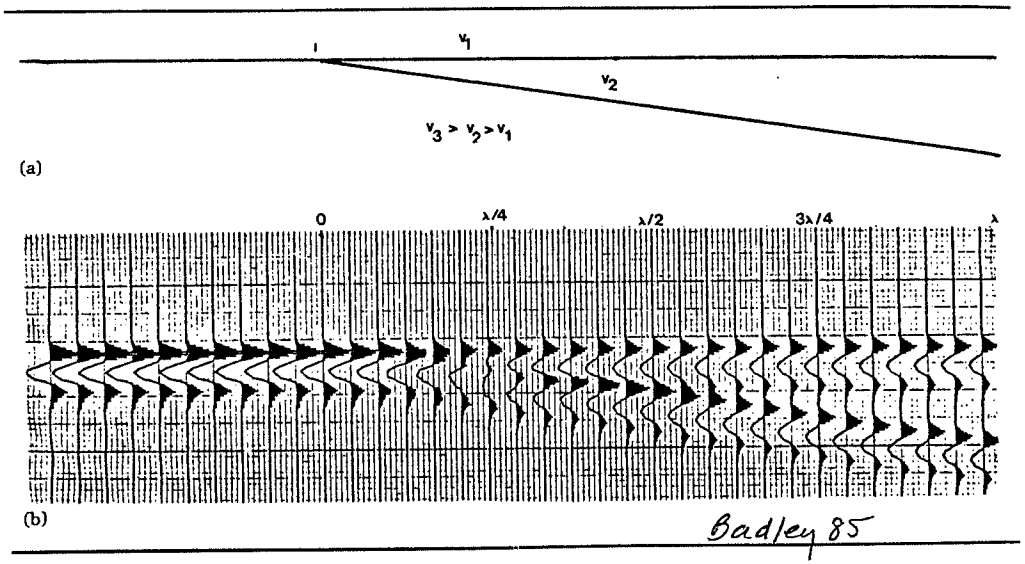

FIGURE 2.16 *Reflection from a wedge of acoustic impedance intermediate in magnitude between that of the over- and underlying units. The thickness of the wedge is indicated as a fraction of the dominant wavelength. Note that there is still a reflection beyond the limit of the wedge due to the contrast in acoustic impedance between the over- and underlying layers.* (a) *Model.* (b) *Seismic section. Reprinted by permission of the EAEG from Sheriff, 1975, fig. 6.9, p. 128.*

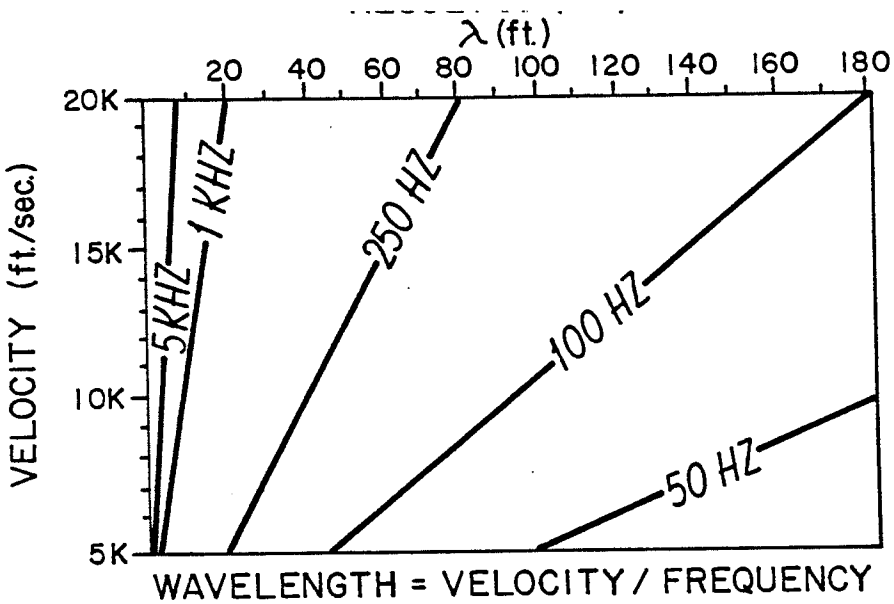

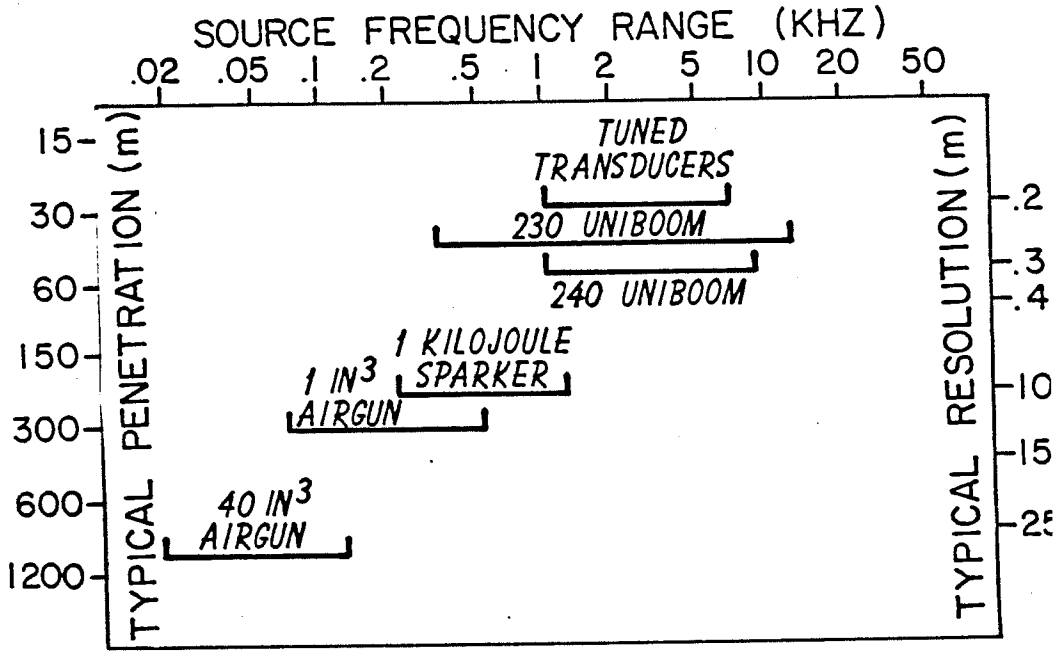

USGS High Res Profiling Short Course Notes

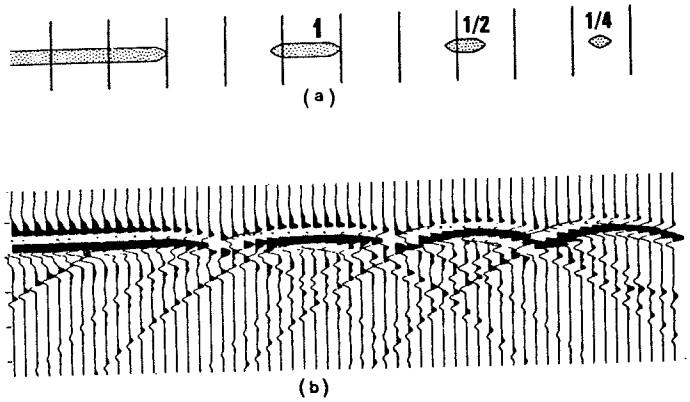

Figure 6.15. Reflections from reflectors of limited dimensions. (a) Cross section of model; vertical lines are spaced by the Fresnel-zone size (specific dimensions are not included because the effect is dimensionless). (b) Seismic section resulting from traverse over the model. The peak amplitude of the four reflections are, respectively, 100%, 87%, 55%, and 40%. (After Meckel and Nath, 1977; reprinted by permission of The American Association of Petroleum Geologists) Sheriff 80

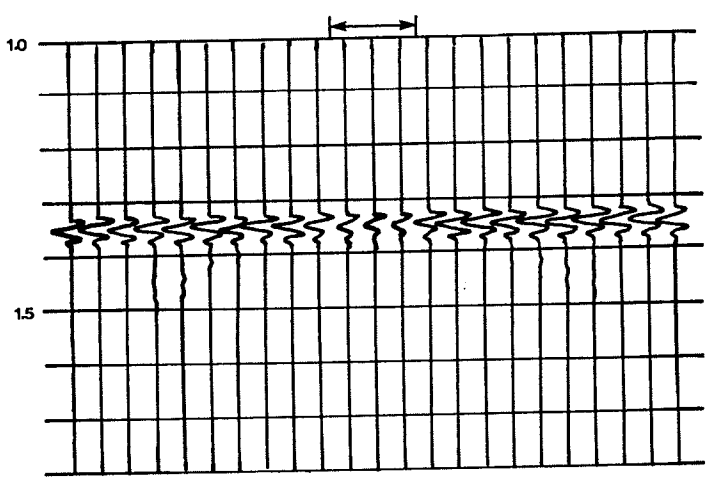

Figure 6.17. Reflection from a reflector containing a hole whose width is three trace intervals (indicated by arrow at top). (From Sheriff, 1977a; reprinted by permission of The American Association of Petroleum Geologists) Sherriff 80

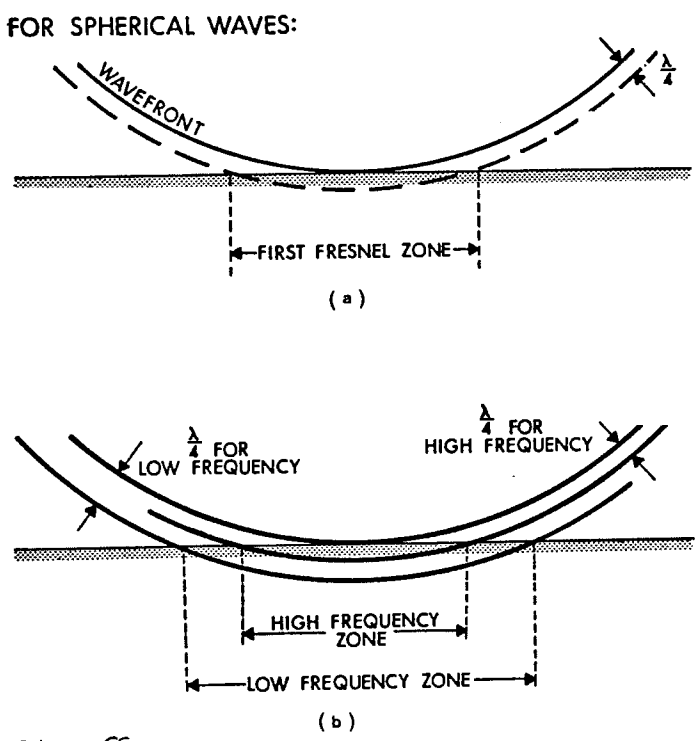

Sheriff 80

Figure 6.14. Fresnel zone. (a) The first energy to reach a geophone from a plane reflector is from the point where a wavefront is first tangent to the reflector; the area of the reflector from which energy can reach the geophone within the next half-cycle is limited by the circle that the wavefront a ¼-wavelength later makes with the reflector. (b) The Fresnel zone is larger for low-frequency components than for high-frequency ones. (From Sheriff, 1977a; reprinted by permission of The American Association of Petroleum Geologists)

Scan

Table 1-1. Typical Limits of Visibility and Separability for a range of geologic situations.

Brown, '99, AAPG Mem 42 (5th ed)

			Age of rocks		VERY YOUNG	YOUNG	MEDIUM	OLD	VERY OLD
			Depth of target		VERY SHALLOW	SHALLOW	MEDIUM	DEEP	VERY DEEP
			Formation Velocity (m/s)		1600	2000	3500	5000	6000
			Predominant Frequency (Hz)		70	50	35	25	20
			Wavelength (m)	λ	23	40	100	200	300
			LIMIT OF SEPARABILITY	$\frac{\lambda}{4}$	**6**	**10**	**25**	**50**	**75**
LIMIT OF VISIBILITY	Poor S/N	e.g.	Water sand poor data	$\sim\frac{\lambda}{8}$	**3**	**5**	**13**	**25**	**38**
	Moderate S/N	e.g.	Water or oil sand fairly good data	$\sim\frac{\lambda}{12}$	**2**	**3**	**8**	**17**	**25**
	High S/N	e.g.	Gas sand good data	$\sim\frac{\lambda}{20}$	**1**	**2**	**5**	**10**	**15**
	Outstanding S/N	e.g.	Gas sand excellent data	$\sim\frac{\lambda}{30}$	**<1**	**1**	**3**	**7**	**10**

units are meters

Fine scale heterogeneities

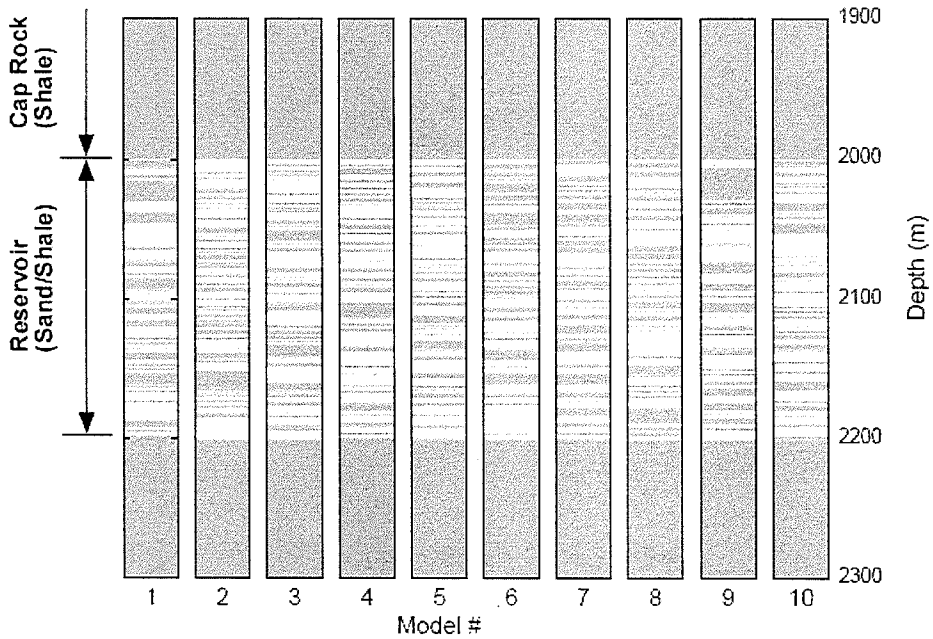

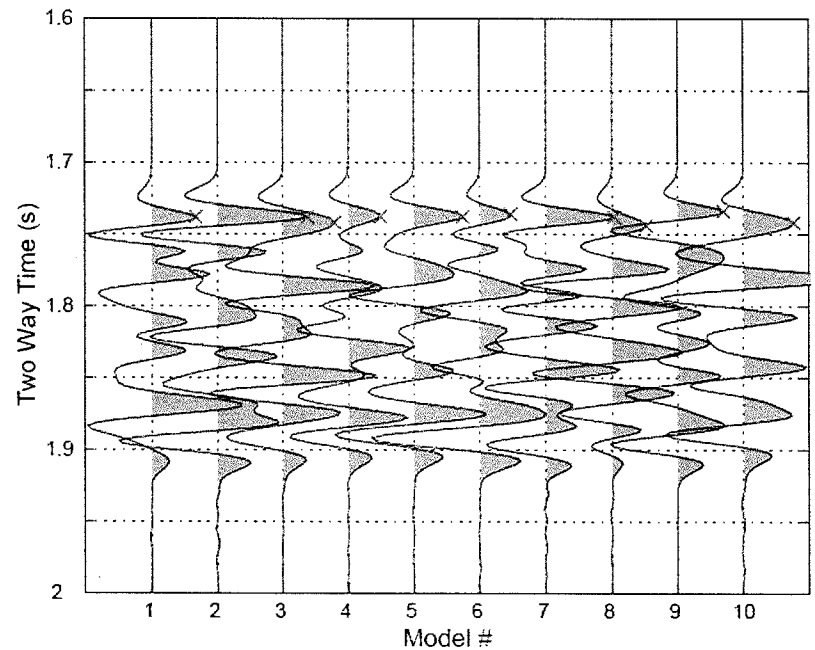

Takahashi, 2000

(OUTCROP MODELS AS TESTS OF RESOLUTION)

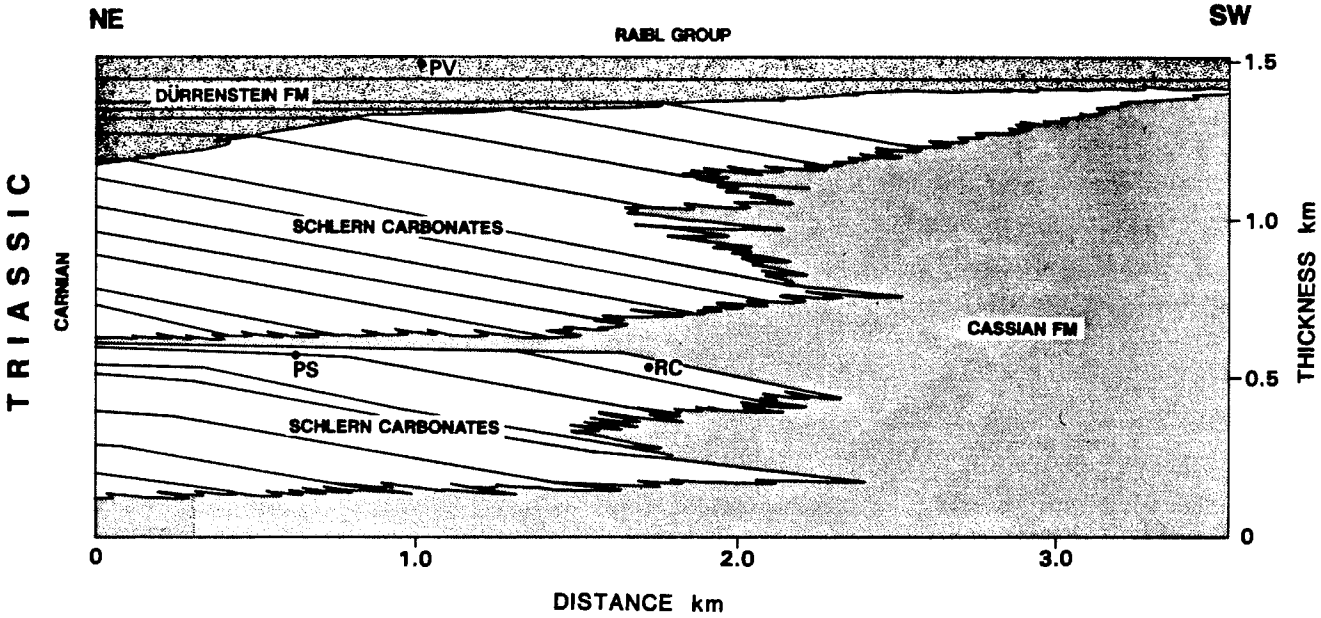

Figure 2—Stratigraphic terminology used in this study for the Picco di Vallandro area. PV = Picco di Vallandro, PS = Punta di Serla, RC = Rocce della Chiesa. The Raibl Group shown at the top of the diagram overlies the Dürrenstein Formation, but is not exposed due to erosion at Picco di Vallandro. Line and plane of section shown in Figure 6.

Biddle et al, 1992, AAPG Bull

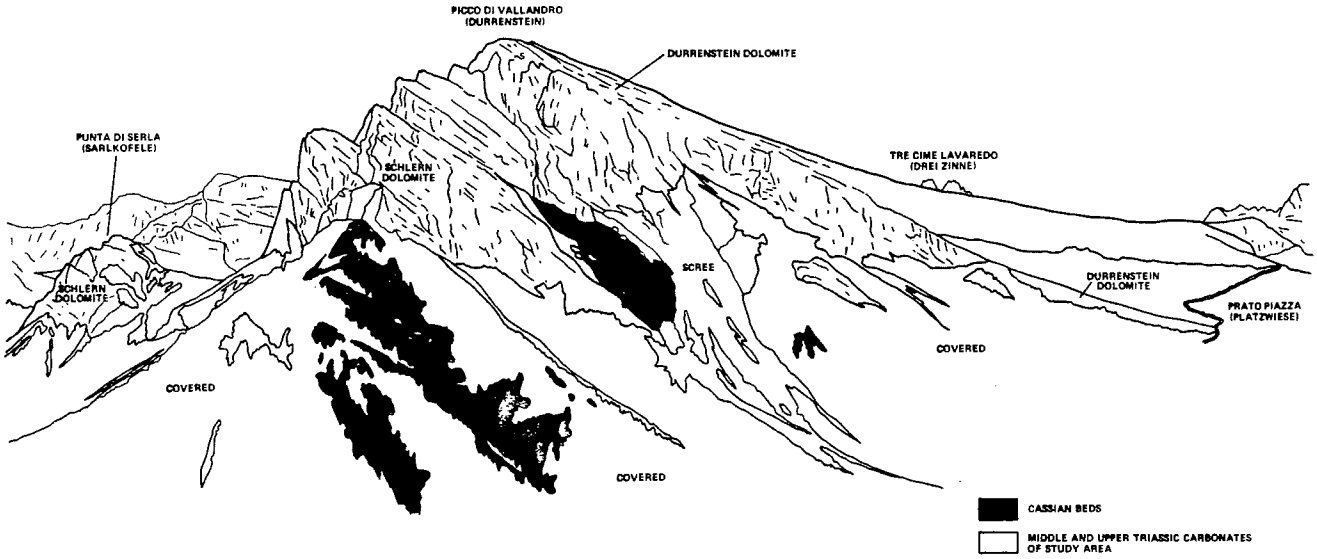

Figure 3—Line drawing of Picco di Vallandro looking toward the east (see Figure 4) showing distribution of, and relationships between, the stratigraphic units discussed in the text.

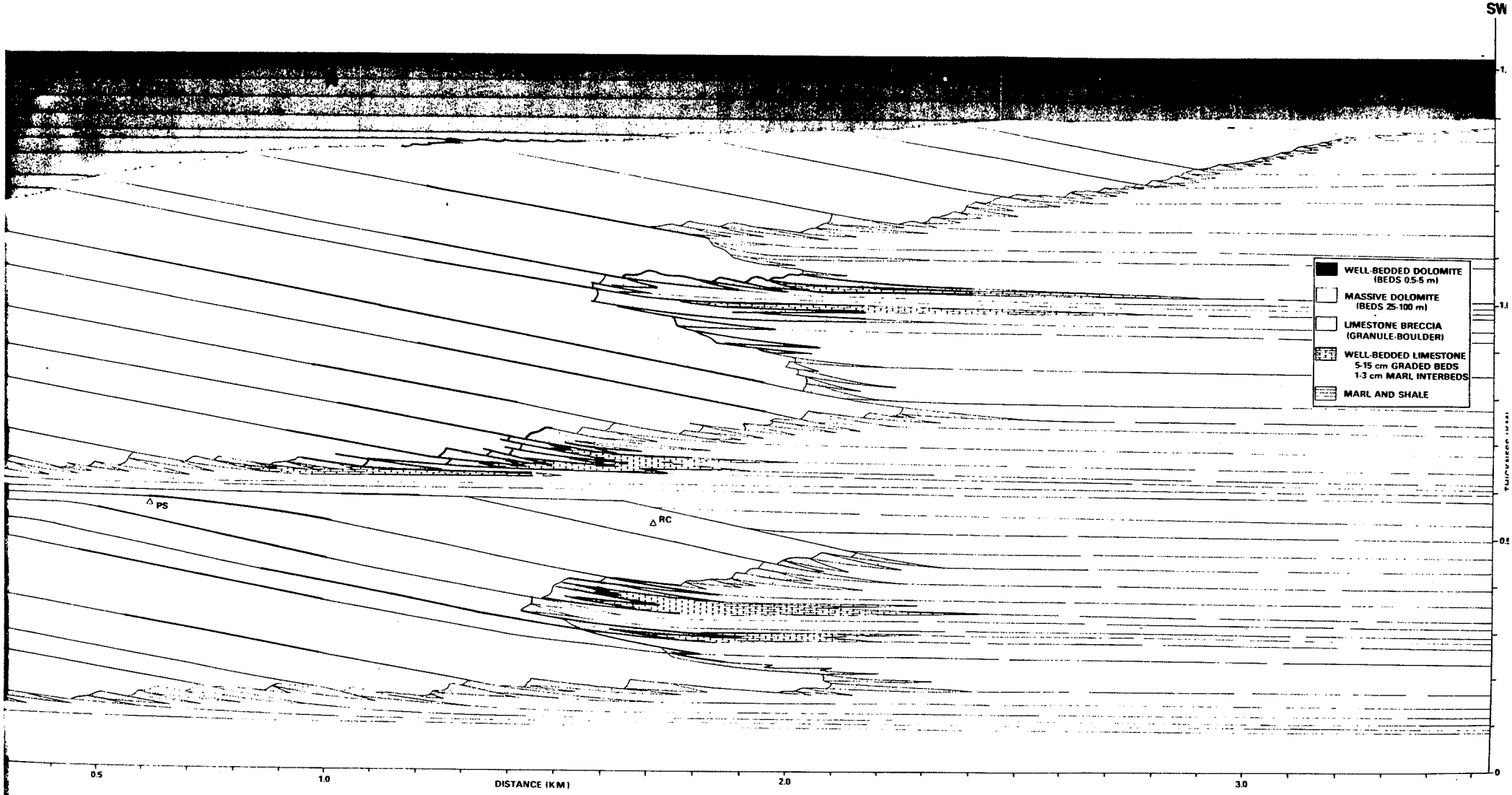

...section, Picco di Vallandro area. Heavier lines represent areas of on-ground ...and lithology in other areas have been projected from photographs and other ...di Vallandro, PS = Punta di Serla, RC = Rocce della Chiesa. See text for discussion. Line ...n in Figure 6.

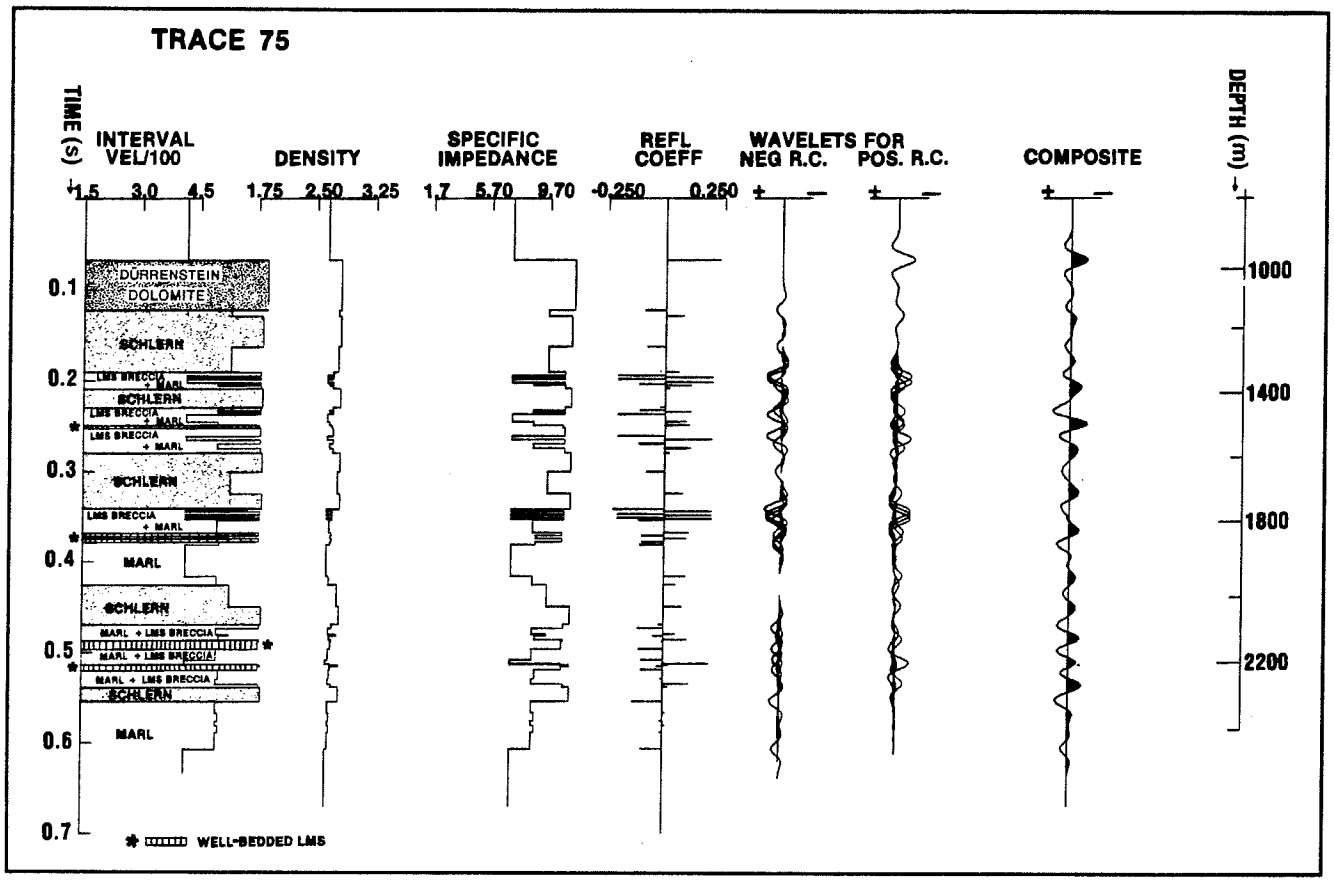

Figure 13—Detailed impedance-reflection plot, trace 75. Trace location is shown on Figures 10–11. Interval velocity is in km/s. Abbreviations as in Figure 12. See text for discussion.

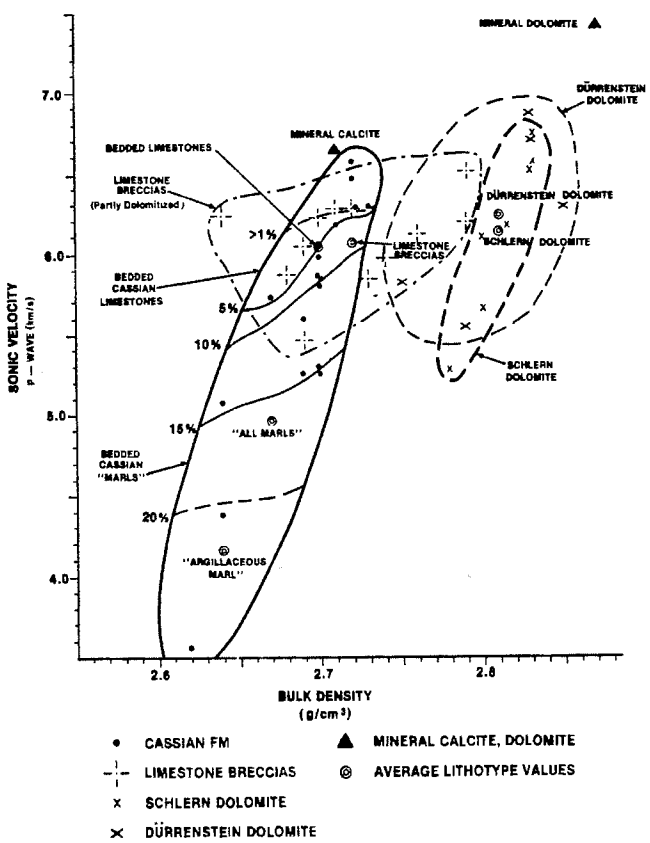

Figure 7—Sonic velocity vs. bulk density for Picco di Vallandro samples (Rudolph et al. 1989). Samples are plotted by stratigraphic unit or lithotype. Enclosed areas represent the field covered by each stratigraphic or lithologic unit. Mean values were calculated for each field, with three means calculated for the Cassian Formation: one for bedded limestones, one for all marls, and one for argillaceous marl. Contours in the Cassian Formation field represent percent noncarbonate material (see Table 1). Velocity and density of mineral calcite and dolomite are given for reference (from Simmons and Wang, 1971; Sumino and Anderson, 1984).

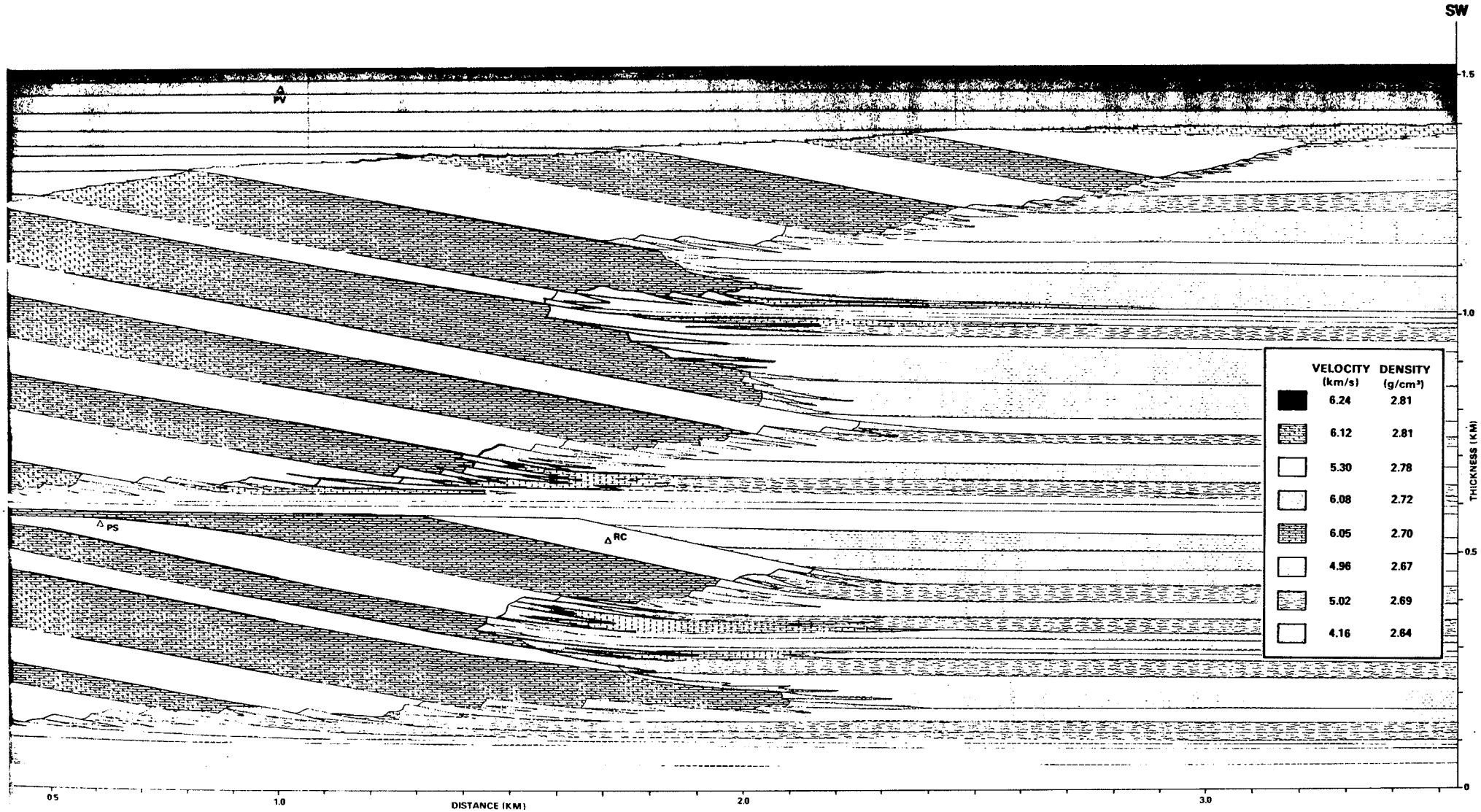

section. Picco di Vallandro area. This cross section provides the basic input Vallandro. PS = Punta di Serla, RC = Rocce della Chiesa. See text for discussion. igure 6.

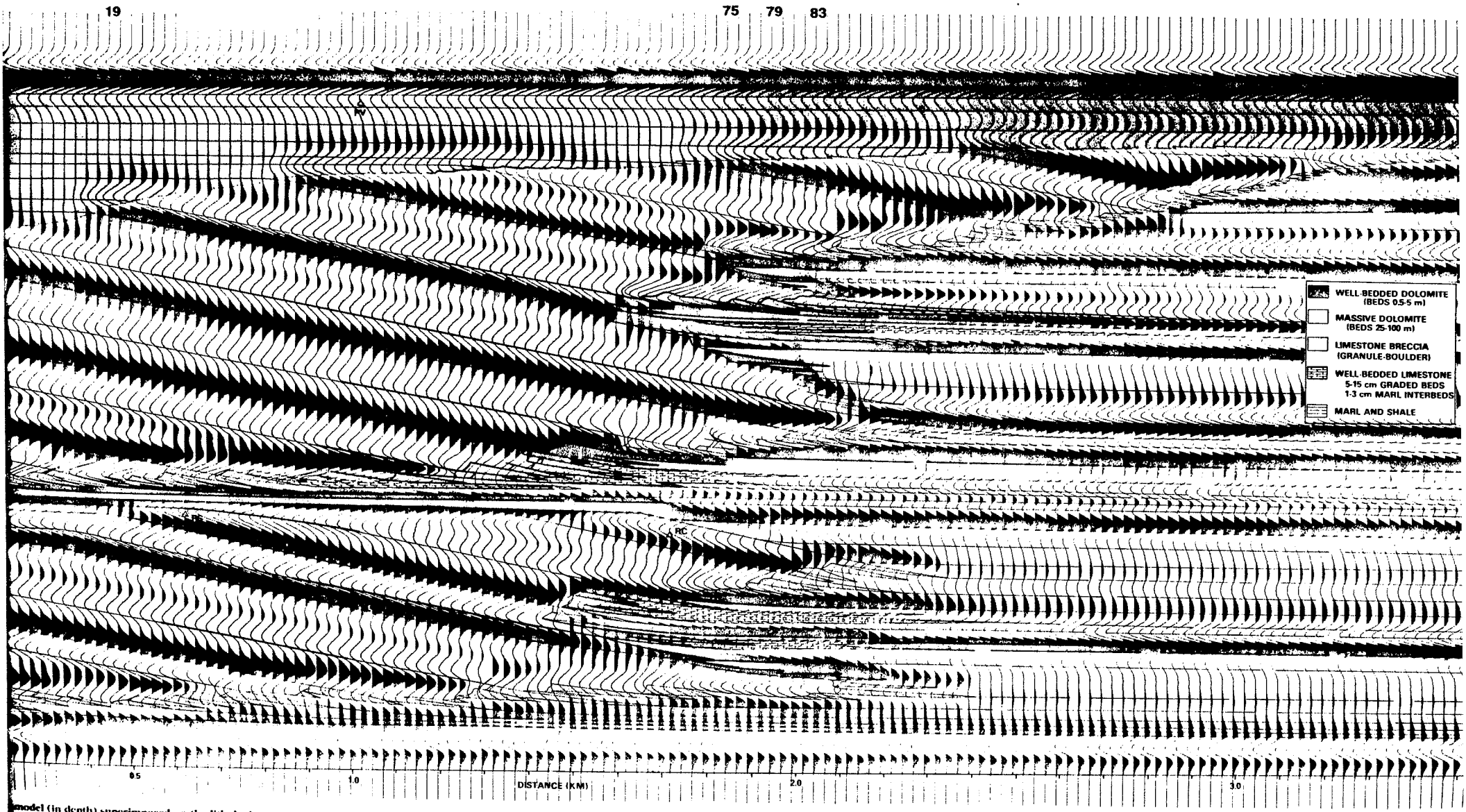

model (in depth) superimposed on the lithologic cross section of the Picco di Vallandro area. the top of the model show the positions of the detailed traces illustrated in Figures 12–15. PV). PS = Punta di Serla, RC = Rocce della Chiesa. See text for dicussion. Line and plane of section

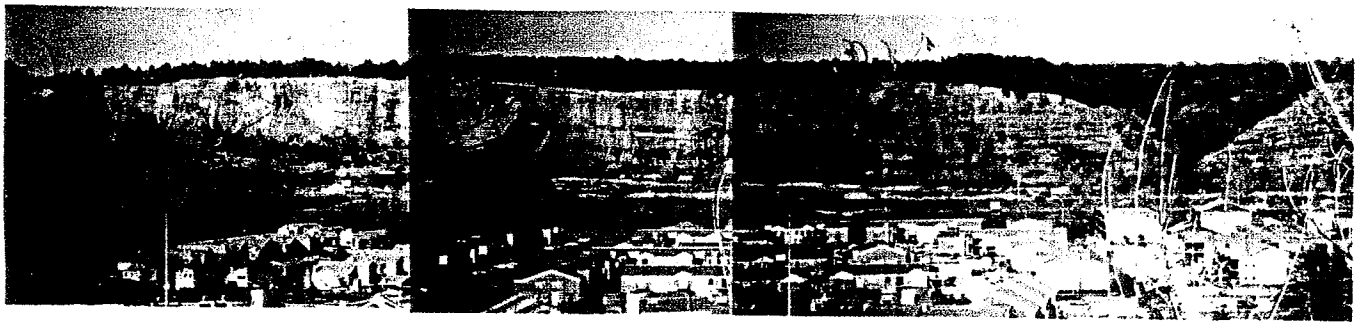

Figure 2—Photomosaic of Big Rock Quarry face (location of profile shown on Figure 1).

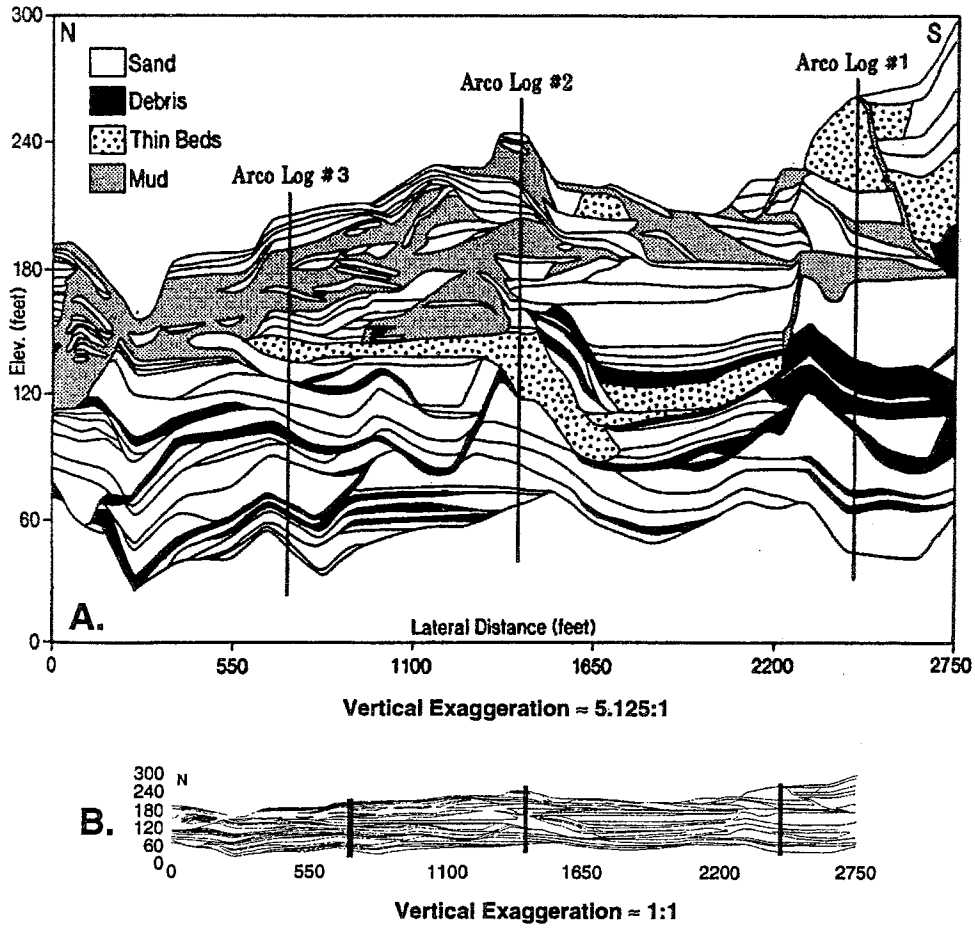

Figure 3—(A) Correlation diagram from quarry photo mosaic (original scalar distortion) (from Bouma and Cook, 1994, used by permission). (B) Correlation diagram from quarry photo mosaic (differentially "squeezed" to approximate photomosaic and seismic aspect ratio and scale) (simplified from Bouma and Cook, 1994).

Coleman et al, 2000, AAPG Mem 72, p. 119-126.

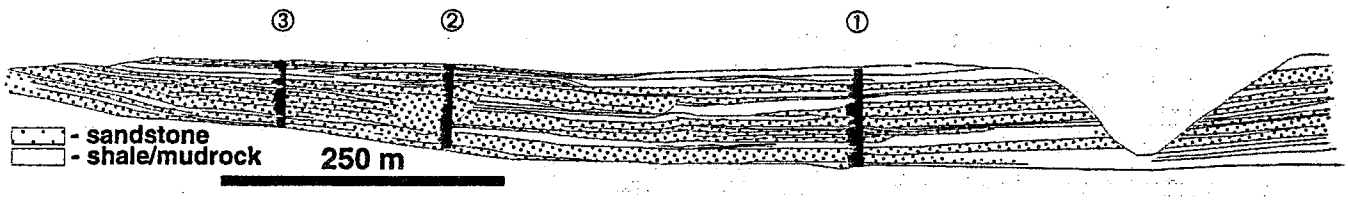

Figure 4—Line drawing from photomosaic of Big Rock Quarry face, with outcrop gamma-ray logs from Jordan et al. (1991).

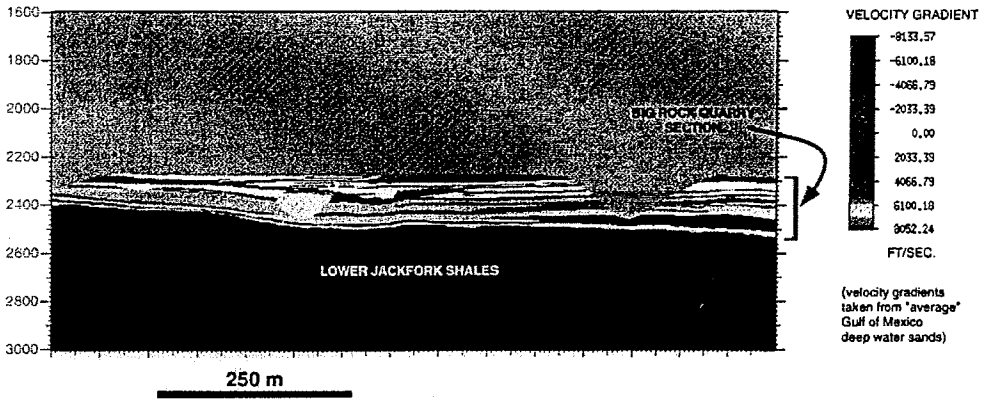

Figure 5—Seismic velocity model for synthetic seismic line of Big Rock Quarry face.

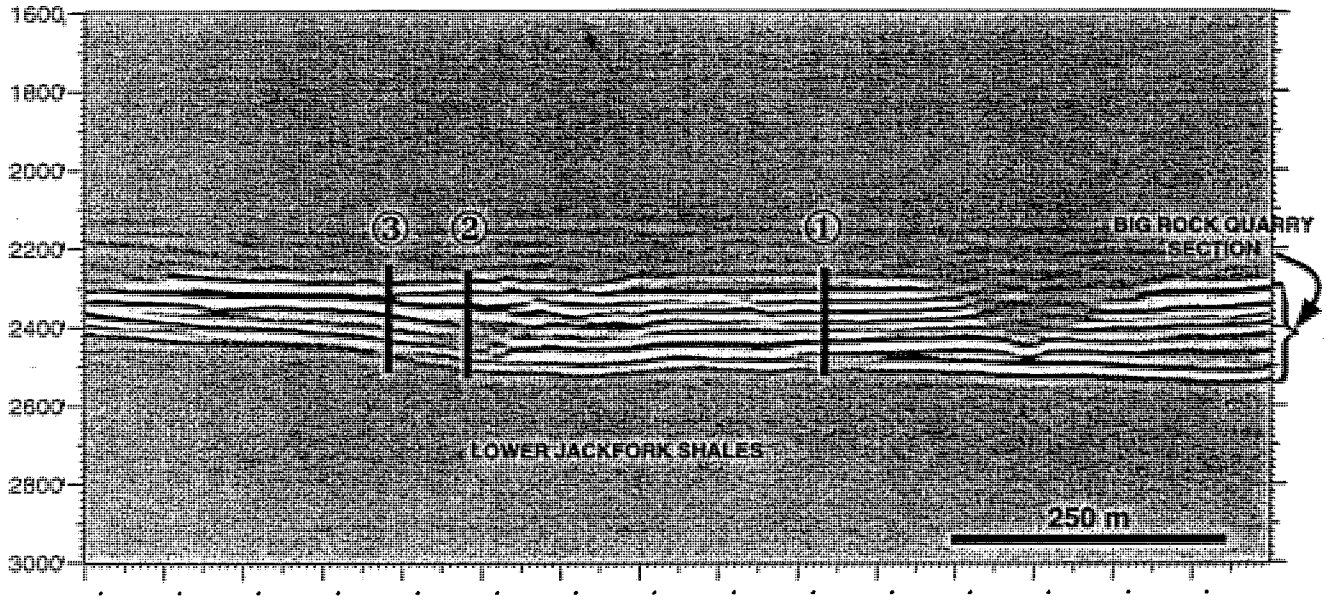

Figure 6—A 300-Hz synthetic seismic line, Big Rock Quarry face, with location of ARCO's outcrop gamma-ray logs from Jordan et al. (1991).

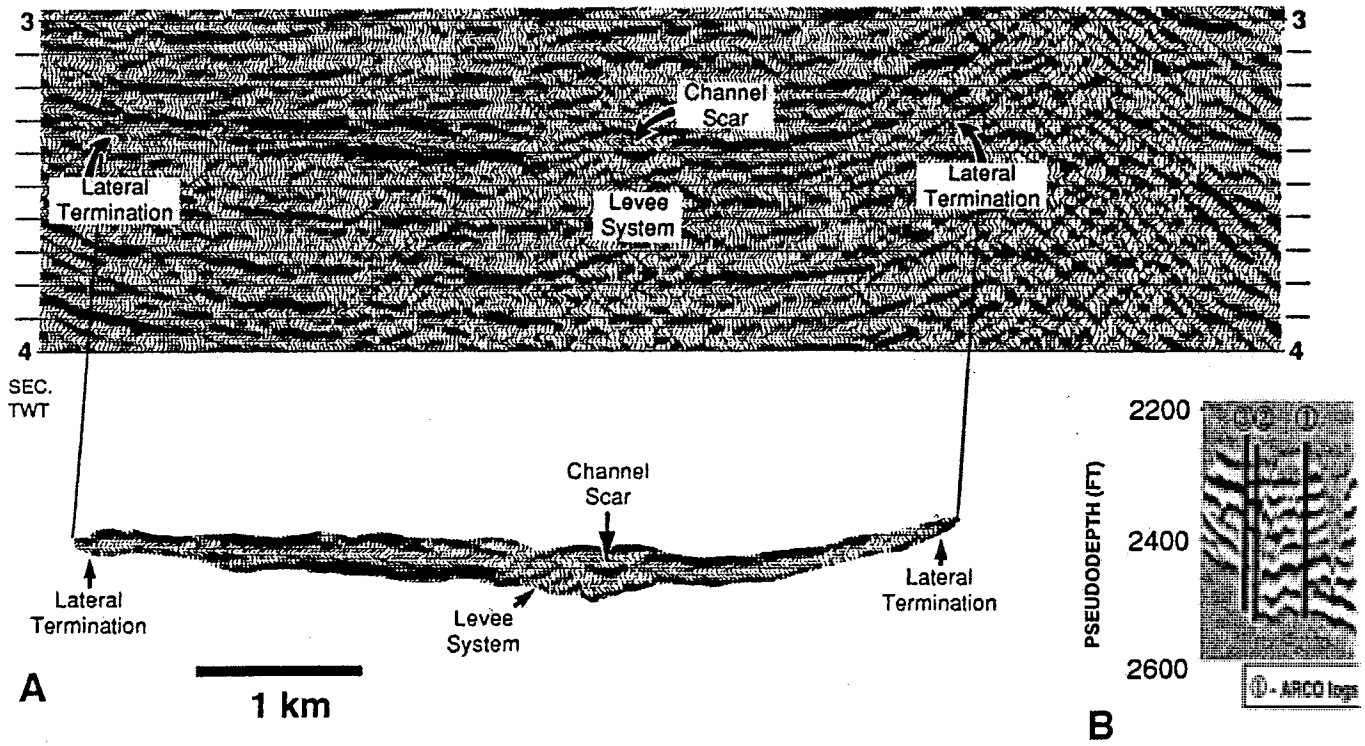

Figure 8—(A) Selected portion of a seismic line in Green Canyon Block 136 illustrating seismic facies character of a profile across a submarine channel/levee complex (modified from Geitgy, 1990, reproduced with permission of the Gulf Coast Sections Society of Economic Paleotologists and Mineralogists Foundation). (B) A 300-Hz synthetic seismic line of Big Rock Quarry face (Figure 6) displayed at approximately the same

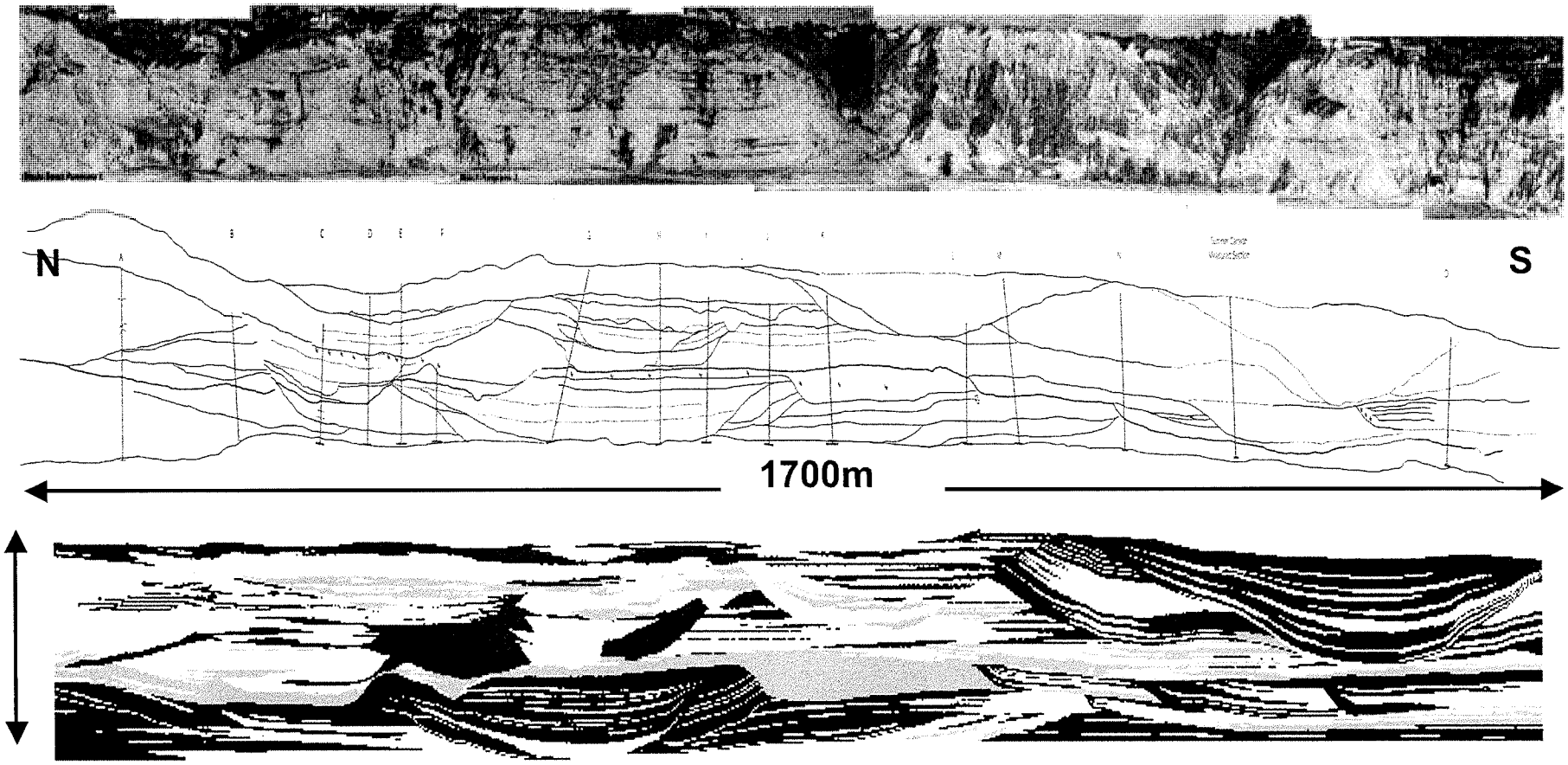

L. Stright 2008

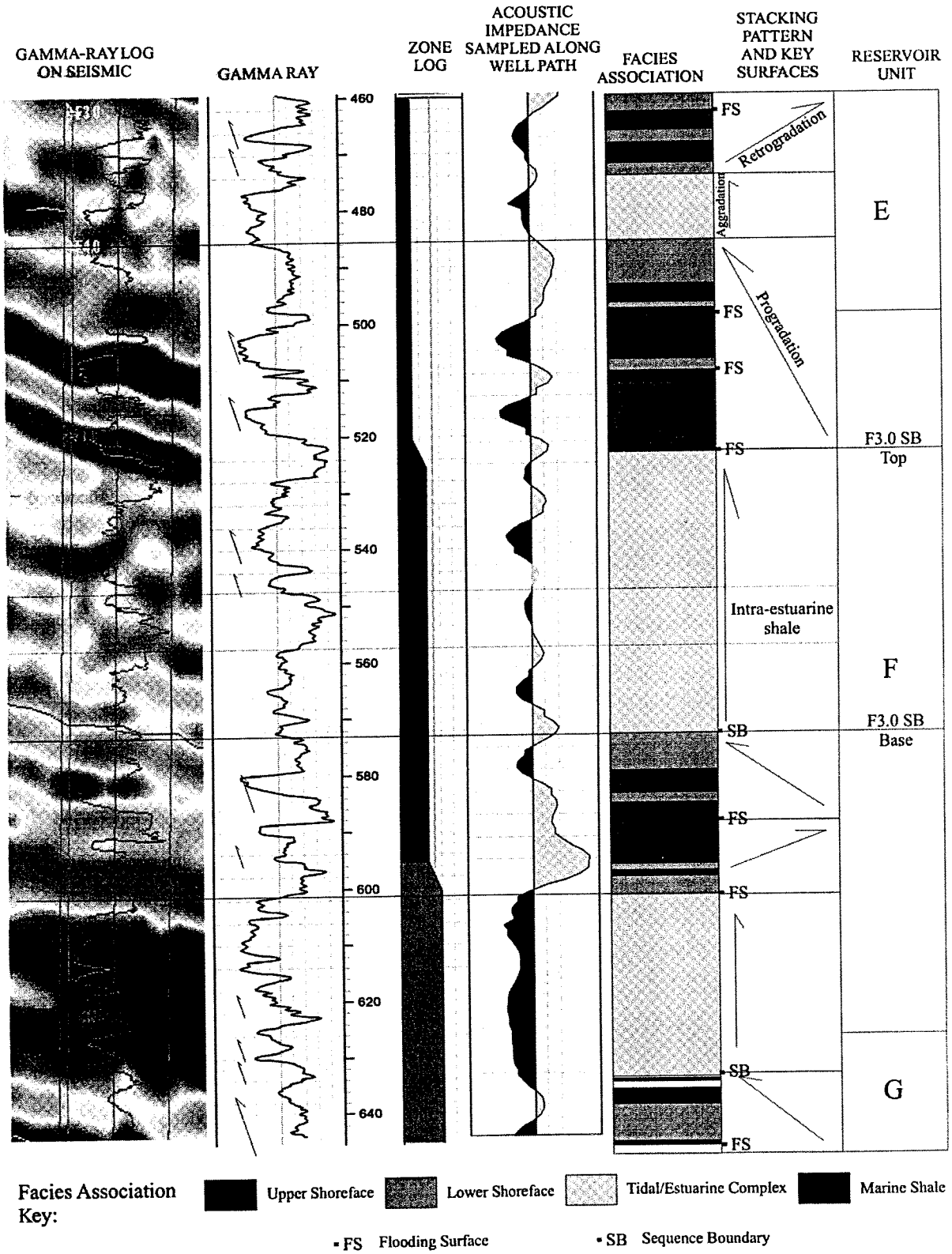

Figure 5. Example well showing seismic to well tie and sedimentological sequence stratigraphic analysis. Note the 1:1 correspondence between coarsening-upward shoreface parasequences at 500–520 m on the gamma-ray log and black, negative acoustic impedance events. Also note the distinctive fuzzy seismic character of the tidal-estuarine complex. See text for full discussion.

AAPG Bull, v. 85, p. 433–458

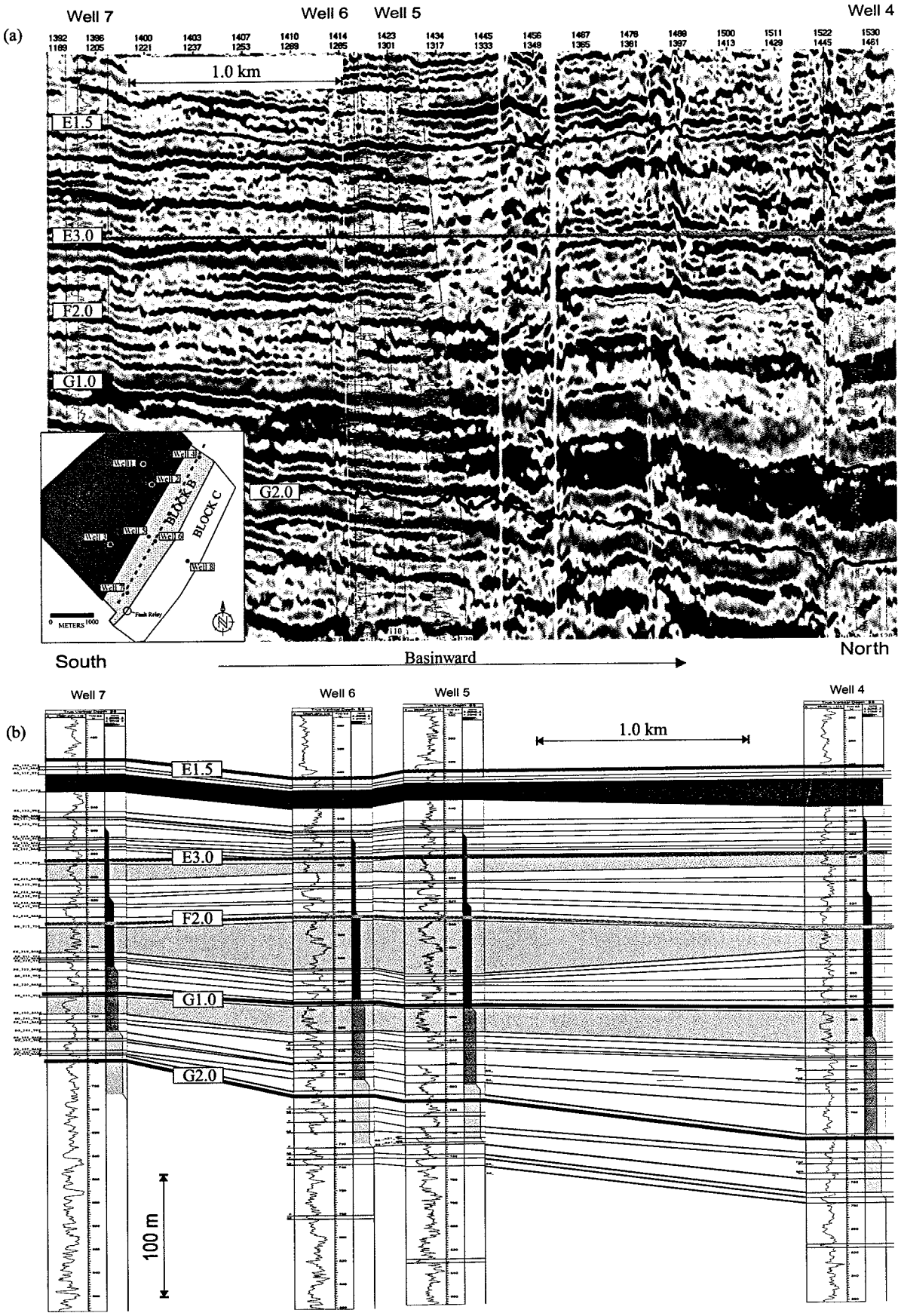

AAPG Bull, v. 85, p. 433-458

EXTENDING RESOLUTION BY INTEGRATING GEOLOGY, PETROPHYSICS & SEIS RESPONSE

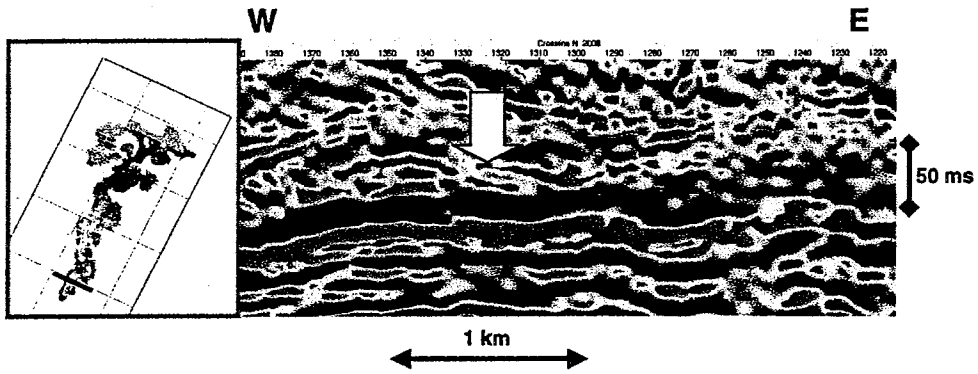

Figure 6.10: Seismic section intersecting the southern Grane fan. We observe seismic signatures of vertical and lateral stacking of separate channelized depositional units.

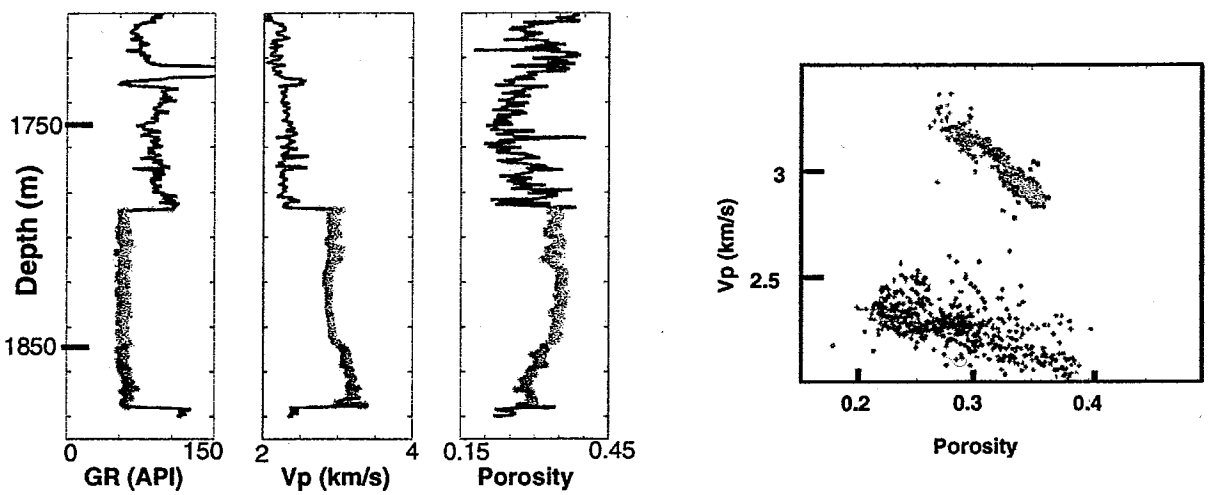

Figure 6.15: Gamma ray, Vp, and porosity in well #2 (location, see Figure 5.2). Cross plot of Vp versus porosity is shown to the right. The lower zone of the reservoir sands has higher velocities and lower porosities than the upper zone. This textural change is related to sorting/packing (c.f., Chapter 2), and explains the internal reflector observed in the seismic section in Figure 6.19.

Avseth, Stanford PhD thesis, 2000

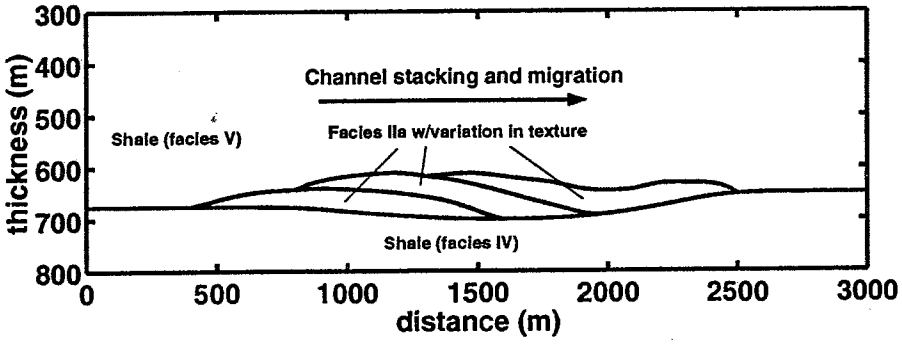

Figure 6.16: Geologic model showing lateral migration/stacking of channel sands.

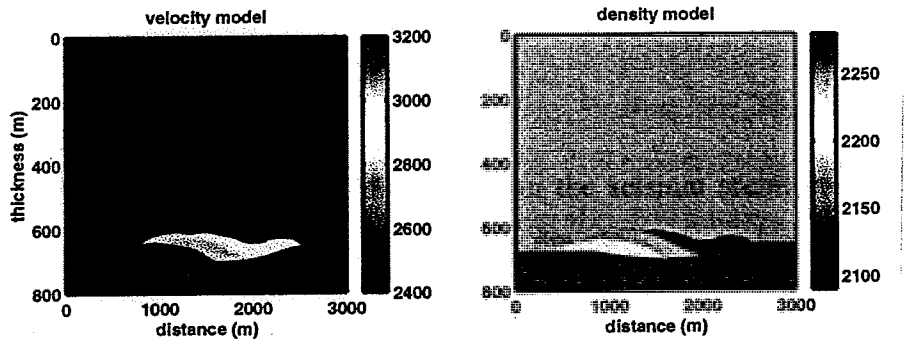

Figure 6.17: Velocity and density models of a laterally stacked channel-complex.

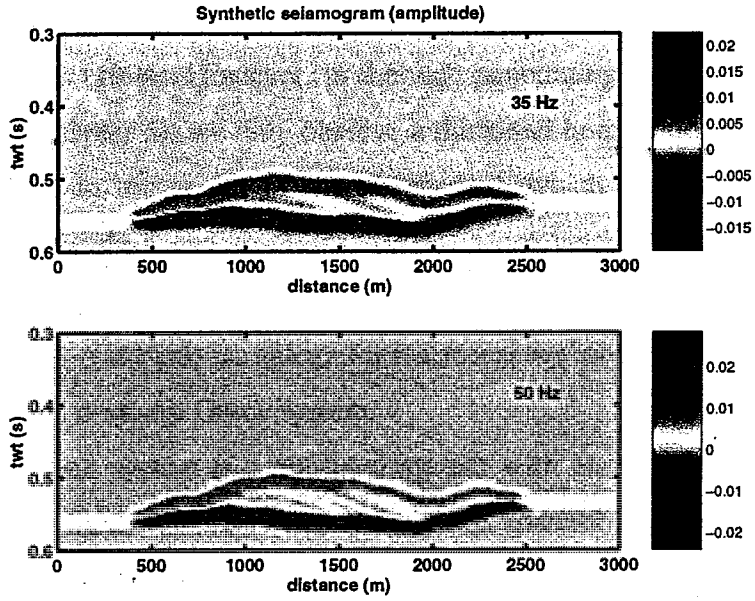

Figure 6.18: Synthetic seismic sections, one with a 35 Hz wavelet (upper) and one with a 50 Hz wavelet (lower). The results show that internal reflectors can occur due to sandstone texture in the studied turbidite system, even at 35 Hz. The top sand reflector is in general a strong positive amplitude, whereas the erosive base causes a strong negative amplitude.

Molasse Basin, Austria

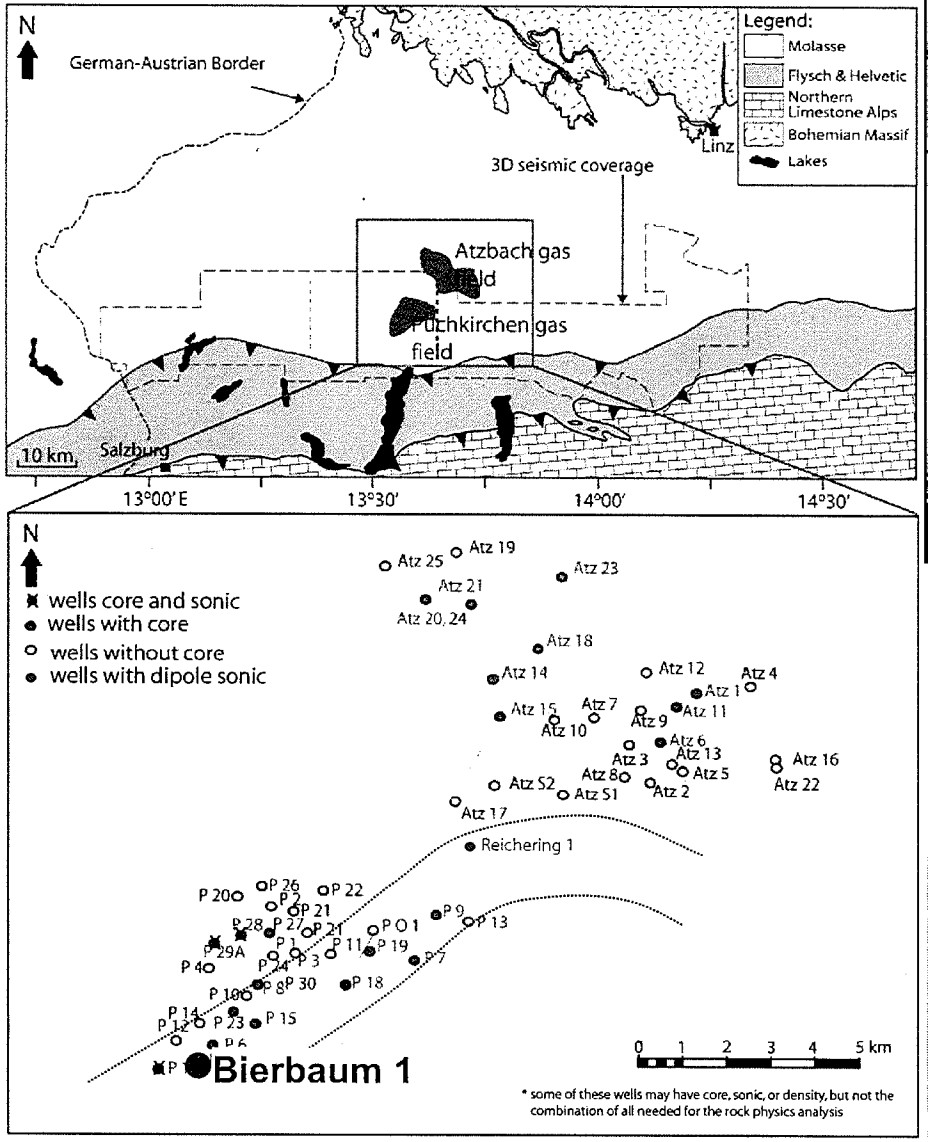

de Ruig, 2006

Hubbard, 2006

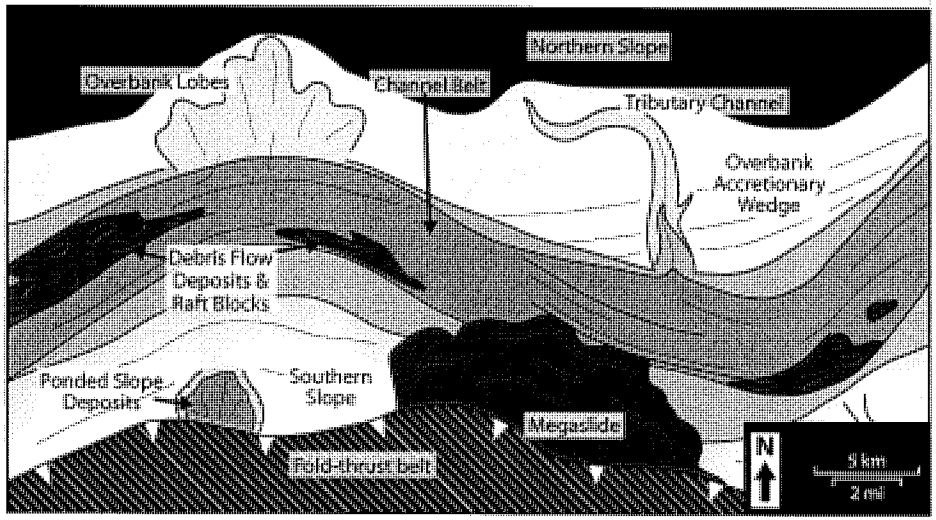

Inverted P-Impedance and the A1 sand contoured from logs and cores

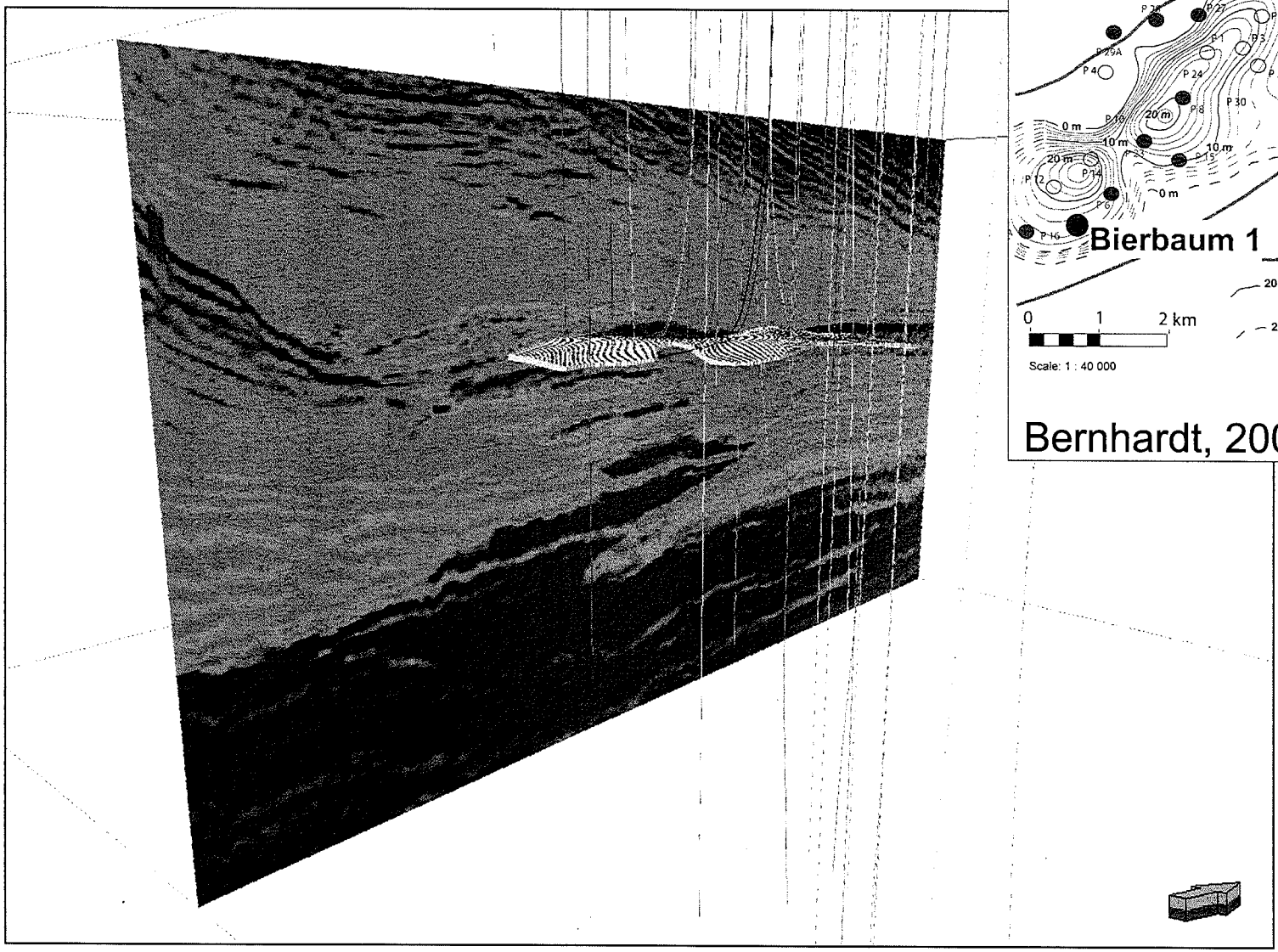

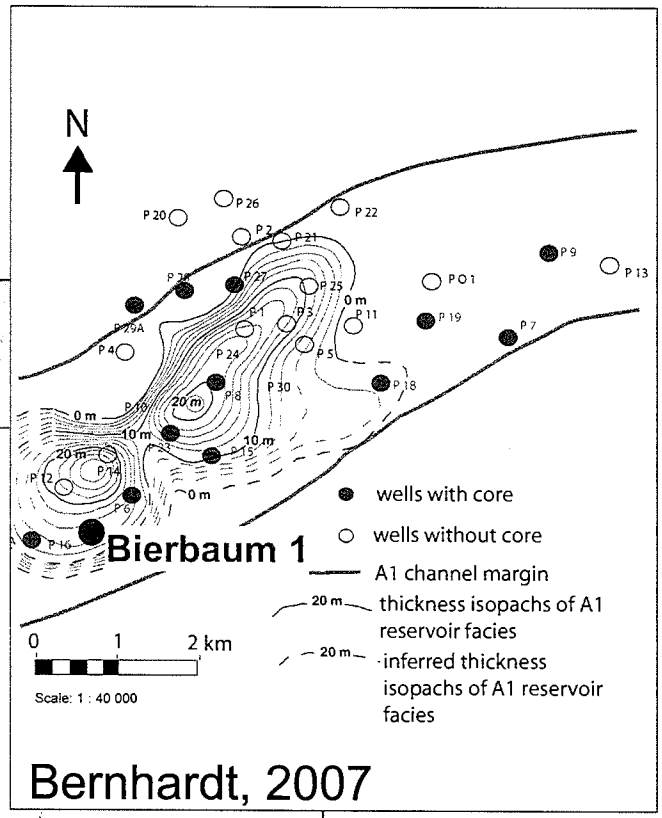

Bernhardt, 2007

L. Stright 2008

Traditional Calibration

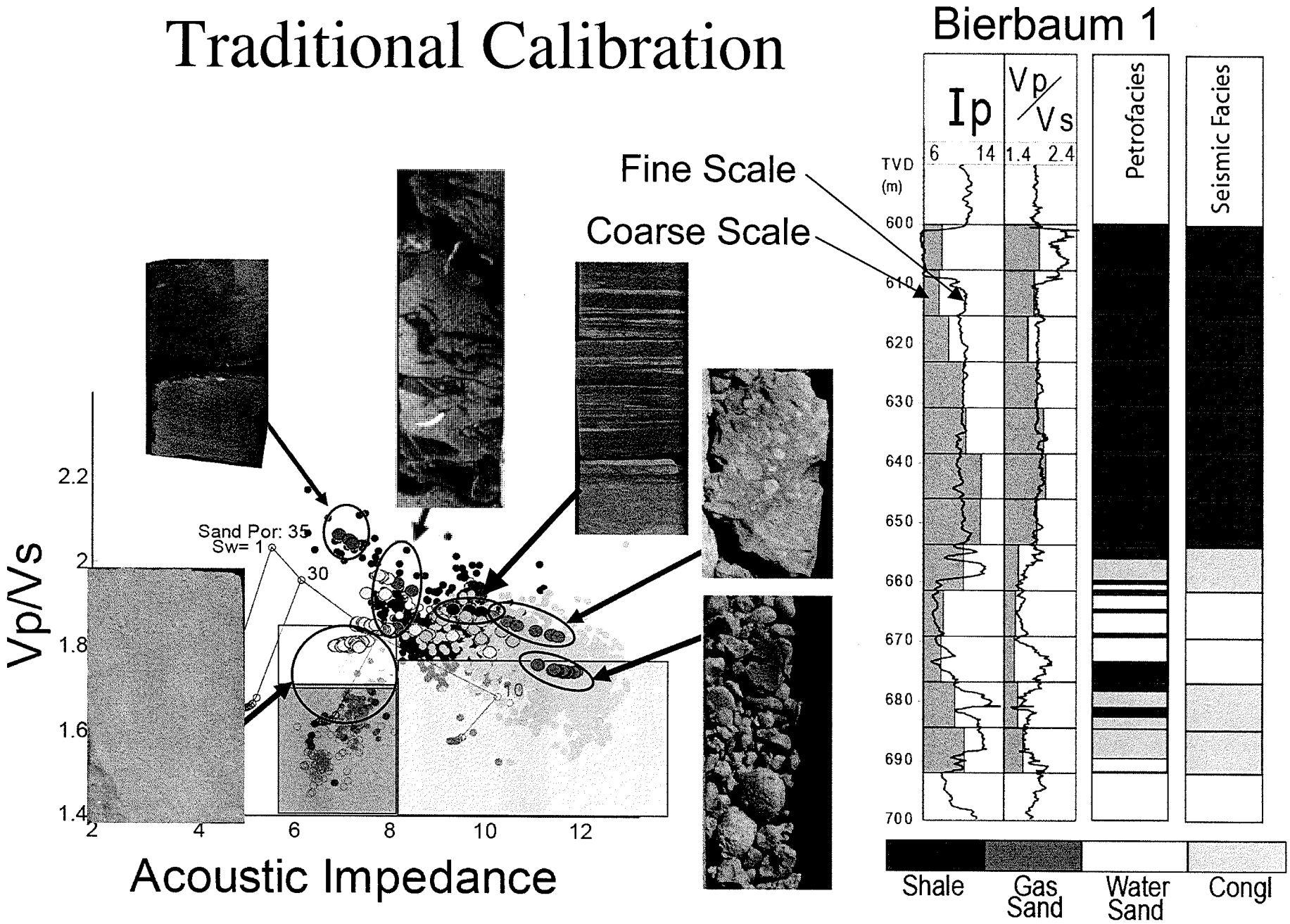

L. Stright 2008

Fine scale heterogeneities

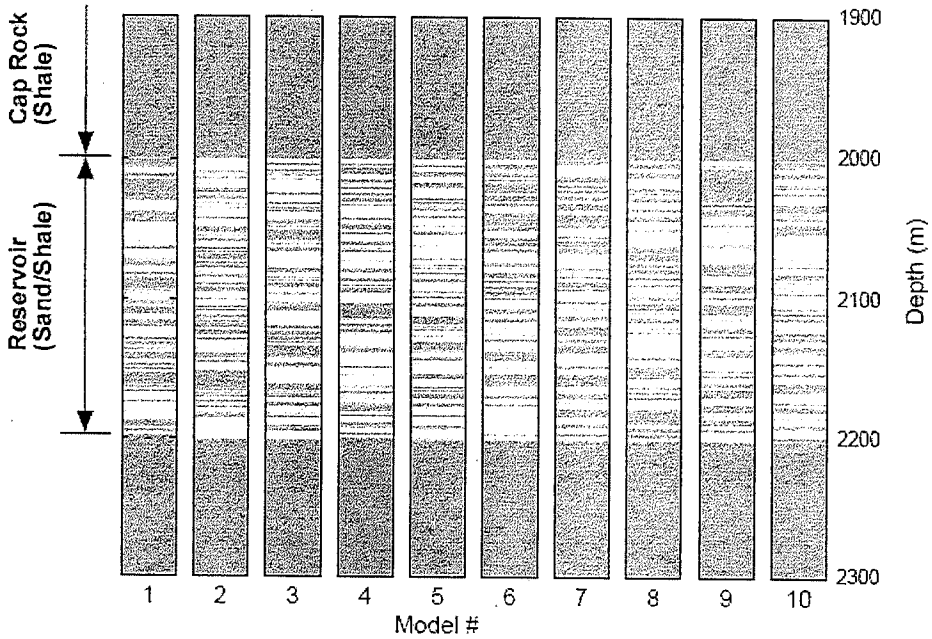

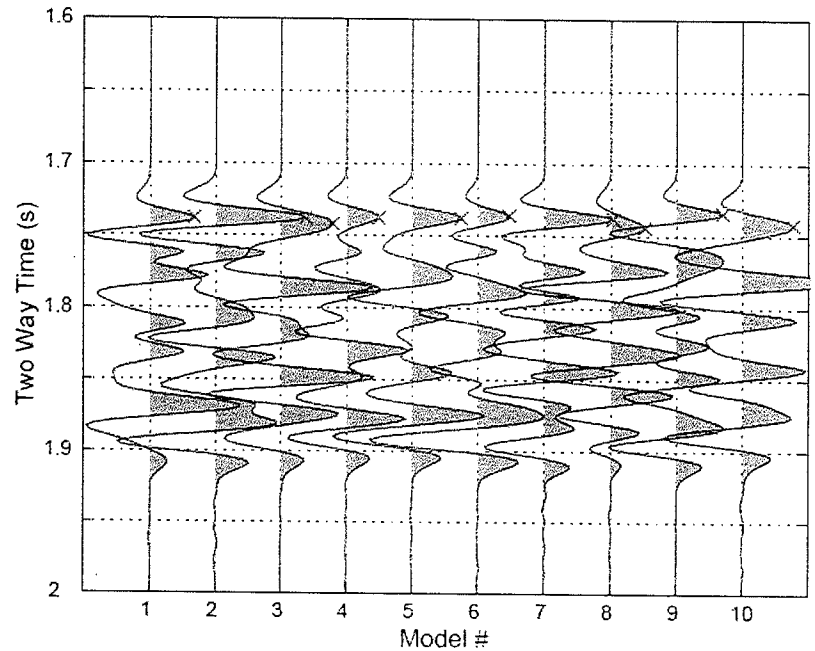

Takahashi, 2000

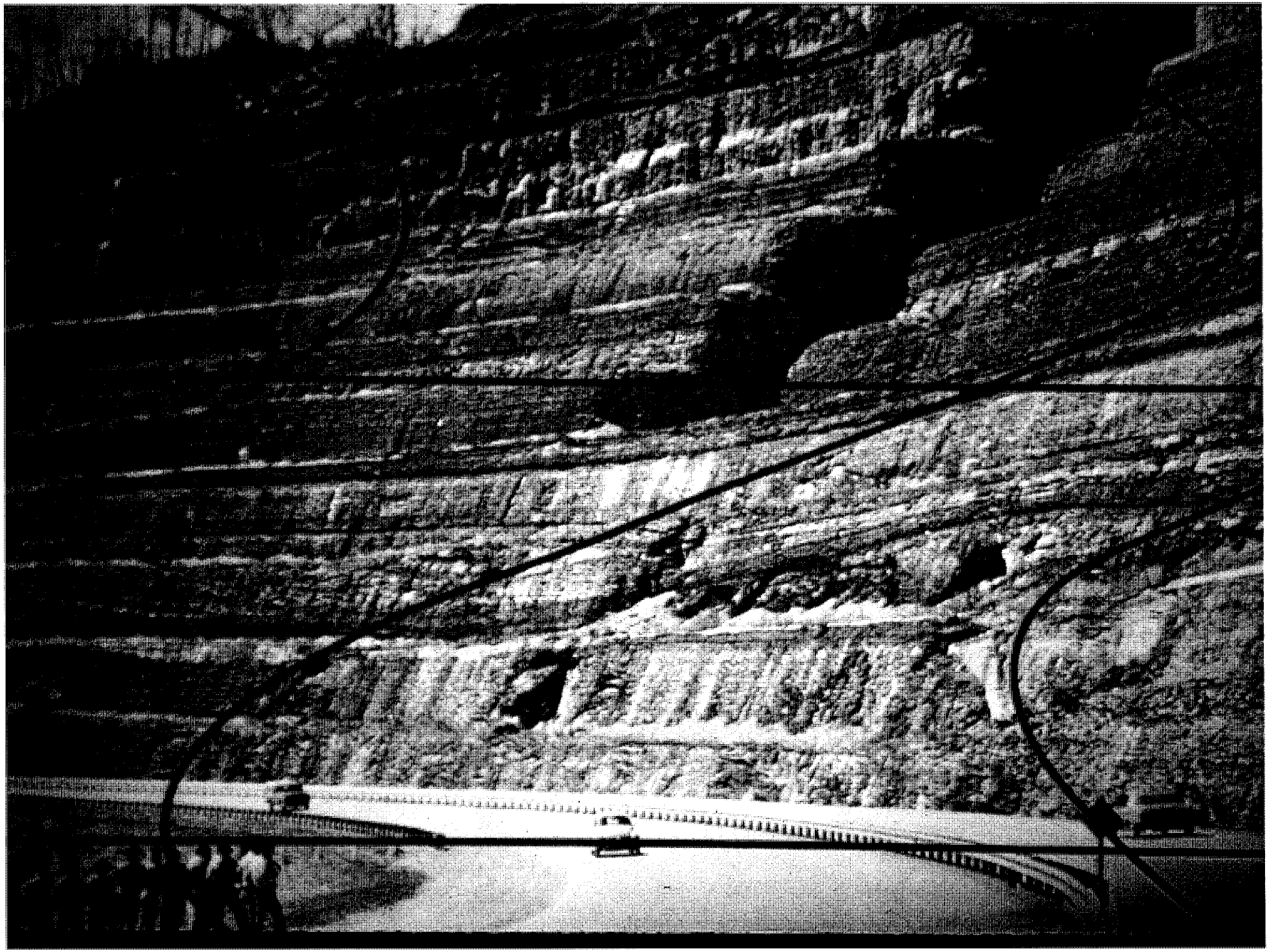

SEISMIC FACIES (Exxon concepts and approaches)

- Erect sequences as packages of concordant reflectors (defined by reflectors terminated at sequence boundaries)

- Note internal character of sequence
  - -configuration of reflectors
  - -continuity of reflectors
  - -amplitude of reflectors
  - -frequency
  - -interval velocity

- External form of sequence

REFLECTION TERMINATIONS (AT SEQUENCE BOUNDARIES)	REFLECTION CONFIGURATIONS (WITHIN SEQUENCES)		EXTERNAL FORMS (OF SEQUENCES AND SEISMIC FACIES UNITS)
LAPOUT	PRINCIPAL STRATAL CONFIGURATION		
BASELAP	PARALLEL		SHEET
ONLAP	SUBPARALLEL		SHEET DRAPE
DOWNLAP	DIVERGENT		WEDGE
TOPLAP	PROGRADING CLINOFORMS		BANK
TRUNCATION	SIGMOID		LENS
EROSIONAL	OBLIQUE		MOUND
STRUCTURAL	COMPLEX SIGMOID-OBLIQUE		FILL
CONCORDANCE	SHINGLED		
(NO TERMINATION)	HUMMOCKY CLINOFORM		
	CHAOTIC		
	REFLECTION-FREE		
	MODIFYING TERMS		
	EVEN	HUMMOCKY	
	WAVY	LENTICULAR	
	REGULAR	DISRUPTED	
	IRREGULAR	CONTORTED	
	UNIFORM		
	VARIABLE		

In practice:

Single line (2-D) analysis => Grid analysis => Full interpretation

Table 1. Geologic Interpretation of Seismic Facies Parameters.

REFLECTION TERMINATIONS (AT SEQUENCE BOUNDARIES)	REFLECTION CONFIGURATIONS (WITHIN SEQUENCES)		EXTERNAL FORMS (OF SEQUENCES AND SEISMIC FACIES UNITS)
LAPOUT	PRINCIPAL STRATAL CONFIGURATION		
BASELAP	PARALLEL		SHEET
ONLAP	SUBPARALLEL		SHEET DRAPE
DOWNLAP	DIVERGENT		WEDGE
TOPLAP	PROGRADING CLINOFORMS		BANK
TRUNCATION	SIGMOID		LENS
EROSIONAL	OBLIQUE		MOUND
STRUCTURAL	COMPLEX SIGMOID-OBLIQUE		FILL
CONCORDANCE	SHINGLED		
(NO TERMINATION)	HUMMOCKY CLINOFORM		
	CHAOTIC		
	REFLECTION-FREE		
	MODIFYING TERMS		
	EVEN	HUMMOCKY	
	WAVY	LENTICULAR	
	REGULAR	DISRUPTED	
	IRREGULAR	CONTORTED	
	UNIFORM		
	VARIABLE		

Table 2. Seismic Reflection Parameters Used in Seismic Stratigraphy, and Their Geologic Significance.

SEISMIC FACIES PARAMETERS	GEOLOGIC INTERPRETATION
REFLECTION CONFIGURATION	• BEDDING PATTERNS • DEPOSITIONAL PROCESSES • EROSION AND PALEOTOPOGRAPHY • FLUID CONTACTS
REFLECTION CONTINUITY	• BEDDING CONTINUITY • DEPOSITIONAL PROCESSES
REFLECTION AMPLITUDE	• VELOCITY-DENSITY CONTRAST • BED SPACING • FLUID CONTENT
REFLECTION FREQUENCY	• BED THICKNESS • FLUID CONTENT
INTERVAL VELOCITY	• ESTIMATION OF LITHOLOGY • ESTIMATION OF POROSITY • FLUID CONTENT
EXTERNAL FORM & AREAL ASSOCIATION OF SEISMIC FACIES UNITS	• GROSS DEPOSITIONAL ENVIRONMENT • SEDIMENT SOURCE • GEOLOGIC SETTING

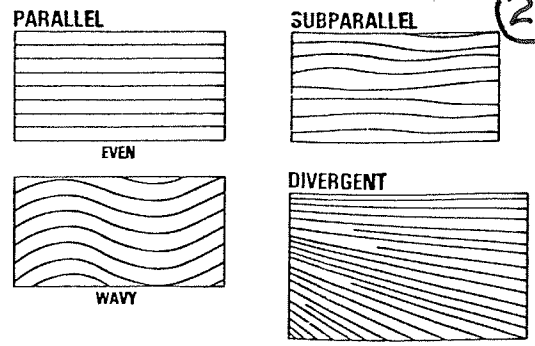

FIG. 4—Parallel, subparallel, and divergent seismic reflection configurations.

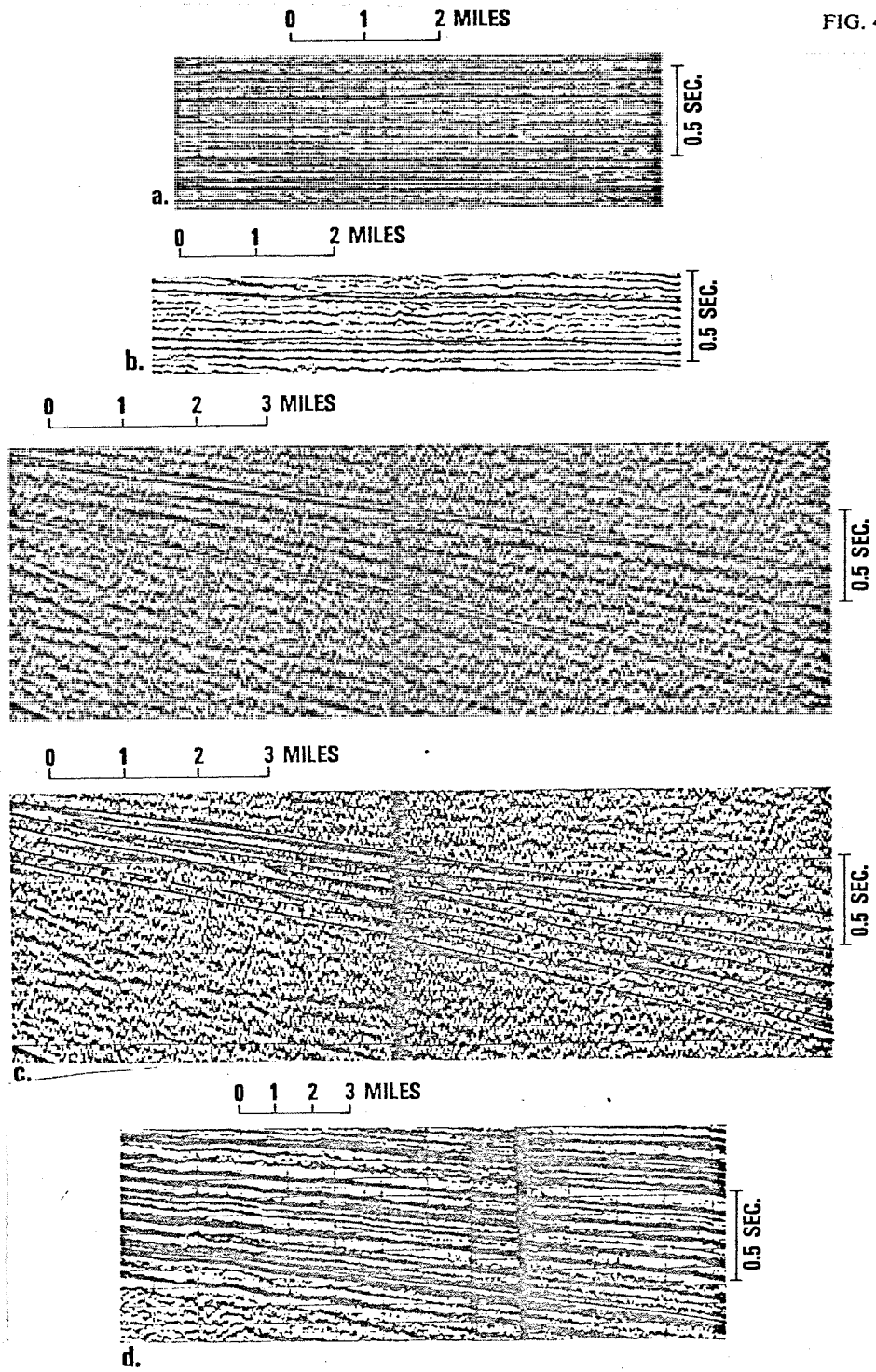

FIG. 5—Parallel, subparallel, and divergent seismic reflection configurations: **a** is a parallel configuration with good continuity and high to medium amplitude; **b** is subparallel configuration with good to fair continuity and high to medium amplitude; **c** and **d** are divergent configurations, with thickening of individual reflection cycles in direction of divergence. Nonsystematic reflection terminations occur in direction of thinning.

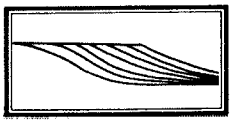

OBLIQUE (FIGURE 14)

THIS PROGRADATIONAL REFLECTION CONFIGURATION IS INTERPRETED AS A PROGRADING CLINOFORM PATTERN, CONSISTING IDEALLY OF A NUMBER OF STEEP-DIPPING STRATA TERMINATED UPDIP BY TOPLAP AT OR NEAR A BASICALLY FLAT UPPER SURFACE, AND DOWNDIP BY DOWNLAP AGAINST THE LOWER SURFACE. SUCCESSIVELY YOUNGER FORESET SEGMENTS OF STRATA BUILD ALMOST ENTIRELY LATERALLY IN A DEPOSITIONALLY DOWNDIP DIRECTION. THEY BUILD OUT FROM A RELATIVELY CONSTANT UPPER SURFACE DUE TO THE LACK OF TOPSET STRATA BUT ARE CHARACTERIZED BY PRONOUNCED TOPLAP TERMINATIONS OF FORESET STRATA.

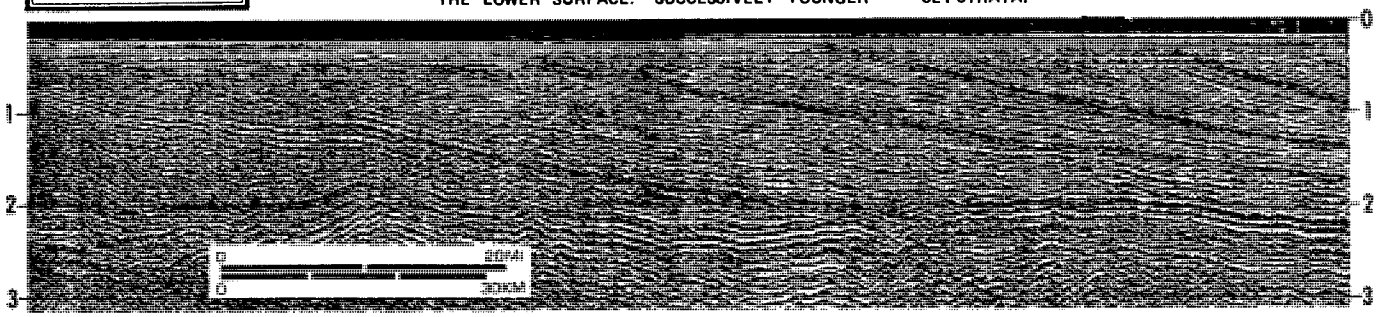

THIS IS AN EXAMPLE OF OBLIQUE SEISMIC REFLECTION CONFIGURATION. THIS CONFIGURATION IMPLIES DEPOSITIONAL CONDITIONS WITH SOME COMBINATION OF RELATIVELY HIGH SEDIMENT SUPPLY, SLOW TO NO BASIN SUBSIDENCE, AND A STILLSTAND OF SEA LEVEL TO ALLOW RAPID BASIN INFILL AND SEDIMENTARY BYPASS WITH SOME EROSION OF THE UPPER DEPOSITIONAL SURFACE.

FIGURE 15

Abbott 79

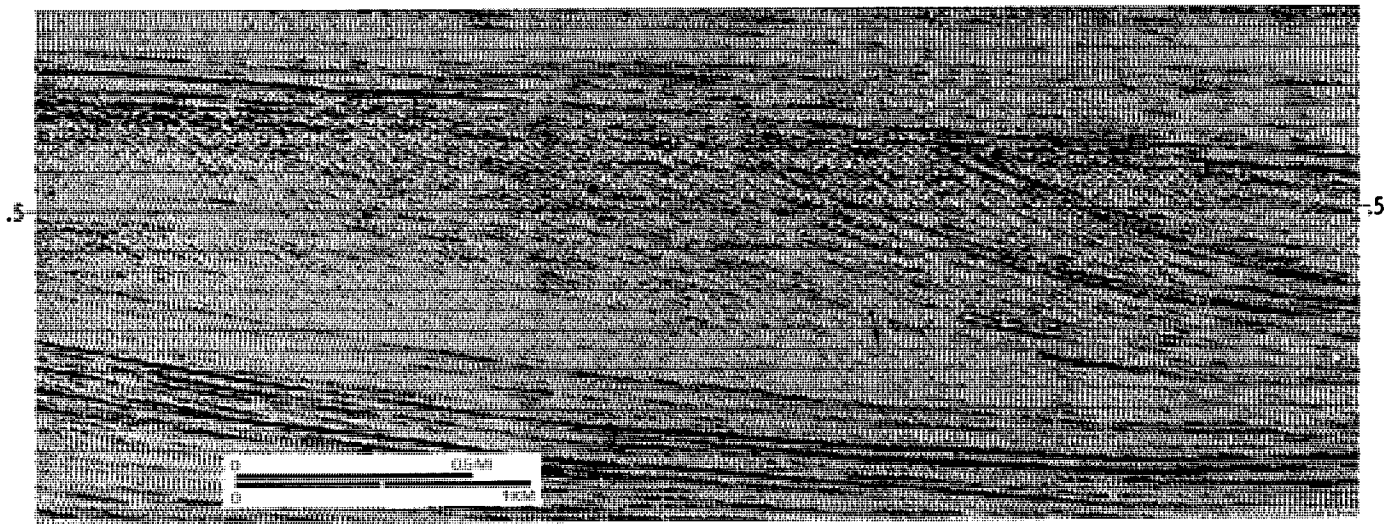

THIS FIGURE IS ANOTHER EXAMPLE OF AN OBLIQUE SEISMIC REFLECTION CONFIGURATION PATTERN.

FIGURE 16

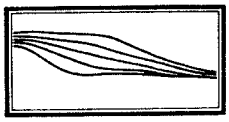

SIGMOID (FIGURE 9)

THIS PROGRADATIONAL CONFIGURATION IS A PROGRADING CLINOFORM FORMED BY SUPERPOSED "S" SHAPED REFLECTIONS INTERPRETED AS STRATA WITH THIN, GENTLY DIPPING UPPER AND LOWER SEGMENTS, AND THICKER, MORE STEEPLY DIPPING MIDDLE SEGMENTS. THE LOWER SEGMENTS OF THE STRATA APPROACH THE LOWER SURFACE OF THE FACIES UNIT AT VERY LOW ANGLES, AND THE SEISMIC REFLECTIONS SHOW DOWNLAP TERMINATIONS AS THE STRATA TERMINATE OR BECOME TOO THIN TO BE RECOGNIZED ON SEISMIC SECTIONS.

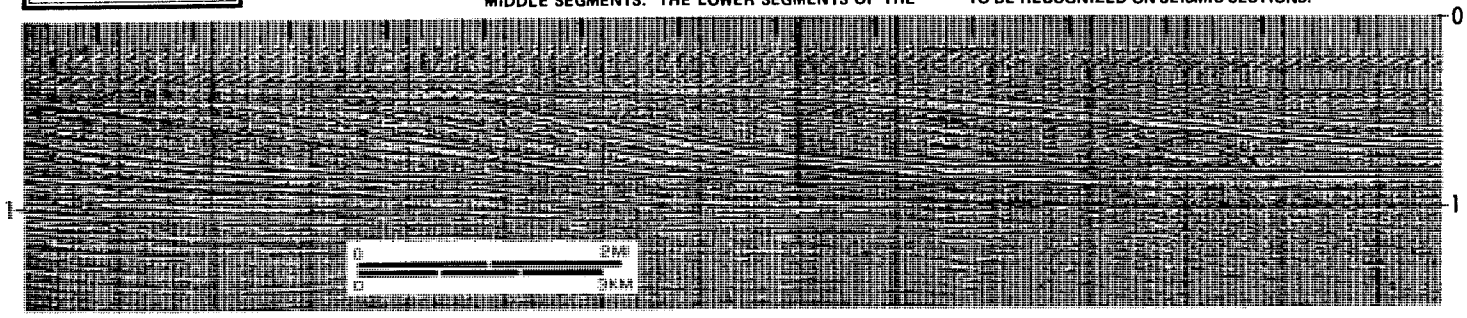

THIS FIGURE IS AN EXAMPLE OF SIGMOID SEISMIC REFLECTION CONFIGURATION. THIS CONFIGURATION IMPLIES RELATIVELY LOW SEDIMENT SUPPLY WITH RELATIVELY RAPID BASIN SUBSIDENCE AND/OR RAPID RISE IN SEA LEVEL TO ALLOW DEPOSITION AND PRESERVATION OF THE TOPSET BEDS.

FROM GROEN, 1972.

FIGURE 10

Abbott #79

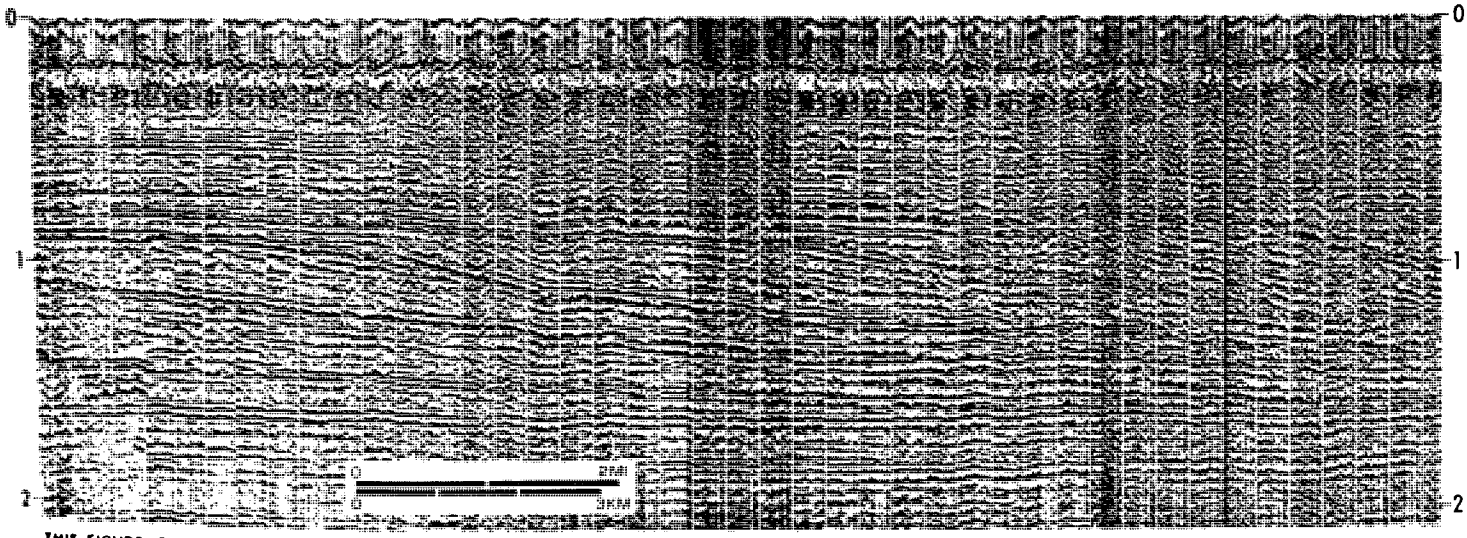

THIS FIGURE IS AN EXAMPLE OF SIGMOID SEISMIC REFLECTION CONFIGURATION WITH SOME SEGMENTS OF COMPLEX SIGMOID-OBLIQUE.

FIGURE 11

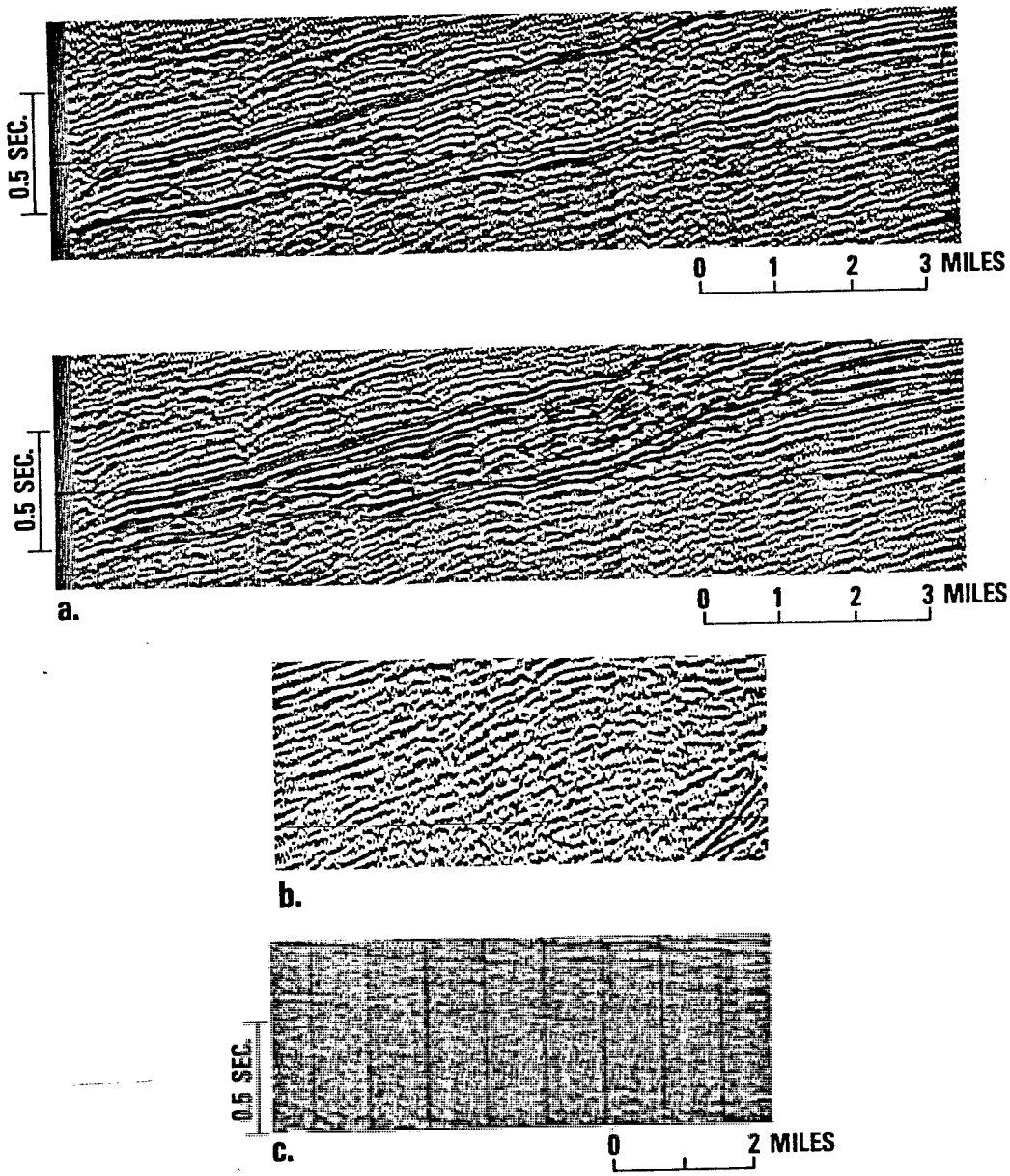

FIG. 10—Examples of chaotic and reflection-free seismic configuration. In **a** reflections may be interpreted as contorted stratal surfaces; in **b** no stratal patterns may be reliably interpreted; **c** is largely reflection-free, where no or very few reflections occur in seismically homogeneous shale.

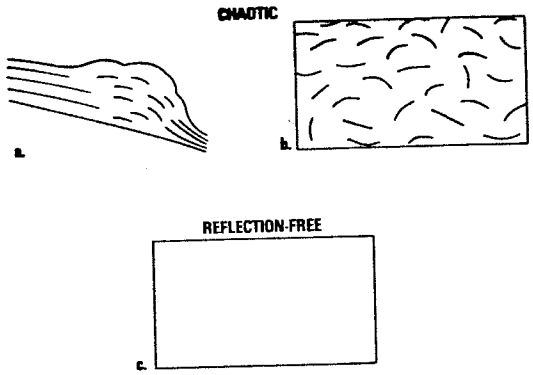

FIG. 9—Diagrams of chaotic and reflection-free seismic reflection patterns. **a** represents a chaotic pattern which may be interpreted as original stratal features still recognizable after penecontemporaneous deformation; in **b** reflections may not be interpreted in any recognizable stratal pattern; **c** represents a reflection-free area.

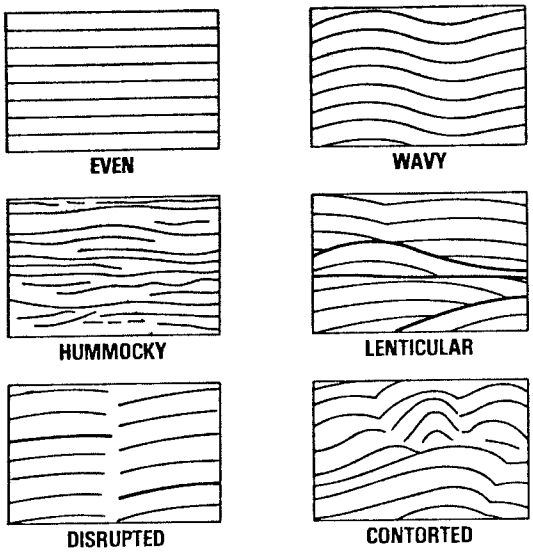

FIG. 11—Some modifying seismic reflection configurations.

Table 1. Geologic Interpretation of Seismic Facies Parameters.

REFLECTION TERMINATIONS (AT SEQUENCE BOUNDARIES)	REFLECTION CONFIGURATIONS (WITHIN SEQUENCES)		EXTERNAL FORMS (OF SEQUENCES AND SEISMIC FACIES UNITS)
LAPOUT	PRINCIPAL STRATAL CONFIGURATION		
BASELAP	PARALLEL		SHEET
ONLAP	SUBPARALLEL		SHEET DRAPE
DOWNLAP	DIVERGENT		WEDGE
TOPLAP	PROGRADING CLINOFORMS		BANK
TRUNCATION	SIGMOID		LENS
EROSIONAL	OBLIQUE		MOUND
STRUCTURAL	COMPLEX SIGMOID-OBLIQUE		FILL
CONCORDANCE	SHINGLED		
(NO TERMINATION)	HUMMOCKY CLINOFORM		
	CHAOTIC		
	REFLECTION-FREE		
	MODIFYING TERMS		
	EVEN	HUMMOCKY	
	WAVY	LENTICULAR	
	REGULAR	DISRUPTED	
	IRREGULAR	CONTORTED	
	UNIFORM		
	VARIABLE		

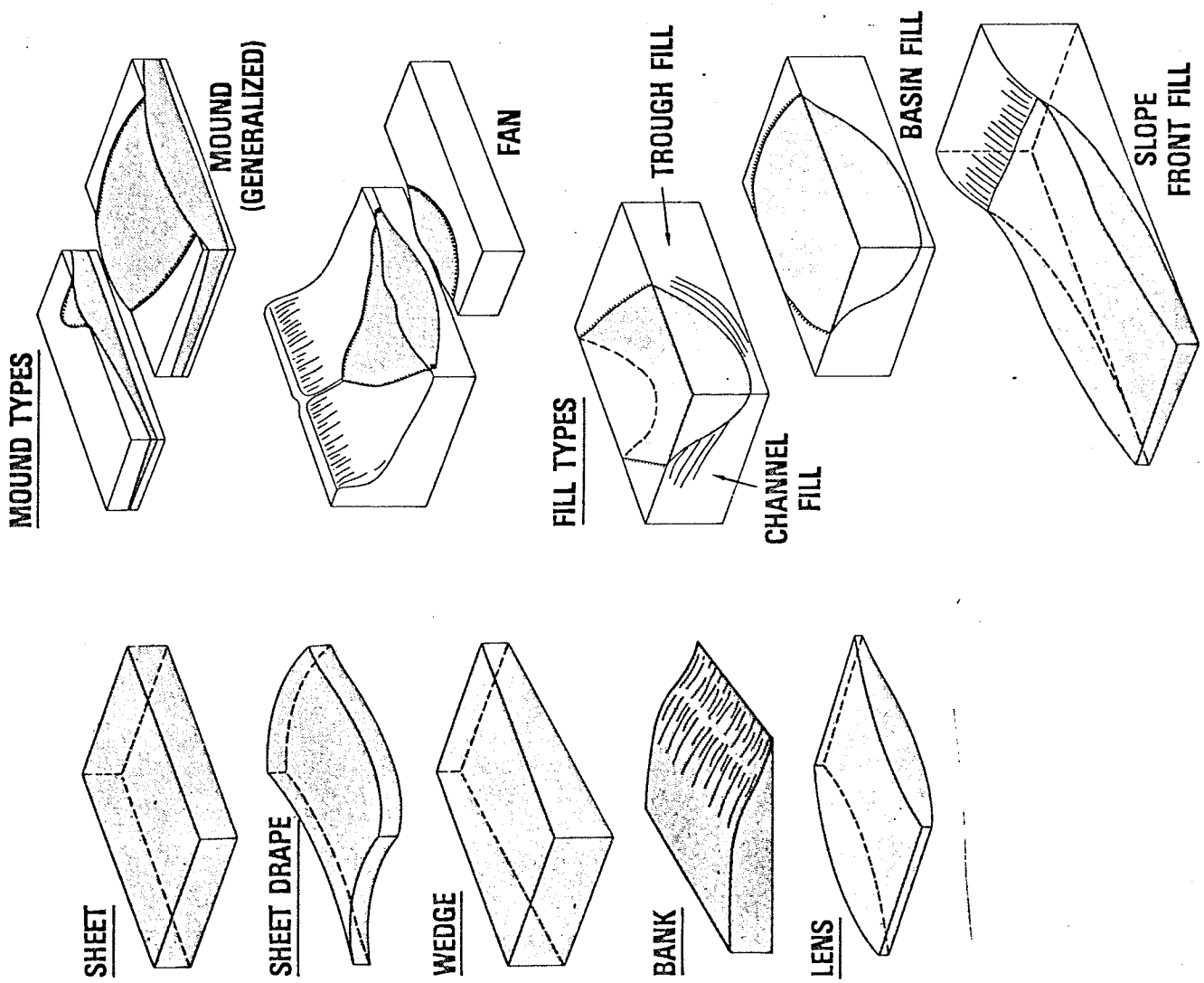

FIG. 12—External forms of some seismic facies units.

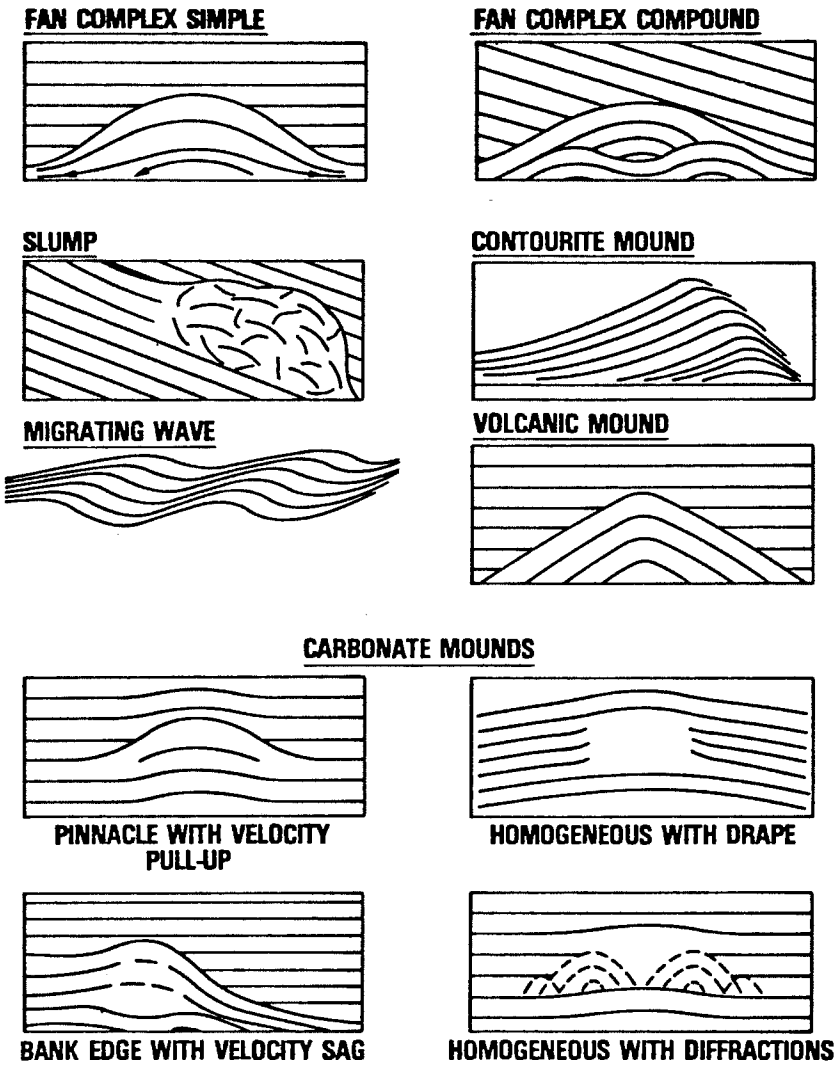

FIG. 13—Some mounded seismic facies units.

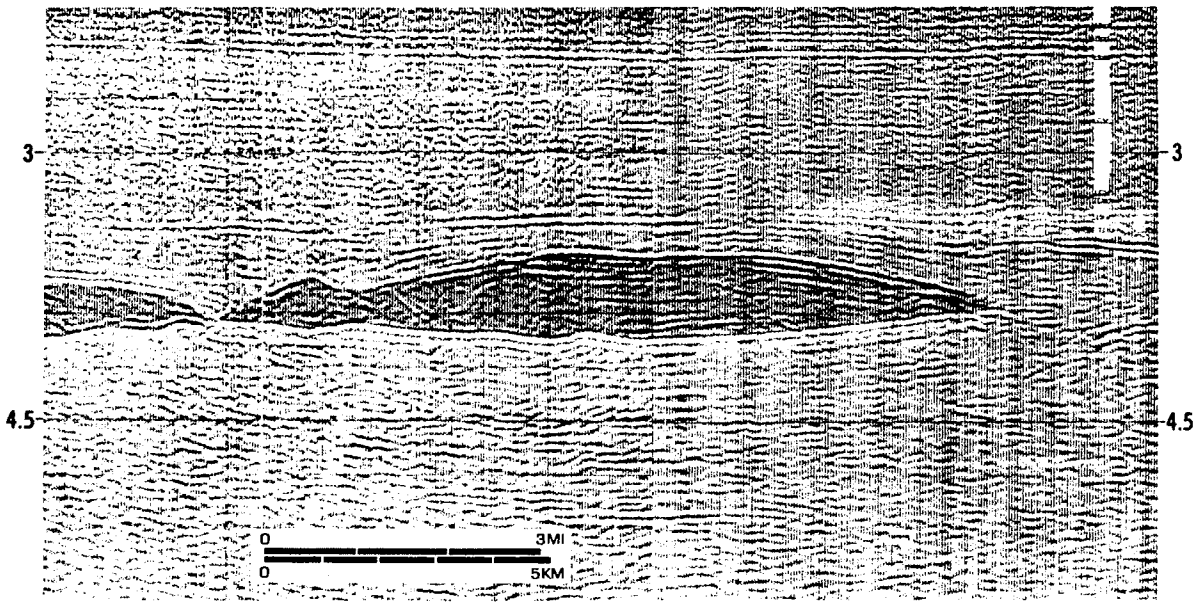

LENS SEISMIC FACIES UNIT – THIS FIGURE ILLUSTRATES A LARGE SALT LENS BASED ON WELL DATA WHICH IS CLEARLY DEFINED BY A HIGH AMPLITUDE REFLECTION.

Abbott 79

FIGURE 34

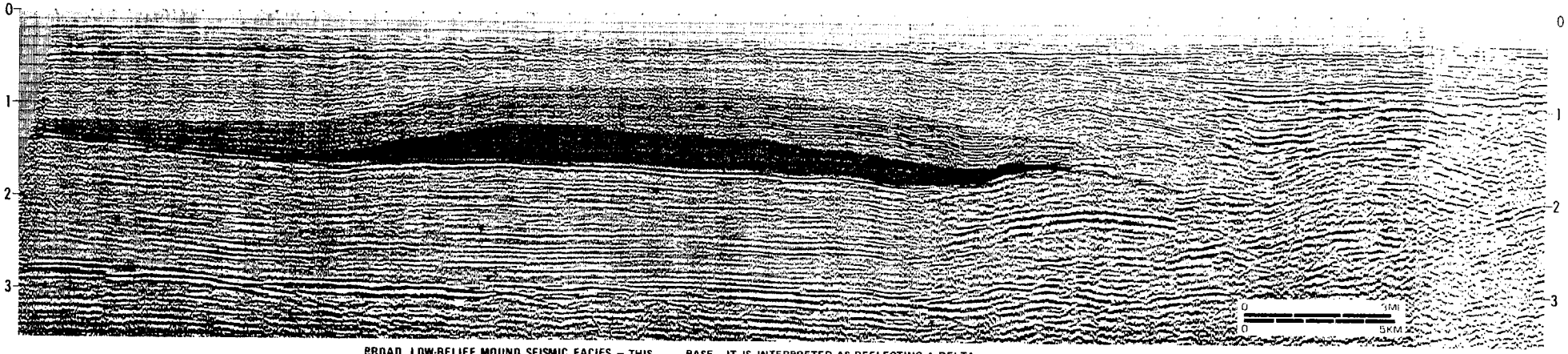

BROAD, LOW-RELIEF MOUND SEISMIC FACIES – THIS FIGURE ILLUSTRATES A MOUNDED EXTERNAL FORM WITH REFLECTIONS CONCORDANT AT THE TOP AND DOWNLAPPING IN OPPOSITE DIRECTIONS AT THE BASE. IT IS INTERPRETED AS REFLECTING A DELTA LOBE FORMED ON A SUBSIDING SHELF.

Abbott '79

FIGURE 23

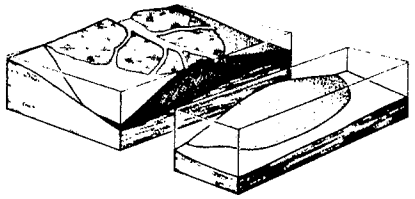

DELTA LOBE

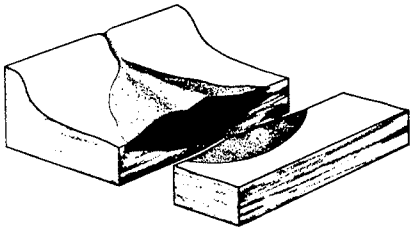

DEEP SEA FAN

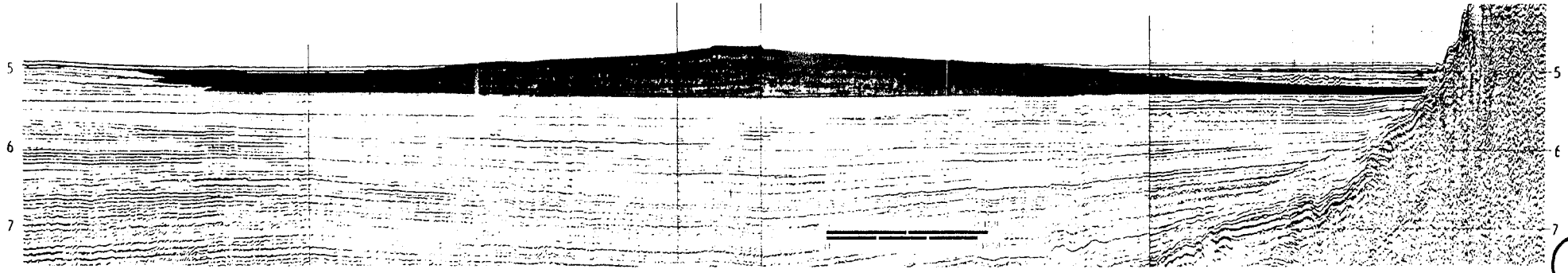

A VERY BROAD SYMMETRICAL LOW-RELIEF MOUND SEISMIC FACIES – THIS FIGURE ILLUSTRATES A CROSS-SECTION VIEW OF A LARGE DEEP SEA FAN NEAR MID-TO-OUTER FAN POSITION. IT IS CHARACTERIZED BY PARALLEL, HUMMOCKY, WAVY AND CHAOTIC REFLECTION CONFIGURATION PATTERNS TYPICAL OF A CHANNEL-LOBE COMPLEX. NOTE THE ONLAP OF THE OVERLYING STRATA WHICH FILLS IN AROUND THE MOUND. ALSO NOTE THE DEEP SEA ONLAP AND BUTTRESS SURFACE AGAINST OLDER ROCKS ON THE RIGHTHAND SIDE OF THE FIGURE.

Abbott 79

FIGURE 24

3) BANK CONFIGURATIONS

A BANK SEISMIC FACIES UNIT IS A UNIT WITH A BAN EXTERNAL FORM WITH A CLINOFORM OR "BANK-F LEADING EDGE THAT COMMONLY MARKS A SHELF BREAK.

Abbott 79

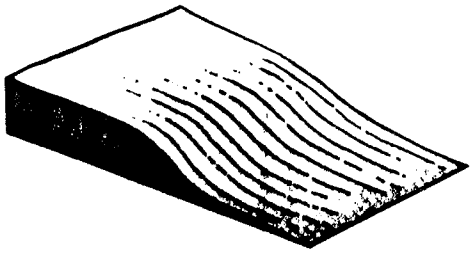

BANK

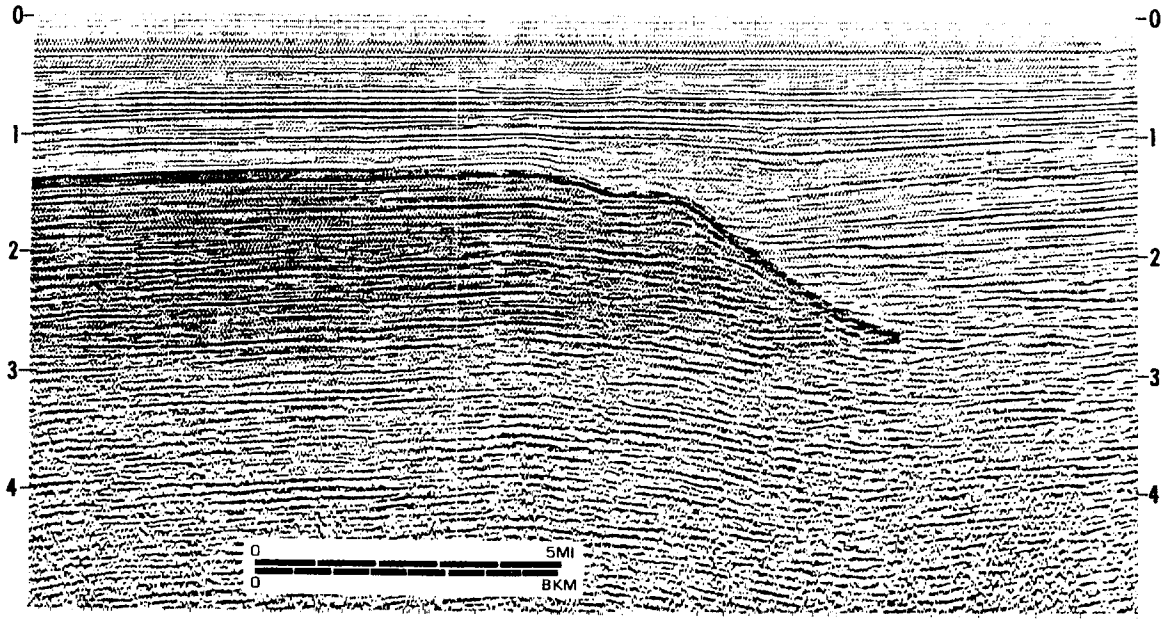

BANK SEISMIC FACIES UNIT – THIS FIGURE ILLUSTRATES A BANK EXTERNAL FORM WITH A WELL-DEFINED CLINOFORM MARKING THE SHELF-SLOPE, FROM THE ONLAPPING BASIN FILL.

FIGURE 31

MIGRATING WAVE

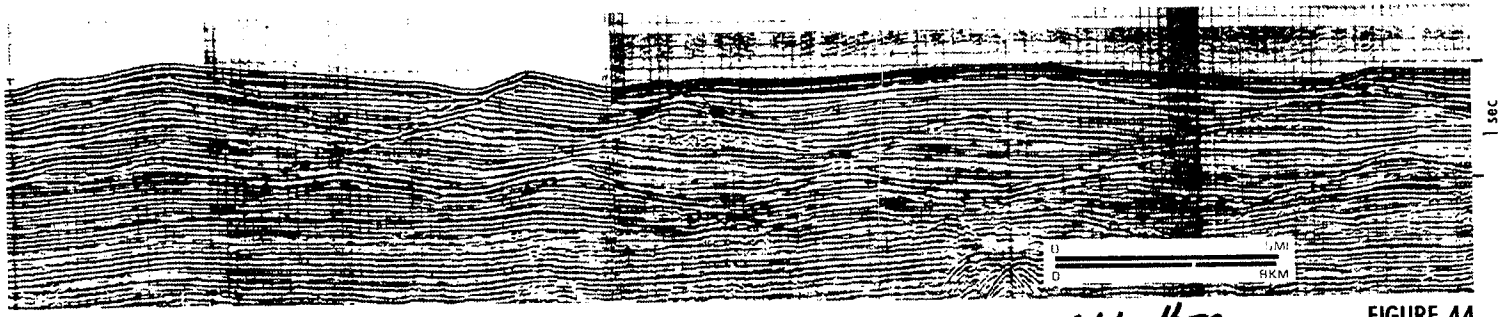

Abbott 79

FIGURE 44

208

2) FILL CONFIGURATIONS

Abbott '79

FILL CONFIGURATION PATTERNS ARE INTERPRETED AS STRATA FILLING NEGATIVE-RELIEF FEATURES IN THE UNDERLYING STRATA. THE INCISED OR UNDERLYING REFLECTIONS GENERALLY SHOW EROSIONAL TRUNCATION ALONG THE BASAL SURFACE OF THE FILL. FILL FORMS OR UNITS HAVE BEEN CLASSIFIED BY THEIR EXTERNAL FORM SUCH A CHANNEL FILL, TROUGH FILL, BASIN FILL OR SLOPE-FRONT FILL. THEY ALSO SHOW A VARIETY OF INTERNAL REFLECTION CONFIGURATIONS, SOME OF WHICH ARE ILLUSTRATED IN FIGURES 28 THROUGH 30.

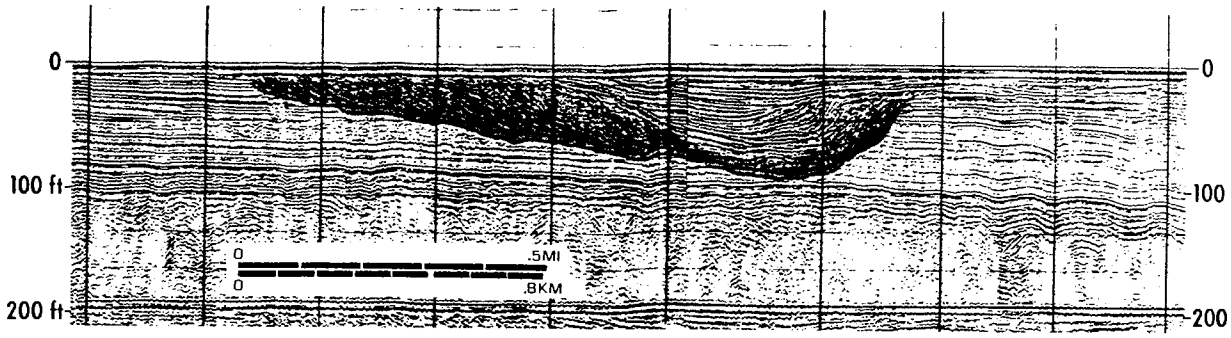

FILL SEISMIC REFLECTION CONFIGURATION – THIS FILL REFLECTION CONFIGURATION PATTERN IS INTERPRETED TO BE A DISTRIBUTARY CHANNEL COMPLEX INCISED INTO DELTA FRINGE SILTS AND CLAYS. THE DEPOSITIONAL CYCLE OCCURRING WITHIN THIS DISTRIBUTARY CHANNEL IS AN ACTIVE CHANNEL SEDIMENTATION PHASE AT THE BASE FOLLOWED BY AN ABANDONED CHANNEL FILL AT THE TOP. THE CHANNEL CONTACT IS SHARP (CONTINUOUS HIGH AMPLITUDE REFLECTION) AND EROSIONAL AGAINST THE ADJOINING "BED ROCK." SEDIMENTS ARE SAND IN THE BOTTOM OF THE CHANNEL AND IN THE PROGRADING CLINOFORM PATTERN ON THE LEFT. THE MIDDLE AND UPPER PART, WHICH REPRESENTS THE ABANDONED FILL STAGE, CONSISTS MAINLY OF THIN-BEDDED CLAY. THE ACOUSTIC RESPONSE FROM THE SAND IS A RANDOM, DISORGANIZED PATTERN SIMILAR TO A NOISE PATTERN. THE CLAY APPEARS TO CAUSE A SONIC RESPONSE WHICH IS MORE CONTINUOUS AND CRISP. THE FRINGE SILTS AND CLAY EVENTS REPRESENT FLAT-LYING STRATA THAT GENERALLY EXTEND ACROSS LONG SEGMENTS OF THE SPARKER LINE.

FROM KING, 1973. FIGURE 2

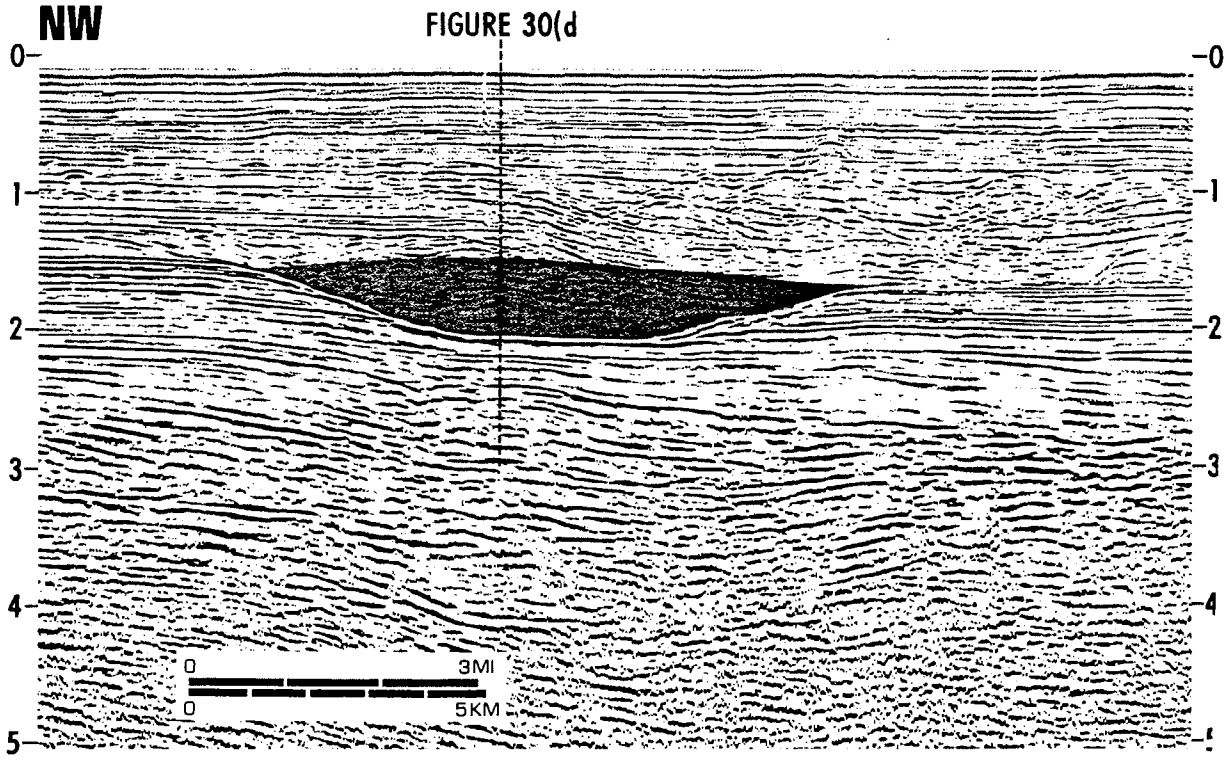

Abbott 79 FIGURE 30 (c)

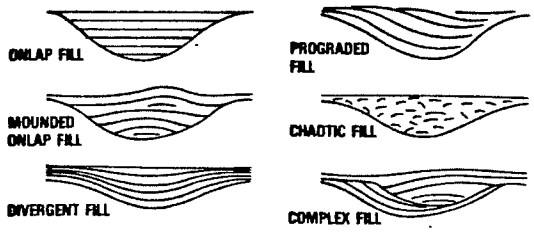

FIG. 15—Some fill seismic facies units.

Interpretation methodologies

Basic approaches to interpreting stratigraphic relations on 2-D lines have already been covered (e.g., recognizing onlap, downlap).

Now, we'll take a look at some of the issues concerning optimum stratigraphic interpretation of 3-D seismic data.

< STRATIGRAPHIC SEQUENCES ARE 3-D! >

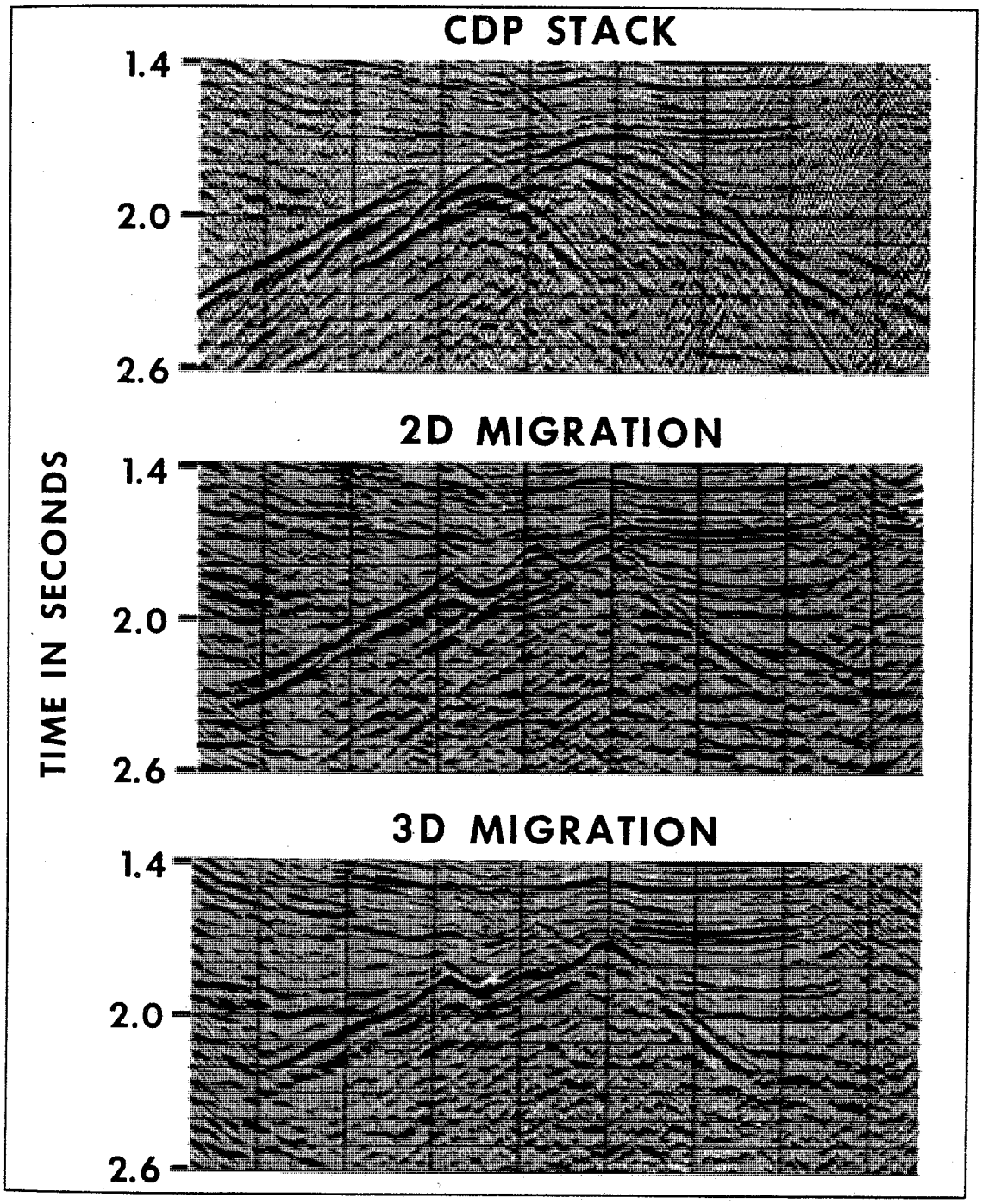

Fig. 1-9. Improved structural continuity of an unconformity reflection resulting from 2-D and 3-D migration.

Brown, 1999, AAPG Mem 42 (5th ed)

Fig. 1-15. Areal coverage of a 3-D survey compared to the coverage of a grid of five 2-D lines, and the ability of each to delineate a meandering channel.

Brown, 1999, AAPG Mem 42 (5th ed)

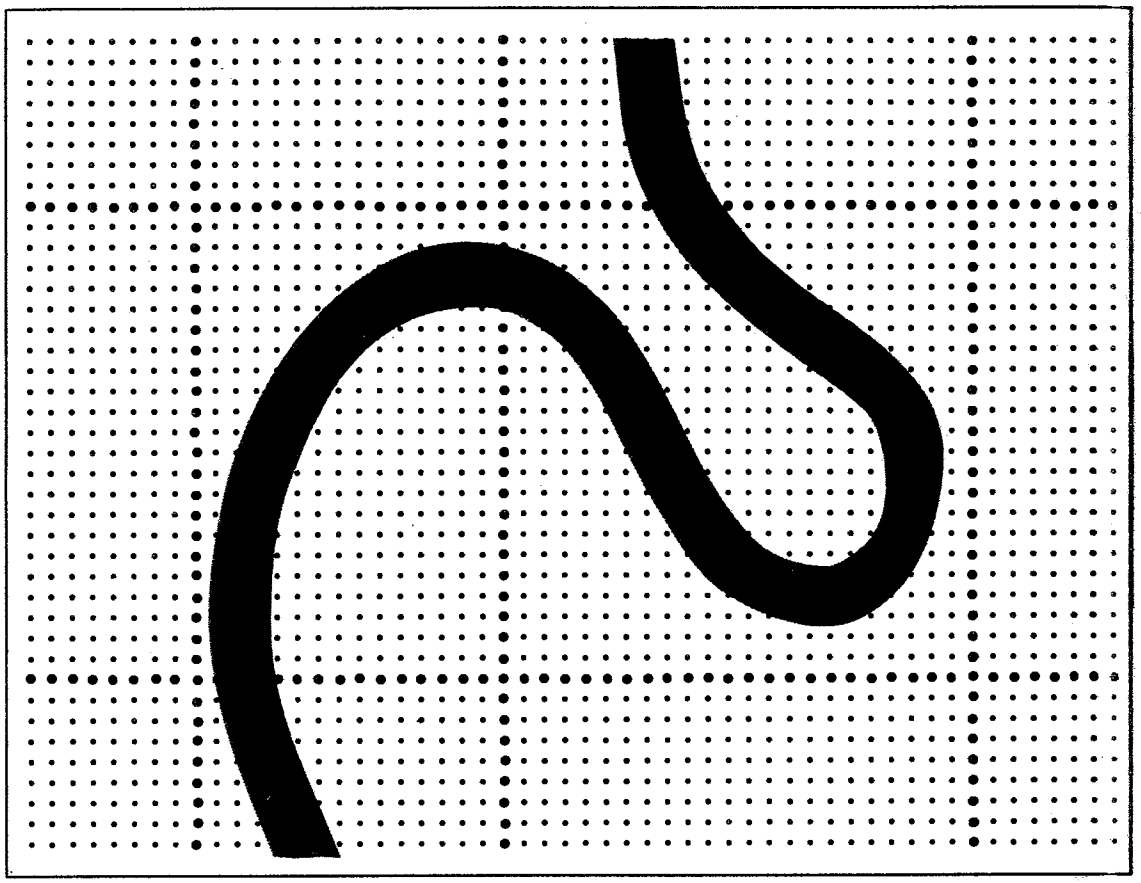

The challenge of identifying small strat features in vertical section, vs. the benefits of horizontal slices

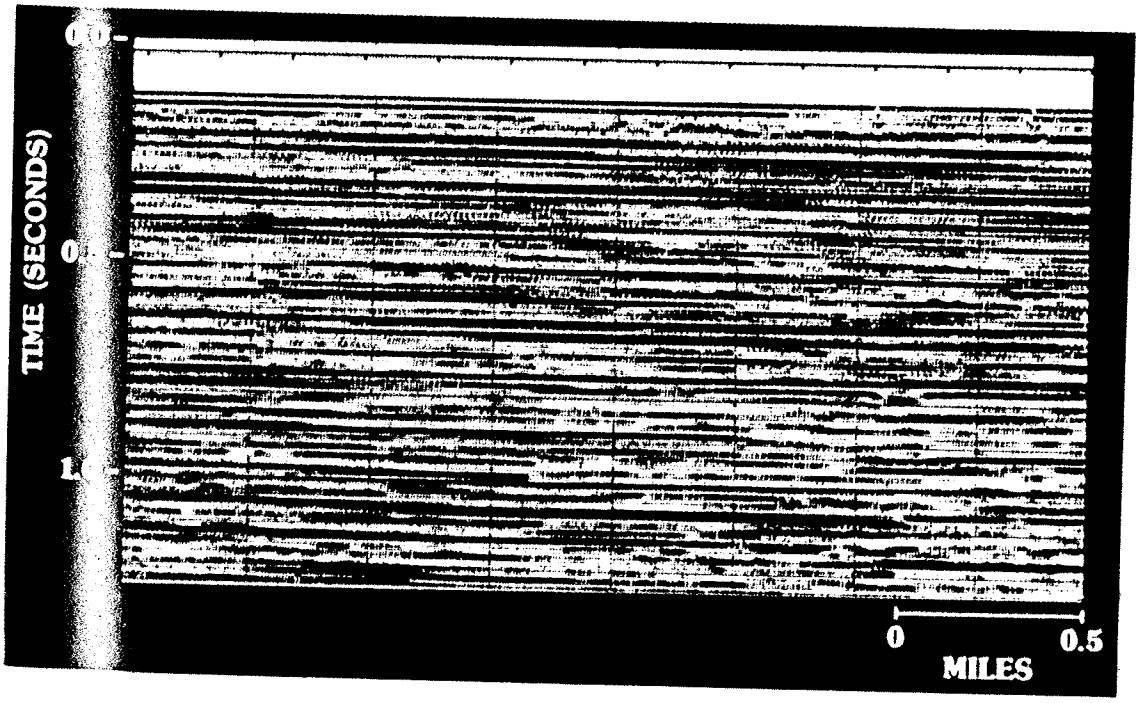

Fig. 4-21. Horizontal section from Matagorda Block 668, offshore Texas, showing prominent channel. It is a useful and interesting challenge to locate the channel intersection on the vertical section of Figure 4-22. (Courtesy ARCO Oil and Gas Company.)

Fig. 4-22. Vertical section from Matagorda Block 668, offshore Texas. (Courtesy ARCO Oil and Gas Company.)

Brown, 1999, AAPG Mem 42 (5th ed)

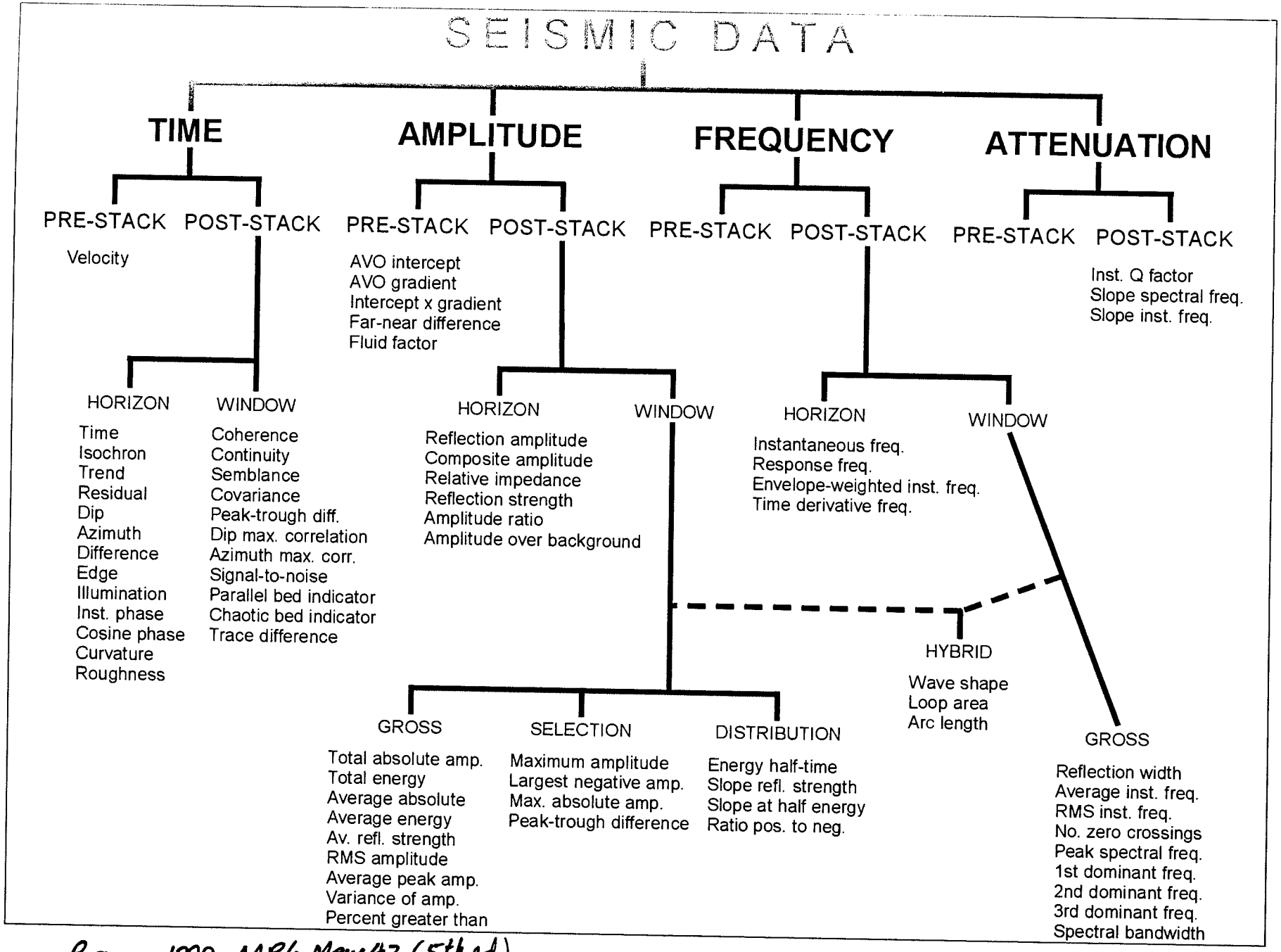

Brown, 1999, AAPG Mem 42 (5th ed)

Fig.8-1. Seismic attributes derived from or related to the basic seismic information of time, amplitude, frequency and attenuation. Window can be constant time interval, constant interval hung from one horizon or interval between two horizons.

3-D affords ability to choose among multiple attributes for best definition.

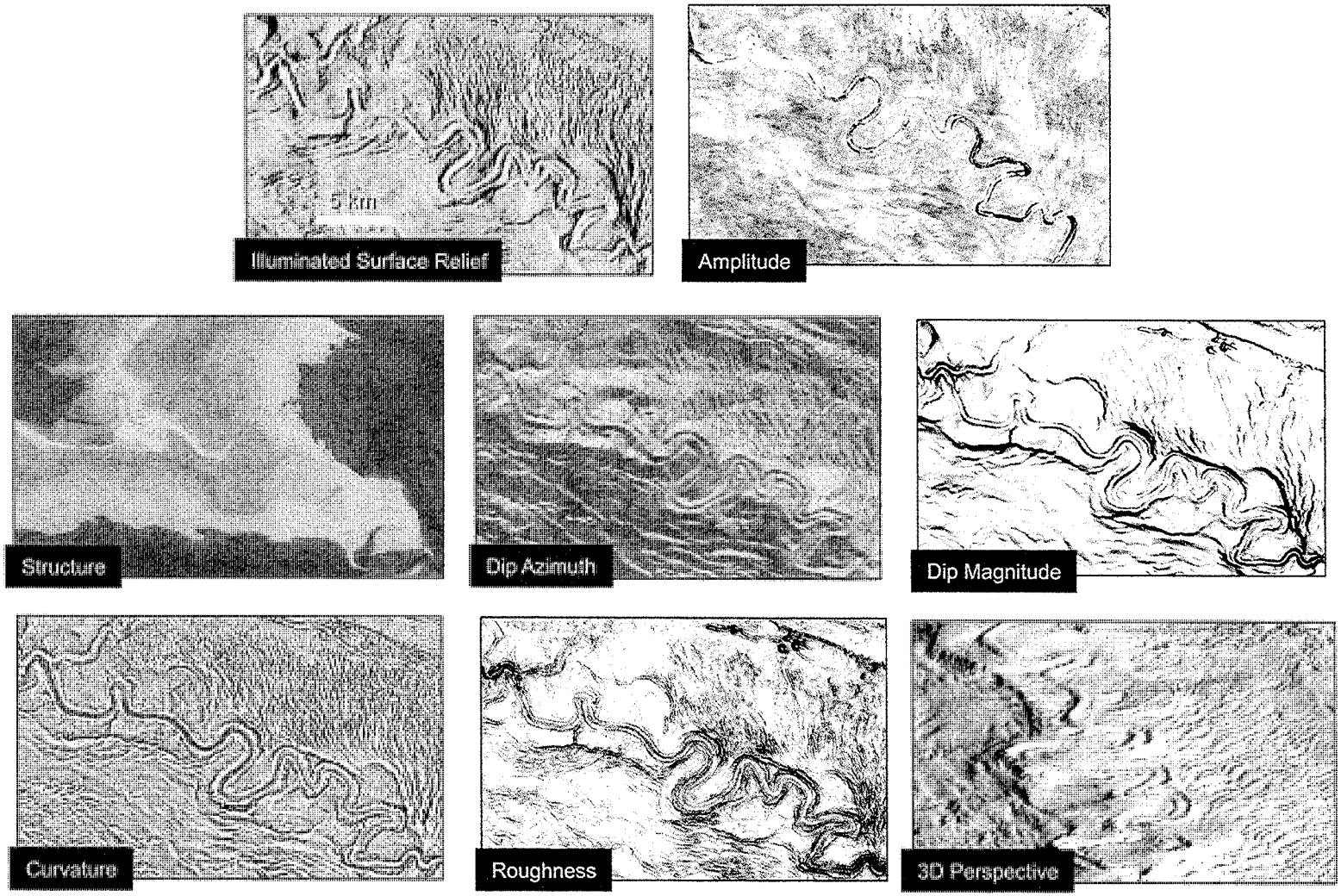

Fig. 11. Various horizon-based attributes extracted from the upper bounding surface of a deep-water turbidite channel, Gulf of Mexico. Each attribute affords the interpreter different and potentially valuable insights regarding depositional elements.

Posamentier et al, 2007

Fig. 8-30. Coherence time slice at 1250ms from Gulf of Mexico showing channels and faults (after Bahorich and Farmer, 1995). Note the channels indicated by the red arrows, how the channels are cut by faults, and also the point bars where one of the channels changes direction. (Courtesy Amoco Corporation. Data courtesy Geco-Prakla.)

Brown, 1999, AAPG Mem 42 (5th ed)

Fig. 8-31. Time slice at 1250ms from Gulf of Mexico for comparison with Figure 8-30 (after Bahorich and Farmer, 1995). (Courtesy Amoco Corporation. Data courtesy Geco-Prakla.)

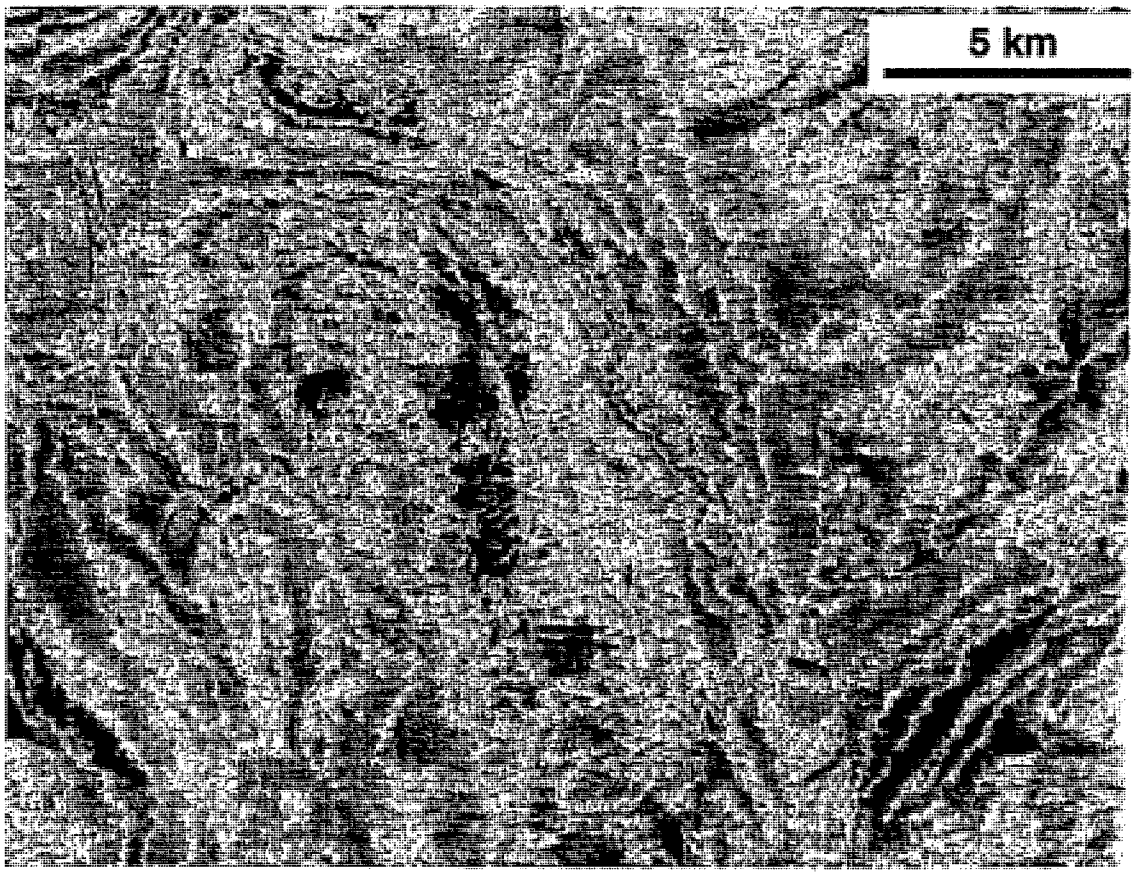

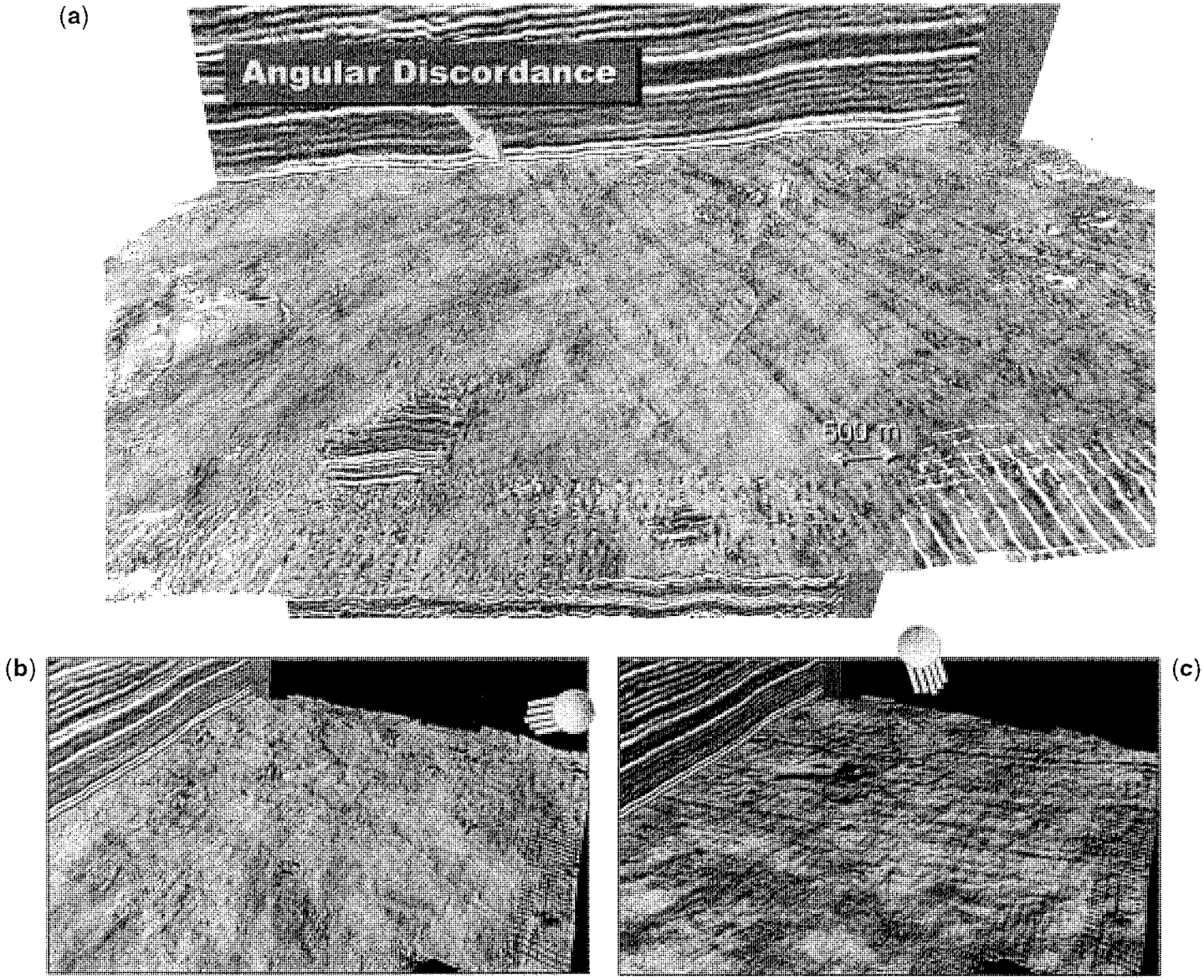

Fig. 3. (**a**) Illuminated unconformity surface in perspective view with channel and ridge-form erosional remnants (i.e. cuestas). (**b**) The same unconformity surface with lighting from the right – parallel to the trend of the ridge-form erosional remnants. (**c**) The unconformity surface with lighting from the top. Note that the ridge-form erosional remnants are far better visible when the lighting is orthogonal to the ridges.

Posamentier et al, 2007

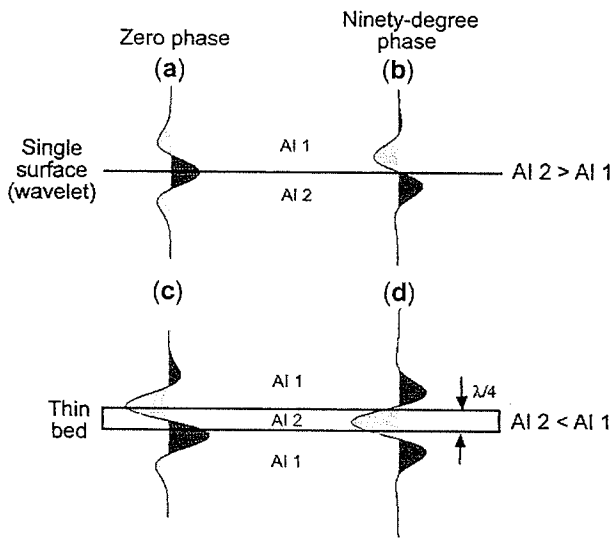

Fig. 3. Phase control of seismic waveform to a geological object. Corresponding to a (0° phase) Ricker wavelet, seismic reflection is symmetrical to a single surface (**a**), but is antisymmetrical to a seismically thin bed ($\lambda/4$ in this case, (**c**). In contrast, a 90° phase Ricker wavelet results in a reflection that is antisymmetrical to a single surface (**b**) but symmetrical to a thin bed (**d**). The 90° phase data are optimal for thin-bed lithological interpretation because the maximum amplitude (trough) points to the centre of the bed, seismic polarity approximates lithology, and stratigraphical resolution is higher (narrower side lobes).

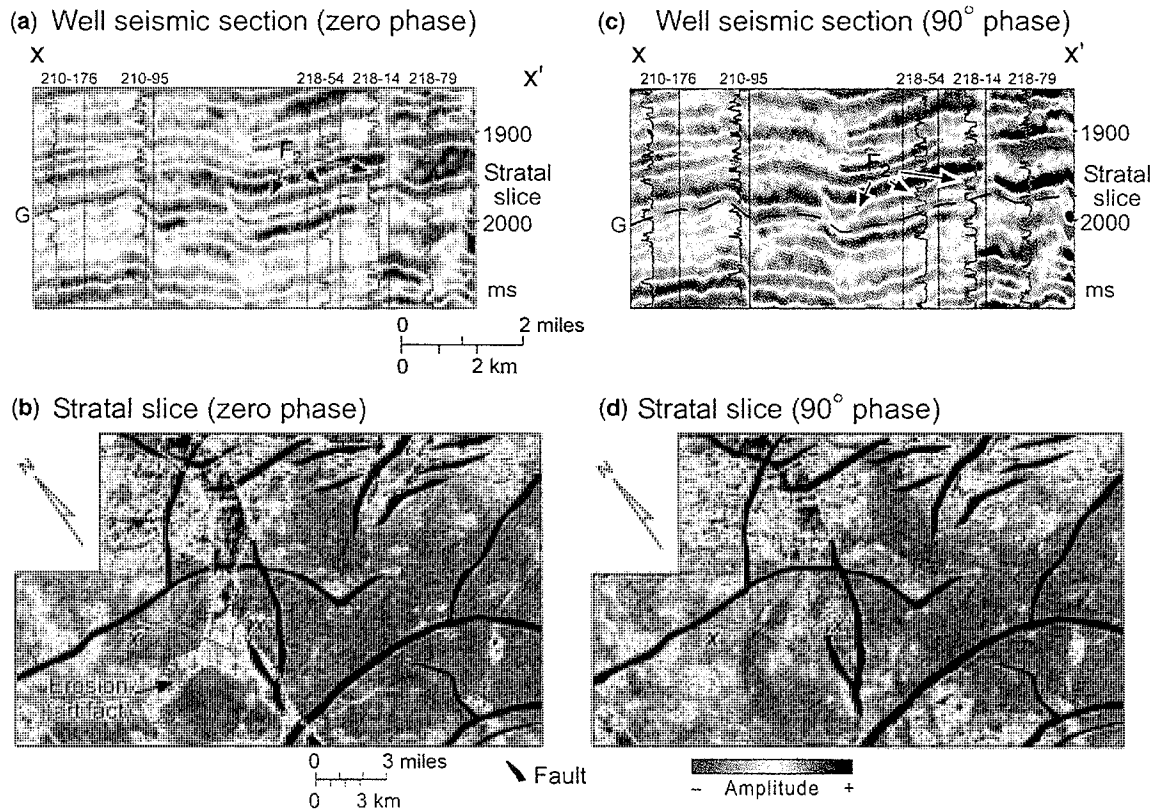

Fig. 4. Seismic interpretation example showing advantages of 90° phase seismic wavelets (modified from Zeng & Backus 2005*b*). (**a**) C_{clay} log section (X–X′) projected to zero-phase seismic data. Amplitude traces are not tied to lithology. A false, unconformable contact between the two sequences is visually apparent. (**b**) Stratal slice roughly following the seismic trough at upper G sandstone depicts a channel-like erosional feature wherever F_2 sandstone exists, creating an interpretive pitfall. (**c**) C_{clay} log section (X–X′) is tied to 90°-phase seismic data (red is sandstone; black is shale). The 'unconformable' contact observed in the zero-phase data disappears. (**d**) Stratal slice following seismic trough at the centre of G unit uncovers no seismic artefact.

Zeng, 2007

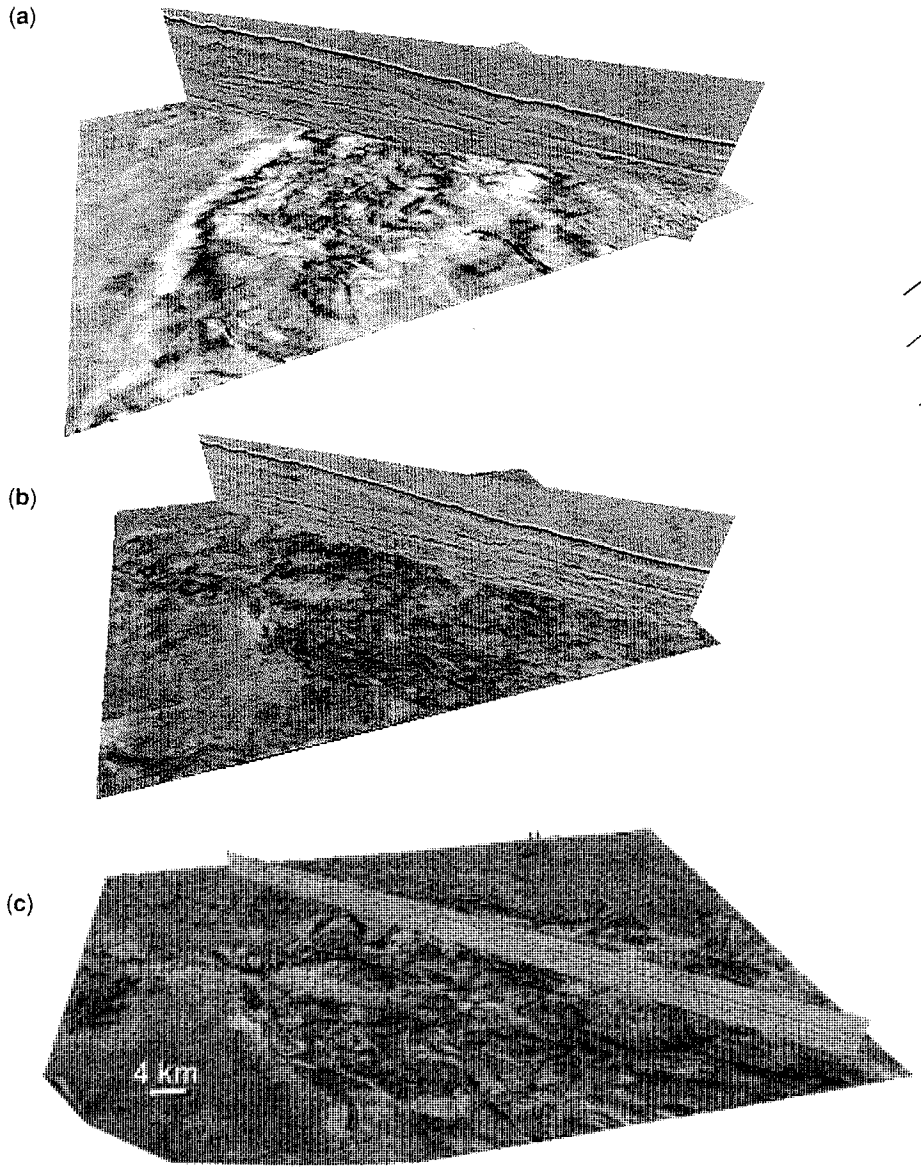

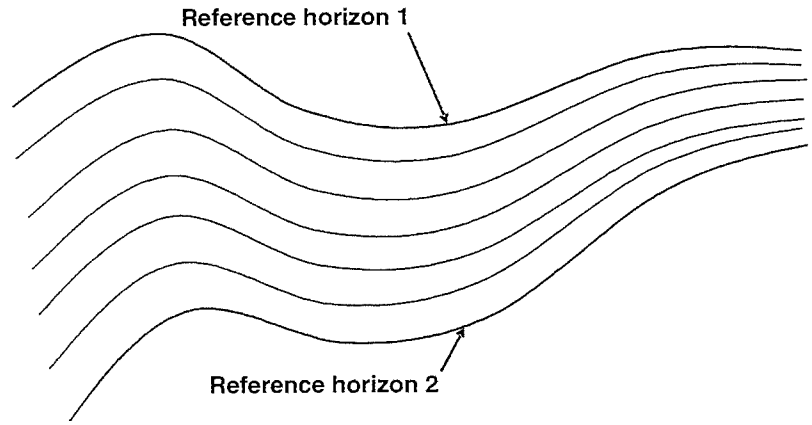

Posamentier et al, 2007

Fig. 5. (**a**) Seismic amplitude extraction along time slice through southeast-dipping reflections. Part of a frontal splay (i.e. lobe) turbidite system in the deep-water Gulf of Mexico is imaged. (**b**) Seismic amplitude extraction along dipping planar slice oriented approximately parallel to seismic reflections. More of the depositional system is imaged. (**c**) Seismic amplitude extraction along horizon-parallel slice, also referred to as horizon slice or stratal slice. This slice achieves the best possible image of the depositional system.

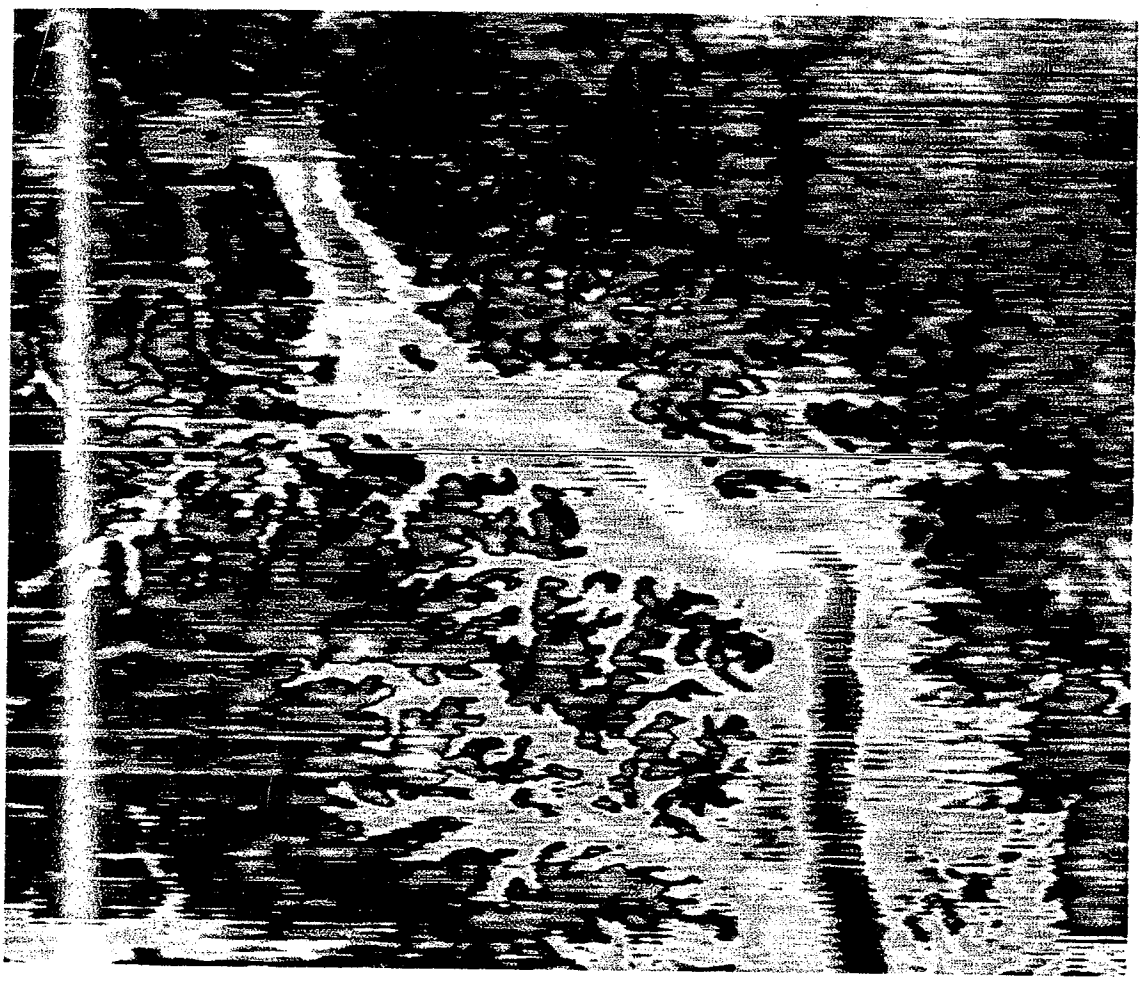

Fig. 4-19. Horizontal section at 104 ms from Nubi 3-D survey recorded in the Mahakam delta offshore Kalimantan, Indonesia. Note the dendritic patterns of incised canyons. (Courtesy Total Indonesie.)

Brown, 1999, AAPG Mem 47 (5th ed)

Note especially the fine detail of dendritic drainage pattern impossible to define on vertical sections.

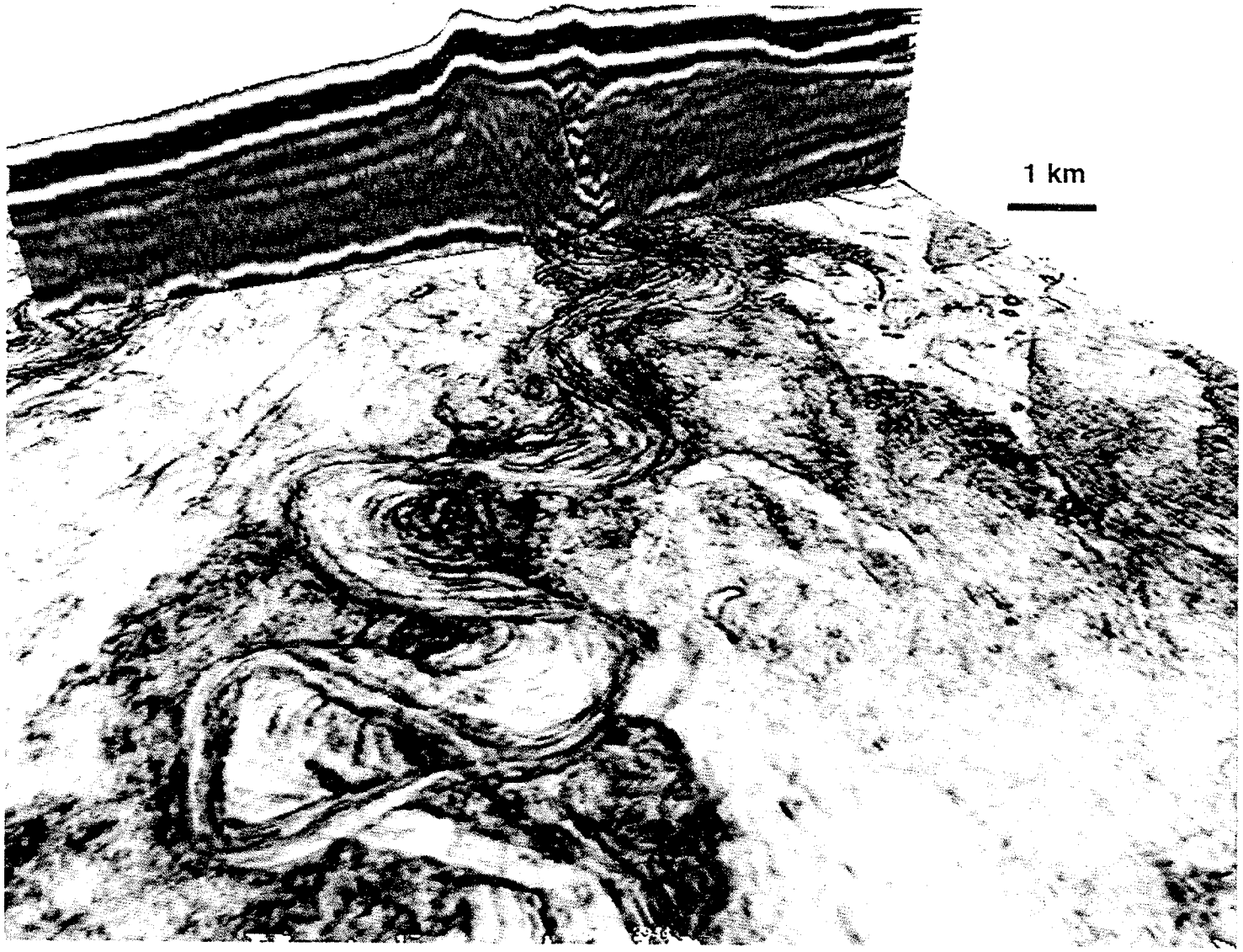

Fig. 14. Co-displayed coherence (in plan view, i.e. time slice) and reflection amplitude (in cross section view).

Posamentier et al, 2007

Calibration of 3-D images

Fig. 4-17. Horizontal section at 100 ms from Peciko 3-D survey recorded in the Mahakam delta offshore Kalimantan, Indonesia. The deltaic features seen here are about 18,000 years old. (Courtesy Total Indonesie.)

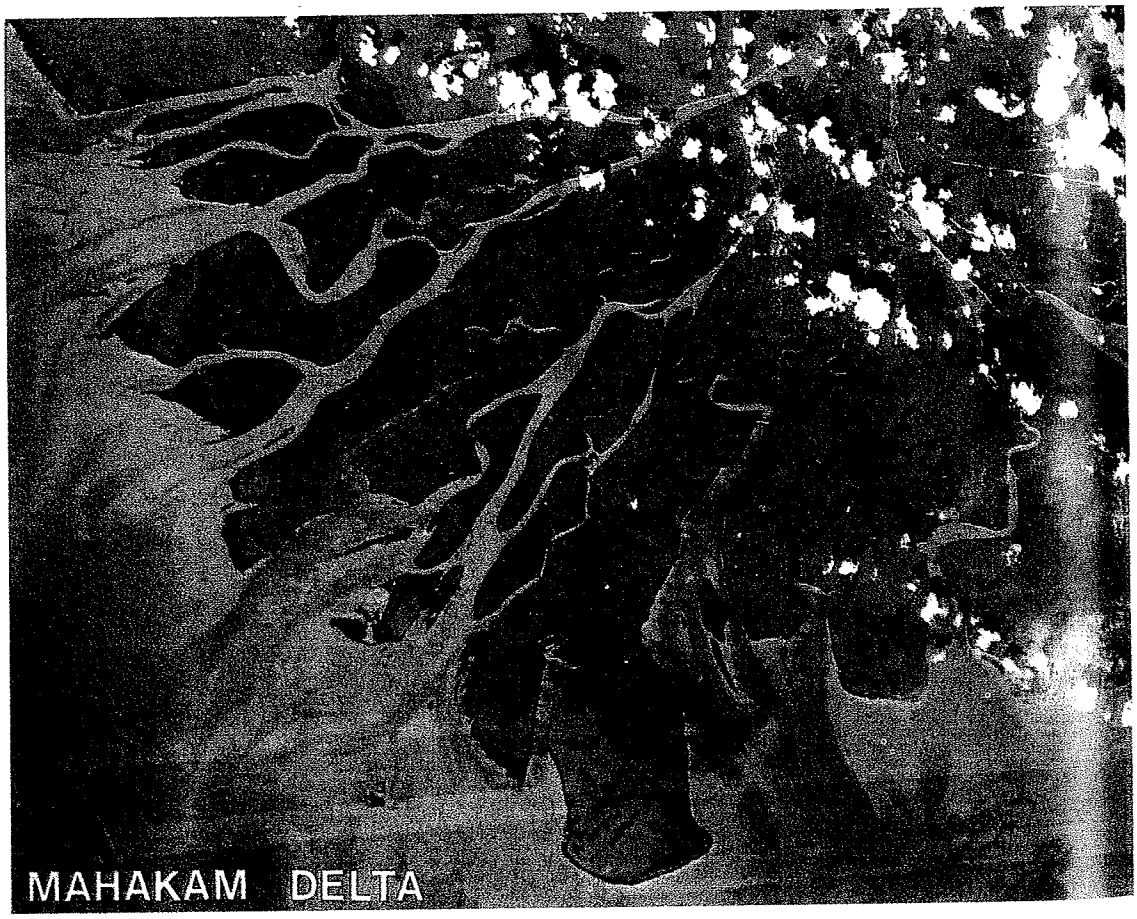

Fig. 4-18. Satellite photograph of part of present Mahakam delta for comparison with Figure 4-17. (Courtesy Total Indonesie.)

Seismic imaging of nonmarine, coastal and shallow marine settings

NONMARINE, COASTAL & SHELFAL DEPOSITIONAL SYSTEMS

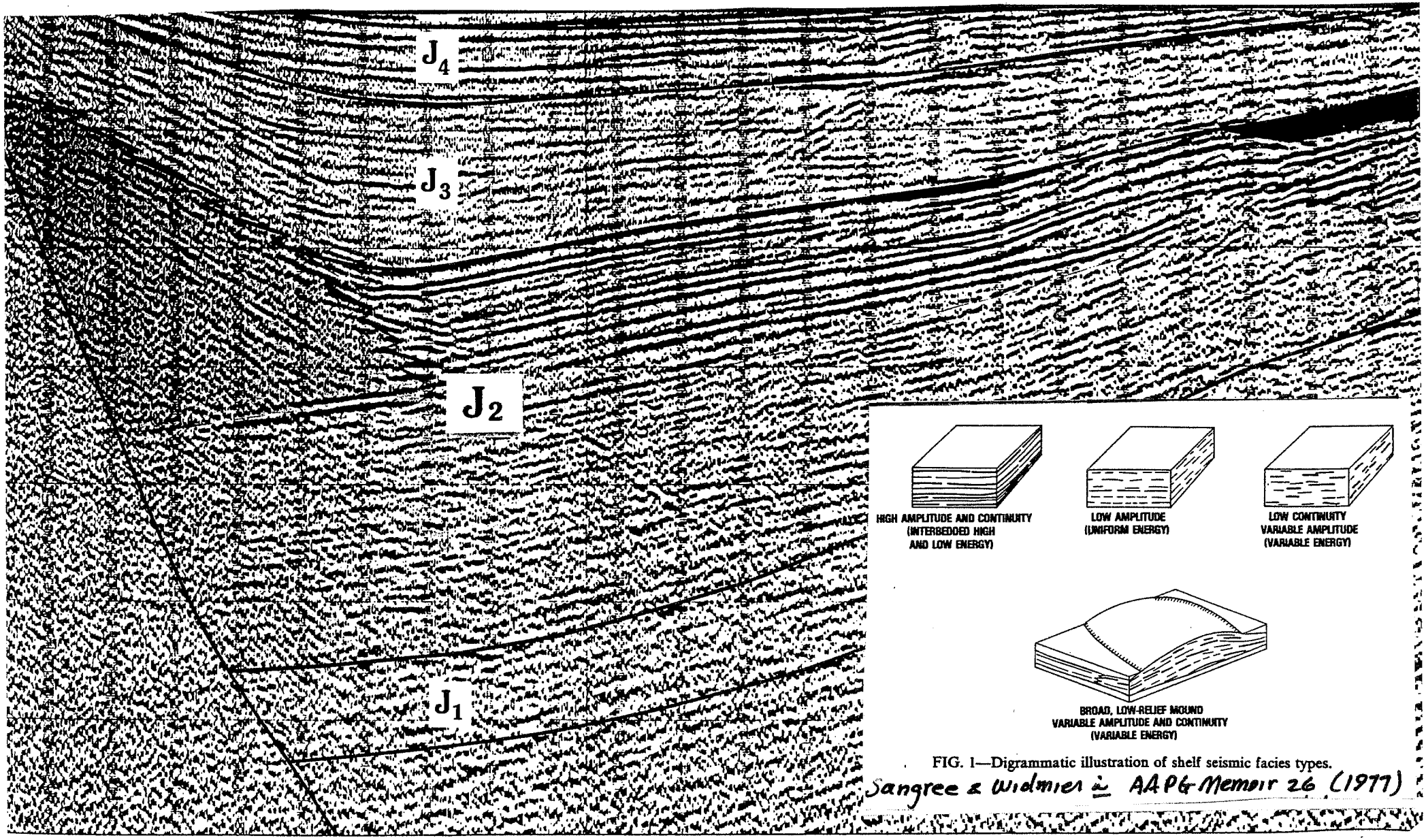

FIG. 1—Digrammatic illustration of shelf seismic facies types.

Sangree & Widmier in AAPG Memoir 26 (1977)

Hubbard etal 1985b

0 5

Reality checks from nonmarine, coastal, deltaic and shallow marine settings

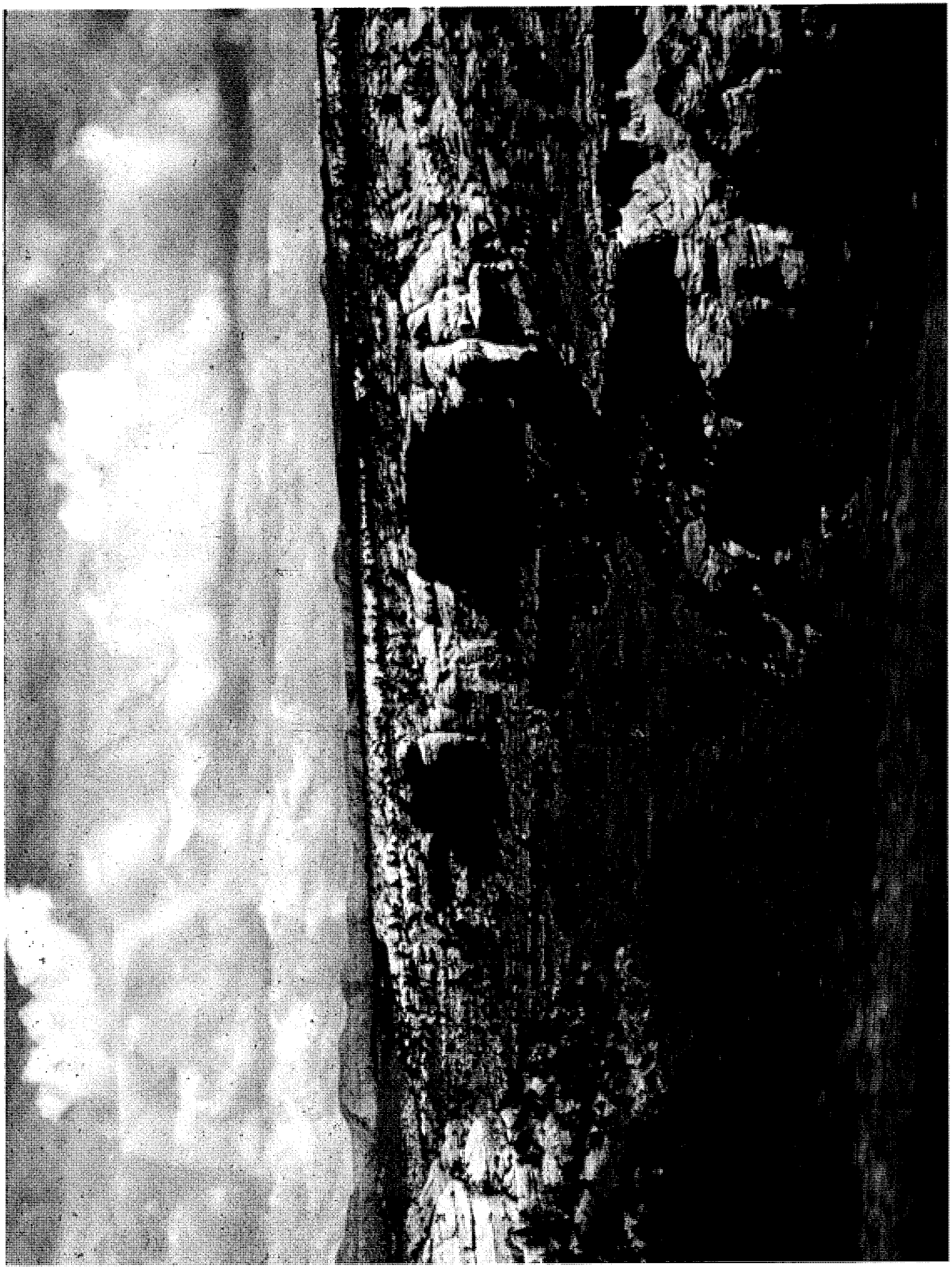

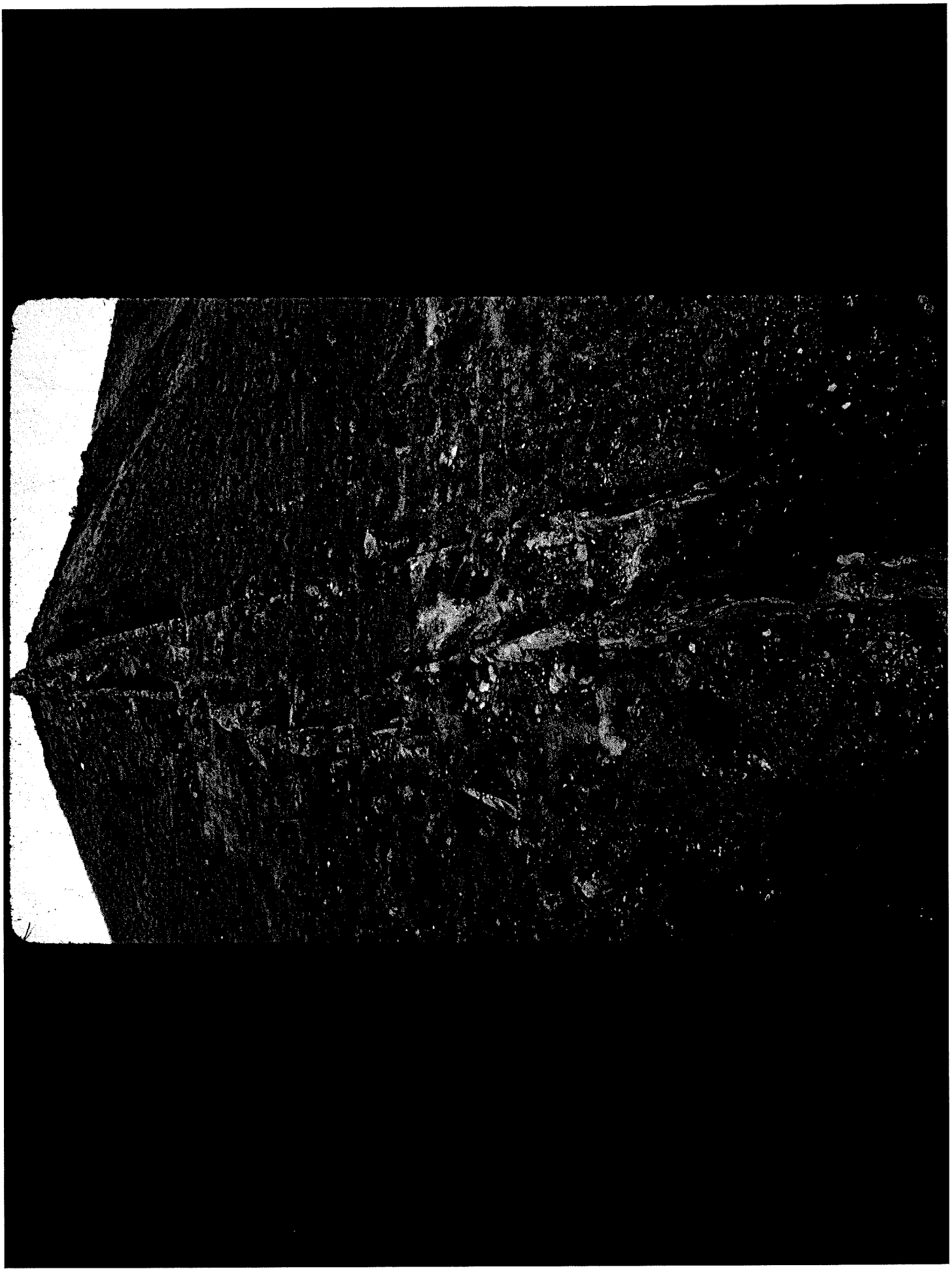

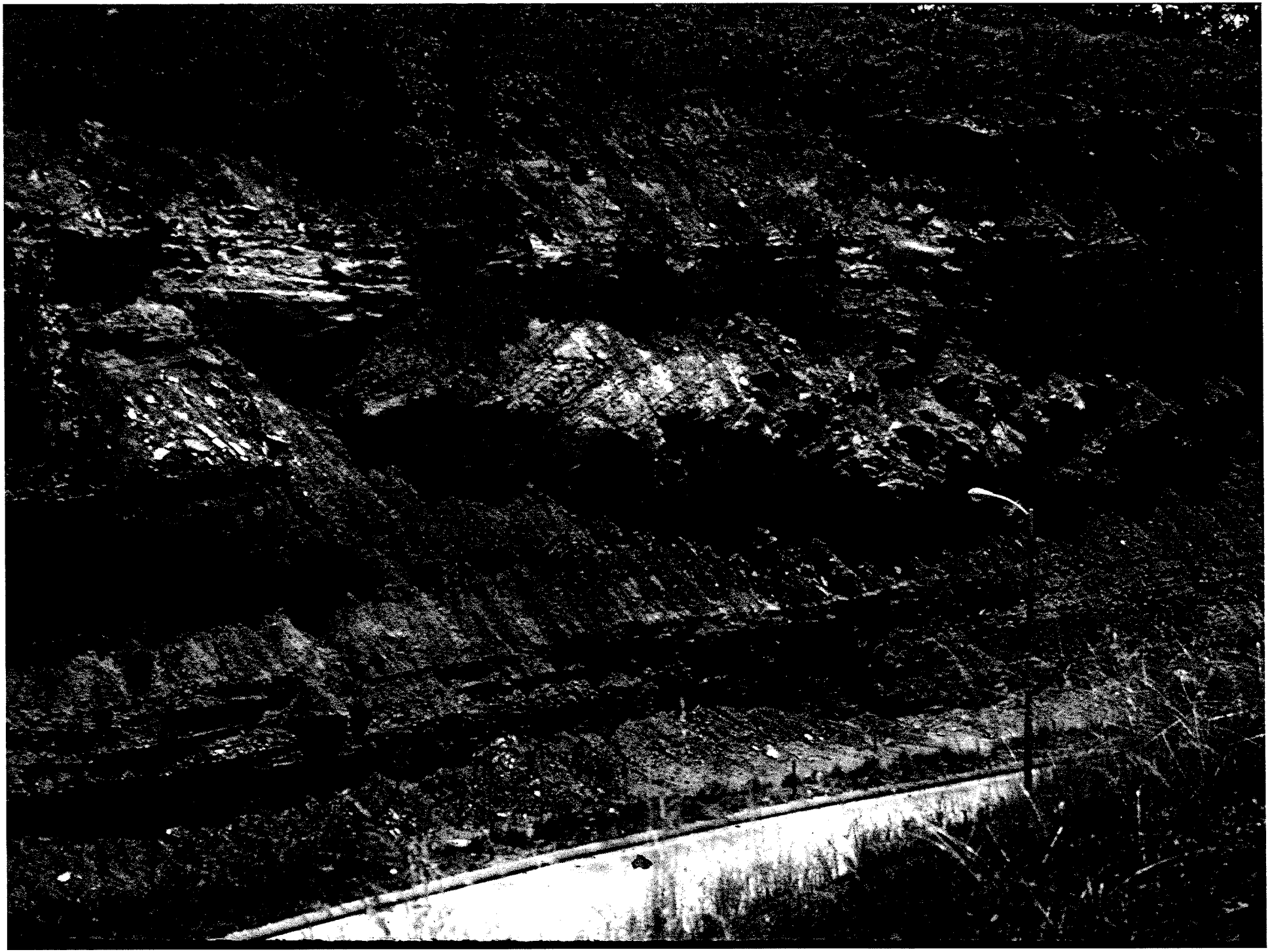

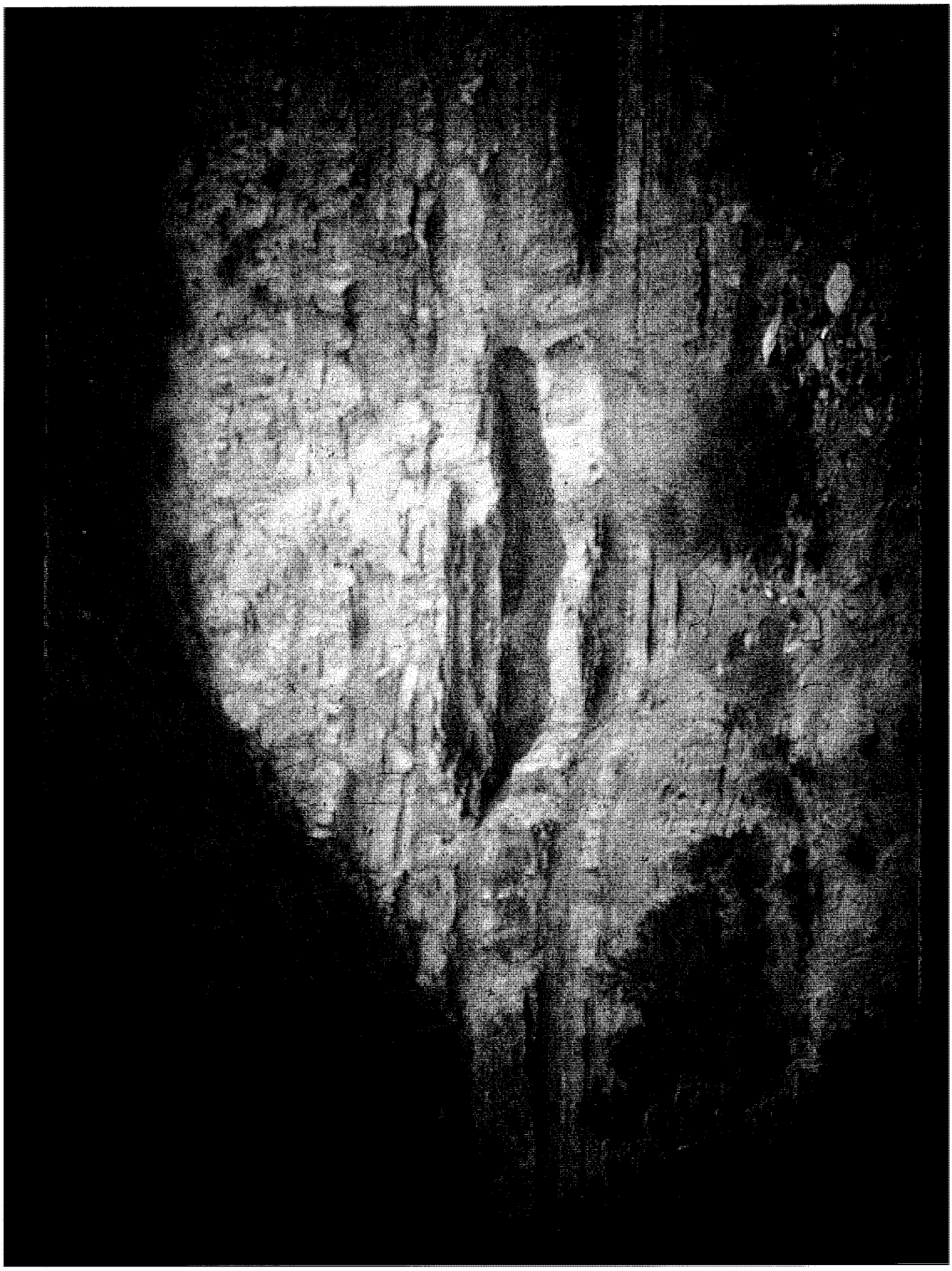

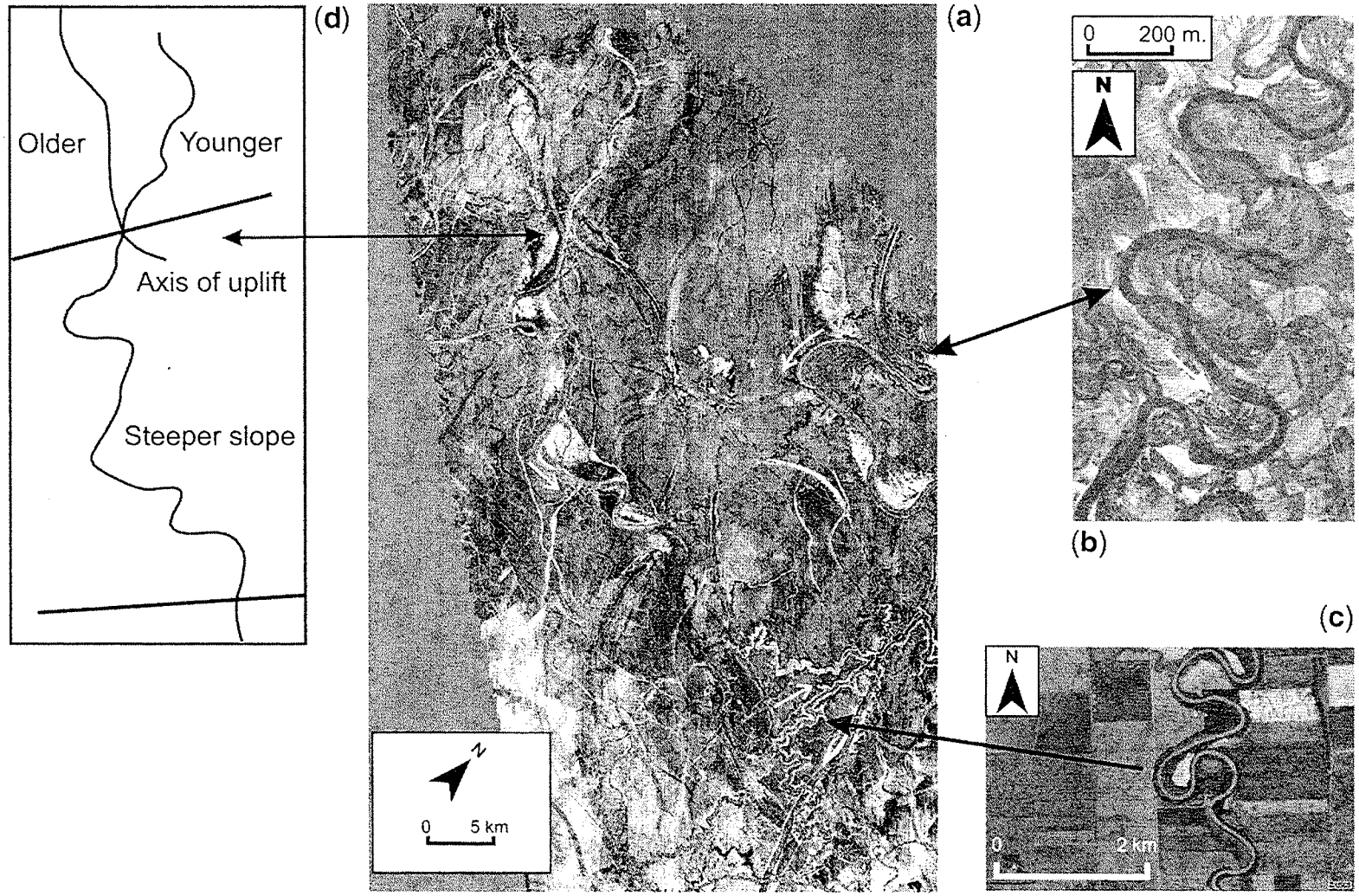

Fig. 15. (**a**) Seismic slice (Miall 2002, his fig. 3). (**b**) Comparison with similar, but smaller modern equiwidth stable, sinuous stream displaying scroll bar topography, Henry's Fork River, Idaho (modified from Brice 1982). (**c**) Comparison with similar, but smaller modern equiwidth, incised stream, Red River of northern Michigan (modified from Brice 1982). (**d**) Tracing of the large imaged channel that shows change from lower to higher sinuosity downstream and interpretation of possible palaeo-tectonic tilting.

Ethridge and Schumm, 2007

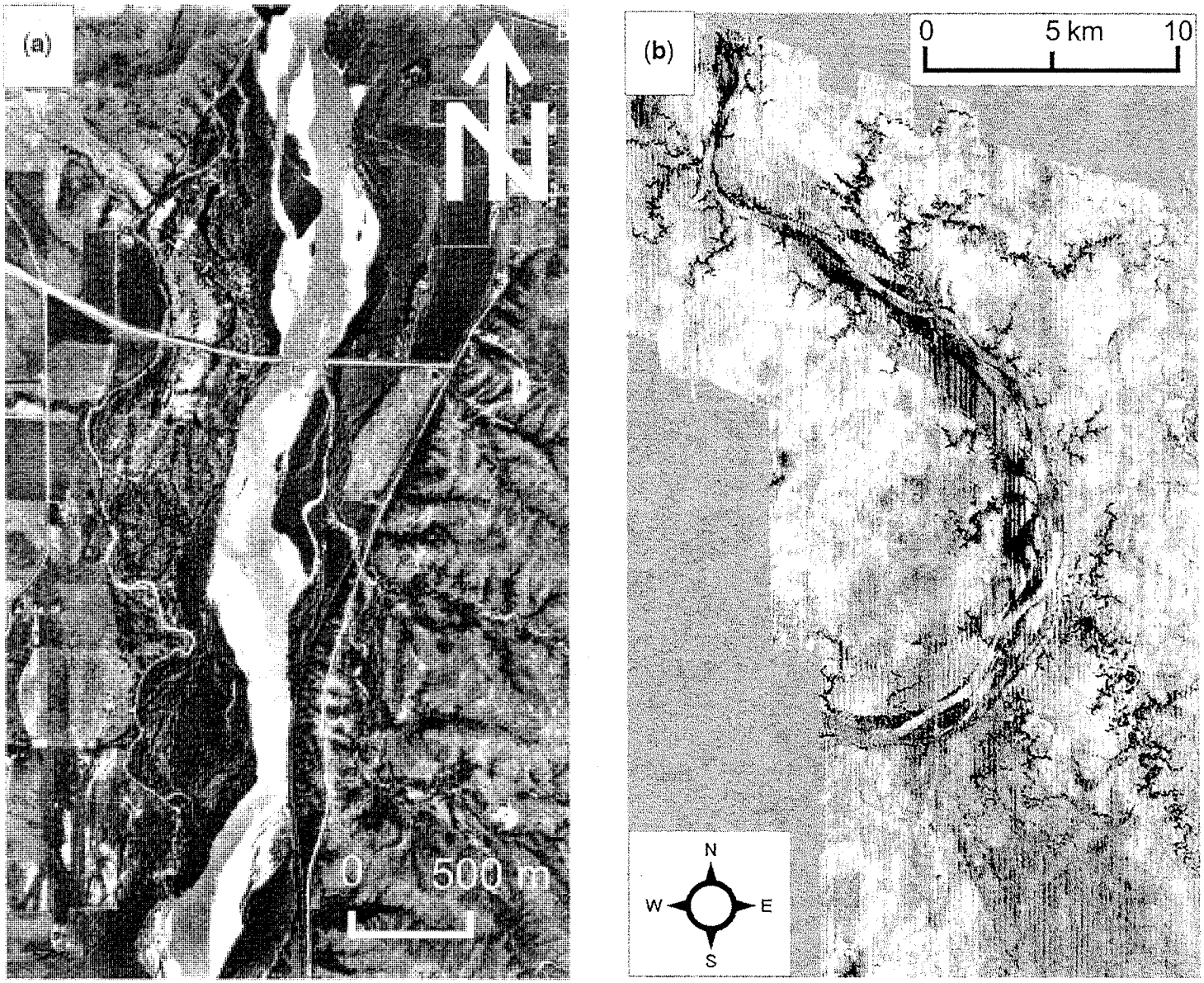

Fig. 13. (**a**) Modern Niobrara River, northeastern Nebraska showing small tributary drainages on interfluve. (**b**) An 84 ms time slice through 3D seismic volume, Java Sea Shelf, offshore NW Java (modified from Posamentier 2001). Note the same type of small tributary drainages on interfluves adjacent to the trunk incised valley.

Ethridge and Schumm, 2007

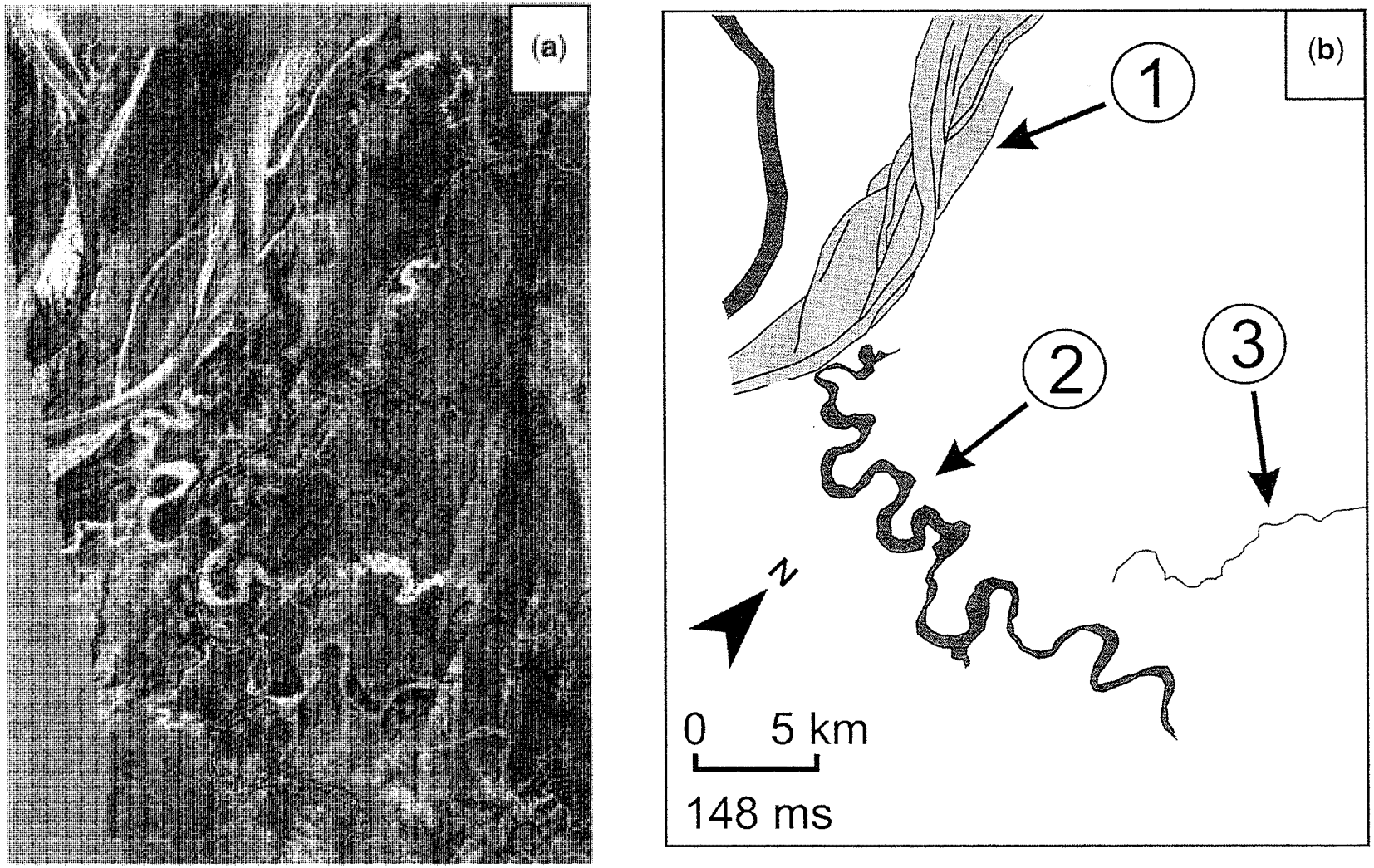

Fig. 14. (**a**) Seismic image showing a portion of the 148 ms slice from Pleistocene deposits in the Malay basin, Gulf of Thailand (Miall 2002). (**b**) Interpreted channels in the portion of 148 ms seismic image shown in (a). The base of the large braided river in the NW corner is interpreted to mark a sequence boundary within the succession (modified from Miall 2002; his fig 8). Numbers 1–3 refer to interpretations discussed in text (seismic slice provided by A. Miall).

Ethridge and Schumm, 2007

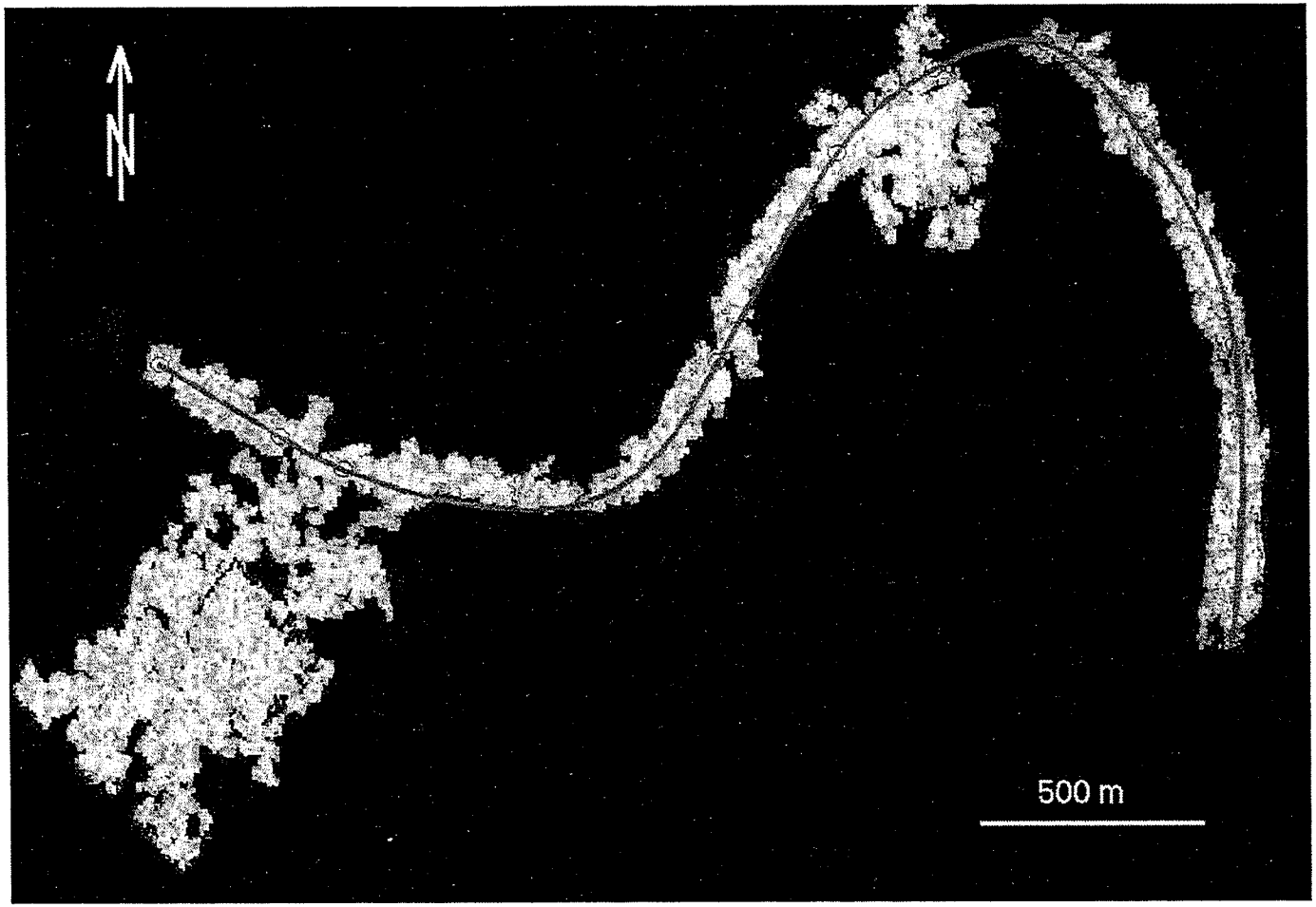

Fig. 4. Plan view of a channel with possible crevasse splays (left and top) extracted with the voxel-growing method.

Rabelo et al, 2007

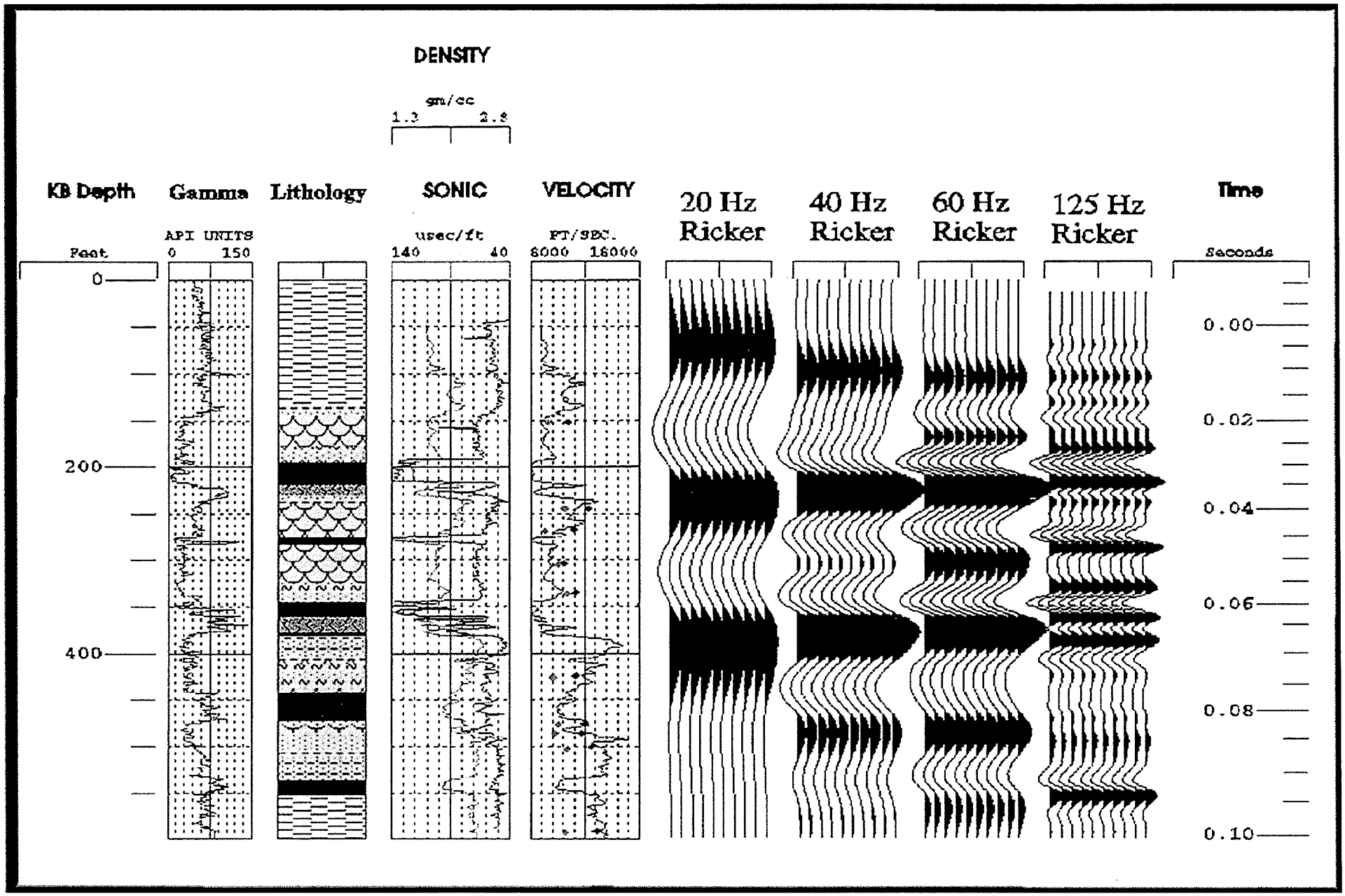

Courtesy of Richard Moiola

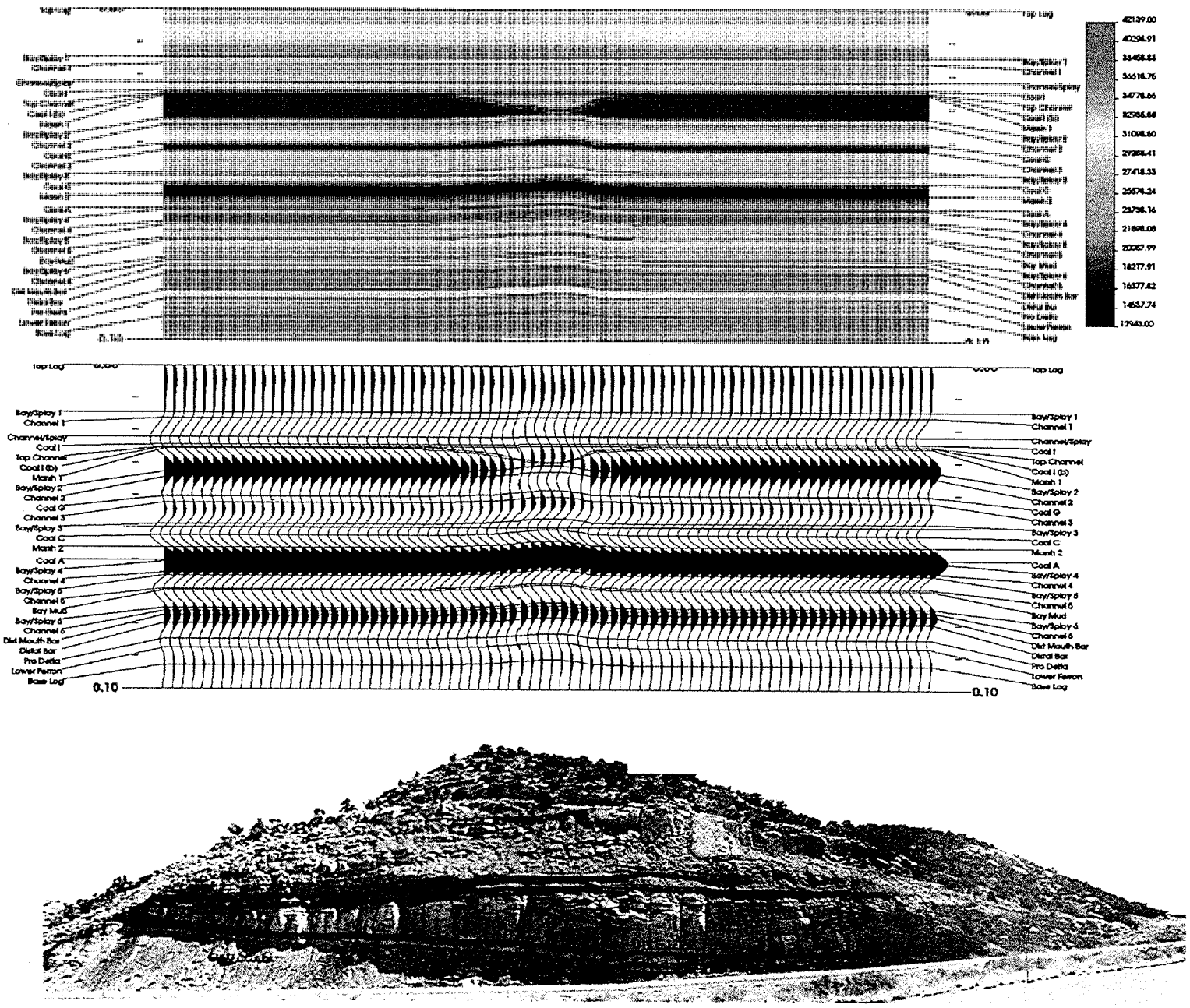

Courtesy of Richard Moiola

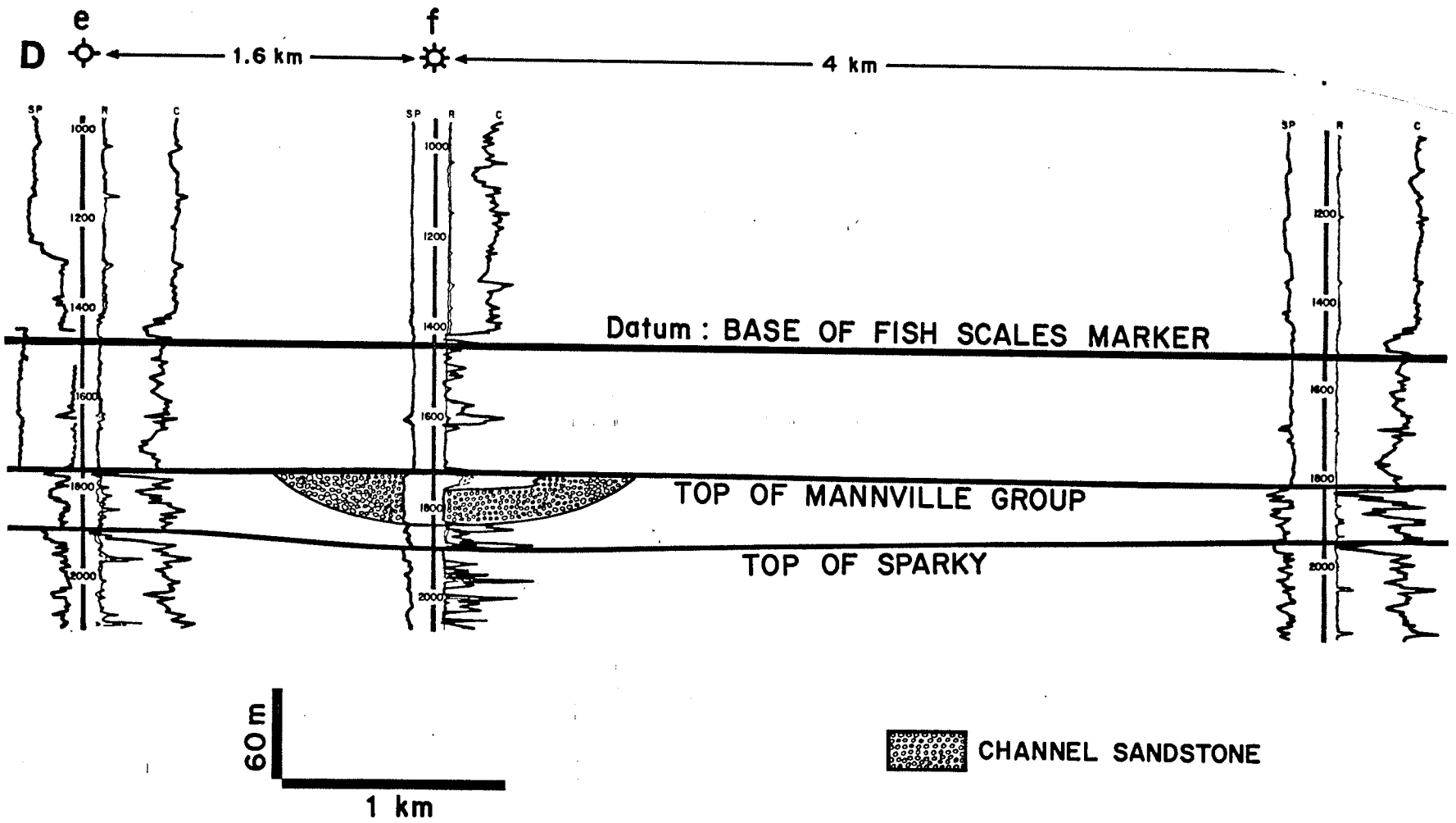

FIG. 7—Stratigraphic cross section oriented along seismic line shown in Figure 6 (modified after Putnam and Oliver, 1980).

Peter E. Putnam
AAPG Bull April 82

218

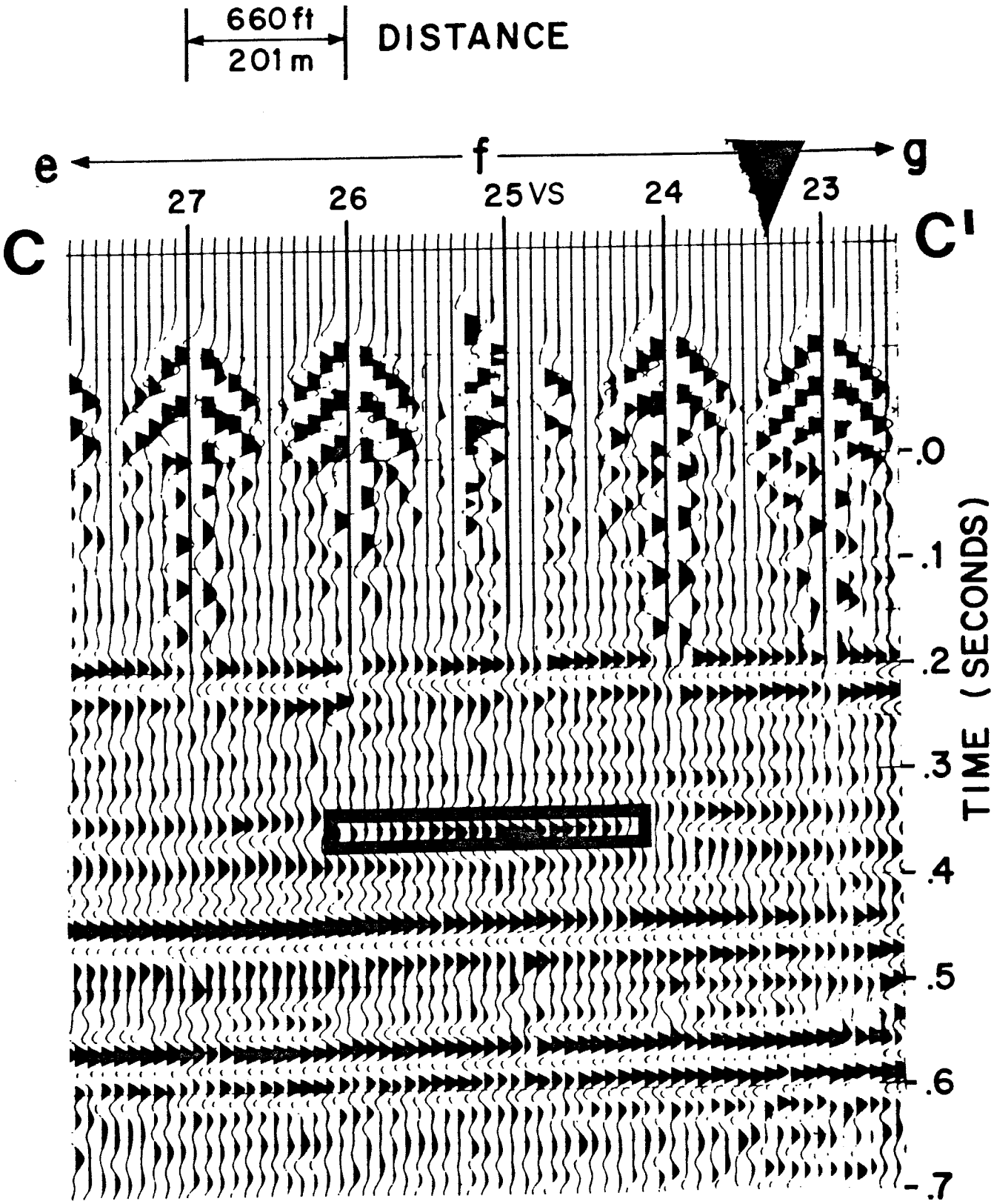

FIG. 6—Seismic section showing "bright spot" oriented across channel sandstone in east-central Alberta (from Putnam and Oliver, 1980).

Conventional 'Vibroseis' Data

Erosional Unconformity, River Channel
W.L. Chapman
conoco

Energy Source: Vibroseis ®
Stacking Multiplicity: 24
Number of Channels Recorded: 48
Interval between Input Channels: 220'
Minimum Offset Distance: 880'
Maximum Offset Distance: 5940'
Static Corrections: Adaptive & Elevation
Deconvolution: 11-55 Hz
Frequency Filtering: 11-58 Hz
Other:
Migration: No
Source of Velocities for Processing: Data Derived

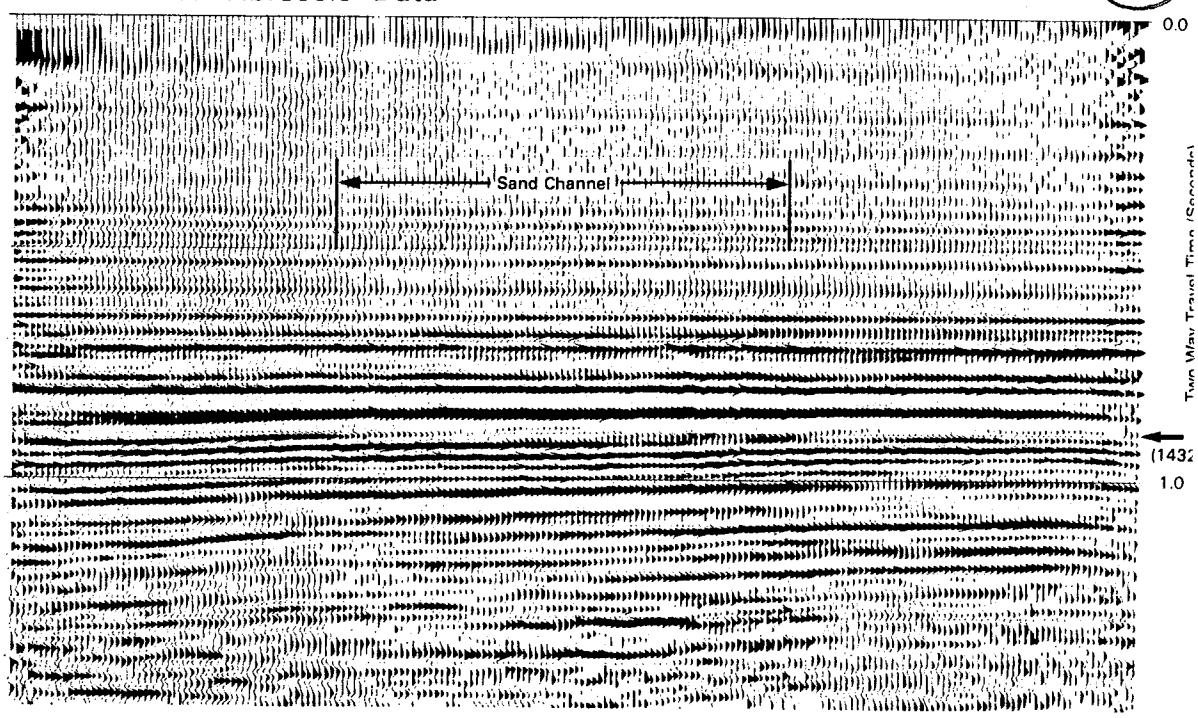

Figure 1

One Kilometer

One Mile

Bally 1.2.1-31

Time Section

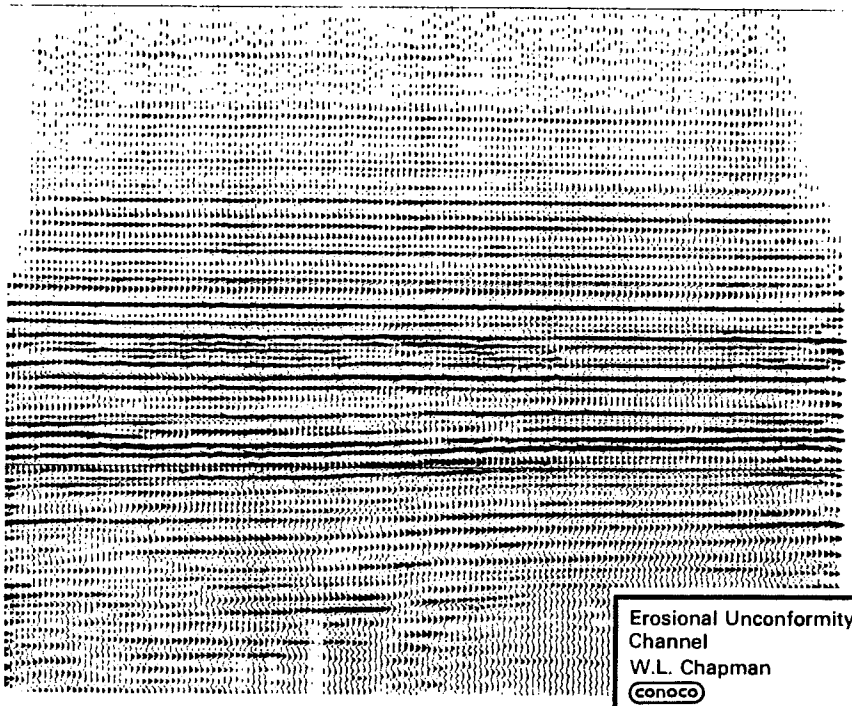

Figure 2

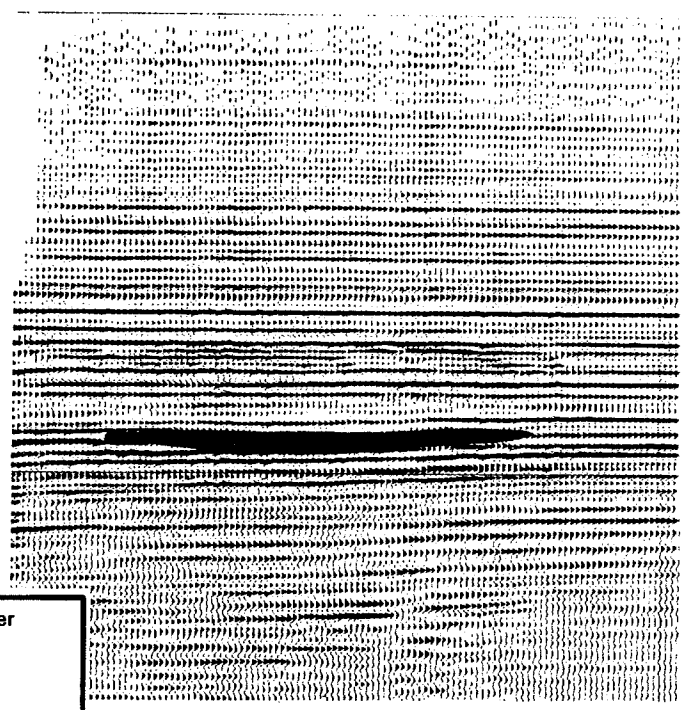

Figure 3

One Kilometer

One Mile

Erosional Unconformity, River Channel
W.L. Chapman
conoco

Energy Source: Vibroseis ®
Stacking Multiplicity: 24
Number of Channels Recorded: 48
Interval between Input Channels: 110'
Minimum Offset Distance: 330'
Maximum Offset Distance: 2860'
Static Corrections: Adaptive & Elevation
Deconvolution: 25-90 Hz
Frequency Filtering: 25-80 Hz
Other:
Migration: No
Source of Velocities for Processing: Data Derived

Bally 1.2.1-32

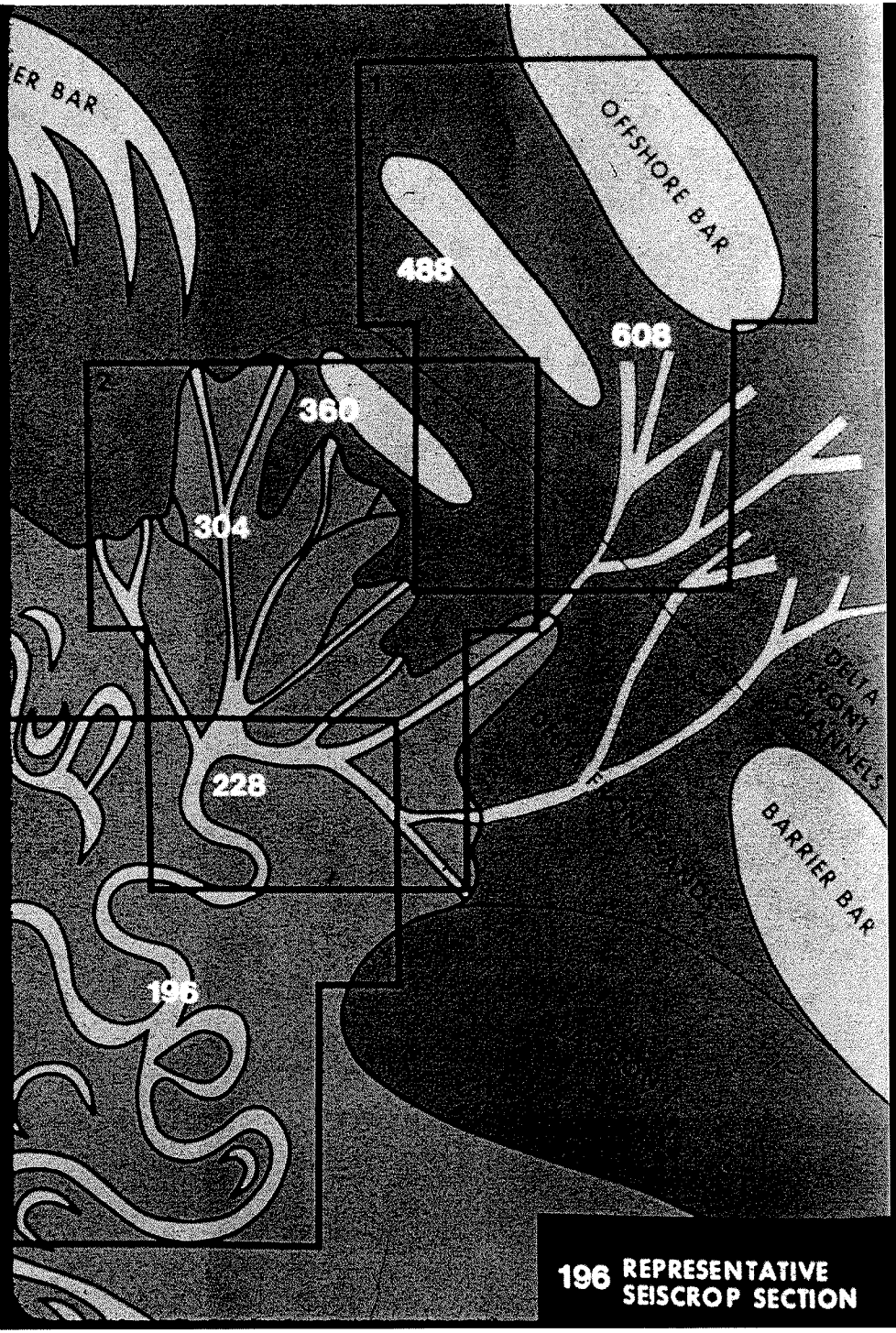

196 REPRESENTATIVE SEISCROP SECTION

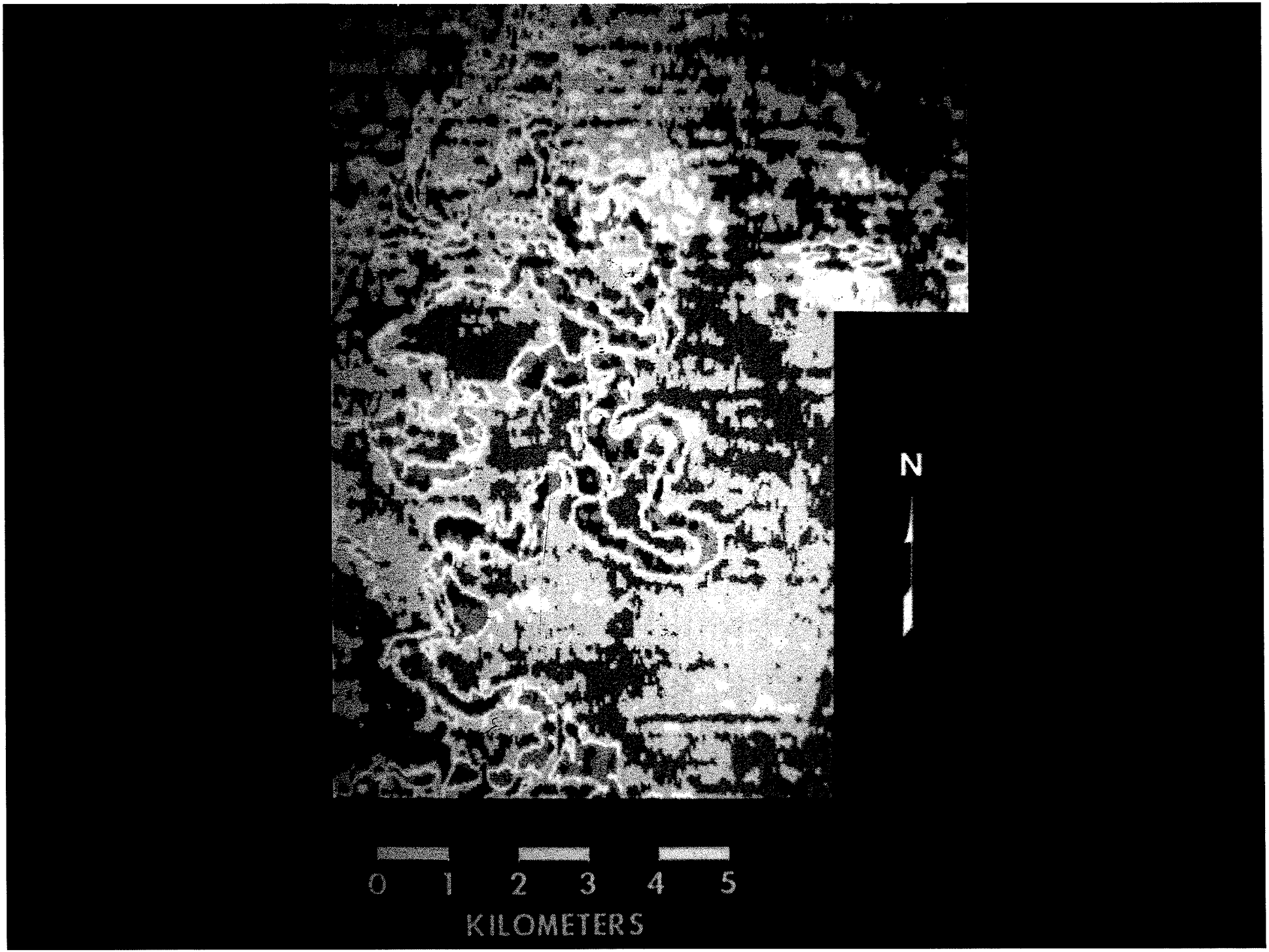
N
0 1 2 3 4 5
KILOMETERS

THE 3-D SOLUTION TO FINDING CHANNELS (BUT SAND-FILLED OR NOT??)

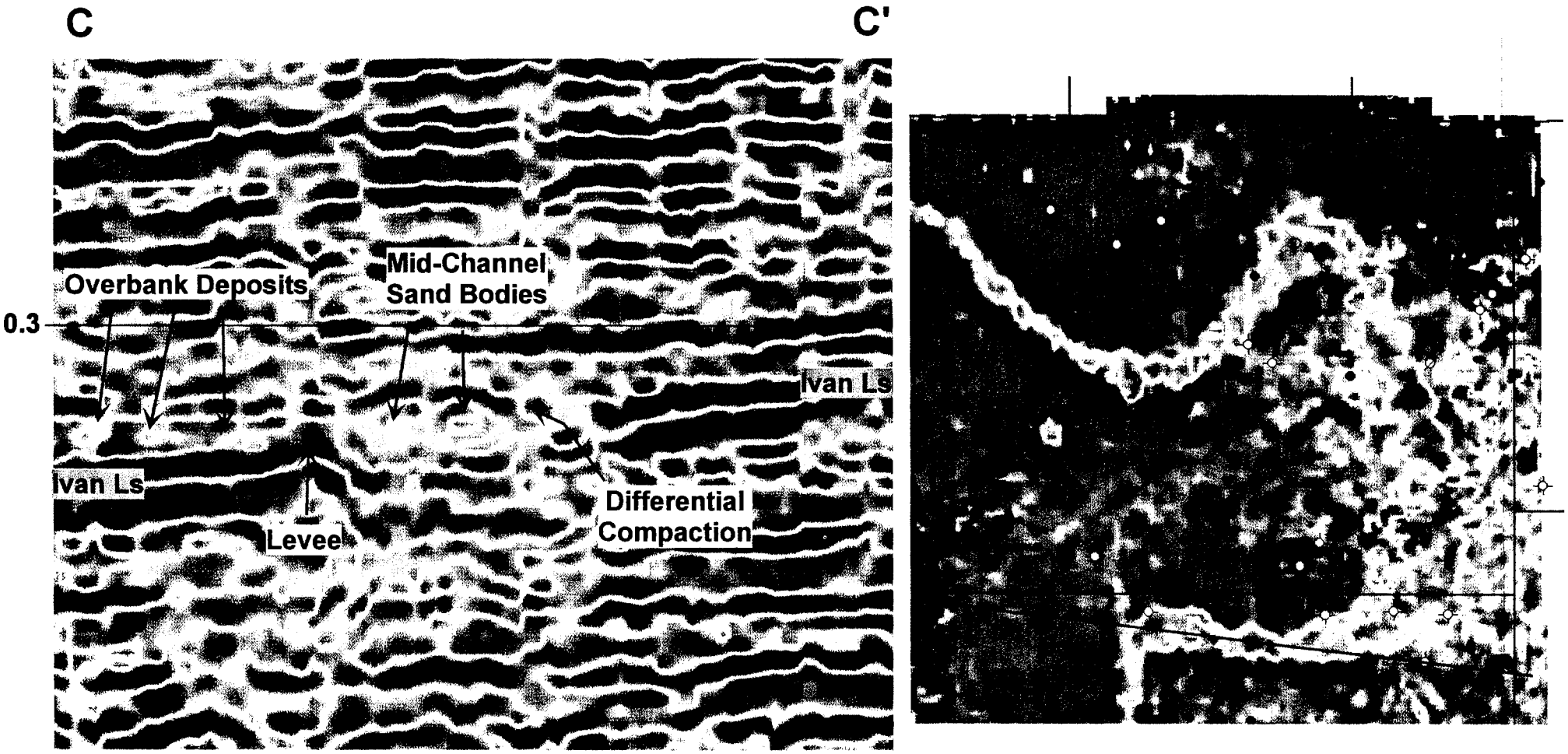

FIGURE 9A. Arbitrary line along channel axis showing mid-channel sand bodies, levee, overbank deposits, and differential compaction.

DELTA TYPES

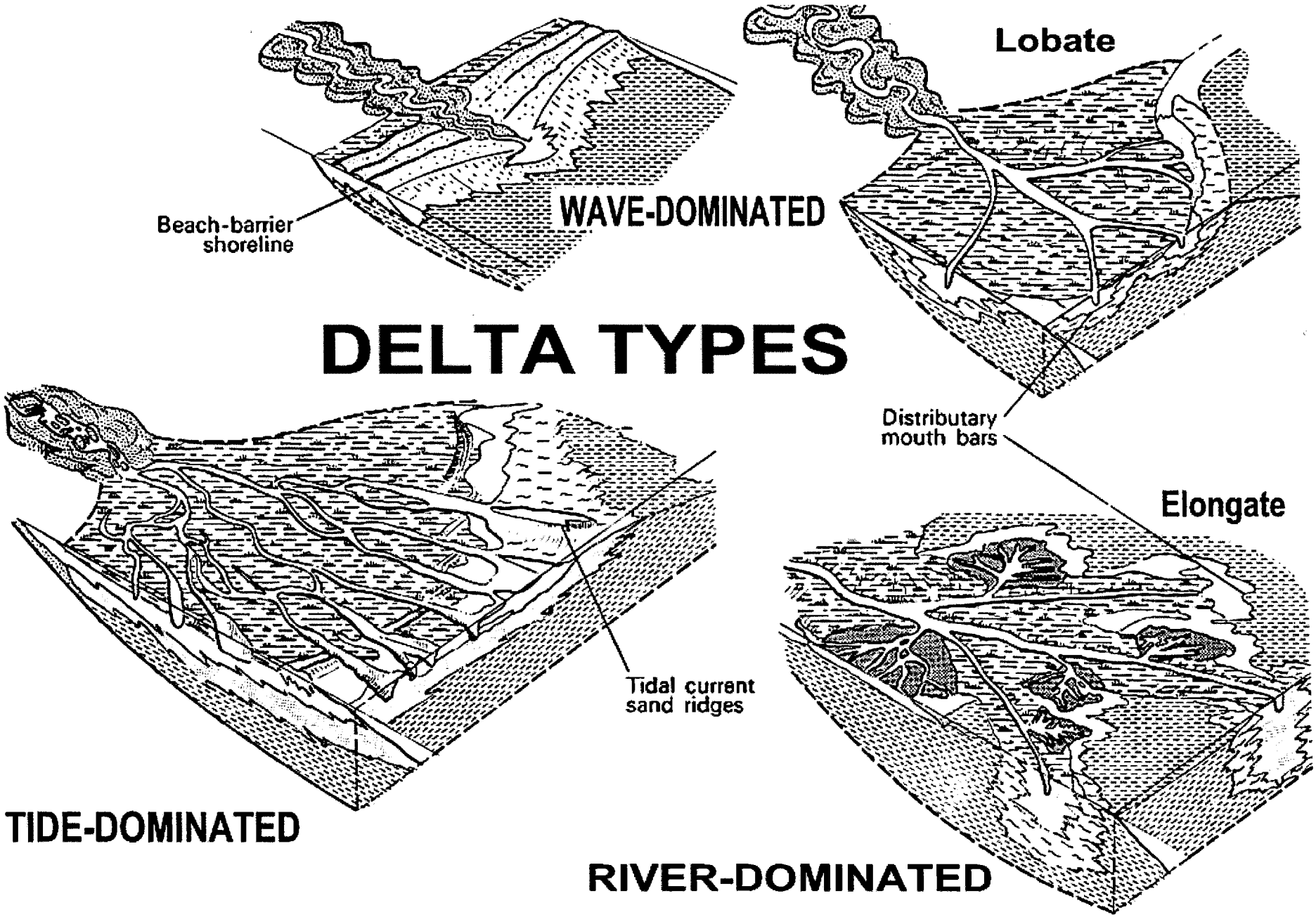
Beach-barrier shoreline
WAVE-DOMINATED
Lobate
Distributary mouth bars
Elongate
Tidal current sand ridges
TIDE-DOMINATED
RIVER-DOMINATED

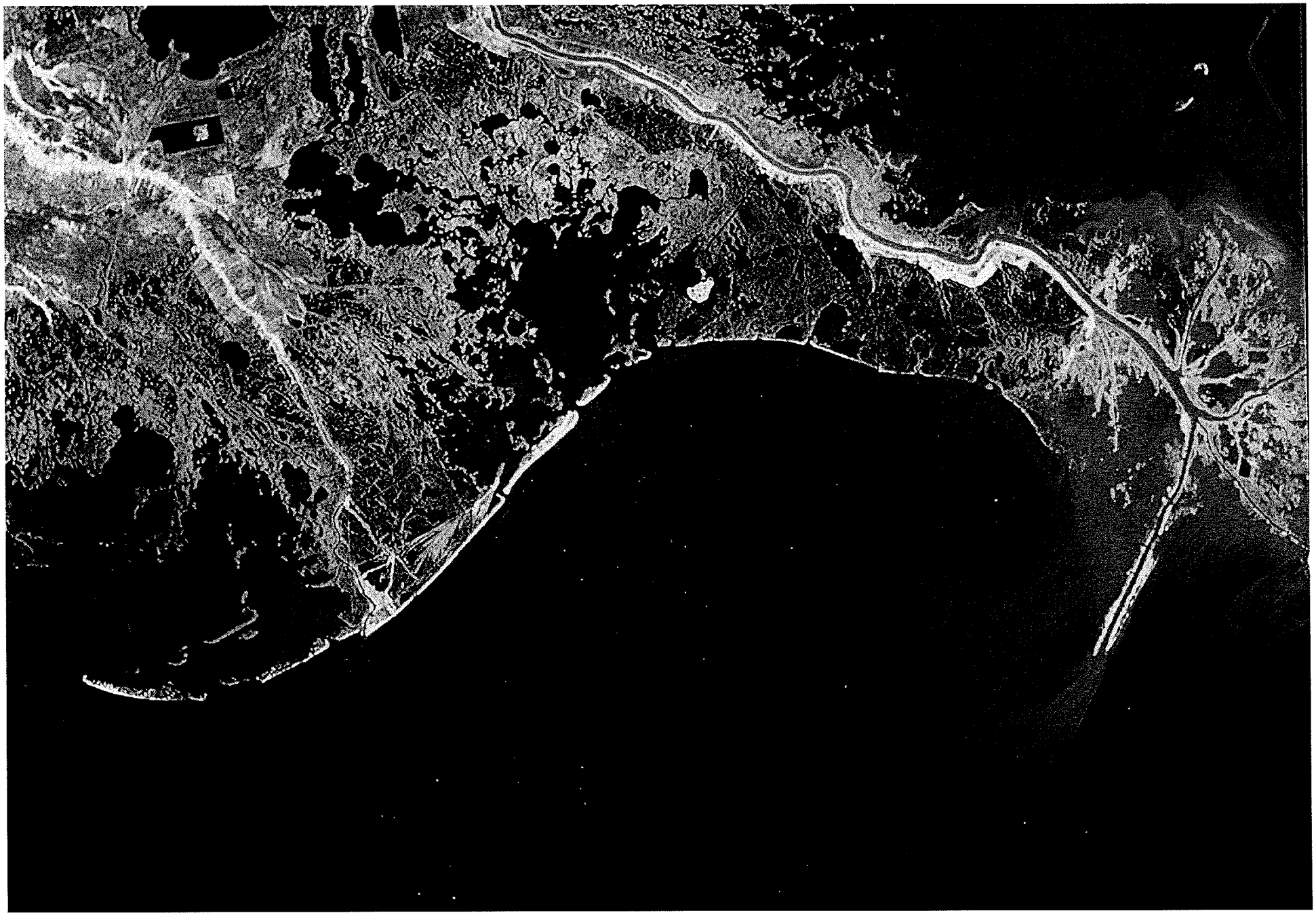

Fig. 8-32. Coherence horizon slice covering time range 1100 ms to 1400 ms using small analysis window to further emphasize stratigraphic features seen in Figure 8-30. Scale is same as Figure 8-30 and its outline is here in red. Horizon slice is calculated over ±8 ms window around smoothed picked horizon. (Courtesy Amoco Corporation. Data courtesy Geco-Prakla.)

RIVER-DOMINATED DELTAS

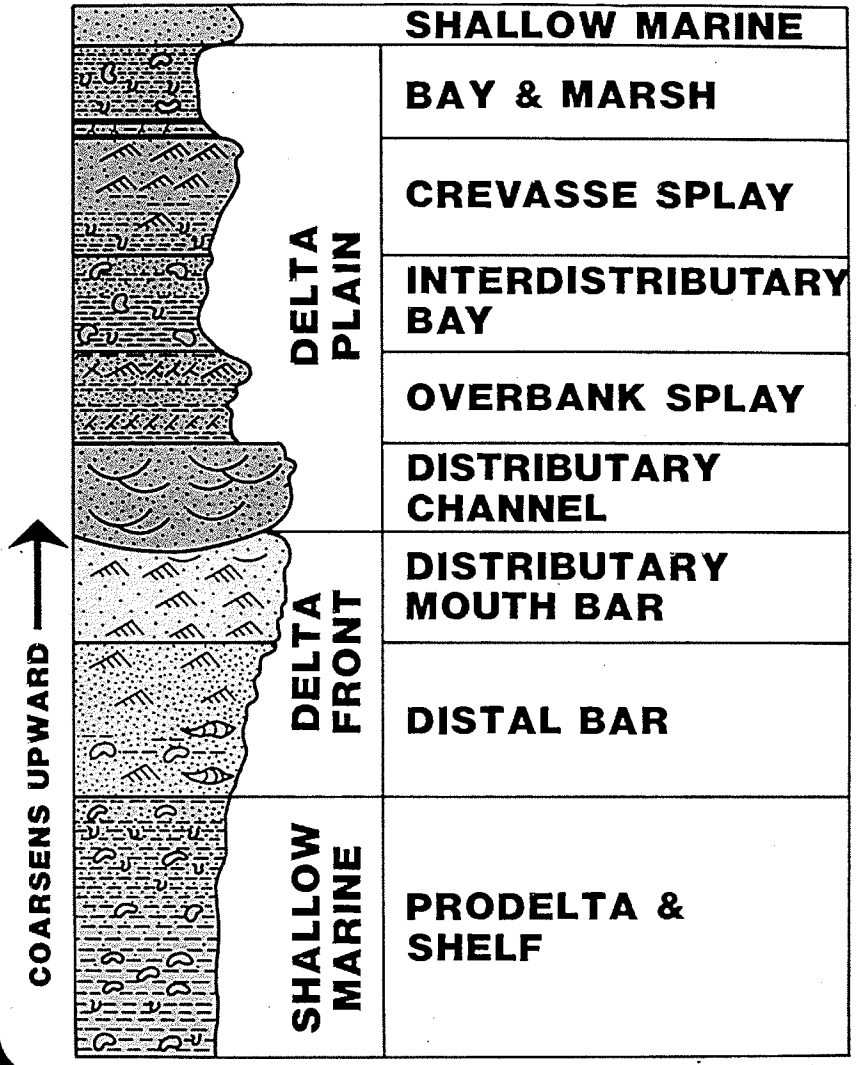

Ferron Sandstone: Outcrop Belt

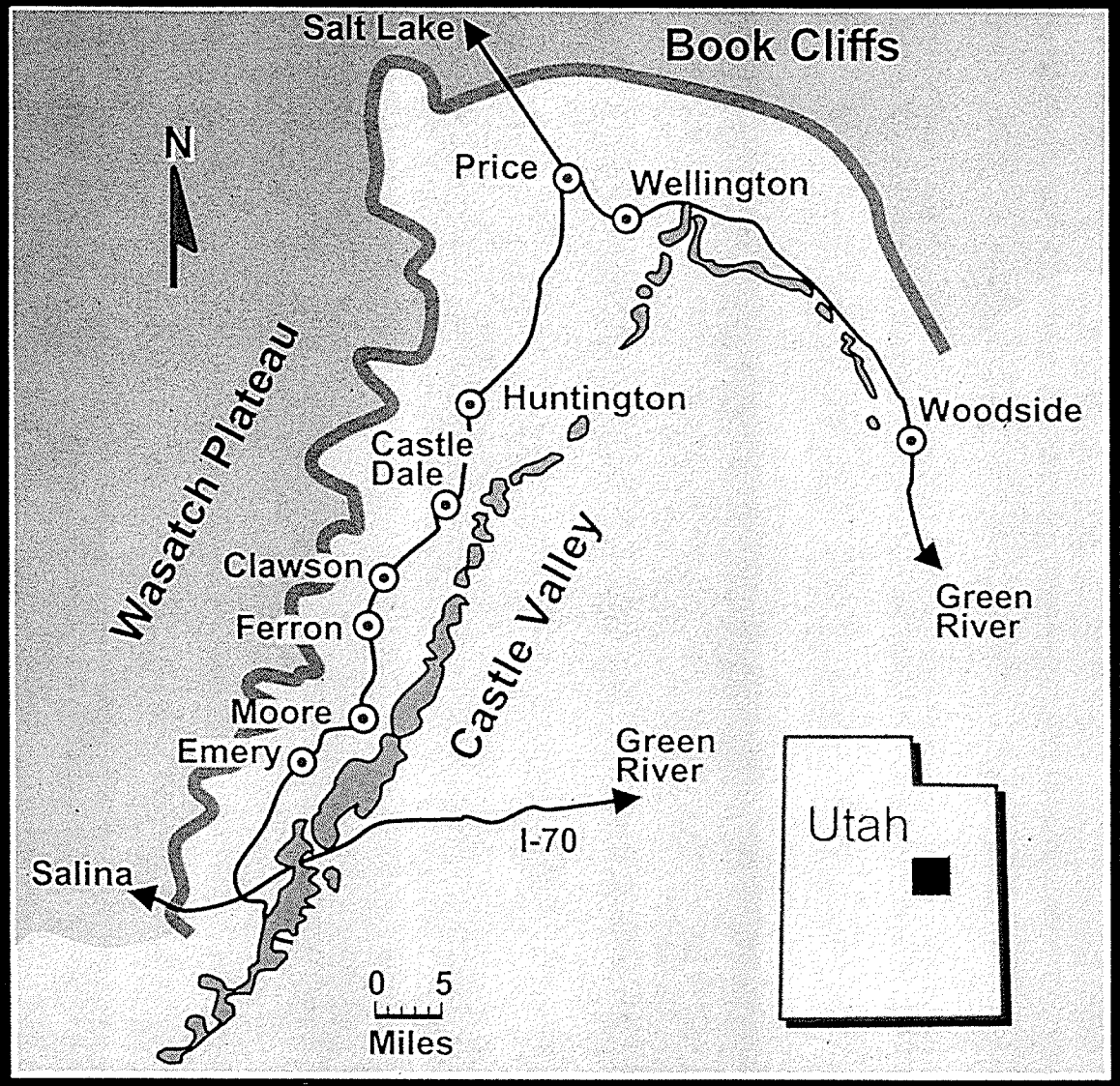

Courtesy of Richard Moiola

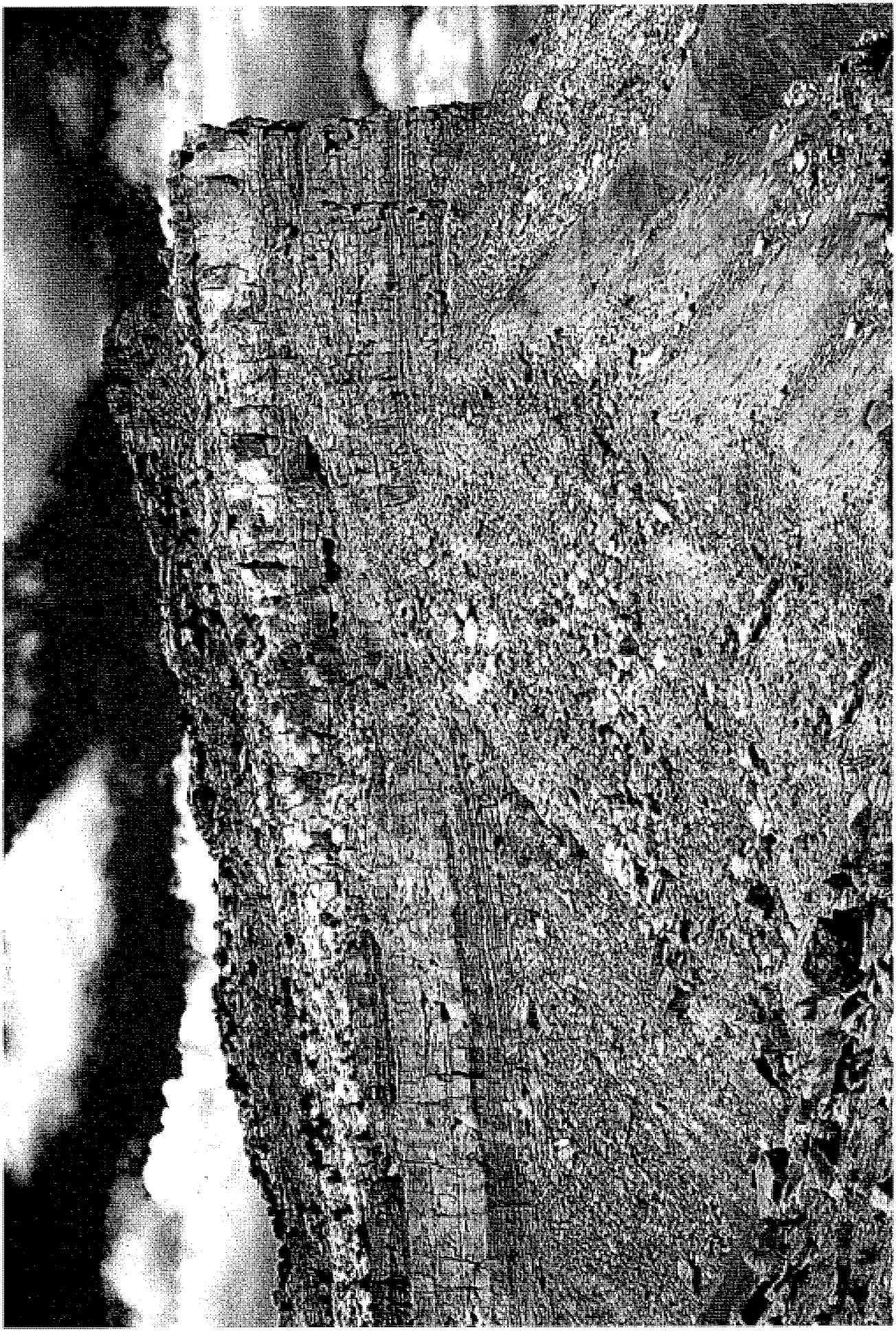

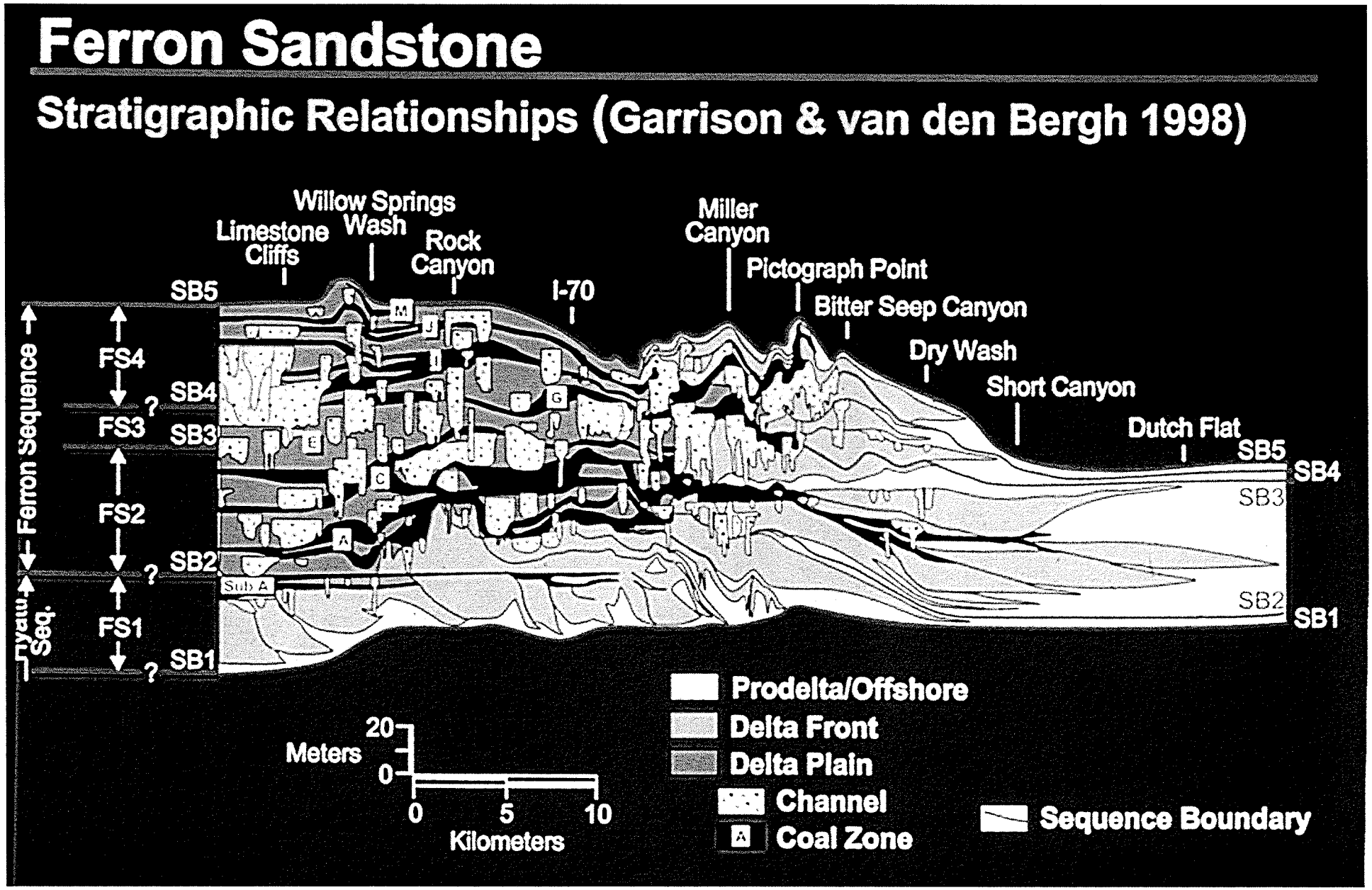

Courtesy of Richard Moiola

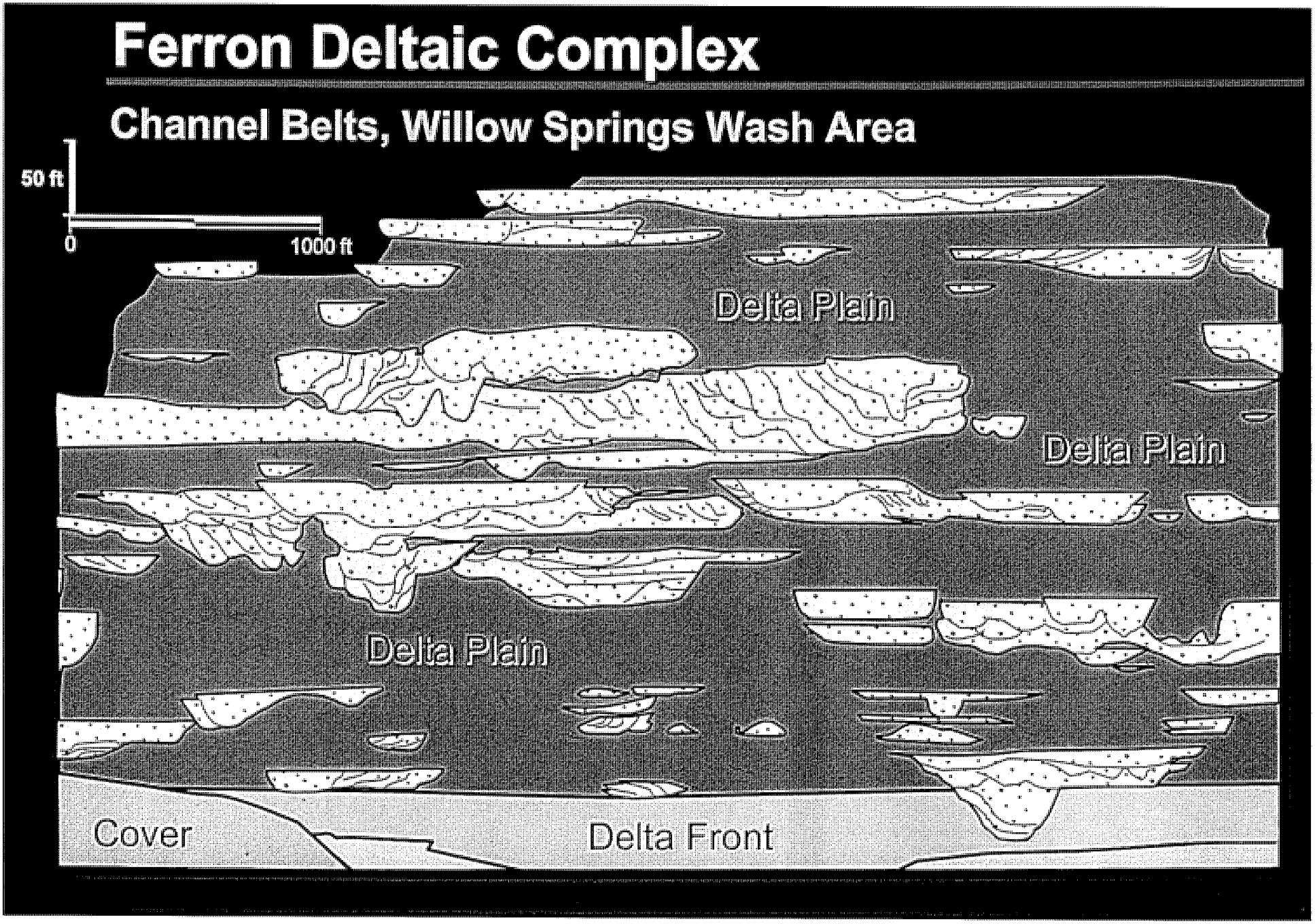

Courtesy of Richard Moiola

<DELTAS>

Helland-Hansen et al 91
Basin Research V. 6, 181-191.

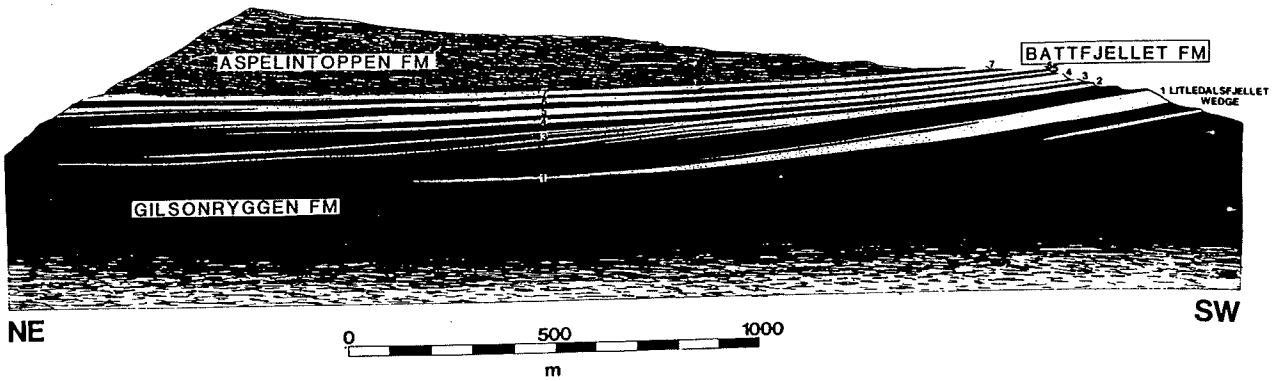

Fig. 4. Geometrical model (drawing from photograph in Fig. 2). Black indicates shale, mudstone and siltstone; dots indicate sandstone (excerpt from Helland- Hansen, 1992).

THE CLINOFORM & ITS ORIGINS

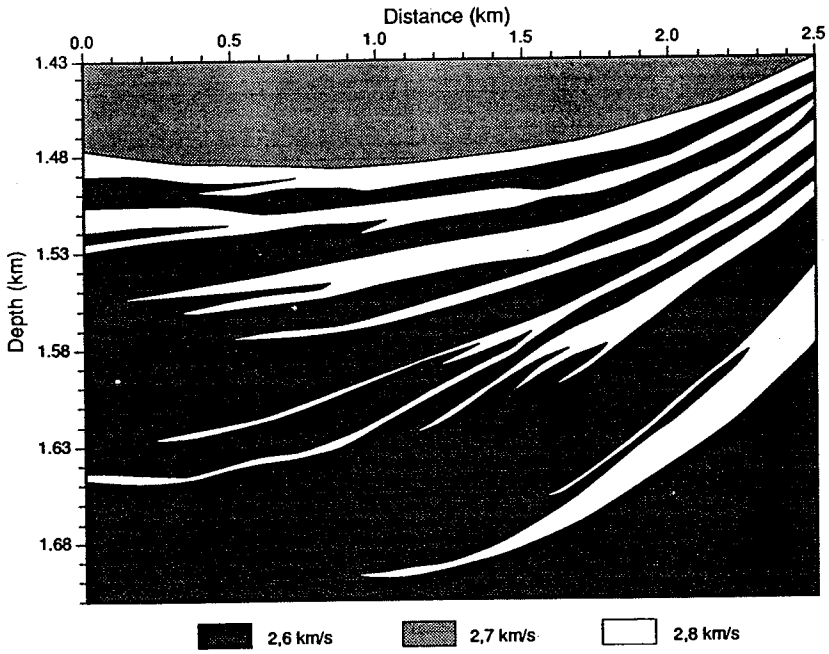

Fig. 6. Model geometry and velocity layer distribution, Model 1.

Helland-Hansen et al 94
Basin Research v6, 181-191

'ig. 8. Constant-velocity layer model of synthetic sections. (a) Time arrivals; (b) 100-Hz minimum phase Ricker wavelet; (c) 50-Hz ıinimum phase Ricker wavelet; (d) 30-Hz minimum phase Ricker wavelet.

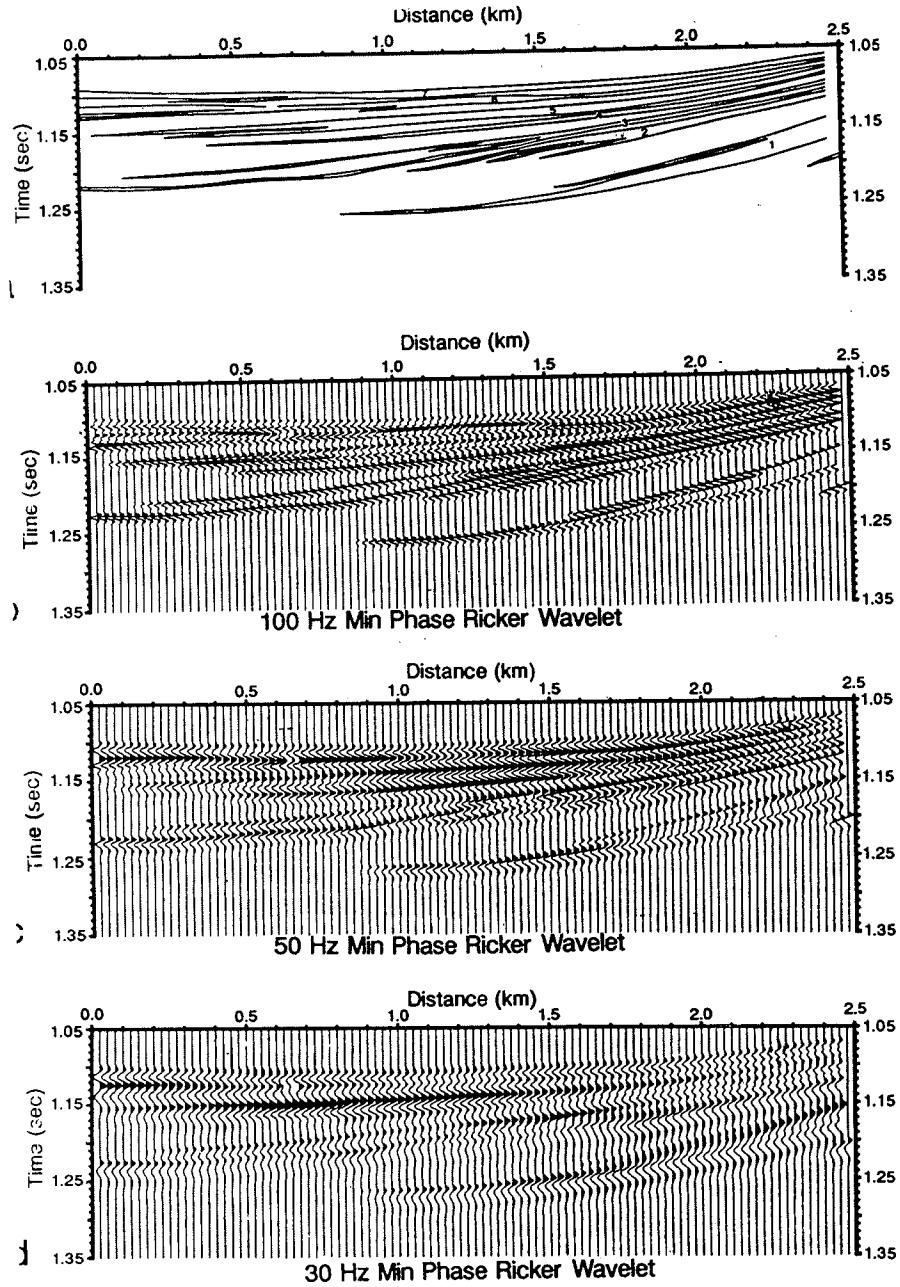

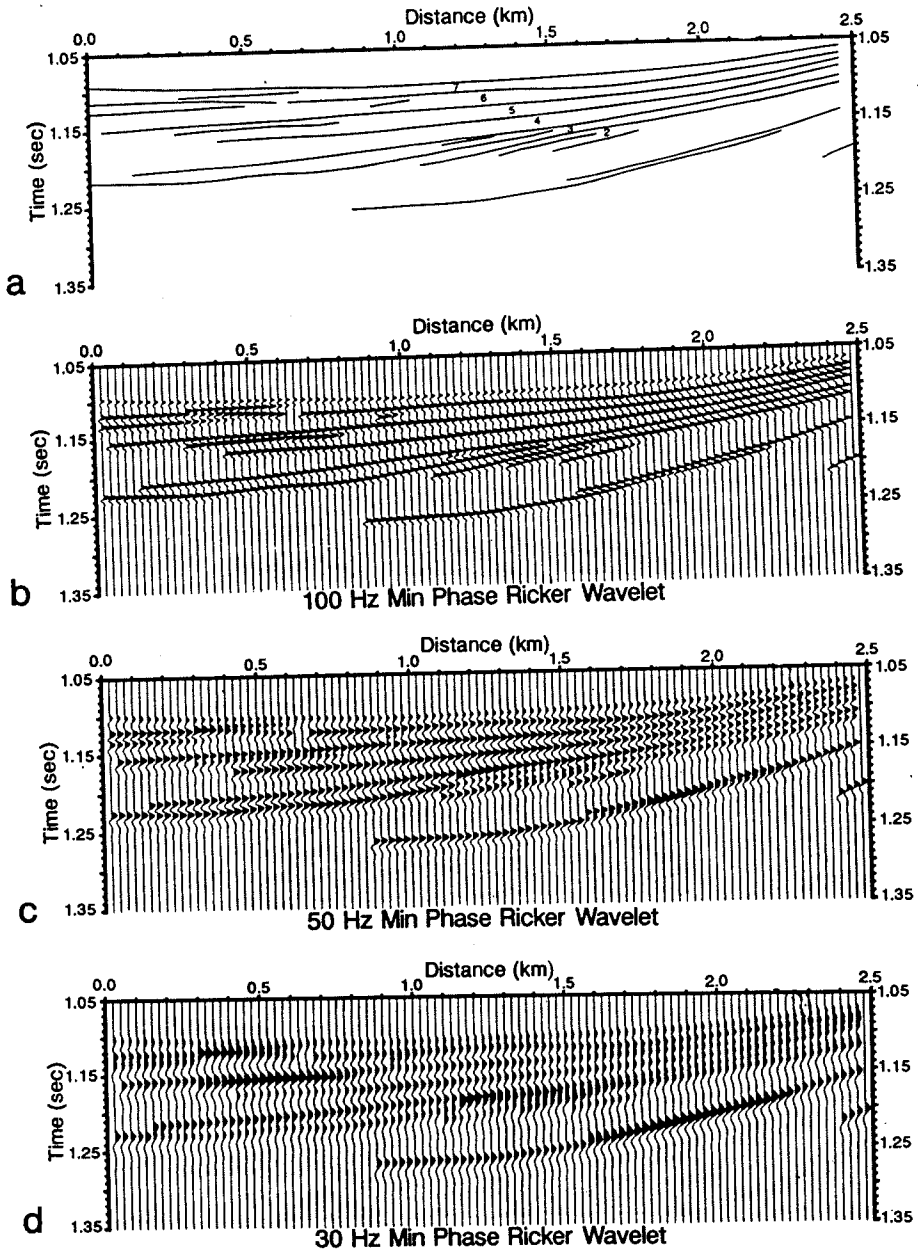

Fig. 9. Variable-velocity layer model of synthetic sections. (a) Time arrivals; (b) 100-Hz minimum phase Ricker wavelet. (c) 50-Hz minimum phase Ricker wavelet; (d) 30-Hz minimum phase Ricker wavelet.

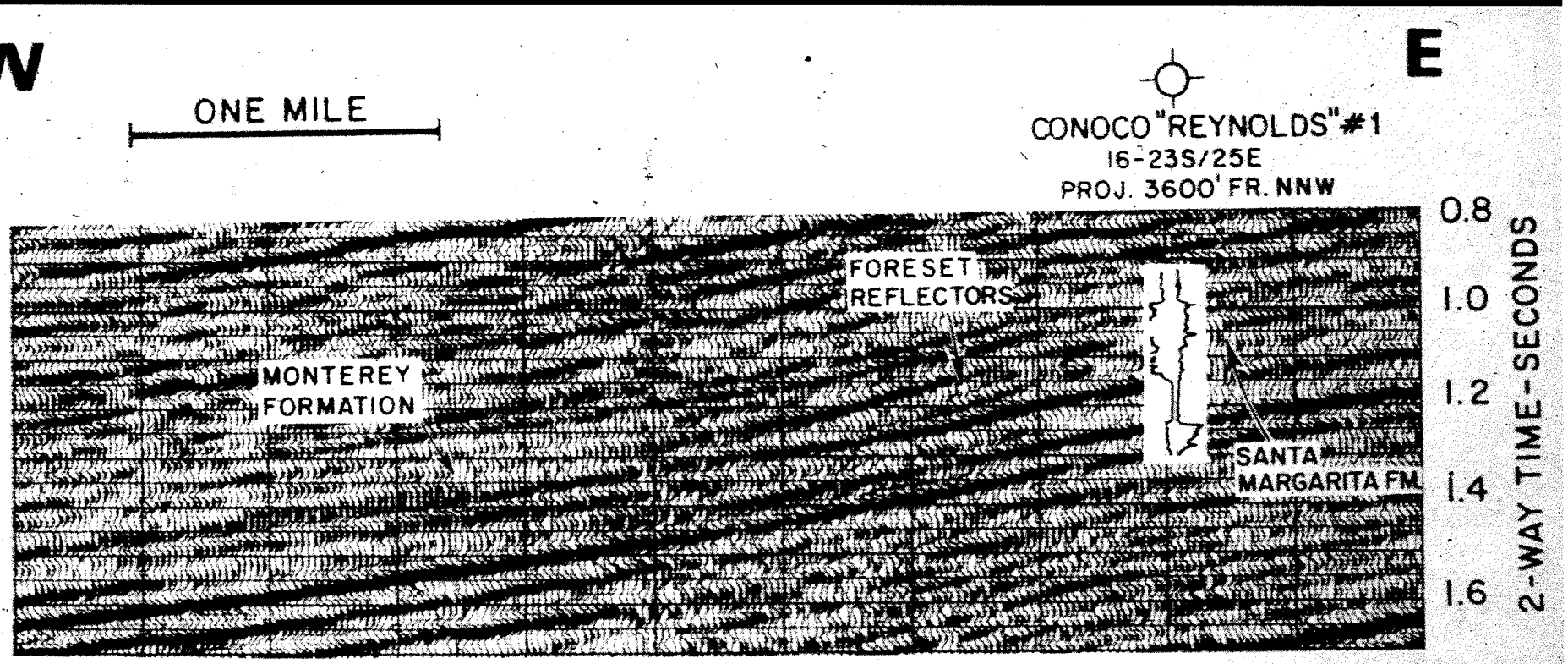
W
E
ONE MILE
CONOCO "REYNOLDS" #1
16-23S/25E
PROJ. 3600' FR. NNW
FORESET
REFLECTORS
MONTEREY
FORMATION
SANTA
MARGARITA FM.
0.8
1.0
1.2
1.4
1.6
2-WAY TIME-SECONDS

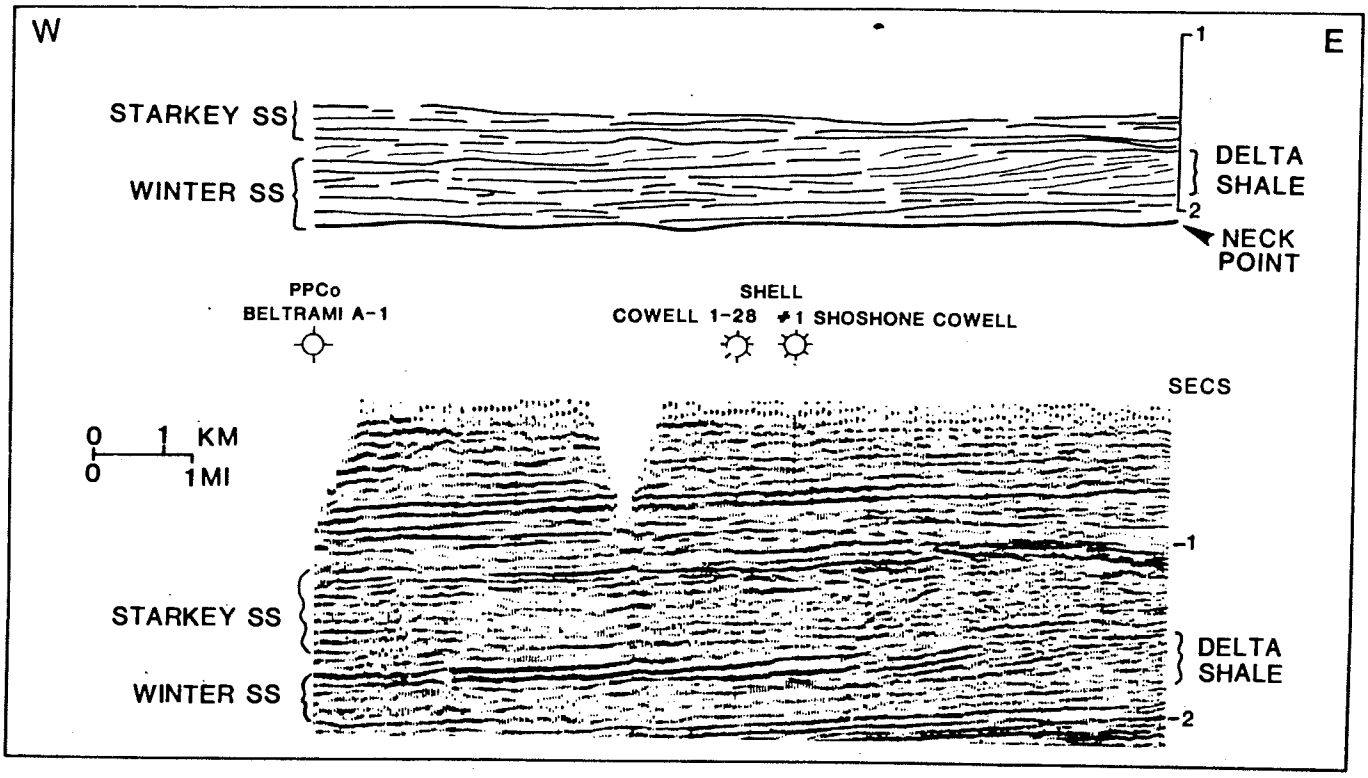

FIG. 22—Seismic section in southern Sacramento Valley, California, showing seismic character and interpretation of seismic sequences of Upper Cretaceous Starkey sandstone, Delta shale, and Winters sandstone. See Figure 21 for approximate location of section.

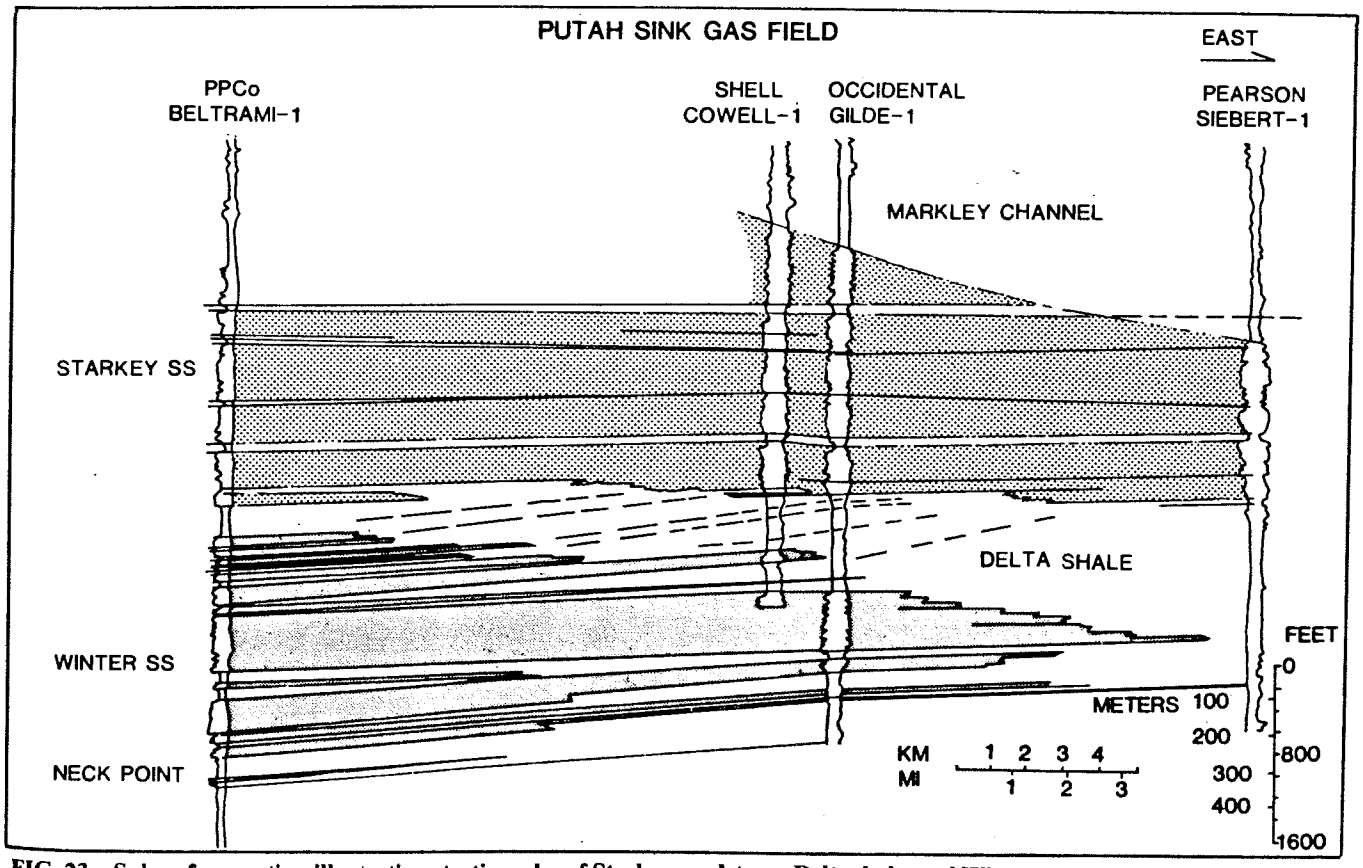

FIG. 23—Subsurface section illustrating stratigraphy of Starkey sandstone, Delta shale, and Winters sandstone and their relation to each other. Section also shows stratigraphic trap in turbidite sands of Putah Sink gas field (modified from Drummond et al, 1976). See Figure 21 for approximate location of section.

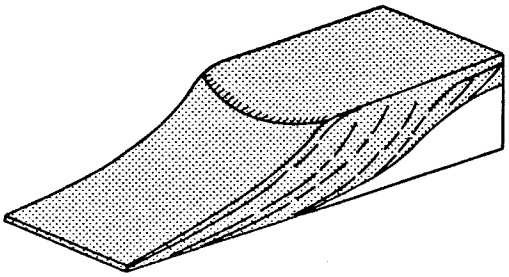

OBLIQUE PROGRADATIONAL
(HIGH ENERGY)

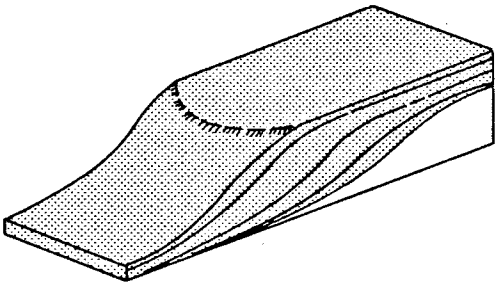

SIGMOID PROGRADATIONAL
(LOW ENERGY)

FIG. 5—Shelf-margin and prograded-slope seismic facies types.

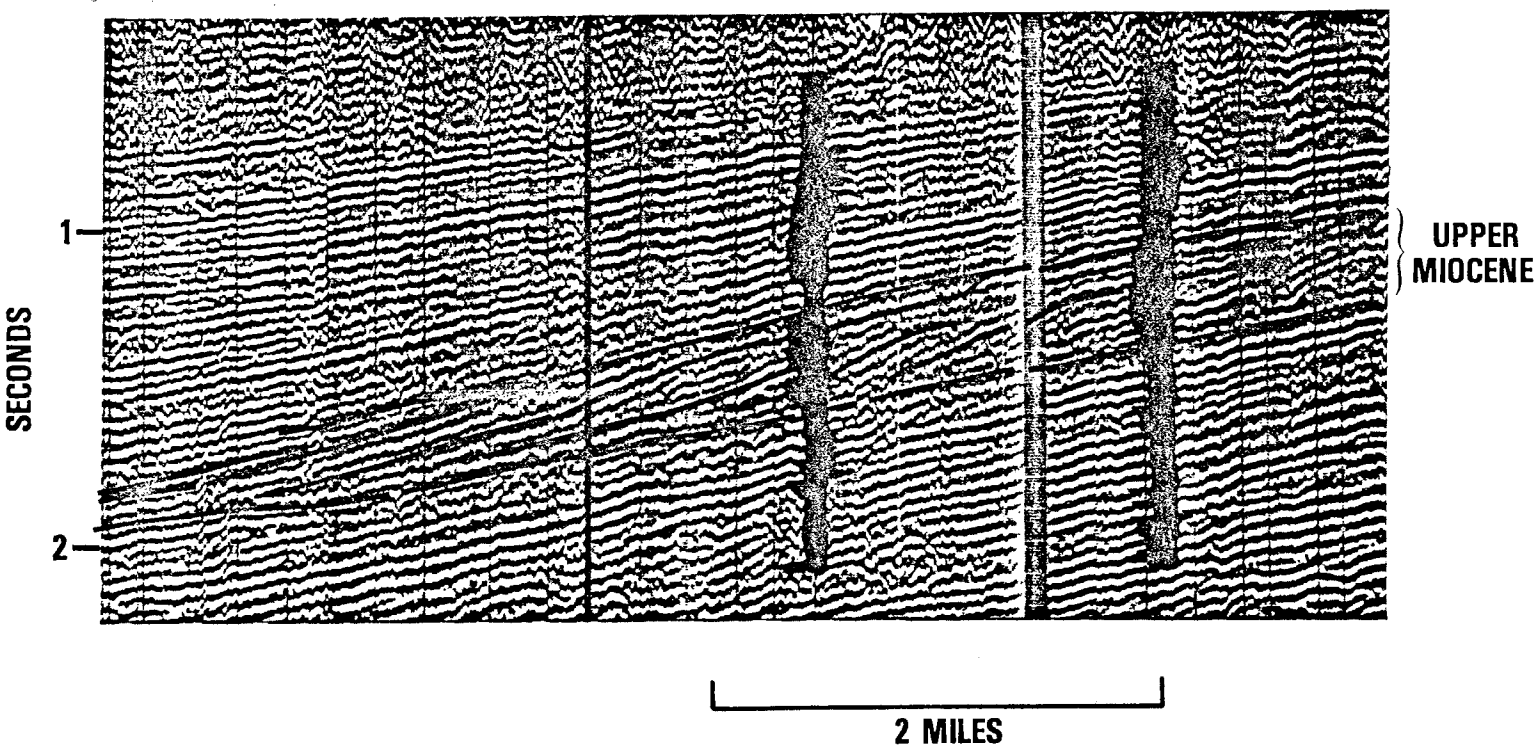

FIG. 6—Oblique-progradational seismic facies, Miocene example. Upper Miocene deposits form prominent, basinward-thinning, oblique-prograding facies unit. Two wells located along line contain abundant reservoir quality sandstone in facies.

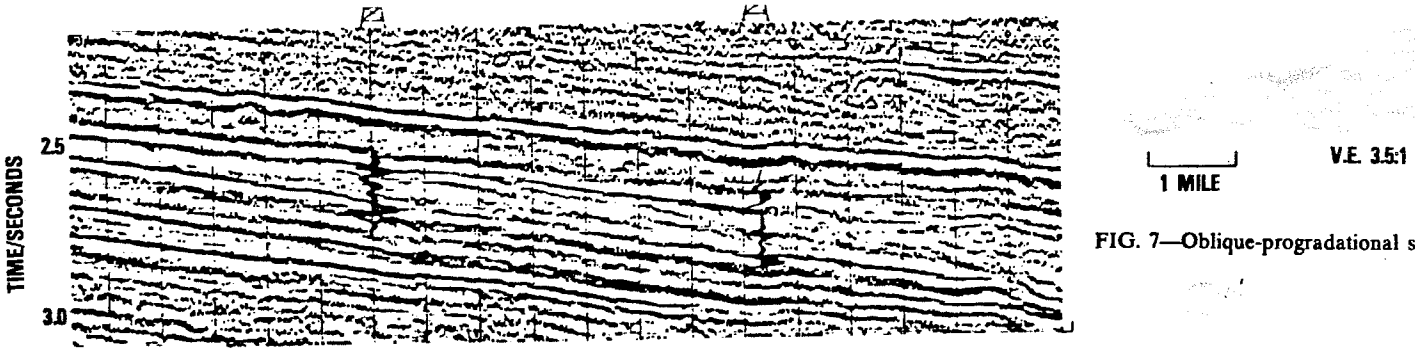

FIG. 7—Oblique-progradational seismic facies.

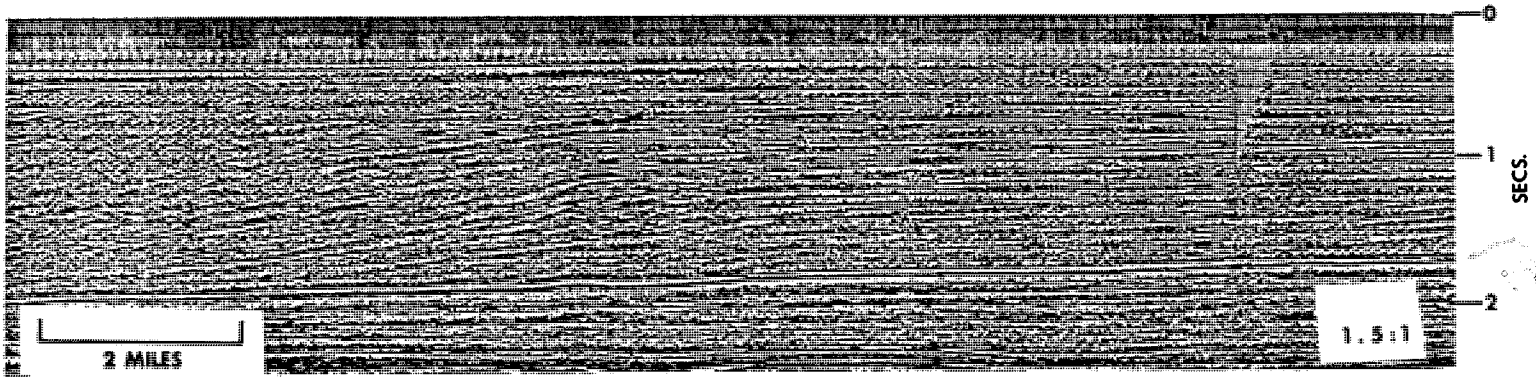

FIG. 8—Sigmoid-progradational seismic facies, offshore eastern Canada. Section shows striking sequence boundary at about 1.8 sec (on right) separating parallel reflections below from sigmoid-prograding reflections above.

DELTAIC DETAILS: CHANNELS & LOBES

Fig. 4-11. Schematic diagram of delta prograding across the Gulf of Thailand 3-D survey area between mid-Miocene and Pleistocene.

Brown 86

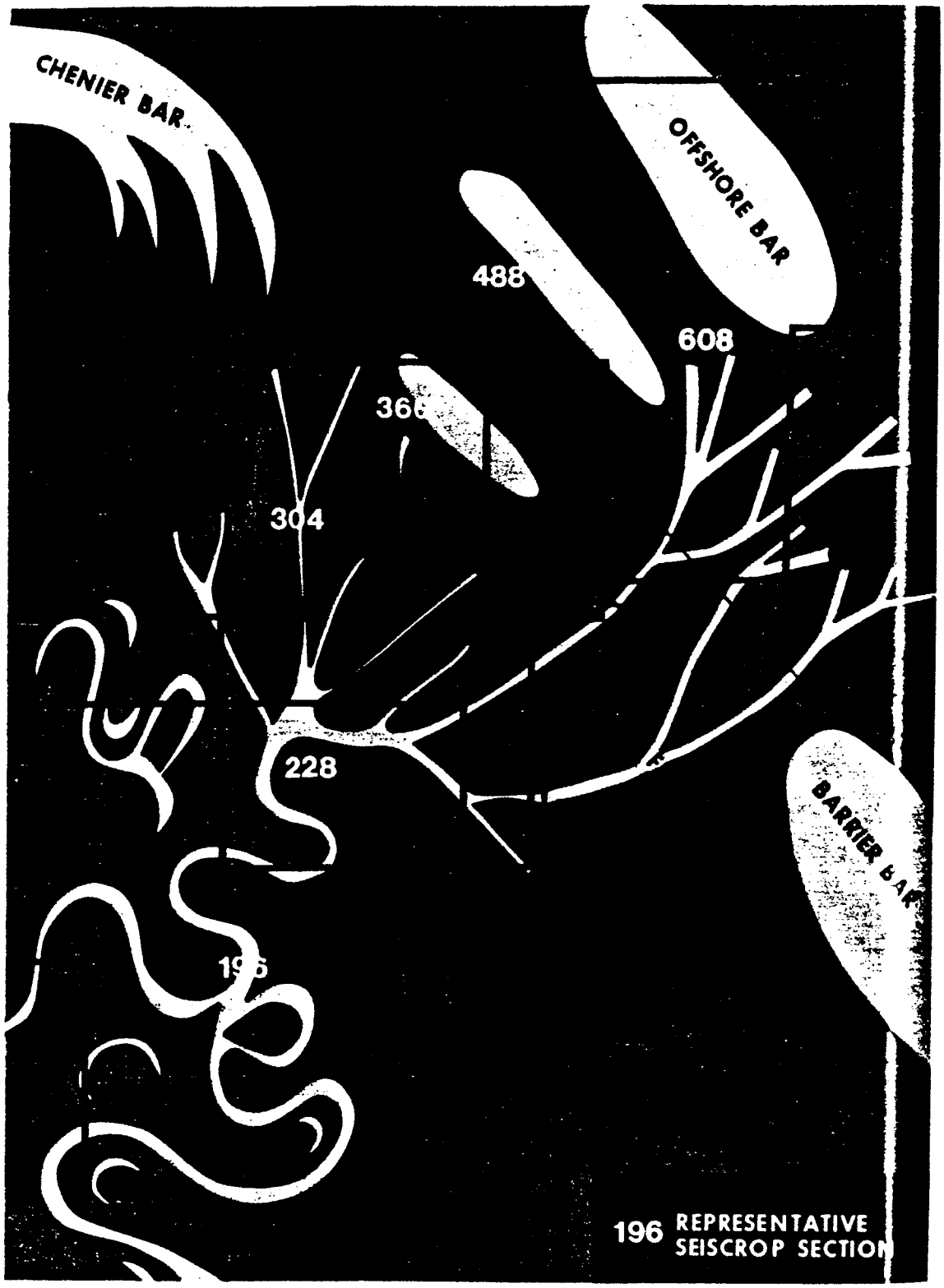

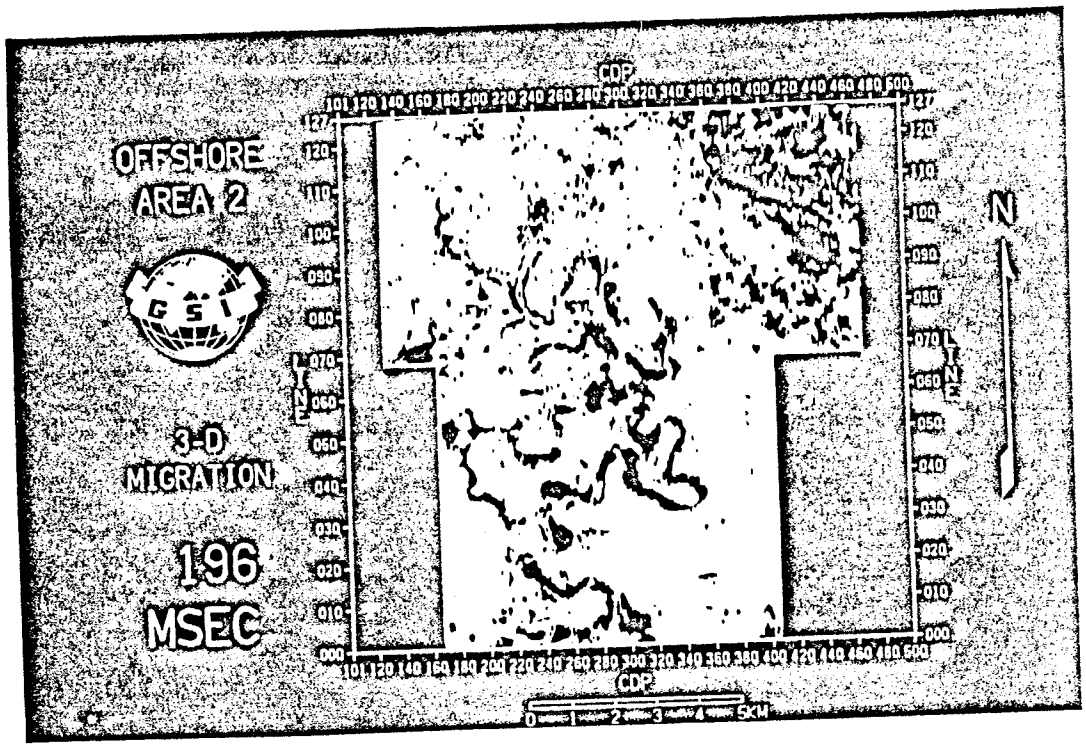

FIG. 27 - SHALLOW SEISCROP AT 0.196 SECONDS.

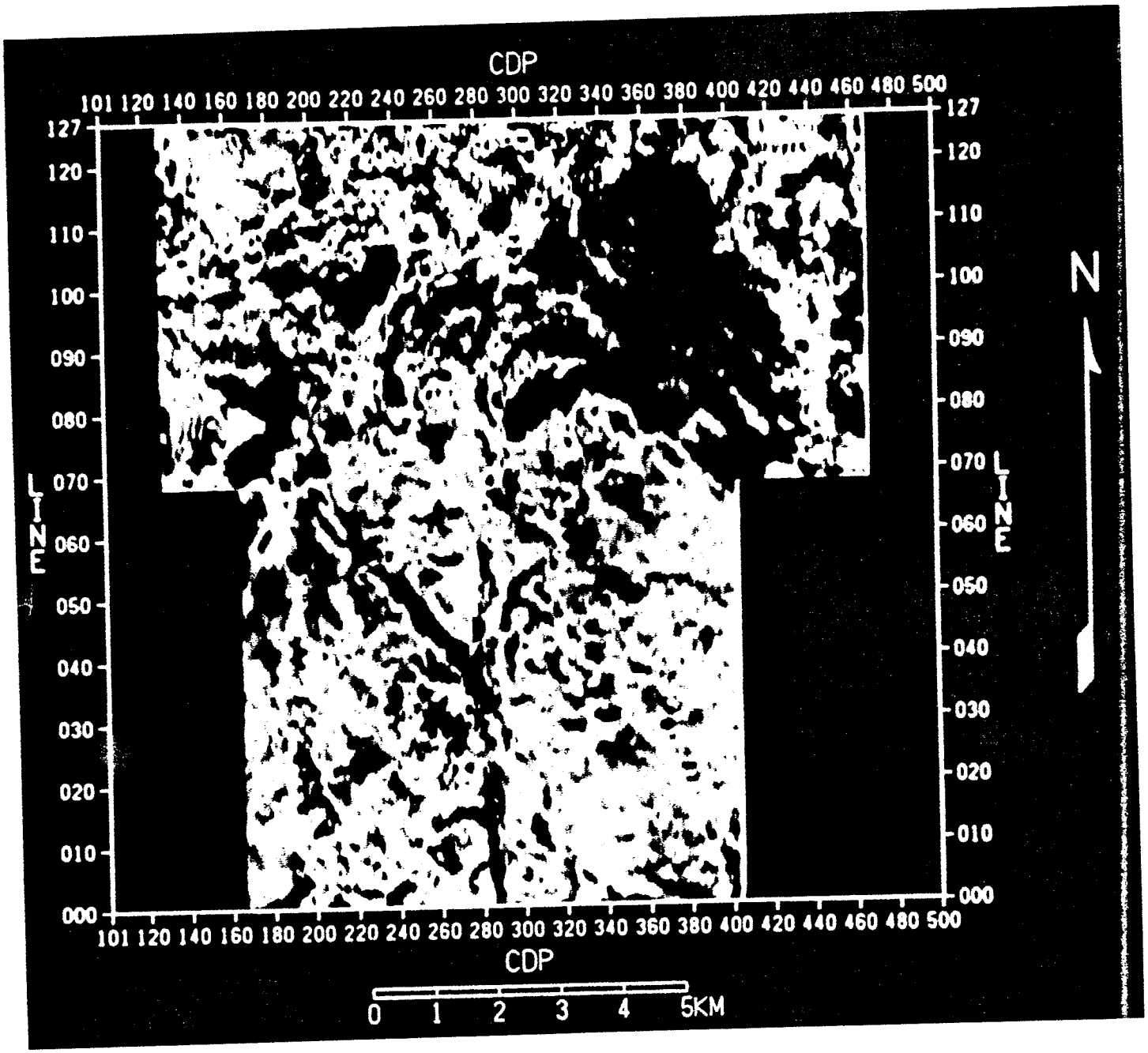

Fig. 4-15. Seiscrop section at 304 ms from Gulf of Thailand showing a Chenier bar and distributary channels (Courtesy Texas Pacific Oil Company Inc.) Brown 86

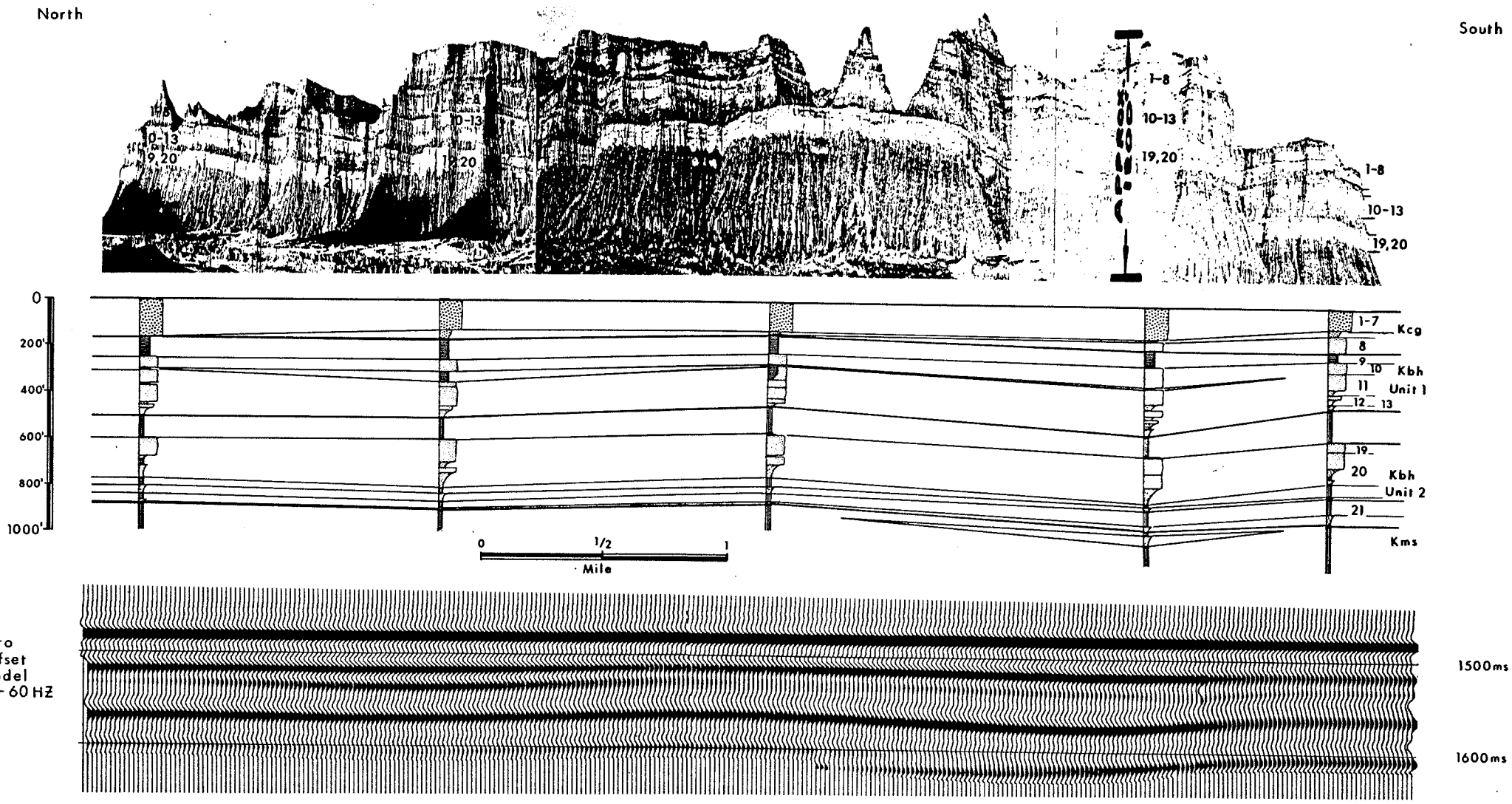

Leblanc et al in Bally

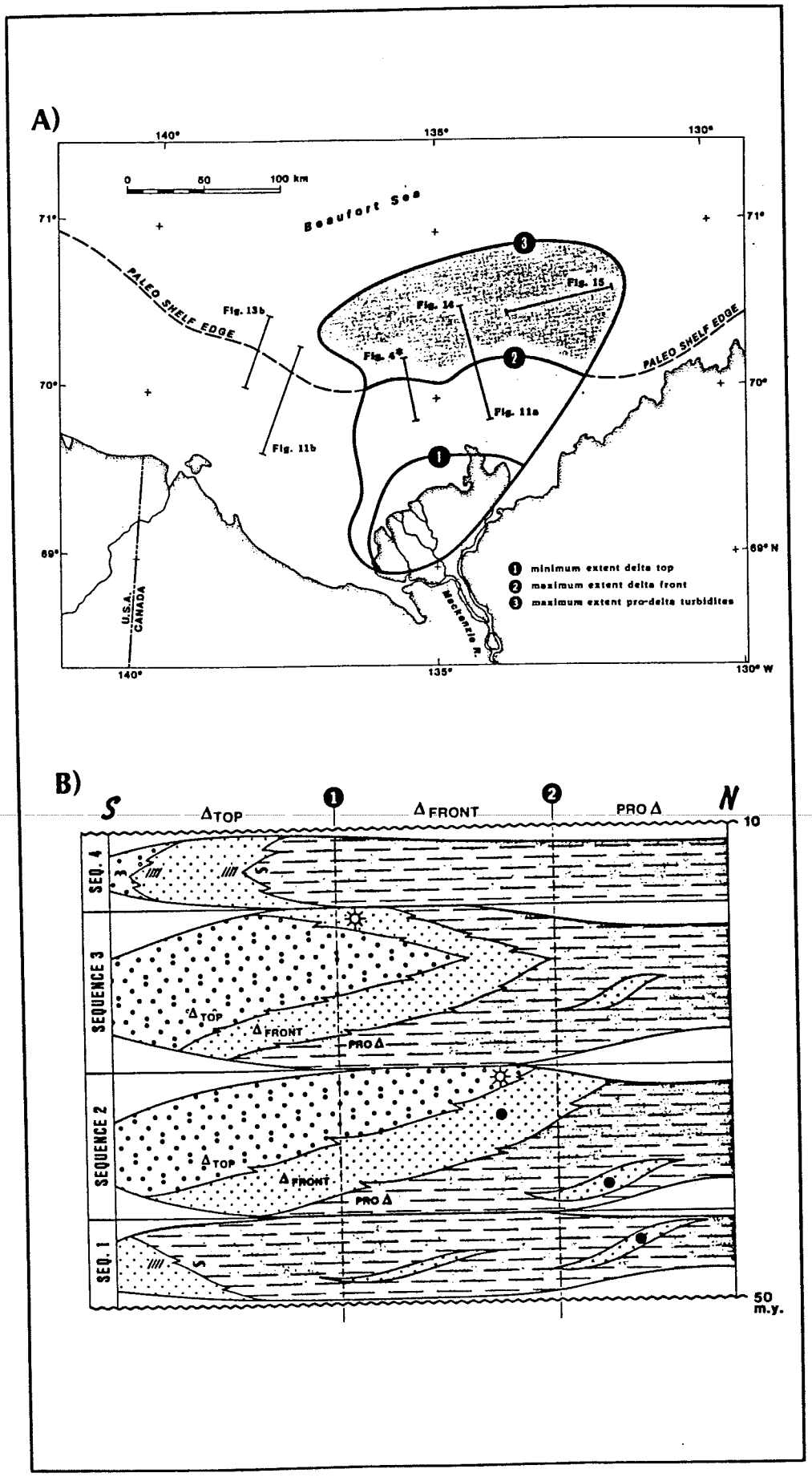

LONG-TERM DELTA CONSTRUCTS

Figure 12. Figure 12a shows a location map for the Eurekan megasequence in the Beaufort Sea and the seismic line locations of figures shown elsewhere in the text. Figure 12b is a chronostratigraphic diagram of the Eurekan megasequence within the deltaic depocenter shown on Figure 11a and on Figure 4 of Hubbard, Pape, and Roberts (1985; this volume). Three Eurekan hydrocarbon play fairways are distinguished on the basis of dominant depositional environment. Delta top depositional environments are shown in green, delta front depositional environments are shown in yellow and pro-delta depositional environments in brown. Oil accumulations are restricted to the deeper stratigraphic levels and are trapped in turbidite and delta front sands of Sequences 1 and 2. Gas accumulations are trapped at shallower stratigraphic levels, primarily in the delta top and delta front environments of Sequences 2 and 3. Note that Sequences 1 and 4 equate more to depositional environments in a linear prograding shelf system rather than to the lobate delta environments of Sequences 2 and 3. To the west and east of the major deltaic depocenter all sequences equate more to the prograding shelf system (Figures 11b and 13).

Hubbard et al 1985b

B)

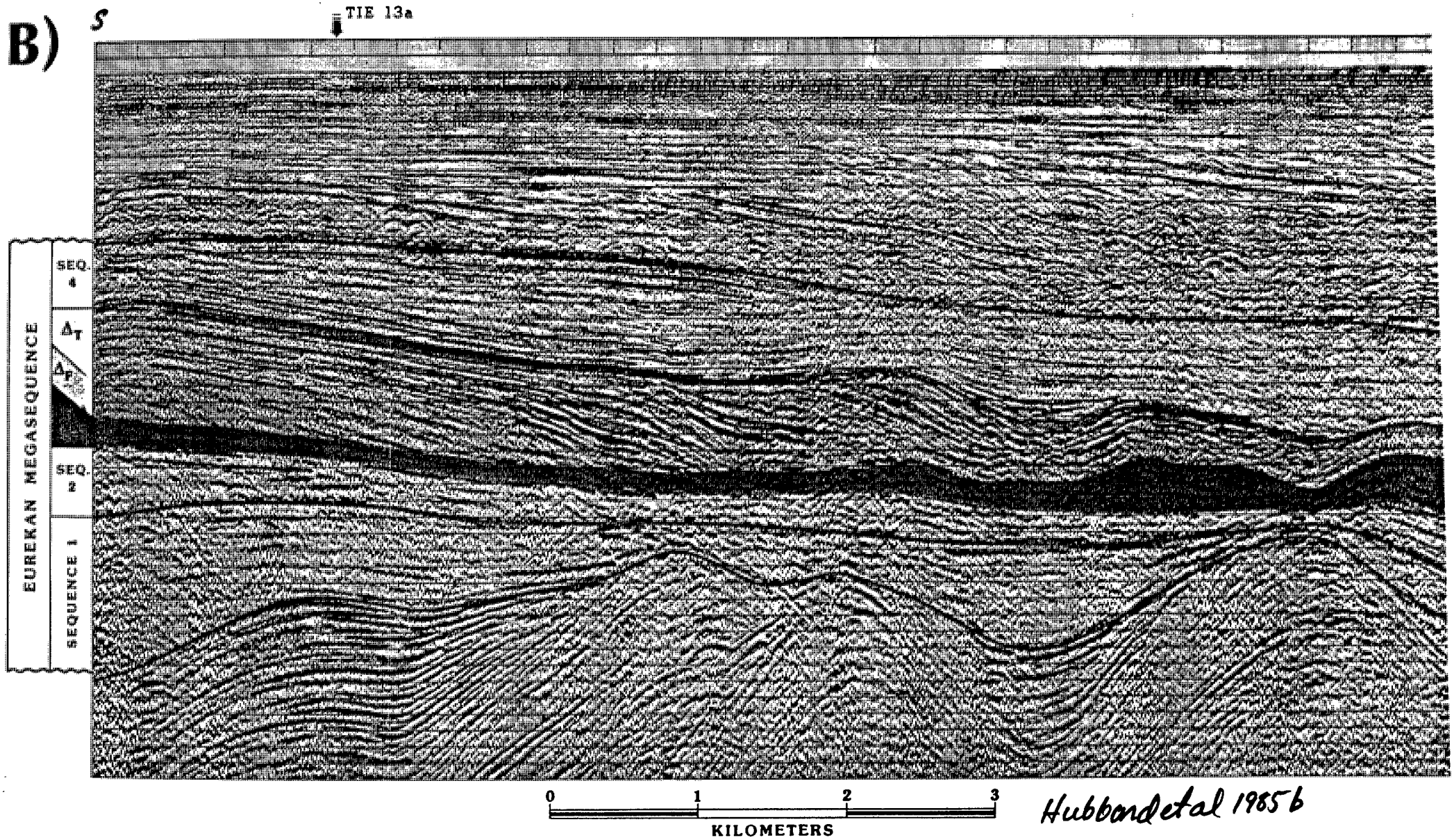

Hubbard et al 1985b

226

STRATIGRAPHIC SEQUENCES ON THE SHELF

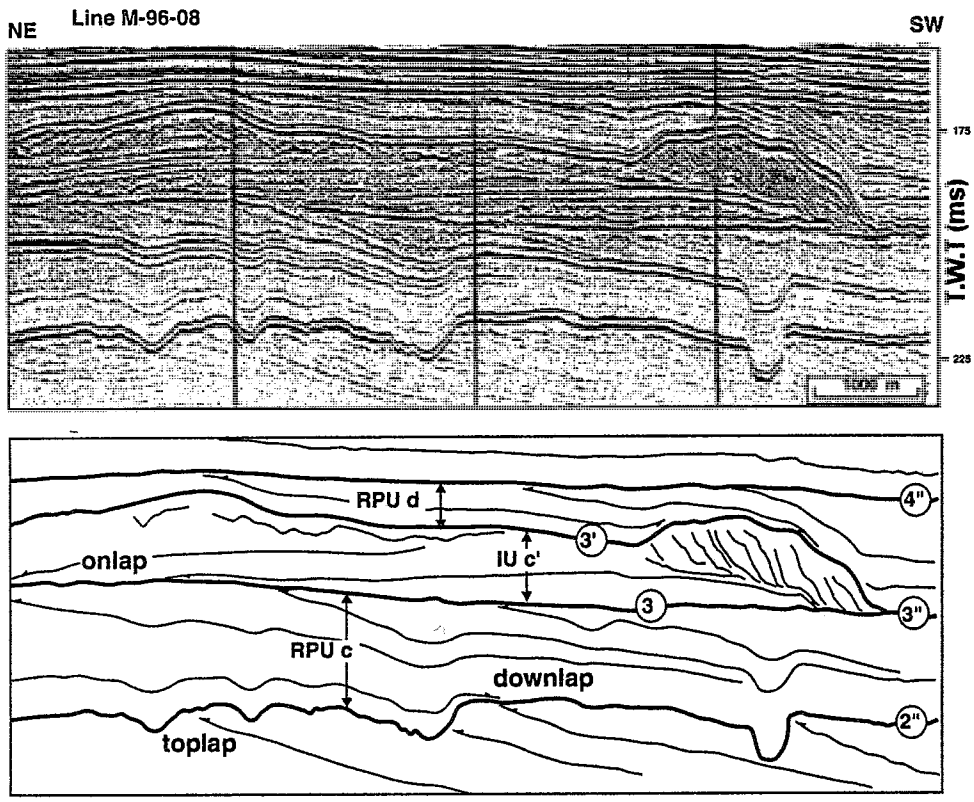

Figure 4—Uninterpreted (top) and interpreted (bottom) seismic section illustrating the principal unconformities and associated reflection terminations. Each regional unconformity (1″, 2″, 3″ etc.) is polygenetic and separates locally into two surfaces (1, 2, 3, etc., and 1′, 2′, 3′, etc.). The seismic units are of two types: regional prograding units (RPU) and intercalated units (IU), each exhibiting specific external shape and internal configuration (see text for further discussion and Figure 2 for location).

Tesson et al, 2000, AAPG Bull, v84 p119-150.

(NOTE SCALE!)

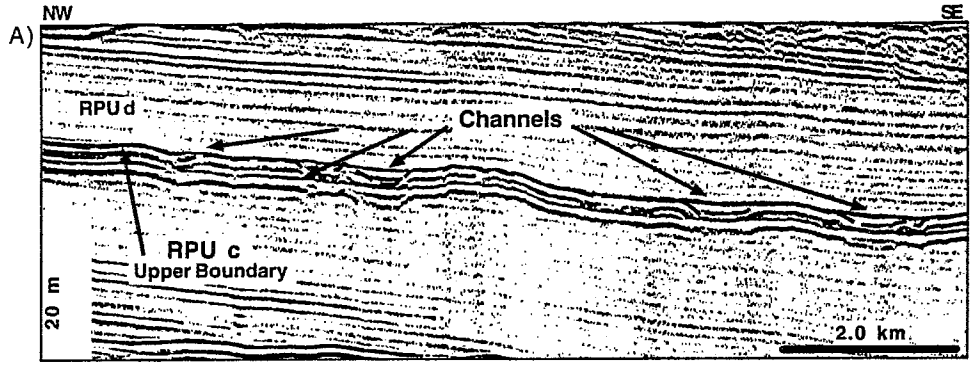

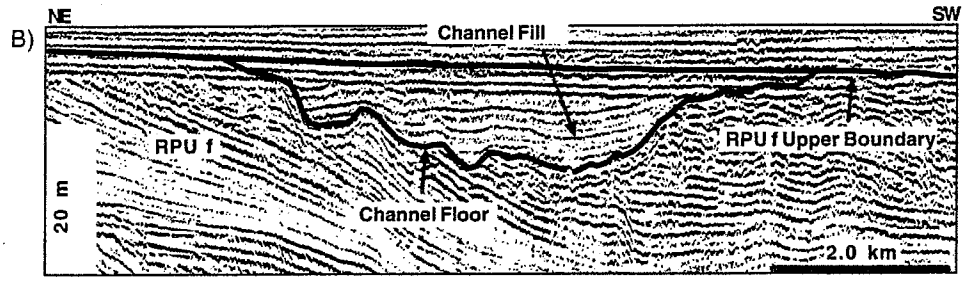

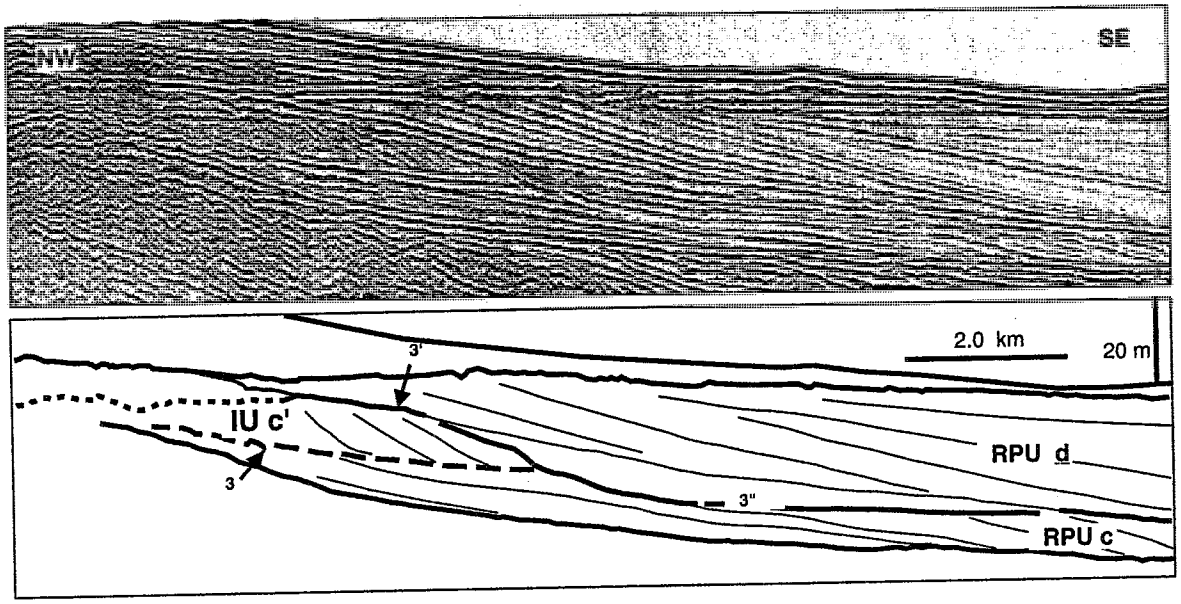

Figure 15—Seismic section (uninterpreted and interpreted) illustrating the external and internal geometry of a proximal intercalated unit (pIU c'). This stratigraphic unit is characterized by oblique to oblique-tangential reflections. The reflections dip seaward with a moderate to strong angle (up to 5–7°). On the interpreted section (bottom) the lower boundary (3) is an erosional and subhorizontal surface (dashed line). The upper boundary (3') is convex upward.

Tesson et al, 2000, AAPG Bull, v 84, p 119-150.

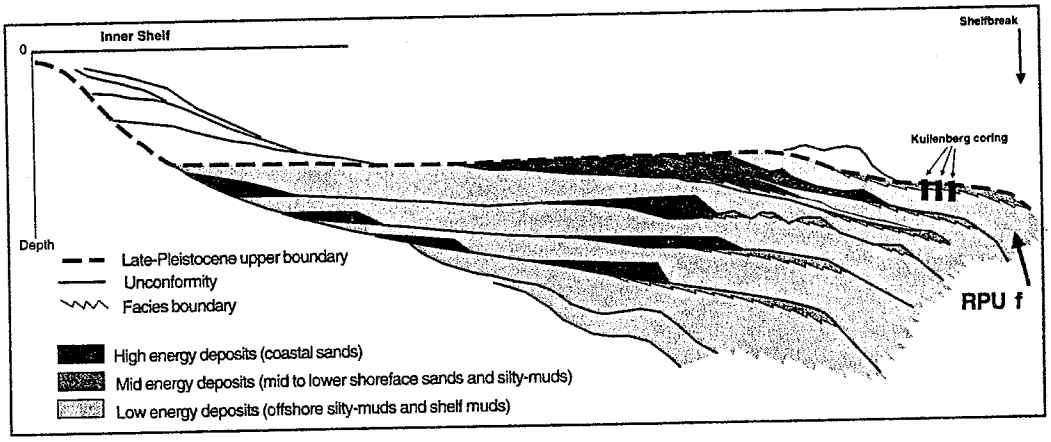

Figure 16—Schematic pattern of late Pleistocene lithology. Interpretation is inferred from seismic facies analysis and calibrated with core data from the uppermost units. Location of samples for C_{14} dating of the uppermost regressive progradational unit (RPU f) (Kullenberg core K-89-16) is given in Table 1.

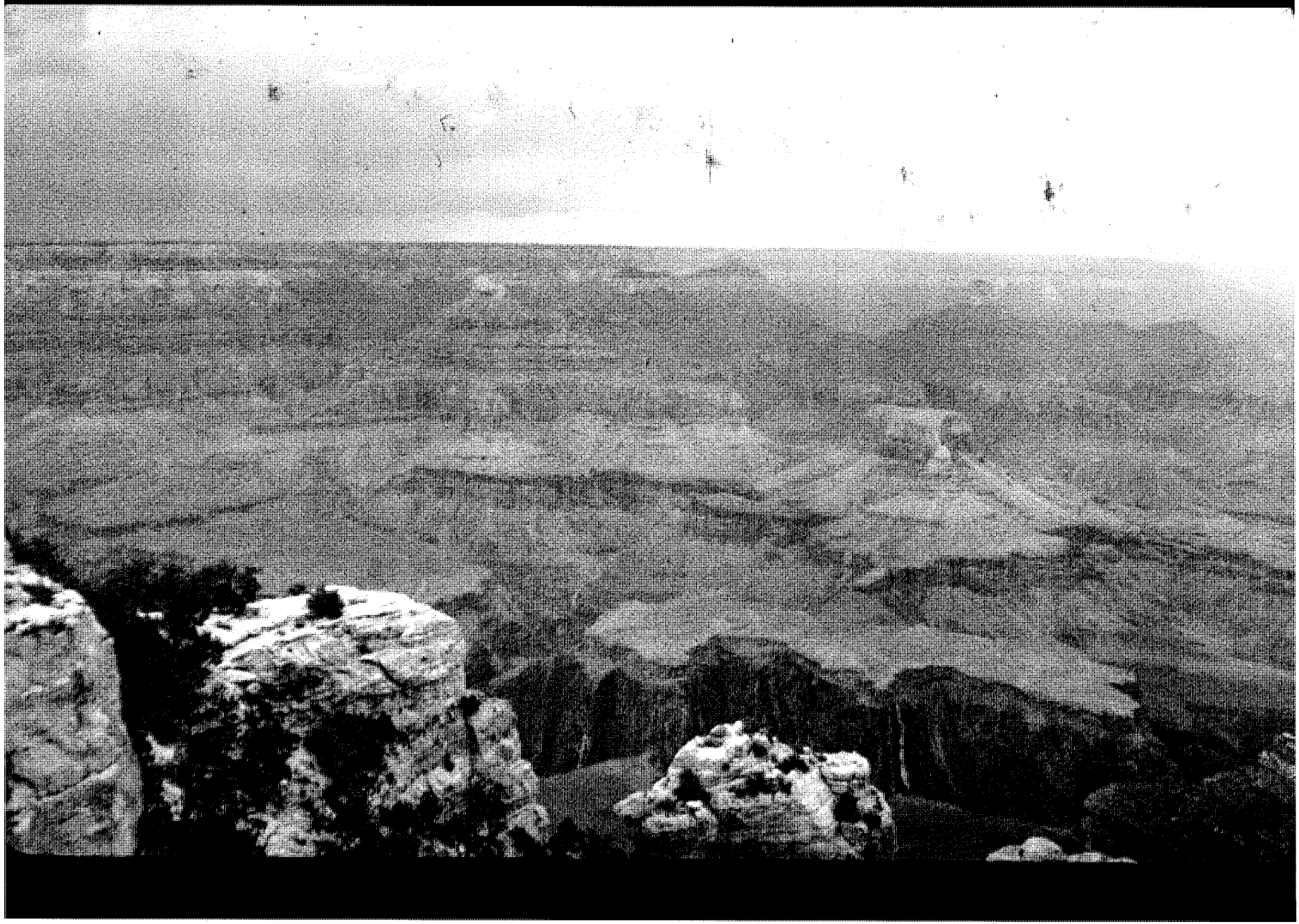

THE CHALLENGE OF RECOGNIZING BASAL TRANSGRESSIVE SANDS

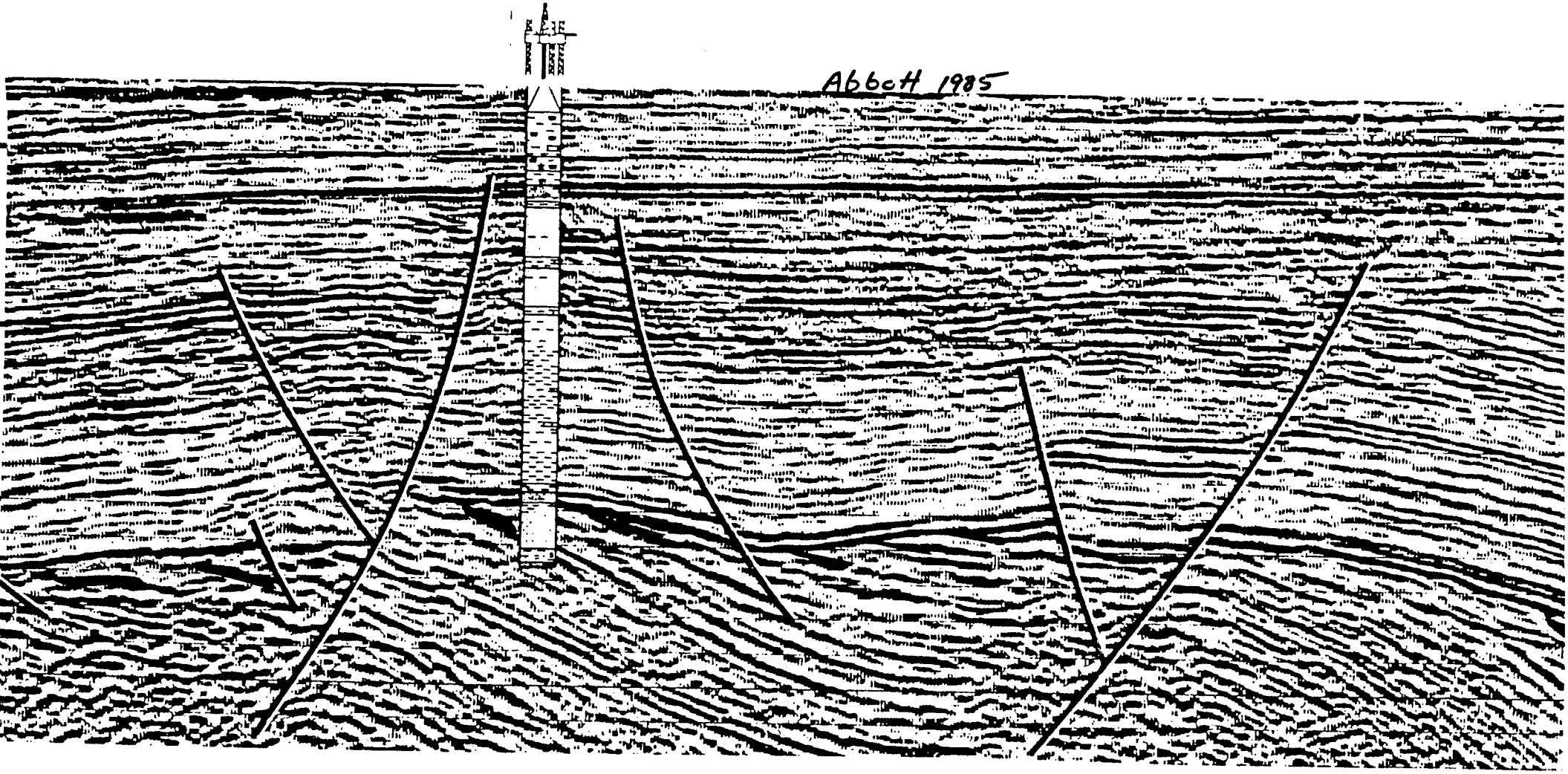

Reality checks from marine slope and basin settings

Strike-Slip Margin off of Los Angeles, California

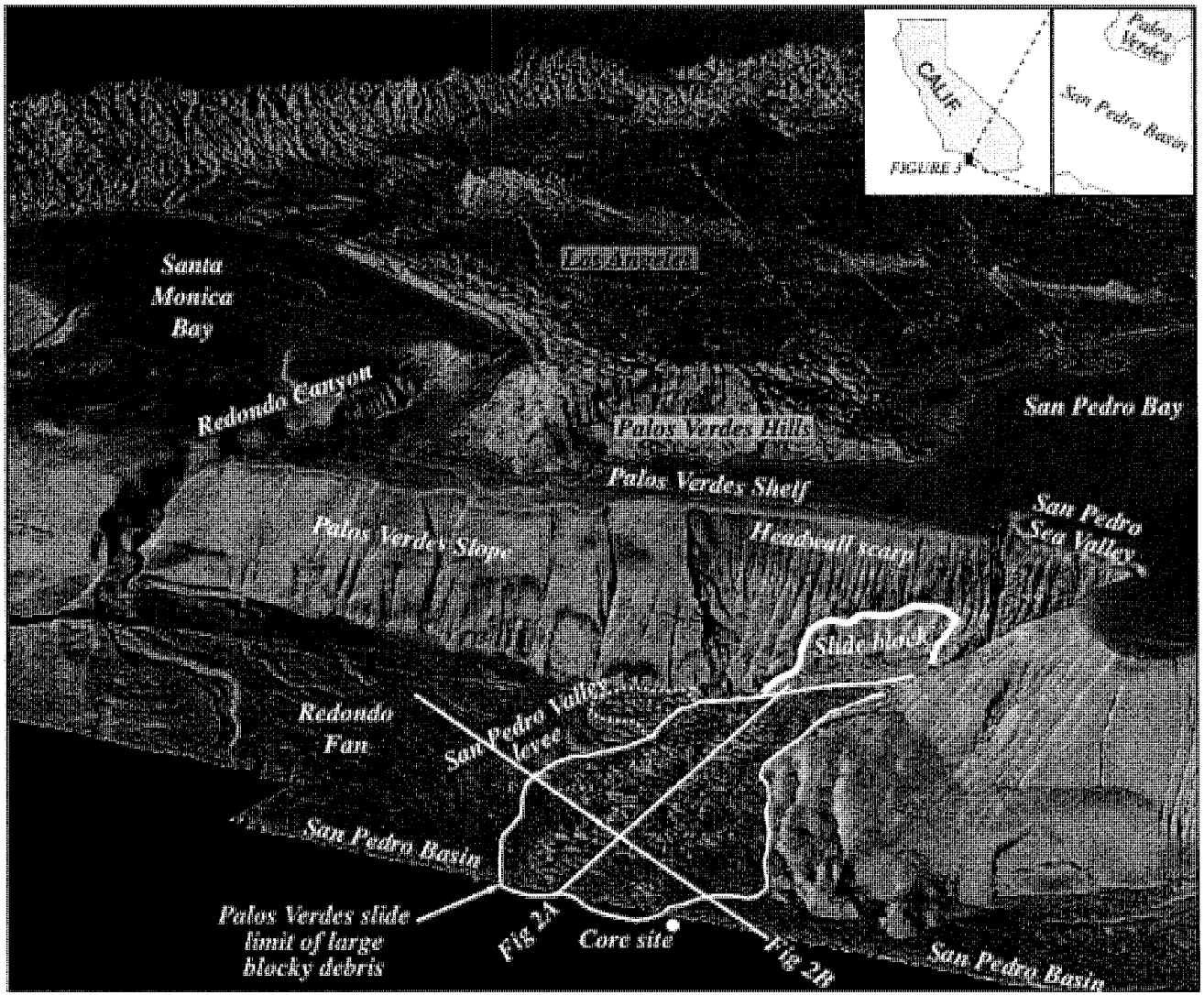

Slope canyon features:

- Localized by shelf incision
- Localized by faulting
- Localized by slope slumping
- Narrow shelves promote access to littoral drift sand

Source:
Bill Normark, USGS

‘Mature’ Rifted Margin Dominated by Salt Tectonics

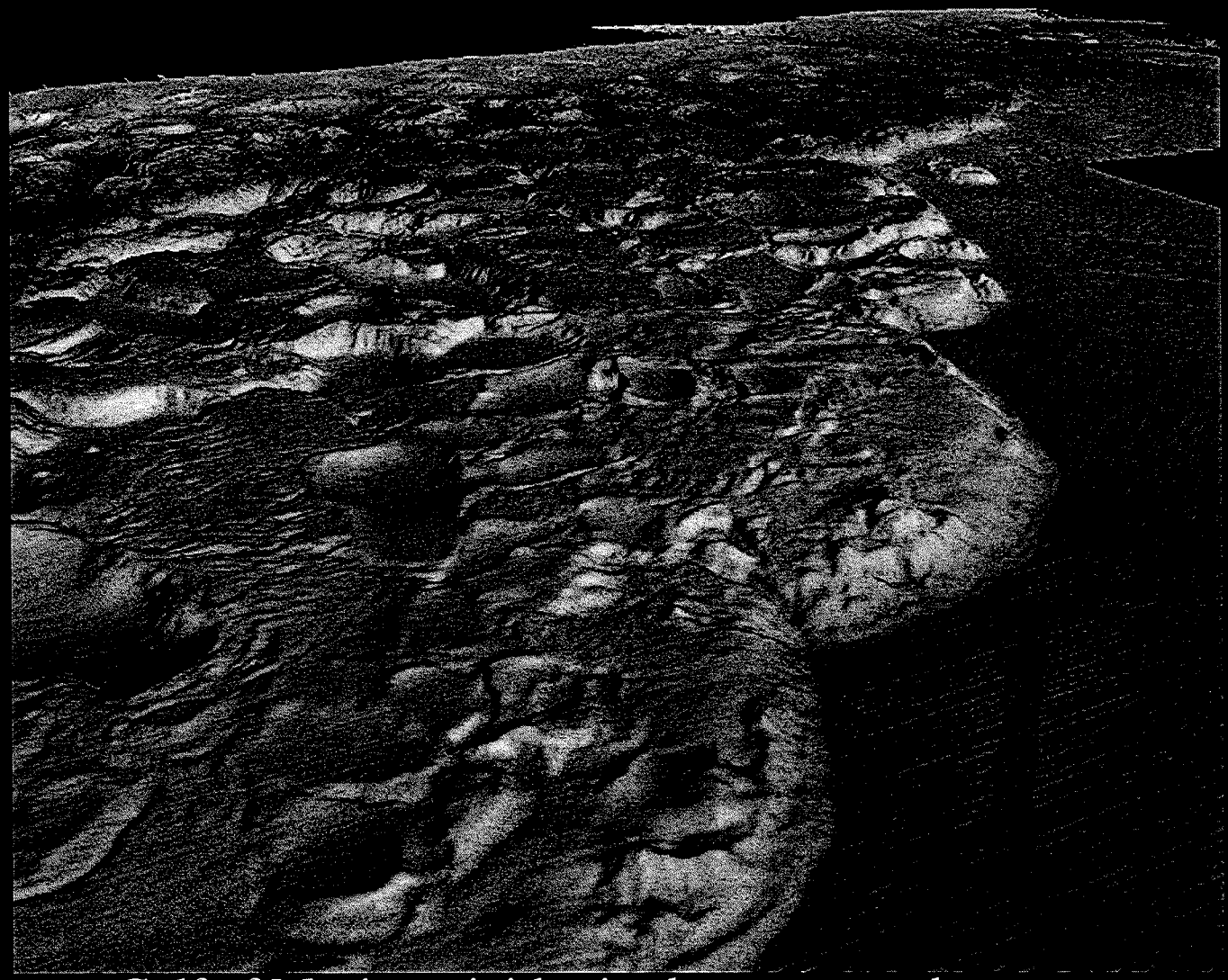

Gulf of Mexico mini-basin slope topography

Source: Lincoln Pratson

Convergent Margin of Oregon

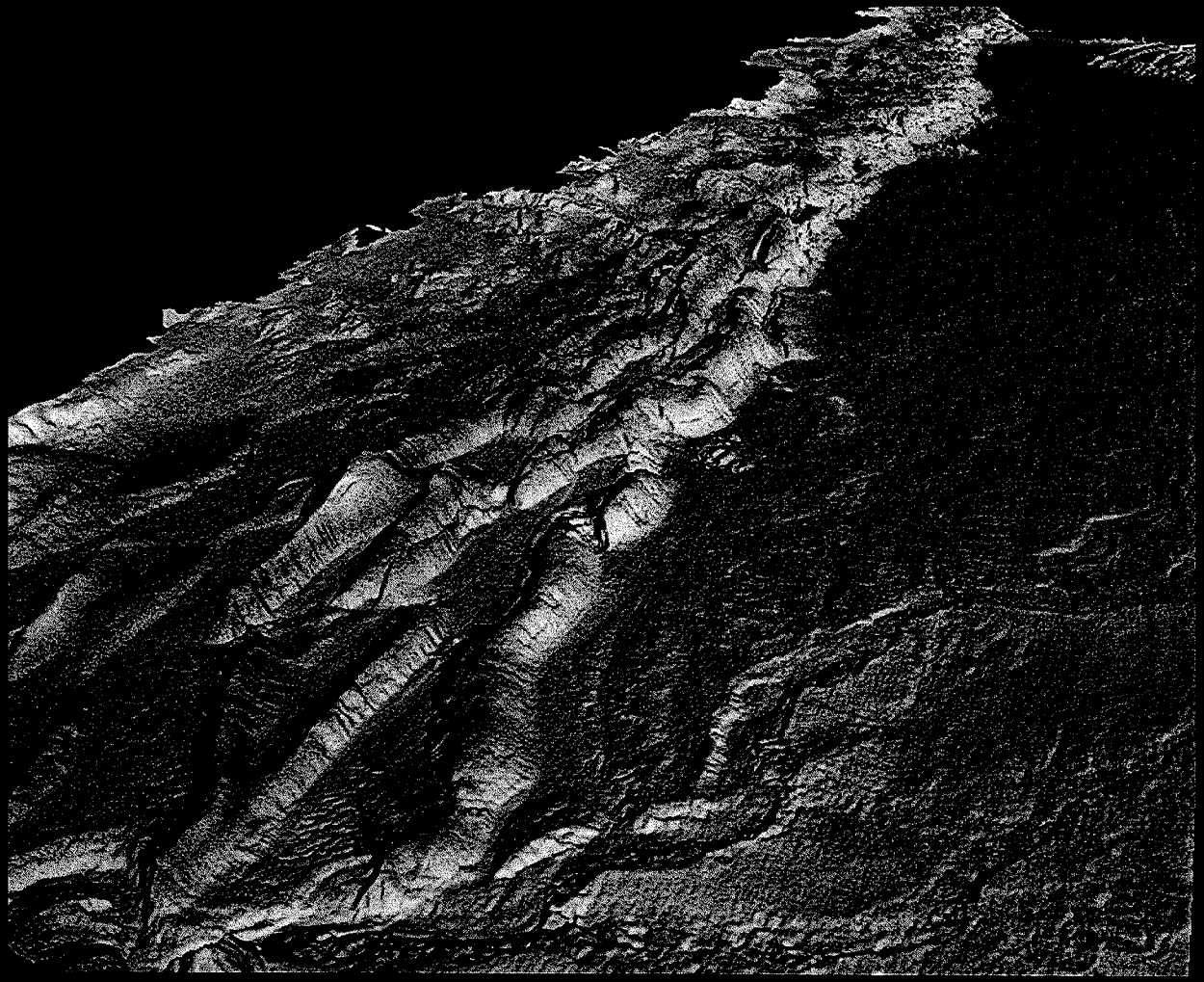

Ponded basins on slope arise
from subduction-related faulting,
as well as large-scale slumping

Source: Lincoln Pratson

THE SLOPE ENVIRONMENT: SHELF TO BASIN TRANSITION.

CANYON & NON-CANYON EXAMPLES

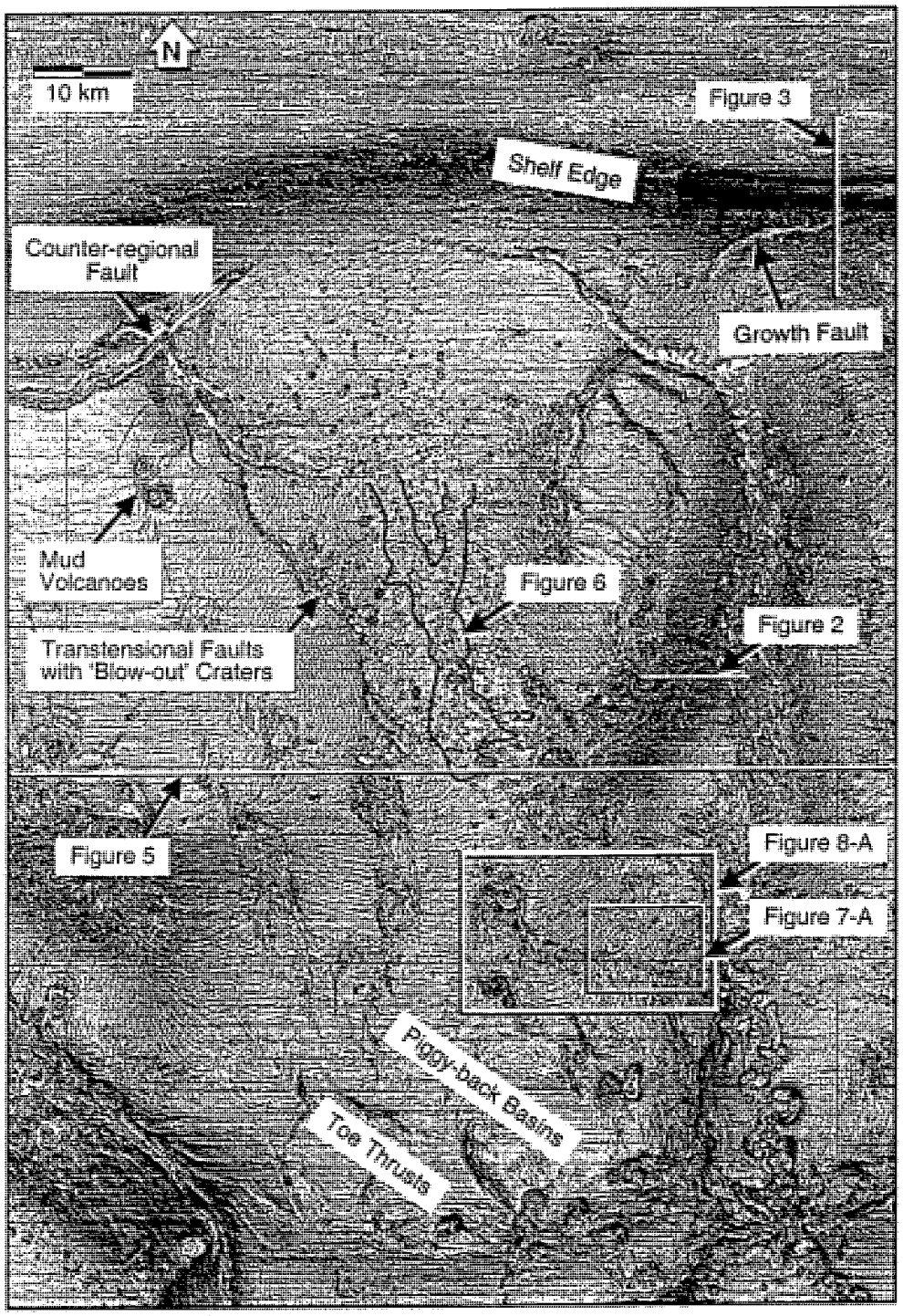

Figure 4—Shaded bathymetric map of the entire study area (Figure 1) displayed to emphasize linear trends. The featureless plain at the north is the shelf. Shaded relief accentuates the shelf edge, counter-regional growth faults, growth faults, transtensional fault zones along the margins of the megaslide, small-scale sea-floor craters, mud volcanoes, piggyback basins, and the toe-thrust zone. The bold outline locates the turbidite system, shown in Figure 6A, within the sea-floor "slide valley."

Armentrout et al, 2000
AAPG Mem 72, p93-108

Sylvester:
http://see-atlas.leeds.ac.uk:8080/
CGG Veritas
Niger Delta

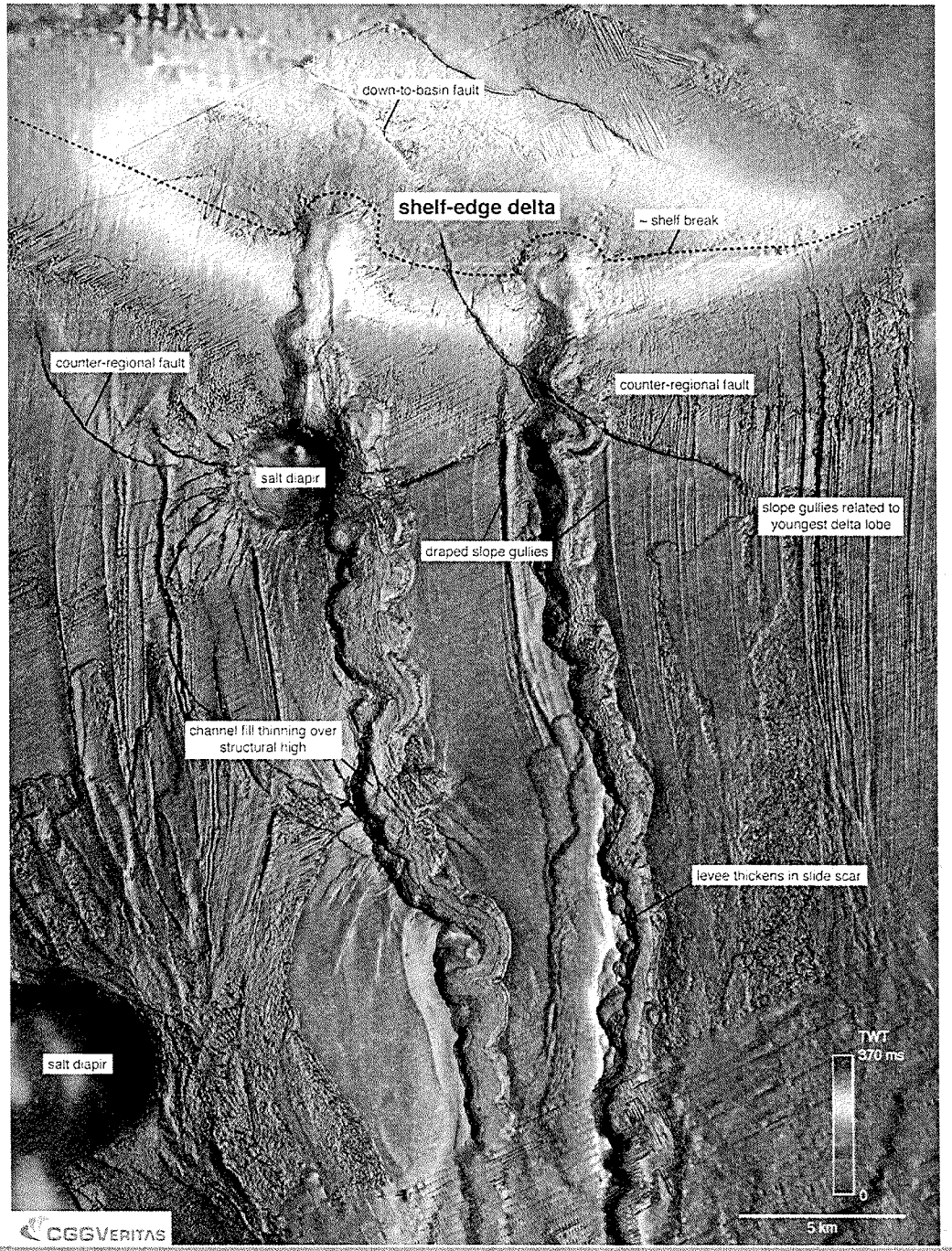

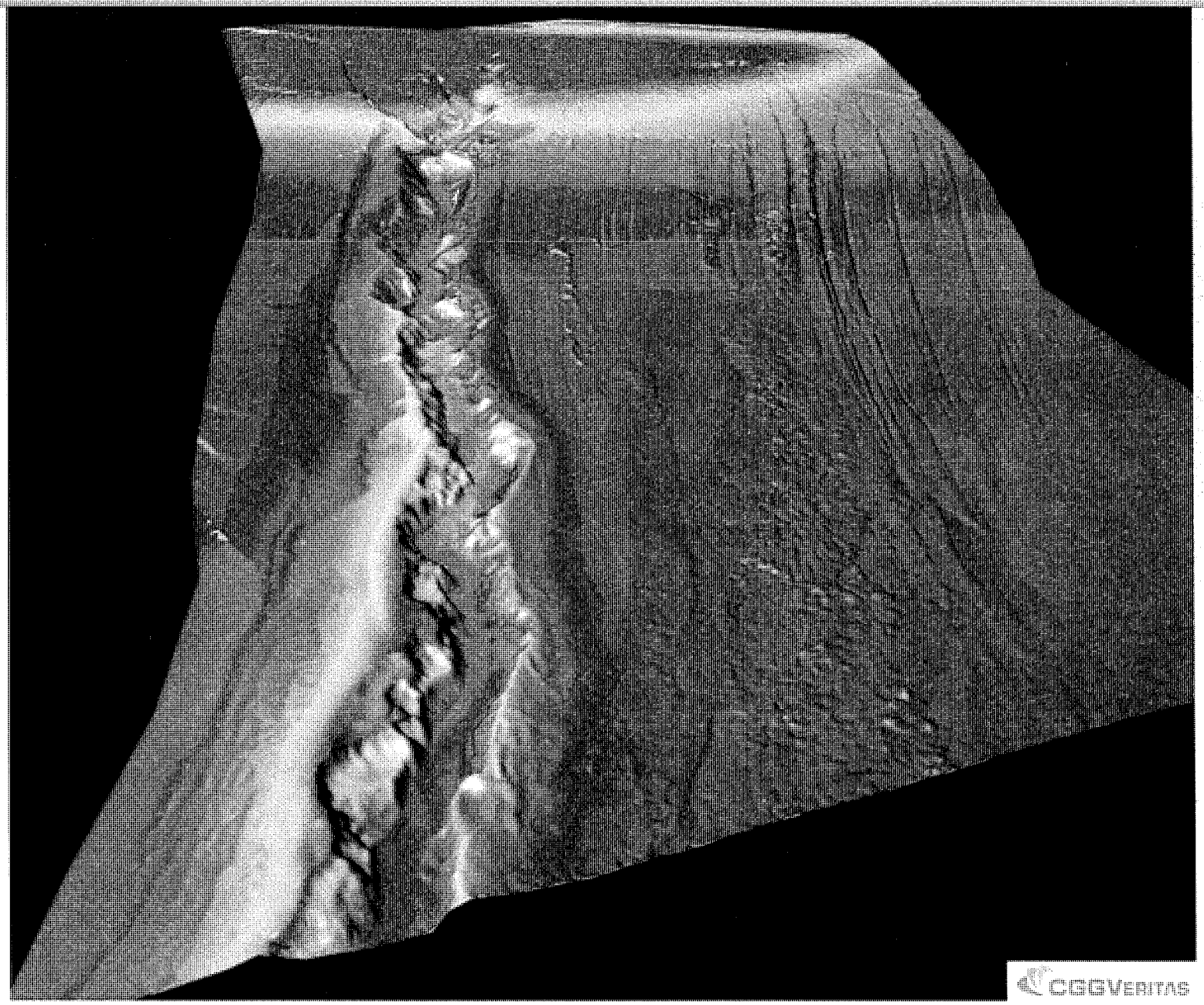

Sylvester: http://see-atlas.leeds.ac.uk:8080/ CGG Veritas Niger Delta slope

Sylvester:
http://see-atlas.leeds.ac.uk:8080/
CGG Veritas
Niger Delta

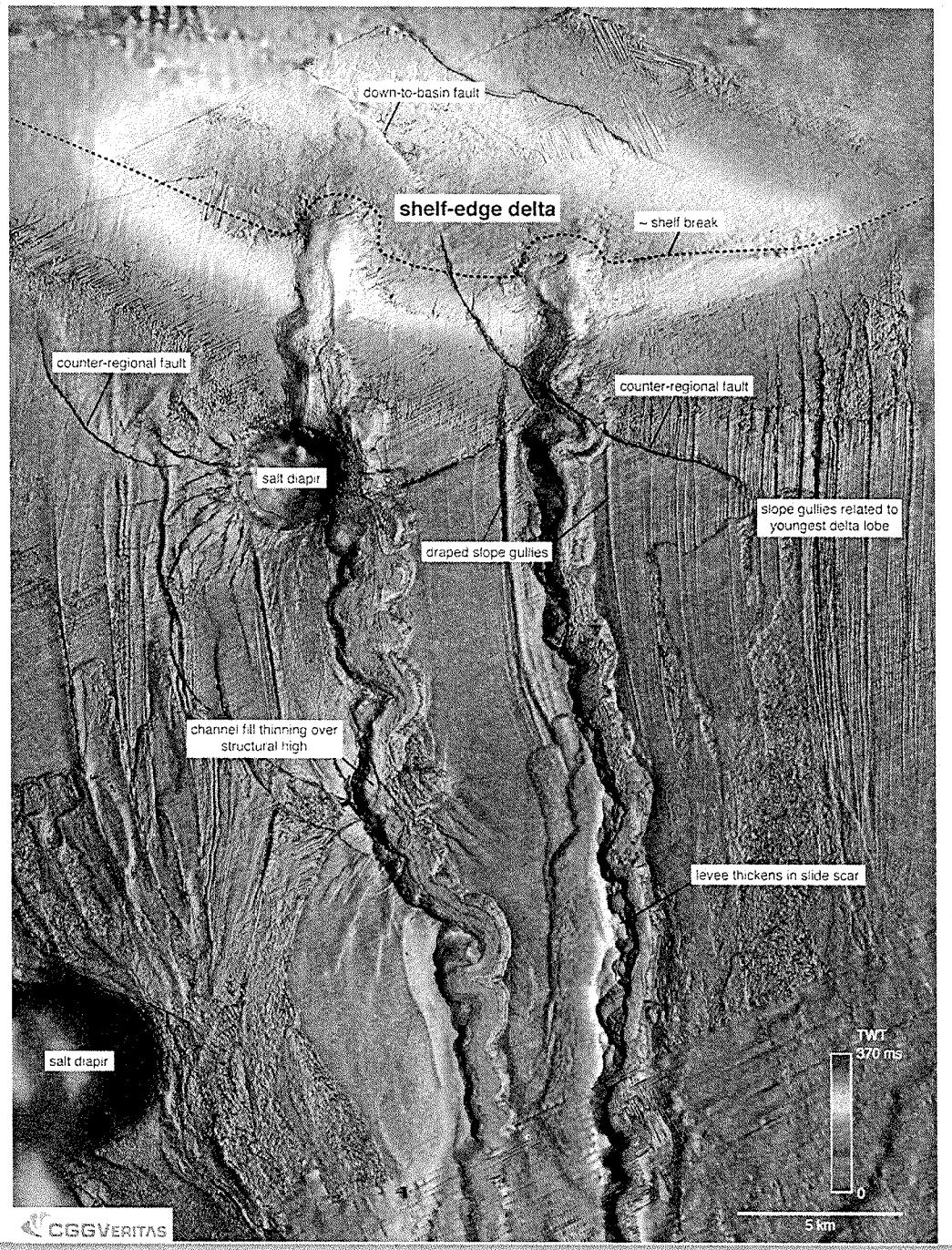

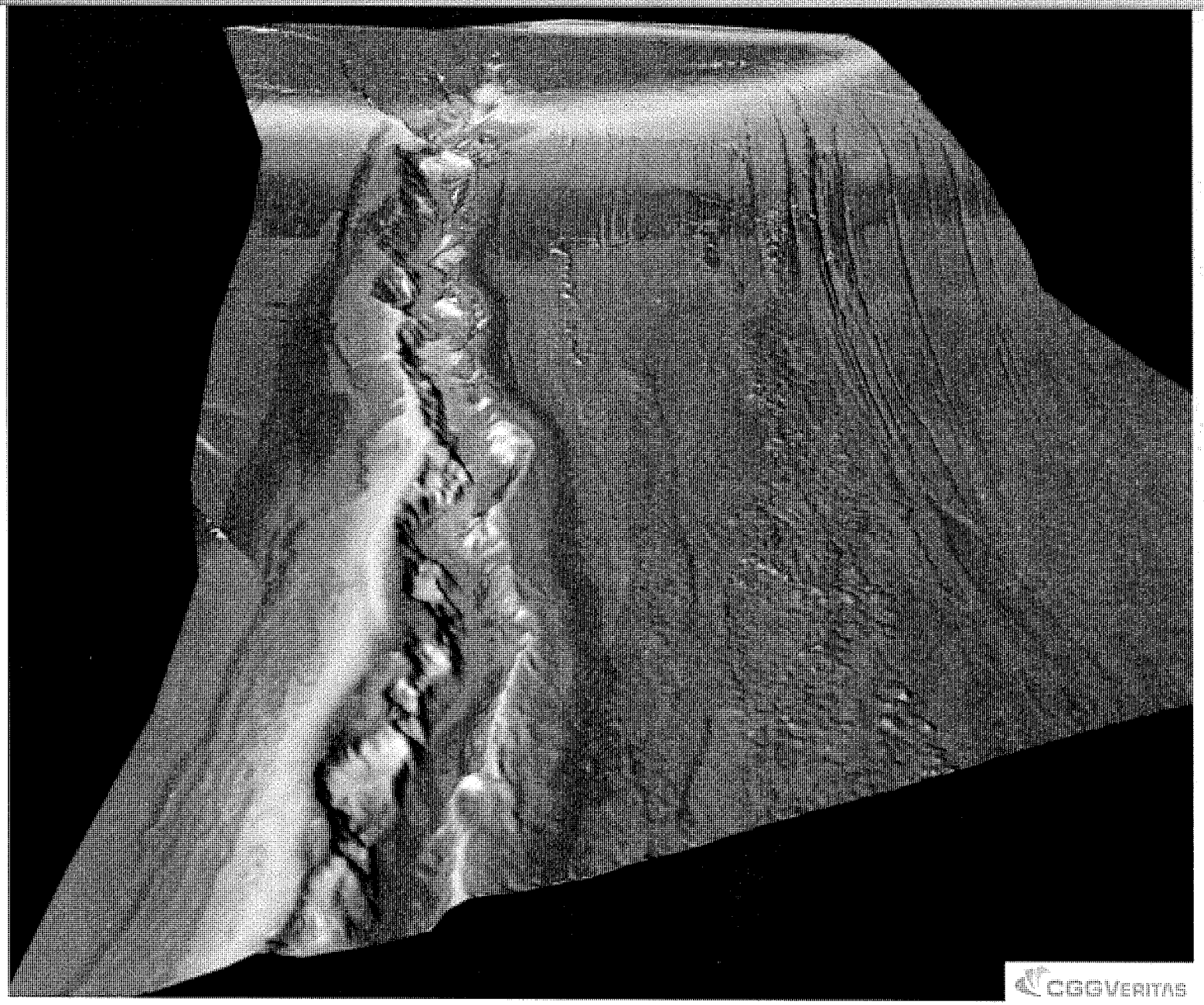

Sylvester: http://see-atlas.leeds.ac.uk:8080/ CGG Veritas Niger Delta slope

Jobe: http://see-atlas.leeds.ac.uk:8080/ Equatorial Guinea slope

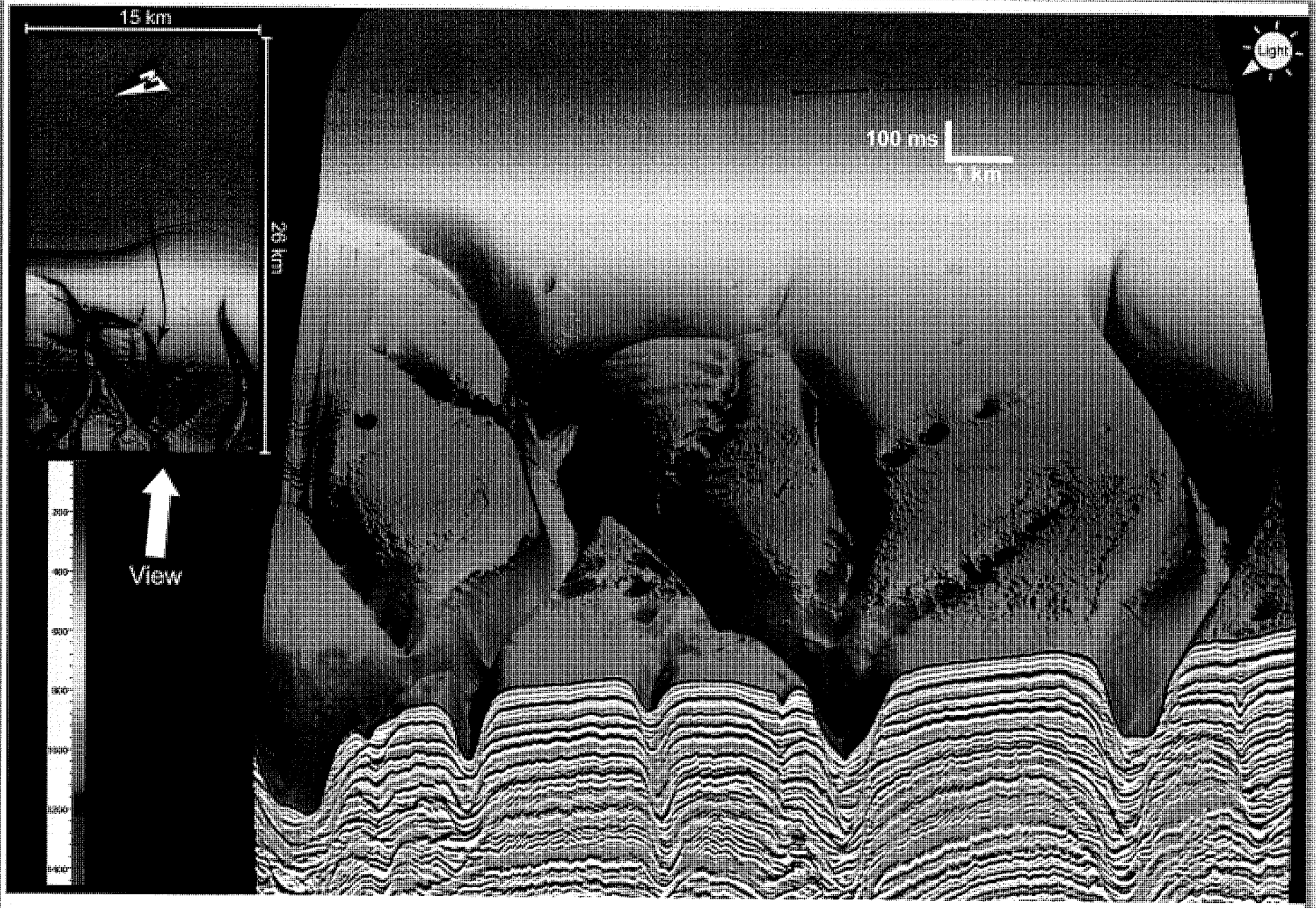

Jobe: http://see-atlas.leeds.ac.uk:8080/ Equatorial Guinea slope

Mixed Sand and Mud System:

Mahakam Channel-Levee Complex

Seismic imaging of failure-dominated submarine slopes

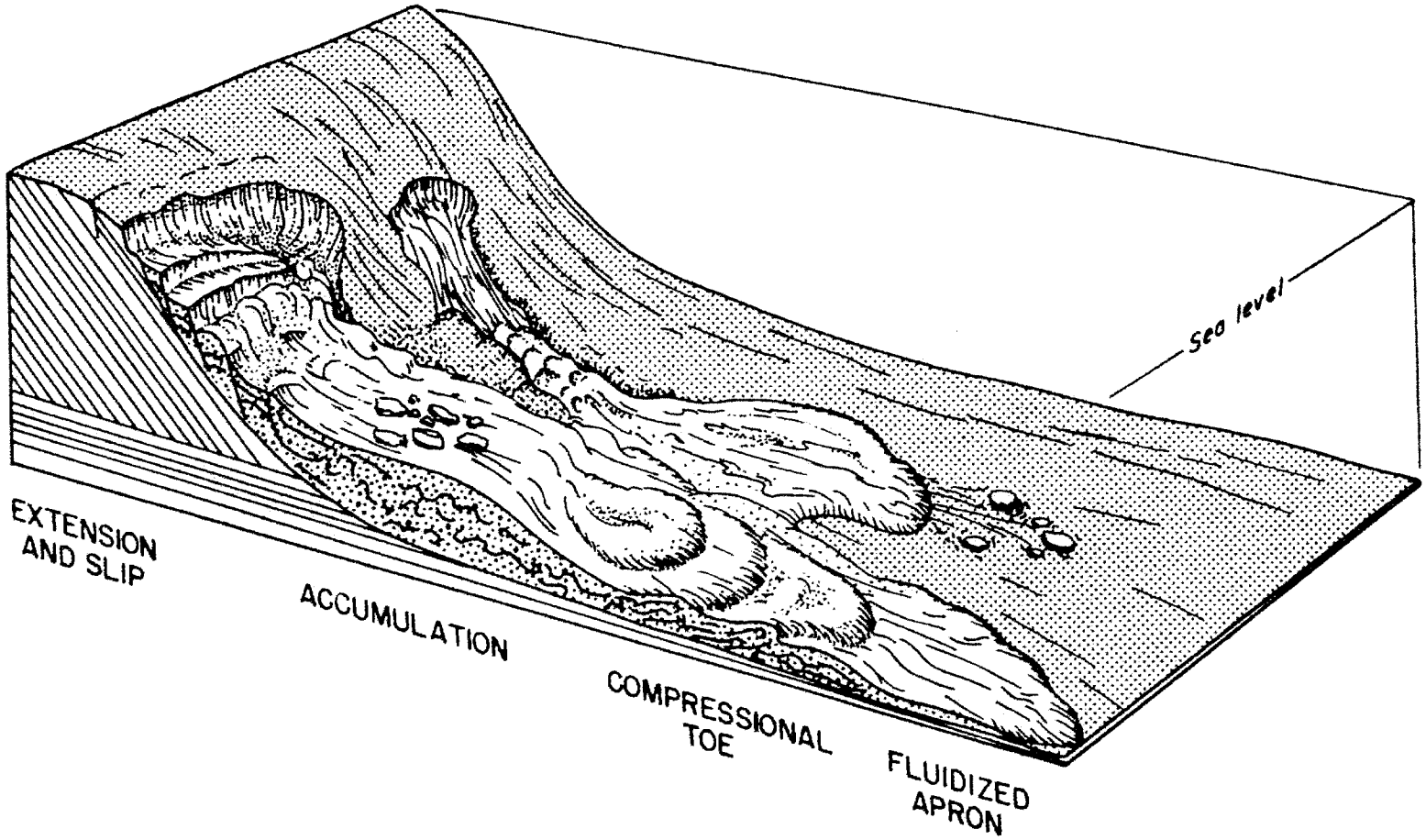

Galloway, 1998, AAPG Bull. V. 82, p. 569-595.

Continental Slopes

- Ancient slope successions:

-often characterized by slump deposits and accumulations of sand that were strongly influenced by slope topography

- turbidity currents also play an important role in shaping the slope environment, particularly in supplying relatively 'clean', well-sorted sand

Slumped mudstone-rich blocks and lenticular packages of turbiditic sandstone, Tres Pasos Formation, Chile

Miocene, Taranaki Basin, New Zealand

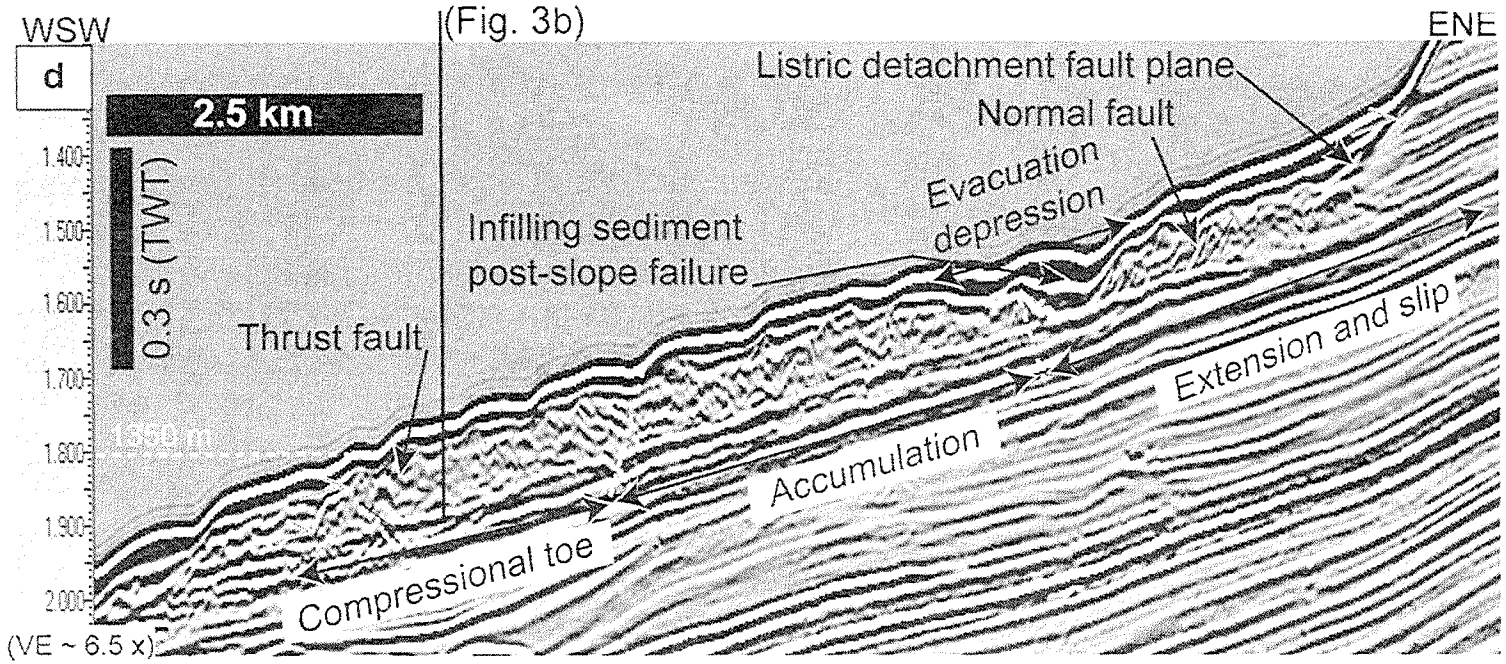

Fig. 3. Seismic profiles showing downslope variations in the morphology of the southernmost tributary slope channel system. (**a**) Strike seismic profile in the upper slope. (**b**) Strike seismic profile in the middle slope. (**c**) Strike seismic profile in the lower-middle slope. (**d**) Seismic profile in the upper slope showing a slope failure on a tributary interfluve. Note this is a dip profile, perpendicular to Figure 3(b). (**e**) Seabed bathymetric map of area I showing the seismic profile locations of Figure 3(a–d). Refer to Figure 2 for location of area I within the study.

Schwab et al., 2007

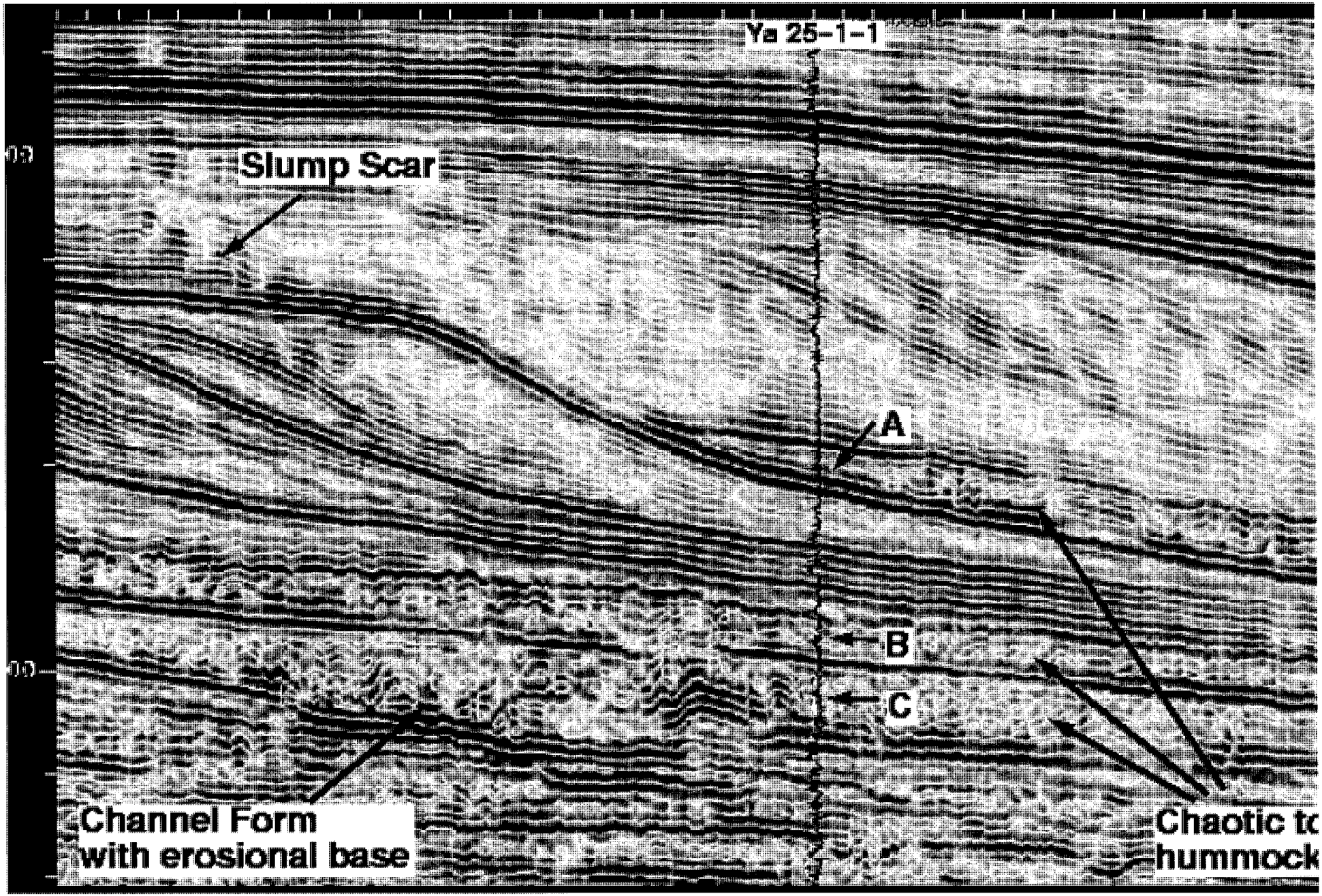

Plio–Pleistocene Shelf Progradation and Basinal Wedges, South China Sea

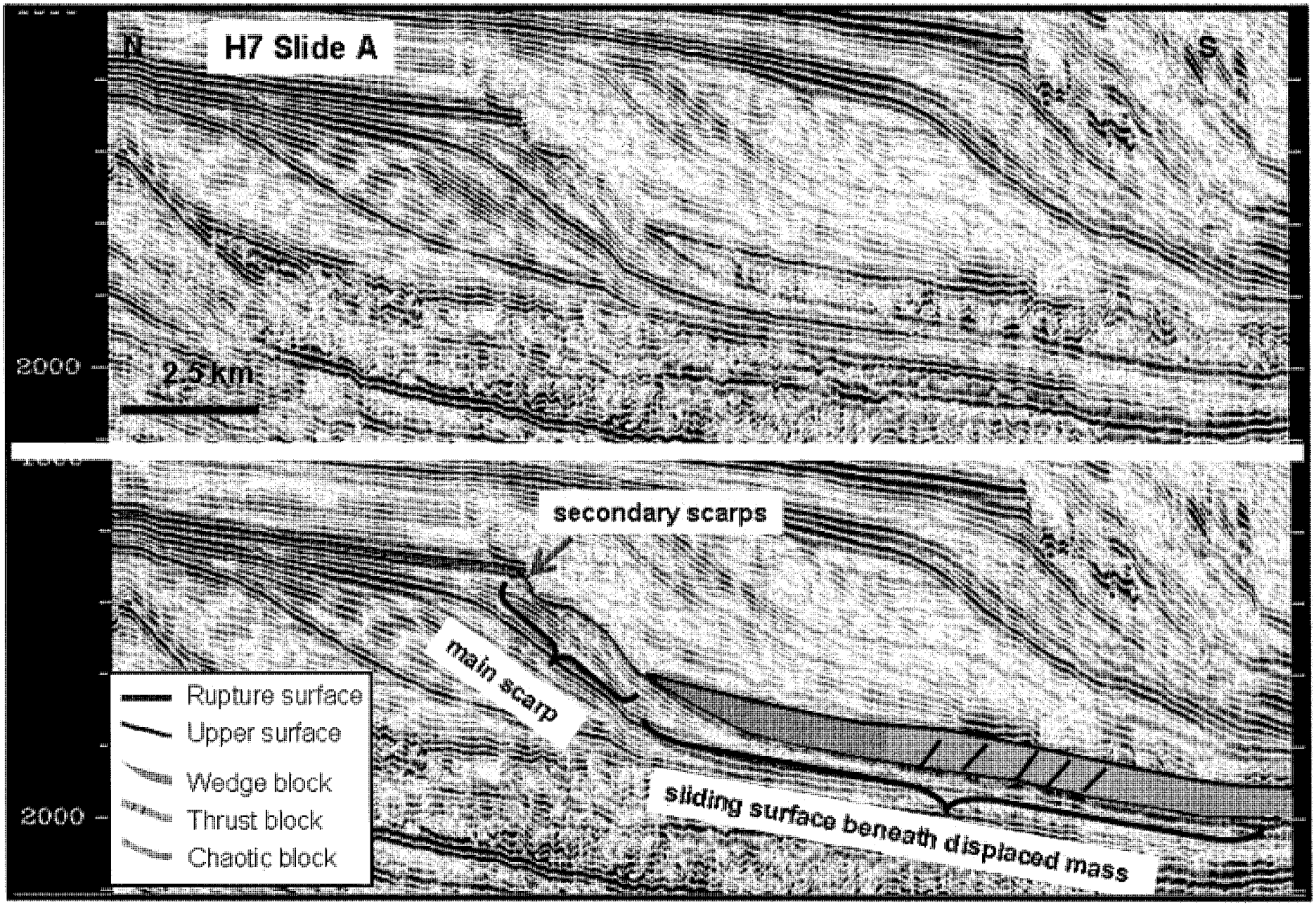

Fig. 11 Dip section of Elements of submarine landslide A along the Horizon 7

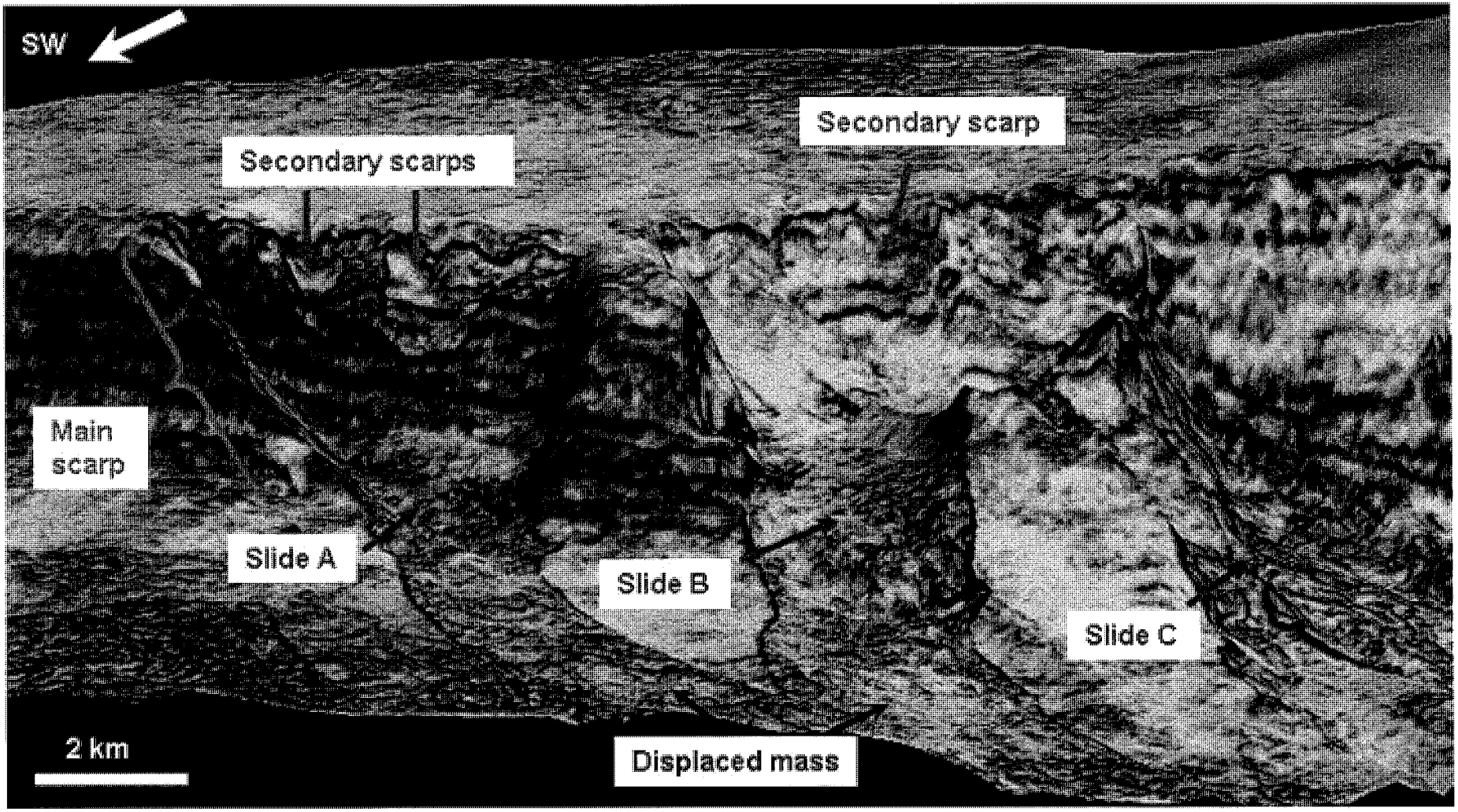

Fig. 9 3-D amplitude extraction map of the submarine landslides along the Horizon 7

Seismic imaging of submarine canyons

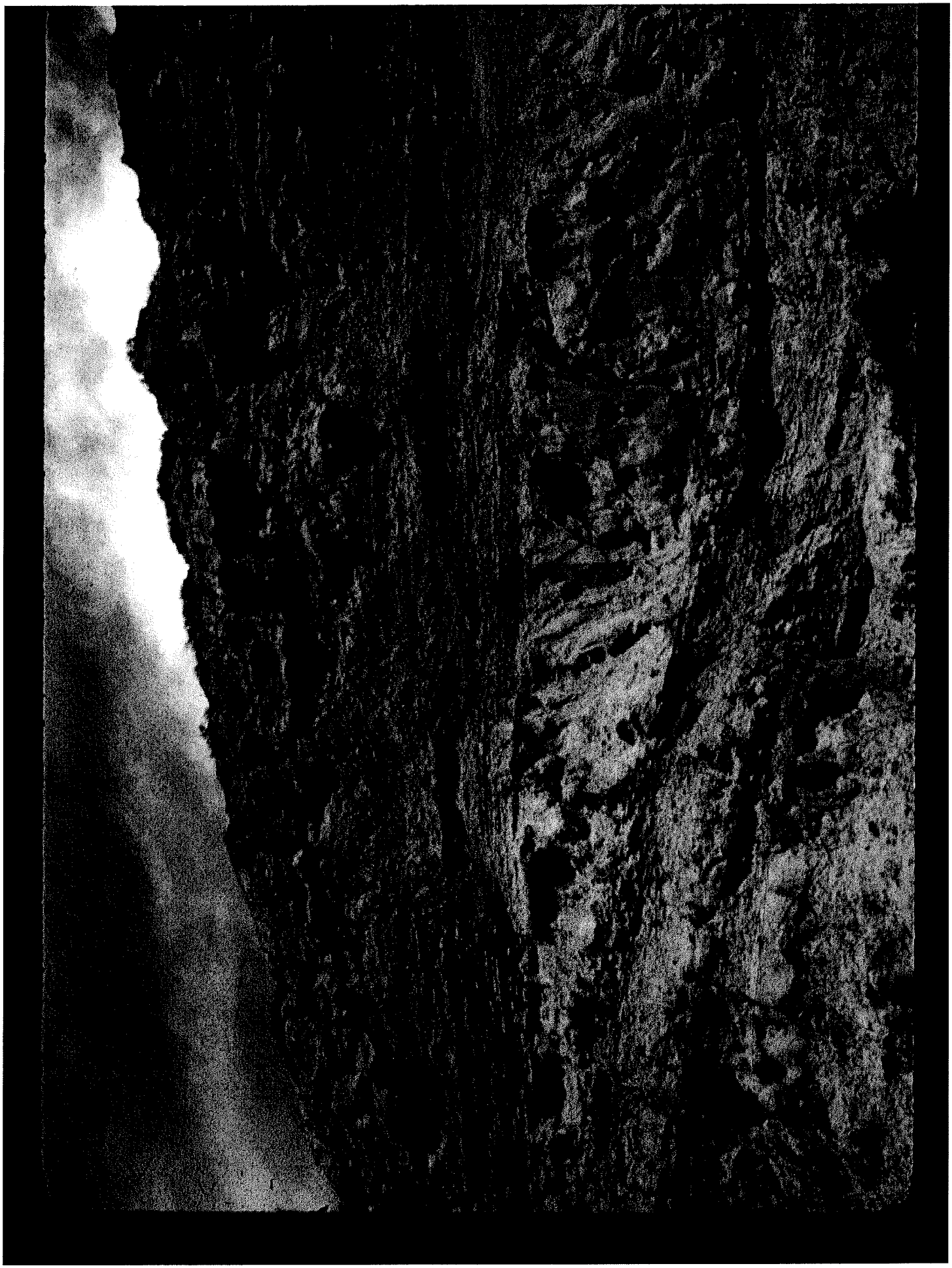

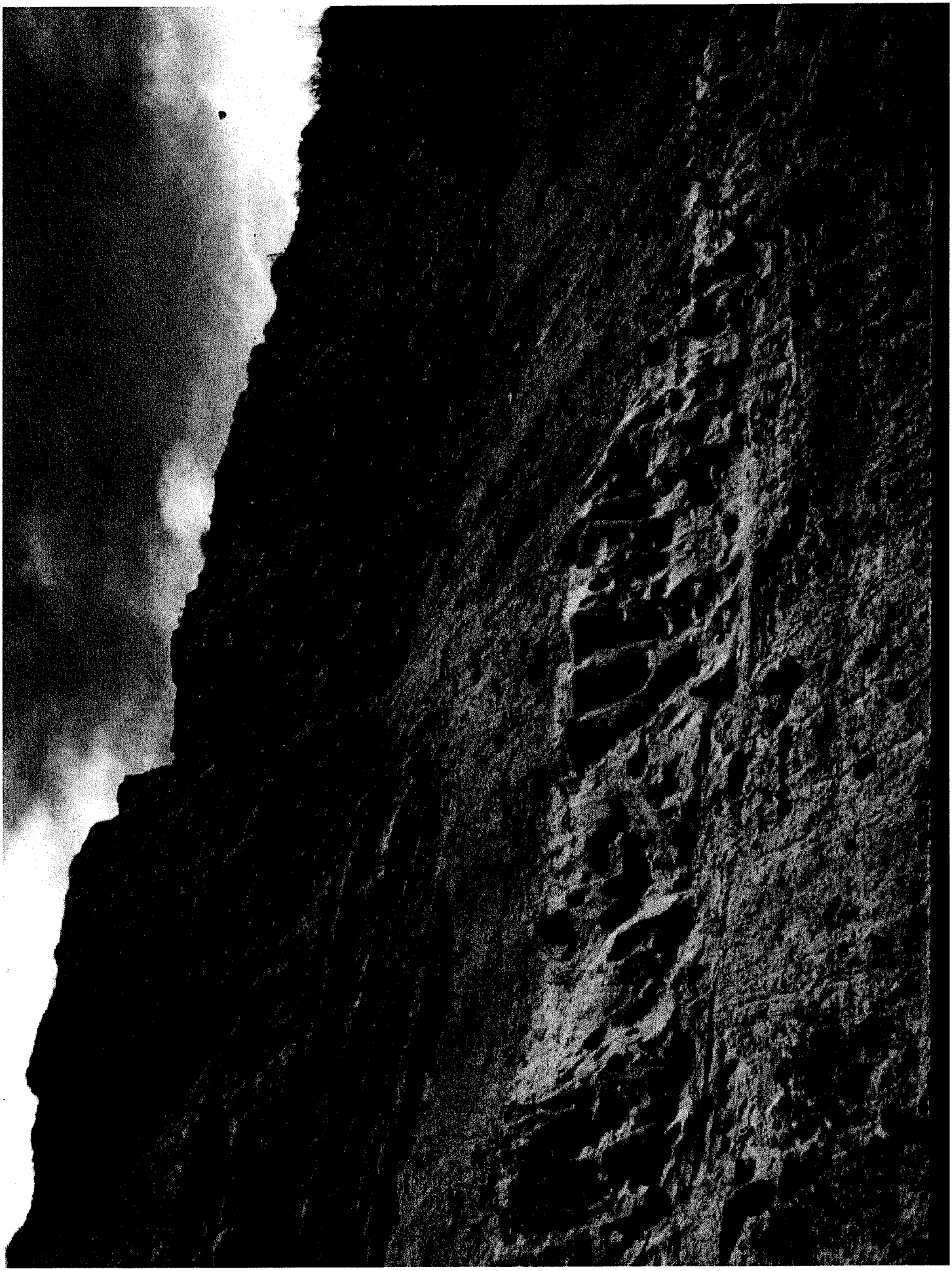

FIGURE 3.5.3-5
(After Farr, 1976)
(Courtesy Western)

Anstey —
Seismic explor
For ss reserv.

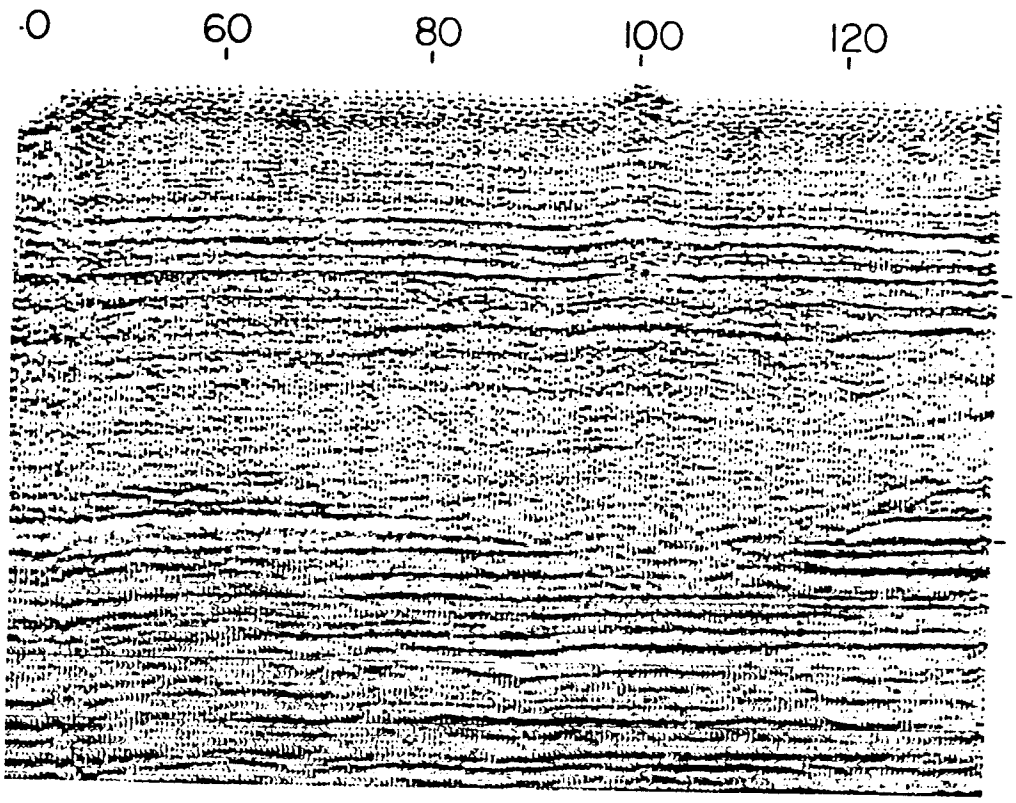

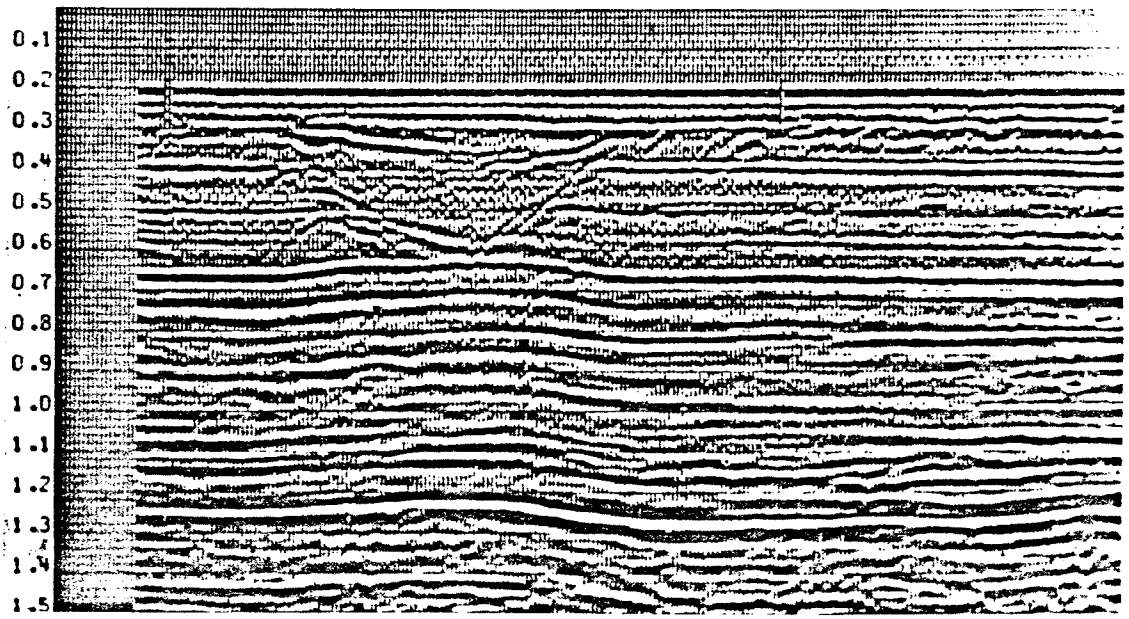

FIGURE 3.5.3-1

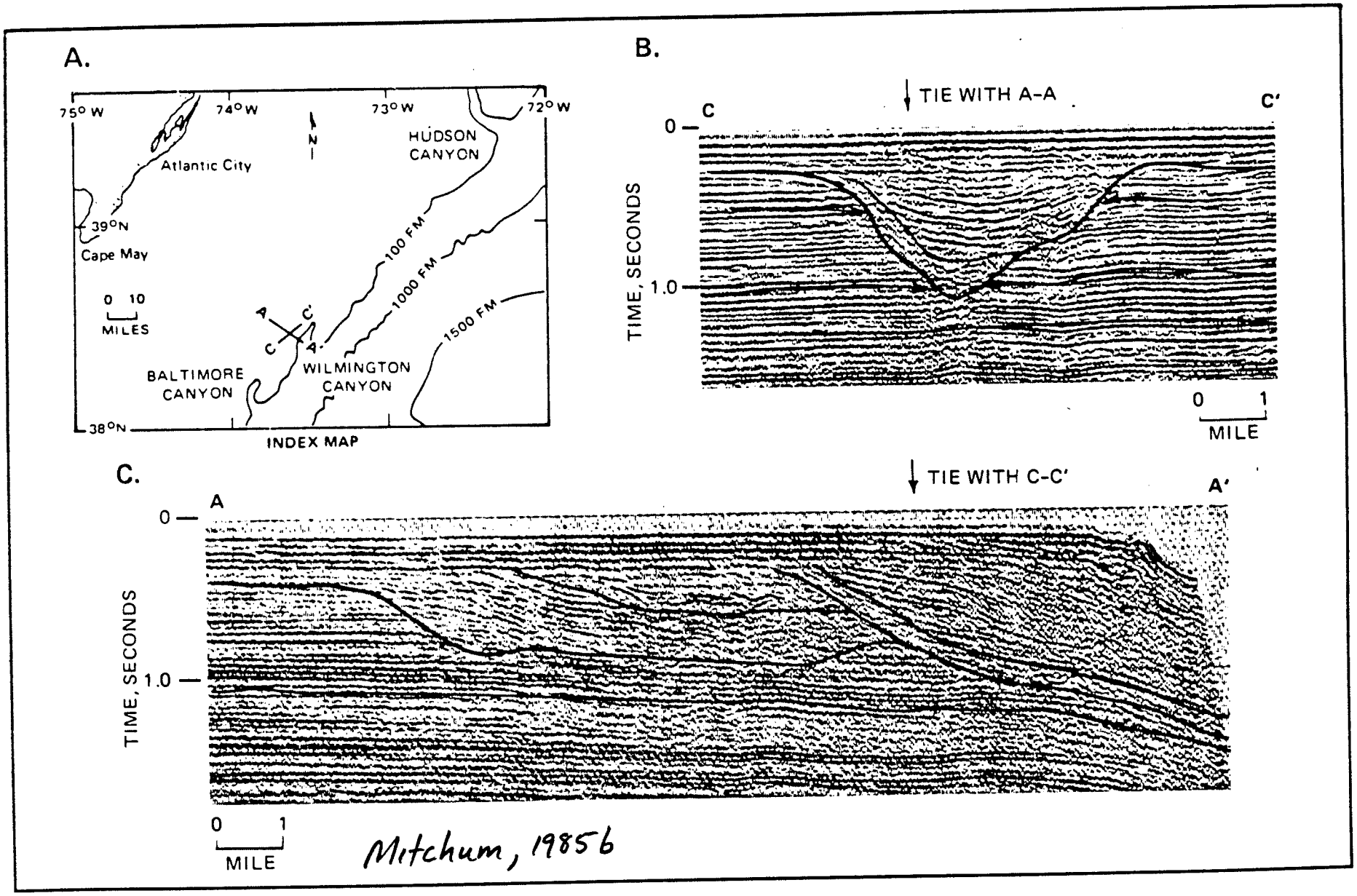

Mitchum, 1985b

e Field

in Graham (ed) 1981
← Pacific Section AAPG Volume 50

NE

232

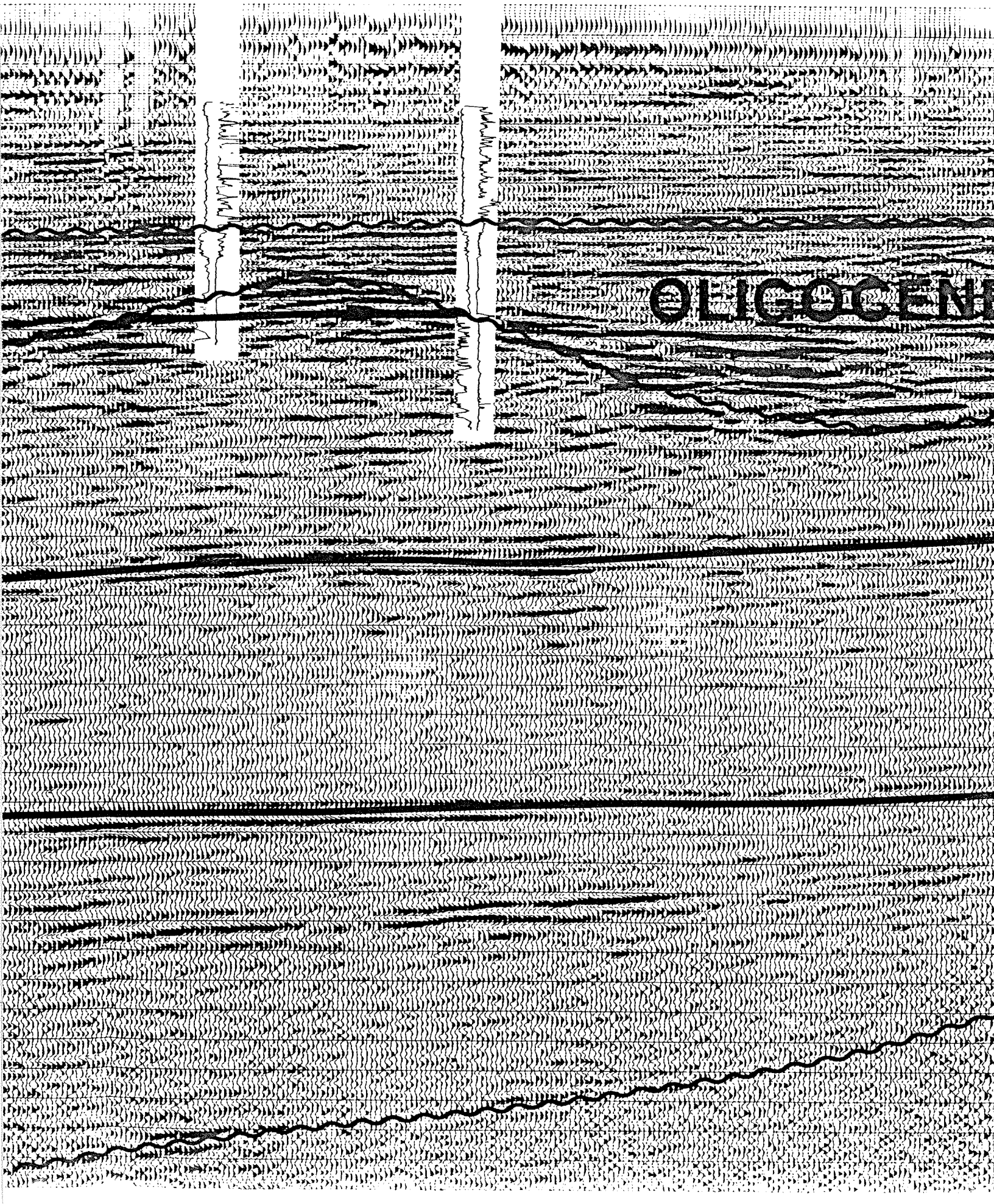

Seismic Evidence for Submarine Canyons

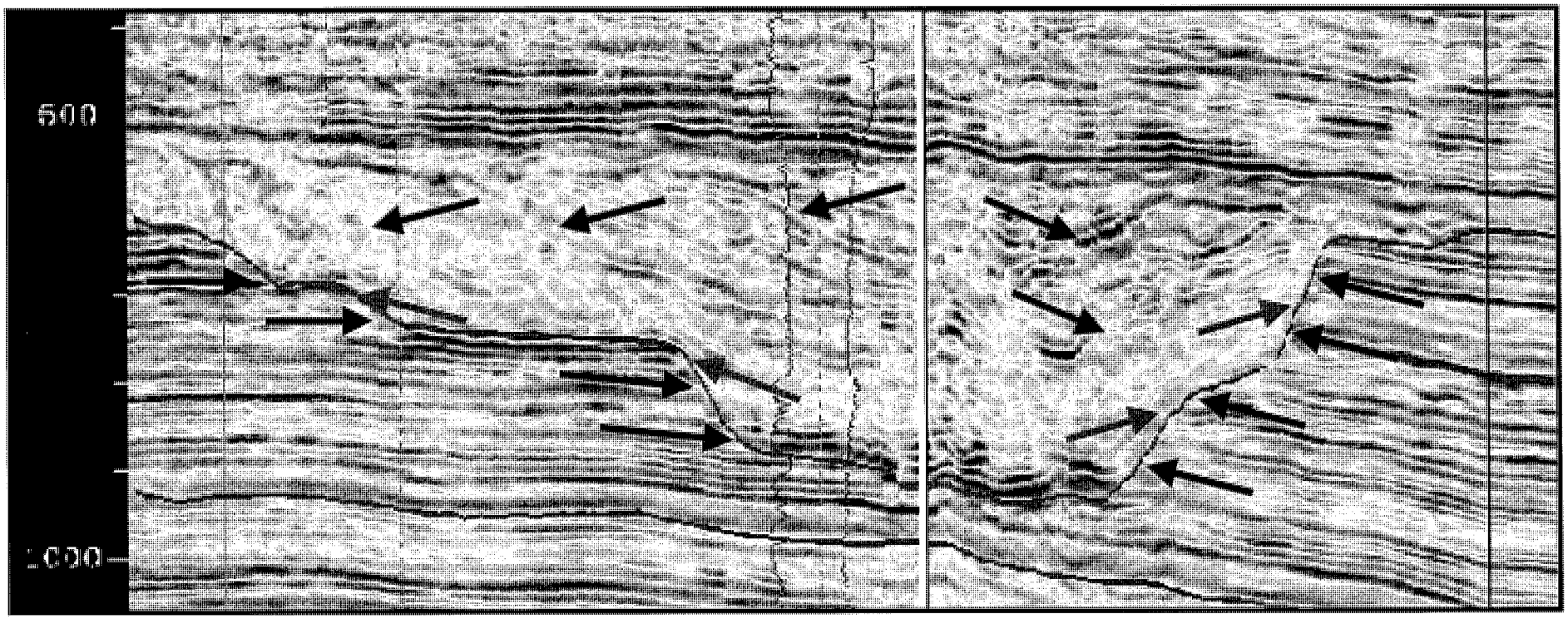

Truncation of underlying reflections

Onlap of overlying reflections

Drape of overlying reflections

Dip discordance across unconformity

TRM 3/20/2001

ARCHITECTURAL ELEMENTS

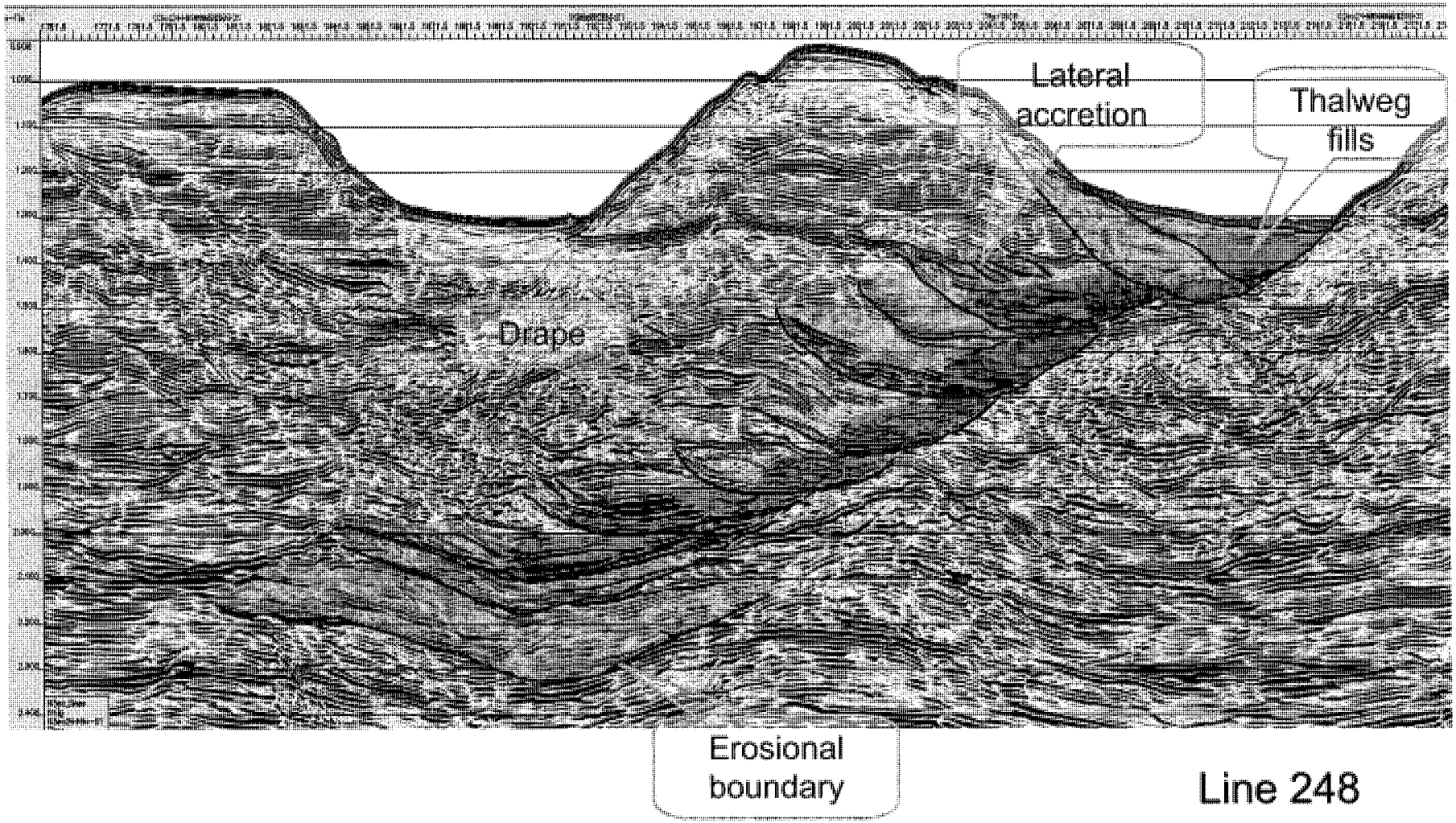

DEEP-WATER DEPOSITIONAL SYSTEMS

230

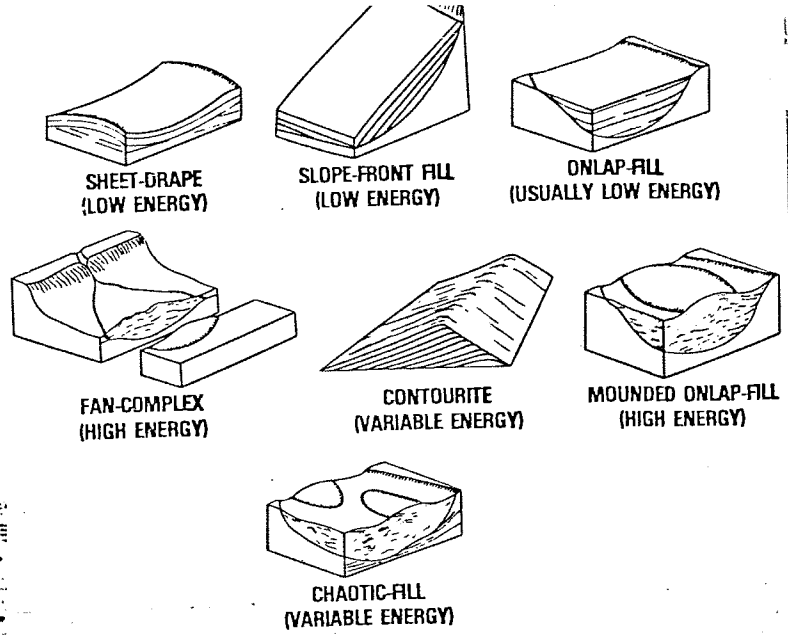

FIG. 9—Basin slope and floor seismic facies types.

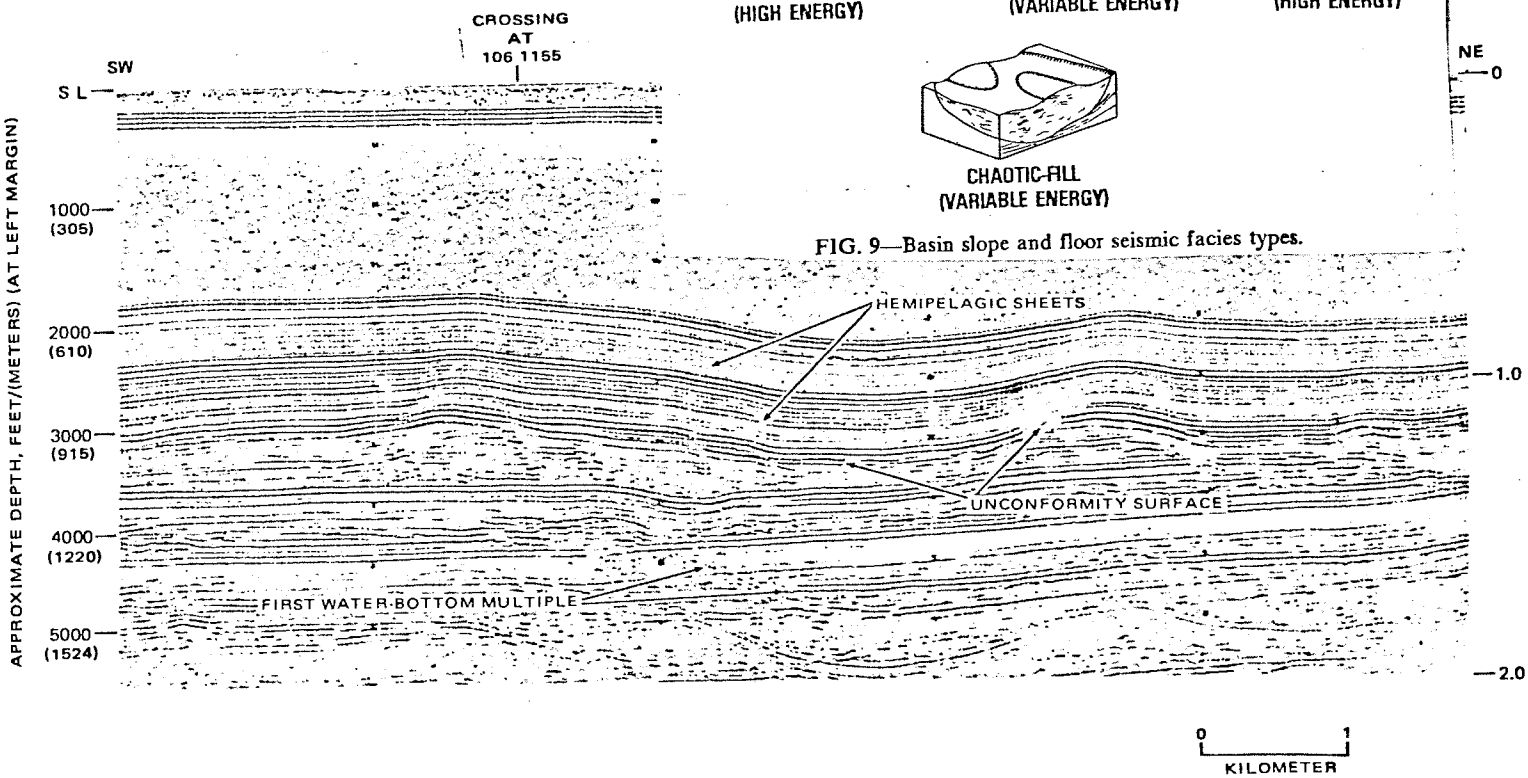

FIG. 10—Sheet-drape seismic facies, Gulf of Mexico. Near-surface reflectors display strong drape over several hundred feet of topographic relief.

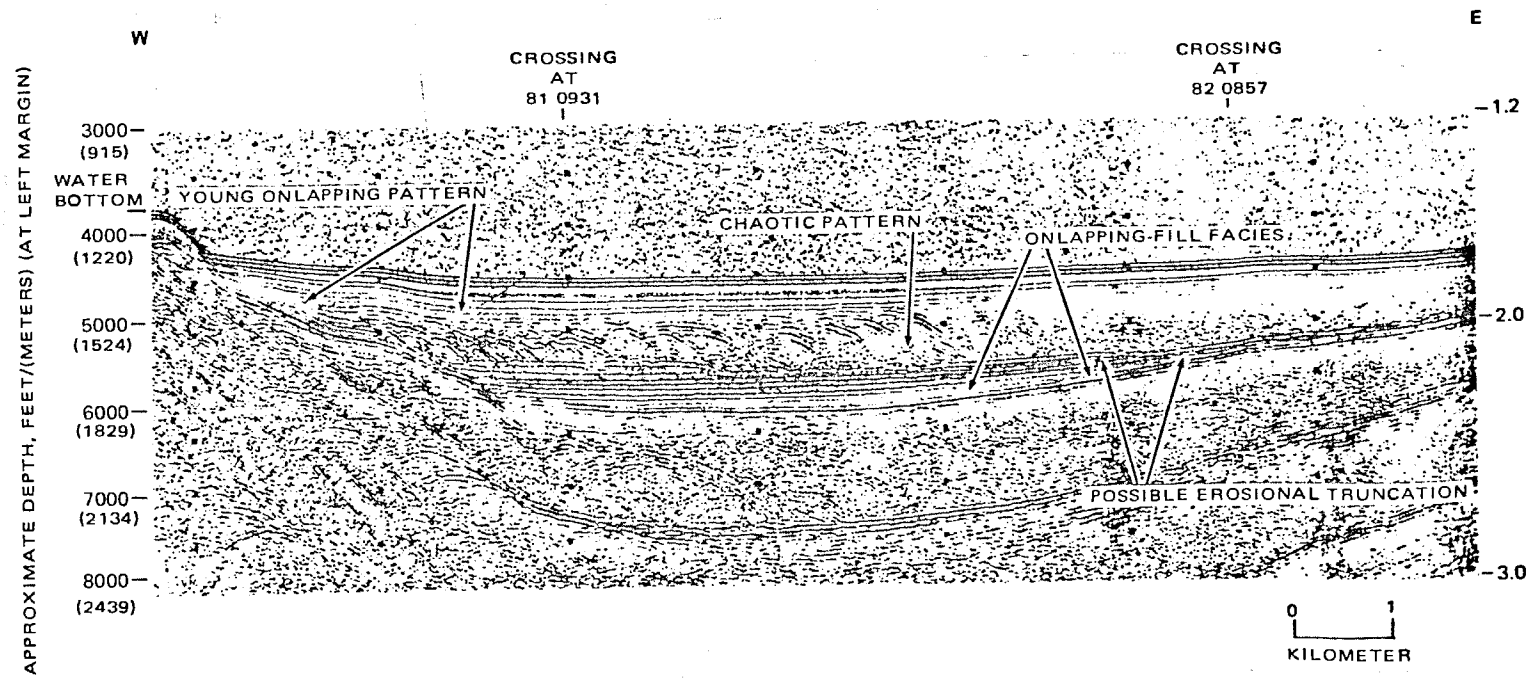

FIG. 11—Onlapping-fill seismic facies. Onlapping seismic cycles are even and uniform at base, and, with increasing amplitude, merge upward into one or two less-continuous cycles. Layered onlapping pattern gives way to chaotic pattern.

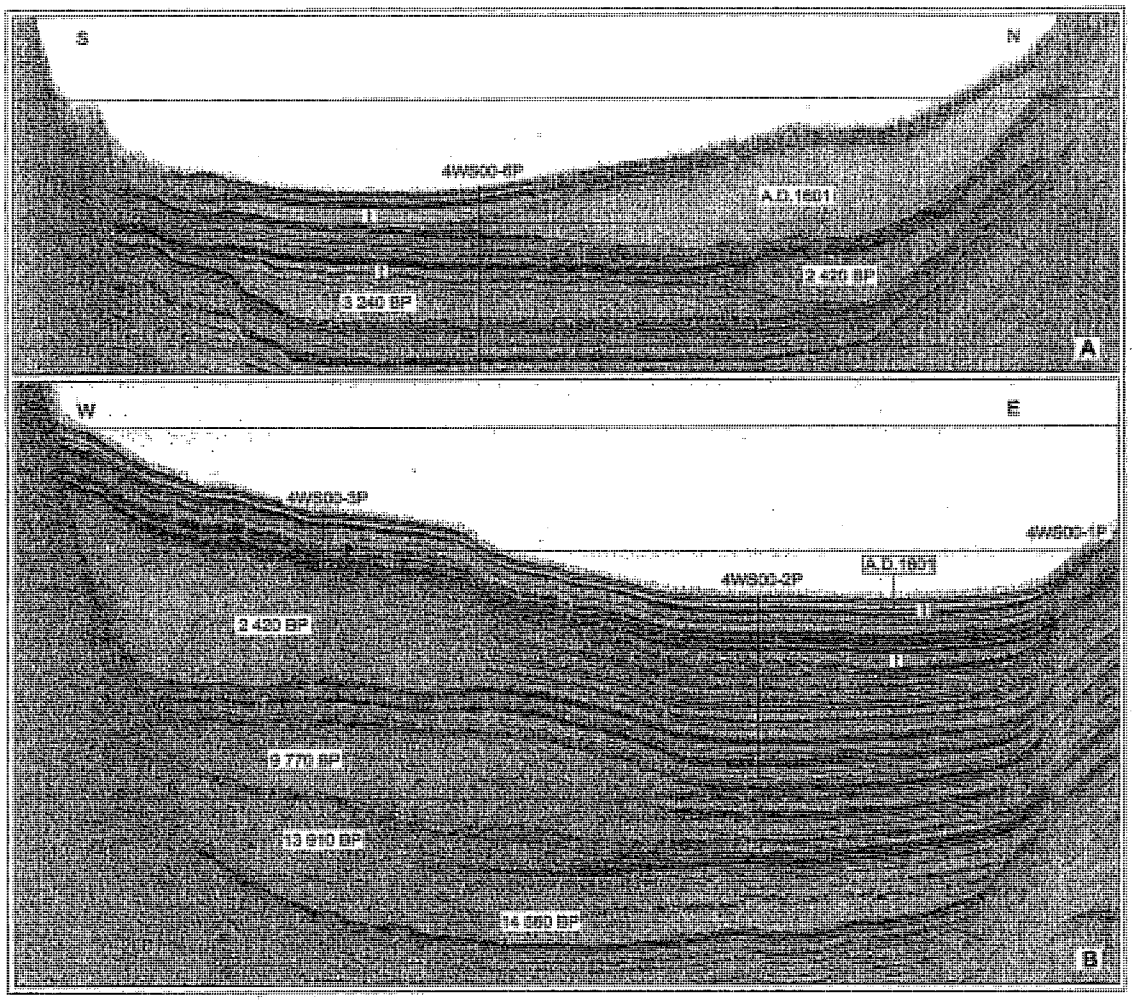

Figure 2. 3.5 kHz seismic profiles across (A) Vitznau and (B) Chrütztrichter subbasins of Lake Lucerne. For exact location of profiles, see Figure 3A. Discussed event horizons with related slump deposits and megaturbidites (t) are outlined in color. Ages: BP is calendar yr B.P. Vertical black lines indicate position of piston cores.

Schnellman et al, 2002, Geology, v. 30, 1131-34

Seismic imaging of marine basin settings and submarine fans

Strike-Slip Margin off of Los Angeles, California

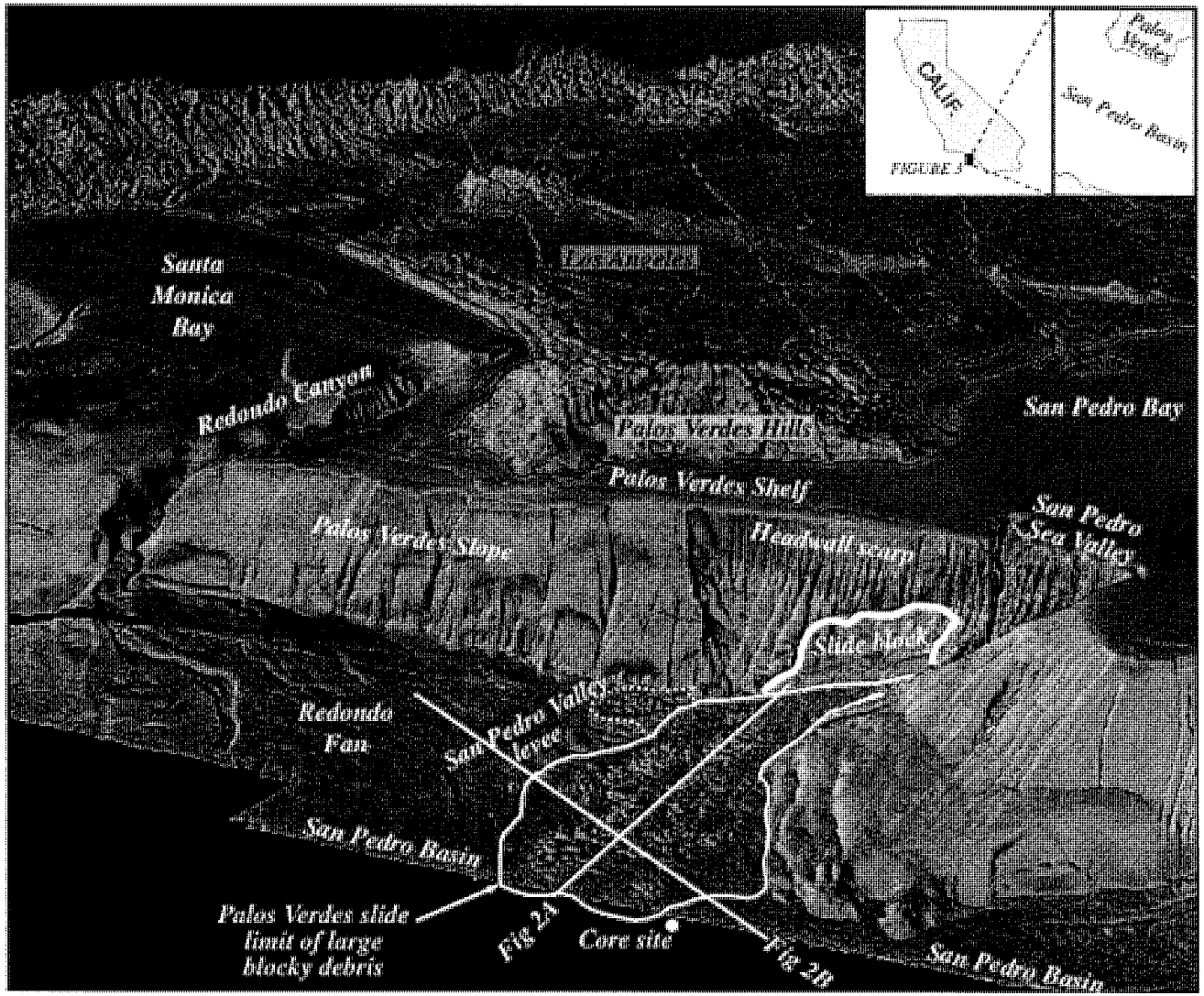

Slope canyon features:

- Localized by shelf incision
- Localized by faulting
- Localized by slope slumping
- Narrow shelves promote access to littoral drift sand

Source:
Bill Normark, USGS

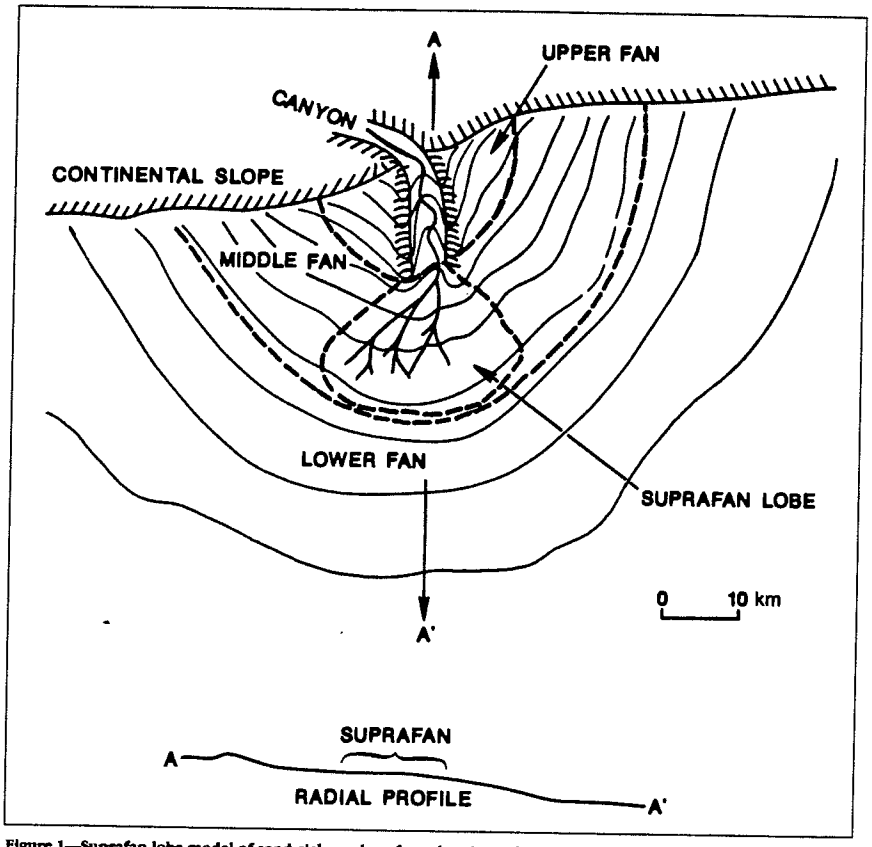

Figure 1—Suprafan lobe model of sand-rich modern fans showing a depositional bulge in radial profile. Simplified after Normark (1970, 1978).

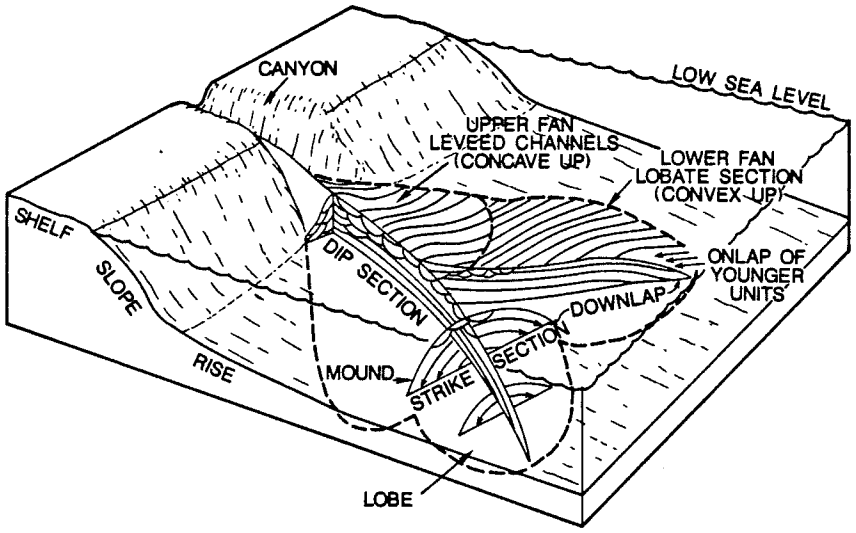

Figure 12—A model of seismic expression of ancient submarine fans. Modified after Mitchum (1985).

sequence stratigraphic architecture

SUBMARINE FAN DEPOSITIONAL SYSTEMS

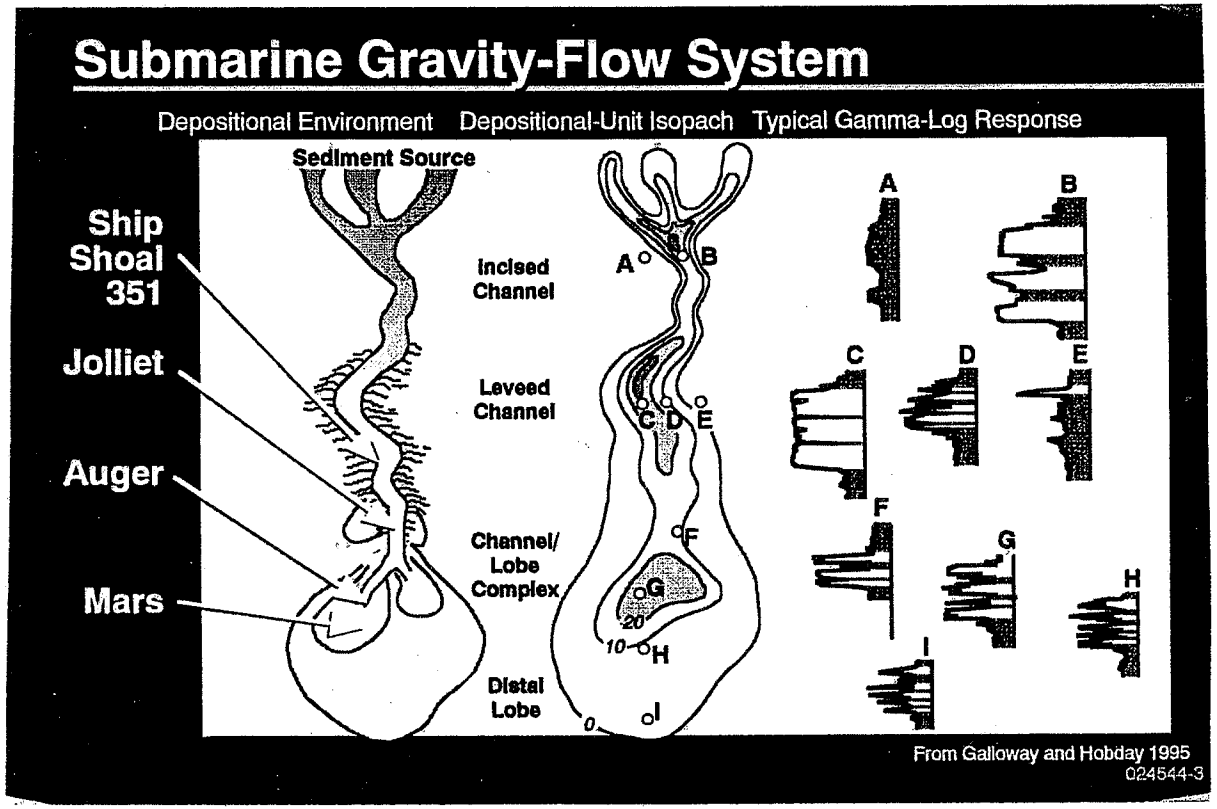

Figure 2. A general model for submarine gravity-flow systems from Galloway and Hobday (1995).

Armentrout - Short Course Notes, 2000

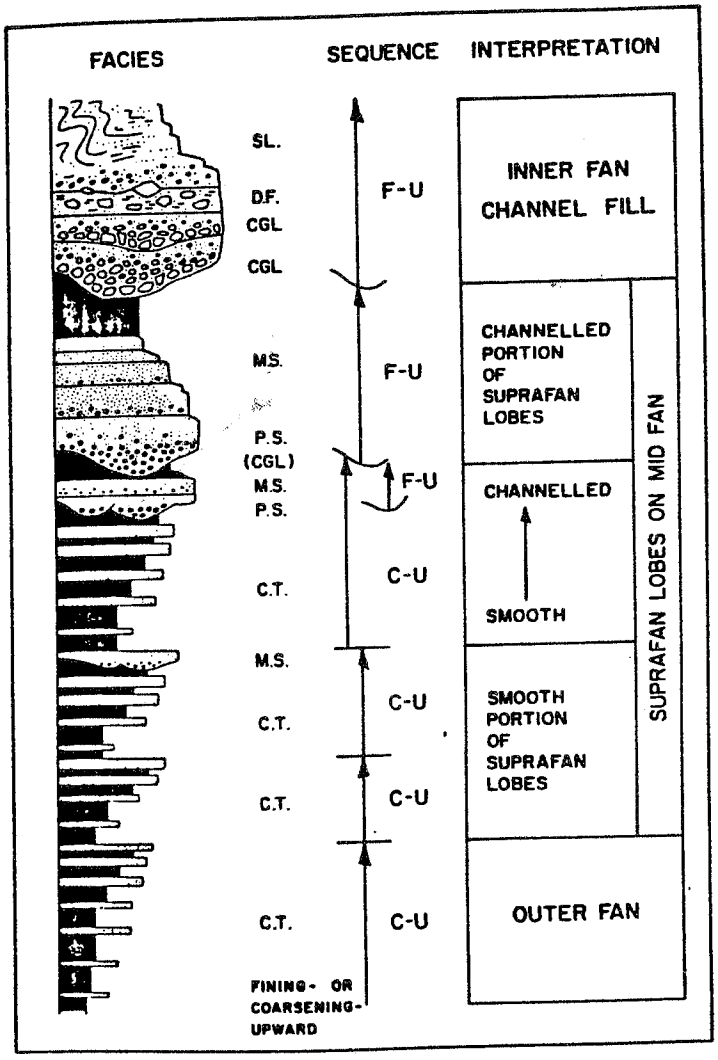

Figure 14
Hypothetical submarine fan stratigraphic sequence produced by fan progradation. C T., classical turbidite, M.S., massive sandstone. P S., pebbly sandstone; D.F., debris flow. Arrows show thickening- and coarsening-upward sequences (C-U) and thinning- and fining-upward sequences (F-U). See text for details.

<SEQUENCE STRATIGRAPHIC ARCHITECTURE>

in Weimer & Link 1991

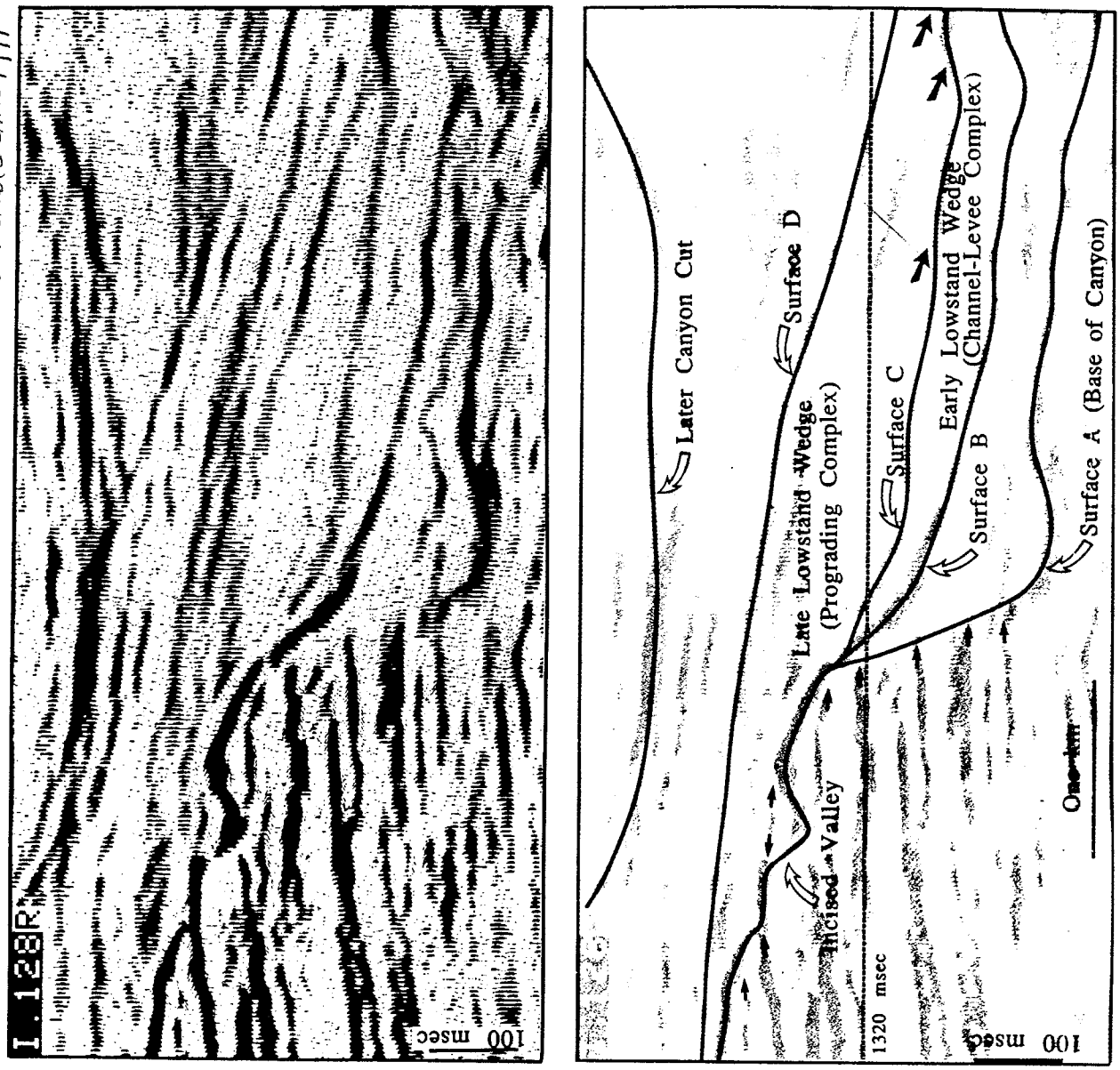

Figure 6.5. Multifold seismic data from a three-dimensional seismic grid illustrates early and late lowstand-wedge deposits in a submarine canyon, offshore Australia. This transverse section (A and B) through the canyon illustrates a complex cut and fill history. Surface A represents the erosional base of the canyon. The canyon subsequently became site of deposition before being incised once again, forming surface B. The canyon was then filled by the early and late lowstand-wedge units separated by a downlap surface (surface C). The external mounding of the early lowstand wedge may represent either axes of leveed channels or mounded slump deposits derived from adjacent canyon walls. A tie slice at 1320 msec illustrates the canyon and prograding complex in plain vie (C and D). The stratal geometries are similar to those shown schematically Figure 6.1. Note that the prograding complex builds into the canyon from th side. A deltaic depositional system can be recognized clearly in the embayme at the side of the canyon. In cross-sectional view (A and B), the upper bounda of the late lowstand wedge is indicated by surface D.

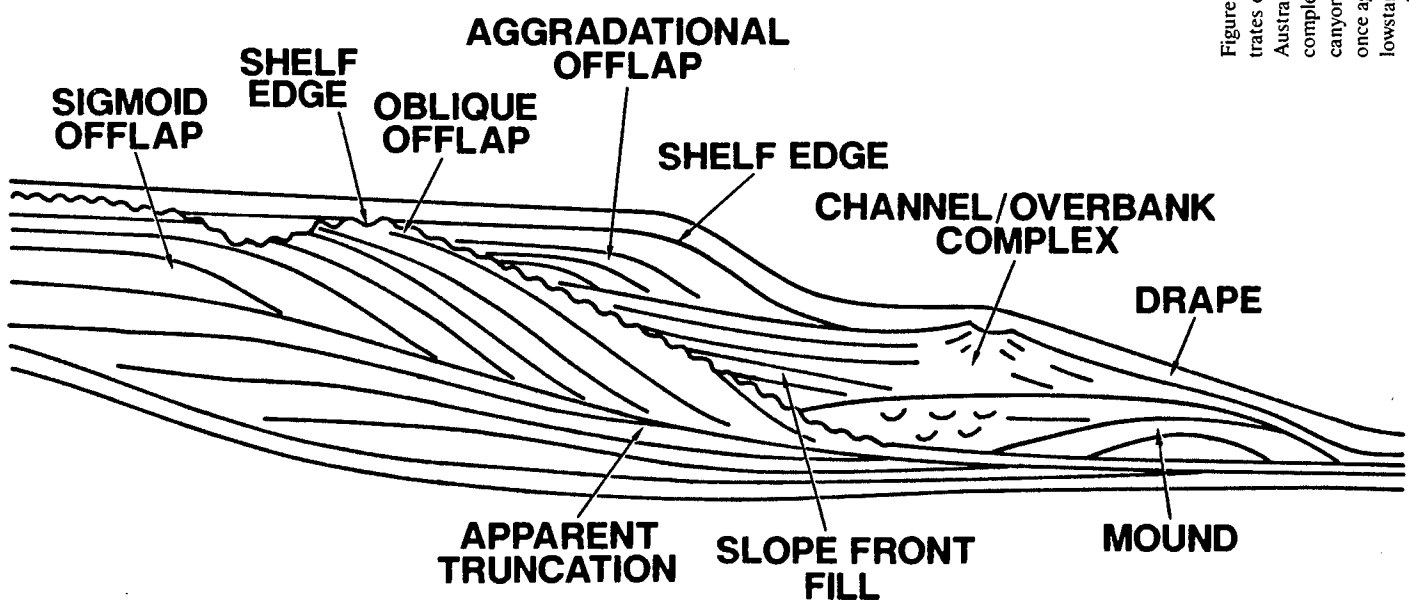

Figure 6. Diagram showing simulated seismic section with common seismic facies patterns. Vail in Bally

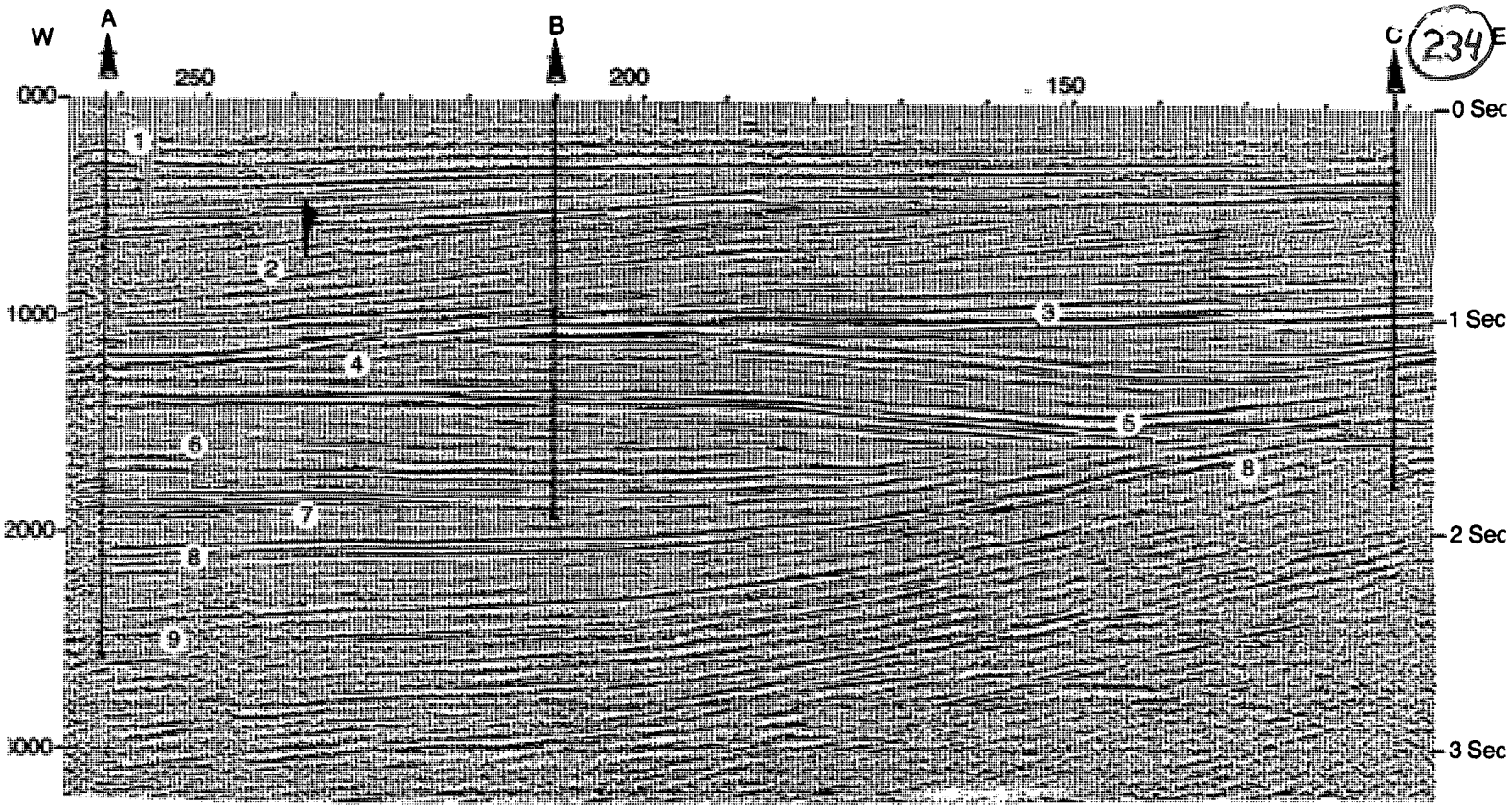

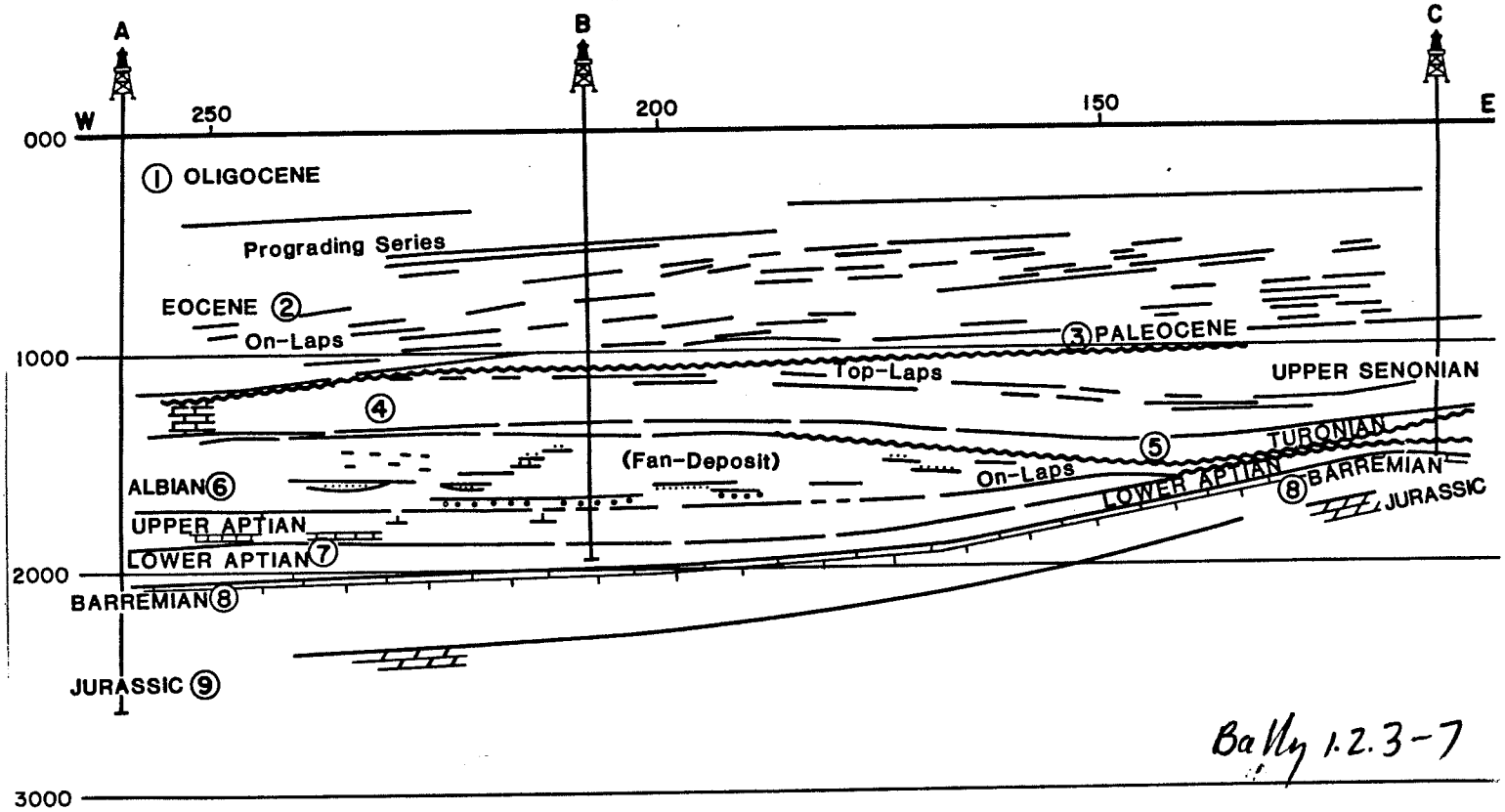

Figure 3

TOTAL DEPTH IN METERS — FEET

A — 3481 m — 11417'
B — 3163 m — 10311'
C — 2950m — 9676'

ALBIAN FAN DEPOSITS

R. CURNELLE - R. MARCO

ELF AQUITAINE (SNEA-P)

AQUITAINE BASIN (Parentis) - FRANCE

What level of detail can be seen?

(RESOLVING INTERNAL DETAILS OF SUBMARINE FANS)

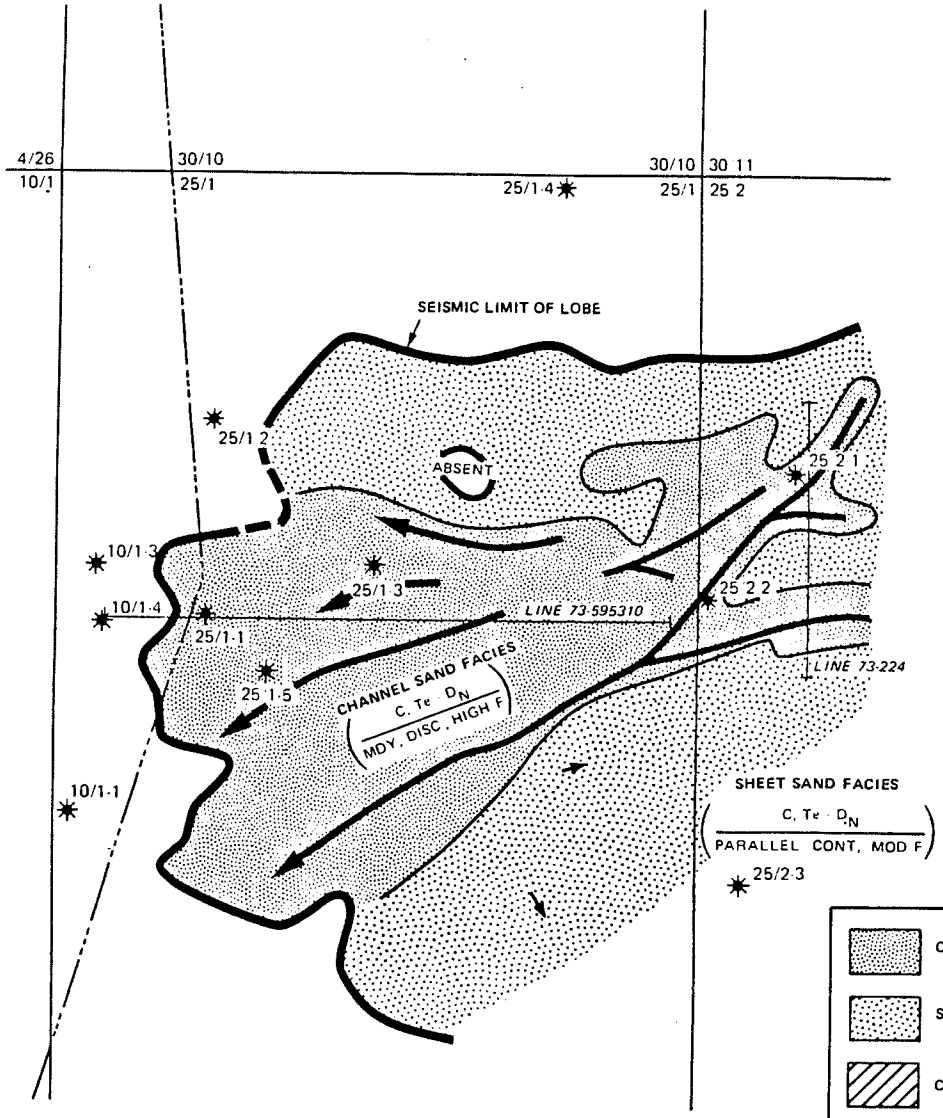

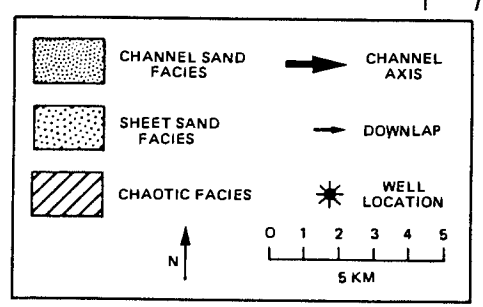

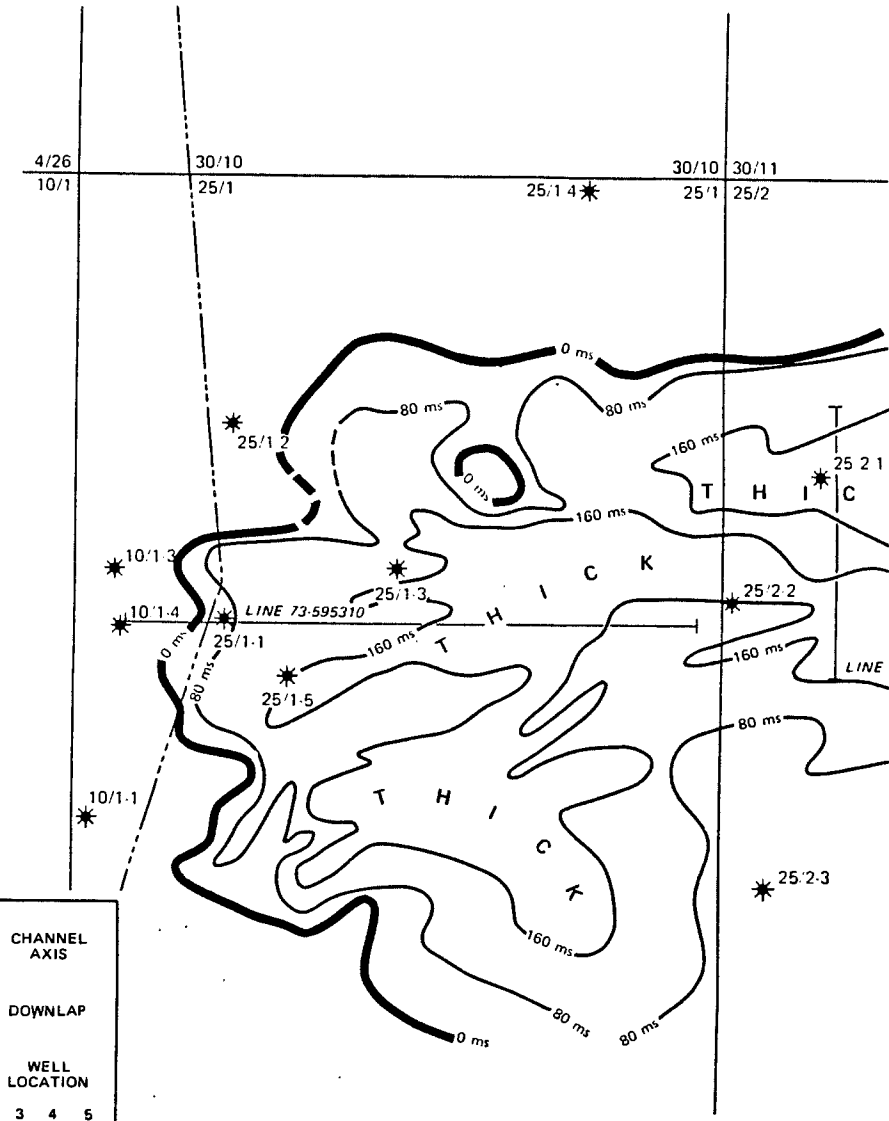

Figure 8. Isochron and facies map, East Frigg lobe.

McGovney & Radovich 1985

AAPG Memoir 32

WHAT DETAIL IS RESOLVABLE?

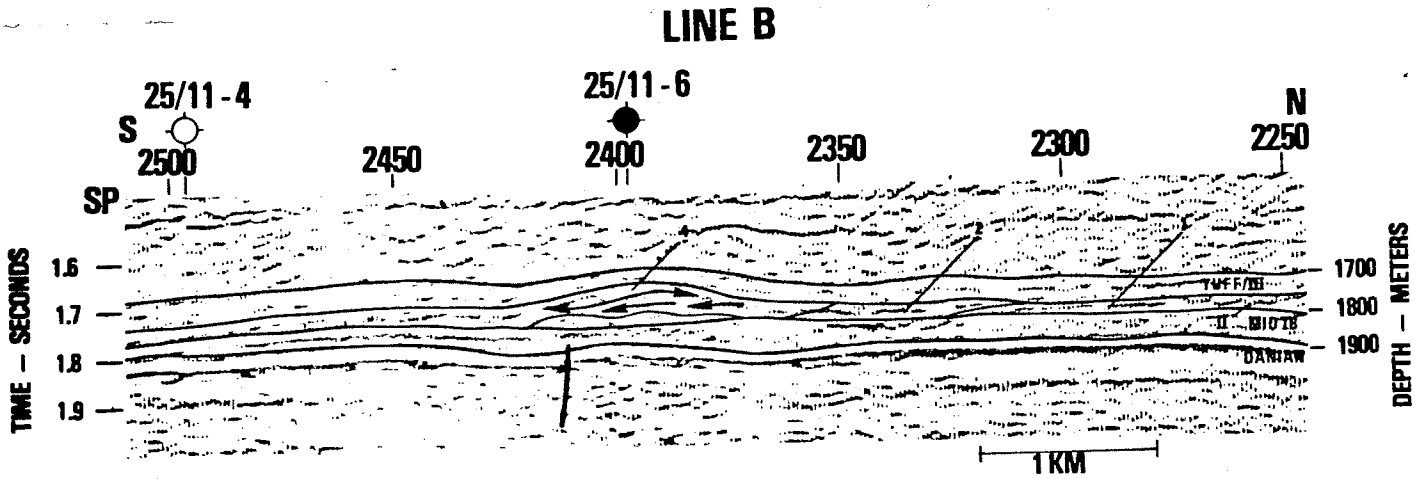

Fig. 4—North-to-south seismic line displaying southward progradation of individual suprafan lobes (1, 2, 4) within the II sequence.

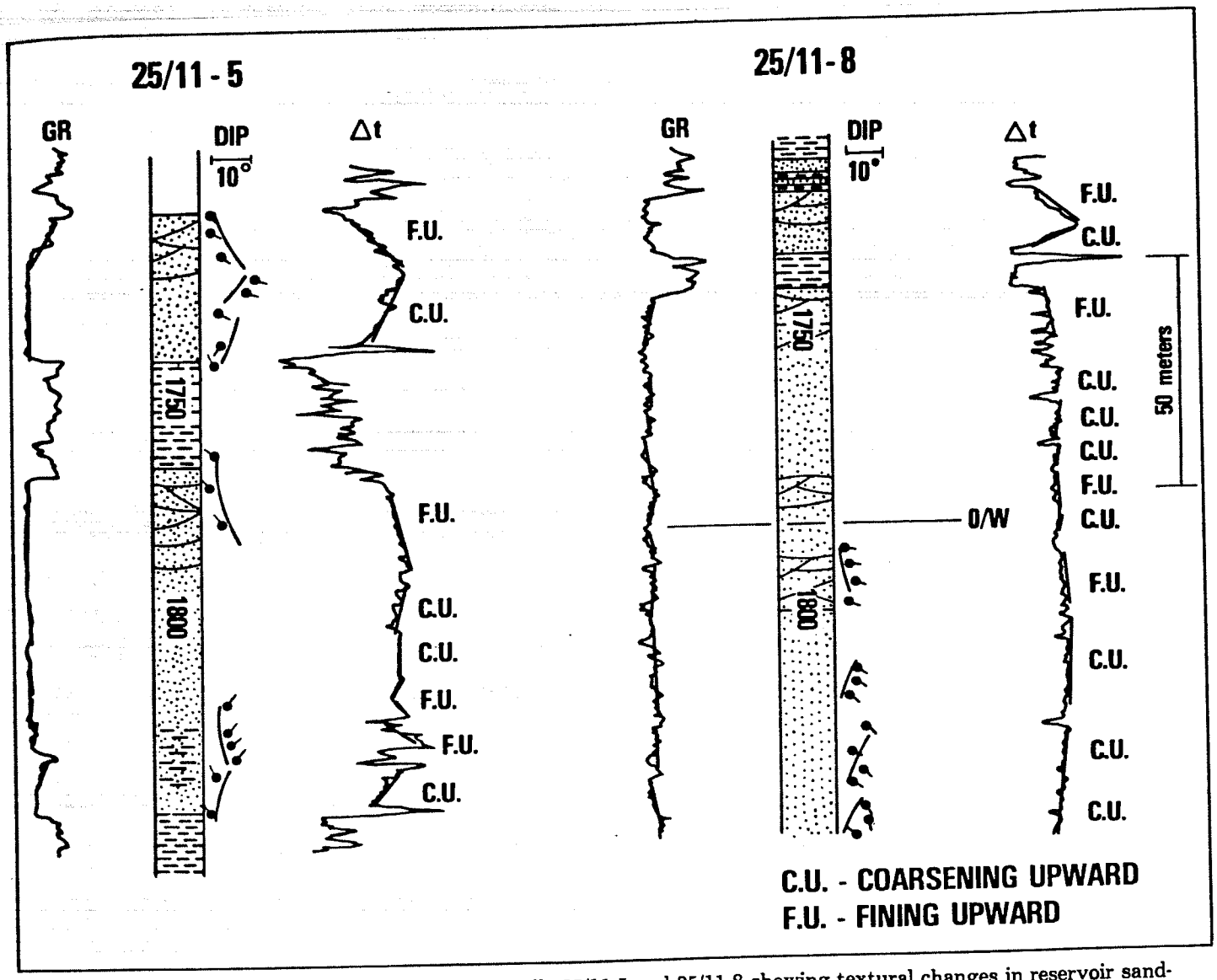

Fig. 5—Gamma ray/sonic and dipmeter logs from wells 25/11-5 and 25/11-8 showing textural changes in reservoir sandstones. A decrease in transit time together with a decrease in gamma value and an increase in dip suggest a coarsening-upward fan-fringe sequence. An increase in transit time with an increase in gamma value and decrease in dip suggest a fining-upward inner fan channel sequence.

Imaging submarine fan channels

Channel - Lobe Transition

Deepwater Mahakam Delta, Indonesia

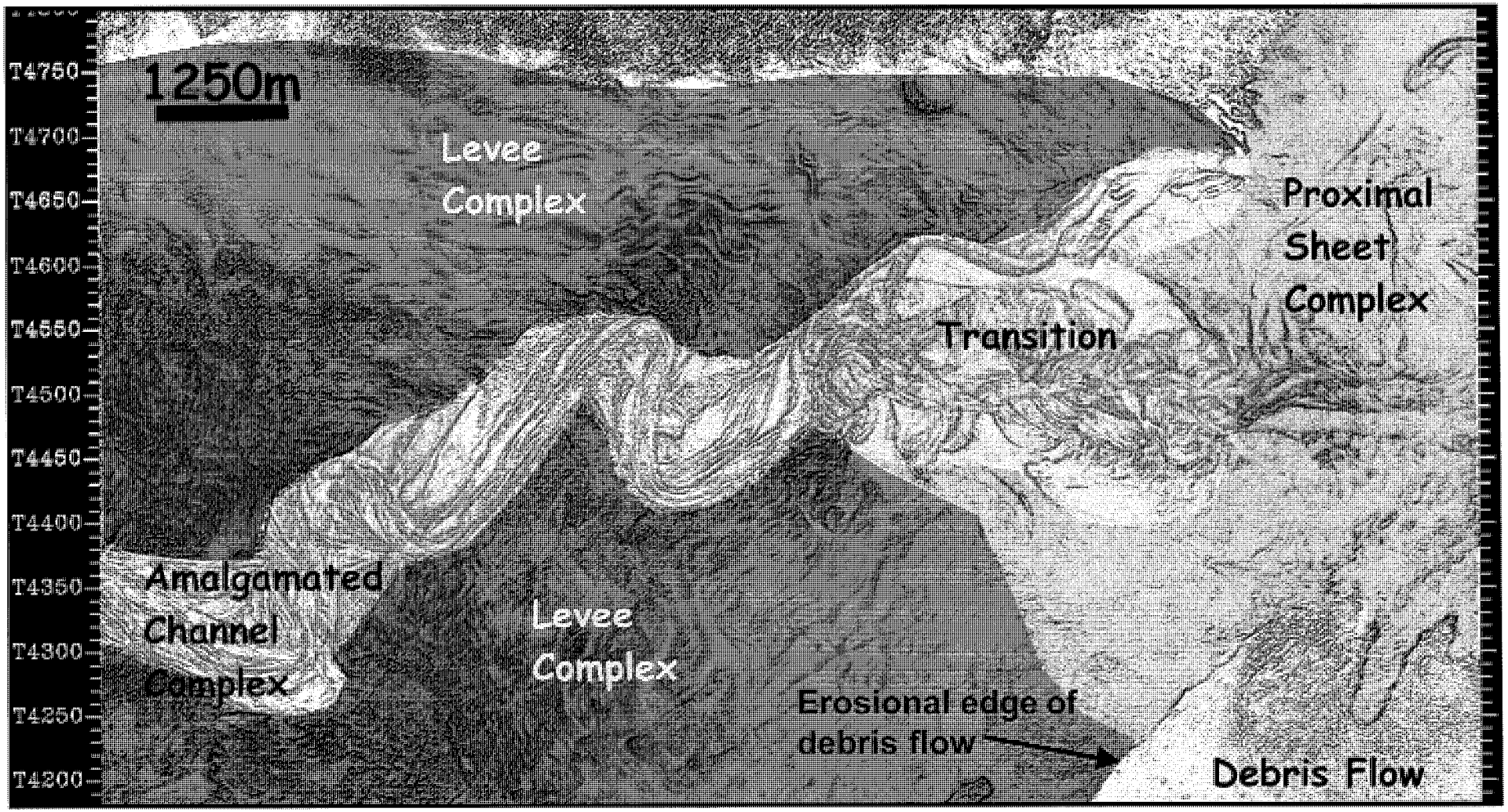

Edge Horizon slice through 14 kms of a near-surface analog (150ms below mudline).

T. McHargue, EPTC Quantitative Stratigraphy Team, 11/2001

Figure 18.3. Location of the channel valleys of the 17 channel-levee systems identified in the Mississippi Fan. Channels are numbered from 1 to 17 (oldest to youngest). Within any CLS, relative ages are lettered from oldest to youngest (a, b, . . .). Trend of youngest channel (#17) southeast of middle fan DSDP sites is from EEZ Scan 85 Scientific Atlas (1987). Approximate ages for five sequence boundaries are from Walters (1985). Channels illustrated in Figures 8.4–8.16 are shown by shaded pattern. Map modified from Weimer and Buffler (1988). Weimer, 1991 in Weimer & Link

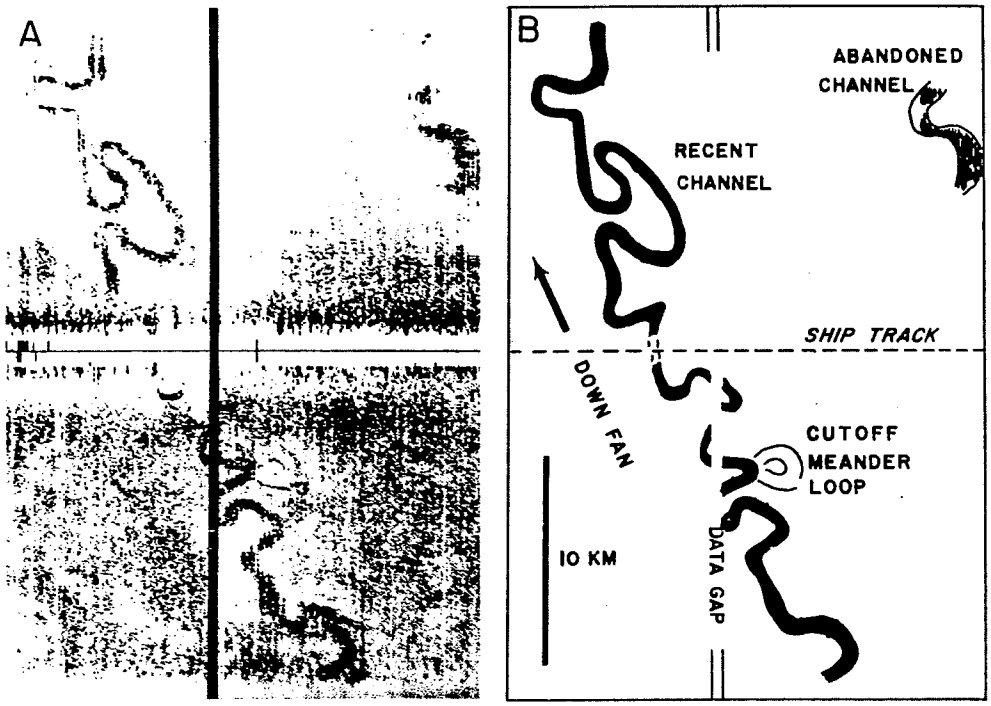

Figure 23.3. Long-range side-scan sonar (GLORIA) record (A) and interpretation (B) of a sinuous channel segment on the middle fan. Note the less-reflective cutoff meander loop in the lower center of the illustration and the small section of abandoned channel to the left of the illustration. The channel turns more than 180° to trend upfan; however, depth along channel increases uniformly along this segment. Location in Figure 23.7. Flood et al 91 in Weimer & Link

Mahakam Channel-Levee Complex

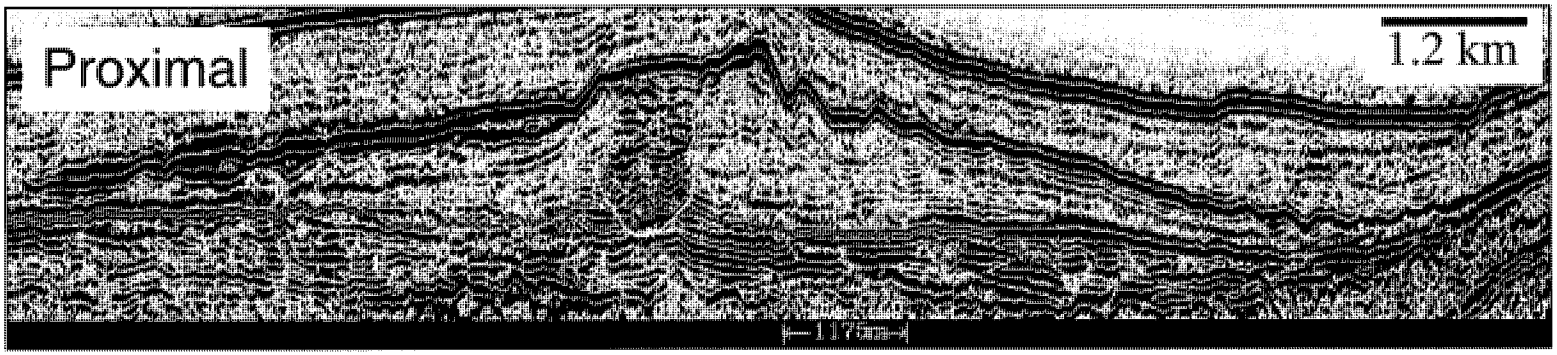

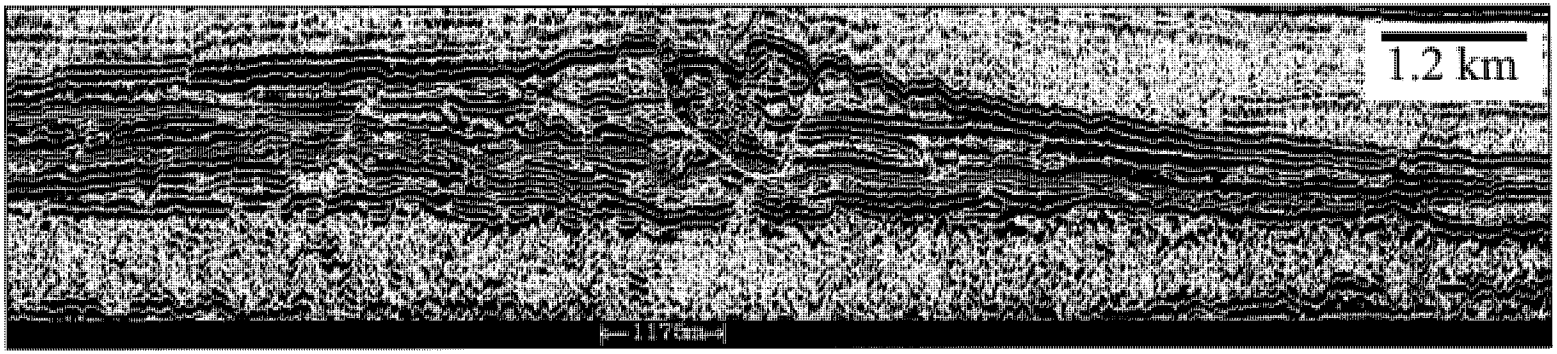

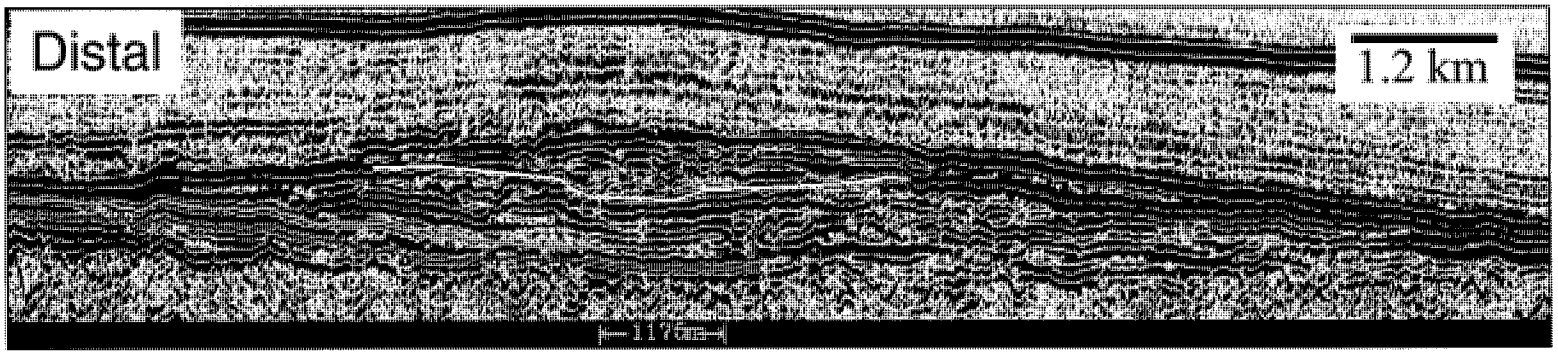

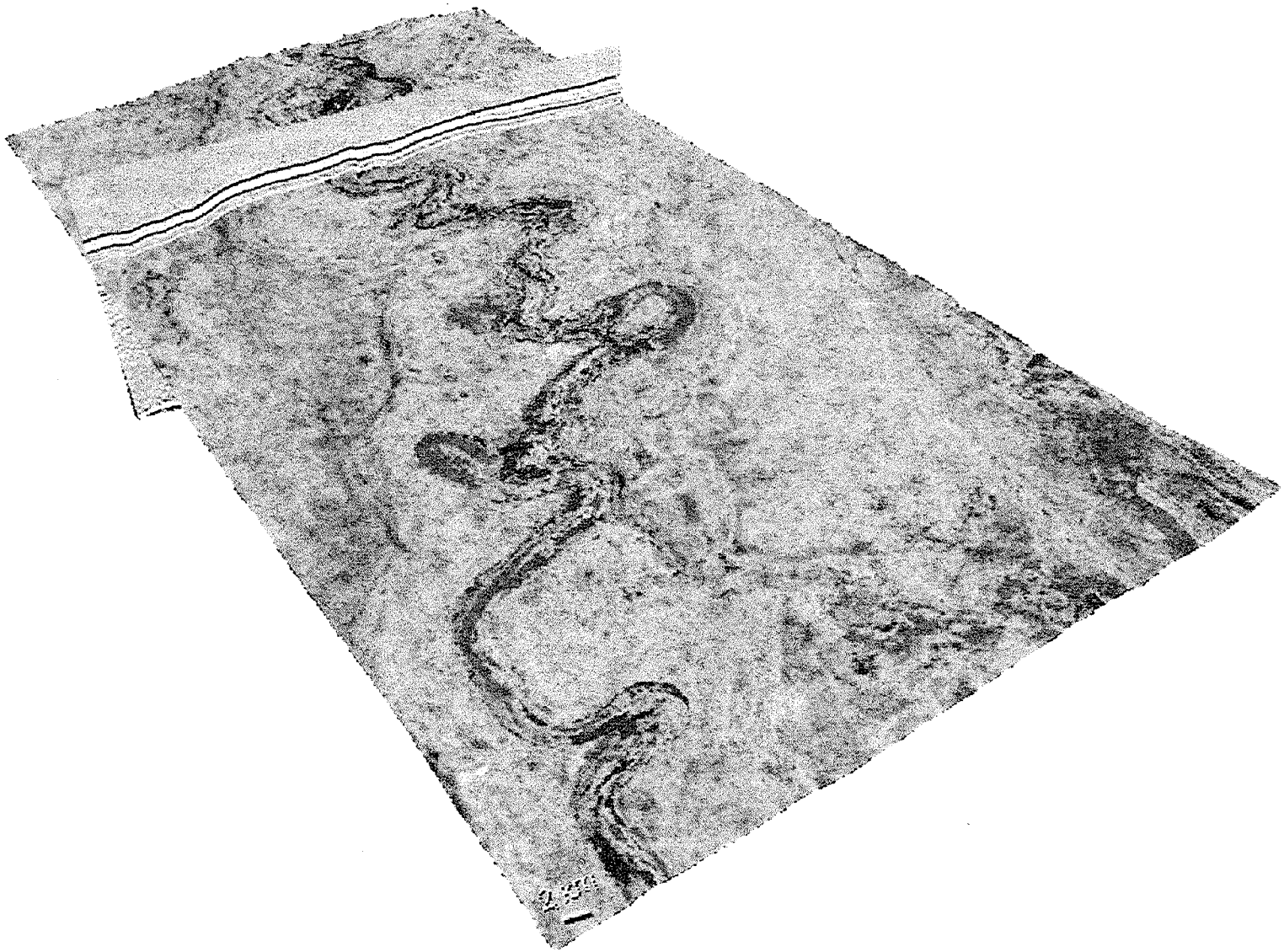

Fig. 2. Reflection amplitude draped on interpreted horizon suggesting presence of sand within deep-water turbidite channel, Gulf of Mexico.

Posamentier et al., 2007

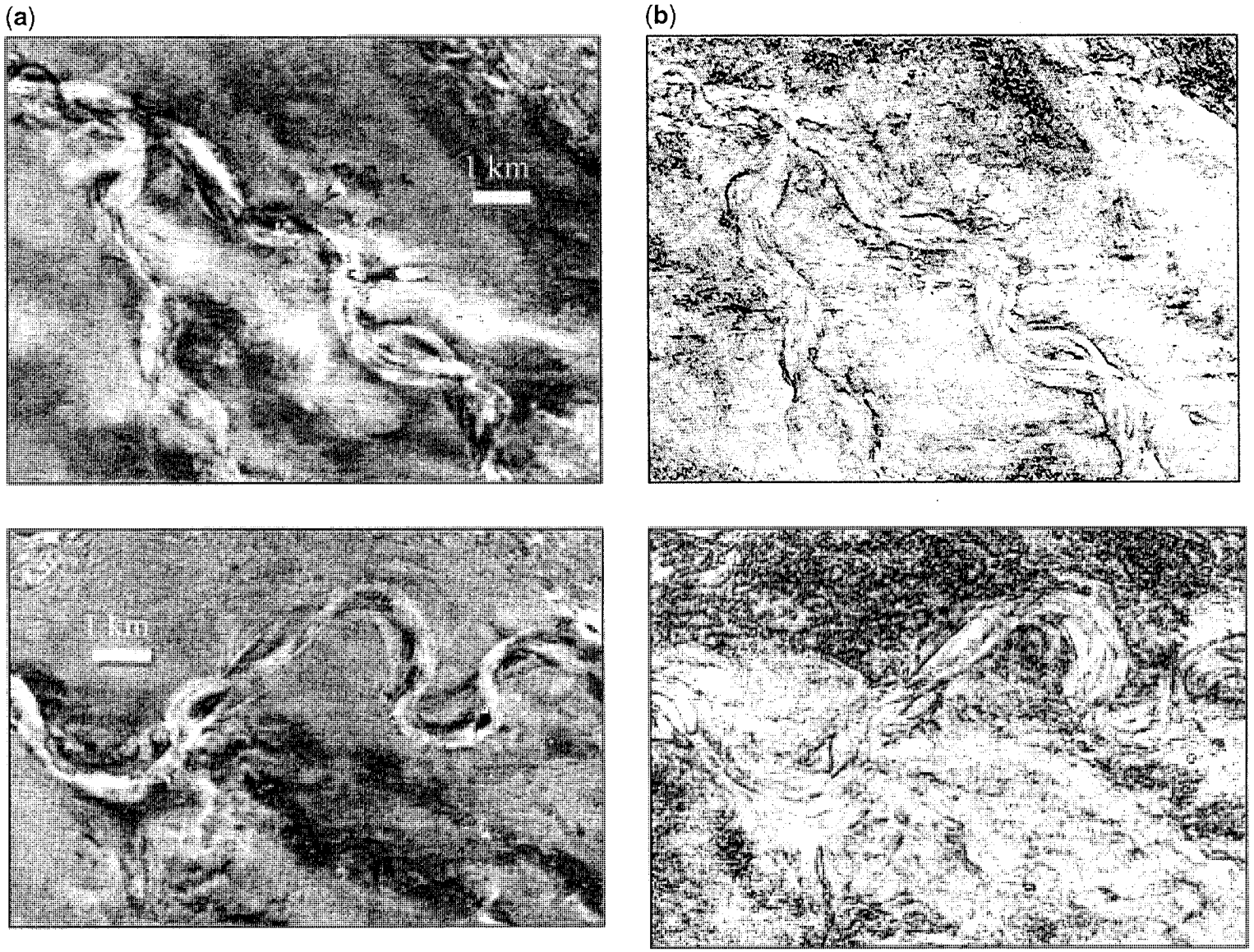

Fig. 12. Amplitude (**a**) and coherence (**b**) time slices illustrating a deep-water turbidite channel, Gulf of Mexico. The amplitude reflection attribute is an indicator of acoustic properties of the channel fill, whereas the coherence attribute highlights the edges of the channel.

Posamentier et al., 2007

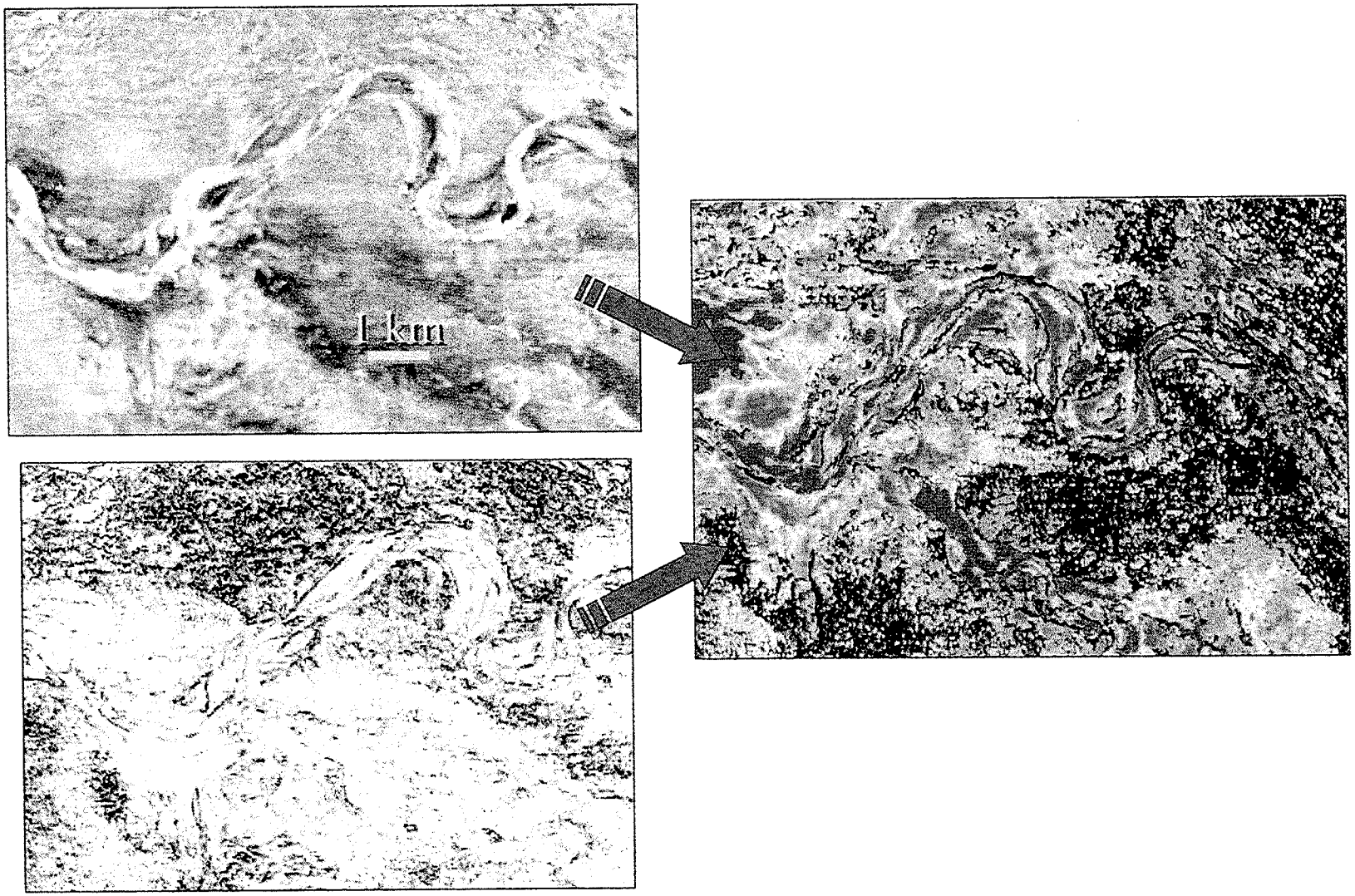

Fig. 13. Co-rendered amplitude and coherence image of a deep-water turbidite channel, Gulf of Mexico.

Posamentier et al., 2007

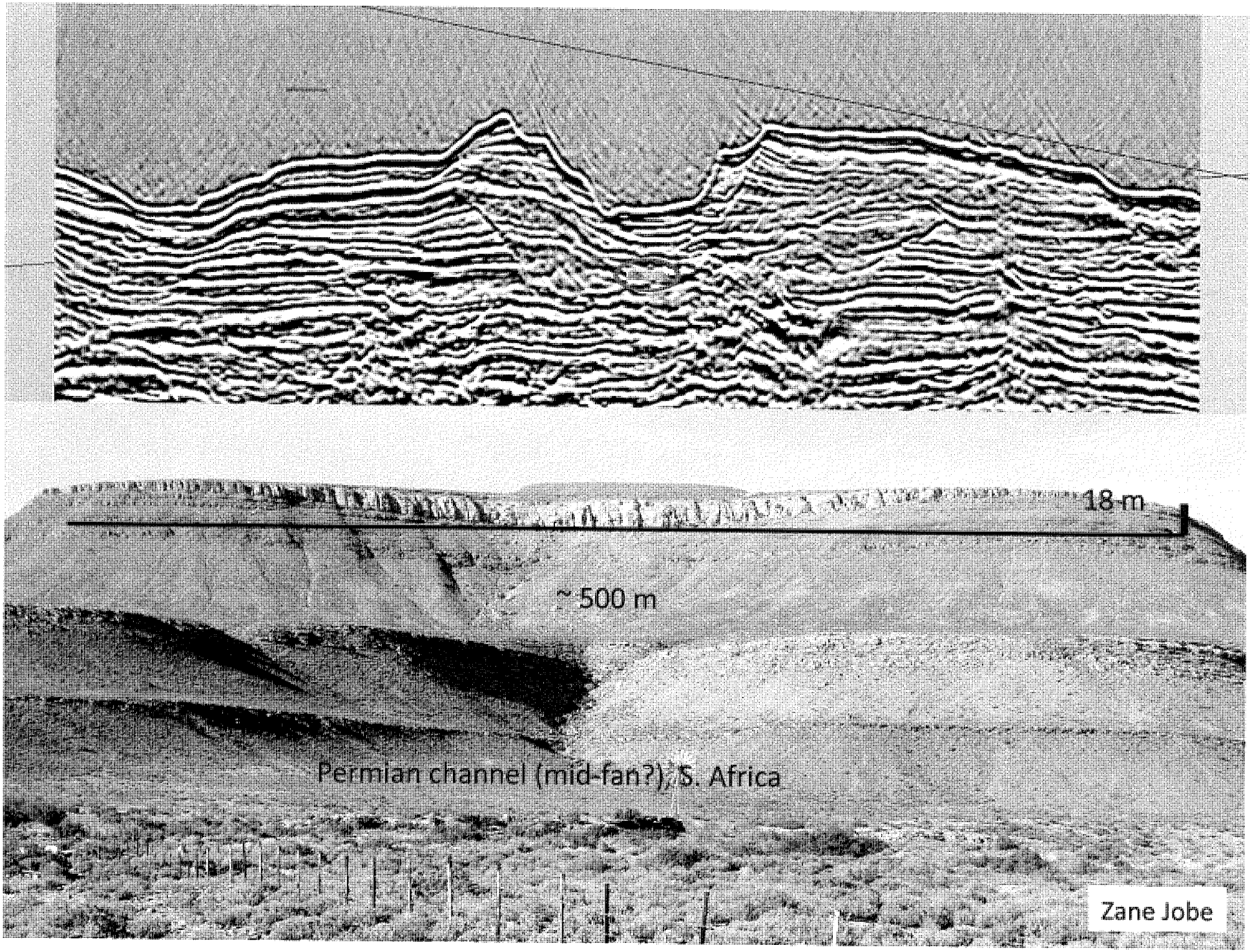
18 m
~500 m
Permian channel (mid-fan?), S. Africa
Zane Jobe

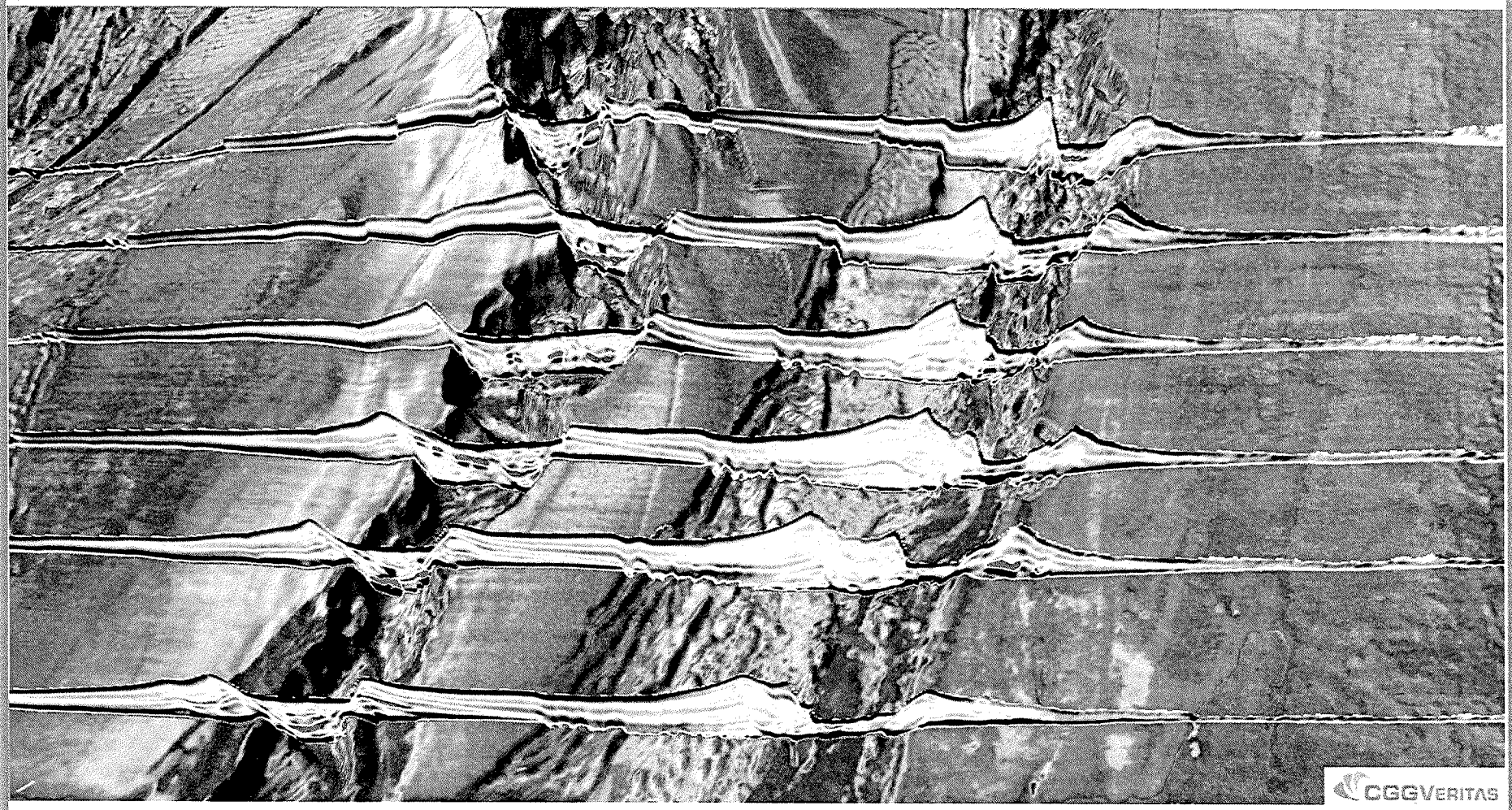

Sylvester: http://see-atlas.leeds.ac.uk:8080/ CGG Veritas Niger Delta slope

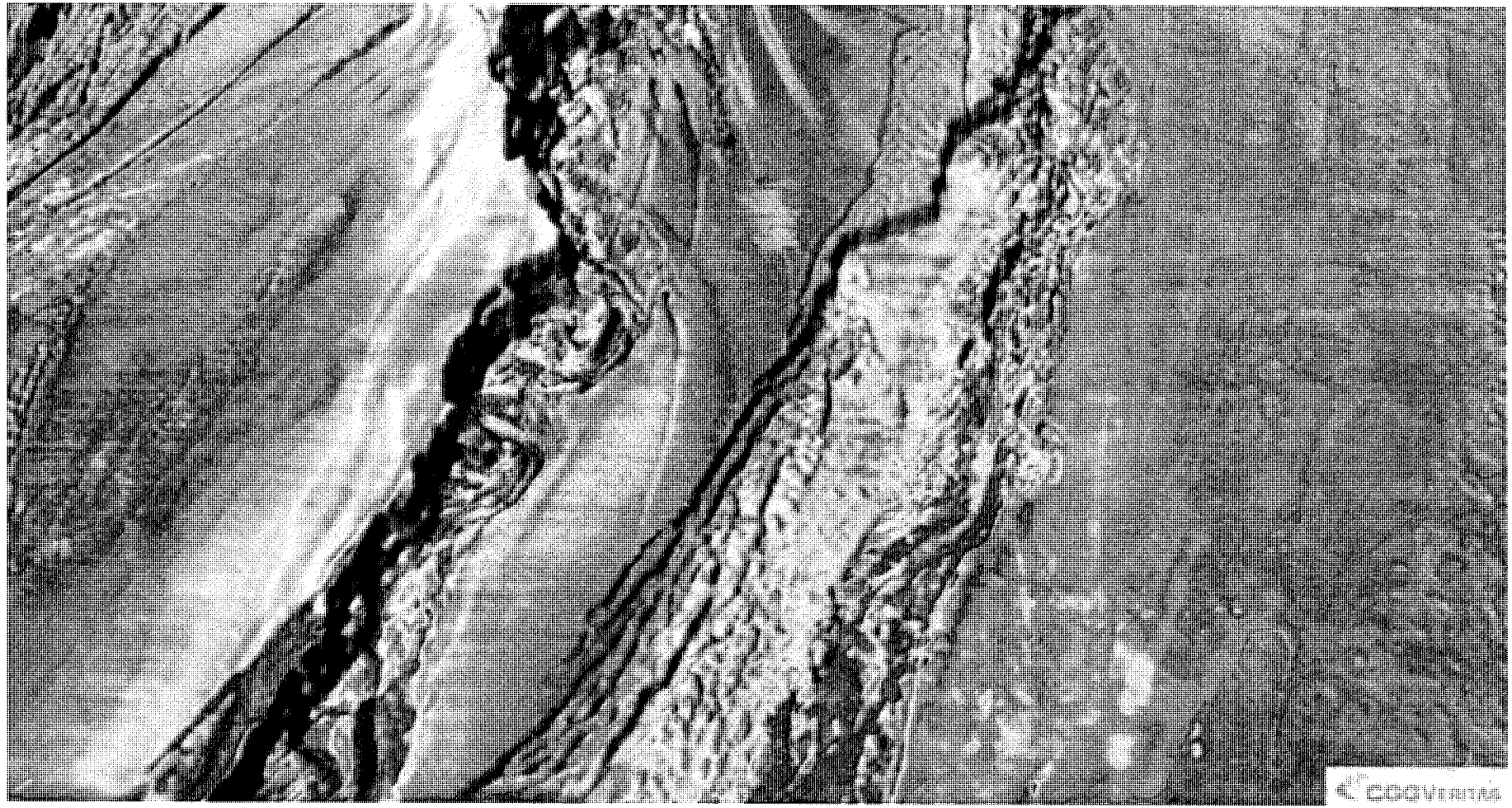

Sylvester: http://see-atlas.leeds.ac.uk:8080/ CGG Veritas Niger Delta

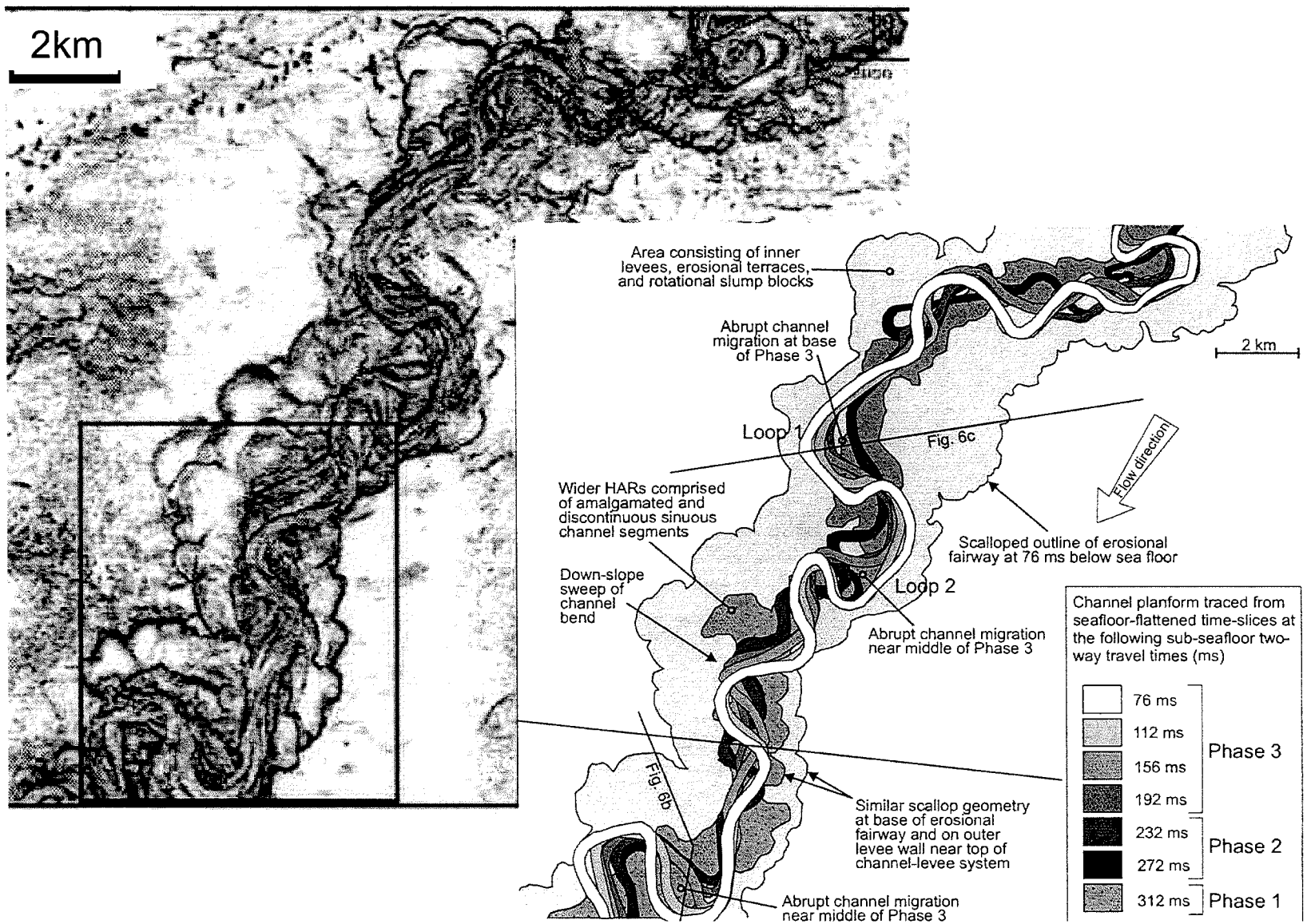

Deptuck, M.E., G.S. Steffans, M. Barton, and C. Pirmez, in press, Architecture and evolution of upper fan channel-belts on the Niger Delta slope and in the Arabian Sea.

Lateral accretion package (LAP)

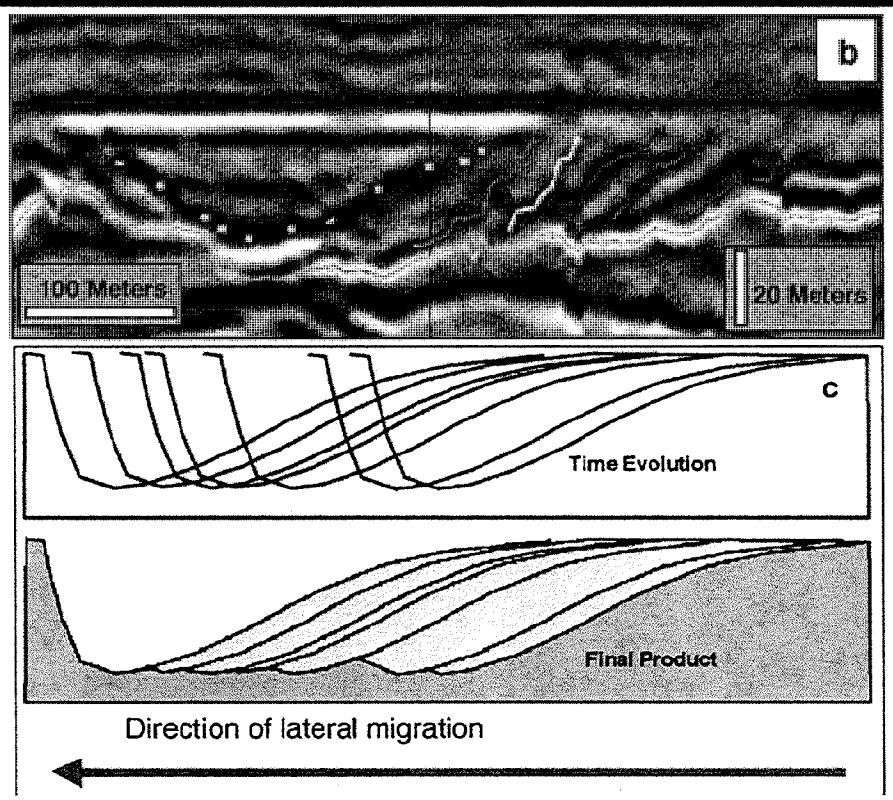

Fig. 26. (a) Fluvial point-bar model (modified from Galloway & Hobday, 1983). (b) The cross-section view of a LAP in a deepwater, sinuous, erosionally confined channel resembles the geometry of a fluvial point-bar. (c) Depositional model proposed for the LAPs. The accretion surfaces would be formed by relatively continuous lateral sweep of channel bends by systematic erosion of the outer banks and deposition along inner banks (the classic point-bar model).

Abreu et al 2003

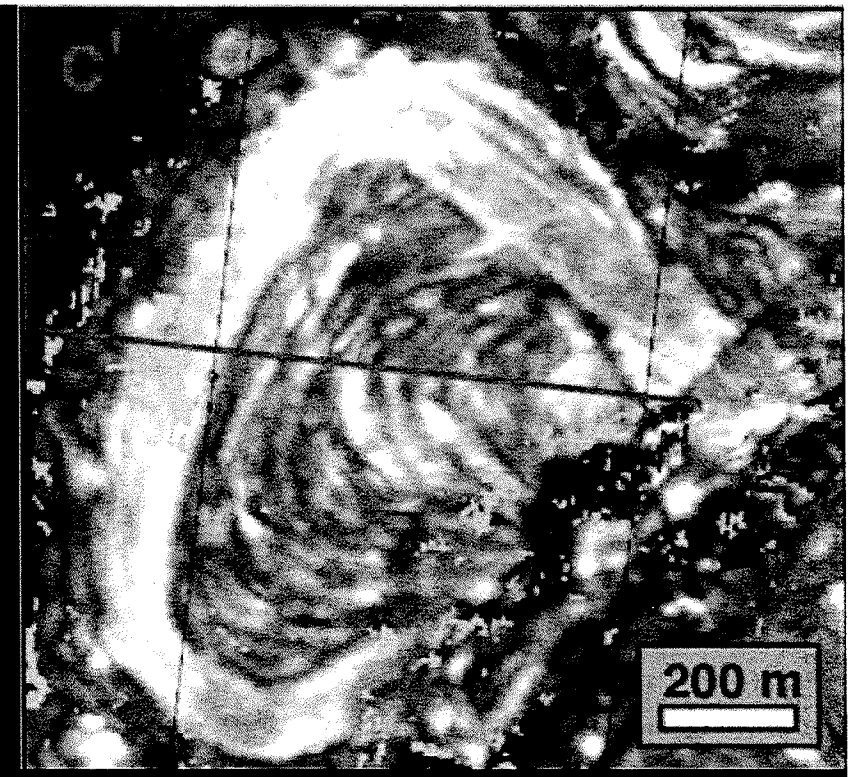

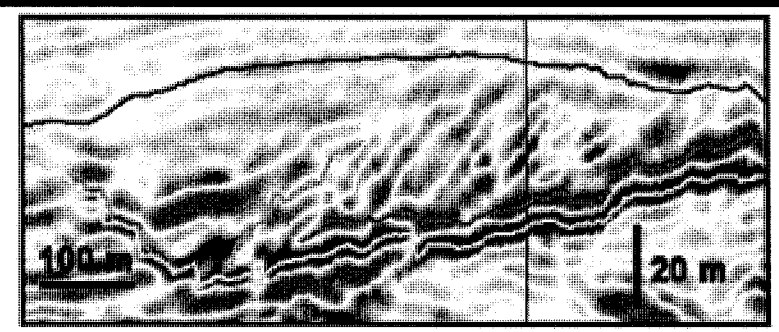

Conglomeratic to Coarse Grain Sands

Sandy Turbidites

Muddy Turbidites

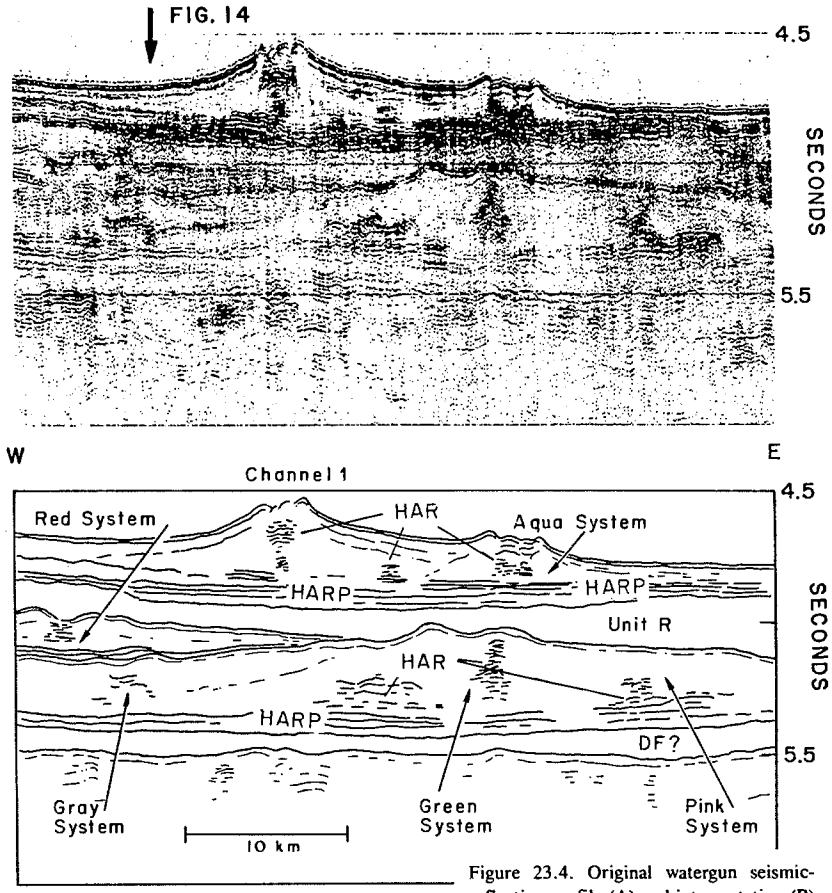

Figure 23.4. Original watergun seismic-reflection profile (A) and interpretation (B) from the middle fan at 3450 m showing the relationship between the different seismic facies observed on the fan. Note the high-amplitude reflections (HAR) within the levee of Channel 1 and the flatter-lying high-amplitude reflection packets (HARP) that lie beneath the channel-levee system. Similar acoustic facies are also observed associated with other channel-levee systems (with color names as given by Manley and Flood, 1988) both at the fan surface and at depth. Unit R, which separates the Upper Levee Complex (ULC) from the Middle and Lower Levee Complexes (MLC and LLC), appears to be a debris-flow deposit. An inferred debris-flow deposit (marked DF?) separates the LLC from the more deeply buried Bottom Levee Complex (BLC). Arrow marks crossing point of Figure 23.14. The paths of the buried (color named) channel-levee systems are shown in Figure 23.5. Profile location shown on Figures 23.5 and 23.16.

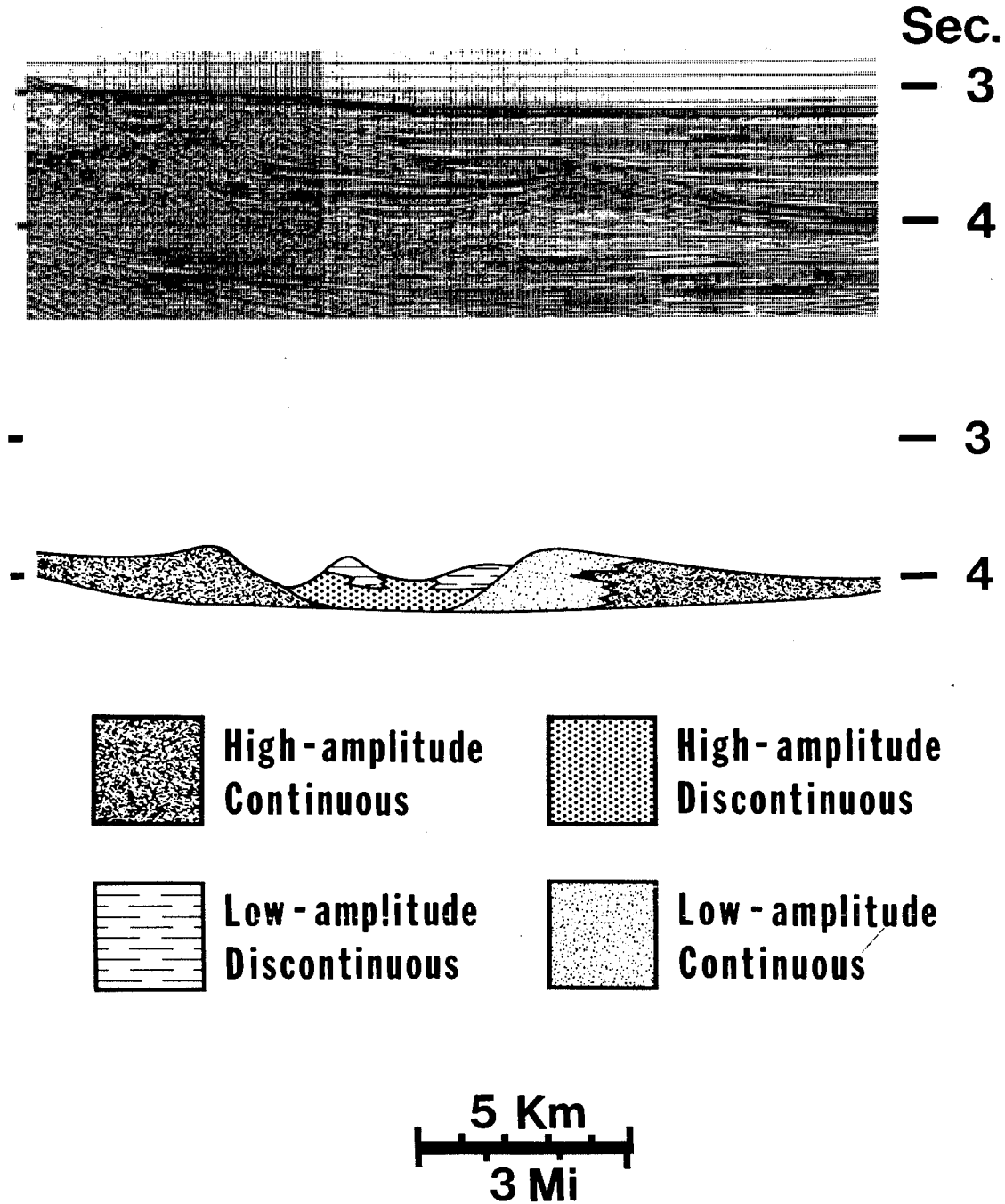

Figure 22.3. Internal seismic facies of aggradational channel-levee complexes of the Indus inner fan. Characteristics of these facies are summarized in Table 22.1. Only the high-amplitude discontinuous facies is considered to be sand prone.

McHargue '91 (w/ Bally)

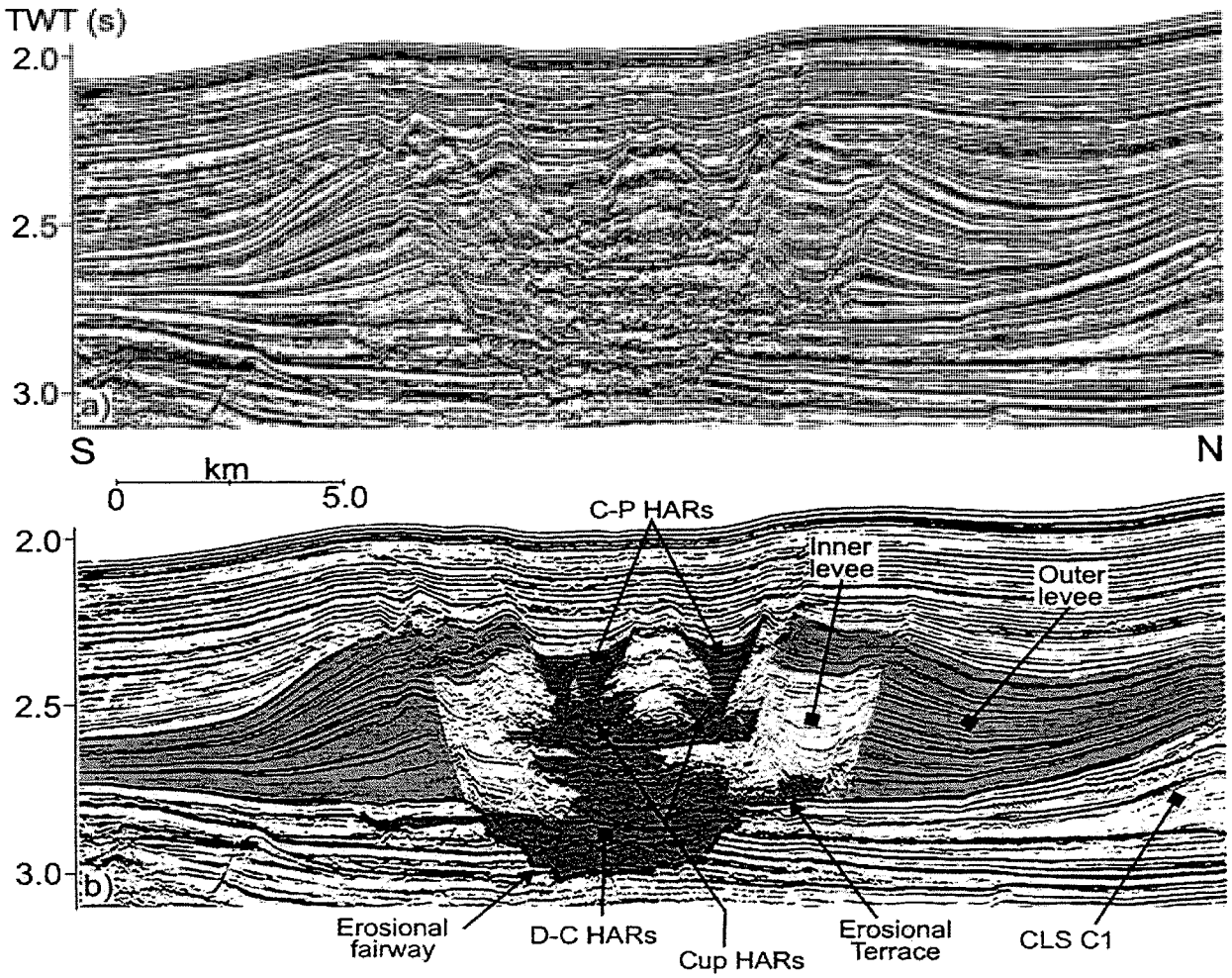

Deptuck, M.E., G.S. Steffans, M. Barton, and C. Pirmez, in press, Architecture and evolution of upper fan channel-belts on the Niger Delta slope and in the Arabian Sea.

Fig. 7. Seismic amplitude extraction along a horizon slice through a deep-water crevasse splay (note the distributive channel pattern), Gulf of Mexico. Reflection amplitude suggests that the channels are sand-prone.

Posamentier et al., 2007

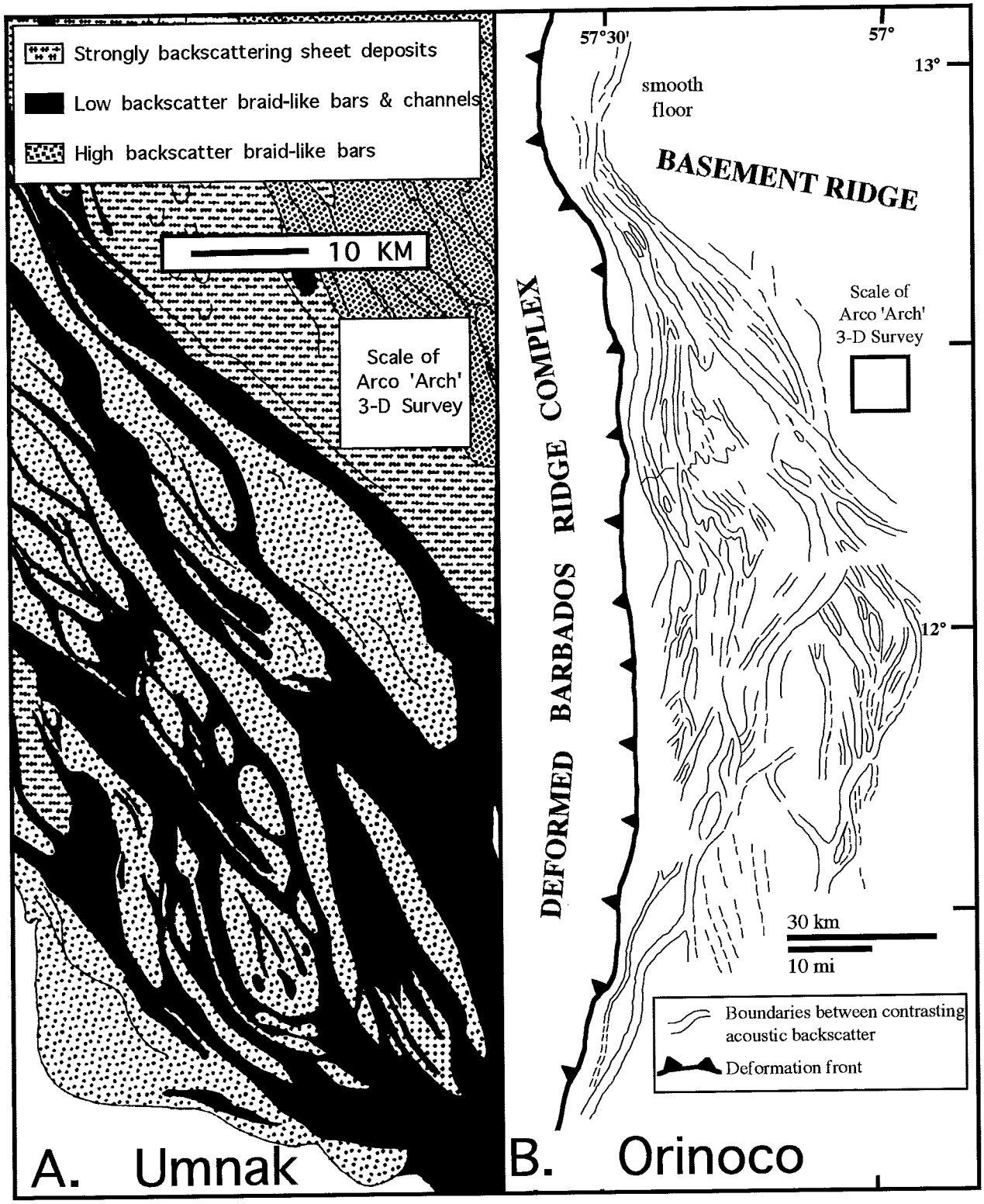

Harrison & Graham, 1999, AAPG Bulletin

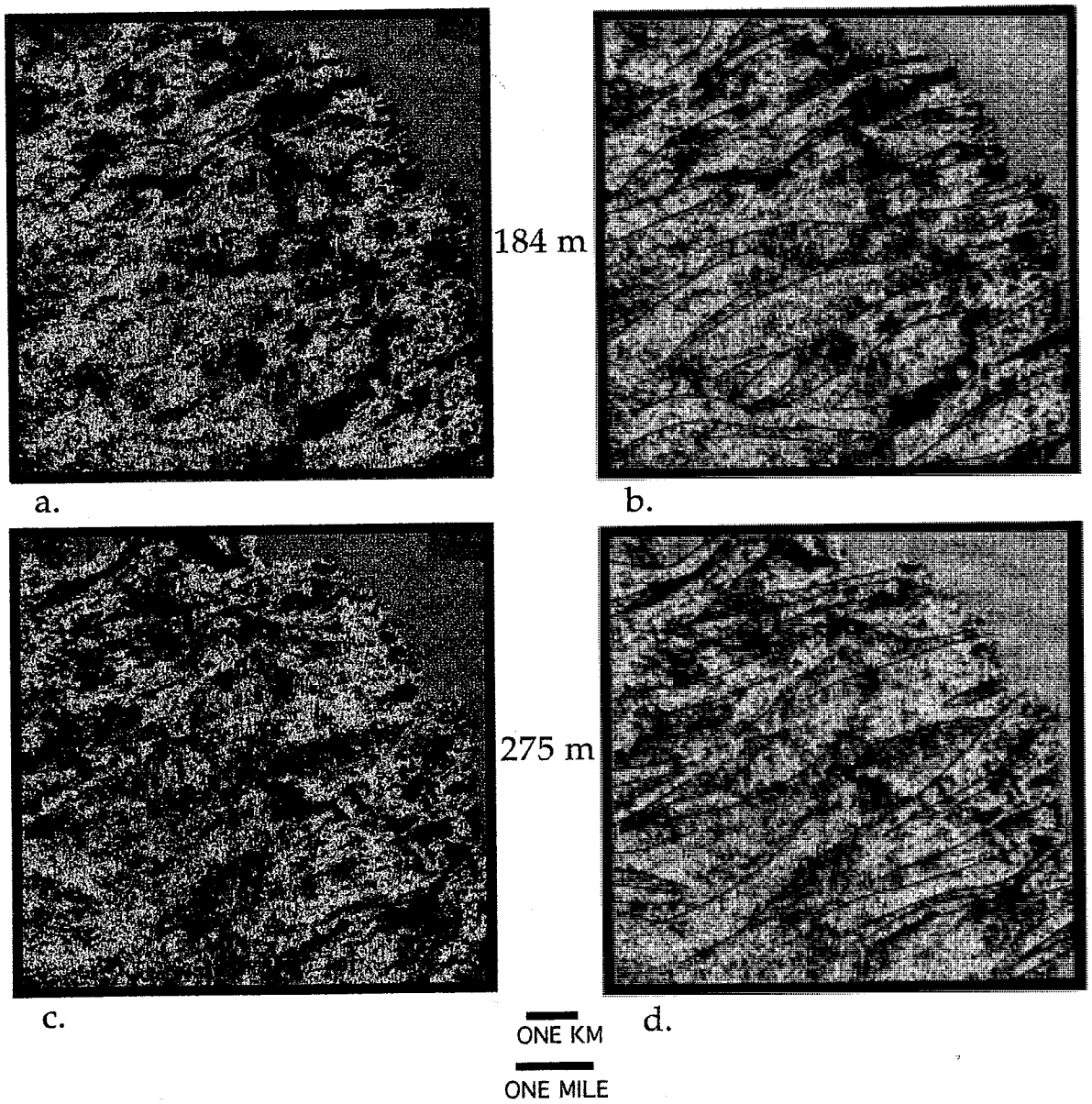
184 m
a.
b.
275 m
c.
d.
ONE KM
ONE MILE

Imaging submarine fan lobes & sheets

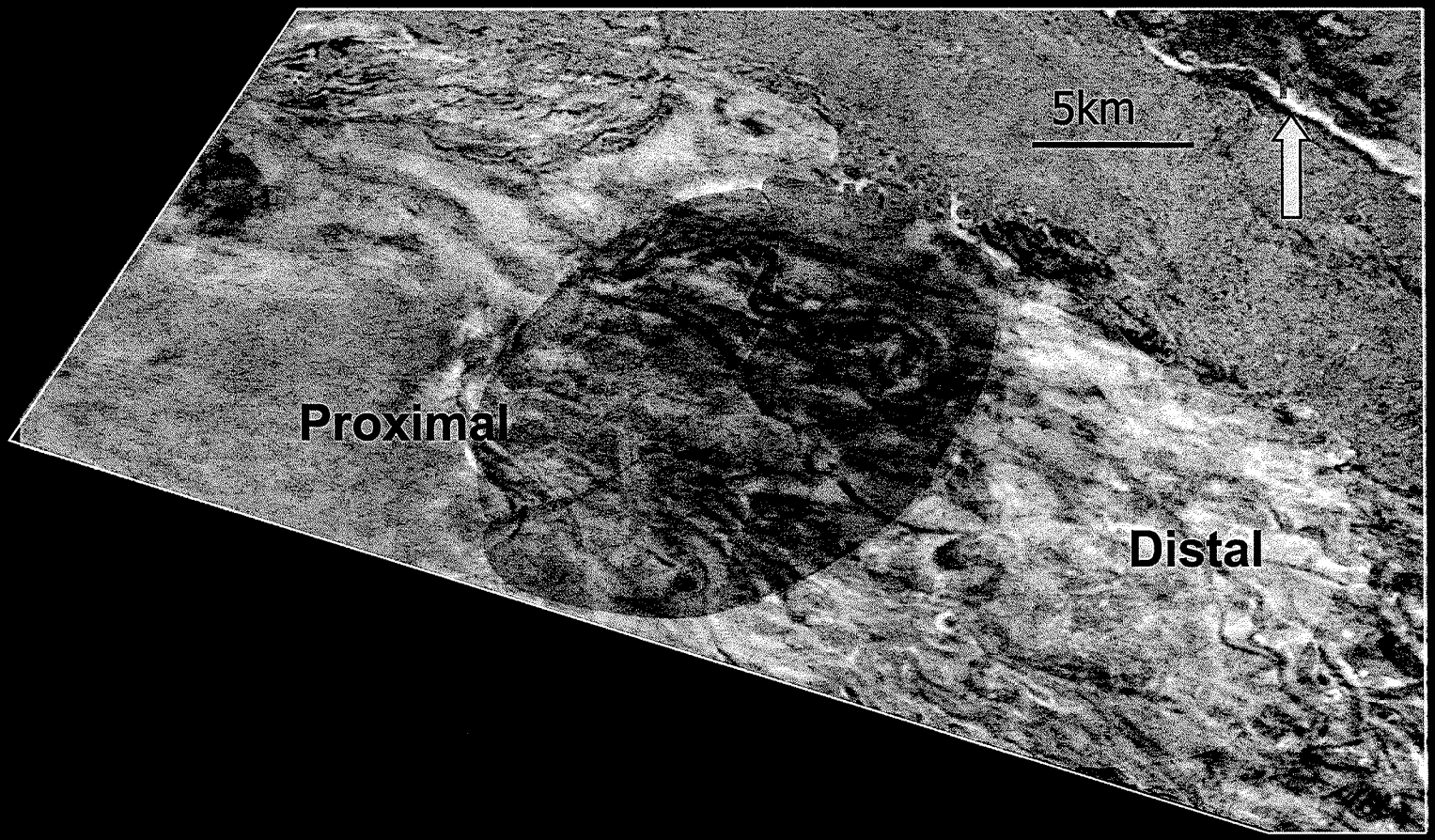
5km
Proximal
Distal

Channel - Lobe Transition

Deepwater Mahakam Delta, Indonesia

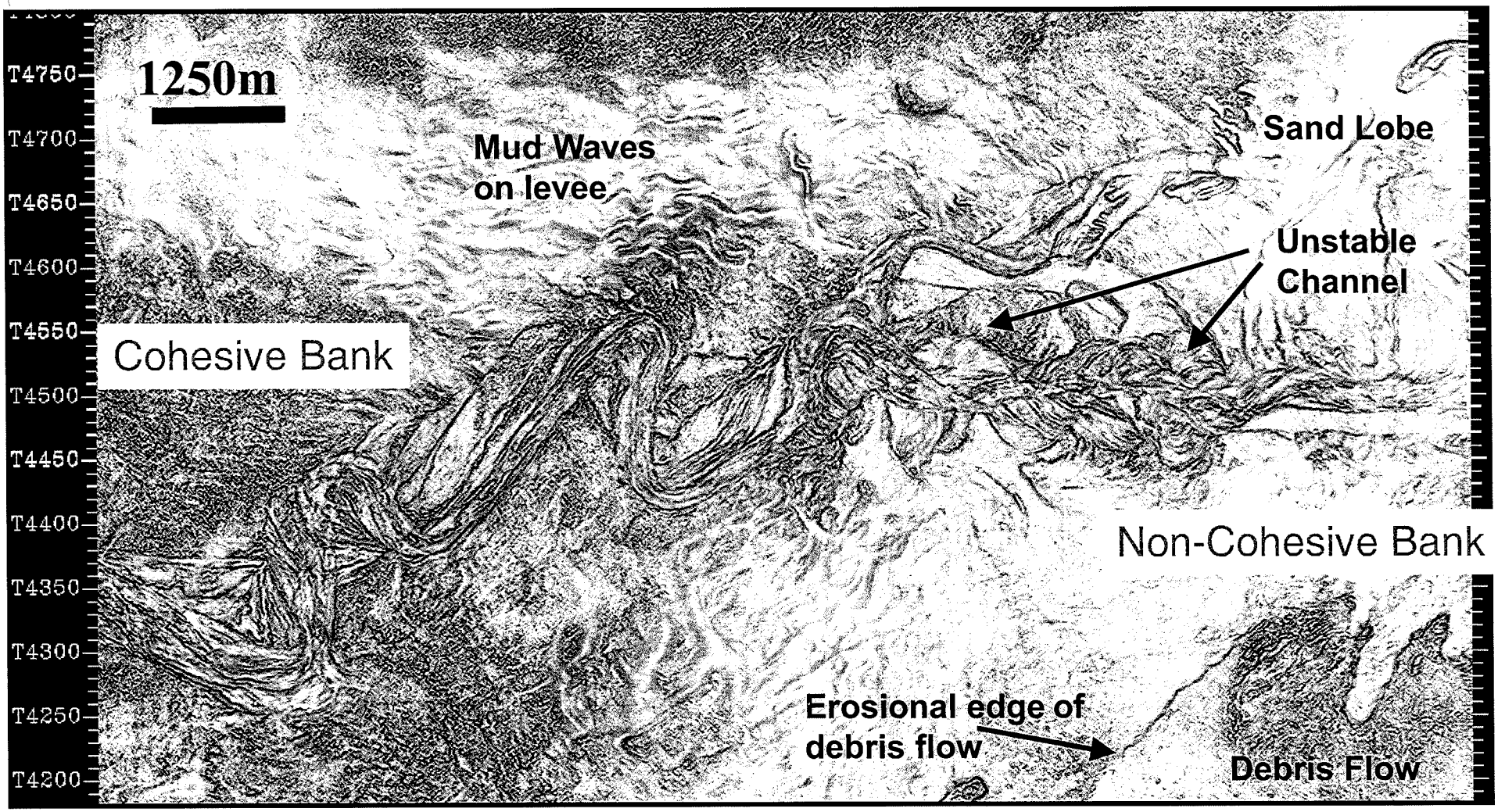

Edge Horizon slice through 14 kms of a near-surface analog (150ms below mudline).

shallowedge.gif

T. McHargue, EPTC Quantitative Stratigraphy Team, 11/2001

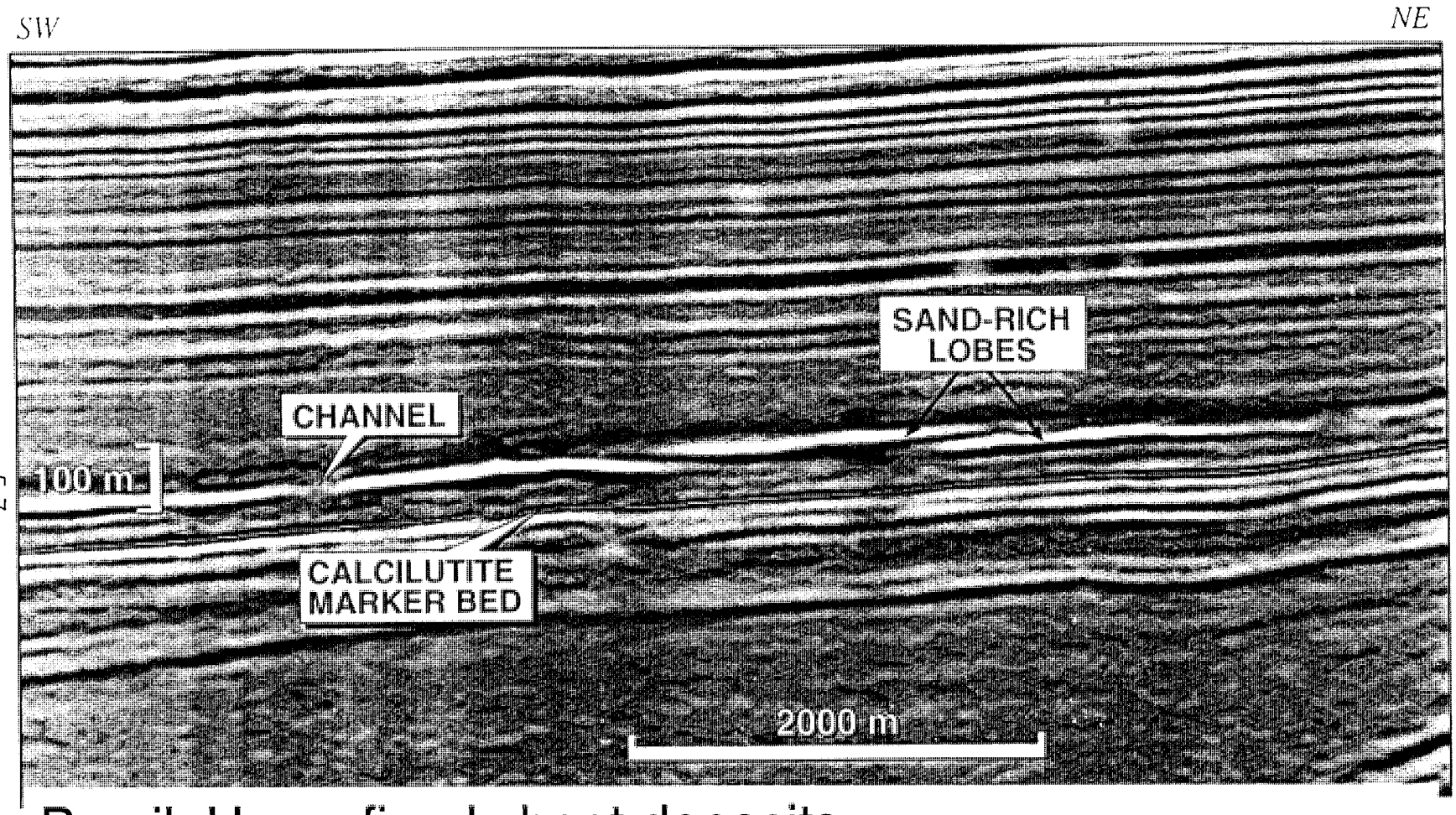

Brazil: Unconfined sheet deposits. Typically, a sheet (lobe) is 5-60m thick, 1-8 km. Wide, and 2-12 km. Long. Amalgamation of stacked lobes can result in sand-rich units (<10% mud) up to 125 m thick. Usually deposited in intra-slope basins.

From: C.H.L. Bruhn, 1998, Petroleum Geology of Rift and Passive Margin Turbidite Systems: Brazilian and Worldwide Examples, Part 2: Deep Water Reservoirs from the Eastern Brazilian Rift and Passive Margin Basins. AAPG International Conference Course Notes #6,

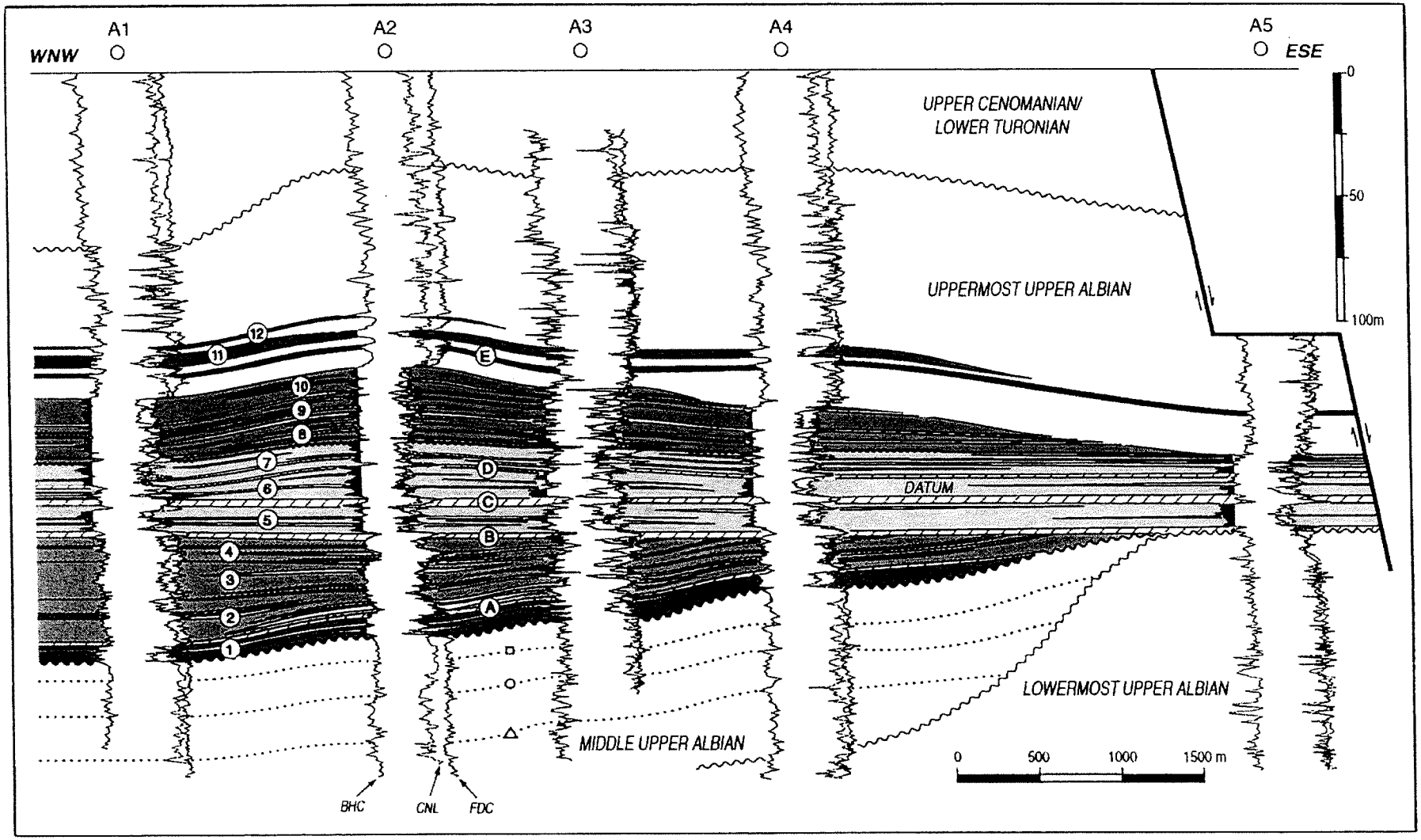

Albacora Field, Brazil: stacked to amalgamated turbidite sheets (colors). 12 reservoir units are separated either by widespread beds of hemipelagic mud or debris flows deposits (white).

From: C.H.L. Bruhn, 1998, Petroleum Geology of Rift and Passive Margin Turbidite Systems: Brazilian and Worldwide Examples, Part 2: Deep Water Reservoirs from the Eastern Brazilian Rift and Passive Margin Basins. AAPG International Conference Course Notes #6,

Submarine fan evolution

A submarine fan (or frontal splay) from the shallow Gulf of Mexico

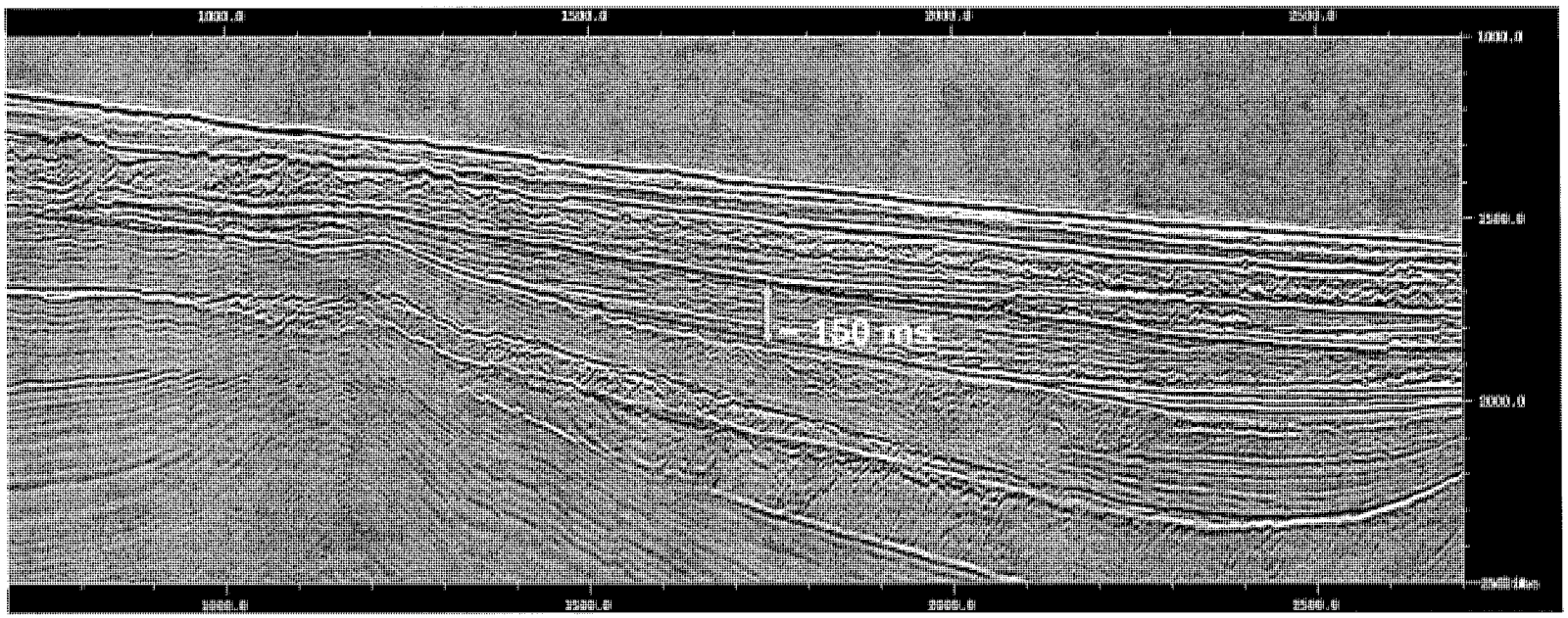

Courtesy Dominic Armitage

Seismic as a guide to well-log interpretations

Oligocene Puchkirchen Formation - Background

Stratigraphy

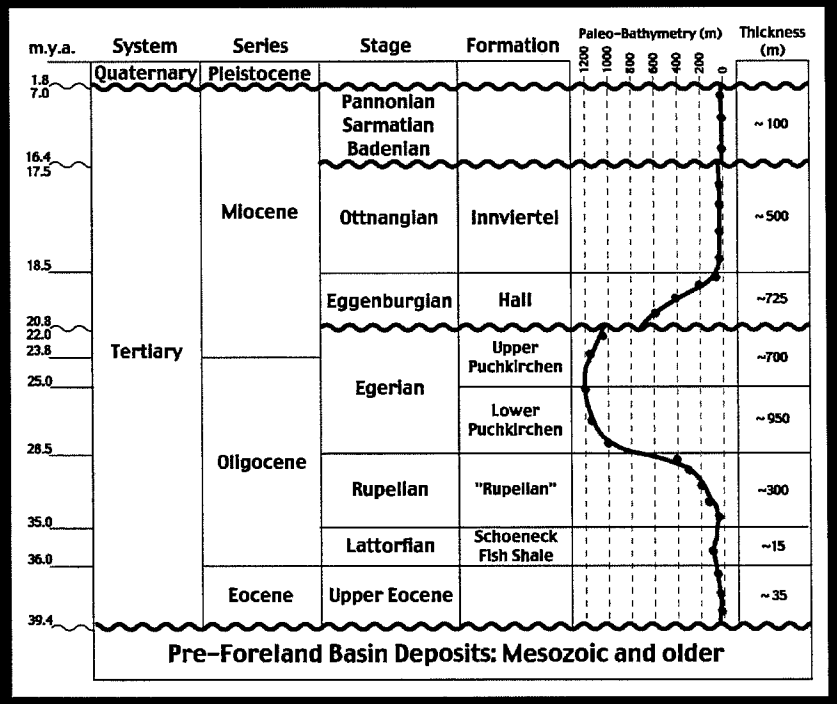

Database

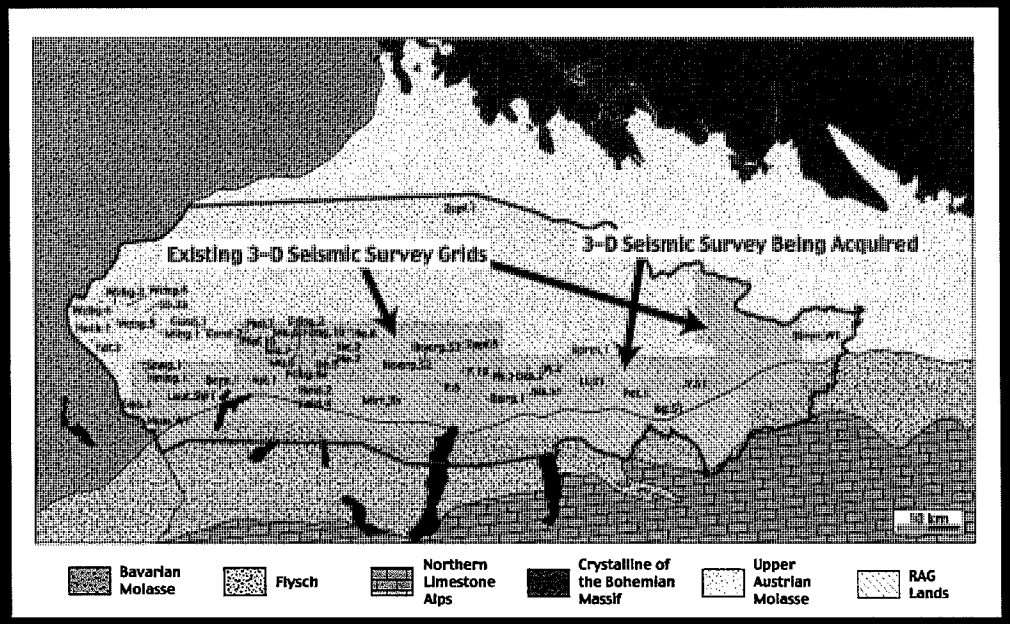

Study Area (modified from Homewood et al., 1986)

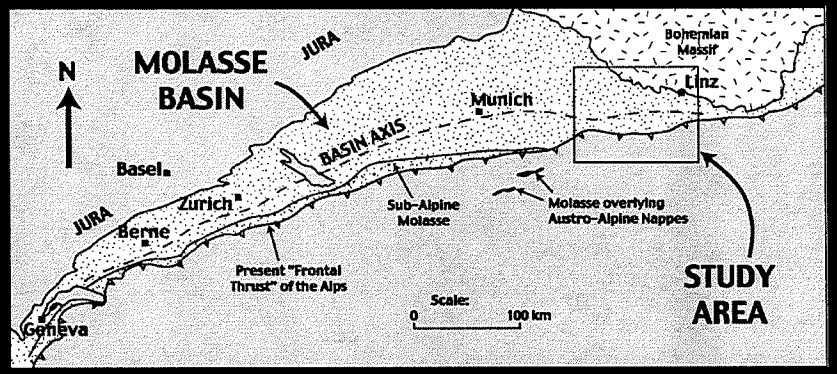

Paleogeography (modified from Sissingh, 1997)

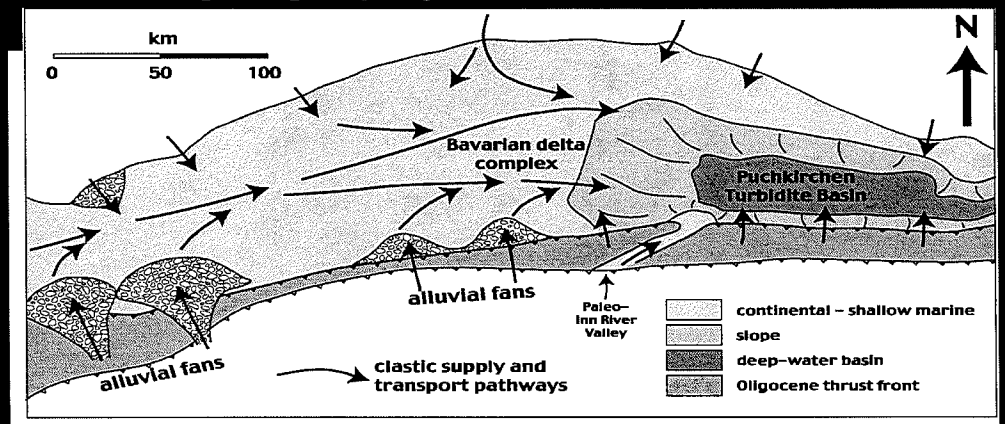

Hubbard, 2003

RMS semblance & RMS amplitude

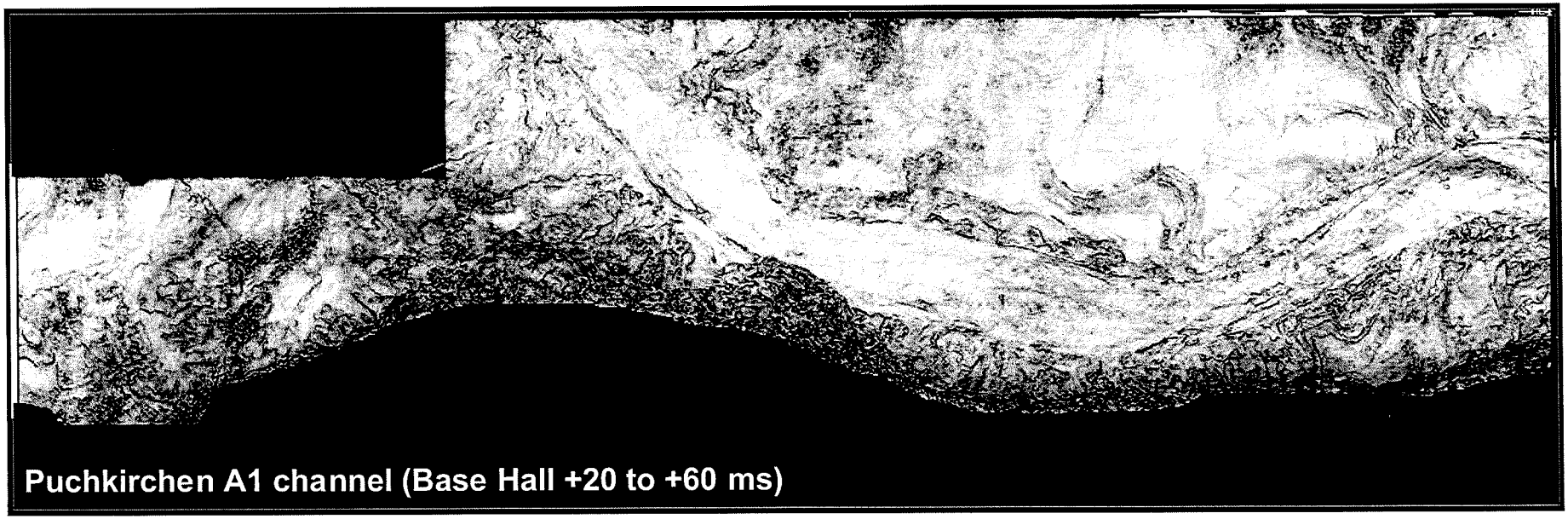

Puchkirchen A1 channel (Base Hall +20 to +60 ms)

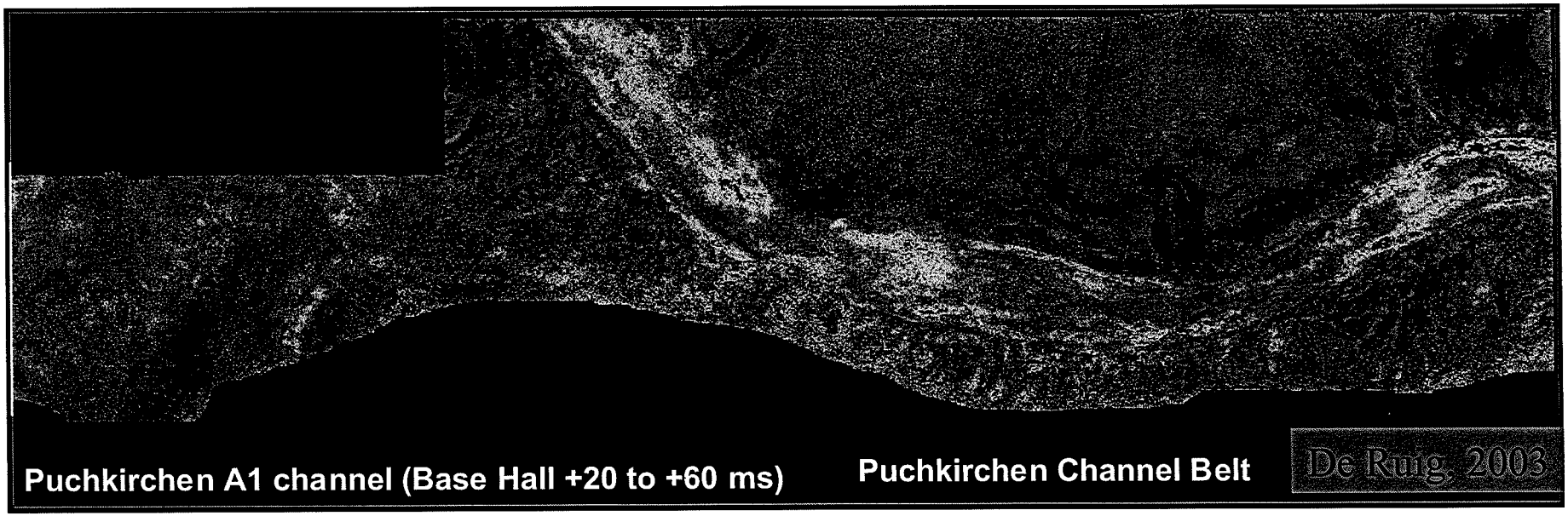

Puchkirchen A1 channel (Base Hall +20 to +60 ms)

Puchkirchen Channel Belt

De Ruig, 2003

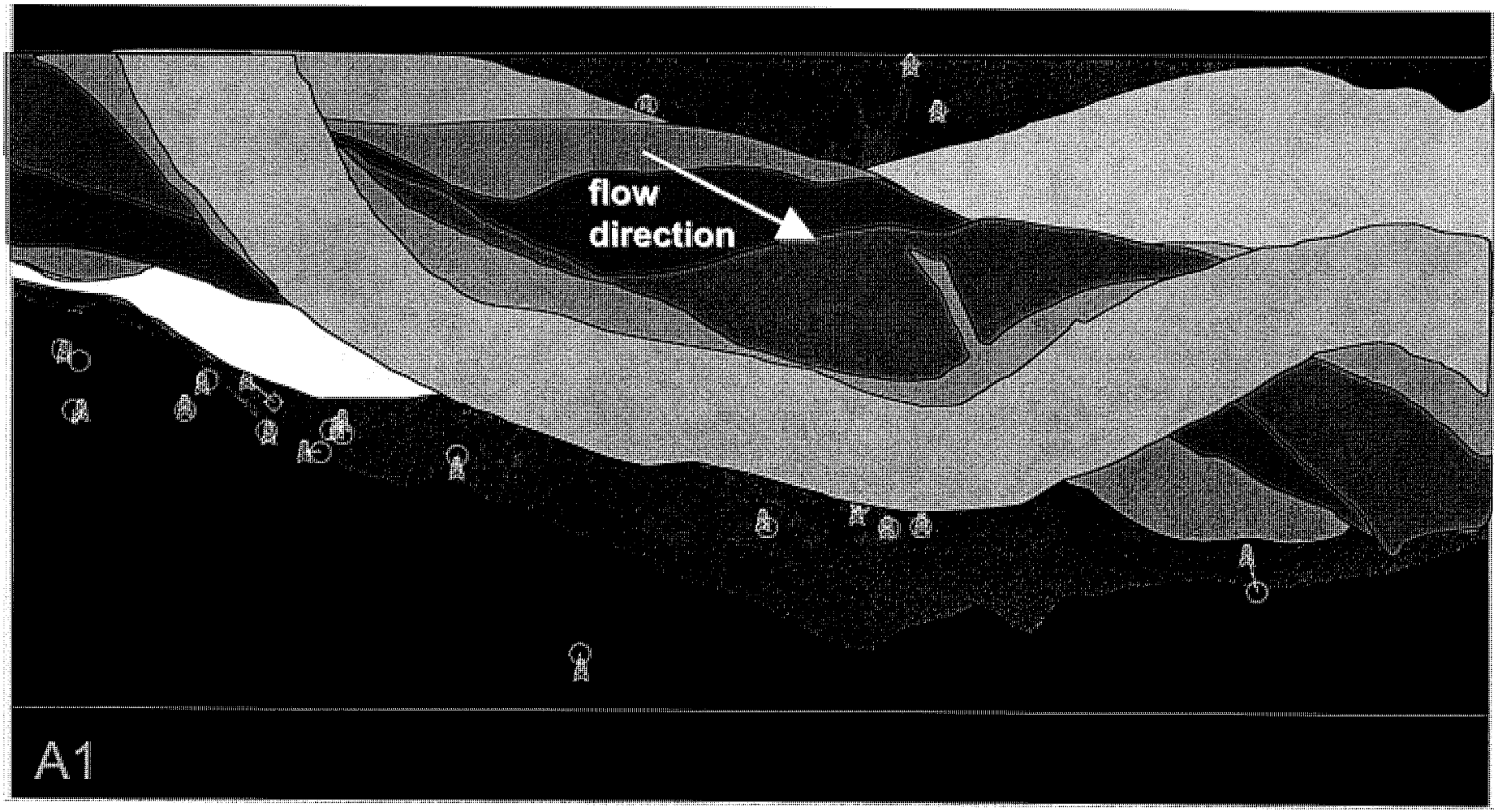
flow
direction
A1

Architectural Element Analysis

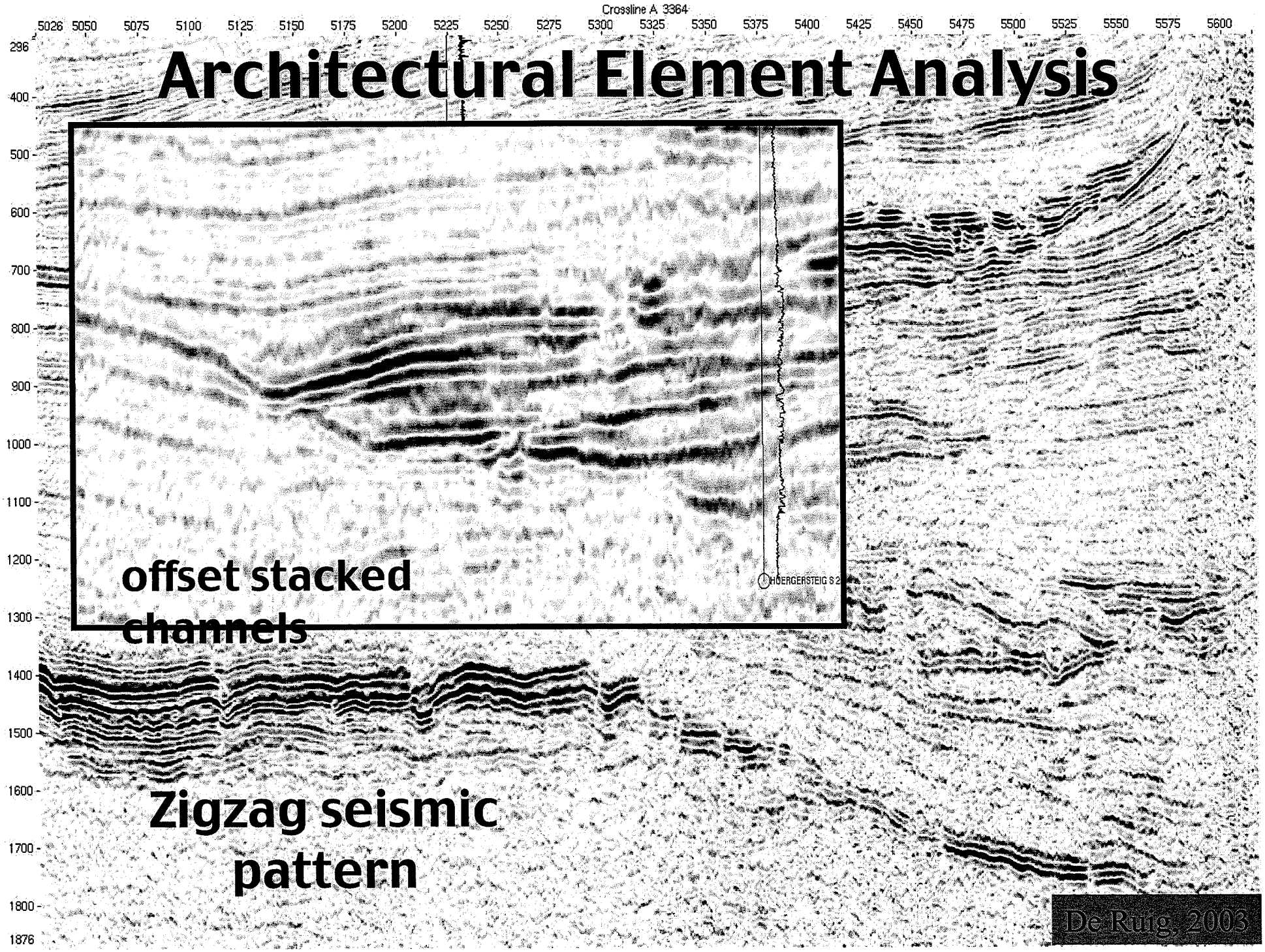

De Ruig, 2003

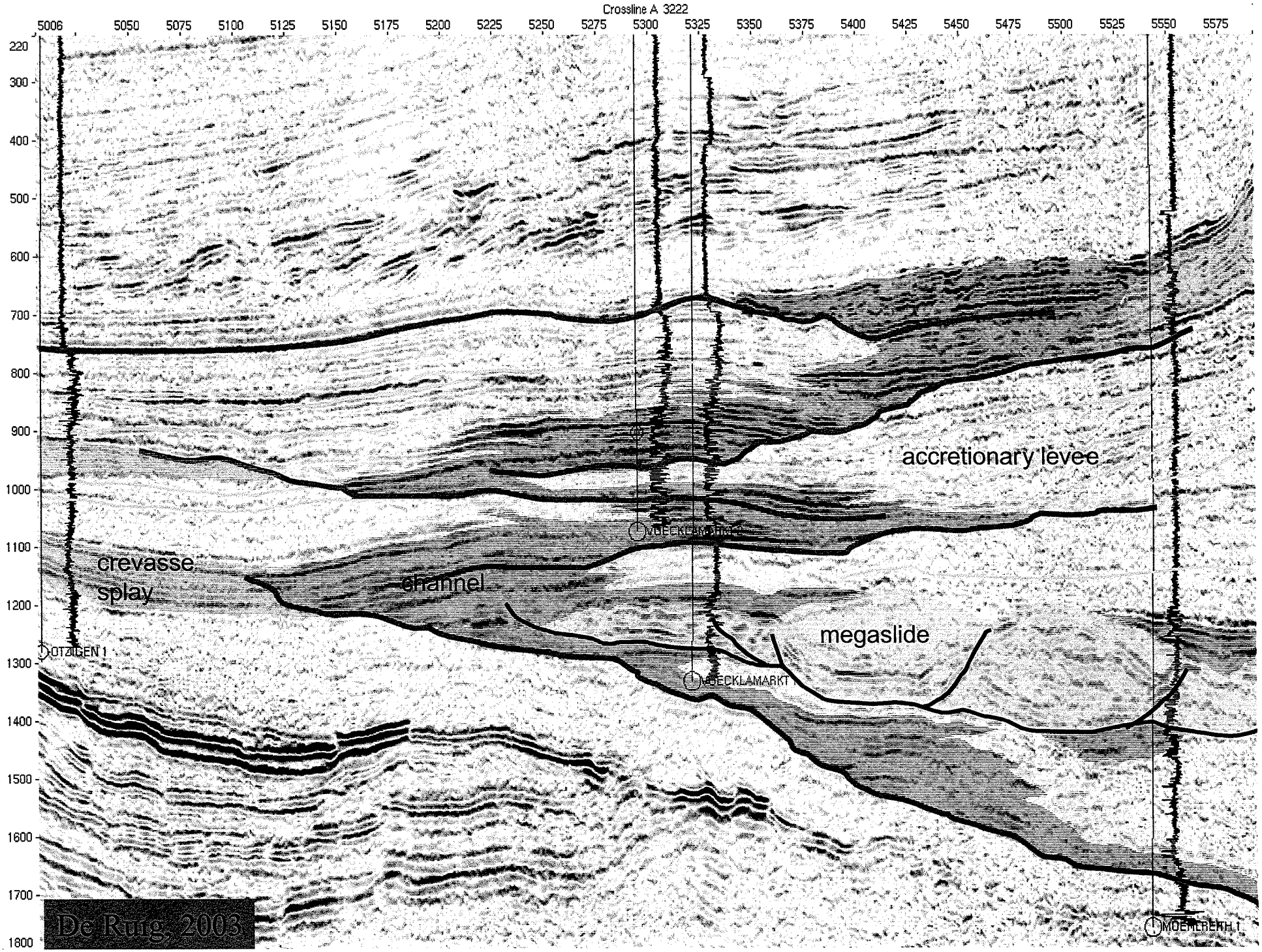
Crossline A 3222
5006
5050
5075
5100
5125
5150
5175
5200
5225
5250
5275
5300
5325
5350
5375
5400
5425
5450
5475
5500
5525
5550
5575
220
300
400
500
600
700
800
900
1000
1100
1200
1300
1400
1500
1600
1700
1800
accretionary levee
crevasse
splay
channel
megaslide
OTZIGEN 1
MOECKLAMARKT
MOEMLREHH 1
De Ruig, 2003

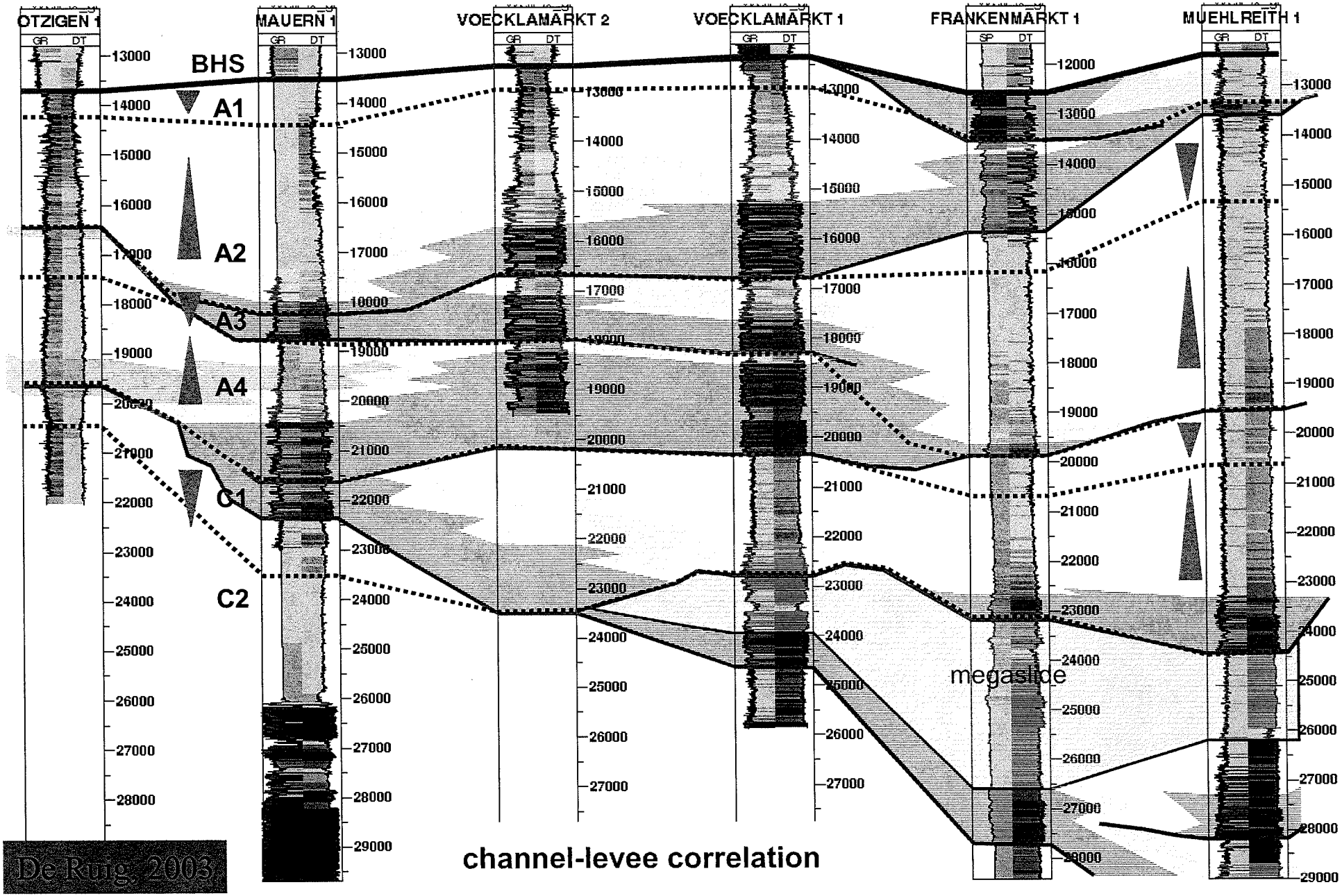

channel-levee correlation

Use the right model

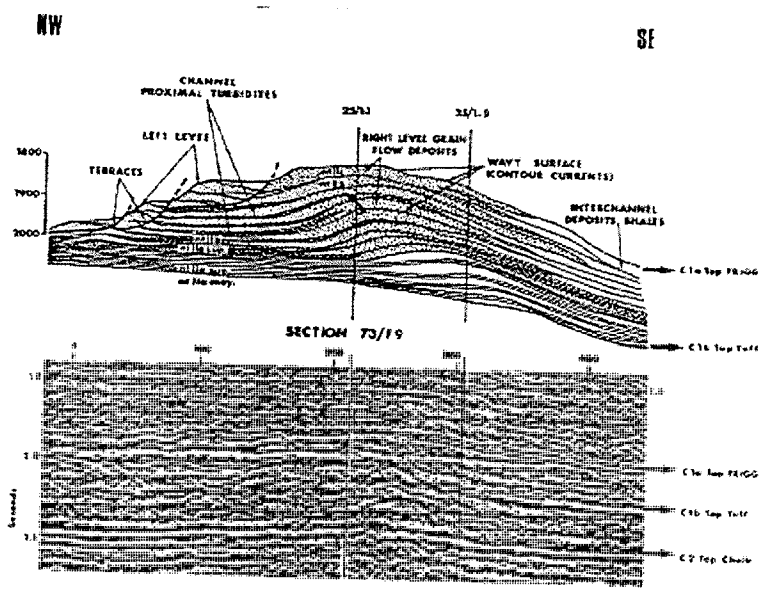

Figure 21: Channel-levee interpretation of seismic data from Frigg field, North Sea ('flat spot' in center of section just above 2.0 seconds is a water/petroleum contact). Compare with modern channel-levee analog example in Figure 20 (Heritier . others, 1979).

An example from the North Sea where things didn't quite work out….

A mound is not always what it seems….

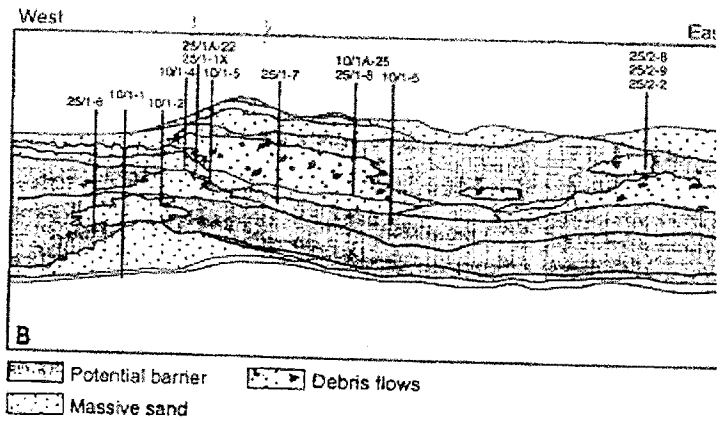

Figure 10—(A) Seismic section across Frigg field showing sheet mound geometry (see the top Frigg sa 9, SSL survey, 1973. (B) General stratigraphic model for the Frigg field. Core from the Elf 25/2-8 well study. Palynozones are shown by nflb, nflla-u, etc. Note discontinuous nature of debris-flow sands. Si Brewster (1991).

Table 2. Summary of "Pitfalls" in Recognition of Submarine Fans *Mitchum 1985 b*

FEATURE WITH SUPERFICIAL FAN SHAPE	CHARACTERISTICS SIMILAR TO THOSE OF FAN	DIAGNOSTIC CRITERIA FOR SEPARATION FROM FAN
Prograding clinoform slope lobes (most common "pitfall") (Fig. 13 A and B)	Mounded shape in strike (transverse) direction, commonly enhanced by local erosion	Prograding clinoform morphology in dip (longitudinal) direction; recognition of erosional truncation
Arcuate detached normal fault in outer shelf-upper slope position (Fig. 13 C)	"Roll-over" on downthrown limb produces mound shape; complex faulting produces "chaotic" character	Seismic map grid shows fault pattern and absence of "fan" shape; possible internal prograding character in fault blocks
Shale-prone mounded chaotic-fill seismic facies produced by slump and creep onslope (Fig. 13 D)	Superficial mound shape (commonly mappable) on or at the base of slope, or in small slope basins; possible apparent "canyon"	Poorly organized internal fan configuration with chaotic to internal "mounded" configuration; little amplitude difference with surrounding units; commonly associated with slump scars on slope; slump may produce apparent "canyon"; associated with large shelf-edge failures, growth faults, and diapirism in rapidly prograding deltaic areas (Mississippi delta)
Contourites or "depositional anticlines" (Fig. 13 E)	"Mounded" shape in transverse section; deep-water associations along continental margins	Very consistent internal reflections in longitudinal section; internally asymmetric, with long gentle, and short steep flank; larger than most fan; possible gentle toplap; Elongate map shape along continental margins; preferred position where contour currents are focused; commonly remote from sand source

Many Exploration Disappointments Result From

Using the Wrong Model!

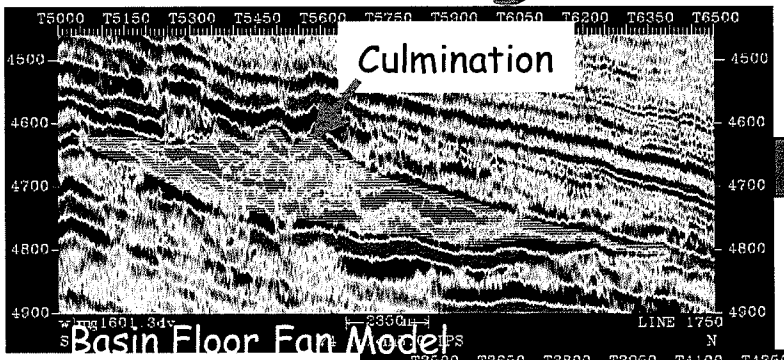

Initial Estimate of
Net-to-Gross: 70 - 90%

COMPARE TO SHALLOW ANALOG

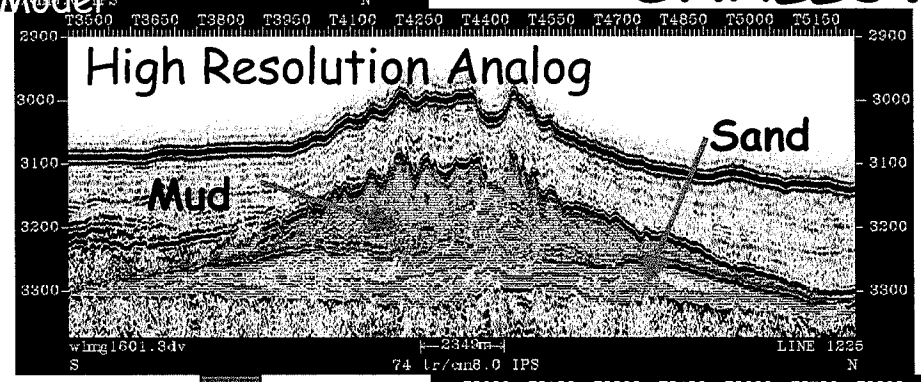

RE-INTERPRET

- Revised Estimate of
  Net-to-Gross: 40 -70%
- Move the well location.

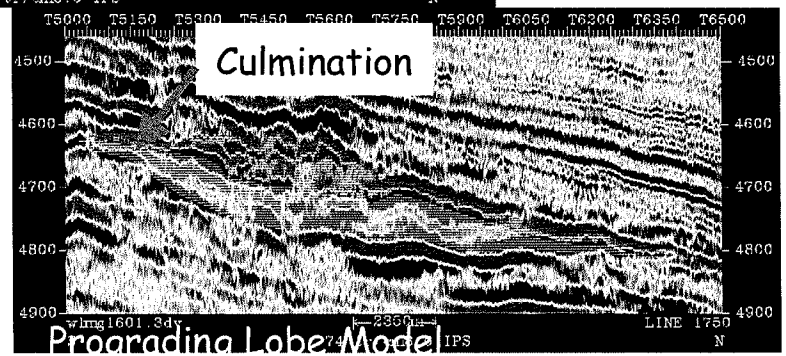

SEISMIC STRATIGRAPHIC INTERPRETATION OF "FRAMEWORK" (NON DETRITAL) CARBONATE BUILD-UPS

SIMPLIFIED GENETIC TYPES:

1. "REEF" - POSITIVE RELIEF FRAMEWORK FEATURE
2. "BANK" - PILE-UP (NOT EXTENSIVELY BOUND IN FRAMEWORK) OF SKELETAL REMAINS (& RELATED SEDIMENT) OF COMMUNITY OF GREGARIOUS ORGANISMS.

PROBLEM: CAN'T TELL THESE APART SEISMICALLY. AT BEST CAN ONLY DETECT POSITIVE RELIEF & CARBONATE COMPOSITION. HENCE, MORE USEFUL APPROACH

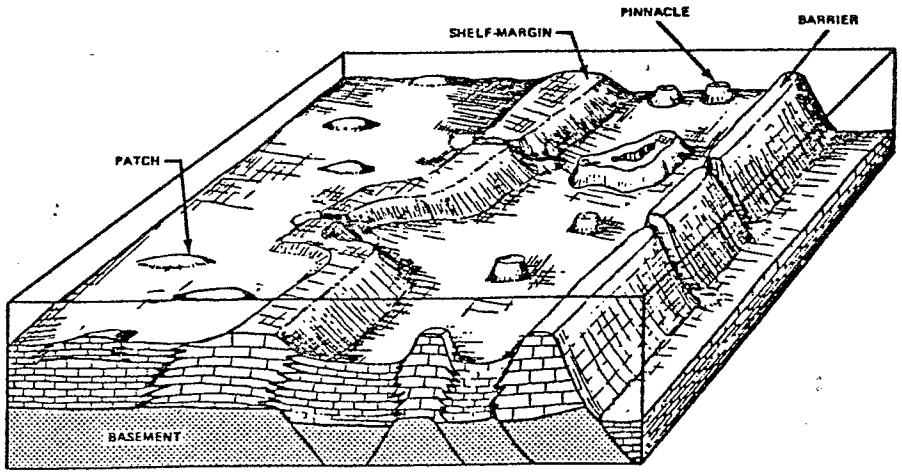

FIG. 1—Types of carbonate buildups most easily recognized from seismic interpretation. Conventional classification of reefs and banks, although preferred, is not easily applicable to seismic data.

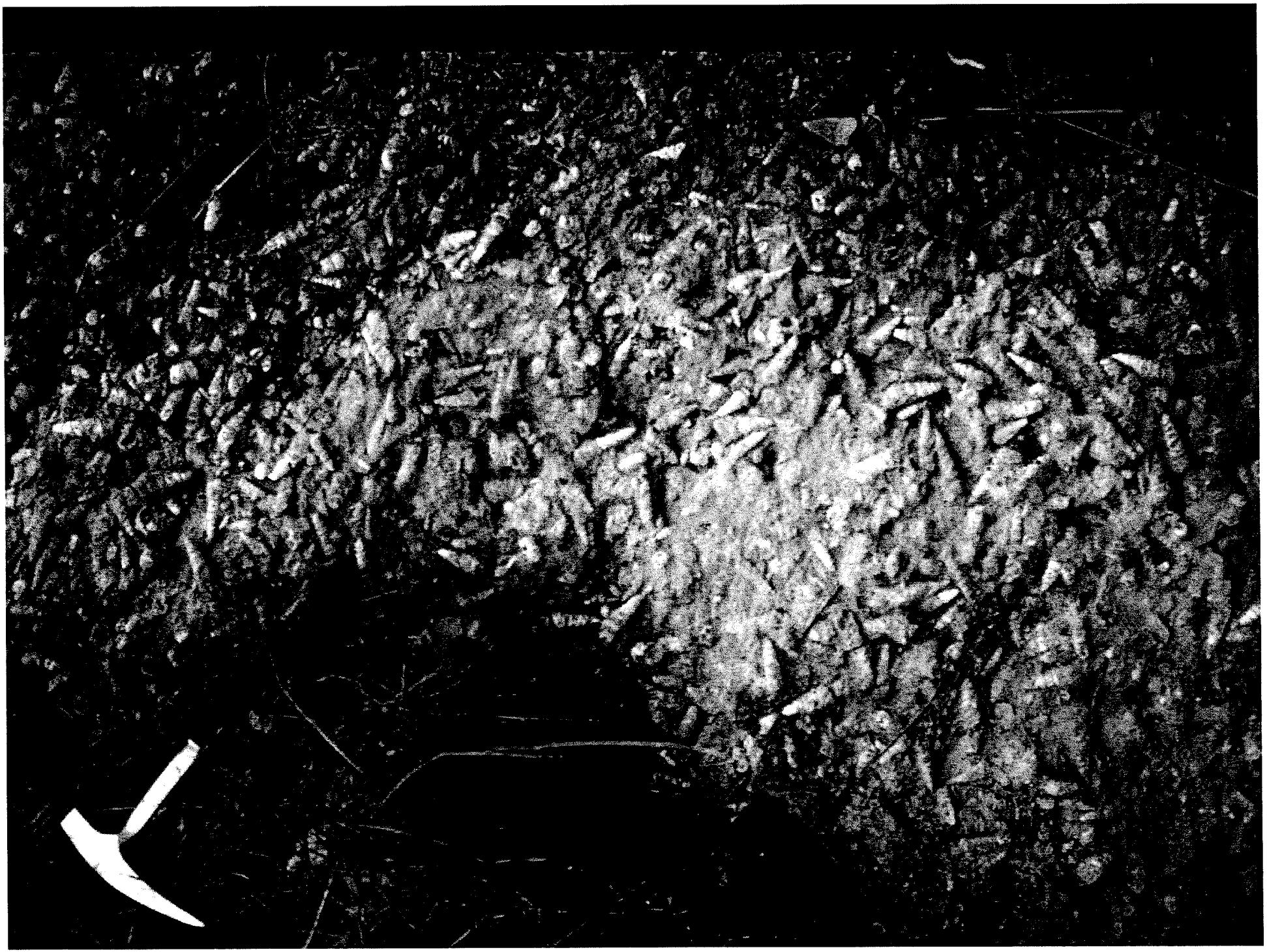

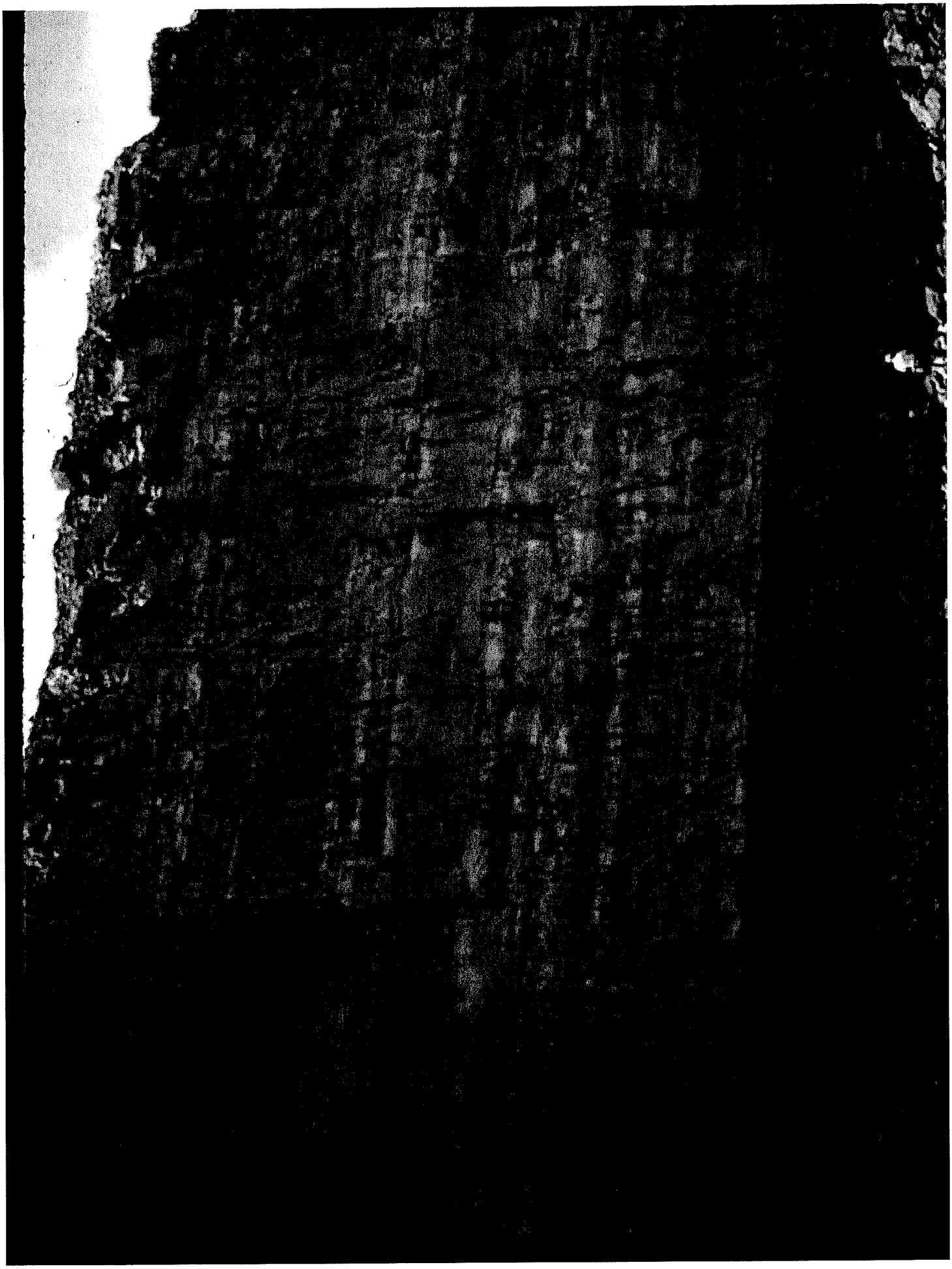

Reality checks from carbonate settings

AAPG Bull Feb'81

247

Actualistic basis for interpreting carbonate systems by refl. seis.

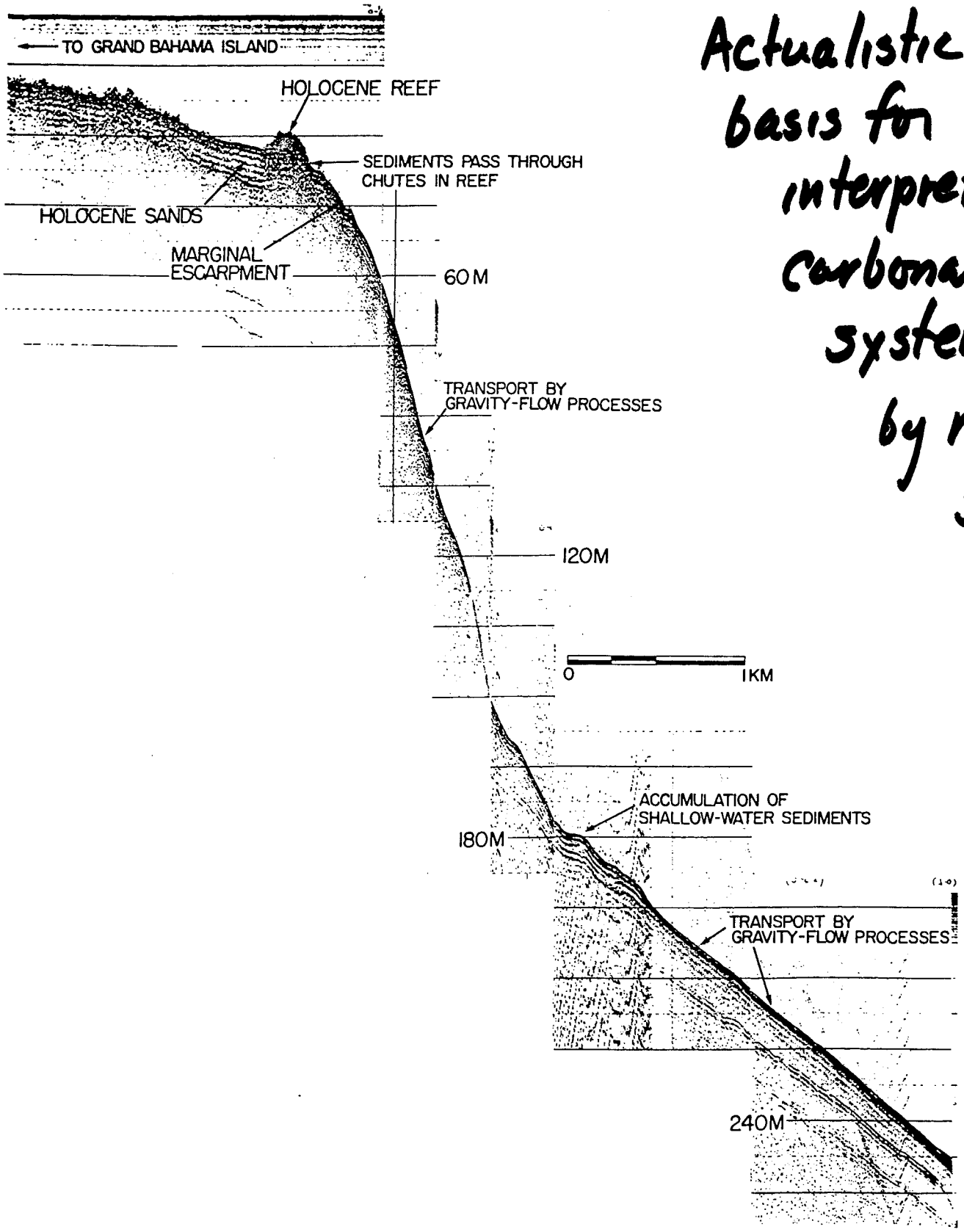

FIG. 20—Seismic profile 30 (Fig. 2A) illustrates progress of shallow-water sands carried to deep.

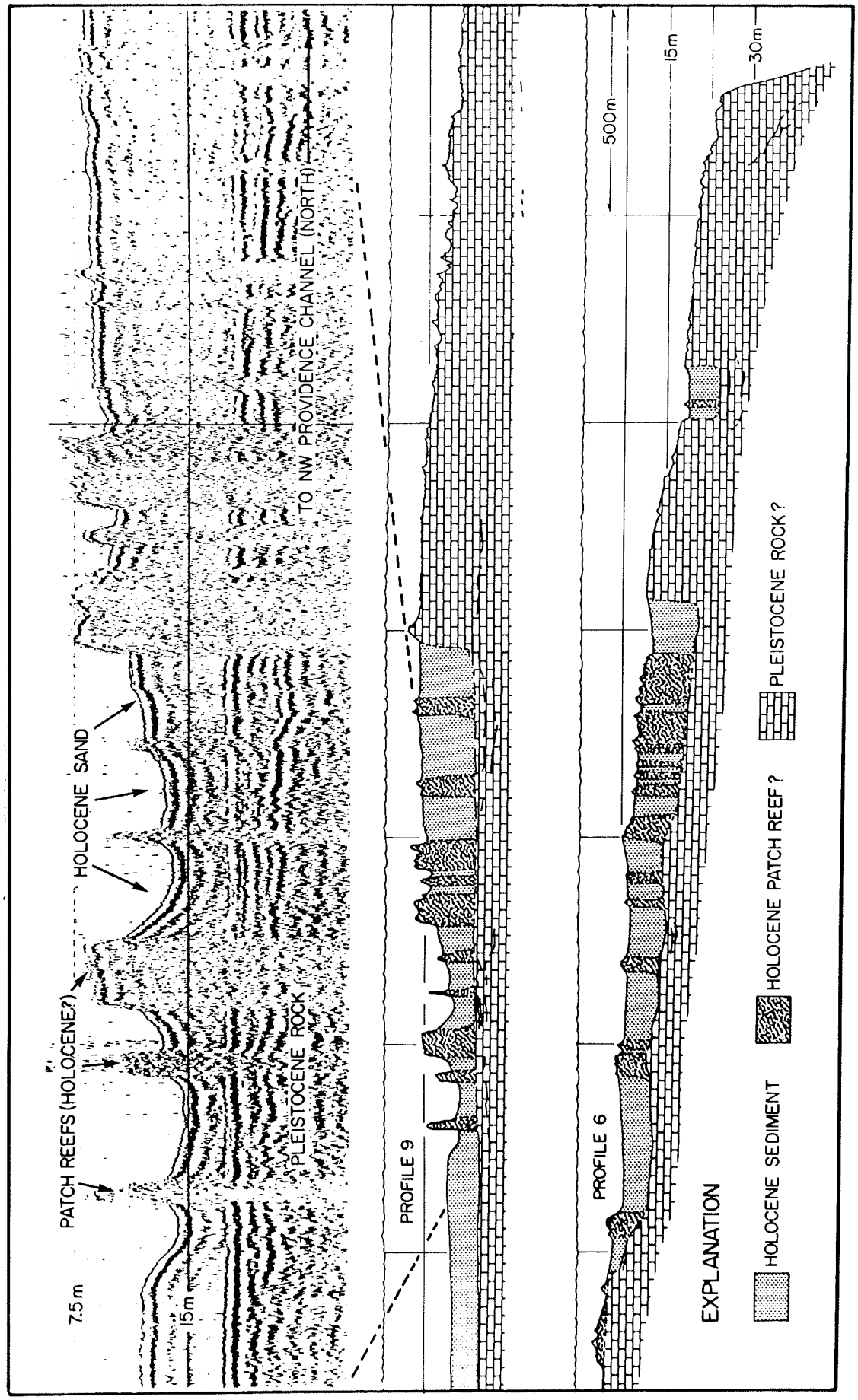

FIG. 9—Seismic profile 9 (Fig. 2A) and interpretation, with profile 6 interpretation. This unusual area is zone of patch reefs and thick sediment accumulation. Bank top shows extensive vertical growth.

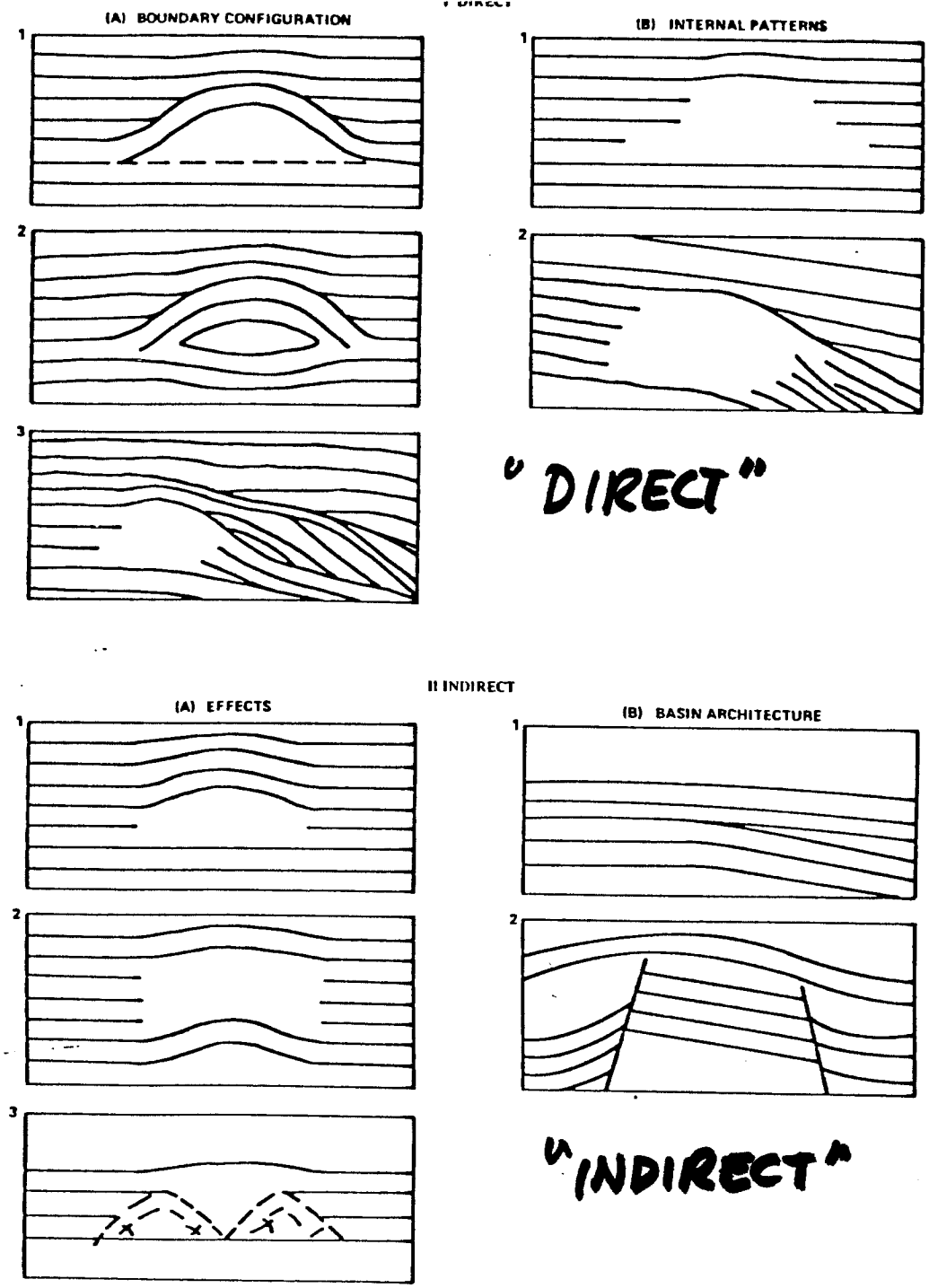

FIG. 3—Seismic criteria for recognizing carbonate buildups. Criteria for directly outlining buildups include reflections from top and sides of buildups and onlap of overlying reflections onto buildups (I-A); and patterns of seismic facies change between buildup and enclosing strata (I-B). Criteria that indirectly outline or infer presence of buildup include drape, velocity anomalies, and spurious events (II-A), and determination of optimum basin positions for buildups (II-B).

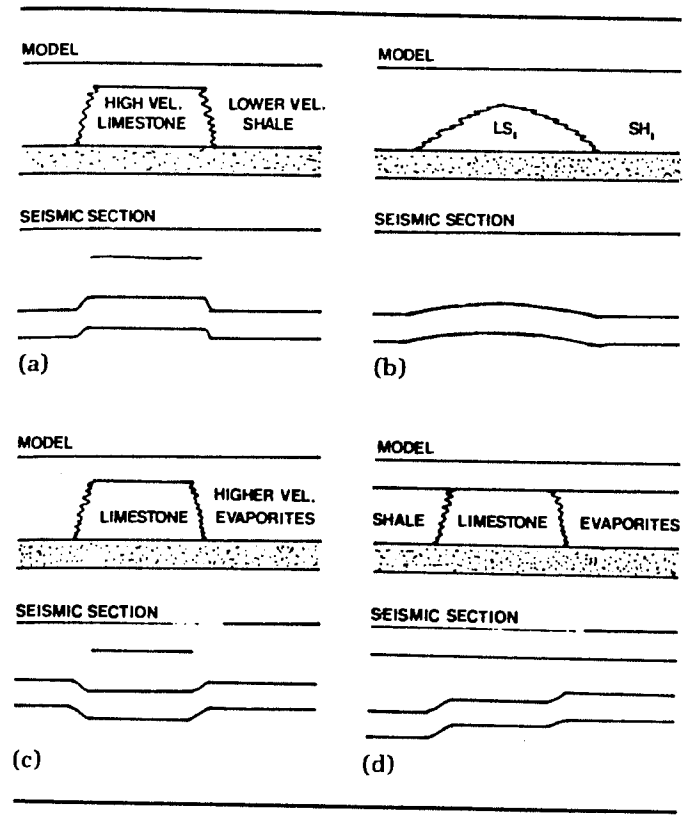

FIGURE 3.36 *Velocity anomalies beneath reefs.* (a) *A reef composed of high-velocity limestone encased in lower-velocity shales produces a velocity pull-up on underlying reflections.* (b) *Same as (a), except the reef has a more rounded form.* (c) *A reef encased in an evaporitic sequence with high interval velocity produces a velocity push-down on underlying reflections.* (d) *A reef with low-velocity basinal shales to its left and high-velocity backreef evaporites to its right produces a push-down beneath the shales and pull-up beneath the evaporites. Reprinted by permission of IHRDC Press from Sheriff, 1980a, fig. 5.17, p. 115.* Badley 85

METHODS OF RECOGNIZING CARBONATE SYSTEMS

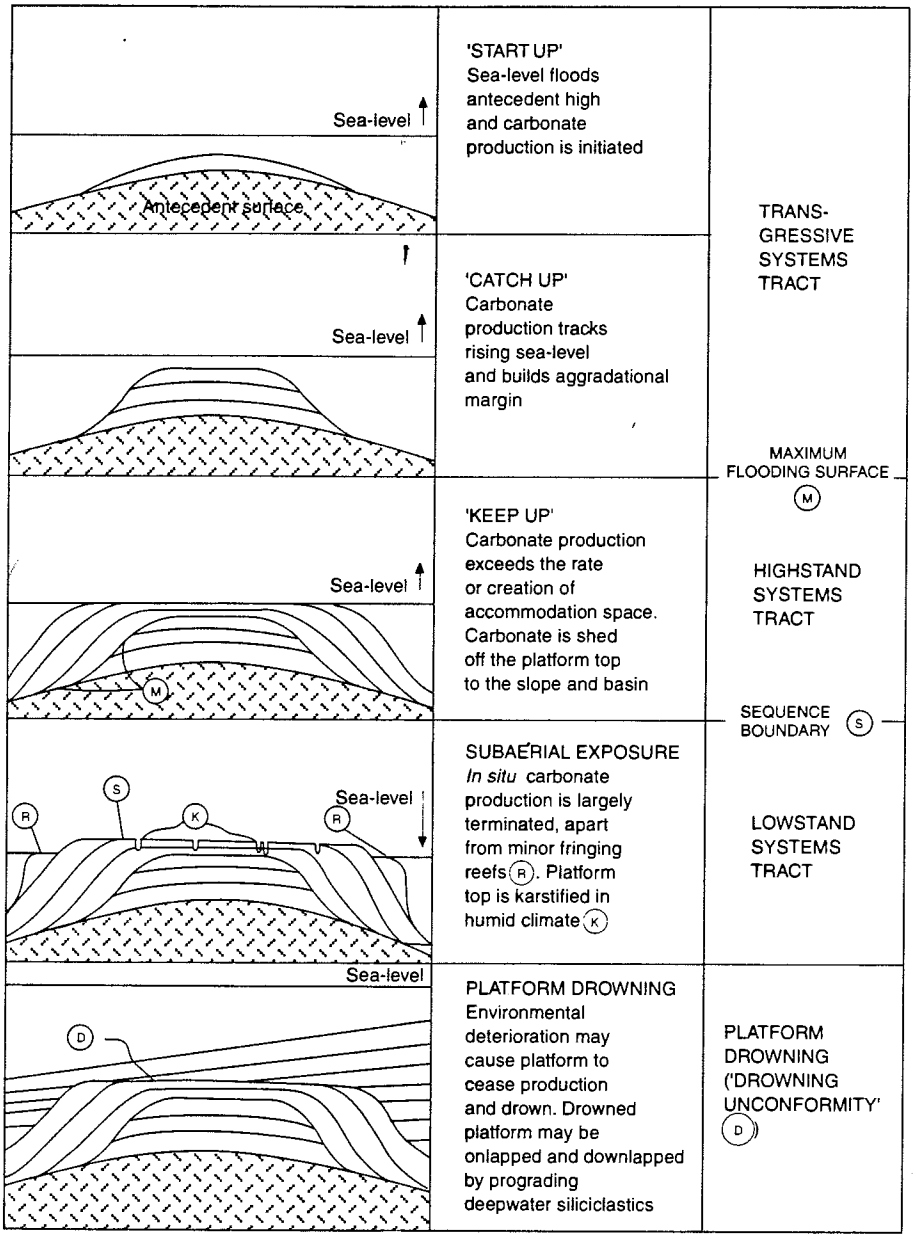

Emery & Myers 96

Fig. 10.6 Schematic model for an isolated carbonate platform, showing idealized systems tract geometries and platform drowning

Basis for sequence stratigraphic architecture of carbonate systems

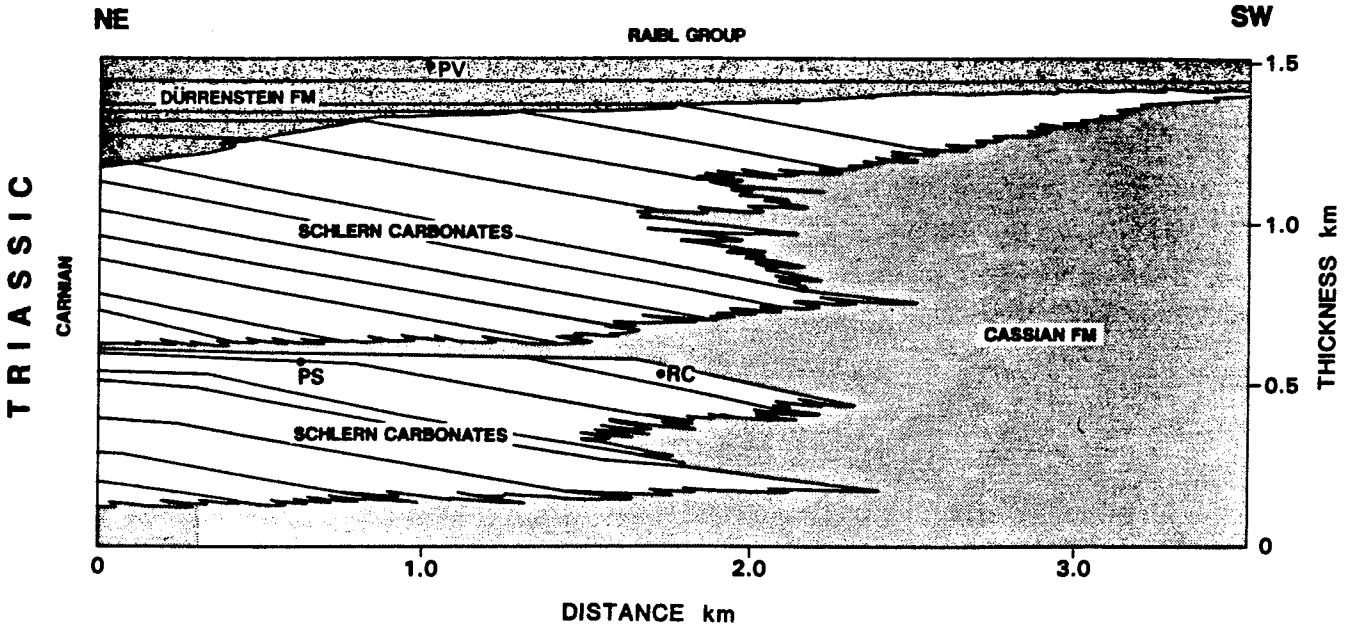

Figure 2—Stratigraphic terminology used in this study for the Picco di Vallandro area. PV = Picco di Vallandro, PS = Punta di Serla, RC = Rocce della Chiesa. The Raibl Group shown at the top of the diagram overlies the Dürrenstein Formation, but is not exposed due to erosion at Picco di Vallandro. Line and plane of section shown in Figure 6.

example from Biddle et al. 92

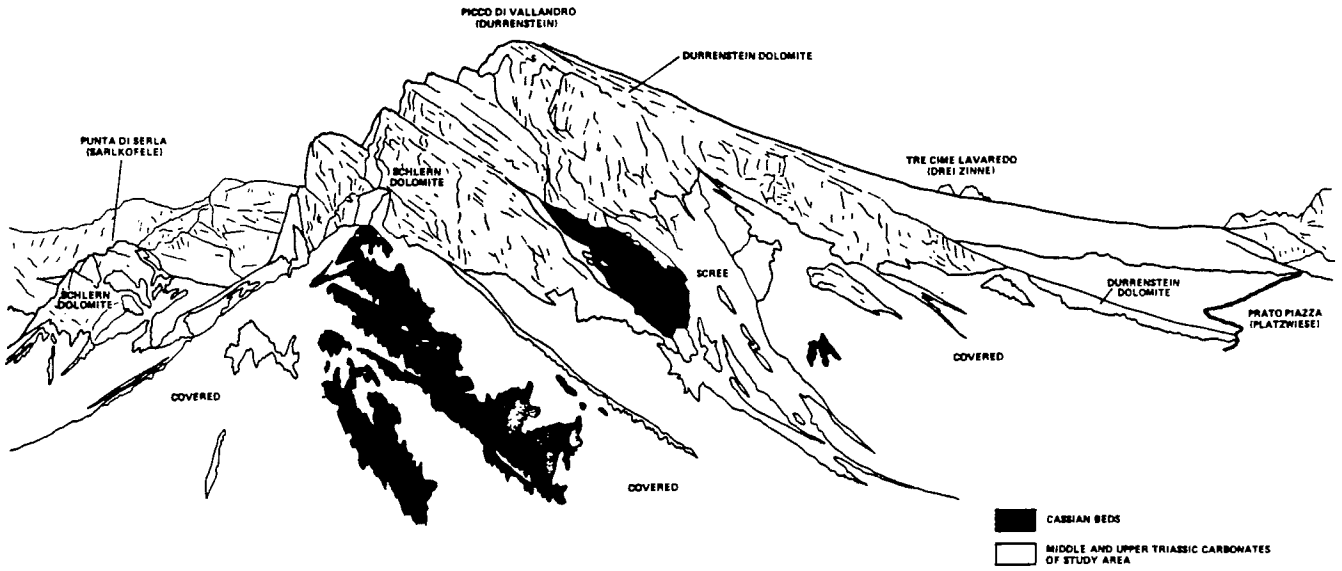

Figure 3—Line drawing of Picco di Vallandro looking toward the east (see Figure 4) showing distribution of, and relationships between, the stratigraphic units discussed in the text.

CALIBRATION ... CARBONATE PLATFORM MARGIN DEPOSITIONAL SYSTEMS

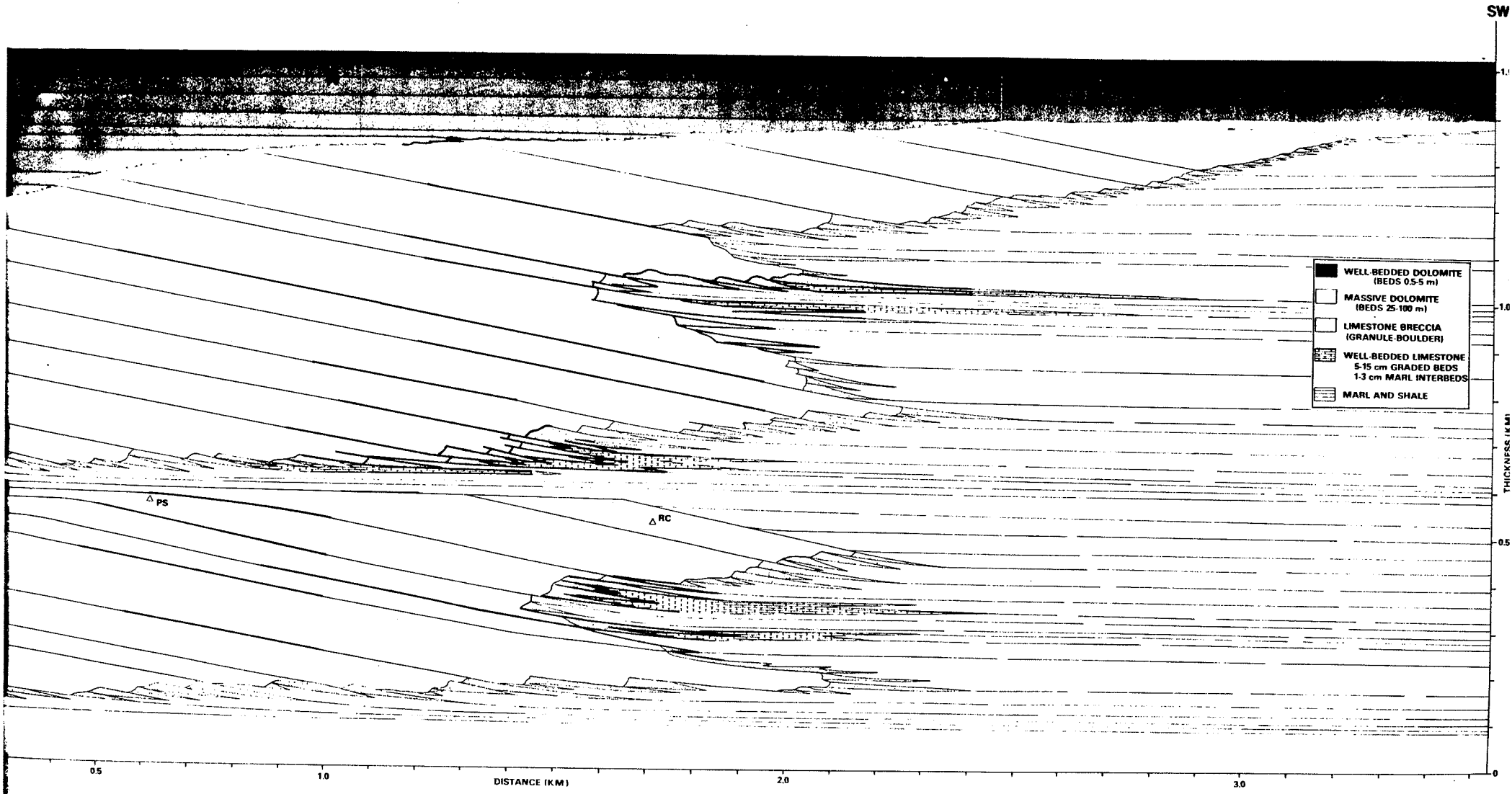

section, Picco di Vallandro area. Heavier lines represent areas of on-ground and lithology in other areas have been projected from photographs and other Vallandro. PS = Punta di Serla, RC = Rocce della Chiesa. See text for discussion. Line in Figure 6.

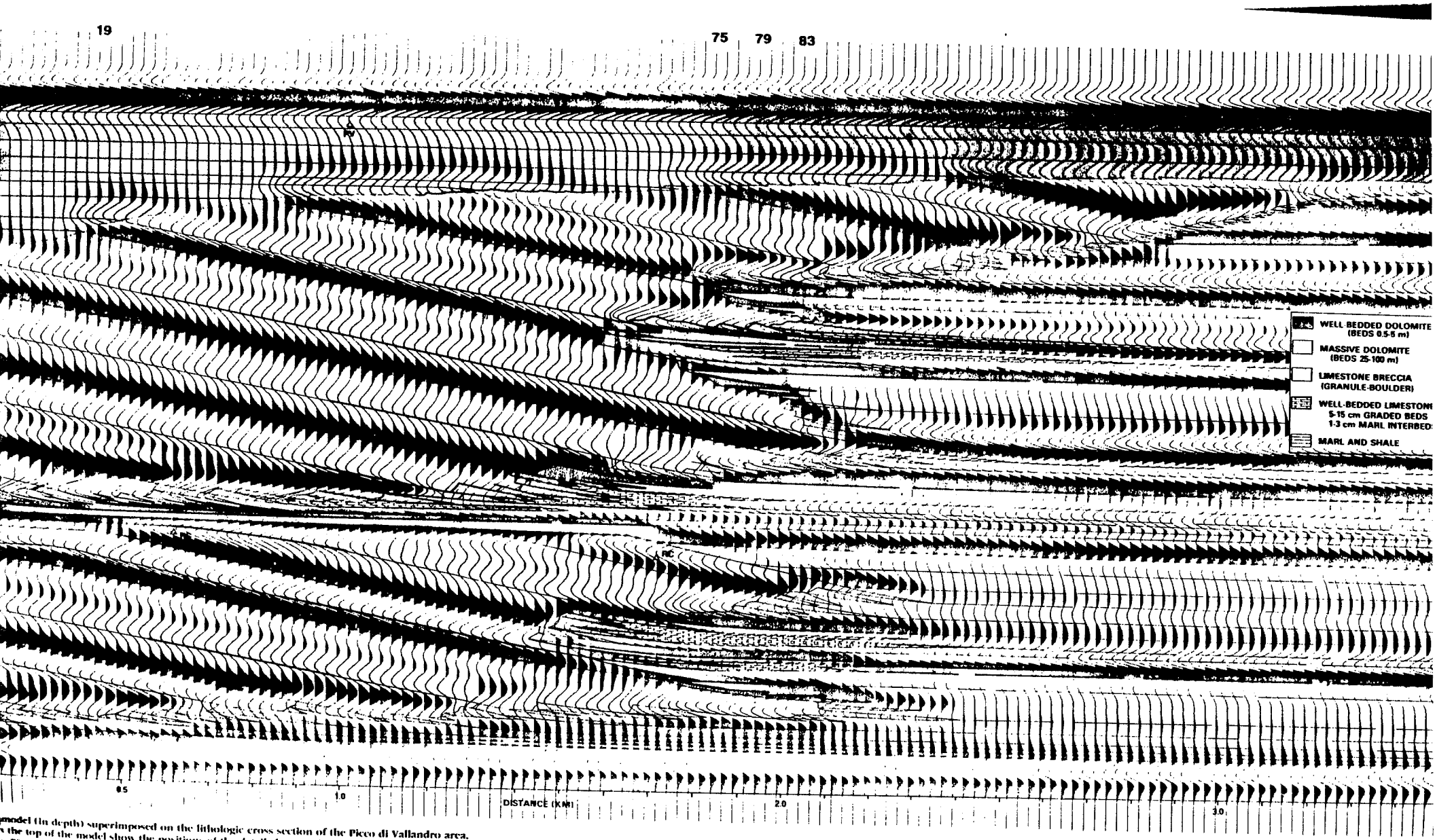

model (in depth) superimposed on the lithologic cross section of the Picco di Vallandro area. the top of the model show the positions of the detailed traces illustrated in Figures 12–15. PV). PS = Punta di Serla, RC = Rocce della Chiesa. See text for dicussion. Line and plane of section

EXAMPLES OF CARBONATE MARGIN SYSTEMS ..

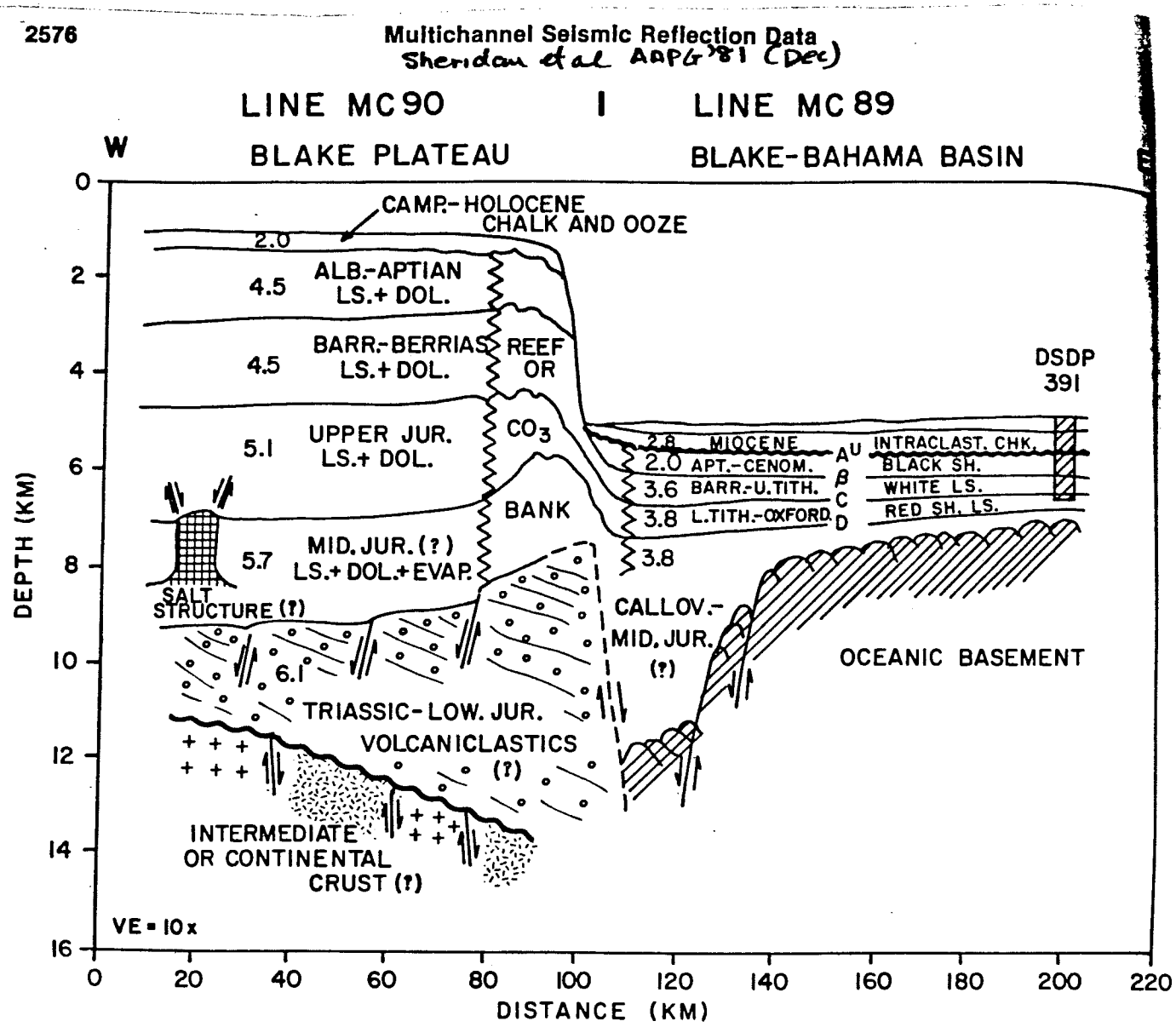

FIG. 4—Structural cross section across edge of Blake Plateau and Blake-Bahama Basin based on depth conversion of lines MC 89 and MC 90. Seismic interval velocities used for depth-section conversion are given in km/sec. Correlations with DSDP Site 391 are shown.

Seismic Recognition of Carbonate Buildups

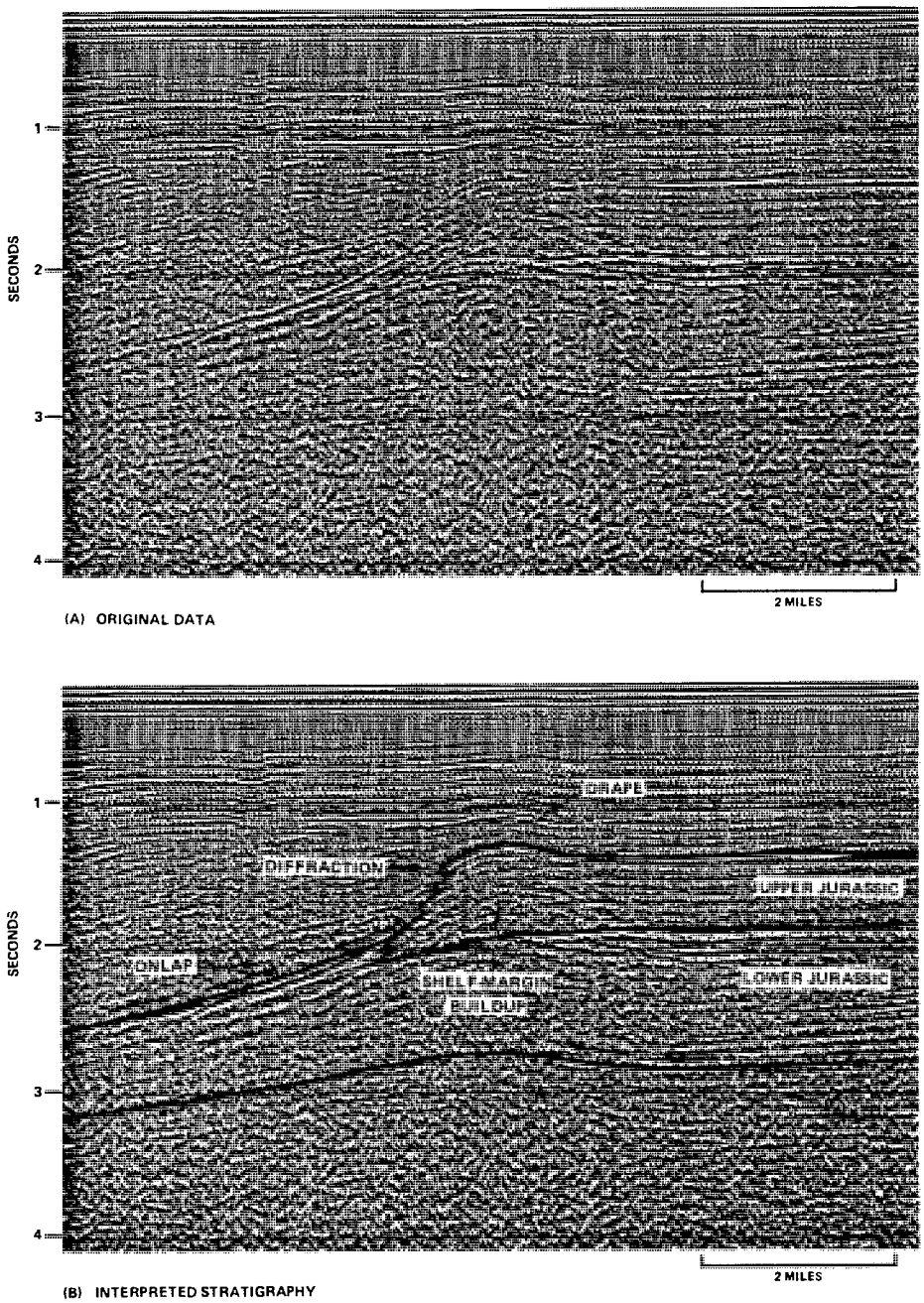

FIG. 6—Offshore West Africa (12-fold CDP Aquapulse® data). Shelf-margin carbonate buildup can be seen by (1) reflection from top and front of buildup, (2) onlap of cycles onto buildup, (3) change from continuous, parallel reflectors into discontinuous reflectors, (4) numerous diffractions, (5) drape over buildup, and (6) abrupt change in dip of reflectors.

Wells encountered series of Mesozoic shelf-margin buildups along eastern Atlantic continental margin off Africa. Buildup displayed on this line is interpreted as Late Jurassic.

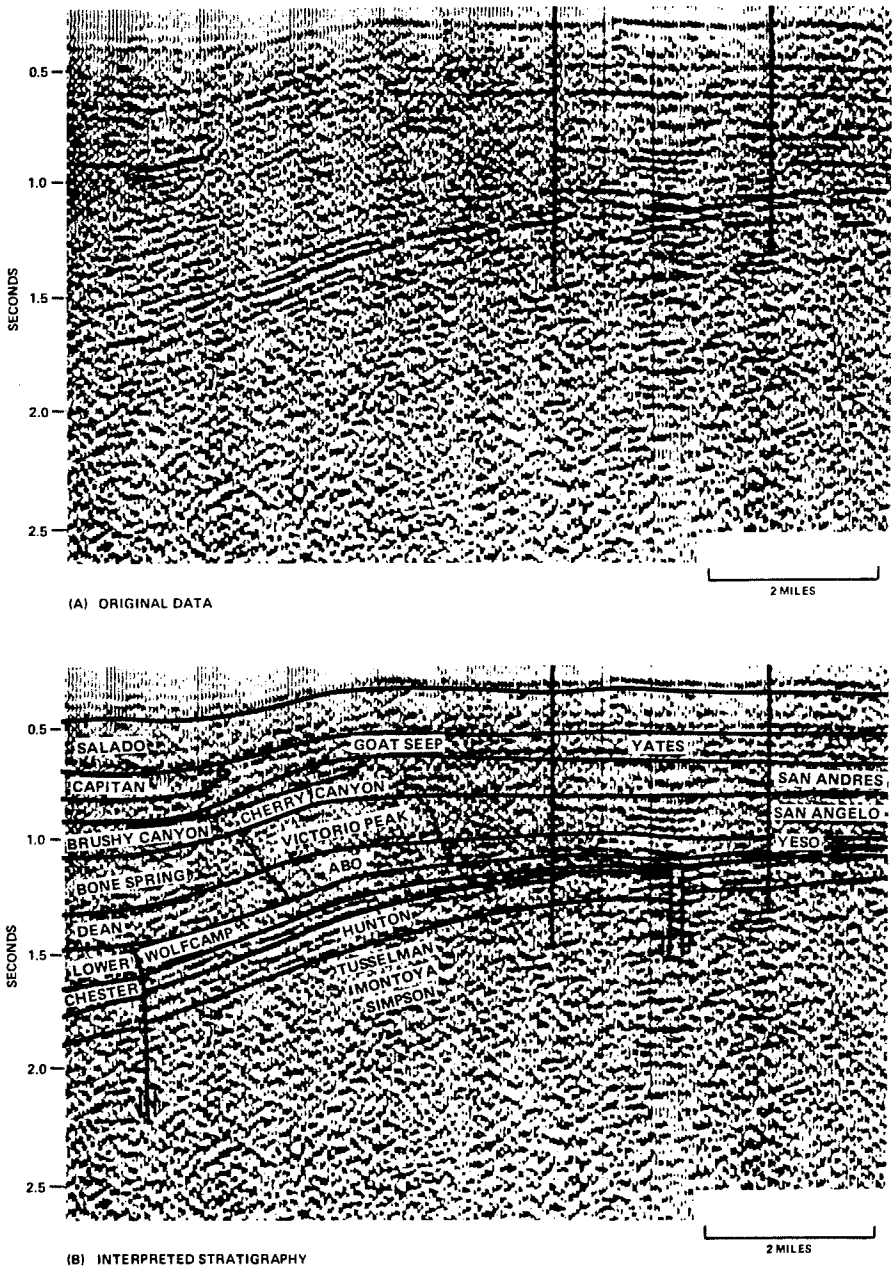

FIG. 9—Central basin platform, Lea County, New Mexico (12-fold CDP Vibroseis® data). Shelf-margin carbonate-bank buildup on this line is indicated by (1) abrupt change in dip at shelf edge, and (2) seismic facies change from high-amplitude, continuous reflections to low-amplitude to nearly reflection-free zone at shelf edge.

Leonardian and Guadalupian shelf-margin banks, composed mainly of dolomitized skeletal limestones of the Abo, Victorio Peak, Goat Seep, Getaway, and Capitan Formations, are documented by wells in this part of Permian basin. Basinward of shallow-water banks are siltstones, shales, and micritic limestones of Dean, Bone Spring, Brushy Canyon, and Cherry Canyon Formations; shelfward of banks are thin-bedded, dolomitized micritic and dolomitized algal-laminated limestones and sandstones of the Yates, Seven Rivers, Queen, Grayburg, San Andres, San Angelo, and Yeso Formations.

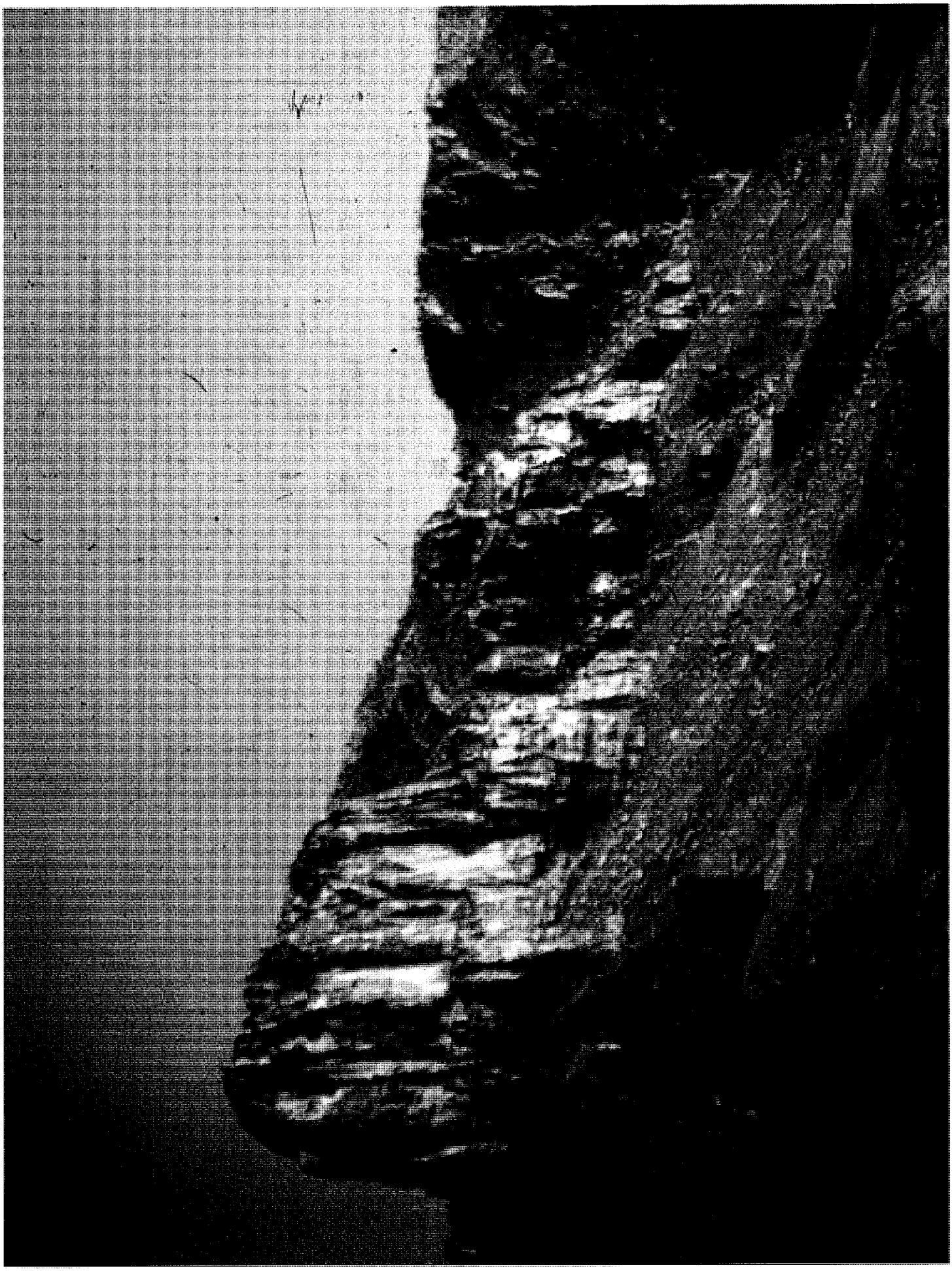

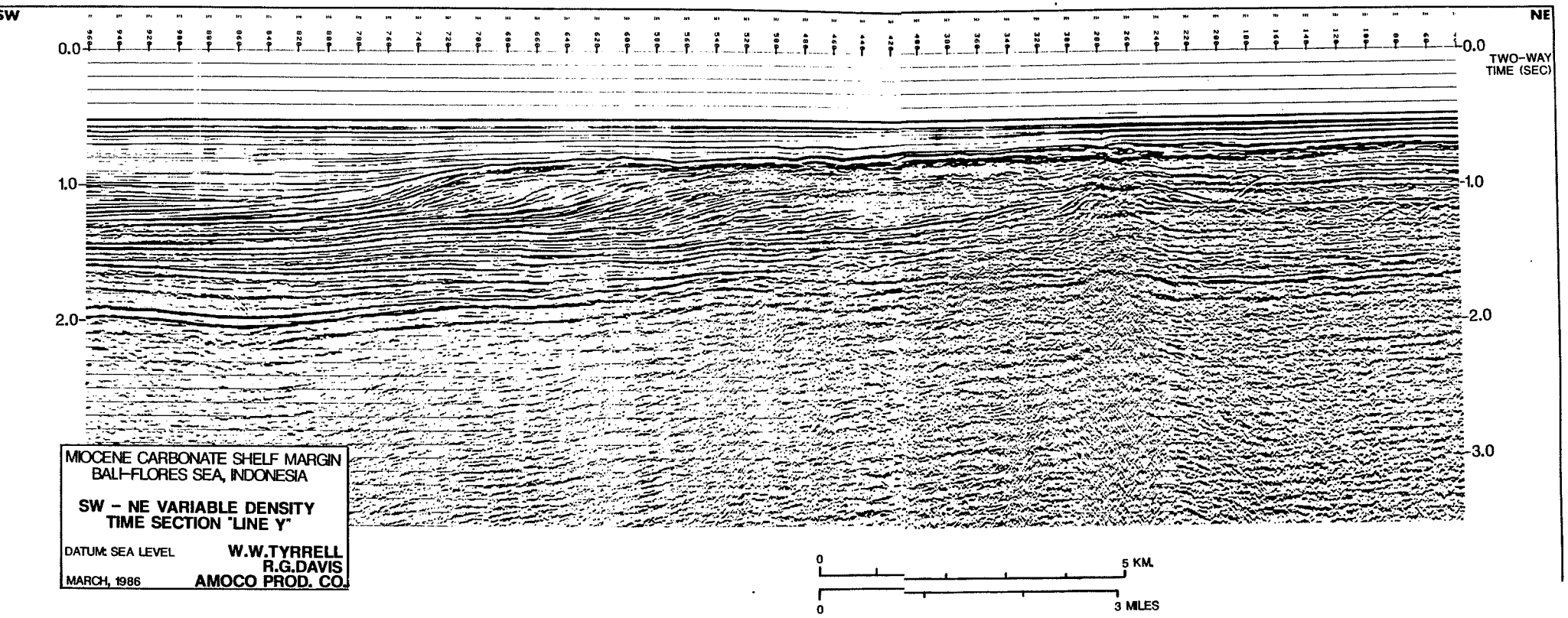

Figure 2. Southwest–northeast variable density time section, line Y. Tyrrell & Davis in Bally

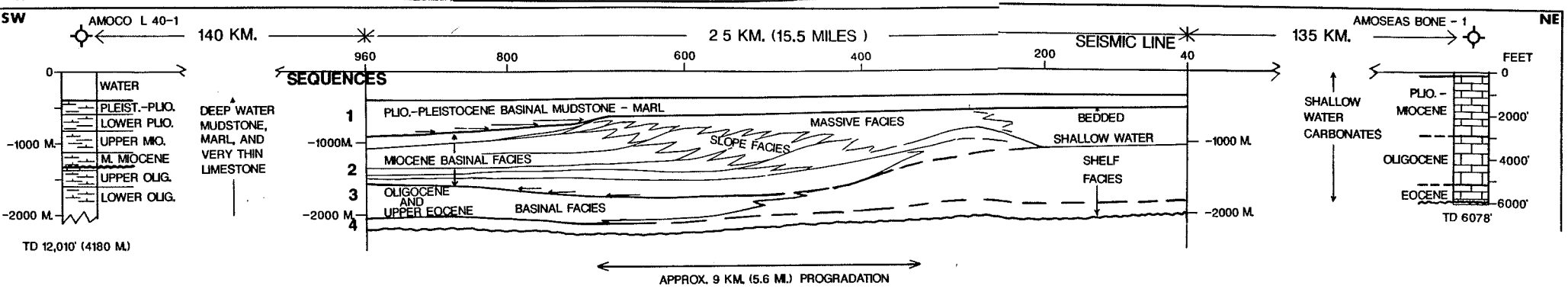

EXAMPLES OF LOCAL CARBONATE BUILD-UPS ...

Seismic Recognition of Carbonate Buildups

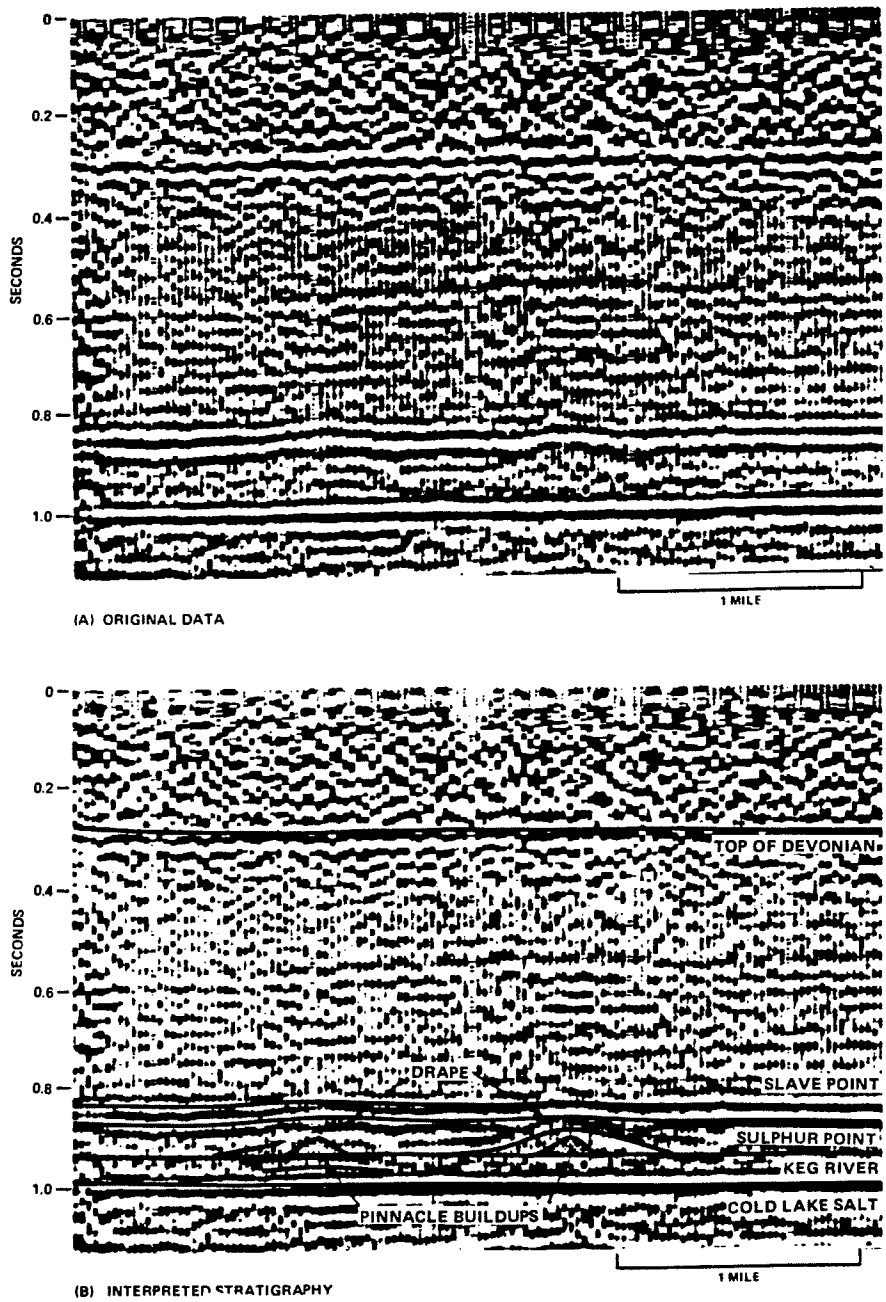

FIG. 10—Rainbow-Zama area, Alberta (6-fold CDP dynamite data, section datumed on Cold Lake salt reflection—a near-basement horizon). Presence of two small pinnacle reefs is indicated by small amount of drape in reflectors above reefs and by one cycle of onlap (?).

Buildups indicated on section are Middle Devonian Keg River Formation pinnacle reefs. Drape seen in overlying Sulphur Point and Slave Point Formations is probably due both to differential compaction and to subsequent removal of Muskeg salt deposited in interreef areas. Recoverable reserves in Rainbow-Zama area are estimated at 800 million bbl of oil. Pool size is variable; some are smaller than 8 ha., others are larger than 2 sq km, but average is 20 to 30 ha. Pay thickness is variable.

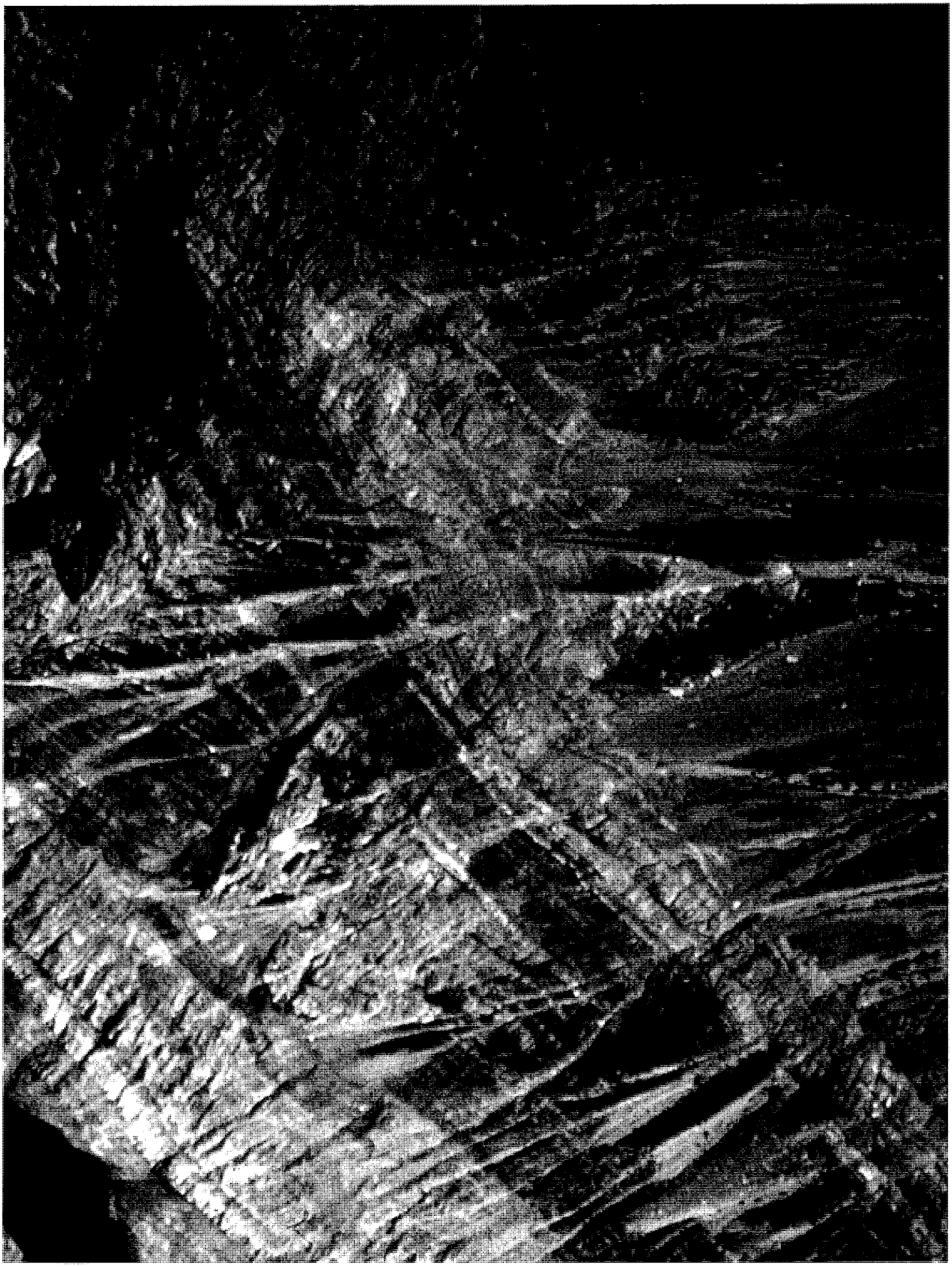

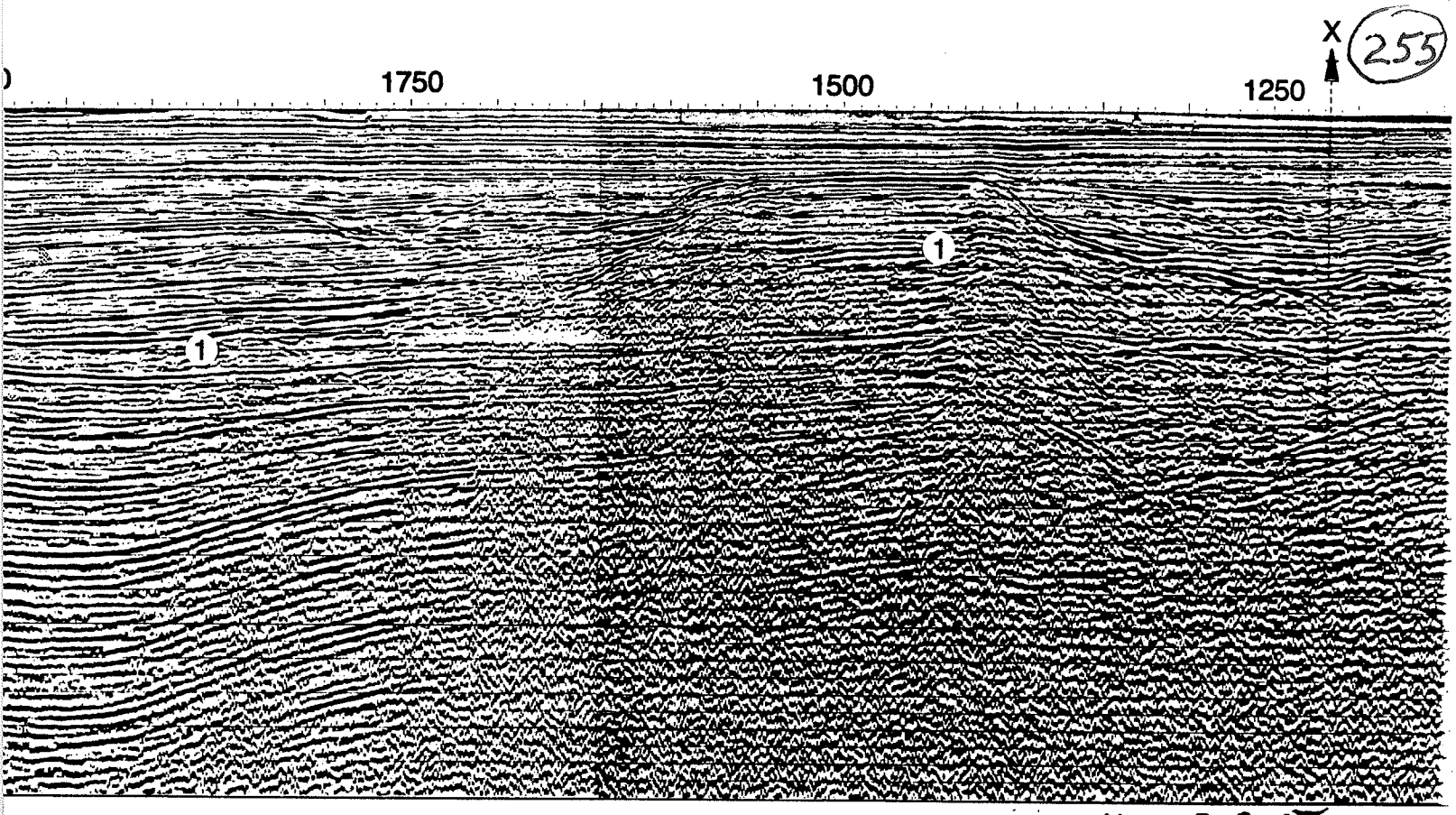

Bally 1.2.3-5

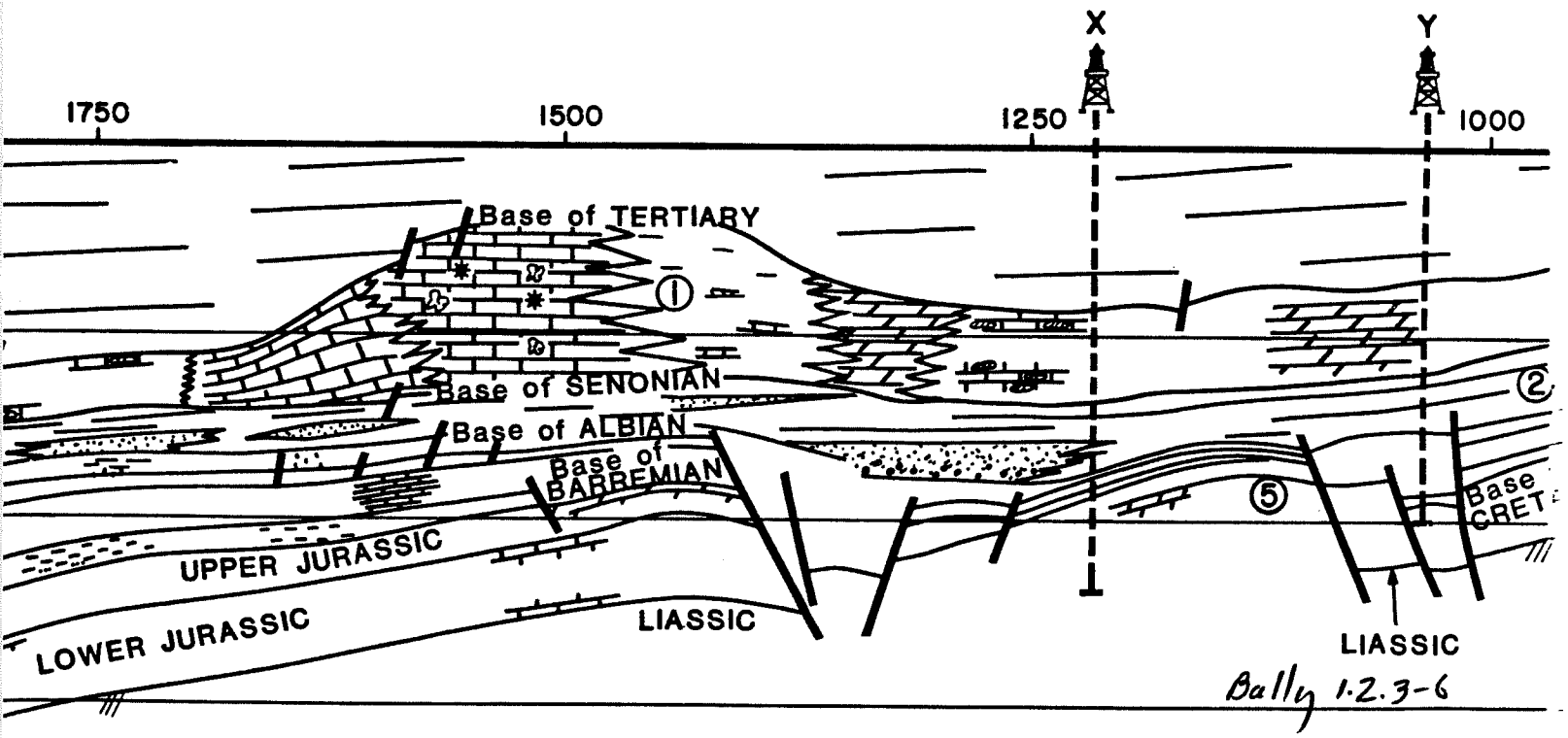

Bally 1.2.3-6

TOTAL DEPTH IN METERS — FEET

X — 4533 m — 15065'
Y — 3366 m — 11043'

VELOCITY AS A TOOL...

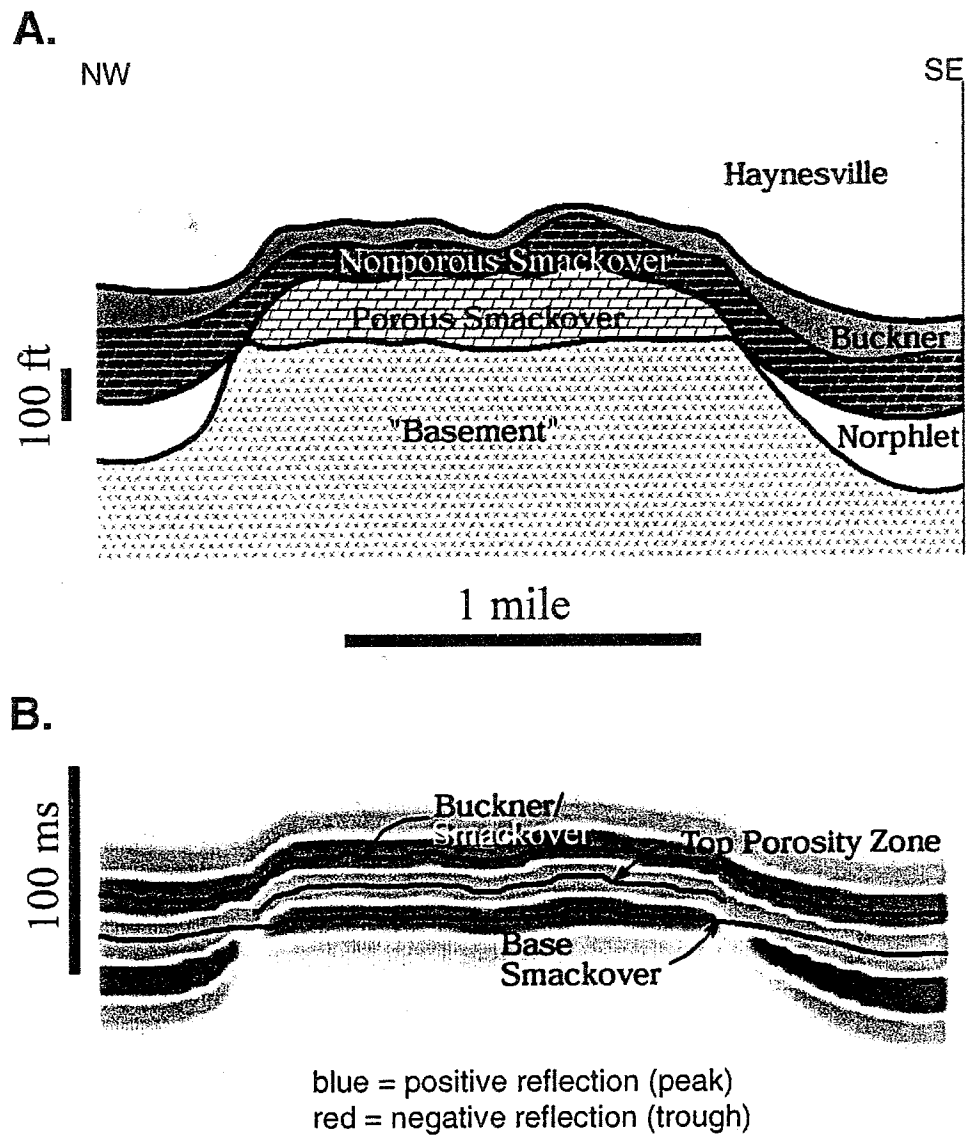

Figure 8. (A) Geologic model used in seismic modeling of Figure 7 and (B) seismic section of the structure at Appleton field (modified from Balch and Hart, 2000). Geologic model and seismic section correspond to structure cross section AA′ in Figure 3. See Table 1 for physical properties of rocks.

Table 1. Average Smackover and Associated Rock Physical Properties*

Horizon	Velocity (ft/sec)	Density (g/cm3)
Haynesville siliciclastics	14,925	2.53
Buckner anhydrite	19,354	2.96
Upper nonporous Smackover carbonates	20,513	2.80
Porous Smackover carbonates	16,160	2.65
Norphlet siliciclastics	13,000	2.60
Paleozoic basement (igneous)	19,802	2.77

*Modified from Hart and Balch (2000).

VALUE OF 3-D SEISMIC (VS. 2-D) IN IDENTIFYING LOCAL CARBONATE BUILD-UPS - - - -

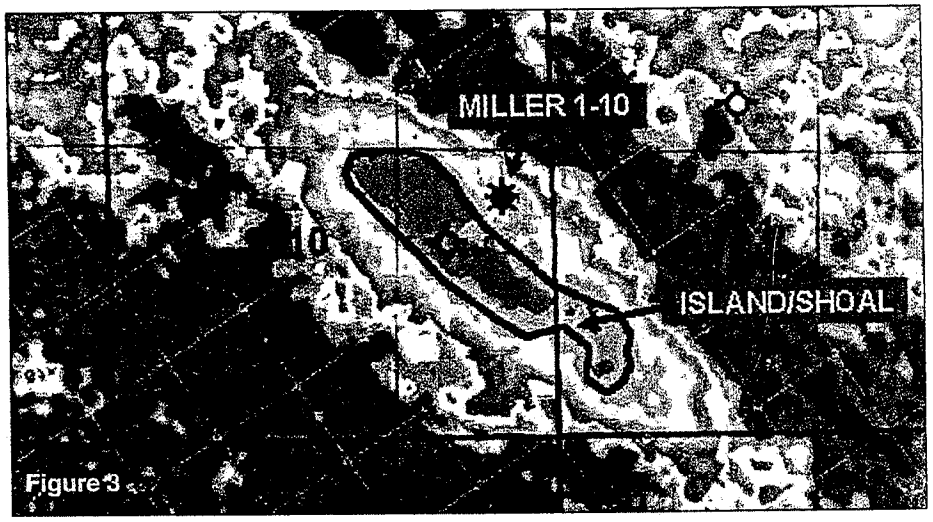

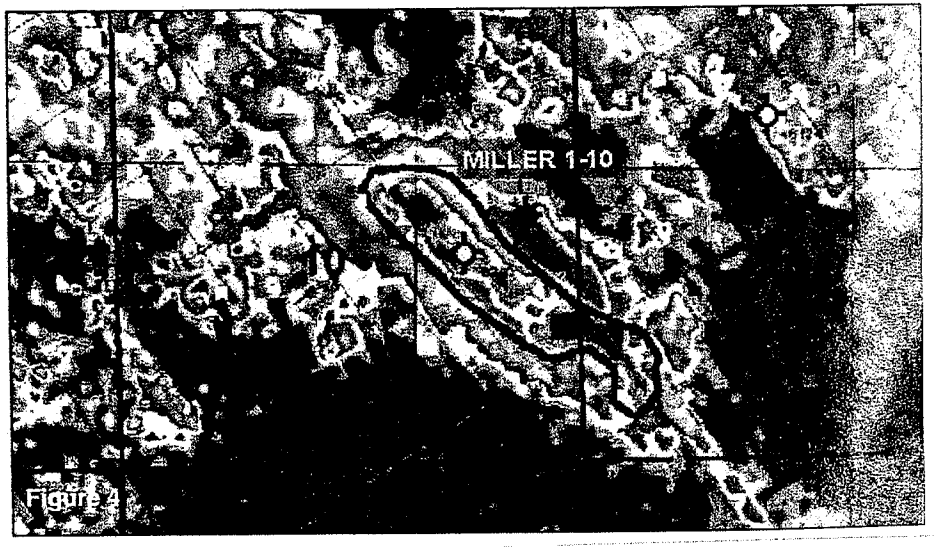

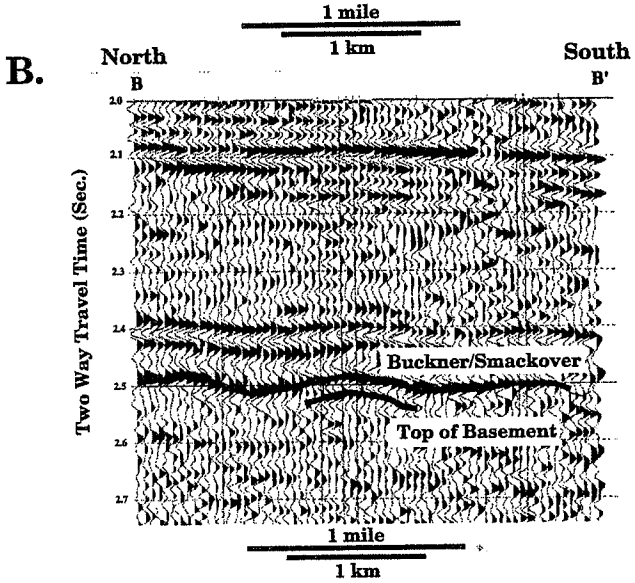

Figure 5. Seismic reflection profile BB′ across Appleton field: uninterpreted line (A) and interpreted line (B). See Figure 3 for location of seismic reflection profile BB′.

Johnson et al, 2001, AAPG Explorer, March issue, p. 34-35.

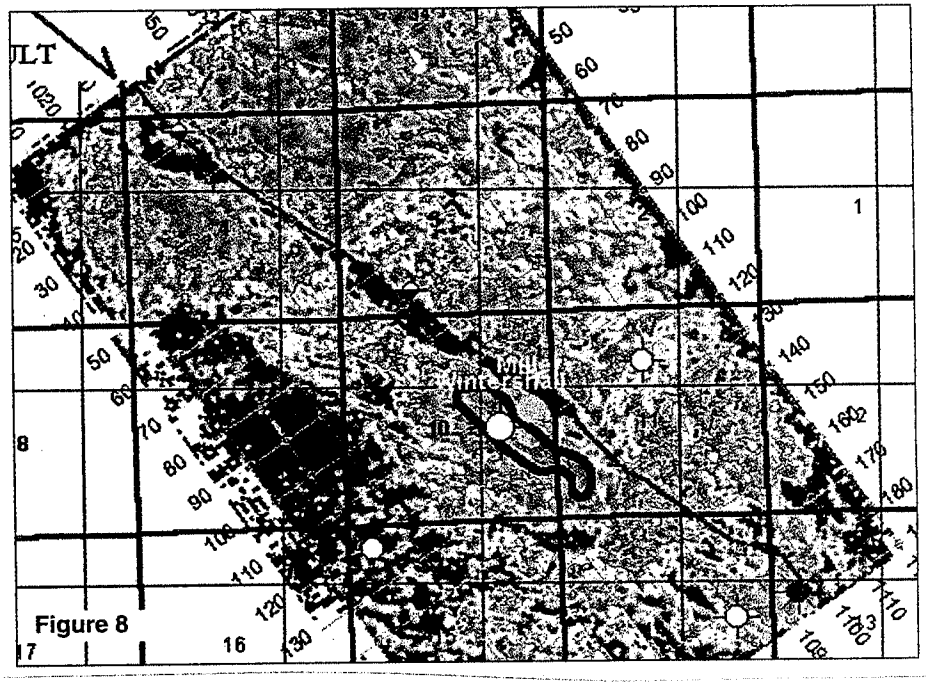

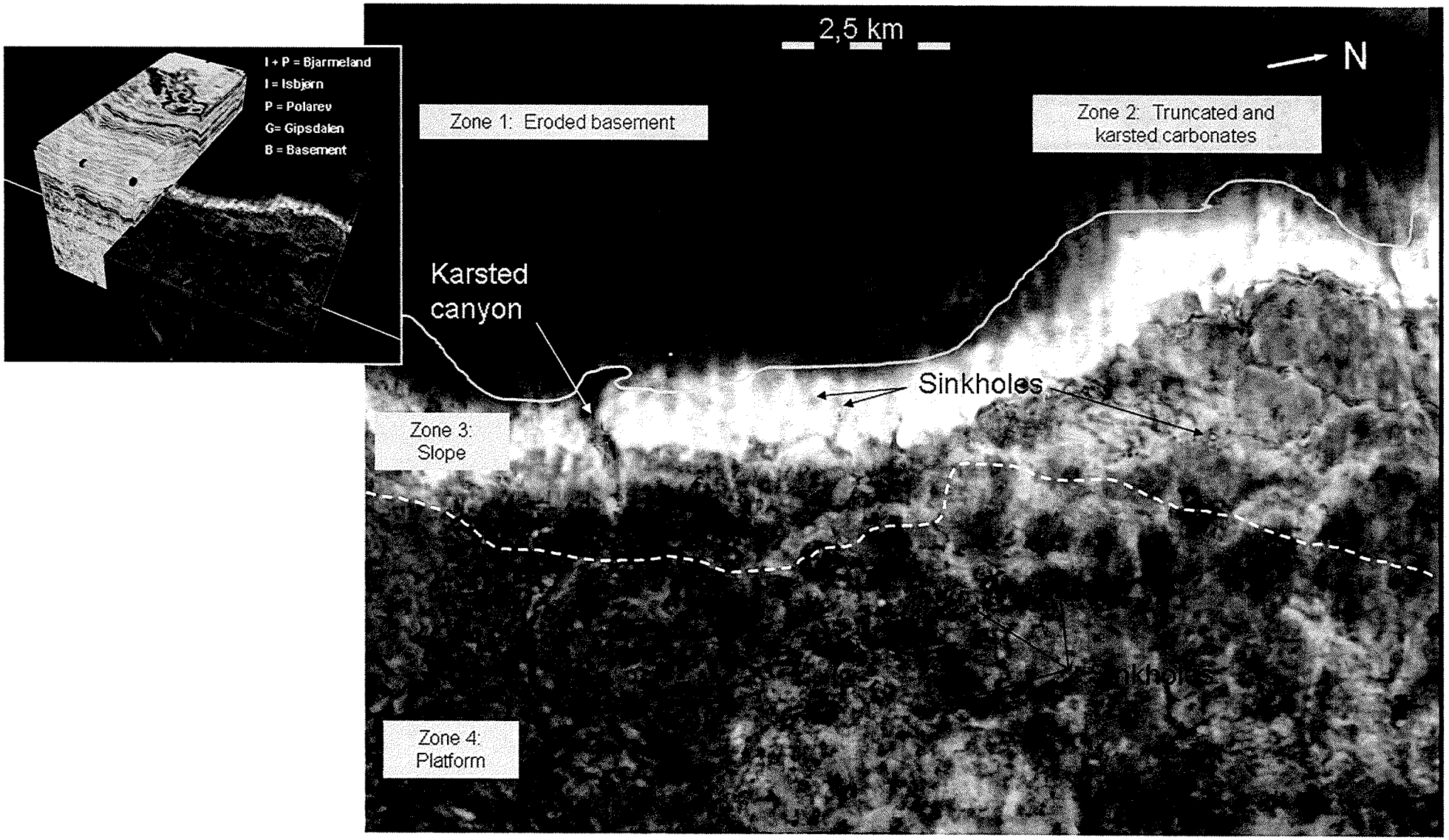
I + P = Bjarmeland
I = Isbjørn
P = Polarev
G= Gipsdalen
B = Basement
2,5 km
N
Zone 1: Eroded basement
Zone 2: Truncated and karsted carbonates
Karsted canyon
Sinkholes
Zone 3: Slope
Zone 4: Platform

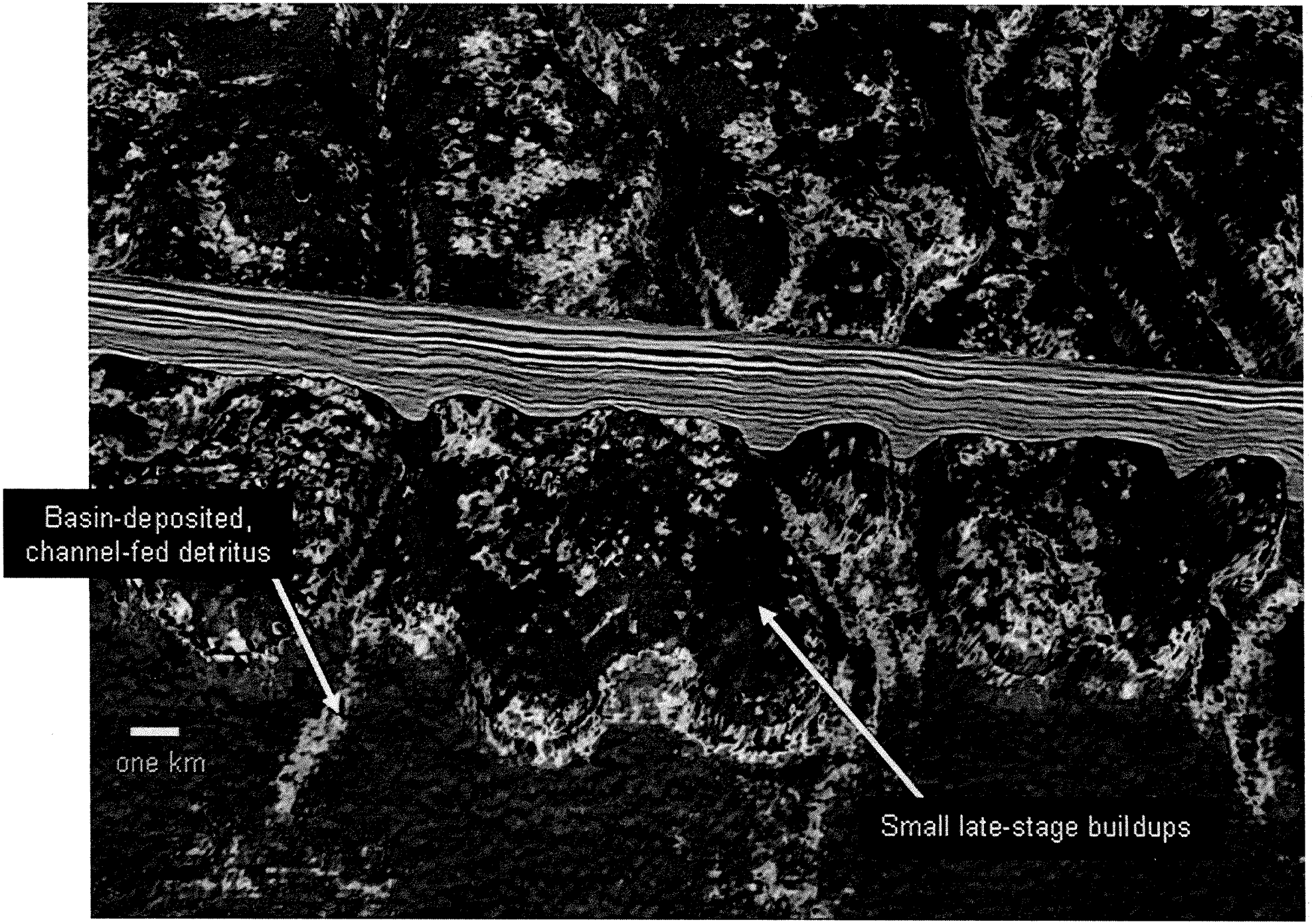
Basin-deposited,
channel-fed detritus
one km
Small late-stage buildups

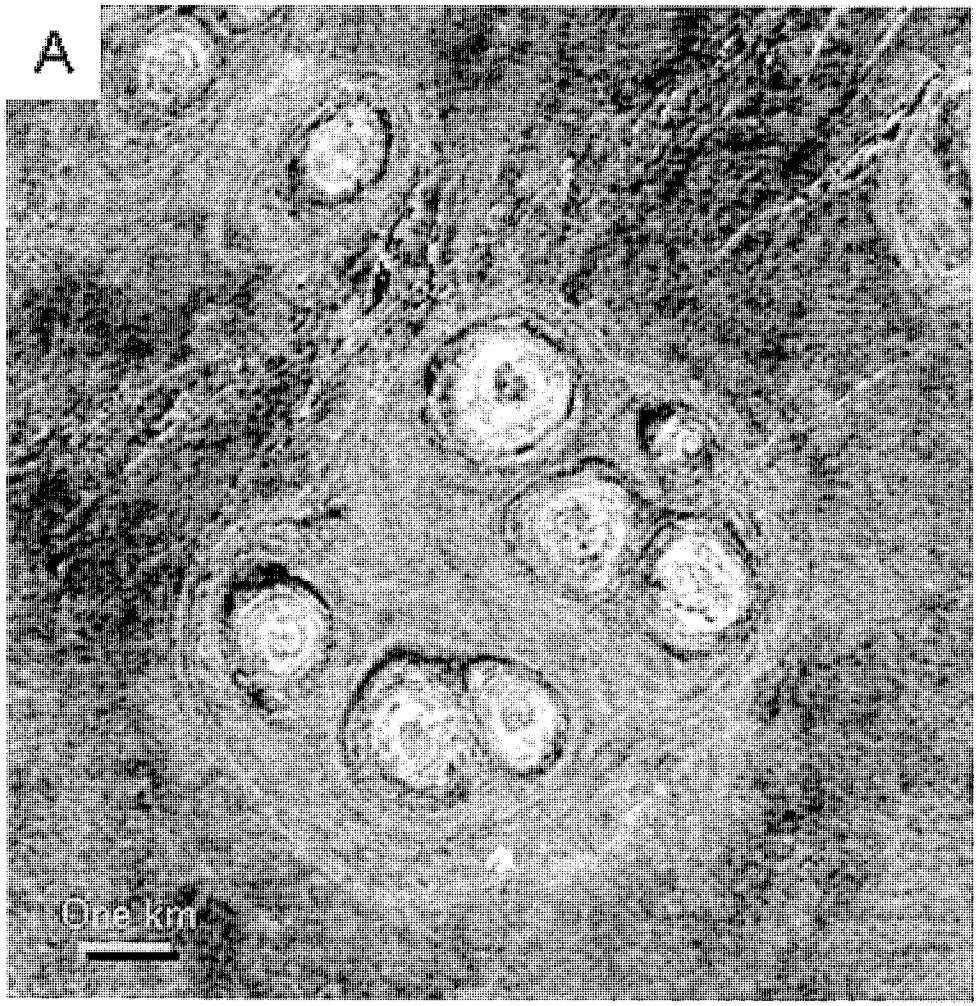
A
One km

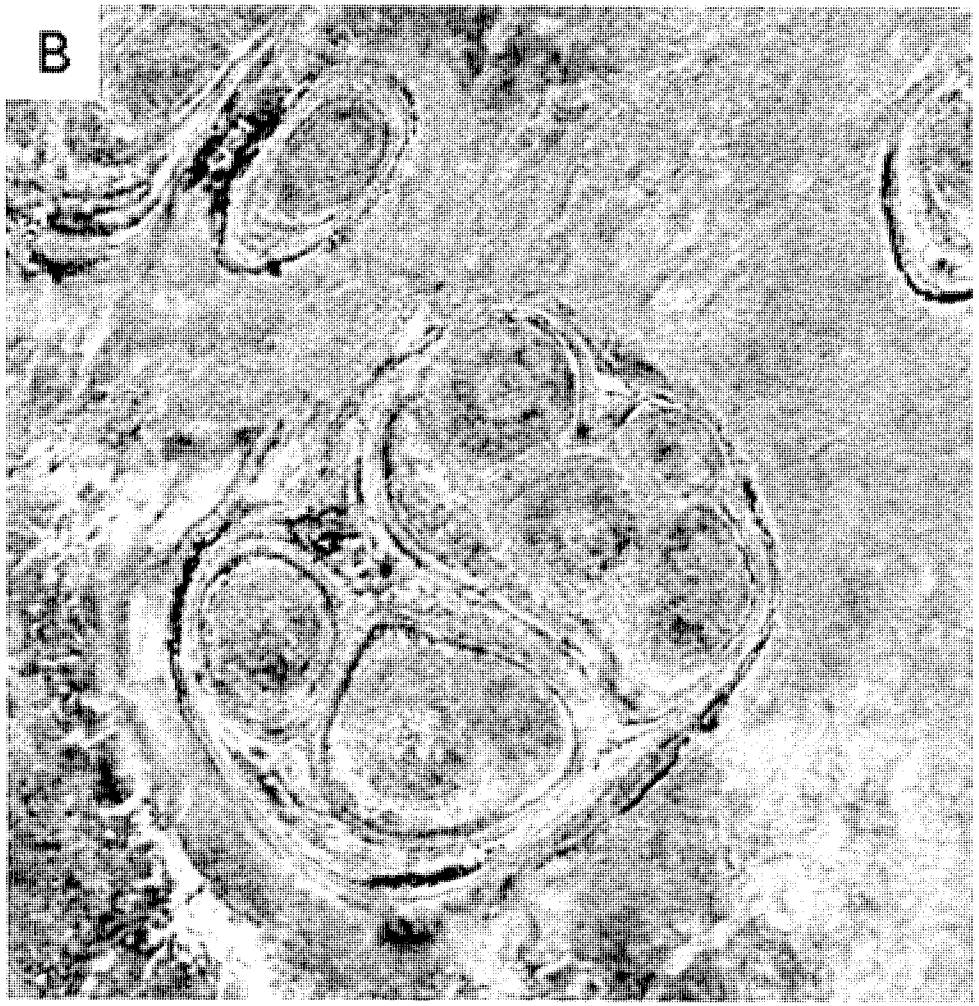
B

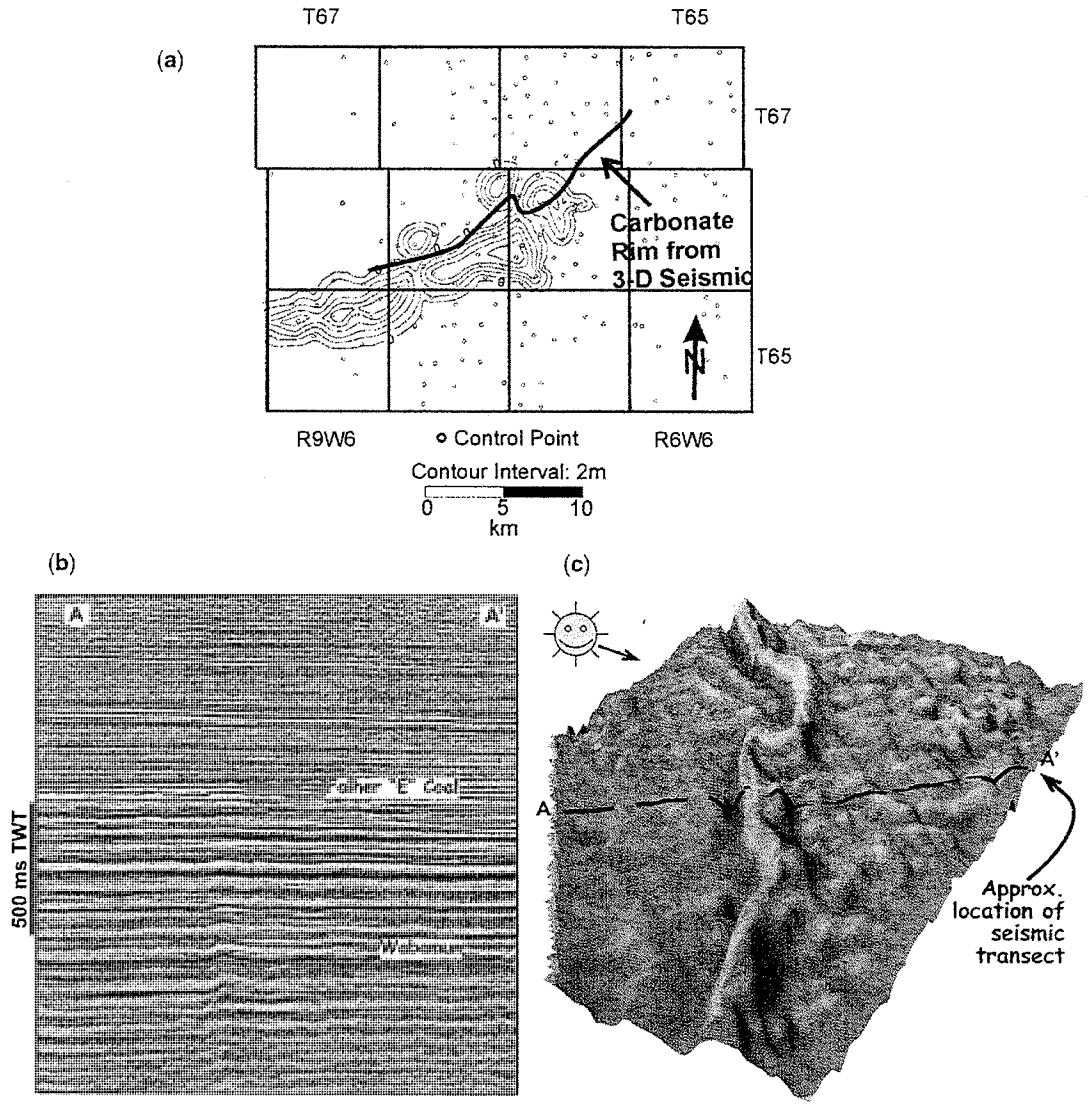

Fig. 7. (**a**) Net porosity map (meters) of the Falher F trend (lower Cretaceous, Deep Basin of western Canada) showing a SW–NE linear trend associated with the presence of productive and porous shoreface and beachface conglomerates (cf. Nodwell & Hart, 2006). (**b**) Seismic transect showing the relative positions of the Lower Cretaceous Falher Member (here defined using a reflection from a prominent coal in the Falher) and the Devonian Wabamun Formation in the Deep Basin, central Alberta (Canada). Approximate location of seismic transect shown in (**c**). (c) Dip curvature display, draped over illuminated rendered surface of the Wabamun Formation. The seismic data image the northwestern flank of the Gold Creek Reef trend. Note the presence of a well-defined rim. The conglomerate trend shown in (a) directly overlies the rim of the platform.

Hart and Sagan, 2007

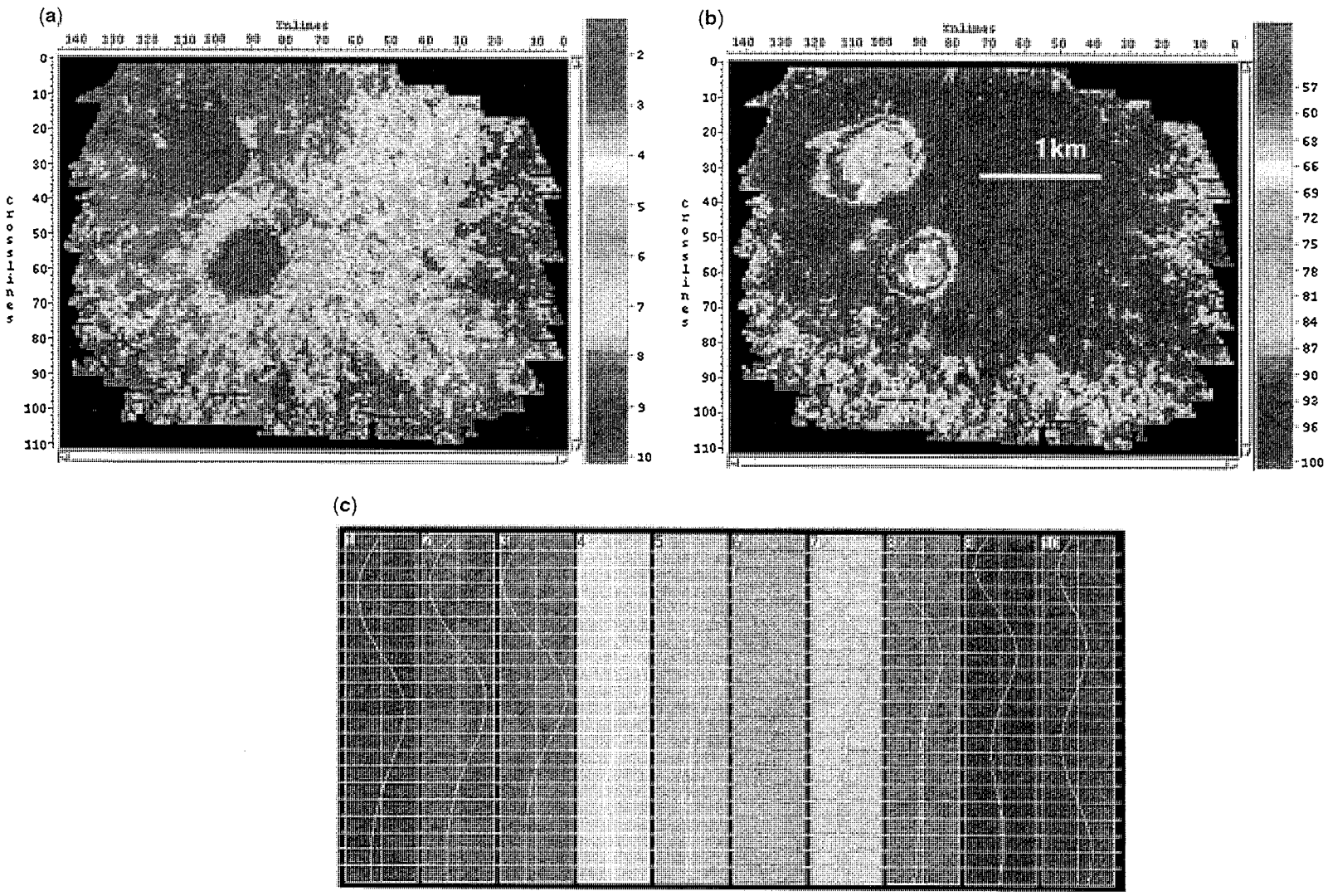

Fig. 9. Seismic facies mapping of two Devonian pinnacle reefs, western Canadian sedimentary basin. (**a**) Seismic facies map illustrating that all seismic traces within the reefs are assigned to a single facies class. (**b**) Seismic facies correlation map wherein each trace is compared with class 3 (c). Note the more detailed seismic and therefore geological expression of the reefs. (**c**) The neural-network-derived 10 seismic facies classes upon which the analysis was based (Stratimagic software by Paradigm Inc.).

Hart and Sagan, 2007

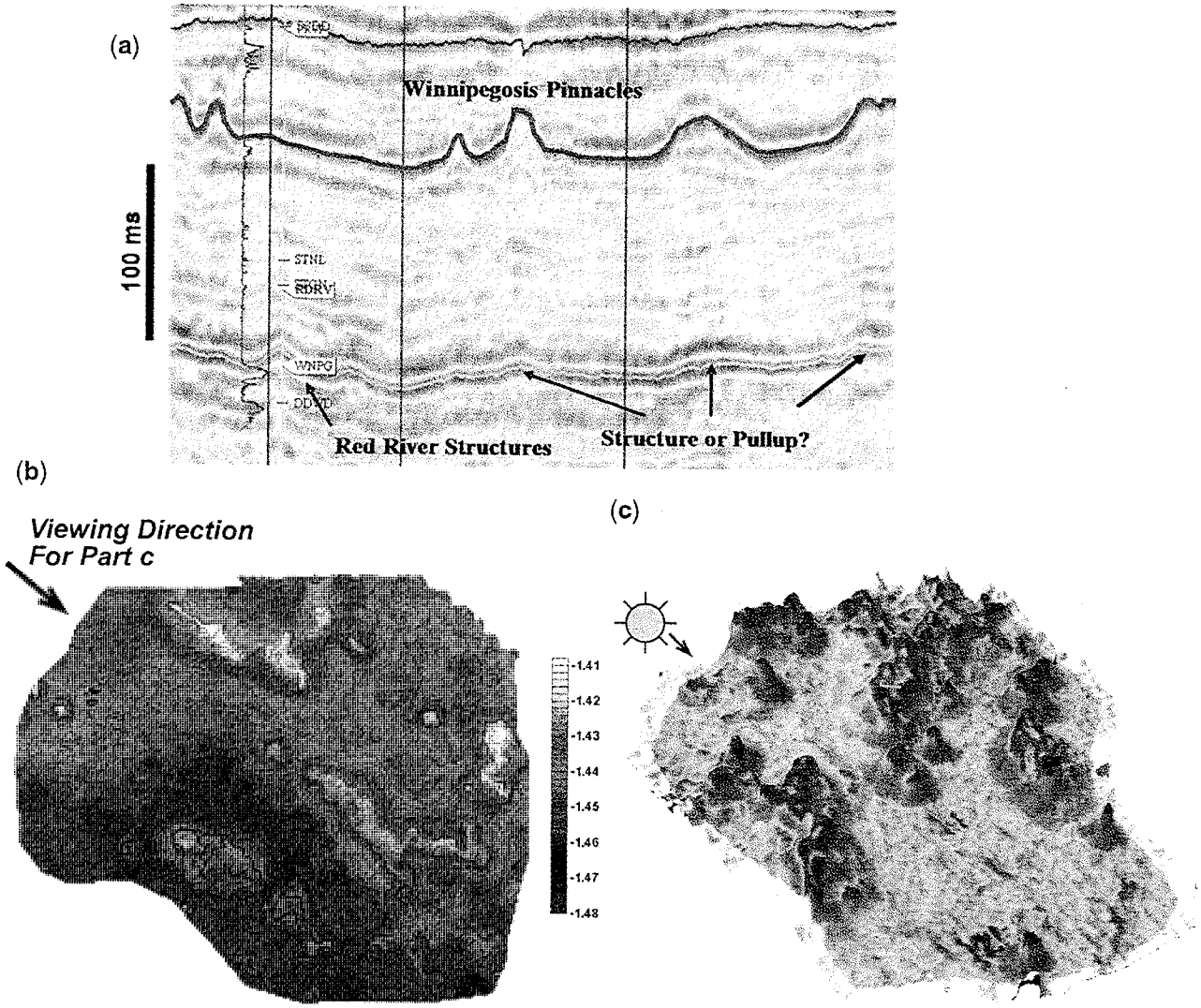

Fig. 6. (**a**) Seismic transect from the Williston Basin (SE Saskatchewan, Canada) showing (Devonian) pinnacle reefs at the Winnipegosis level and subtle apparent structures at an underlying (Ordovician) level that could be either real or related to velocity pull-up beneath the pinnacle reefs (drilling in the area has encountered both possibilities). (**b**) Time-structure map showing Devonian pinnacle reefs identified in (a). Note the subtle regional dip to the south (bottom of the page). (**c**) The same surface shown in 3D with a dip curvature drape and illumination. This image removes the effects of regional dip and highlights the morphology of the individual pinnacles.

Hart and Sagan, 2007

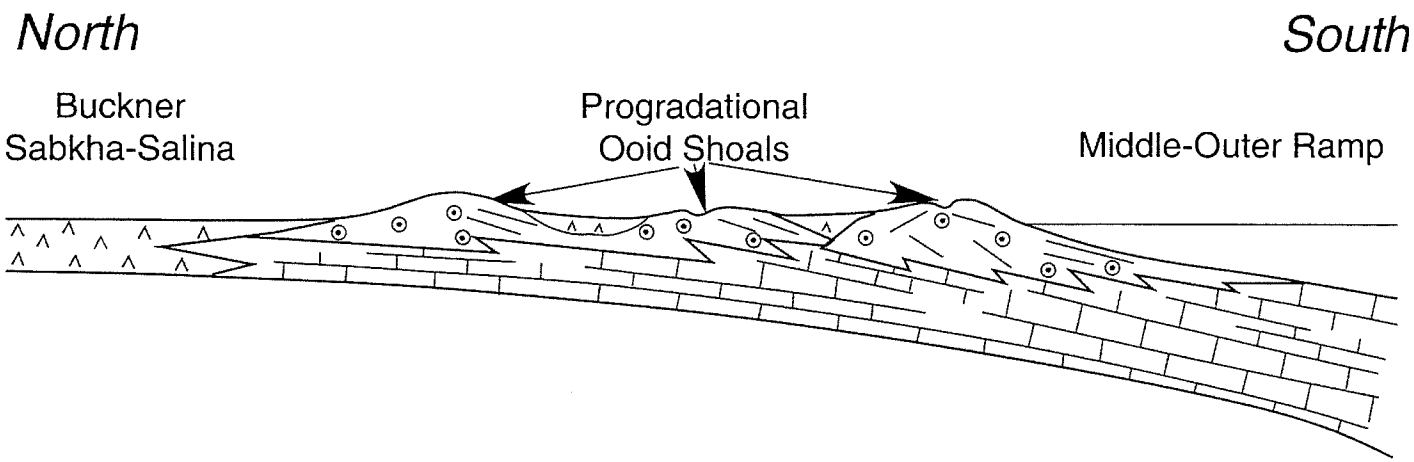

Fig. 4. Schematic depositional model of the Smackover-Buckner formations is based upon Ahr (1973), Baria *et al.* (1982), Harris & Dodman (1982) and others.

Handford and Baria, 2007

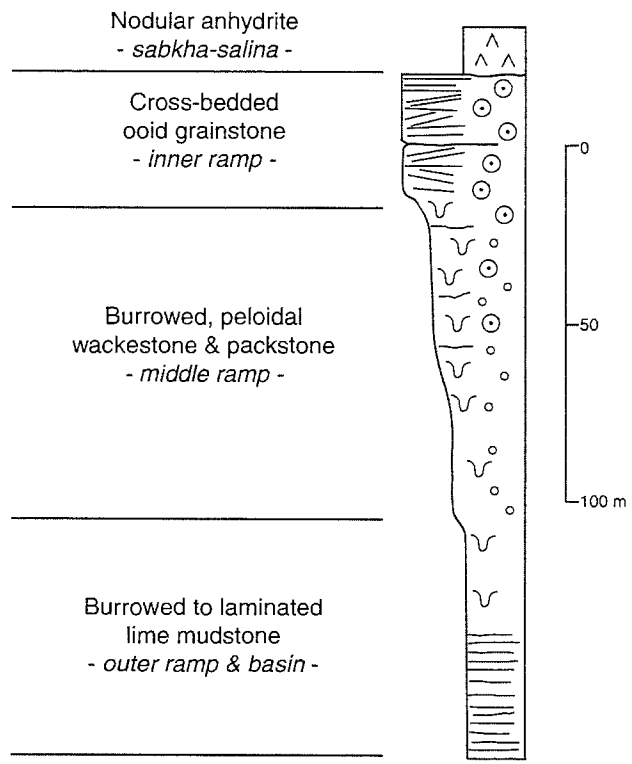

Fig. 3. Schematic diagram showing typical vertical succession of Smackover lithofacies in the northern Gulf Coast area of Louisiana and Arkansas.

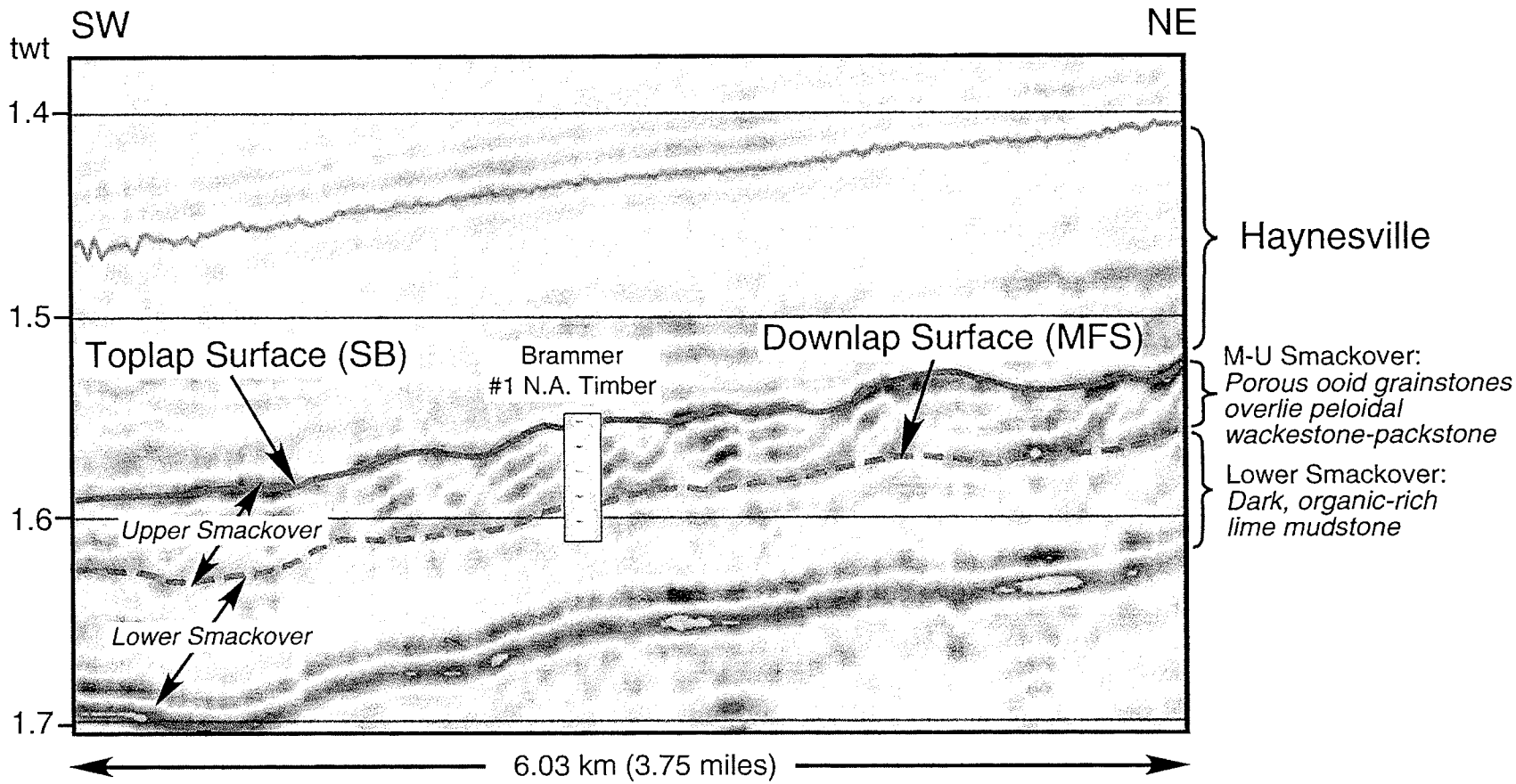

Fig. 5. Arbitrary NE–SW line through seismic survey shows Smackover-Haynesville formations. Clinoforms lie within the middle to upper Smackover Formation. Downlap and toplap surfaces are identified and a general 'tie' with a Smackover well log that lies along the line. No synthethic seismogram was available for the Brammer well (inset). All seismic data are in two-way travel time (twt) in seconds.

Handford and Baria, 2007

Use the appropriate model

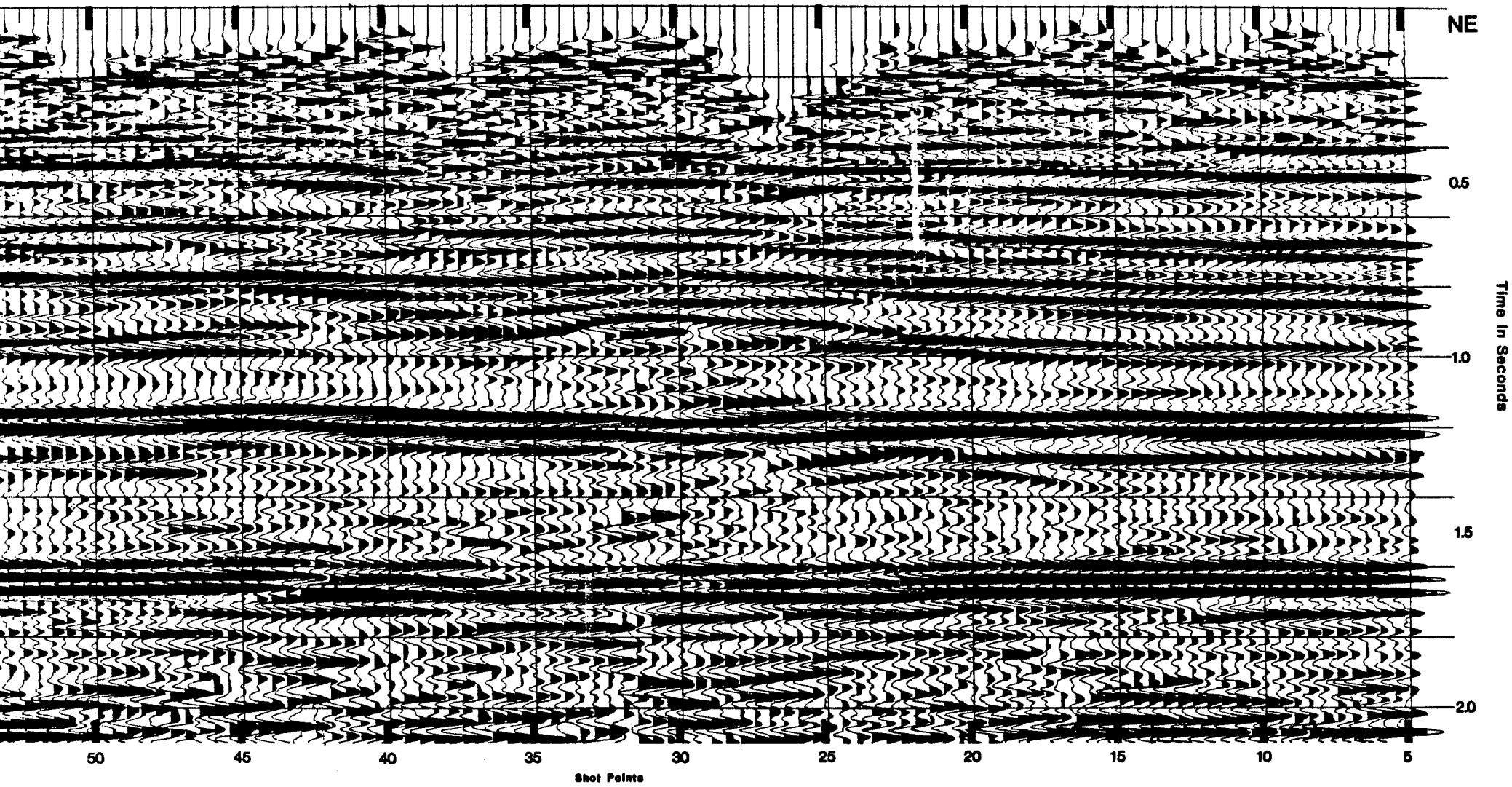

Igneous Structures

Bally 1.3-8

CARBONATE BUILD-UP OR PITFALL?

256

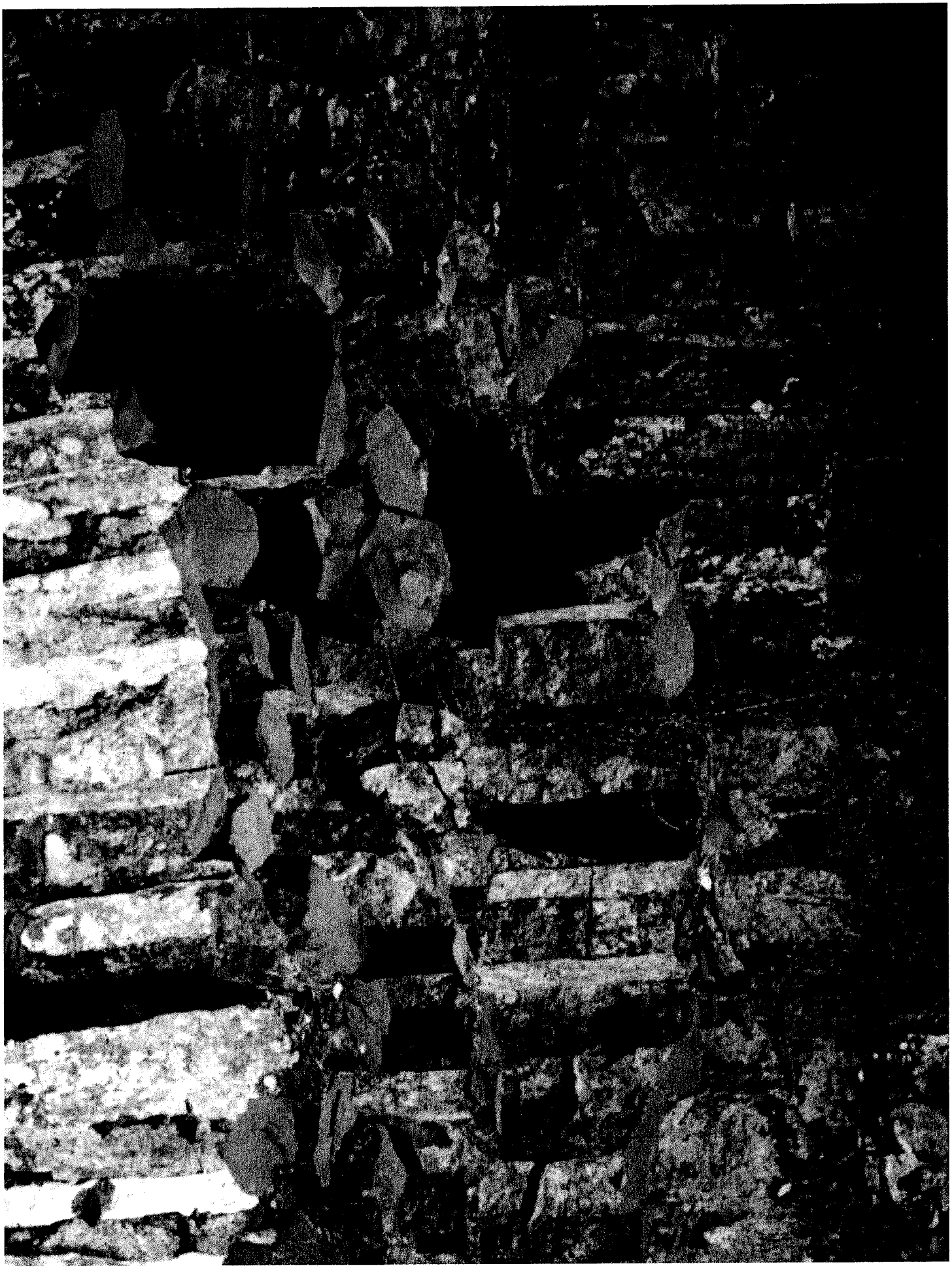

Inter-relationships between tectonics and sedimentation, as imaged by the seismic method

Relationships between Structure and Stratigraphy

In a variety of circumstances, structure may control sedimentation (and resulting stratigraphy) and vice versa. On the scale of most seismic studies, though, it is structure which influences sedimentation. This sort of thing occurs in all structural settings. The message to interpreters: Never interpret structure without attention to stratigraphy, and never interpret stratigraphy without attention to structure.....to do so is to invite poor interpretations.

A few examples follow.....

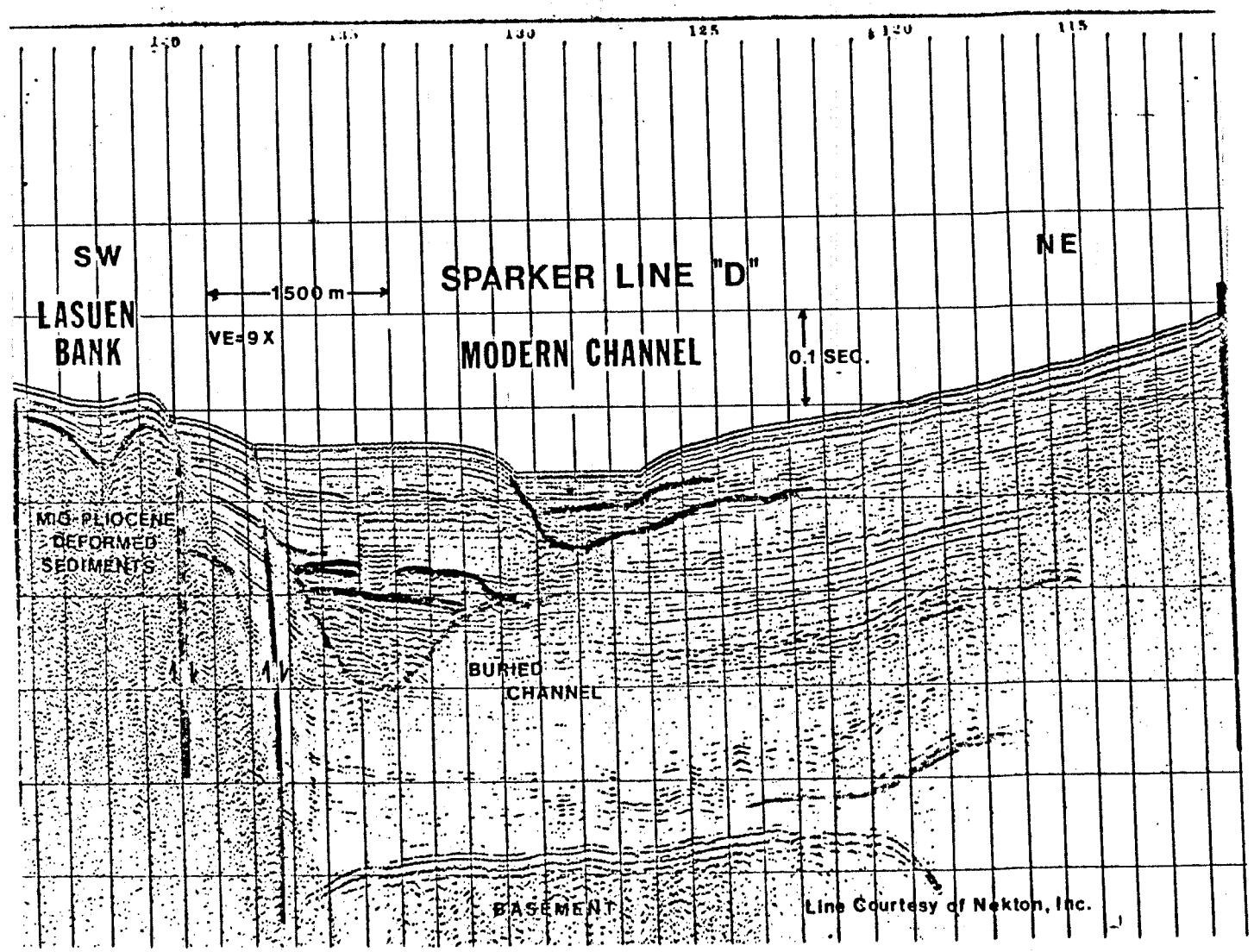

Graham & Bachman, AAPG Jan '83

258

Sylvester:
http://see-atlas.leeds.ac.uk:8080/
CGG Veritas
Niger Delta slope, dip magnitude

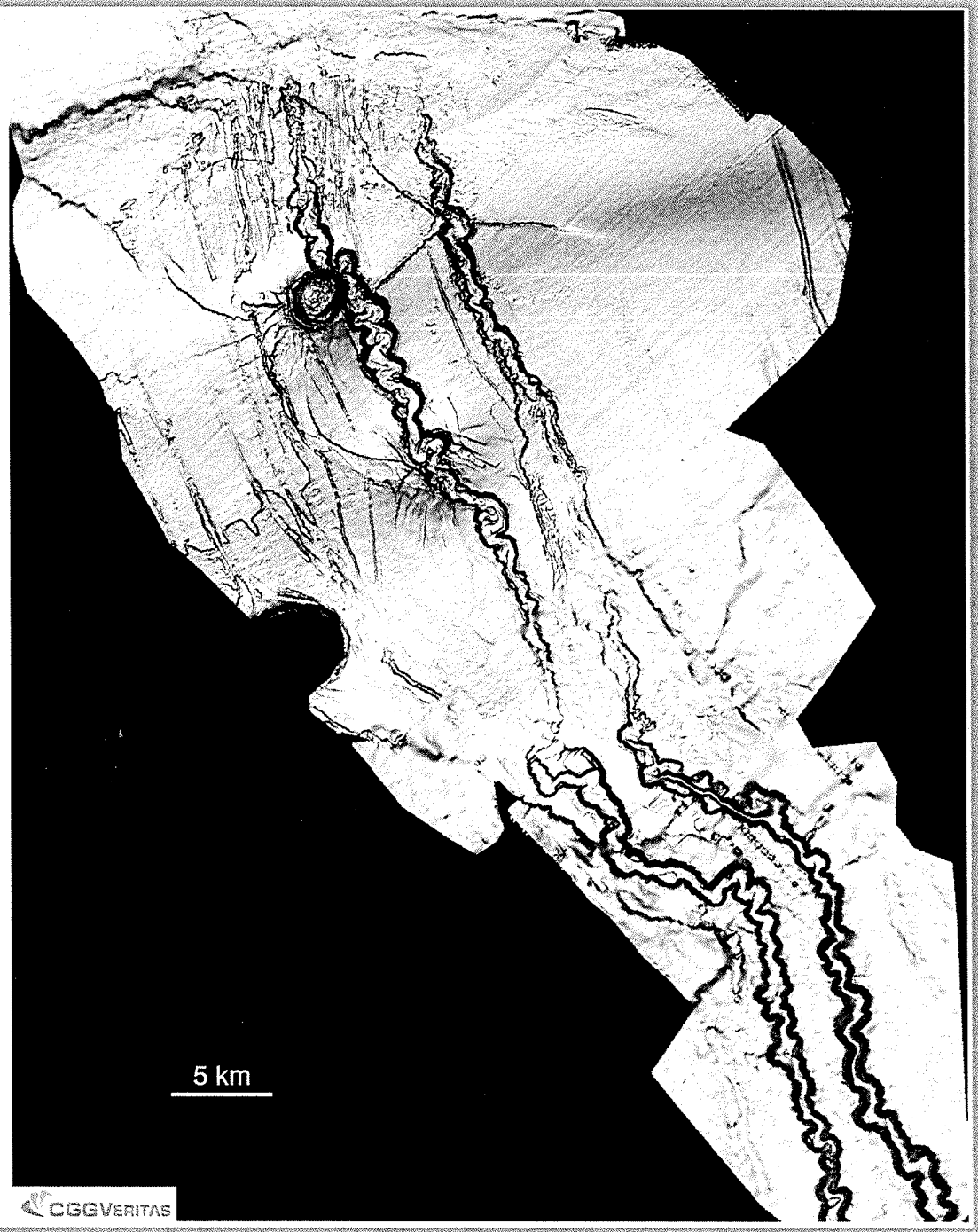

Sylvester:
http://see-atlas.leeds.ac.uk:8080/
CGG Veritas
Niger Delta

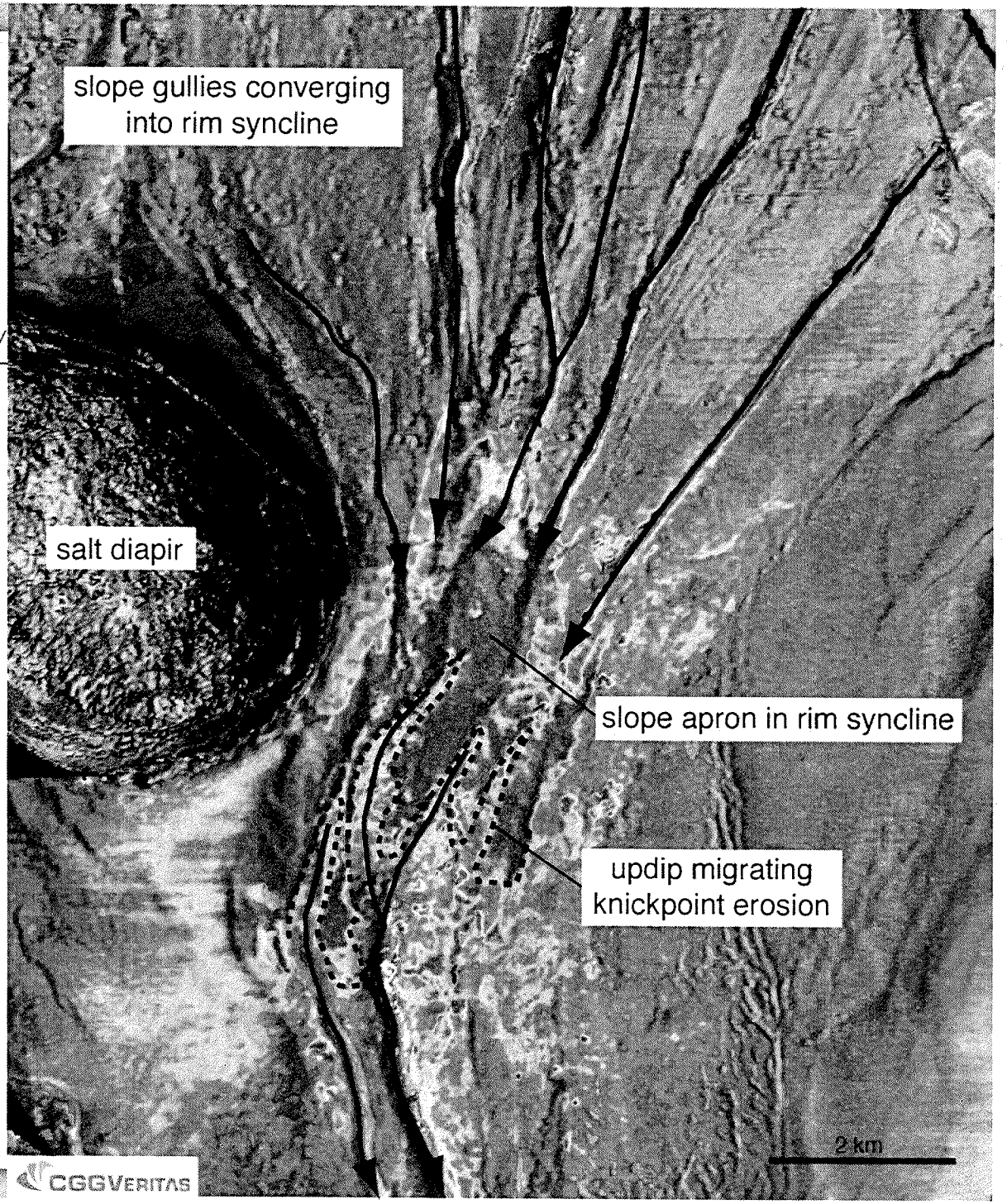

Nigeria - Horizon Slice (Time 252ms)

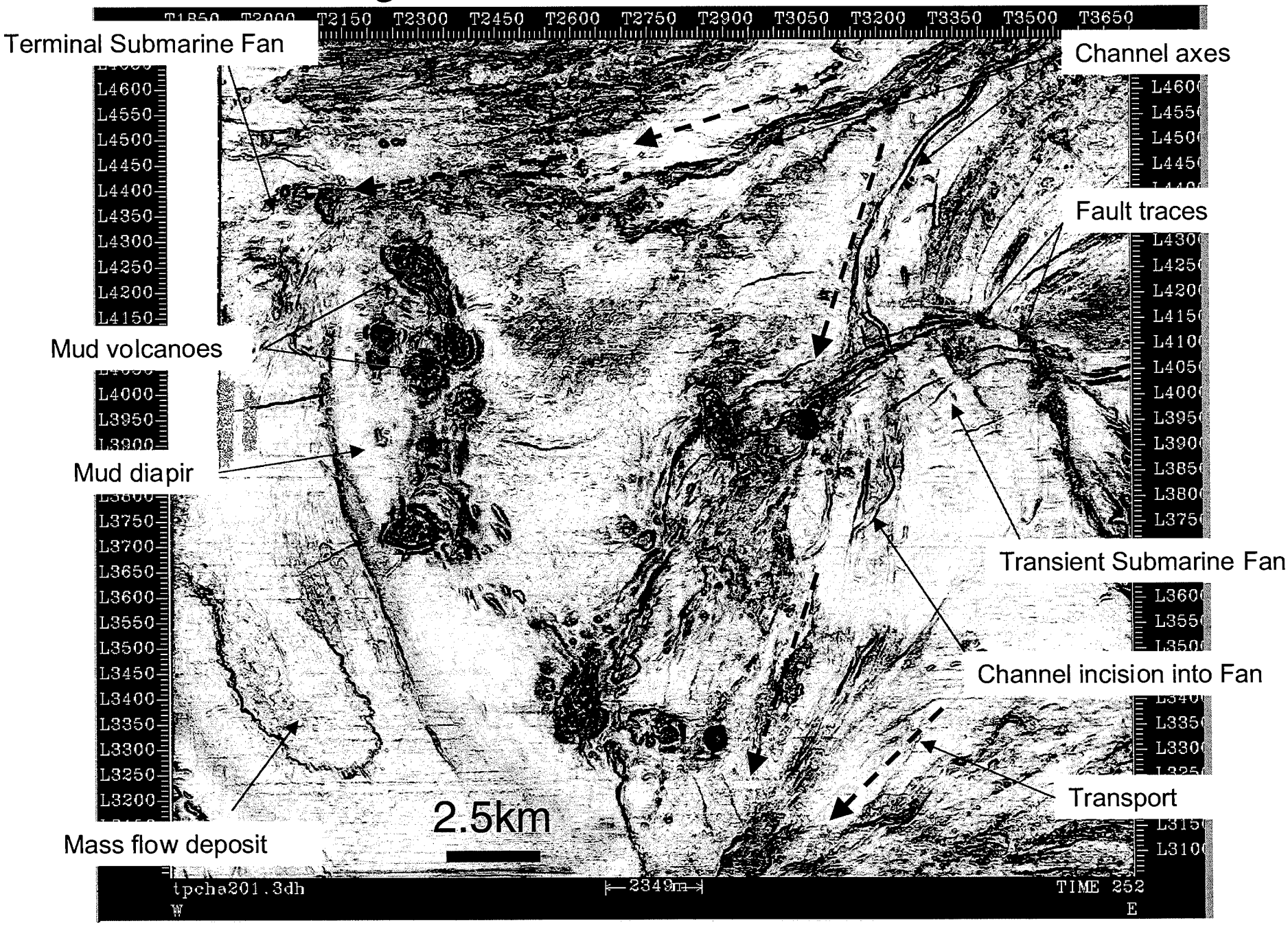

incised channels in sheet sands

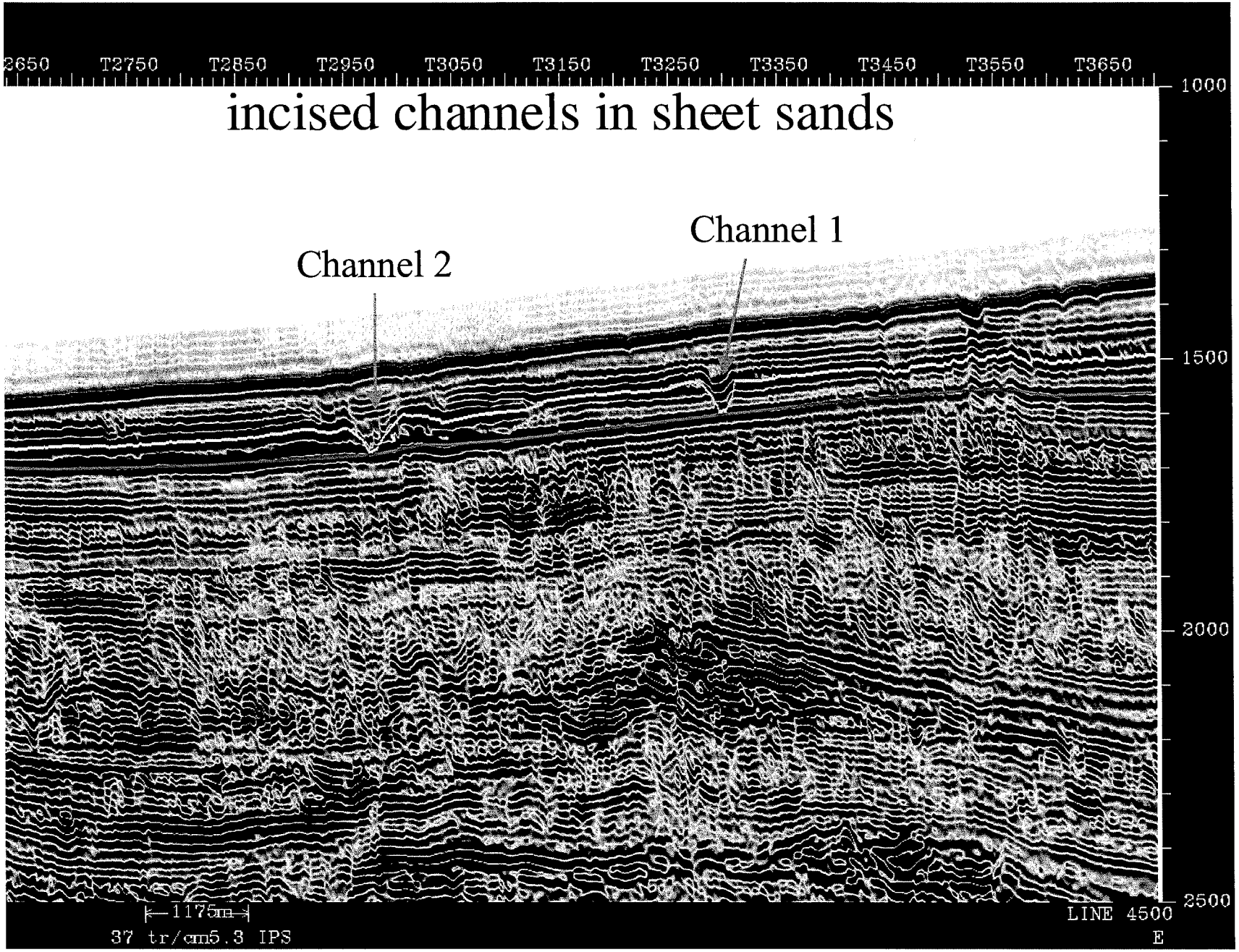

Nigeria - Near Sea Floor

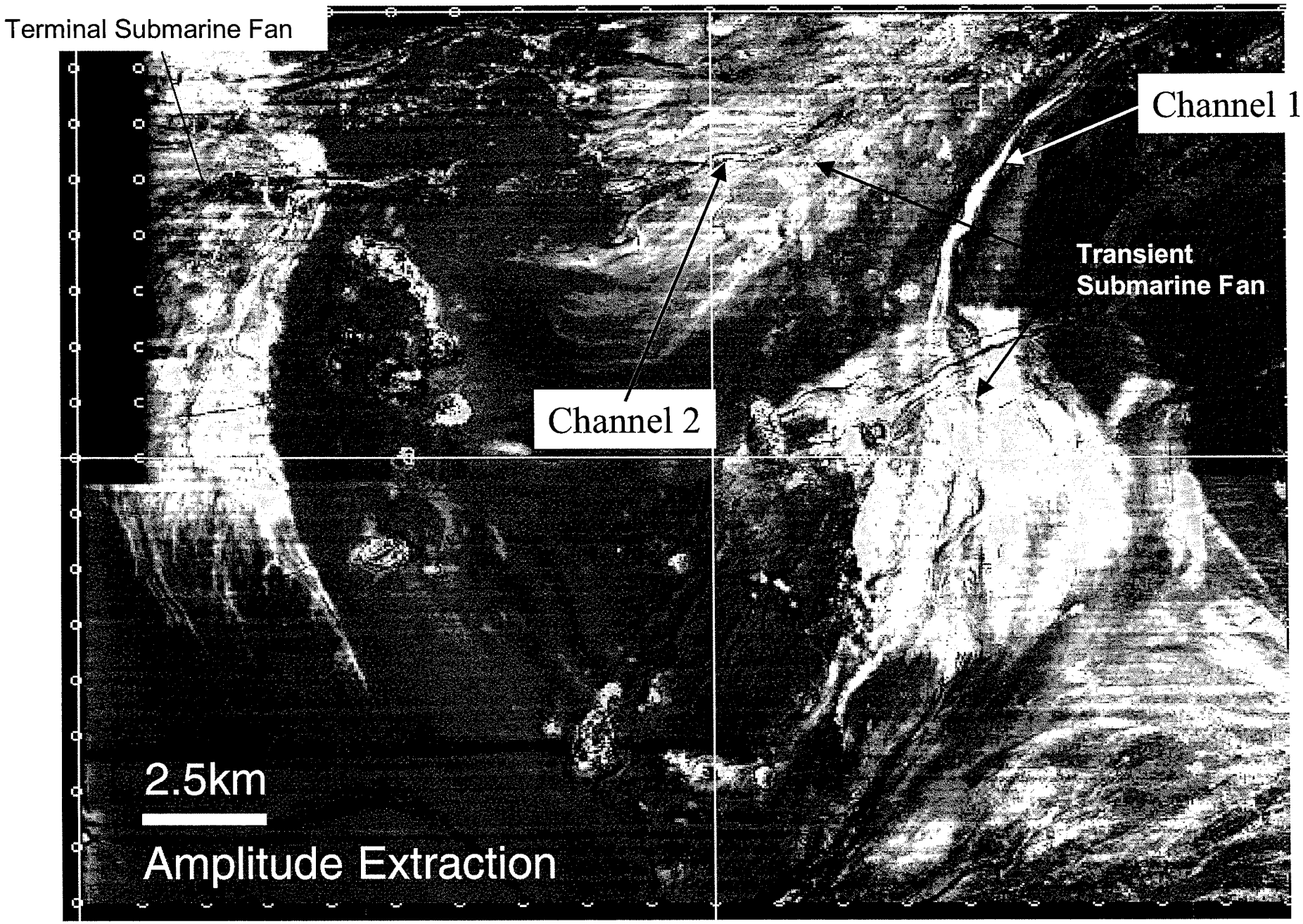

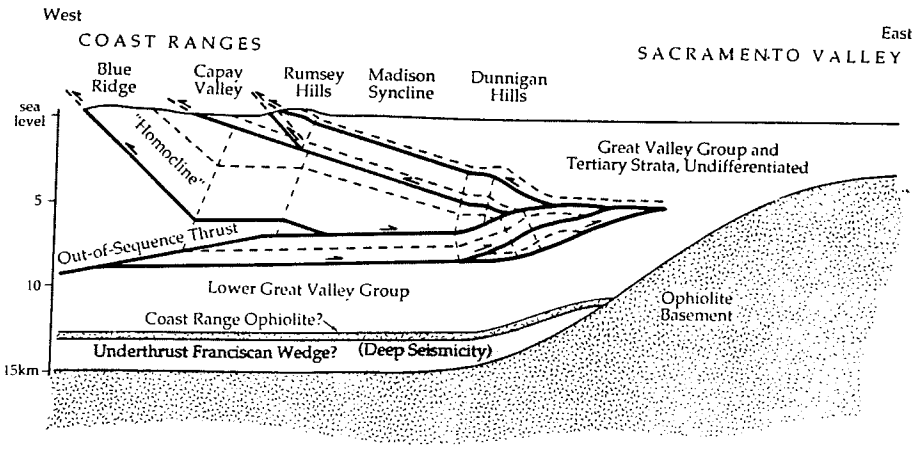

Fig. 7. Schematic model for the blind thrust system beneath the southwestern Sacramento Valley based on tectonic-geomorphic development, patterns of microseismicity, and analysis of seismic reflection data. Uplift of the eastern Coast Ranges and homoclinal eastward tilting at the mountain front is attributed to the growth and propagation of a triangle zone. Folding east of the mountain front is due to movement on an east-vergent out-of-sequence thrust and movement on west-vergent backthrusts that root in the out-of-sequence thrust. The model also speculatively attributes deep microseismicity (10-13 km) to thrusting within an underthrust wedge of Franciscan assemblage, as proposed for the western San Joaquin Valley by Wentworth et al. [1984] and Wentworth and Zoback [1989].

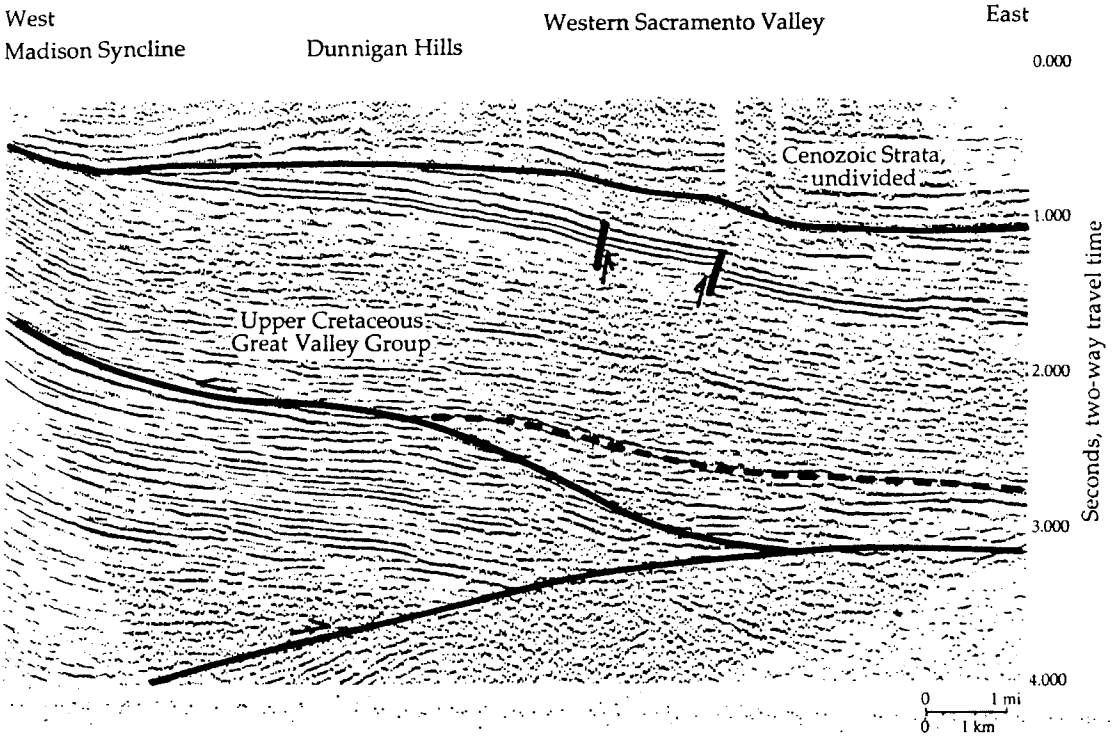

Fig. 6b. Interpretation of the major structures in the ARCO profile (Figure 6a). The blind east-vergent thrust beneath the eastern Rumsey Hills visible in the Chevron profile (Figure 5) extends eastward beneath the Dunnigan Hills. A west-vergent thrust roots in the blind east-vergent thrust and ramps up to the west. Fault-bend folding in the hanging wall of the west-vergent thrust is apparent from the deformation of a high-amplitude seismic marker at approximately 2.7-2.8 s depth beneath the eastern Dunnigan Hills, and by folding of the angular unconformity between the Mesozoic Great Valley strata and overlying Cenozoic strata.

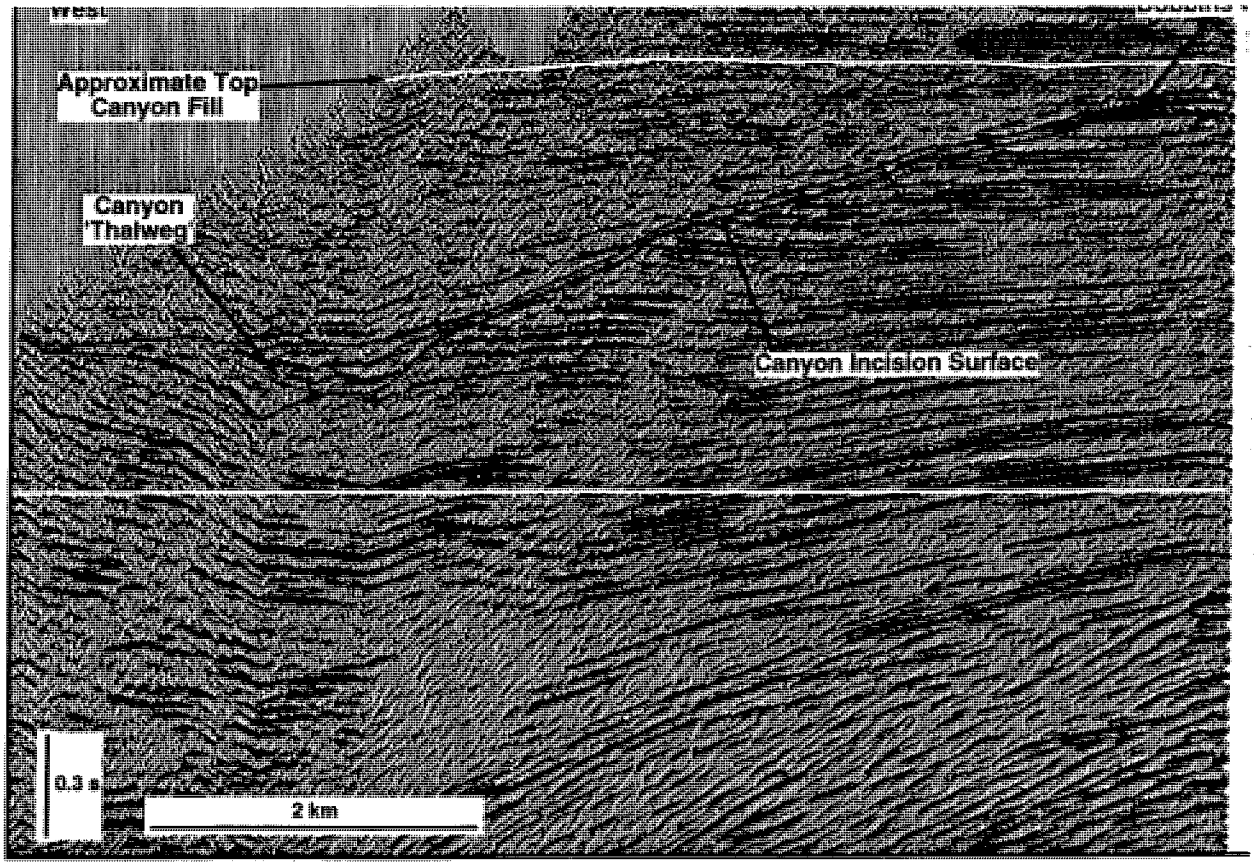
WEST
Approximate Top Canyon Fill
Canyon 'Thalweg'
Canyon Incision Surface
0.3 s
2 km

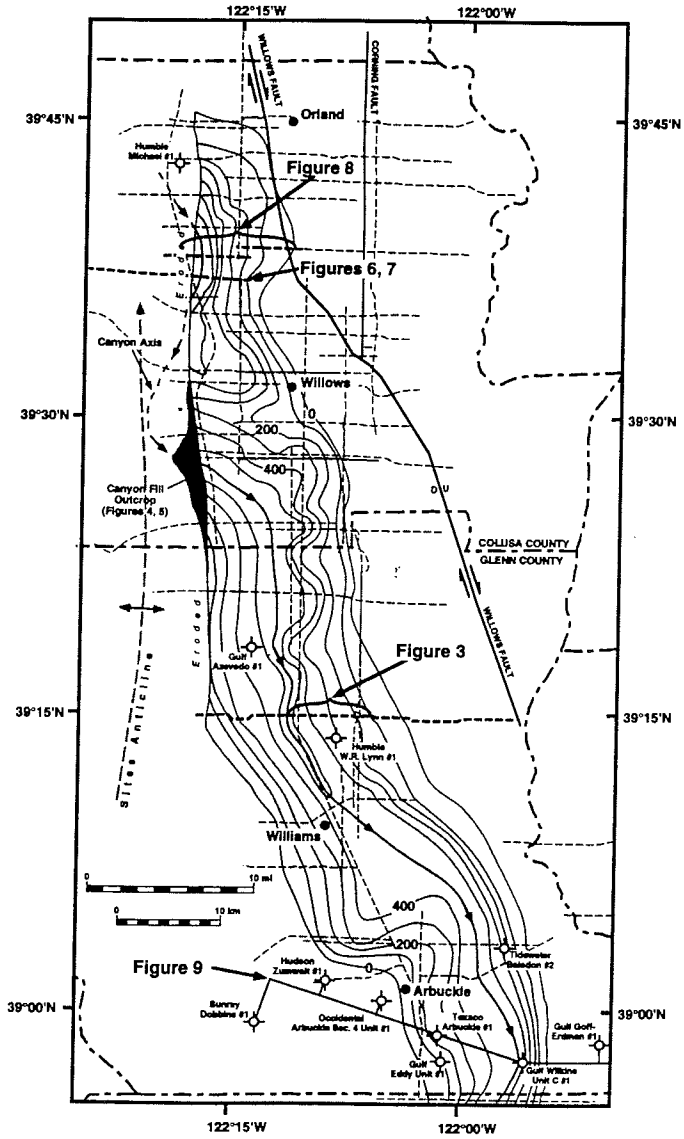
122°15'W
122°00'W
39°45'N
39°30'N
39°15'N
39°00'N
WILLOWS FAULT
CORNING FAULT
Orland
Humble Michael #1
Figure 8
Figures 6, 7
Canyon Axis
Willows
0
200
400
Canyon Fill Outcrop (Figures 4, 5)
COLUSA COUNTY
GLENN COUNTY
Eroded
Stony Anticline
Gulf Azevedo #1
Figure 3
Humble W.R. Lynn #1
Williams
0
10 mi
0
10 km
400
200
0
Figure 9
Hudson Zumwalt #1
Tidewater Baladon #2
Arbuckle
Sunray Dobbins #1
Occidental Arbuckle Sec. 4 Unit #1
Texaco Arbuckle #1
Gulf Goff-Erdman #1
Gulf Eddy Unit #1
Gulf Wilkins Unit C #1

SEISMIC STRATIGRAPHY IN THE LARGEST SENSE.

- DRAW TOGETHER LOCAL SEQ & STRUCTURE TO PRODUCE REGIONAL SETTING & HISTORY

- DRAW TOGETHER MANY SUCH REGIONAL STUDIES TO DETECT GLOBAL PATTERNS IN SEQUENCES

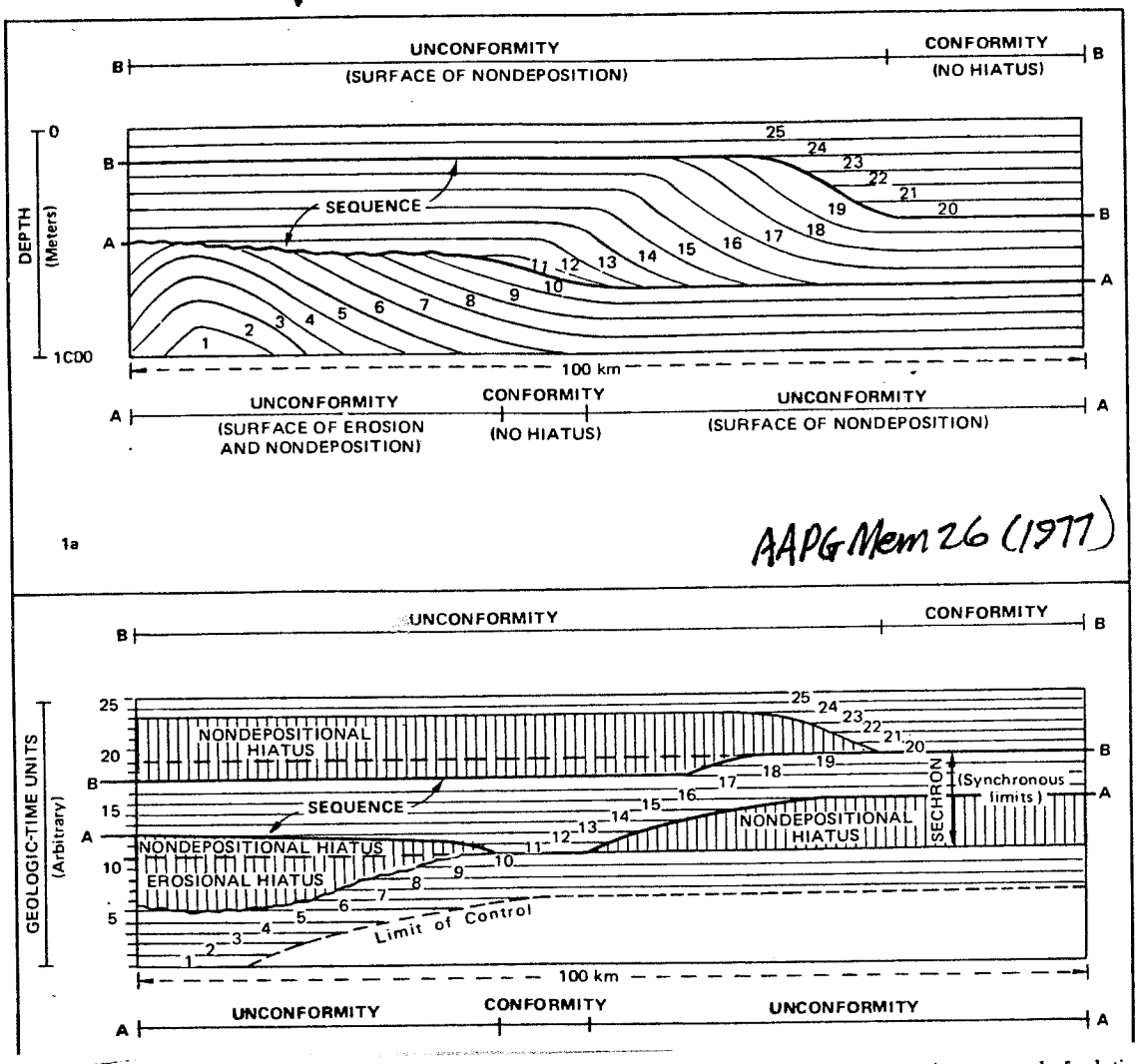

FIG. 1—Basic concepts of depositional sequence. A depositional sequence is a stratigraphic unit composed of relatively conformable successions of genetically related strata and bounded at its top and base by unconformities or their correlative conformities.

A. Generalized stratigraphic section of a sequence. Boundaries defined by surfaces A and B which pass laterally from unconformities to correlative conformities. Individual units of strata 1 through 25 are traced by following stratification surfaces, and assumed conformable where successive strata are present. Where units of strata are missing, hiatuses are evident.

B. Generalized chronostratigraphic section of a sequence. Stratigraphic relations shown in A are replotted here in chronostratigraphic section (geologic time is the ordinate). Geologic-time ranges of all individual units of strata given as equal. Geologic-time range of sequence between surfaces A and B varies from place to place, but variation is confined within synchronous limits. These limits determined by those parts of sequence boundaries which are conformities. Here, limits occur at beginning of unit 11 and end of unit 19. A sechron is defined as maximum geologic-time range of a sequence.)

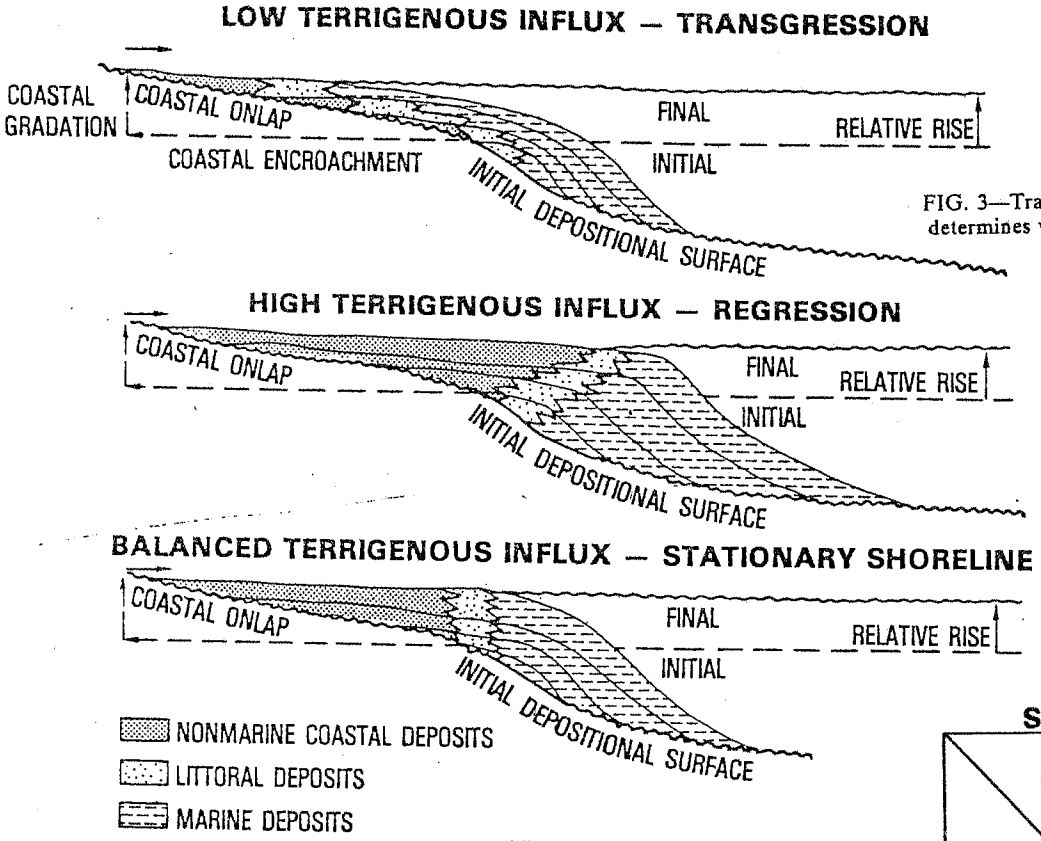

FIG. 3—Transgression, regression, and coastal onlap during relative rise of sea level. Rate of terrigenous influx determines whether transgression, regression, or stationary shoreline is produced during relative rise of sea level.

AAPG Mem 26 (1977)

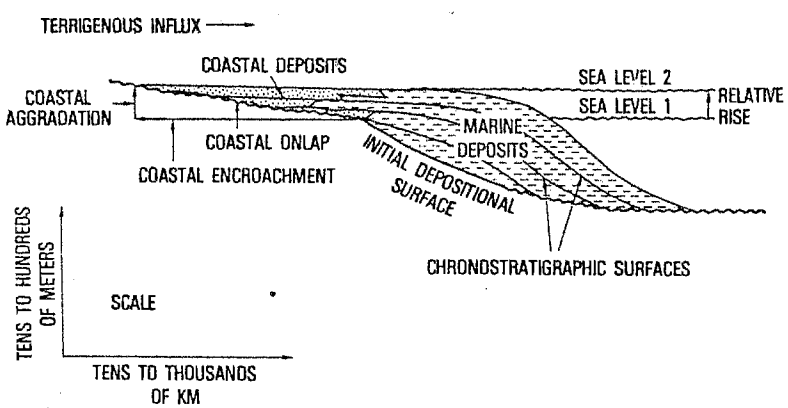

FIG. 2—Coastal onlap indicates a relative rise of sea level. Relative rise of base level allows coastal deposits of a maritime sequence to aggrade and onlap initial depositional surface.

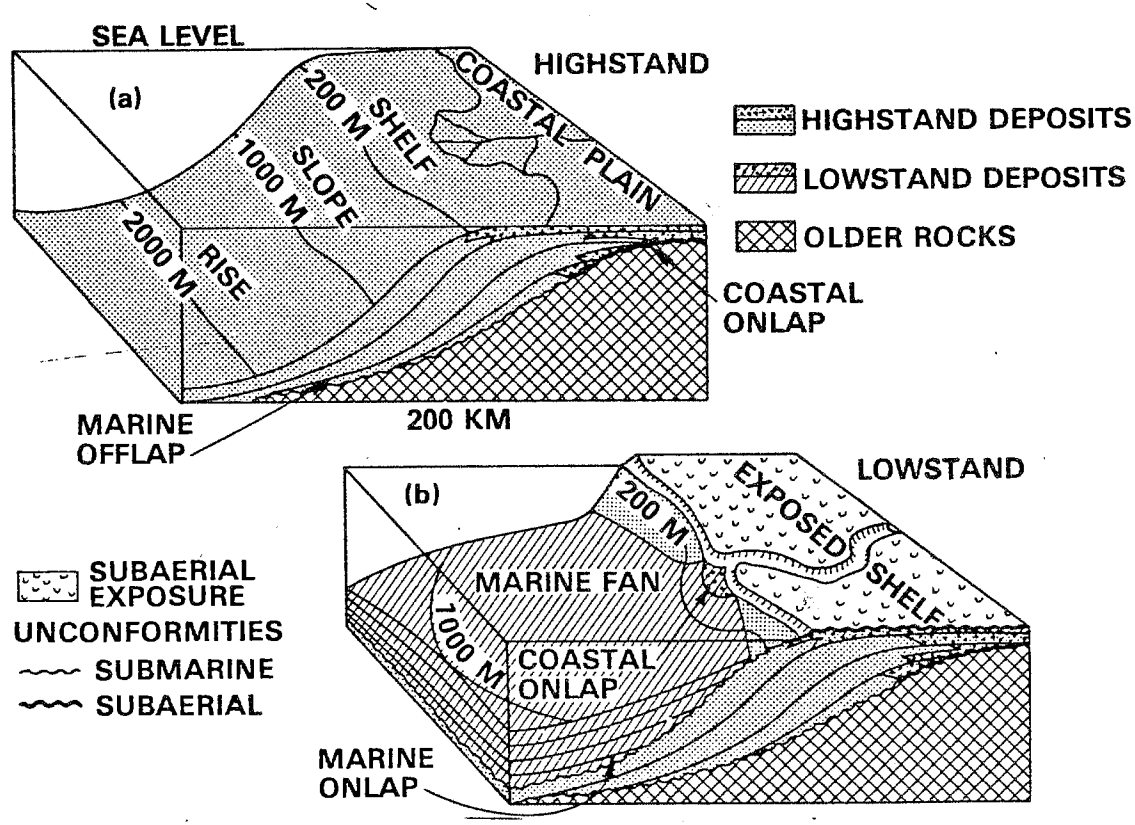

FIG. 9—Depositional patterns during highstand (a) and lowstand (b) of sea level.

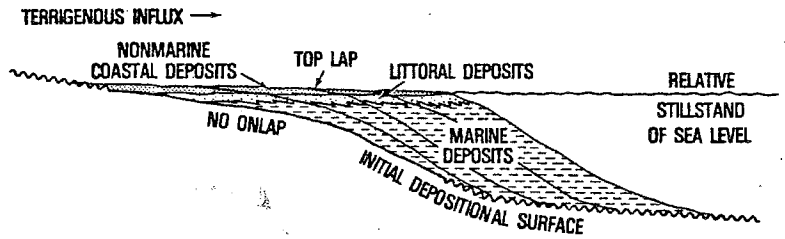

FIG. 6—Coastal toplap indicates relative stillstand of sea level. With no relative rise of base level, nonmarine coastal and/or littoral deposits cannot aggrade, so no onlap is produced; instead, by-passing produces toplap.

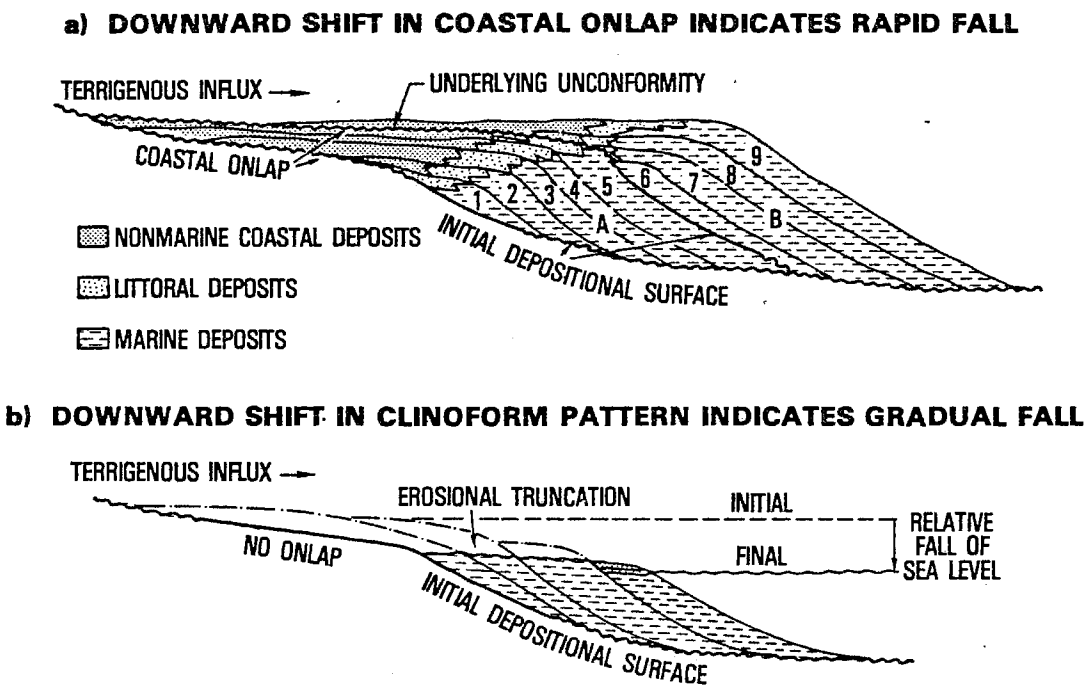

FIG. 8—Downward shift of coastal onlap indicates relative fall of sea level. With relative fall of base level, erosion is likely: deposition is resumed with coastal onlap during subsequent rise. (a) Downward shift in coastal onlap indicates rapid fall observed in all cases studied so far. (b) Downward shift in clinoform pattern (after Weller, 1960), indicates gradual fall; but has not been observed on seismic data.

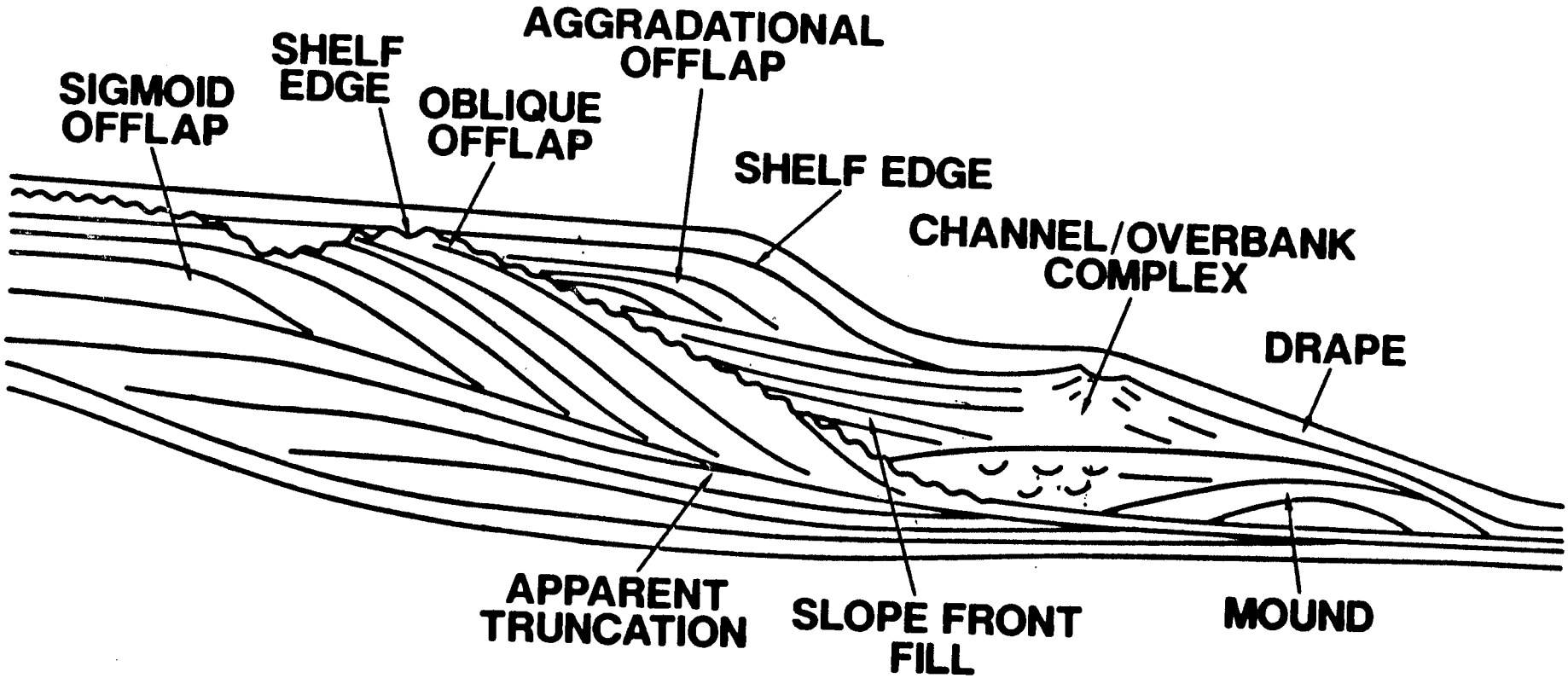

Figure 6. Diagram showing simulated seismic section with common seismic facies patterns.

P. Vail, 1988 in Seis Strat. Atlas (Bally, ed)

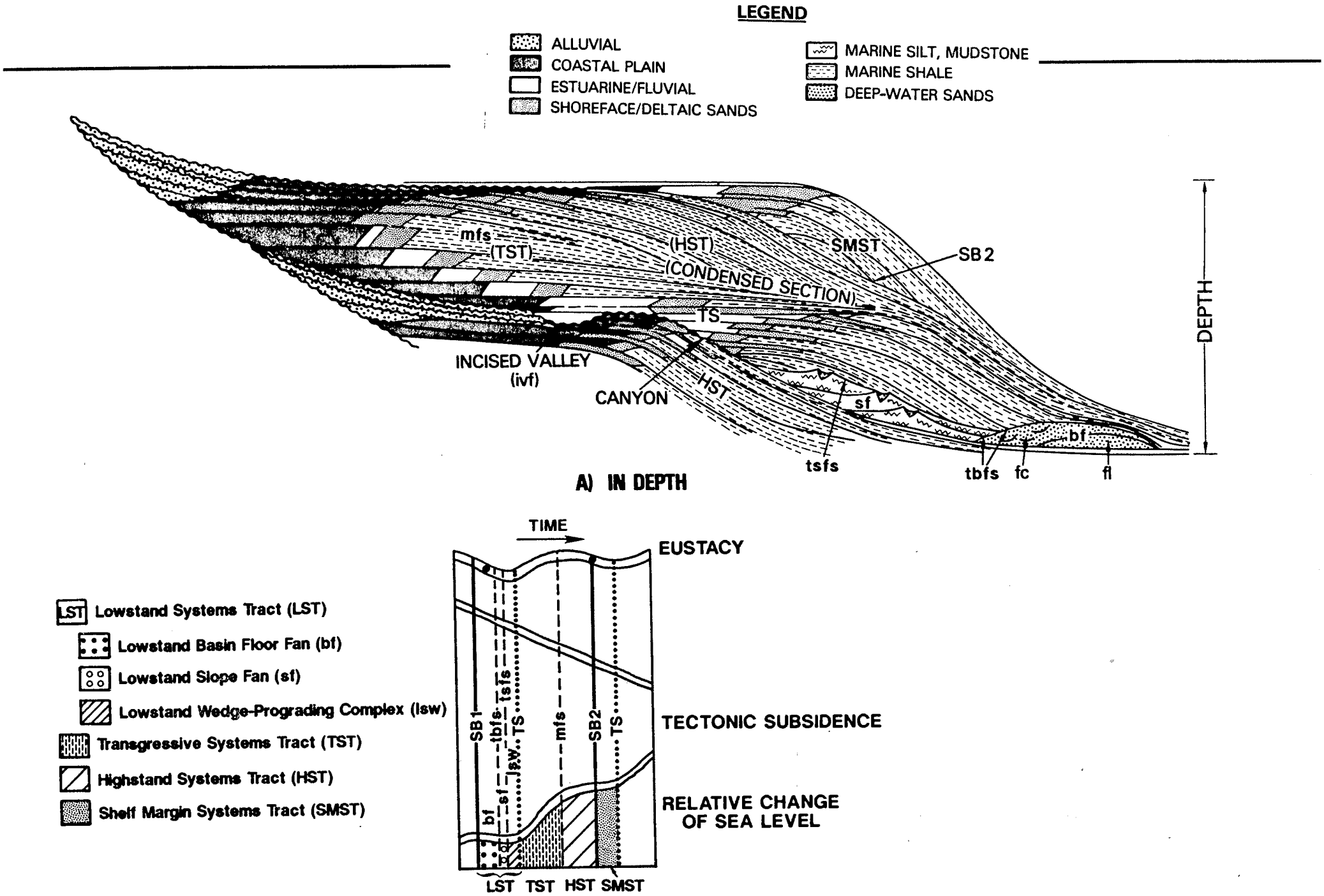

Vail, 1988 in Bally "Seis Strat Atlas" v. 2.

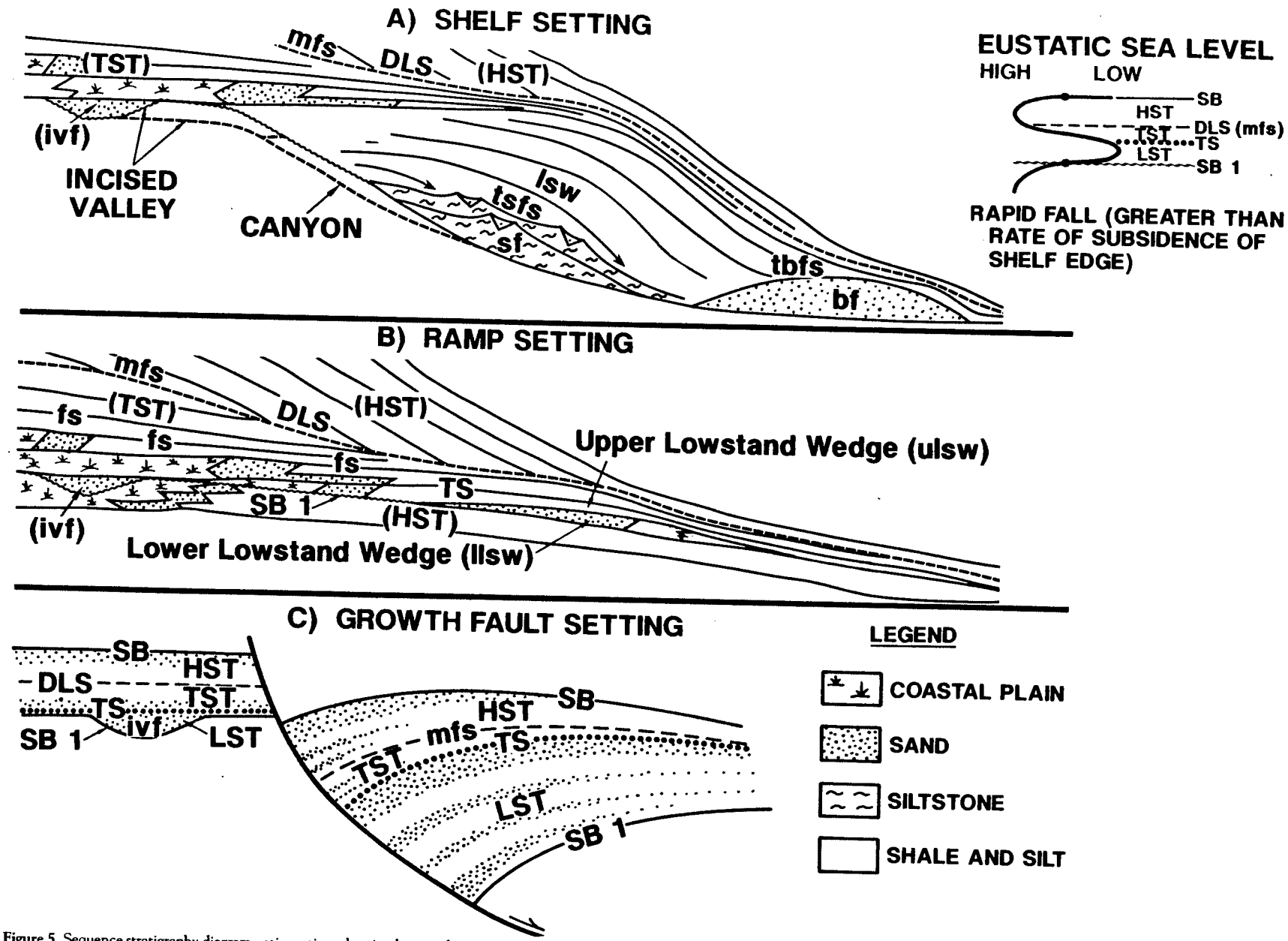

Figure 5. Sequence stratigraphy diagrammatic section, showing lowstand systems tracts in shelf, ramp and growth fault settings.

Vail & Baly

Stratigraphic sequences occur in a scaled hierarchy.

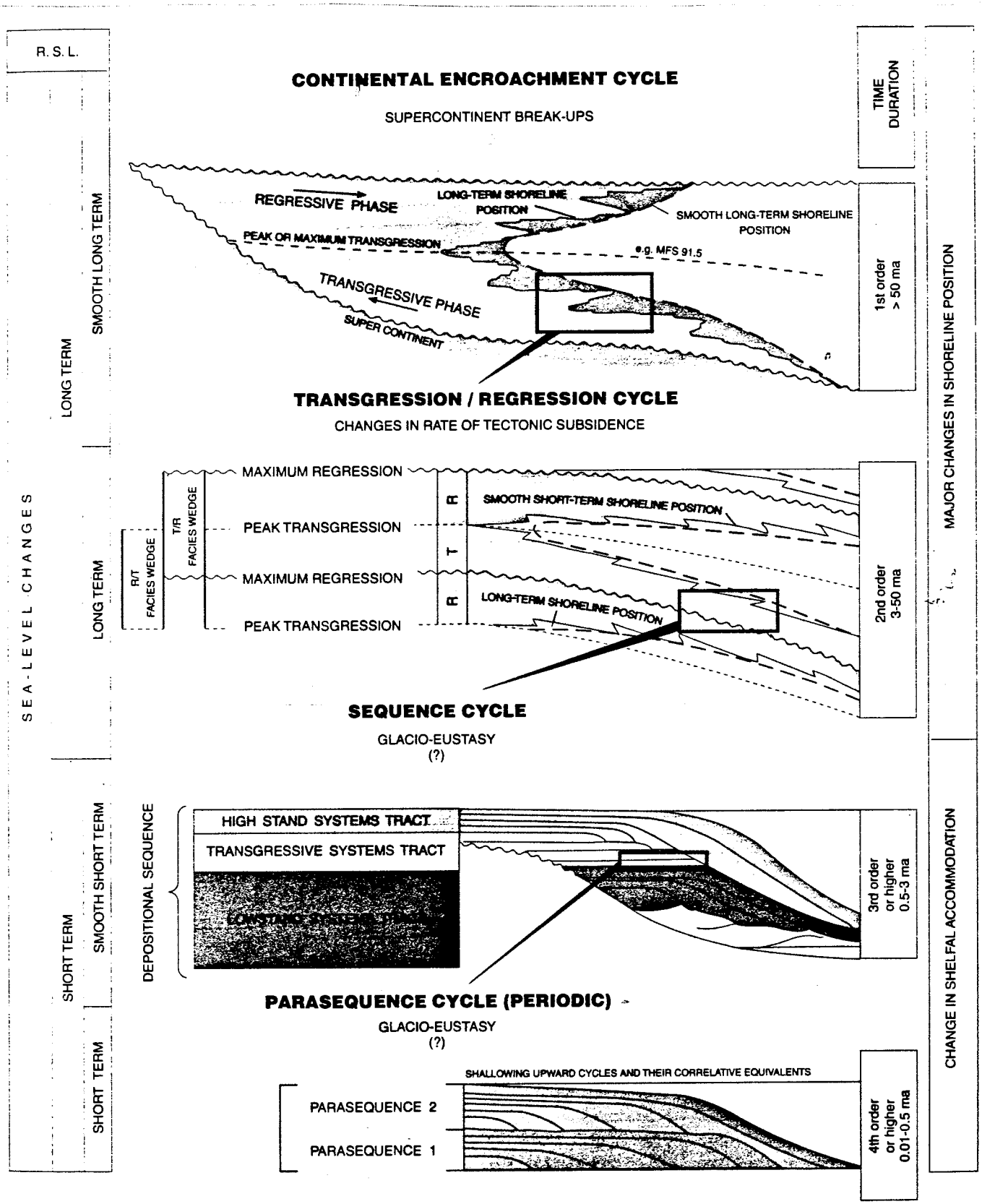

Fig. 2.9 Hierarchy of stratigraphic cycles (after Duval *et al.*, 1992)

MORE ON SECTION ANALYSIS AT A REGIONAL LEVEL THRU AN EXAMPLE FROM THE WEST AFRICAN CONTINENTAL MARGIN.

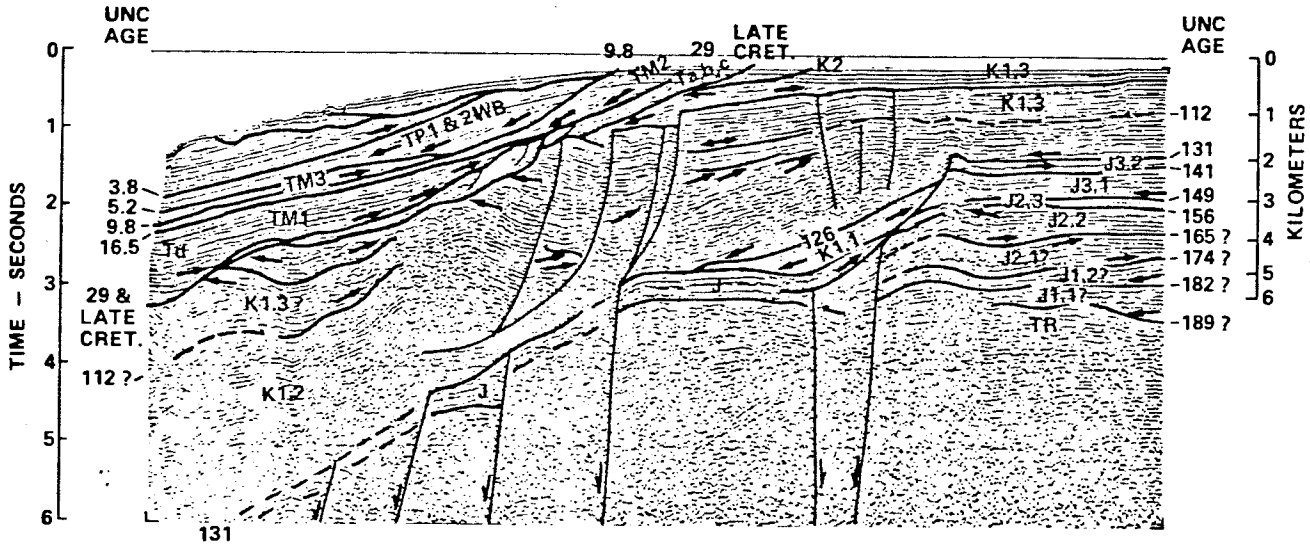

Fig. 2. Seismic section from offshore northwest Africa showing sequences defined by seismic reflections. Systematic reflection termination patterns are used to determine downlap, onlap, truncation, and toplap of strata at sequence boundaries. Geologic ages of sequences determined from wells on section and in surrounding area. Sequence and sequence boundary notations, e.g. J2.3 and 131, and the ages they represent are listed in Fig. 1 and explained in the text.

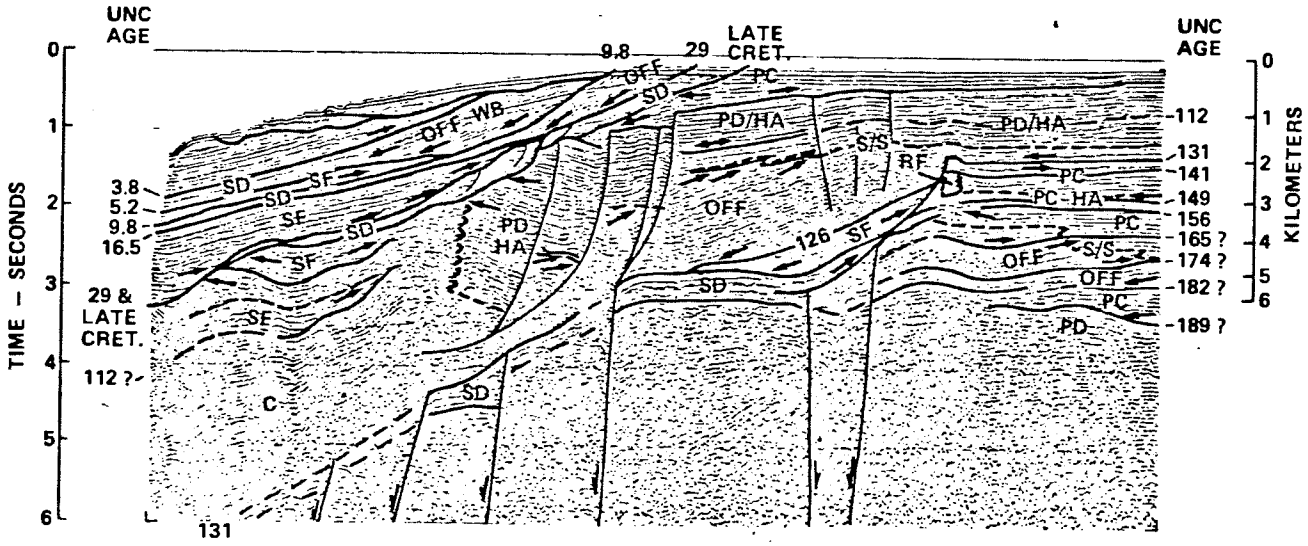

Fig. 3. Seismic section, same as Fig. 2, showing seismic facies units.

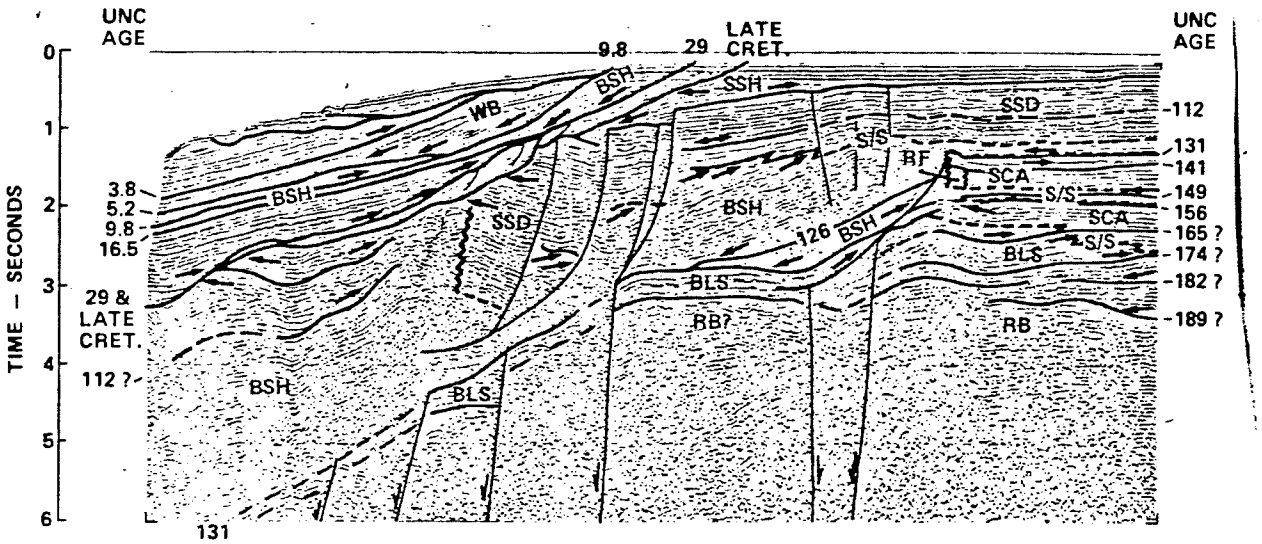

Fig. 4. Seismic section, same as Fig. 2, showing geologic facies.

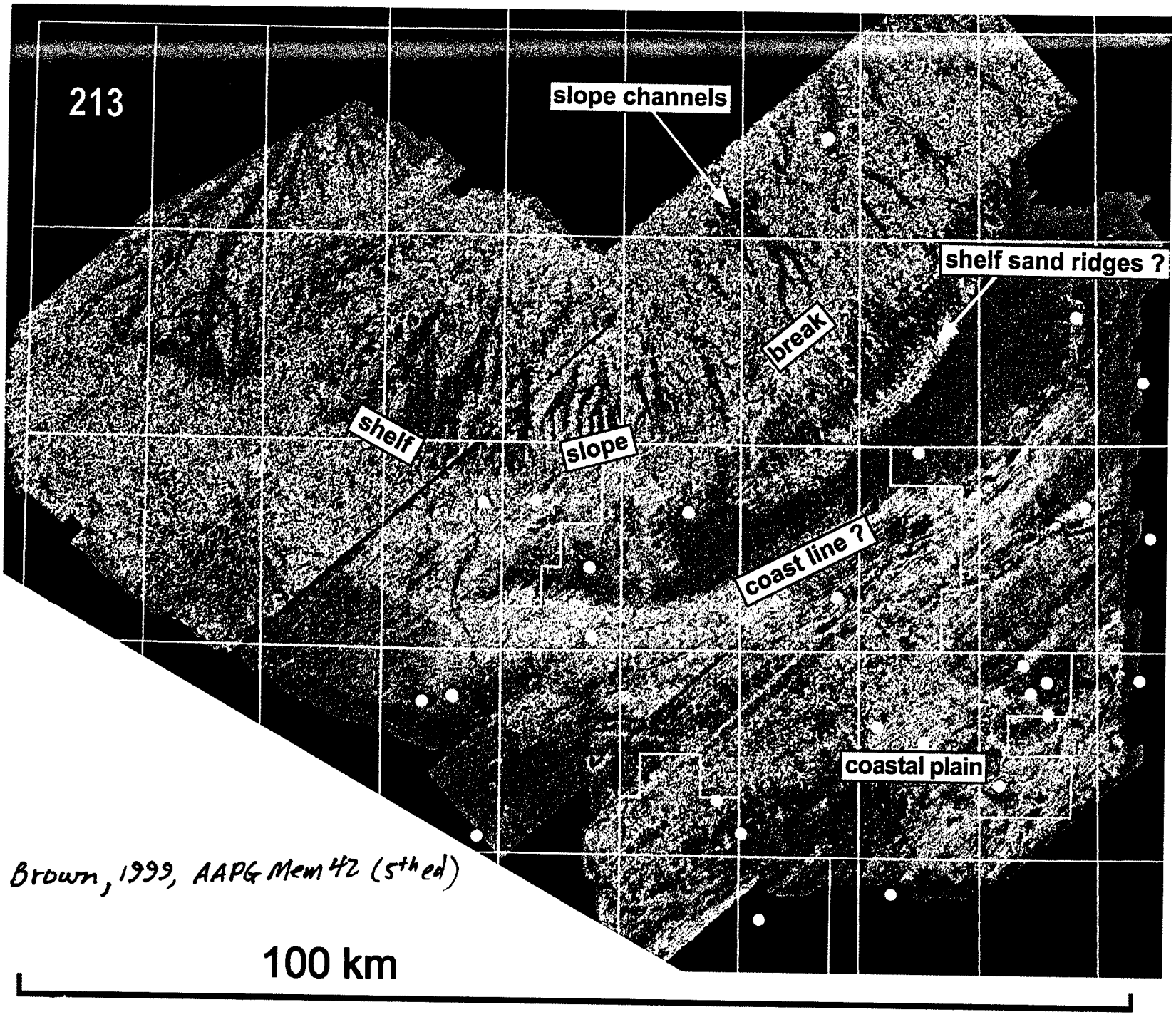

Brown, 1999, AAPG Mem 42 (5th ed)

WITH THESE CONCEPTS IN MIND, YOU CAN SET OUT TO ANALYZE COMPLEX STACKS OF SEQUENCES?

1. SEIS-STRAT SECTION
   - DEFINE SEQS.
   - INFER FACIES

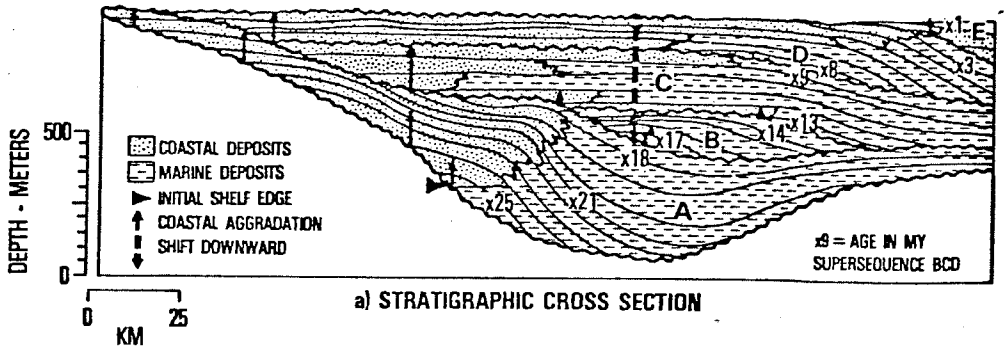

a) STRATIGRAPHIC CROSS SECTION

2. CONSTRUCT CHRONOSTRATIGRAPHY

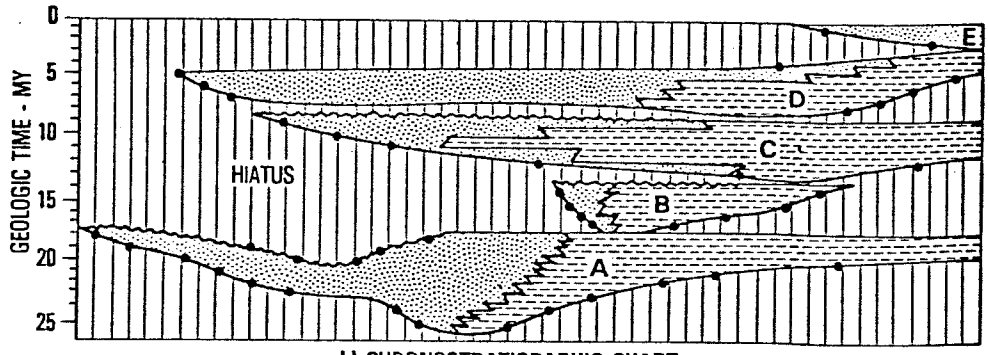

b) CHRONOSTRATIGRAPHIC CHART

3. PLOT TIME VS. THICKNESS CHANGES RELATIVE TO SOME REFERENCE TO TRACK $ CHANGE (RELATIVE) THRU TIME.

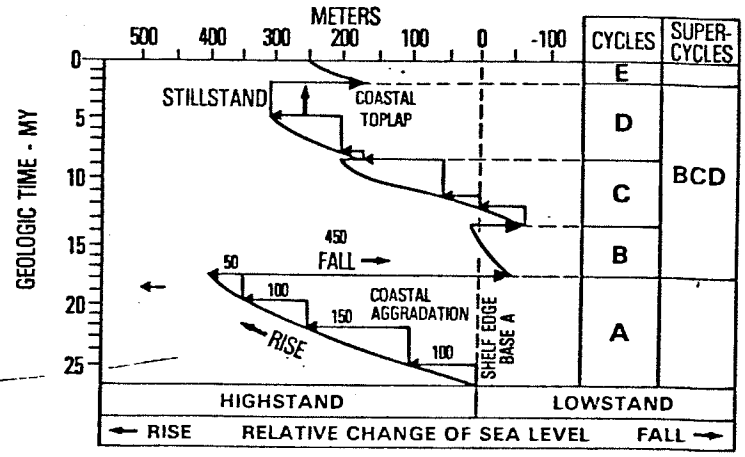

c) REGIONAL CHART OF CYCLES OF RELATIVE CHANGES OF SEA LEVEL

FIG. 13—Procedure for constructing regional chart of cycles of relative changes of sea level.

ARE THE PATTERNS IN 13C) A REFLECTION OF REGIONAL TECTONICS OR GLOBAL EUSTACY?

TO HELP ANSWER THAT QUESTION, MUST COMPARE $ CURVE W/ CURVES FROM OTHER REGIONS & OTHER TECTONIC SETTINGS.

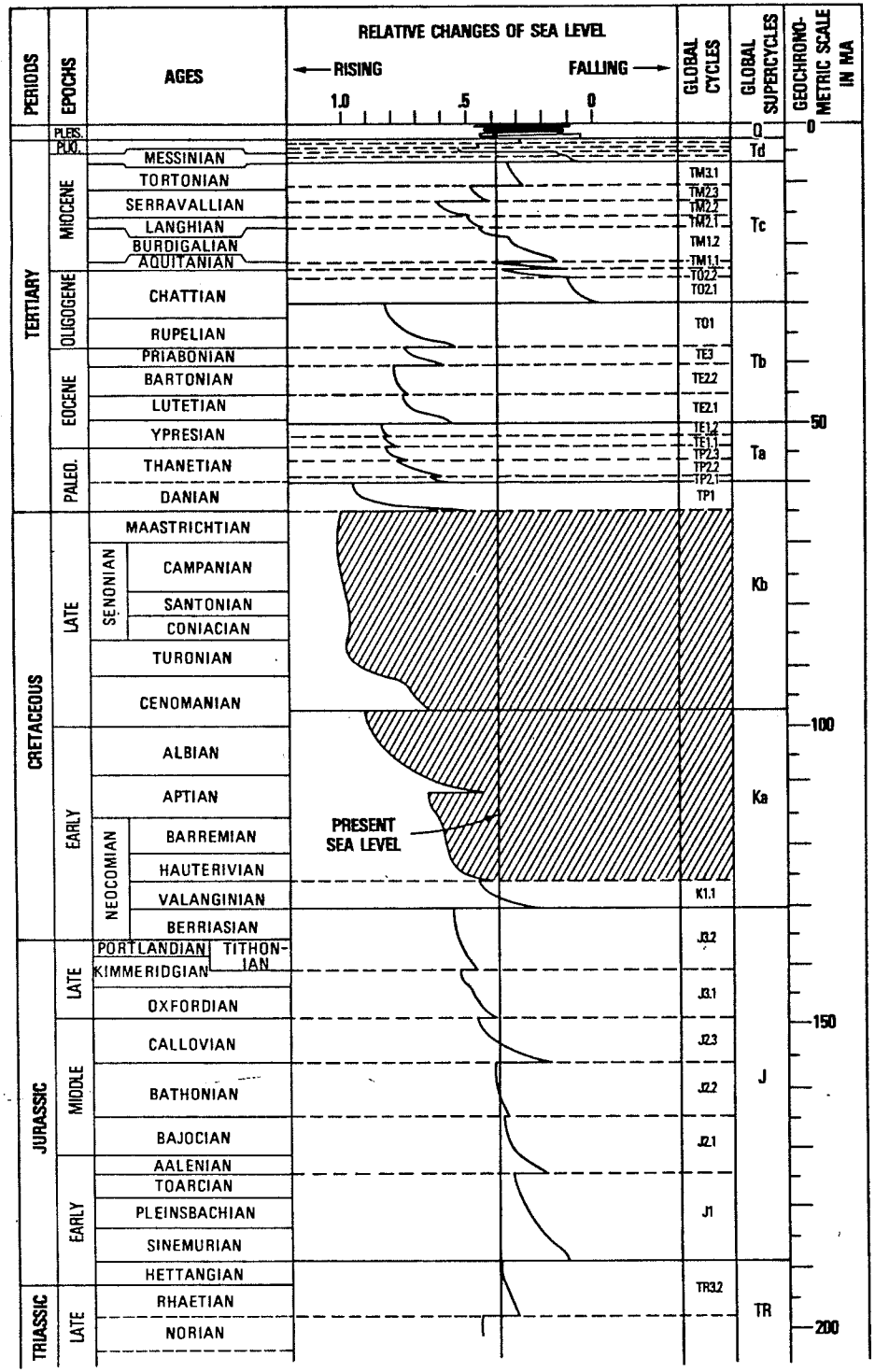

Jurassic-Cretaceous time scale after Van Hinte 1976 a, b

FIG. 2—Global cycles of relative change of sea level during Jurassic-Tertiary time. Cretaceous cycles (hatchured area) have not been released for publication.

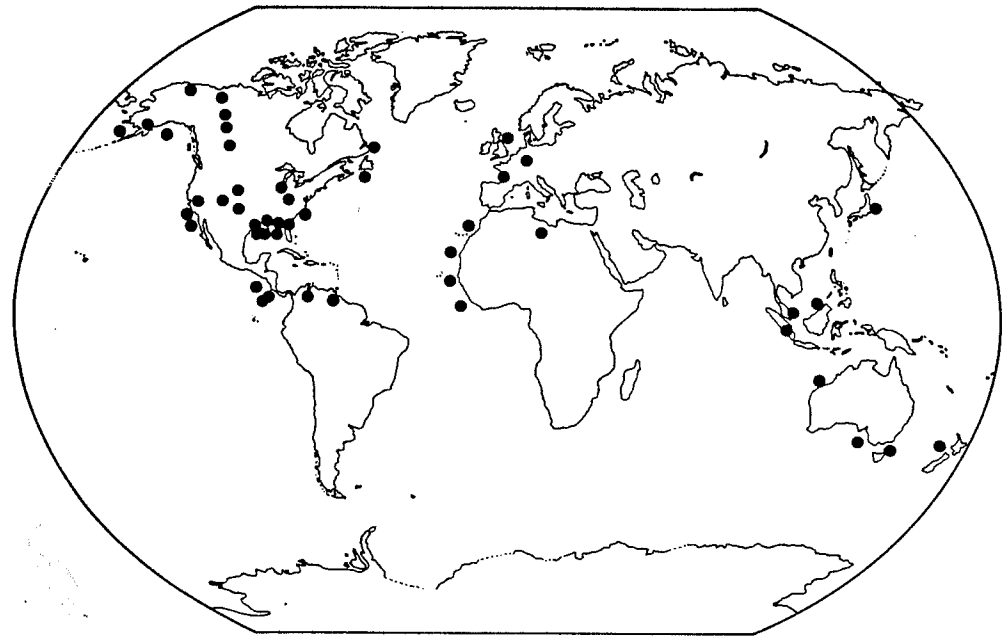

FIG. 4—Location of regional studies of seismic stratigraphy used in construction of global cycle chart for Phanerozoic time.

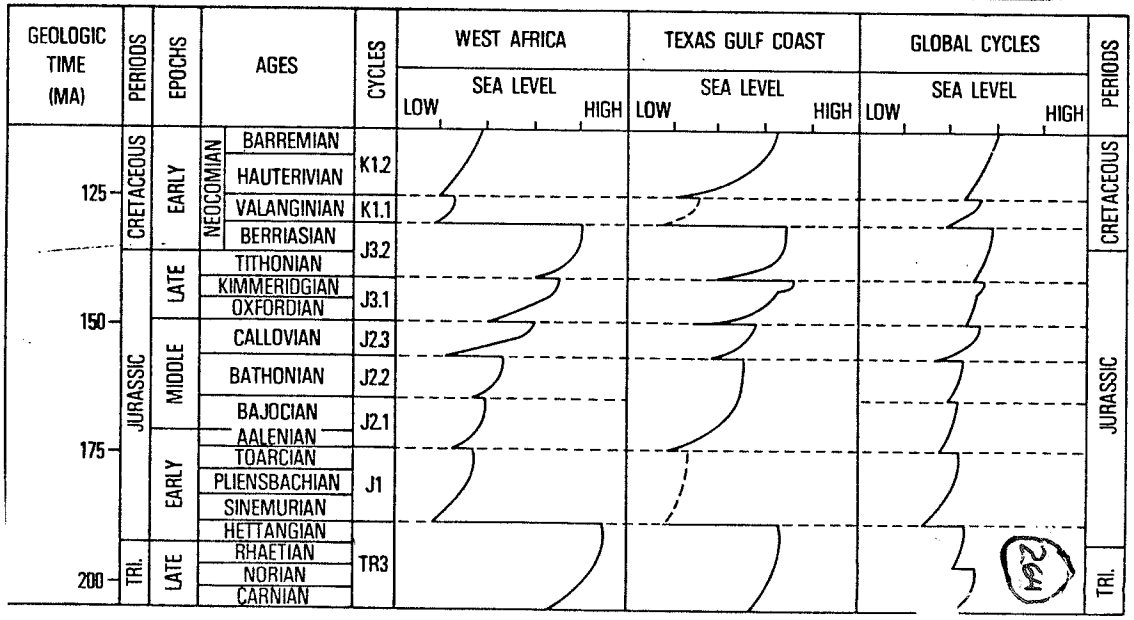

FIG. 14—Comparison of regional cycle charts offshore West Africa and Texas Gulf Coast with global cycle chart.

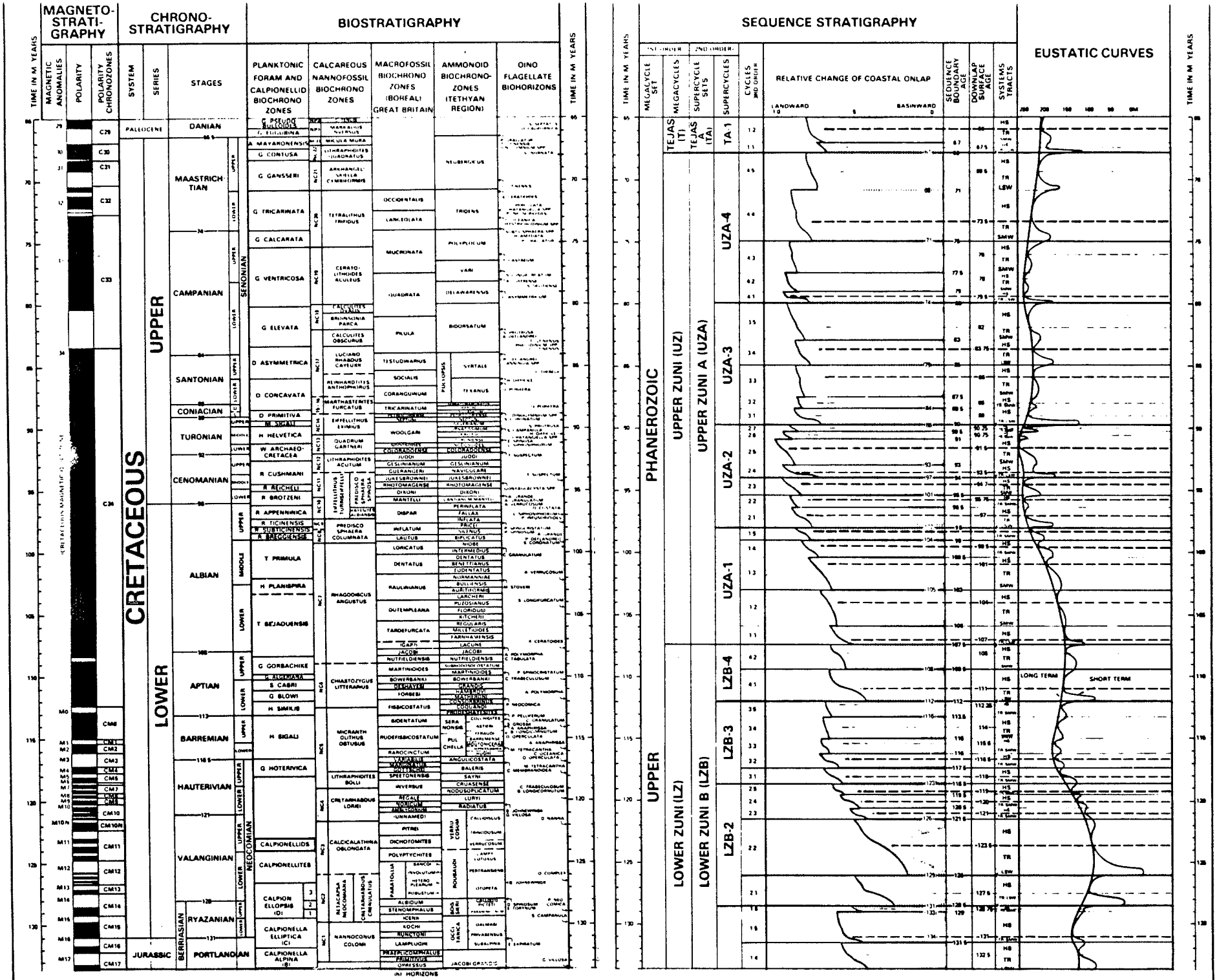

Hag et al '87 Science v. 235

Excerpts from Emery & Meyers (96)

On coastal onlap curves ....

Variations in relative sea-level can be read from the coastal onlap curve. Landward movement of coastal onlap implies rising relative sea-level, whereas seaward movement implies static or falling relative sea-level. This can be seen on Fig. 5.4, where landward shifts in coastal onlap within the lowstand wedge, highstand and transgressive systems tracts are associated with rising relative sea-level, whereas the fall in relative sea-level accompanying deposition of the fans is associated with a basinward movement in coastal onlap. The magnitude of the lateral movement in coastal onlap depends partly on the magnitude of the relative sea-level change, and partly on the basin topography, and is equal to the relative sea-level change divided by the tangent of the topographic slope. It is difficult therefore to deduce the magnitude of relative sea-level changes from a coastal onlap curve, although the frequency of the changes is recorded. Note, however, that these changes may not all be recorded on any one seismic line. A particular line may not intersect a lowstand wedge, for example, and the relative sea-level history associated with that lowstand would not be apparent on the chronostratigraphic chart constructed from that line. A three-dimensional chronostratigraphic analysis is needed to understand fully the relative sea-level history of an area. Also a long-duration period of erosion may remove evidence for previous relative sea-level variations.

Coastal onlap curves were produced for a number of basins by workers in Exxon in the 1970s, and used to construct the composite global coastal onlap curve published by Haq *et al.* (1988). The 'saw-tooth' nature of this curve is an artefact of the plotting process, and the abrupt basinward shifts in coastal onlap represent the boundaries between onlapping topsets of the highstand systems tract and onlapping topsets of the lowstand systems tract (although in some cases the onlap patterns in the lowstand fans were also included in the coastal onlap plot). This asymmetry in the variations in coastal onlap should not be construed as an asymmetry in relative sea-level variations, with rapid falls and slow rises. Asymmetric coastal onlap cycles will result from sine-wave variations in relative sea-level, as a function of the sedimentary response.

One sea-level curves ....

A relative sea-level curve may be constructed by plotting the vertical movement of the topsets through time. This is based on the assumption that topsets were deposited as relatively flat units close to sea-level. Obviously this assumption is not valid in detail, because even paralic topsets will have had some depositional slope. It is probably a good enough assumption in practice for measuring large-scale variations in relative sea-level. For more accuracy, the vertical movement of the offlap break could be measured, based on the assumption that the offlap break occurred at a constant depth during relative sea-level changes. Again this probably is not valid in detail, because the depth of the offlap break is a function of the balance between fluvial supply and marine reworking, a balance that will change during a relative sea-level cycle.

Rising relative sea level causes the topsets and the offlap break to rise with time, with respect to the underlying surfaces, whereas falling relative sea-level causes the offlap break to fall, and the topsets to be displaced downwards. A plot of relative sea-level therefore can be constructed from the vertical movement of the topsets and/or the offlap break. Details of the relative sea-level history will be lost if any of the topsets are removed by erosion.

On problems w/ $ curves...

There are a number of aspects of the Haq *et al.* (1987) chart that have excited comment:

1 The data to support the Haq chart have never been published fully, in particular the evidence for the global correlatability of the sequence boundaries. Miall (1986, 1992) has been a consistent critic of the Haq *et al.* curve, stating:

> The basic premise of the Exxon cycle chart, that there exists a globally correlatable suite of third order eustatic cycles, remains unproven...There are some specific cases where global synchroneity is suggested by detailed stratigraphic documentation (e.g. 4th- and 5th-order glacioeustatic cycles in the Neogene and, possibly the late Palaeozoic; 1st- and 2nd-order cycles related to changing rates of global sea floor spreading), but for the greater part of the Phanerozoic column no such proof is available. (Miall, 1991)

Miall also points out that it is arguable whether global biostratigraphic control is accurate enough to correlate third-order relative sea-levels unambiguously. Thus, for the moment, the global synchroneity of eustatic cycles has to remain to a degree an article of scientific faith rather than scientific fact.

2 The mechanism for generating third-order-scale eustatic sea-level changes is problematic in certain periods of geological time. Increases in the global ice volume during glaciations provide a mechanism for eustatic falls in sea-level in the late Cenozoic and late Palaeozoic, but no such mechanism exists for the (presumed) ice-free Cretaceous and Jurassic. Cloetingh *et al.* (1985) have proposed intraplate stress as a tectonic mechanism for generating third order plate-wide relative sea-level cycles. Finally, it is not accepted universally that the eustatic signal will be visible in all basins, and several stratigraphers believe that it may be obscured by a tectonic signal (e.g. Hubbard, 1988).

However, work is continuing to date basin-margin unconformities more accurately and to correlate these with the Neogene oxygen isotope record and hence directly to ice volume changes (e.g. Miller *et al.*, 1991, 1993). Also, various projects are underway to accurately date and correlate sequence boundaries on a regional scale in Europe, e.g. De Graciansky *et al.* (1993).

PLEDGE OF ALLEGIANCE
TO
SEQUENCE STRATIGRAPHY

I TOTALLY AND COMPLETELY ENDORSE AND EMBRACE
THE SEQUENCE CONCEPT
AS PROMULGATED AND PROMOTED
BY VAIL AND HIS DISCIPLES

I WHOLLY AND FIRMLY BELIEVE THAT
EUSTATIC SEA LEVEL
IS RESPONSIBLE FOR EVERYTHING,
INCLUDING THE PRICE OF TEA IN CHINA

I ABJURE, DENOUNCE, CONDEMN, AND REJECT
ALL NON SEQUENCE-KEYED GEOLOGIC INTERPRETATIONS

(To be said before showering in the morning while facing towards offshore Morocco, with right hand on the latest cycle chart (Memoir 26 for NPA's))

[Version 1A]

272